

**Carbon–Carbon Sigma Bond Activation:
Functionalizing C–C and C–CN Bonds via Carboacylation and Cyanoamidation**

A DISSERTATION SUBMITTED TO
THE FACULTY OF THE UNIVERSITY OF MINNESOTA
BY

Ashley Michelle Dreis

IN PARTIAL FULFILLMENT OF THE REQUIREMENTS FOR THE DEGREE OF
DOCTOR OF PHILOSOPHY

Advisor: Christopher J. Douglas

January 2015

© Ashley M. Dreis 2015

DEDICATION

To my nephew Aidan

– May you always be curious –

I love you, monkey

ACKNOWLEDGEMENTS

Thank you to everyone who believed in me.

ABSTRACT OF THE DISSERTATION

Chapter One. The content of this chapter broadly describes the growing area of carbon–carbon (C–C) sigma bond activation. The barriers to bond activation and the strategies employed to overcome these barriers will be summarized. Examples of stoichiometric and catalytic reactions utilizing strained systems and other thermodynamic driving forces are presented in addition to kinetic strategies enforced through cyclometalation.

Chapter Two. The focus of the second chapter is on my discoveries in quinoline-directed C–C bond activation. A series of catalytic intramolecular carboacylation reactions with both alkenes and alkynes will be discussed. The mechanism(s) of such transformations were elucidated by researchers at Hope College and will be presented. The intermolecular carboacylation with norbornenes discovered by other Douglas group members will be acknowledged, and preliminary investigations into the idea of migratory insertion (or sigma-bond metathesis) across cyclopropane will be provided.

Chapter Three. The third chapter of this thesis describes my efforts to uncover a synthetically viable directing group for C–C bond activation. Directing groups that are anticipated to be removable and reusable, such as quinoline esters, pyridyl esters, and azaindoles, will be described. Efforts to promote C–C activation with versatile triazene directing groups will be discussed. The strategy of metal-organic cooperative catalysis (MOCC) was explored with guanidines and 2-amino pyrimidine diol derivatives, and the concept of Lewis acid or hydrogen-bond-mediated directing groups will be proposed.

Chapter Four. Chapter four provides a selected review of carbon–nitrile (C–CN) bond activation. Cleavage of alkyl, allyl, alkenyl, aryl, acyl, and carbamoyl C–CN bonds that undergo subsequent functionalization will be reported. Intramolecular variations of such reactions are highlighted in complex molecule syntheses.

Chapter Five. The final chapter will explain my efforts in developing enantio- and diastereoselective routes to 3,3-disubstituted lactams via C–CN bond activation (cyanoamidation). β -, λ -, and δ -lactams are shown to be effectively prepared through this methodology, and attempts to access ϵ -lactams will be discussed.

TABLE OF CONTENTS

Dedication.....	i
Acknowledgements.....	ii
Abstract of the Dissertation.....	iii
List of Abbreviations.....	ix-xii
List of Figures.....	xiii-xv
List of Schemes.....	xvi-xxii
List of Tables.....	xxiii-xxiv

PART ONE

<i>CHAPTER ONE:</i> A Brief Overview of C–C Bond Activation.....	1-39
Introduction.....	1
1.1 Barriers to Bond Activation.....	1-5
1.2 Strategies to Bond Activation.....	6-20
1.2.1 <i>Strained systems</i>	6-13
1.2.2 <i>Aromatization</i>	13-14
1.2.3 <i>Chelation Assistance</i>	14-20
1.3 8-Acylquinolines as a Directing Group.....	20-35
1.3.1 <i>Stoichiometric C–C bond activation reactions</i>	20-29
1.3.2 <i>Catalytic C–C bond activation reactions</i>	29-35
Concluding Remarks.....	35
References.....	36-39

<u>CHAPTER TWO:</u>	Carboacylation with 8-Acylquinoline.....	40-160
Introduction.....		40
2.1	Intramolecular Carboacylation with Alkenes.....	41-85
2.1.1	<i>Research Proposal</i>	41-42
2.1.2	<i>Substrate Syntheses</i>	42-48
2.1.3	<i>Results and Discussion</i>	49-55
2.1.4	<i>Concluding Remarks</i>	55-56
2.1.5	<i>Experimental</i>	56-85
2.2	Johnson's Mechanism Elucidation.....	86-95
2.2.1	<i>Mechanistic Investigations with $RhCl(PPh_3)_3$</i>	86-90
2.2.2	<i>Mechanistic Investigations with $[RhCl(C_2H_4)_2]_2$</i>	91-95
2.3	Intramolecular Carboacylation with Alkynes.....	96-131
2.3.1	<i>Research Proposal</i>	96
2.3.2	<i>Substrate Synthesis</i>	96-102
2.3.3	<i>Results and Discussion</i>	102-107
2.3.4	<i>Concluding Remarks</i>	107
2.3.5	<i>Experimental</i>	108-131
2.4	Intermolecular Carboacylation with Norbornenes.....	131-135
2.5	Carboacylation with 8-Quinoliny Ester.....	136-139
2.5.1	<i>Research Proposal</i>	136-137
2.5.2	<i>Results and Discussion</i>	137-138
2.5.3	<i>Experimental</i>	138-139
2.6	Carboacylation across Cyclopropane.....	140-158
2.6.1	<i>Background</i>	141-151
2.6.2	<i>Research Proposal</i>	151-152
2.6.3	<i>Results and Discussion</i>	153-154
2.6.4	<i>Concluding Remarks</i>	155
2.6.5	<i>Experimental</i>	156-158
References.....		159-160

<u>CHAPTER THREE:</u>	A Search for a More Synthetically Viable Method.....	161-225
Introduction.....		161
3.1	Other Heterocyclic Directing Groups.....	161-168
3.1.1	Substrate Syntheses.....	163-167
3.1.2	Concluding Remarks.....	167-168
3.2	Cleavable Directing Groups.....	169-175
3.2.1	Research Proposal.....	169-171
3.2.2	Results and Discussion.....	172-173
3.2.3	Concluding Remarks.....	173
3.2.4	Experimental.....	174-175
3.3	Metal-Organic Cooperative Catalysis (MOCC)	176-186
3.3.1	Background to MOCC in C–C Bond Activation.....	176-181
3.3.2	Research Proposal.....	181-182
3.3.3	Results and Discussion.....	183-186
3.3.4	Concluding Remarks.....	186
3.4	Triazene: A Versatile Directing Group.....	187-204
3.4.1	Background.....	187-191
3.4.2	Research Proposal.....	191-193
3.4.3	Substrate Syntheses.....	194-196
3.4.3	Results and Discussion.....	197-199
3.4.4	Concluding Remarks.....	200
3.4.5	Experimental.....	200-204
3.5	Hydrogen-Bonding Directed Catalysis.....	205-225
3.5.1	Background and Inspiration.....	205-209
3.5.2	Research Proposal.....	210-212
3.5.3	Results and Discussion.....	212-213
3.5.4	Modified Proposal.....	214-215
3.5.5	Synthetic Efforts Toward Co-Catalyst(s).....	215-220
3.5.6	Concluding Remarks.....	221
3.5.7	Experimental.....	222-223
References.....		224-225

PART TWO

<i>CHAPTER FOUR:</i> A Brief Overview of C–CN Bond Activation.....	226-254
Introduction.....	226-228
4.1 Carbocyanation with Alkynes.....	229-235
4.2 Cyanoacylation with Alkynes.....	236-241
4.3 Carbocyanation with Alkenes.....	242-246
4.4 Cyanoacylation with Alkenes.....	247-250
Concluding Remarks.....	250-251
References.....	252-254

<i>CHAPTER FIVE:</i> Intramolecular Cyanoamidation with Alkenes.....	255-329
Introduction.....	255
5.1 Enantioselective Cyanoamidation.....	256-276
5.1.1 <i>Research Proposal: 3,3-disubstituted δ-lactams</i>	256-258
5.1.2 <i>Substrate Synthesis</i>	258-262
5.1.3 <i>Results and Discussion</i>	262-269
5.1.4 <i>Concluding Remarks</i>	270
5.1.5 <i>Experimental</i>	271-276
5.2 Diastereoselective Cyanoamidation with Chiral Auxiliaries.....	277-329
5.2.1 <i>Research Proposal: 3,3-disubstituted δ-lactams</i>	277-278
5.2.2 <i>Substrate Syntheses</i>	278-279
5.2.3 <i>Results and Discussion</i>	279-292
5.2.4 <i>Concluding Remarks</i>	292-295
5.2.5 <i>Research Proposal: 3,3-disubstituted γ-lactams</i>	296
5.2.6 <i>Substrate Syntheses</i>	297
5.2.7 <i>Results and Discussion</i>	297-300
5.2.8 <i>Concluding Remarks</i>	300
5.2.9 <i>Research Proposal: 3,3-disubstituted β- and ϵ-lactams</i>	301-302

5.2.10	<i>Substrate Syntheses</i>	303-304
5.2.11	<i>Results and Discussion</i>	304-305
5.2.12	<i>Concluding Remarks</i>	306
5.2.13	<i>Experimental</i>	307-328
	References.....	329
	Bibliography.....	330-348
	Appendix.....	349-471
	<i>Chapter Two Spectra</i>	349-423
	<i>Chapter Three Spectra</i>	424-437
	<i>Chapter Five Spectra</i>	438-471

LIST OF ABBREVIATIONS

C–C	carbon–carbon sigma bond
C–CN	carbon–nitrile bond
C–D	carbon–deuterium bond
C–H	carbon–hydrogen bond
C–X	carbon–heteroatom bond
M–C	metal–carbon bond
M–CN	metal–nitrile bond
M–H	metal–hydrogen bond
M–X	metal–heteroatom bond
acac	acetylacetone
brsm	based on recovered starting material
PhH	benzene
BDE	bond dissociation energy
BINAP	(2,2'-bis(diphenylphosphino)-1,1'-binaphthyl
BHT	2,6-di(<i>tert</i> -butyl)-4-methylphenol
CNS	central nervous system
cod	cyclooctadiene
coe	cyclooctene
Cp*	pentamethylcyclopentadienyl
Cy	cyclohexyl

2-DPC	di(pyridin-2-yl) carbonate
DABCO	1,4-diazabicyclo[2.2.2]octane
DCC	<i>N,N'</i> -dicyclohexylcarbodiimide
DCE	dichloroethane
DCM	dichloromethane
DFT	density functional theory
DIBAL-H	diisobutylaluminium hydride
DMAP	<i>N,N</i> -dimethylaminopyridine
DMF	<i>N,N</i> -dimethylformamide
DMPU	<i>N,N</i> -dimethylpropylene urea
DMS	dimethyl sulfide
d1	delay time
de	diastereomeric excess
d.r.	diastereomeric ratio
dba	dibenzylideneacetone
dppb	1,4-bis(diphenylphosphino)butane
dppe	1,2-bis(diphenylphosphino)ethane
dppp	1,3-bis(diphenylphosphino)propane
ee	enantiomeric excess
EtOAc	ethyl acetate
HB	hydrogen bond
HBD	hydrogen bond donor
Hex	hexanes

HOMO	highest occupied molecular orbital
HPLC	high performance liquid chromatography
IR	infrared
IBX	2-iodoxybenzoic acid
LAH	lithium aluminum hydride
LUMO	lowest unoccupied molecular orbital
MCP	methylenecyclopropane
MeCN	acetonitrile
MVK	methyl vinyl ketone
m/z	mass-to-charge ratio
nbd	norbornadiene
NBS	<i>N</i> -bromosuccinimide
N.R.	no reaction
NMO	<i>N</i> -methylmorpholine- <i>N</i> -oxide
NMP	<i>N</i> -methyl-2-pyrrolidinone
NMR	nuclear magnetic resonance
OAc	acetate
OTf	trifluoromethanesulfonate
PCC	pyridinium chlorochromate
PCP	pincer ligand (phosphine, carbanion, phosphine)
PhH	benzene
PhMe	toluene
pin	pinacolato

PMB	4-methoxybenzyl or <i>para</i> -methoxybenzyl
py	pyridine
R _f	retention factor
refl	reflux
rt	room temperature
salen	2,2'-ethylenebis(nitrilomethylidene)diphenol, N,N'-ethylenebis(salicylimine)
SPO	secondary phosphine oxide
T ₁	spin lattice relaxation time
TBD	to be determined
TCE	tetracyanoethylene
TCEO	tetracyanoethyleneoxide
TEA	triethylamine
TFT	α,α,α -trifluorotoluene
THF	tetrahydrofuran
TMP	tetramethylpiperidine
TPAP	tetrapropylammonium perruthenate
TFFA	trifluoroacetic anhydride
TOF	turnover frequency
tol	tolyl
TON	turnover number
Ts	4-toluenesulfonyl
Xantphos	4,5-bis(diphenylphosphino)-9,9-dimethylxanthene

LIST OF FIGURES

CHAPTER ONE

Figure 1. Oxidative Addition.....	2
Figure 2. Steric hindrance: a kinetic barrier for C–H bond activation.....	3
Figure 3. Thermodynamic considerations to bond activation.....	4
Figure 4. Steric hindrance: a kinetic barrier for C–C bond activation.....	5
Figure 5. Orbital interactions with metals.....	8
Figure 6. Cyclometalation.....	15
Figure 7. Pincer-type ligand for C–C bond activation.....	16

CHAPTER TWO

Figure 8. General depiction of carboacylation and hydroacylation.....	40
Figure 9. Scope of the intramolecular carboacylation with alkenes.....	52
Figure 10. Homologated and amino substrates for carboacylation with alkynes.....	97
Figure 11. Phenyl alkyne substrate derivatives 2.123–2.128	100
Figure 12. Scope of the intramolecular carboacylation with alkynes.....	106
Figure 13. Proposed mechanisms for hydrosilylation of vinylcyclopropanes.....	146
Figure 14. Proposed mechanism for hydrosilylation of MCPs.....	148
Figure 15. Proposed mechanism for migratory insertion across cyclopropane.....	150

CHAPTER THREE

Figure 16. Other potential heterocyclic directing groups.....	163
Figure 17. Proposed heterocycles of masked functionality.....	171
Figure 18. Mechanism for MOCC C–C bond activation exchange reaction.....	178
Figure 19. Mechanism for MOCC C–C bond activation ring contractions.....	180
Figure 20. Alternative co-catalyst directing groups for MOCC.....	182
Figure 21. The functional versatility of triazenes.....	188
Figure 22. Mechanism of Neber and Beckmann rearrangements.....	196
Figure 23. Molecular motor catalysts in stereoselective reactions.....	206
Figure 24. Enzymatic molecular recognition mechanism.....	207
Figure 25a. Hydrogen bond directed regioselective benzylic oxidation.....	207
Figure 25b. Regioselective benzylic oxidation of ibuprofen.....	208
Figure 26. Al–SPO5–Ni bimetallic system.....	209
Figure 27. Illustration of Al–SPO5–Ni in hydrocarbamylation.....	209
Figure 28. Proposed C–C bond activation with HB directing group.....	210
Figure 29. Thiosemicarbazone as a potential directing group.....	211

CHAPTER FOUR

Figure 30. Terminology of organonitrile additions across olefins.....	228
--	-----

CHAPTER FIVE

Figure 31. Alkaloids containing 3,3-disubstituted piperidine ring(s).....	258
Figure 32. Phosphoramidite ligands with BINOL backbone.....	261
Figure 33. Phosphoramidite ligands with hydrogenated BINOL backbone.....	262
Figure 34. Phosphoramidite ligands with TADDOL backbone.....	262
Figure 35. Phosphoramidite ligands with miscellaneous backbones.....	262
Figure 36. Proposed mechanism for the formation of side-product 5.14a	282
Figure 37. Additional substrates for intramolecular cyanoamidation.....	290

LIST OF SCHEMES

CHAPTER ONE

Scheme 1. Oxidative addition into cyclopropane.....	7
Scheme 2. Murakami's synthesis of the (\pm)- β -cuparenone.....	9
Scheme 3. Mechanism for tandem C–C bond activation and β -carbon elimination.....	9
Scheme 4. Cyclobutanone C–C bond activation and lactonization.....	11
Scheme 5. Cyclobutanone C–C bond activation and intramolecular carboacylation.....	12
Scheme 6. Ligand bite angle chemoselectivity effects.....	13
Scheme 7. C–C bond activation driven by aromatic stabilization.....	14
Scheme 8. C–C bond activation with pincer-type systems.....	16
Scheme 9. Electronics dictate chemoselectivity in C–H vs C–C bond activation.....	17
Scheme 10. C–C vs. C–H bond activation at room temperature.....	19
Scheme 11. sp^2 – sp C–C bond activation with 8-acylquinoline	21
Scheme 12. Trapping of the sp^2 – sp^3 C–C bond activation adducts.....	23
Scheme 13. Hypothetical C–H bond activation via a six-membered metallacycle.....	24
Scheme 14. Phosphine-promoted reductive elimination and decoordination.....	25
Scheme 15. Failure to promote oxidative addition by PPh_3 adsorption.....	26
Scheme 16. Stereochemistry of oxidative addition and reductive elimination.....	26
Scheme 17. Crossover experiment: homolysis-recombination mechanism.....	27
Scheme 18. Stoichiometric alkyl C–C bond exchange.....	29

Scheme 19. Catalytic alkyl C–C bond exchange.....	30
Scheme 20. Catalytic aryl C–C bond exchange.....	31
Scheme 21. Proposed mechanism of phenyl for ethyl exchange.....	32
Scheme 22. C–C bond activation/cross coupling alkyl-for-aryl exchange.....	33
Scheme 23. C–C bond activation/cross coupling aryl exchange.....	34
Scheme 24. Proposed mechanism for C–C bond activation/cross coupling.....	35

CHAPTER TWO

Scheme 25. Proposed intramolecular carboacylation with 8-acylquinolines.....	42
Scheme 26. Preparation of 8-bromoquinoline and quinolinyl ketone 2.17	43
Scheme 27. Re-routed preparation of allylic ether derivatives.....	43
Scheme 28. Syntheses of oxygen-tethered substrates.....	45
Scheme 29. Syntheses of amino-tethered substrates.....	47
Scheme 30. Syntheses of methylene-tethered substrates.....	48
Scheme 31. Synthesis of pyrrole-linker substrate.....	48
Scheme 32. Competition experiment showing 2.41 does not sequester catalyst.....	53
Scheme 33. Attempts to convert quinolinyl ketone to an ester or amide.....	54
Scheme 34. C–C bond activation/cross coupling strategy for quinoline removal.....	55
Scheme 35a. Intramolecular carboacylation with RhCl(PPh ₃) ₄	87
Scheme 35b. Mechanism for intramolecular carboacylation with RhCl(PPh ₃) ₃	88
Scheme 36. Radical-recombination crossover experiment.....	90
Scheme 37a. Mechanism for intramolecular carboacylation with [RhCl(C ₂ H ₄) ₂] ₂	95
Scheme 37b. Proposed intramolecular carboacylation with alkynes.....	96

Scheme 38. Preparation of alkynyl substrates 2.97–2.100	97
Scheme 39. Attempted synthesis of methylene-tethered alkyne substrates.....	98
Scheme 40. Preparation of alkyne substrate with a pyrrole backbone.....	98
Scheme 41. Preparation of alkynyl substrates 2.113–2.117	99
Scheme 42. Preparation of phenyl alkyne substrates.....	101
Scheme 43. C–C (carboacylation) vs C–H (hydroarylation) bond activation.....	134
Scheme 44. Proposed intramolecular carboacylation with 8-quinoliny ester.....	137
Scheme 45. Ester C–O bond activation with quinoline directing groups.....	138
Scheme 46. Migratory insertion and sigma (σ) bond metathesis.....	140
Scheme 47. Illustration of C–C sigma adduct ($M\cdots C-C$) interaction.....	141
Scheme 48. Rhodacyclobutane-Binor-S complex: $M\cdots C-C$ agostic interaction.....	142
Scheme 49. Rearrangement of hydridocyclopropylrhodium complex.....	144
Scheme 50. Hydrosilylation and ring opening of vinylcyclopropane.....	145
Scheme 51. Hydrosilylation reactions of MCPs.....	147
Scheme 52. Hydrosilylation of vinylcyclopropane.....	149
Scheme 53. Silylboration of vinylcyclopropanes.....	151
Scheme 54. Proposed sigma bond metathesis reactions with cyclopropane.....	152
Scheme 55. Synthesis of quinoliny cyclopropane substrate 2.228	153

CHAPTER THREE

Scheme 56. Attempted syntheses of pyridyl substrate 3.4	164
Scheme 57. Attempted synthesis of benzoxazole substrates 3.6a	165
Scheme 58. Preparation of benzoxazole bromide derivatives.....	166

Scheme 59. Synthetic efforts toward [1,2,4]triazolo[1,5- <i>a</i>]pyridine 3.7	167
Scheme 60. Proposed carboacylation with pyridyl ester directing group.....	170
Scheme 61. Synthesis of pyridyl ester 3.31	170
Scheme 62. Proposed carboacylation with azaindole directing group.....	171
Scheme 63. Reaction screen with pyridyl ester 3.31 and azaindole 3.38	172
Scheme 64. MOCC in hydroacylation reactions.....	177
Scheme 65. MOCC in C–C bond activation alkyl exchange reaction.....	178
Scheme 66. MOCC in C–C bond activation ring contractions.....	179
Scheme 67. Unsuccessful MOCC in intramolecular carboacylation.....	182
Scheme 68. Proposed MOCC carboacylation with amino pyrimidine diols.....	184
Scheme 69. Alternative directing groups for MOCC C–C bond activation.....	185
Scheme 70. C–C bond activation with 2-acylaniline directing group.....	187
Scheme 71. C–H bond activation with triazenes.....	189
Scheme 72. C–H and C–C bond activation reactions with oxazoline.....	190
Scheme 73. Proposed C–C bond activation with triazenes.....	192
Scheme 74. Proposed aryl triazene substrate with aryl-tethered olefin.....	193
Scheme 75. Proposed aliphatic triazene substrate with aryl-tethered olefin.....	193
Scheme 76. Proposed aryl triazene substrate with aliphatic-tethered olefin.....	193
Scheme 77. Preparation of aryl triazene substrate with aryl-tethered olefin.....	194
Scheme 78. Unsuccessful synthesis of aliphatic triazene substrate.....	195
Scheme 79. Preparation of aryl triazene with aliphatic-tethered olefin.....	196
Scheme 80. Hydrocarbamoylation with a chiral Lewis acid directing group.....	208
Scheme 81. Proposed C–C bond activation with HBD directing group.....	211

Scheme 82. Preparation of thiosemicarbazone 3.158a	212
Scheme 83. Michael addition with internal-Lewis-acid-thiourea catalyst.....	214
Scheme 84. Proposed internal-Lewis-acid-assisted HB directing group.....	215
Scheme 85. Unsuccessful syntheses of internal-Lewis-acid HB co-catalyst.....	216
Scheme 86. Unsuccessful syntheses of internal-Lewis-acid HB co-catalyst.....	217
Scheme 87. Preparation of bromosemicarbazone 3.174	218
Scheme 88. Unsuccessful borylations of bromo- and iodosemicarbazone.....	219
Scheme 89. Unsuccessful coupling of iodo-aryltriazene and thiosemicarbazide.....	220
Scheme 90. Michael addition accelerated by pallado-urea catalyst.....	220

CHAPTER FOUR

Scheme 91. C–CN bond activation in Dupont’s adiponitrile synthesis.....	227
Scheme 92. Intermolecular arylcyanation with alkynes.....	231
Scheme 93. Intermolecular alkenyl- and alkynylcyanation with alkynes	232
Scheme 94. Intermolecular alkylcyanation with alkynes.....	233
Scheme 95. Intermolecular allylcyanation with alkynes.....	234
Scheme 96. Intermolecular carbocyanation in the synthesis of plaunotol.....	235
Scheme 97. Intramolecular arylcyanation with alkynes.....	235
Scheme 98. Decarbonylation of acyl nitriles.....	237
Scheme 99. Presumed acylcyanation with terminal alkynes.....	237
Scheme 100. Attempted acylcyanation with internal alkynes.....	238
Scheme 101. Heterocarbonyls in acylcyanation reactions.....	239
Scheme 102. Intramolecular cyanoesterification with alkynes.....	240

Scheme 103. Intramolecular cyanoamidation with alkynes.....	241
Scheme 104. Intermolecular carbocyanation reactions with norbornadiene.....	243
Scheme 105. Intermolecular carbocyanation reaction with 1,2-dienes.....	244
Scheme 106. Enantioselective intramolecular carbocyanation with alkenes.....	245
Scheme 107. Synthesis of (-)-eptazocine via carboacylation with alkenes.....	246
Scheme 108. Synthesis of (-)-esermethole via carboacylation with alkenes.....	246
Scheme 109. Intermolecular cyanoesterification with norbornene.....	247
Scheme 110. Intermolecular cyanoesterification with 1,2-dienes.....	249
Scheme 111. Enantioselective intramolecular cyanoamidation with alkenes.....	250

CHAPTER FIVE

Scheme 112. Proposed intramolecular cyanoamidation: δ - lactams.....	257
Scheme 113. Synthesis of cyanoformamide acid precursor 5.6	259
Scheme 114. Preparation of cyanoformamides 5.1a and 5.1b	260
Scheme 115. Evan's oxazolidinone auxiliary in an asymmetric aldol reaction.....	277
Scheme 116. Proposed diastereoselective cyanoamidation with auxiliaries.....	278
Scheme 117. Re-routed synthesis of acid precursor.....	279
Scheme 118. Preparation of cyanoformamide 5.8d	291
Scheme 119. Preparation of cyanoformamide derivatives 5.8e–g	292
Scheme 120. Enantioselective cyanoamidation: λ - lactams.....	296
Scheme 121. Proposed diastereoselective cyanoamidation: λ -lactams.....	296
Scheme 122. Preparation of cyanoformamides 5.27a–b	297
Scheme 123. Fu's stereoselective synthesis of β -lactams.....	302

Scheme 124. Proposed intramolecular cyanoamidations: β - and ϵ -lactams.....	302
Scheme 125. Synthesis of allylic cyanoformamide 5.35	303
Scheme 126. Synthesis of cyanoformamide 5.37	304
Scheme 127. Cyanoamidation to form β -lactams.....	304
Scheme 128. Unsuccessful cyanoamidation to form ϵ -lactams.....	305

LIST OF TABLES

CHAPTER TWO

Table 1. Reaction optimization for intramolecular carboacylation with alkenes.....	50
Table 2. Linear free-energy relationships with $\text{RhCl}(\text{PPh}_3)_3$	89
Table 3. Linear free-energy relationships with $[\text{RhCl}(\text{C}_2\text{H}_4)_2]_2$	92
Table 4. Alkene substitution effects on the rates of reaction with $[\text{RhCl}(\text{C}_2\text{H}_4)_2]_2$	94
Table 5. Reaction optimization for intramolecular carboacylation with alkynes.....	103
Table 6. Intermolecular carboacylation and hydroarylation.....	133
Table 7. Carboacylation across cyclopropane reaction screen.....	154

CHAPTER THREE

Table 8. Reaction screen of aryl triazene with aryl olefin tether.....	198
Table 9. Reaction screen of aryl triazene with aliphatic olefin tether.....	198
Table 10. Reaction screen of aryl triazene with aliphatic olefin tether (n -1).....	199

CHAPTER FIVE

Table 11. Cyanoamidation reactivity screen: <i>3,3-disubstituted δ-lactams</i>	263
Table 12. Enantioselective reactivity screen with BINOL ligands.....	265
Table 13. Enantioselective reactivity screen with hydrogenated BINOL ligands.....	267

Table 14. Enantioselective reactivity screen with TADDOL ligands.....	268
Table 15. Enantioselective reactivity screen with miscellaneous ligands.....	269
Table 16. Diastereoselective screen [<i>R</i> -phenyl(ethyl)amine]: δ -lactams.....	280
Table 17. Diastereoselective screen [<i>S</i> -phenyl(ethyl)amine]: δ -lactams.....	284
Table 18. Diastereoselective screen [<i>S</i> -naphthyl(ethyl)amine]: δ -lactams.....	285
Table 18. Continued.....	287
Table 18. Continued.....	289
Table 19. Comparing ligand performance between chiral auxiliaries.....	293
Table 20. Diastereoselective screen [<i>S</i> -phenyl(ethyl)amine]: γ -lactams.....	298
Table 21. Diastereoselective screen [<i>S</i> -naphthyl(ethyl)amine]: γ -lactams.....	300

CHAPTER ONE

A Brief Overview of Carbon–Carbon Bond Activation

INTRODUCTION

Following the advent of carbon–hydrogen (C–H) bond activation, the activation of carbon–carbon (C–C) sigma bonds has gained increasing attention from the organometallic community over the past two decades. The ability to selectively cleave carbon–carbon bonds with subsequent functionalization would not only unveil unusual retrosynthetic disconnections, but would also impact industrial hydrocarbon processes. In essence, viewing the C–C sigma bond as a functional group has the ability to change the way chemists think about organic chemistry and how they approach synthetic challenges. For the remaining discourse of this dissertation, bond activation will refer to the oxidative addition of a transition metal into a specified bond.

1.1 BARRIERS TO C–C BOND ACTIVATION

From both a thermodynamic and kinetic perspective, chemists perceive carbon–carbon (C–C) and carbon–hydrogen (C–H) bonds as intrinsically inert. Carbon and hydrogen belong to a small group of elements that contain the same number of valence electrons as the number of valence orbitals. This fundamental characteristic, in turn, reflects the unavailability of both lone pairs and empty orbitals in alkane bonding.

Additionally, the low polarity in C–C and C–H bonds also contributes to the lack of reactivity of alkanes. Moreover, the unreactive nature of C–C bonds and C–H bonds of alkanes resides in the strength of these respective bonds. With bond dissociation energies (BDEs) of 90–110 kcal mol⁻¹, C–C and C–H bonds have low-lying σ bonding orbitals (HOMOs) and high-lying σ^* bonding orbitals (LUMOs), neither of which are easily accessible. In order to react, a reagent must have the ability to either i) donate electron density into σ^* (nucleophilic addition), ii) abstract electron density from σ (electrophilic addition), or iii) accomplish both simultaneously. The strategy to functionalize alkanes that is adopted by radicals, carbenes, and metal complexes accomplishes both feats simultaneously.¹

Considerable advances in fundamentally understanding the ‘oxidative addition’ or ‘bond activation’ reaction were made in the 1960s, in which low-valent transition metal complexes were shown to insert into a variety of X–Y bonds (ex: H₂, HCl, MeI, Cl₂, R₃Si–H) (Figure 1).² This fundamental aspect in organometallic chemistry ultimately changed the way chemists approach synthesis by enabling complexity-building methods such as catalytic hydrogenation, Suzuki, Negishi, Heck, and Sonogashira couplings, and hydrosilylation reactions.

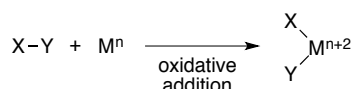


Figure 1. Oxidative addition is a process that increases both the oxidation state and coordination number of the metal center

The activation of H₂ is somewhat unusual based upon typical reactivity trends. Without lone pairs or a polarizable bond, oxidative addition into the H–H bond can best

be regarded as a thermodynamically driven phenomenon. Despite a high bond dissociation energy of $104 \text{ kcal mol}^{-1}$, the activation of H_2 is generally thermodynamically favorable for late d-block transition metals because the resulting metal–hydrogen (M–H) bonds have energies of approximately 60 kcal mol^{-1} (net energetic gain of roughly 15 kcal mol^{-1}) (Figure 2a).³ Although a C–H bond has a similar BDE ($90\text{--}100 \text{ kcal mol}^{-1}$) to that of H–H ($104 \text{ kcal mol}^{-1}$), it is thermodynamically more difficult to activate a C–H bond due to the resulting metal–carbon (M–C) bond (approx. 25 kcal mol^{-1})³ being significantly weaker than a M–H bond (60 kcal mol^{-1}) (Figure 2b).⁴ In addition, the orbital hybridization at carbon imposes an additional barrier to bond activation (which is arguably more important). Unlike the spherical 1s orbital of hydrogen, which can bond in a multidirectional way (Figure 2d), orbital symmetry requires that rotation of the sp^3 -hybridized orbital of carbon must occur in order to effectively overlap with the metal d_{xy} orbital (Figure 2e). Kinetic considerations also render C–H bond activation to be a challenge. The tetrahedral arrangement about carbon creates considerable steric repulsion that disfavors the approach of a ligated metal (Figure 3). The shorter C–H bond length (1.09 \AA), in comparison with readily activated Si–H (1.48 \AA) or C–I (2.14 \AA) bonds, enhances these steric constraints.

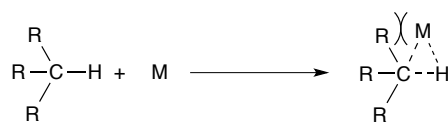


Figure 2. Steric hindrance: a kinetic barrier for C–H bond activation

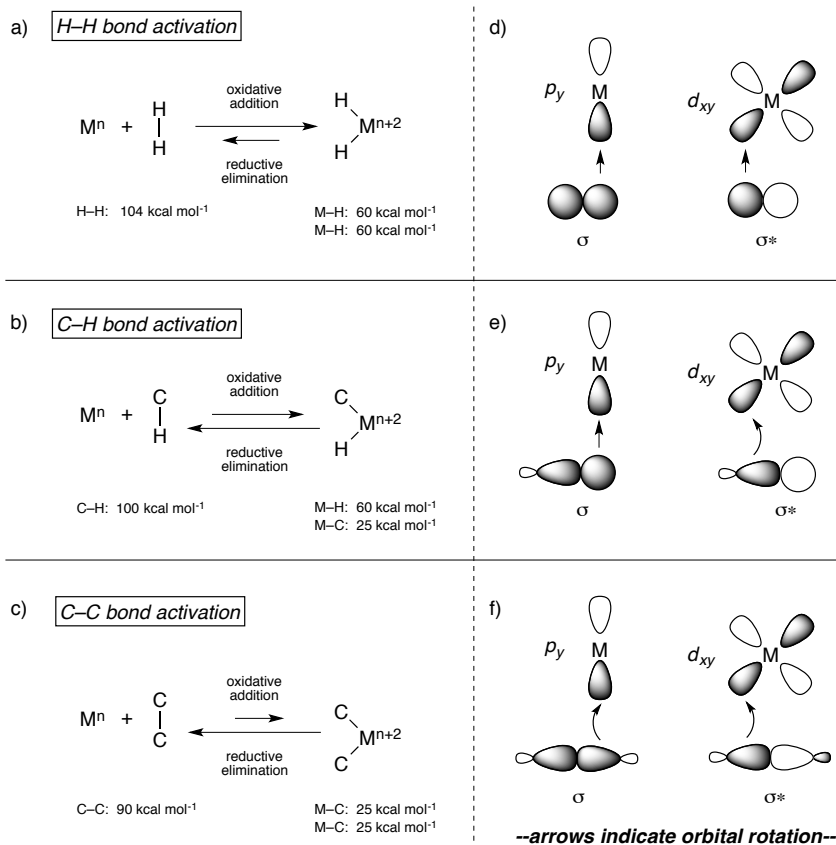


Figure 3. Thermodynamic considerations to bond activation: a) H-H bond activation b) C-H bond activation c) C-C bond activation. Orbital directionality considerations for bond activation: d) H-H bond activation e) C-H bond activation f) C-C bond activation.

From a general thermodynamic standpoint, the activation of C-C bonds is exceedingly more difficult than either C-H or H-H bond activation, despite the weaker C-C bond strength (approx. 90 kcal mol⁻¹). The process of cleaving a C-C bond is significantly endothermic owing to the result of two relatively weak M-C bonds (25 kcal mol⁻¹).^{i,5,6} Moreover, a C-C sigma bond is comprised of two overlapping *sp*³-hybridized orbitals. In order to form covalent bonds with a metal center, both orbitals must rotate substantially.⁷ Although the C-C bond (1.58 Å) is considerably longer than a

ⁱ However, rough estimates for some M-C bond strengths suggest that M-C_{aryl} bonds can be stronger than M-H for rhodium and iridium complexes, thus rendering C-C activation not only thermodynamically feasible, but also more favorable than C-H activation.^{5,6}

C–H bond (1.09 Å), the three-centered transition state for C–C bond activation is further impeded by additional steric hindrance imposed by adjacent tetravalent carbon atoms (Figure 4).

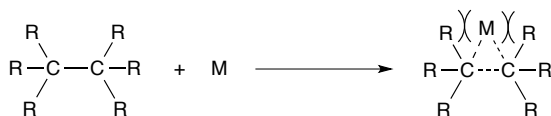


Figure 4. Steric hindrance: a kinetic barrier for C–C bond activation

Both thermodynamic and kinetic barriers make selective C–C bond activation a daunting challenge. Not only is C–C bond activation endothermic by 30–50 kcal mol^{–1}, the energetic preference for the formation of M–H (60 kcal mol^{–1}) over M–C bonds (20–30 kcal mol^{–1}) renders C–C bond activation much less favorable than C–H bond activation. With C–H bonds vastly outnumbering C–C bonds in a typical organic scaffold, and with C–H bonds being more sterically accessible, the selective activation of a C–C bond is at a substantial kinetic disadvantage. The following sections will discuss strategies used to overcome such barriers and demonstrate that selective C–C bond activation can be made feasible.

1.2 STRATEGIES FOR C–C BOND ACTIVATION

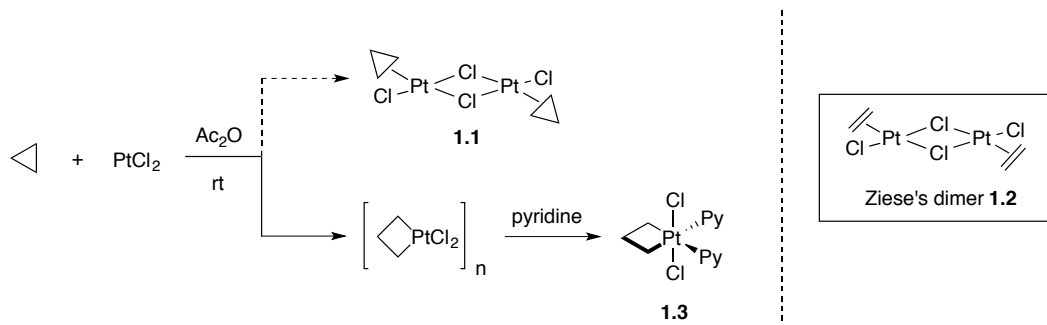
When C–C bond activation is thermodynamically unfavorable, coupling energy-releasing steps such as the relief of ring strain, aromatization, or hydrogenolysis has allowed for the overall transformations to achieve a net gain in enthalpy (Sections 1.3.1 and 1.3.2). With regard to kinetic feasibility, employing a substrate possessing a covalently-bound heteroatom, wherein the heteroatom lone pair may ligate and thus direct the metal into the appropriate bond (chelation assistance), has been demonstrated (Section 1.3.3).

1.2.1 STRAINED SYSTEMS

In 1955, Tipper⁸ serendipitously discovered the first example of oxidative addition of a metal complex into a C–C bond. His research had focused on examining the similarities in reactivity and electronic properties between olefins and cyclopropanes. Tipper had theorized that if the sigma bonds in cyclopropane are more sp^2 -like, as suggested by Walsh,⁹ it would be plausible that cyclopropane would coordinate to a metal center. Efforts to prepare an edge-bound cyclopropane–metal adduct **1.1**, analogous to that of Zeise’s dimer (**1.2**), led to a structure that was later elucidated by Chatt and Mason^{10,11} to be platina(IV)cyclobutane **1.3** (Scheme 1).

Carbon–carbon bond activation in cyclopropane is driven by the energetic release of torsional and angle strain, wherein the total estimated ring strain for cyclopropane is 28 kcal mol^{−1}. In order to accommodate the 60° bond angles in cyclopropane, the orbitals do not overlap linearly but rather are ‘bent.’ These bent bonds are sometimes referred to

as ‘banana bonds.’ The bonds in cyclopropane are neither purely end-on (sigma) nor sidelong (pi) in overlap, but rather somewhere in-between – and thus the orbitals are suggested to be a cross between sp^3 and sp^2 in hybridization. As a consequence, the orbital overlap is less effective, and therefore the C–C bond strength of cyclopropane (60 kcal mol^{-1}) is significantly weaker than a typical C–C sigma bond (90 kcal mol^{-1}).



Scheme 1. Oxidative addition into cyclopropane

As Walsh had suggested, the ‘banana bonds’ in cyclopropane resemble the pi bonds in olefins. In all metal-olefin interactions, the olefinic π -electrons are donated into an empty metal p orbital and electrons from the d_{xy} metal orbital are back-donated (π -backbonding) into the olefinic π^* antibonding orbital, which is illustrated in the Dewar-Chatt-Duncanson model (Figure 5b).¹²⁻¹⁴ Similarly, the p -like orbitals of cyclopropane can donate electron density into the empty metal p orbital. Unlike the traditional sp^3 orbitals of a C–C sigma bond (Figure 5a), the bent geometry of cyclopropane does not require as much orbital rotation in order to achieve effective overlap with the metal (Figure 5c). The major difference between the two models is the relative inaccessibility of the high-lying σ^* antibonding orbital in cyclopropane, which makes back donation from the metal less significant and thus reduces the overall strength

of the agostic interaction. Spectroscopic evidence for this agostic interaction will be further discussed in Chapter 2, Section 2.6.

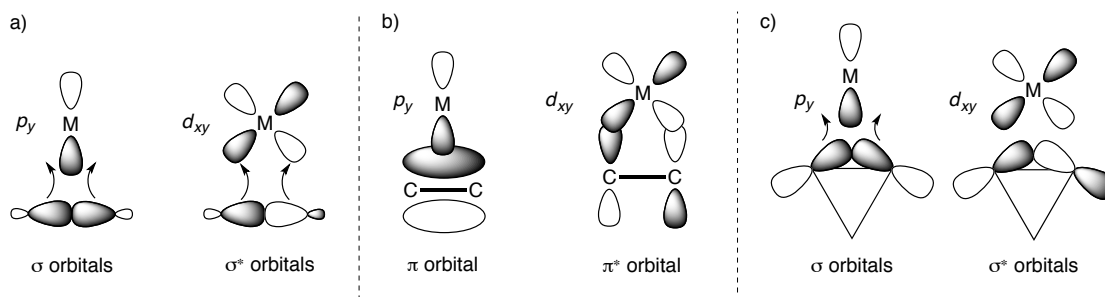
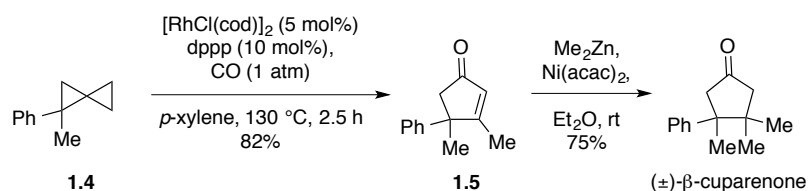


Figure 5. Orbital interactions with metals a) C–C σ bond b) C=C π bond c) C–C σ/π cyclopropane bond

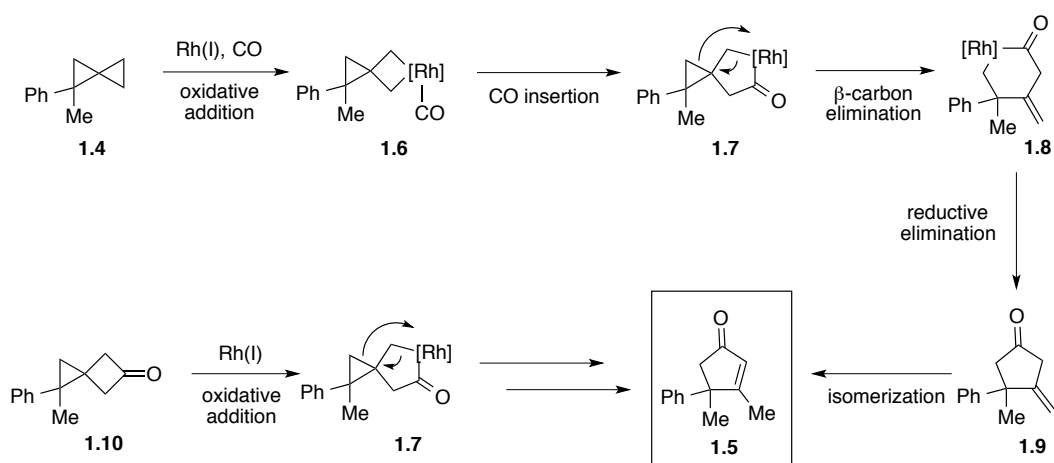
Various 3- and 4-membered systems have been shown to undergo C–C bond cleavage with transition metals.^{15,16} It has been demonstrated that the resulting metallacycles may undergo subsequent skeletal rearrangements and insertion reactions in order to increase molecular complexity. The metallacyclobutane has served as a reactive intermediate in olefin metathesis.^{16,17}

The utility of cyclopropane C–C bond activation is highlighted in Murakami's synthesis of (\pm)- β -cuparenone (Scheme 2).¹⁸ The sesquiterpene contains two contiguous all-carbon quaternary centers, which is a great synthetic challenge to chemists. The intermediate cyclopentene **1.5** was obtained through two successive C–C cleavage processes beginning with spiropentane **1.4**. Oxidative addition into the least hindered cyclopropane C–C bond, with subsequent complexation of a CO ligand, generates the metallocyclobutane **1.6** (Scheme 3). Insertion of carbon monoxide provides rhodacyclopentanone **1.7**, which undergoes selective C–C bond migration – a process known as β -carbon elimination. Reductive elimination of the resulting six-membered rhodacycle **1.8** affords cyclopentanone **1.9** and isomerization of the exocyclic olefin generates cyclopentenone **1.5**. Alternatively, cyclopentenone **1.5** could be obtained

through an analogous reaction with spirocyclic butanone **1.10**. Rhodium insertion into the acyl C–C bond directly provides the rhodacyclopentanone **1.7** that subsequently undergoes β -carbon elimination. Although the release of ring strain contributes to many β -carbon elimination reactions,^{19–24} the process can also be thermodynamically driven by going from a weaker metal–heteroatom bond to the stronger metal–carbon bond.²⁵ In the latter case, wherein the oxidation state of the metal does not change throughout the β -carbon elimination pathway, subsequent oxidative coupling reactions and olefin insertions have been accomplished.²⁶ The remaining discourse will focus on oxidative C–C bond activation, wherein β -carbon elimination reactions are beyond the scope of this dissertation.



Scheme 2. Cyclopropane C–C bond activation in Murakami’s synthesis of (\pm) - β -cuparenone



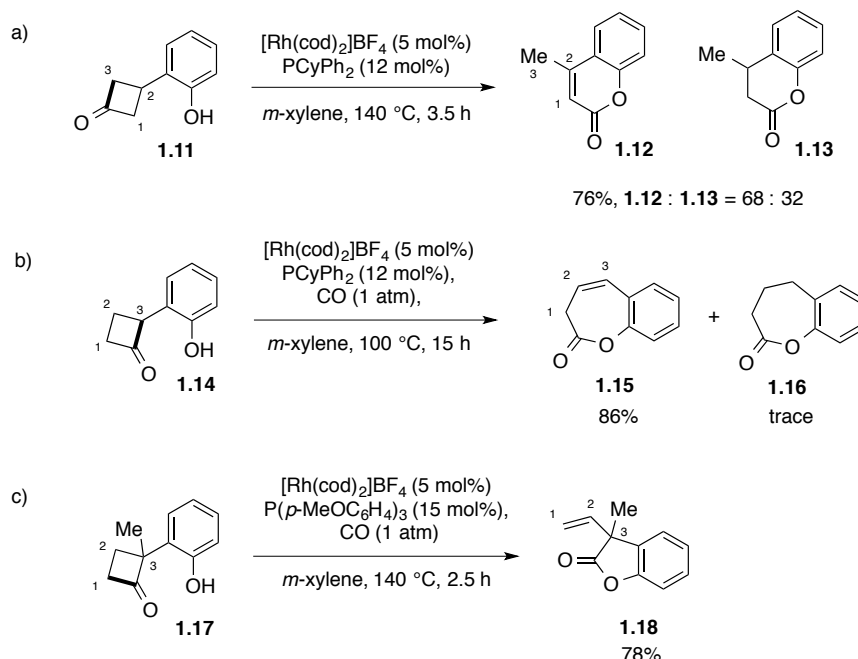
Scheme 3. Mechanism for tandem C–C bond activation and β -carbon elimination en route to (\pm) - β -cuparenone

Murakami's 1994 *Nature* report²⁷ described the selective activation of acyl C–C bonds of cyclobutanones, which were shown to undergo various degradative transformations including decarbonylative ring contractions, β -hydride eliminations, and hydrogenolysis. A complexity-building lactonization methodology was later disclosed that built upon the C–C bond activation of cyclobutanones by incorporating a strategically placed hydroxyl group (Scheme 4).²⁸

The rhodacycle intermediate resulting from the activation of the weaker acyl C–C bond of β -substituted cyclobutanone **1.11** is intercepted by the appended hydroxyl group through a substitution-like displacement (mechanism not shown). The resulting C3 rhodium–hydride can either undergo β -hydride elimination to form chromenone **1.12** with subsequent elimination of H₂, or reductive elimination to produce lactone **1.13**. Alternatively, it is plausible that lactone **1.13** could result from hydrogenation. Products **1.12** and **1.13** were obtained in 76% yield as a 2.1:1 mixture (Scheme 4a).

An analogous reaction of α -substituted cyclobutanone **1.14** proceeded under milder conditions, presumably owing to facilitation by the phenolic hydroxyl group (Scheme 4b). The directing ability of the hydroxyl group also explains the selectivity for activation of the C_{acyl}–C3 bond over the C_{acyl}–C1 bond. In the absence of CO, a mixture of lactones **1.15** and **1.16** were obtained in 22% and 31% yield, respectively, along with 20% of material resulting from decarbonylative ring contraction (not shown). Under an atmosphere of carbon monoxide and extended reaction times, the β,γ -unsaturated lactone **1.15** was obtained in 86% yield with a trace amount of **1.16**, and formation of the cyclopropyl adduct was completely suppressed. Additional steric hinderance imposed by a C3-methyl group on α -substituted cyclobutanone **1.17** overrode the directing group

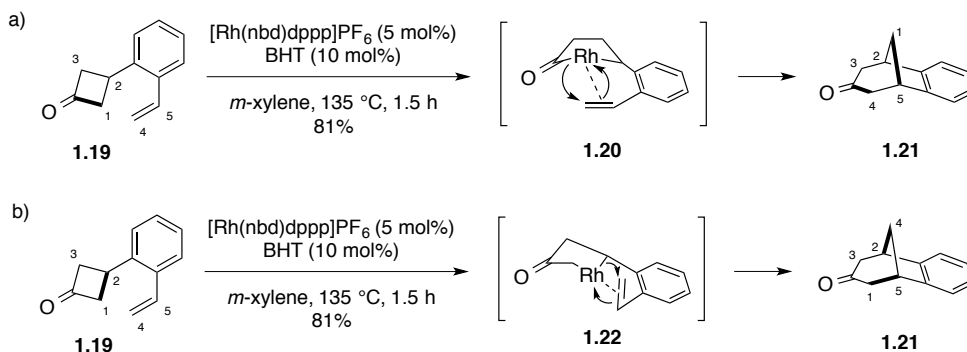
selectivity and thus required higher temperatures (Scheme 4c). The activation of the C_{acyl}–C1 bond resulted in the formation of benzofuranone **1.18** in 78% yield.



Scheme 4. Cyclobutanone C–C bond activation and lactonization methodologies

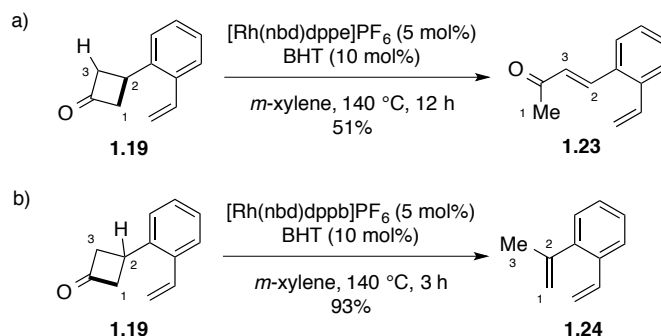
In 2002, Murakami described an intramolecular carboacylation reaction, a process by which a C_{acyl}–C sigma bond is inserted across an olefin.²⁹ Styrenyl cyclobutanone **1.19** was treated with a catalytic amount of [Rh(nbd)(dppp)]PF₆ in *m*-xylene at 135 °C in the presence of BHT as a radical inhibitor. After 1.5 h, benzobicyclo[3.2.1]octan-3-one (**1.21**) was obtained in 81% yield (Scheme 5). The proposed mechanism involves the oxidative rhodium insertion into the cyclobutanone acyl C–C bond followed by olefin coordination. Migratory insertion across the olefin, as depicted by intermediate **1.20**, results in a bridged rhodacycle that undergoes reductive elimination to form the C1–C5 bond (Scheme 5a). Alternatively, **1.20** could conceivably form from the activation of the C1–C2 bond followed by migratory insertion across the olefin as depicted by

intermediate **1.22**. The resulting bridged rhodacycle would form the resulting C1–C5 bond (**1.21**, Scheme 5b). Reaction with ^{13}C -labeled C4 in cyclobutanone **1.19** resulted with the labeled carbon alpha to the carbonyl, thus suggesting path a) as the operable mechanism.



Scheme 5. Cyclobutanone C–C bond activation and intramolecular carboacylation methodology. path a) C_{acyl}–C1 bond activation (operable) path b) C1–C2 bond activation (not operable)

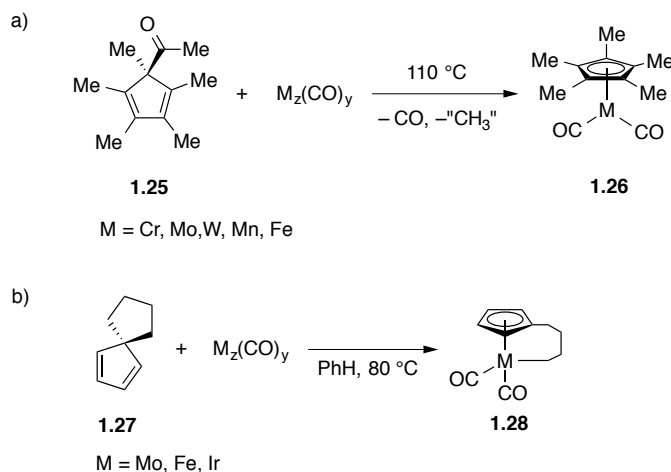
The choice of ligand had a dramatic effect on the outcome of the reaction. Changing the tether length of the bidentate phosphine ligand resulted in β -hydride elimination as the predominant reaction pathway. Treating cyclobutanone **1.19** with $[\text{Rh}(\text{nbd})\text{dppe}]\text{PF}_6$ resulted in enone **1.23** in 51% yield with the remaining material being unreacted **1.19** (Scheme 6a). The proposed mechanism involves the activation of the C1–C2 bond followed by β -hydride elimination of the C3 hydrogen. Treating cyclobutanone **1.19** with $[\text{Rh}(\text{nbd})\text{dppb}]\text{PF}_6$ provided diene **1.24** in 93% yield. The proposed mechanism involves activation of the C_{acyl}–C1 bond followed by decarbonylation and β -hydride elimination of the C2 hydrogen. Although dppe and dppb ligands were ineffective at promoting carboacylation, Cramer was able to develop an enantioselective variant using zwitterionic bisphospholane ligands.³⁰



Scheme 6. Ligand bite angle effects on intramolecular carboacylation of cyclobutanones a) dppe ligand; C1–C2 bond activation and C3 β -hydride elimination b) dppb ligand; C_{acyl} –C1 bond activation, decarbonylation, and C2 β -hydride elimination

1.2.2 AROMATIZATION

In 1971, King demonstrated that the unfavorable thermodynamic equilibrium of activating an unstrained C–C bond could be offset by generating aromatic intermediates. The reaction of cyclopentadiene **1.25** with various carbonylated metals yielded pentamethylcyclopentadienyl (Cp^*) ligated metal complexes **1.26** (Scheme 7a).³¹ Metal carbonyl complexes of chromium, molybdenum, tungsten, manganese, and iron underwent the transformation, but nickel was ineffective. It was later shown that less labile alkyl groups, such as that of spirocyclopentadiene **1.27**, underwent C–C bond cleavage that resulted in an alkyl-bridged cyclopentadienyl (Cp) ligated metal complex **1.27** (Scheme 7b).^{17,32,33} In 1993, Chaudret demonstrated that cholesterol could be aromatized by cleaving the C10 methyl group with a cationic ruthenium species (not shown).³⁴ To date, no other demonstrations of C_{sp^3} – C_{sp^3} bond activation without this strategy have been realized.



Scheme 7. C–C bond activation driven by aromatic stabilization. a) sp^3 – sp^2 C–C_{acyl} bond activation b) sp^3 – sp^3 C–C bond activation

1.3.3 CHELATION ASSISTANCE

The preceding sections described strategies to overcome barriers to bond activation that were mainly thermodynamic in nature. However, subtle kinetic factors also contribute to the success of such highly specified systems. For instance, the ‘bent’ orbital overlap in strained cycloalkanes kinetically facilitates C–C bond activation by reducing the degree in which the bonding orbitals must rotate (see Figure 5c). The strategy for aromatic stabilization is aided by olefin pre-coordination, in which the metal is held in proximity (see Scheme 7). In order to activate unstrained bonds that would not be driven by aromatic stabilization, the strategy of chelation assistance by way of a process known as cyclometalation was developed.

The term ‘cyclometalation’ refers to class of reactions in which a ligand (**1.29**) undergoes an oxidative intramolecular metalation to generate a stable chelate ring (metallacycle) containing a metal–carbon (M–C) bond (**1.30**) (Figure 6).³⁵ The term

‘chelation assistance’ refers to the ability of a functional group to bind or ligate the metal in order for the complex to undergo cyclometalation. With five-membered metallacycles shown to be the most stable, strategic placement of the chelating group achieves selectivity by orienting the metal in proximity of the desired bond to be cleaved. Selective activation of C–H bonds was realized through cyclometalation.³⁶⁻³⁹ Cyclometalation was later applied in the selective activation of C–C bonds and has become a prominent strategy in overcoming the inherent barriers.⁴⁰⁻⁴²

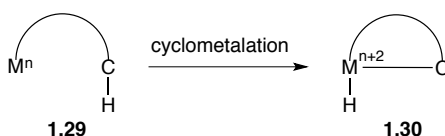


Figure 6. Cyclometalation: A strategy to overcome the kinetic barriers to bond activation

A benchmark in C–C bond activation was demonstrated by Milstein in 1993, in which the oxidative addition into relatively strong, non-strained C–C bonds that did not rely on aromaticity as a driving force was accomplished.⁴³ Pincer ligands (PCP) are powerful chelating agents that tightly bind transition metals through three adjacent sites.⁴⁴ The phosphorylated mesitylene derivatives **1.31** were envisioned as scaffolds that would obtain a pincer-like configuration upon activation of the C_{sp2}–C_{sp3} bond (Figure 7). These C_{aryl}–C_{methyl} bonds are exceptionally strong with a BDE of 101.8 ± 2 kcal mol⁻¹, and are much stronger than the competing benzylic C–H bonds that have a BDE of 88 ± 1 kcal mol⁻¹.⁴⁵ To date, various metal complexes have been reported to afford similar transformations, including Rh^I,^{43,46-49} Ir^I,⁴⁷ Ni^{II},⁵⁰ Pt^{II},^{49,51,52} Ru^{II},⁵² and Os.^{II 53,54}

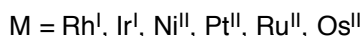
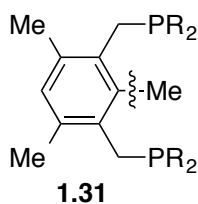
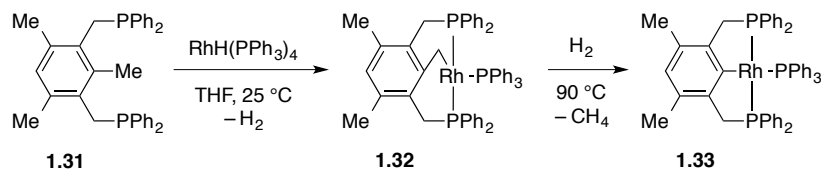


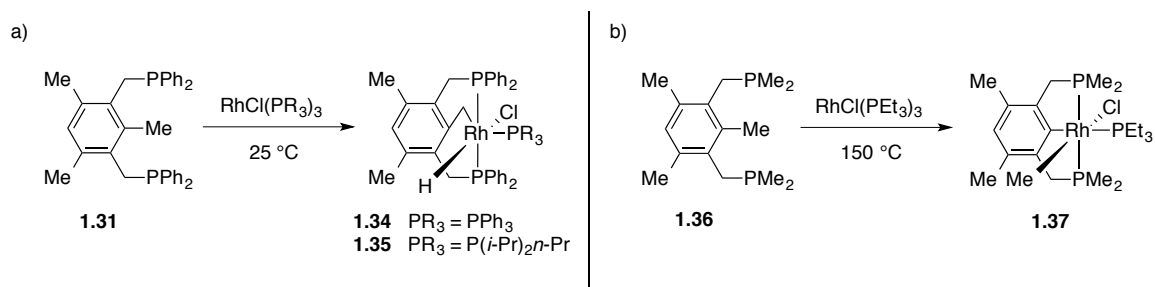
Figure 7. Pincer-type ligand for C–C bond activation

Treating ligand **1.31** with $\text{RhH}(\text{PPh}_3)_4$ exclusively provided the product of C–H activation (**1.32**) upon elimination of H_2 .⁴³ The bis-6-membered chelate **1.32** was shown to be thermally stable, though heating at 90 °C in the presence of H_2 (80 psi) furnished the product of C–C activation (**1.33**), which was accompanied by the release of methane. A plausible mechanism for the transformation of **1.32** to **1.33** is through an oxidative addition of H_2 . The resulting Rh^{III} dihydride complex would be in equilibrium with both **1.32** and **1.31**, and over time, the metal directly inserts into the C–C bond of **1.31**. Reductive elimination of the $\text{C}_{\text{Me}}\text{--Rh--H}$ adduct releases methane and provides pincer complex **1.33**. Milstein had also demonstrated that complex **1.33** could be obtained from **1.32** in which either an aryl halide, silane, or disilane could be used in place of H_2 .^{55,56} These results illustrate that C–C bond activation is thermodynamically feasible. It should be noted that the BDE for a $\text{C}_{\text{aryl}}\text{--Rh}$ bond is about 13 kcal mol^{-1} stronger than a $\text{C}_{\text{alkyl}}\text{--Rh}$ bond, whereas a Rh--H is relatively weak ($<52 \text{ kcal mol}^{-1}$).



Scheme 8. Carbon–carbon bond activation with pincer-type systems

In attempts to observe the fundamental C–C insertion process (prior to methane elimination), Milstein studied the reaction with non-hydrido-based catalysts. Treating **1.31** with $\text{RhCl}(\text{PPh}_3)_3$ or $\text{RhCl}(\text{P}(i\text{-Pr})_2n\text{-Pr})_3$ at room temperature exclusively gave the corresponding C–H activation products **1.34** and **1.35**, respectively, which were shown to be thermally stable at 150 °C (Scheme 9a).⁴⁶ However, the reaction with pincer complex **1.36**, containing the more basic PMe_2 phosphoranes, did not react at room temperature nor upon heating to 90 °C, though after 6h at 150 °C, ligand **1.36** underwent full conversion to the corresponding C–C activation product **1.37** (Scheme 9b). The authors attributed this difference in thermodynamic preference for C–C over C–H activation to the increased electron density at the metal center. The added electron donation from the PMe_2 groups allows for the metal center to more effectively back-bond to the aromatic π^* system, and thus stabilize the $\text{C}_{\text{aryl}}\text{--Rh}$ bond relative to the $\text{C}_{\text{alkyl}}\text{--Rh}$ bond.



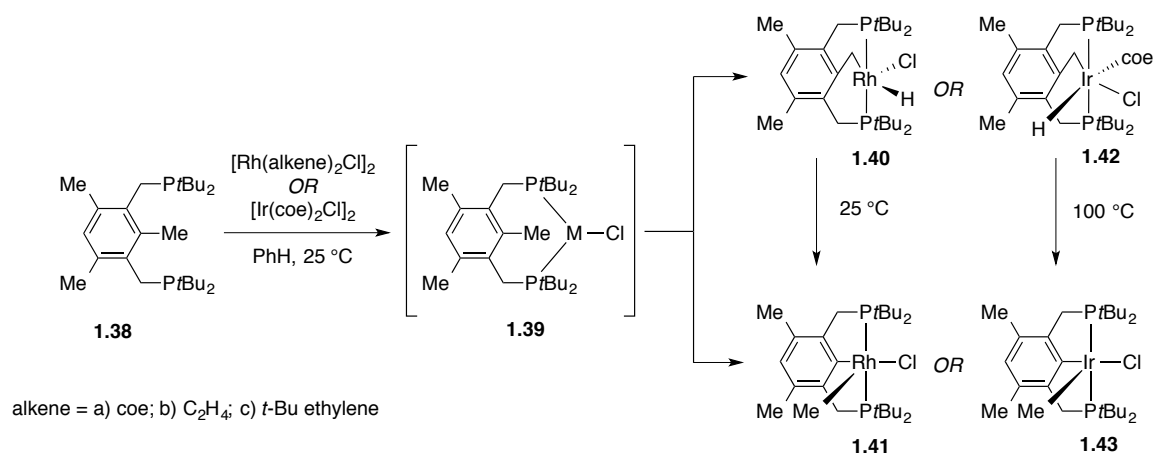
Scheme 9. Differences in electronics dictate chemoselectivity in C–H vs C–C bond activation. a) diphenyl phosphoranes favor C–H bond activation b) dimethyl phosphoranes favor C–C bond activation

Milstein later reported a system in which C–C bond activation was observed at room temperature. Moreover, a direct comparison between the thermodynamic and kinetic preferences for C–C and C–H bond activation was made. Treating PtBu_2 phosphorane **1.38** with $[\text{Rh}(\text{coe})_2\text{Cl}]_2$ for 24 hours at room temperature selectively gave the C–C

activation product **1.41** (Scheme 10).⁴⁷ However, following the reaction by $^{31}\text{P}\{^1\text{H}\}$ NMR revealed parallel formation of the C–H (**1.40**) and C–C (**1.41**) activation products in a 1.25:1 ratio, respectively. Throughout the experiment, only **1.38**, **1.40**, and **1.41** were observed, which implied that ligand exchange to generate intermediate **1.39** might be the rate-determining step. Over time, complex **1.40** was converted into complex **1.41**.

Employing $[\text{Rh}(\text{C}_2\text{H}_4)_2\text{Cl}]_2$ as catalyst resulted in a substantial rate enhancement wherein quantitative conversion was established within 15 min as a 1.25:1 ratio of C–H to C–C activation products (**1.39**:**1.40**). The conversion of **1.39** into **1.40** (via slow C–H reductive elimination, and rapid C–C insertion) was shown to obey first-order kinetics, with $k = 8.59 \times 10^{-5} \text{ s}^{-1}$, corresponding to $\Delta G^\ddagger = 22.4 \text{ kcal mol}^{-1}$. The increase in rate observed with $[\text{Rh}(\text{C}_2\text{H}_4)_2\text{Cl}]_2$ also supports that ligand exchange is the rate-limiting step, whereby ethylene is more labile than cyclooctene. Further evidence to support this claim resides in the sluggish nature of the $[\text{Rh}(t\text{-BuC}_2\text{H}_3)_2\text{Cl}]_2$ catalyst in promoting bond activation.

The reaction with $[\text{Ir}(\text{coe})_2\text{Cl}]_2$ provided **1.42** and **1.43** in a 2:1 ratio and the conversion was found to be three times slower than the analogous reaction with rhodium. Complex **1.42** was isolable and shown to require temperatures above 100 °C in order to afford **1.43**, an observation which may be explained by the greater stability of iridium hydrides. The fact that **1.42** does not convert to **1.43** at room temperature proves that *direct* C–C activation is possible.



Scheme 10. C–C vs. C–H bond activation at room temperature with pincer-type scaffolds

If C–C or C–H bond activation were the rate-limiting step, it would be expected that the reaction with iridium would be faster than with rhodium given that iridium is more easily oxidized. Additionally, it is known that olefins bind more strongly to iridium, which together suggest that ligand exchange is rate limiting. Since the two parallel processes occur through a common intermediate **1.39**, the product ratios directly reflect the ratio between the rate constants of C–H and C–C bond activation, regardless of the overall rate-determining step. The differences in free energies ($\Delta\Delta G^\ddagger$) between C–H and C–C activation were determined to be relatively small, despite theoretical calculations predicting C–C bond oxidative addition to be substantially higher (by 10–20 kcal mol^{–1}). Surprisingly, the kinetic barrier for C–H bond activation was shown to be *higher* than for C–C bond activation by 0.3 kcal mol^{–1} (iridium) and 0.5 kcal mol^{–1} (rhodium). The authors speculate that the thermodynamic and kinetic preference for C–C bond activation in this system can be attributed to the proper choice of ancillary ligand. The more electron-rich *tert*-butyl groups favor C–C bond activation by stabilizing the C_{Ar}–Rh bond

through enhanced back bonding, and the bulkiness orients the metal orbitals to better overlap with the C–C bond.

1.4 8-ACYLQUINOLINE AS A DIRECTING GROUP

The focus of this section will be on chelation assistance using 8-acylquinoline as a directing group for C–C bond activation. This brief review detailing precedent work will serve as an introduction to Chapter 2 and is divided into two parts: stoichiometric and catalytic reactions. Although fundamentally important, the following examples are limited to fragmentation and exchange reactions.

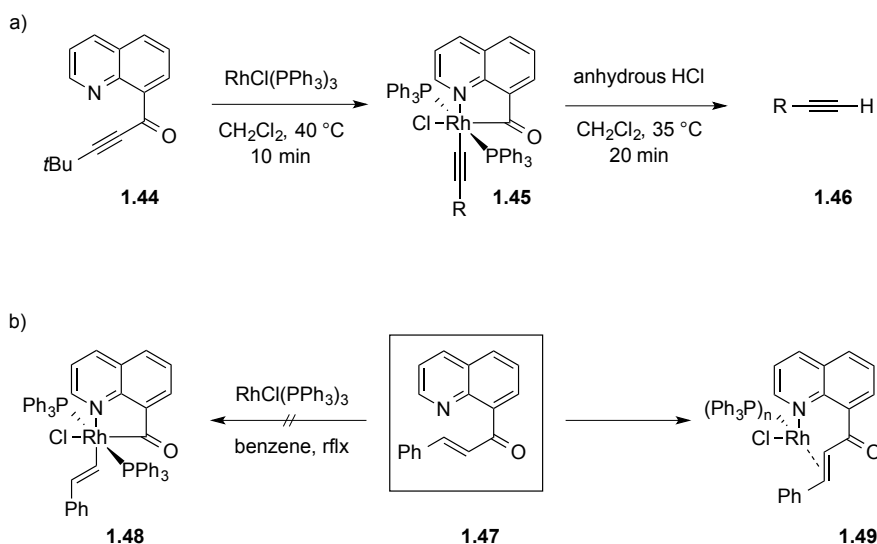
1.4.1 STOICHIOMETRIC C–C BOND ACTIVATION REACTIONS

In 1969, di-alkynyl ketones were shown to decarbonylate by treatment with $\text{RhCl}(\text{PPh}_3)_3$ in refluxing xylenes to yield 1,3-diynes and $\text{RhCl}(\text{CO})(\text{PPh}_3)_2$ by way of an oxidative C–C sigma bond cleavage pathway.^{57,58} More than a decade later, Suggs⁵⁹ discovered that decarbonylation of the Rh(III)ketoacetylide intermediate could be prevented by stabilizing the metal center through cyclometalation.³⁵ The two resulting M–C bonds would have the potential to be controllably functionalized.

The cyclometalation reaction was achieved by treating 8-quinolinyl *t*-butylacetylenyl ketone **1.44** with $\text{RhCl}(\text{PPh}_3)_3$ in CH_2Cl_2 for 10 minutes at 40 °C (Scheme 11a). The resulting stable, yellow solid **1.45** displayed a ketone IR band shifted from 1645 to 1670 cm^{-1} and a ^{31}P NMR doublet at –19.35 ppm, $J_{\text{Rh-P}} = 110$ Hz.⁵⁹ Upon

treatment with anhydrous acid, the Rh(III) compound **1.45** underwent protonation to provide *t*-butylacetylene **1.46** in high yield.

Given that sp^2 – sp C–C bonds of ynones can be readily cleaved by strong reducing agents and/or nucleophiles owing to the low pKa of acetylenes, Suggs questioned whether the less reactive sp^2 – sp^2 C–C bond of an enone could be activated in a similar manner. Attempts to oxidatively add RhCl(PPh₃)₃ into the sp^2 – sp^2 carbon–carbon bond of 8-quinolinyl styrenyl ketone **1.47** did not provide complex **1.48**, even after extended reflux in benzene (Scheme 11b).⁵⁹ The ¹H NMR spectrum of the product showed an olefin multiplet at 4.4 ppm, and the 2-quinolinyl signal shifted downfield at 8.45 ppm, which was consistent with rhodium bound by both the quinoline nitrogen and olefin as depicted in **1.49**. No evaluations of other Rh(I) complexes were reported with **1.47**.



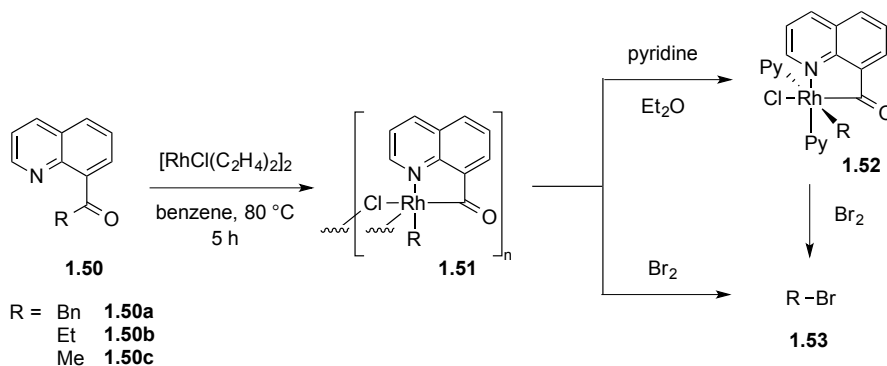
Scheme 11. a) sp^2 – sp C–C bond activation and protonation of rhodium acetylide b) inability to activate sp^2 – sp^2 C–C bond due to alkene coordination

Since the sp^2 – sp^2 α -ketone C–C bond is less reactive than the sp – sp^2 α -ketone C–C bond toward nucleophilic cleavage, one might expect a sp^2 – sp^3 α -ketone C–C bond to be

even less reactive. Perhaps owing to this notion, no reaction of 8-quinolinyl alkylketones **1.50a–c** was observed when treated with $\text{RhCl}(\text{PPh}_3)_3$.⁶⁰ However, reacting **1.50a–c** with $[\text{RhCl}(\text{C}_2\text{H}_4)_2]_2$ in benzene at room temperature provided an insoluble material, which was presumed to be the chlorine-bridged oligomer **1.51a–c** (Scheme 12). The oligomeric complexes were solubilized with excess pyridine and crystallized from ether to give the six-coordinate dipyridyl Rh(III)–acyl complexes **1.52a–c**. The benzyl **1.52a**⁶⁰ and ethyl **1.52b**⁶¹ complexes were confirmed by X-ray crystallography and **1.52b** was independently synthesized via a hydroacylation reaction of 8-quinolinecarboxaldehyde and ethylene.^{61,62} Whether oxidative addition occurred prior to the addition of pyridine was probed by treatment of both **1.51** and **1.52** with bromine. Each reaction gave the corresponding alkyl bromide **1.53**, indicating that pyridine was not necessary for carbon–carbon bond activation to occur.

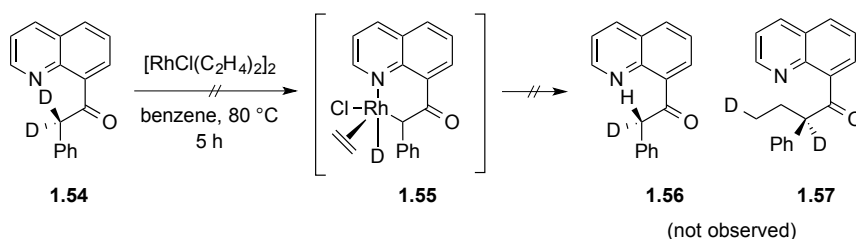
In solution, the five-coordinate mono-pyridyl rhodium complex predominates (not shown). As with other five-coordinate Rh(III) complexes,⁶³ it is likely square pyramidal with the alkyl group in the apical position. With the $\text{Rh}-\text{N}_{\text{pyridine}}$ bond *trans* to the benzyl group 0.13 Å longer than the $\text{Rh}-\text{N}_{\text{pyridine}}$ bond *trans* to quinoline in complex **1.52**, it is likely that the latter pyridine is lost in solution. The Rh(III)–C_{acyl} bond length in **1.52a** was measured at a short distance of 1.949 Å⁶⁰ (1.938 Å⁶⁴ for **1.52b**) relative to other Rh(III)–C_{acyl} bonds (1.971–2.062 Å).⁶⁵ These bond length values are closer to those found for rhodium carbenes (1.968 Å),⁶⁶ though an IR ν_{CO} value of 1633 cm^{–1} portrays **1.52** as the Rh–C_{acyl}. The inherent strength of these shortened bonds could reflect the thermodynamic driving force of the reaction. The strong *trans* effect of the acyl group, in turn, lengthens the Rh–Cl bond by 10% in comparison to typical values.⁶⁷ This

lengthened Rh–Cl bond may play a significant role in the transmetalation step shown in the cross-coupling reaction described in Section 1.4.2 (see Scheme 24).



Scheme 12. Trapping of the sp^2 – sp^3 C–C bond activation adducts and derivatization

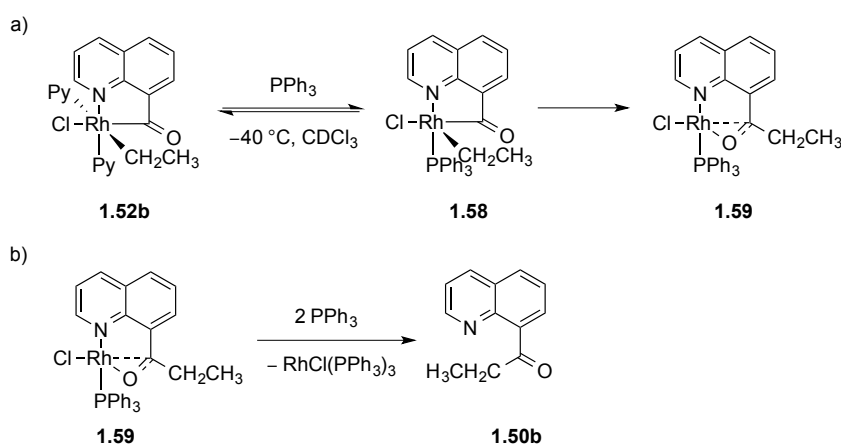
The proximity of the benzylic protons in 8-quinolinyll benzylketone **1.50a** makes it plausible that carbon–hydrogen activation could precede C–C bond activation and thus be a potential competing pathway. In order to probe this, deuterated 8-quinolinyll benzylketone **1.54** was subjected to the reaction conditions (Scheme 13). Should a C–D bond insertion occur via the six-membered metallacycle **1.55**, the resulting Rh(III)–D would presumably undergo migratory insertion onto a bound ethylene ligand. A subsequent β –hydride elimination would generate a Rh(III)–H that could reductively eliminate to give **1.56**. No H/D scrambling was detected and no evidence of the ethylation product **1.57** was observed. This led Suggs and Jun to conclude that C–H bond activation was not occurring. The propensity toward C–C bond activation in this case could be explained by the enhanced stability of five-membered metallacycles in cyclometalation reactions.⁶⁸



Scheme 13. Hypothetical C–H bond activation via a six-membered metallacycle

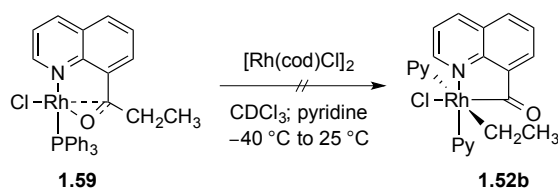
The octahedral dipyriddy Rh(III) complexes **1.52a–c** (Scheme 12) were shown to be stable in solution for extended periods of time. Attempts to promote the reverse reaction (reductive elimination) by the addition of hard ligands such as triethylamine, dimethyl sulfoxide, or *N,N*-dimethylaminopyridine were unsuccessful. This observation was rationalized by Suggs in terms of hard/soft acid base theory. The resulting soft Rh(I) species would be unstable when coordinated to hard ligands. The addition of soft ligands (i.e. phosphines, phosphites, or CO) promoted reductive elimination via Rh(I) stabilization. Alternatively, the lower oxidation state may be stabilized by π -acidic ligands. Treating compound **1.52b** with PPh_3 at -40°C in CDCl_3 allowed for the rapid formation of a five-coordinate monophosphine Rh(III) complex **1.58** characterized by the ^{31}P NMR doublet at 8.3 ppm ($J_{\text{Rh-P}} = 65$ Hz) and the CH_2 carbon as a doublet of doublets ($J_{\text{P-C}} = 82$ Hz and $J_{\text{Rh-C}} = 35$ Hz) in the ^{13}C NMR spectrum (Scheme 14a).⁶⁴ An equilibrium ratio greater than 6:1 favoring compound **1.58** was established within minutes. Over time, the appearance of a second ^{31}P signal at 35.6 ppm with a large coupling constant ($J_{\text{Rh-P}} = 188$ Hz), and the absence of Rh–C and P–C coupling to the CH_2 in the ^{13}C NMR spectrum, indicated the formation of a Rh(I) species via reductive elimination. However, the persisting nonequivalence of the CH_2 protons and appearance of a ^{13}C NMR carbonyl doublet at 99.9 ppm ($J_{\text{Rh-C}} = 15$ Hz) suggested the η^2 -ketone complex **1.59**. In the absence of excess PPh_3 , the bound η^2 -ketone either dissociates or is

displaced by pyridine in solution at temperatures above $-10\text{ }^{\circ}\text{C}$. Kinetic measurements demonstrated a first-order dependence on phosphine, which implied only one phosphine was required to promote reductive elimination. In the presence of excess PPh_3 , complex **1.59** was readily converted to the 8-quinoliny ethylketone **1.50b** and $\text{RhCl}(\text{PPh}_3)_3$ (Scheme 14b). This process was monitored by variations in the coupling constants between rhodium and phosphorus.



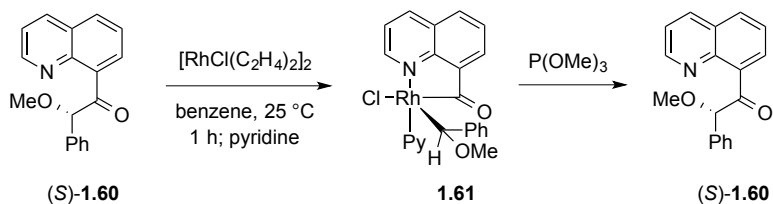
Scheme 14. a) Phosphine-promoted reductive elimination b) Excess phosphine-promoted ligand exchange

With phosphine ligands shown to promote reductive elimination, and phosphine-containing complexes oxidatively unreactive toward substrates **1.50a–c**, Suggs investigated whether removing phosphine from the metal center would encourage oxidative addition. A CDCl_3 solution of **1.59** was treated with $[\text{Rh}(\text{cod})\text{Cl}]_2$ which served as a phosphine sponge (Scheme 15).⁶⁹ Although the ^{31}P resonance of **1.59** rapidly disappeared, no indication of the rhodium insertion product **1.52b** was observed, even upon warming to $25\text{ }^{\circ}\text{C}$.



Scheme 15. Failure to promote oxidative addition by PPh_3 adsorption onto $[\text{Rh}(\text{cod})\text{Cl}]_2$

In order to gain insight into the reaction mechanism of carbon–carbon bond activation, the stereochemical outcome of oxidative addition and reductive elimination was probed. Combining $[\text{RhCl}(\text{C}_2\text{H}_4)_2]_2$ and (*S*)-8-quinoliny α -methoxybenzyl ketone derivative **1.60** ($[\alpha]_{\text{D}} = -117^\circ$) in benzene at room temperature provided the Rh(III)–alkyl complex **1.61** as a single diastereomer (Scheme 16).⁷⁰ Phosphite-promoted reductive elimination regenerated **1.60** ($[\alpha]_{\text{D}} = -111^\circ$). Since reductive elimination is known to proceed with retention of configuration in other systems, it is likely that both steps took place with retention rather than inversion of configuration.

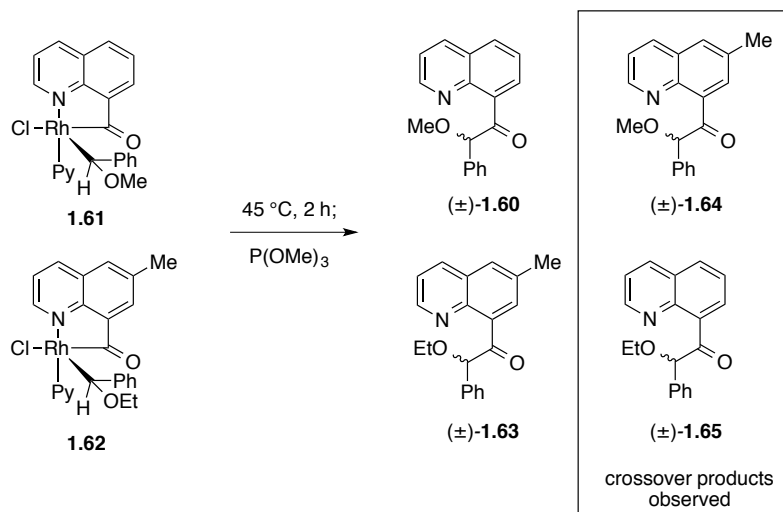


Scheme 16. Stereochemical outcome of oxidative addition and reductive elimination

In the absence of phosphite ligand, benzaldehyde was detected upon thermal decomposition of complex **1.61** at 90°C . The formation of benzaldehyde could readily be explained by homolysis of the rhodium–alkyl bond in that α -alkoxy radicals are known to undergo fragmentation to carbonyl compounds.⁷¹ In the presence of CCl_4 the putative methyl radical was trapped as the methyl chloride under thermolysis conditions.

Lowering the temperature to 45–60 °C prevented radical fragmentation, but was sufficient for homolysis as indicated by the racemization of **1.60**.

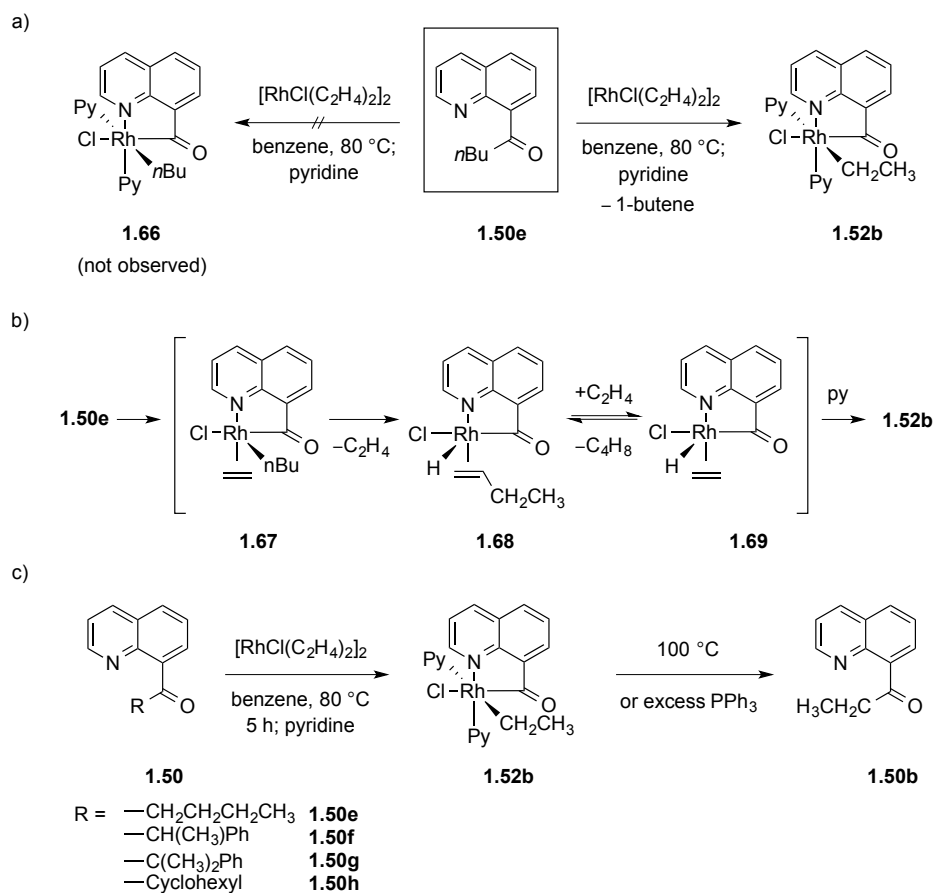
A cage-escape crossover experiment, in which complex **1.61** and the ethoxy derivative **1.62** were heated together at 45 °C, yielded the corresponding racemates of **1.60** and **1.63** along with racemic crossover products **1.64** and **1.65** (Scheme 17). A control experiment in which complexes **1.61** and **1.62** were immediately treated with trimethyl phosphite did not yield crossover products. These observations were interpreted as a result of the radical fragmentation and recombination mechanistic process.



Scheme 17. Crossover experiment: evidence for a Rh–C homolysis-recombination mechanism

The rates of racemization at carbon over the temperature range of 37–52 °C provided an enthalpic value of $\Delta H^\ddagger_{(\text{racemization})} = 32.5 \pm 1.5$ kcal/mol. Assuming the carbon radical has a very low racemization barrier,⁷² the calculated $\Delta H^\ddagger_{(\text{racemization})}$ should reflect the activation enthalpy for homolysis of the Rh–C bond. Should the radical recombination barrier for Rh(II) mirror the value reported for Co(II) systems (ca. 2 kcal mol⁻¹),^{73,74} a Rh–C bond dissociation energy (BDE) of approximately 31 kcal/mol can be estimated.

Subjecting 8-quinolinyll butylketone **1.50e** to reaction conditions with $[\text{RhCl}(\text{C}_2\text{H}_4)_2]_2$ and pyridine did not provide the analogous bipyridyl Rh(III)–butyl complex **1.66** as expected (Scheme 18a).⁷⁵ Instead, the ethyl complex **1.52b** was isolated in >90% yield and 1-butene was observed in the ^1H NMR spectrum. The observation of 1-butene suggested that Rh(III)–butyl complex **1.67** underwent β -hydride elimination to give the Rh(III)–H complex **1.68** (Scheme 18b). Migratory insertion of the metal–hydride across an ethylene ligand (**1.69**) (ethylation) would generate the corresponding Rh(III)–ethyl complex that is subsequently trapped by pyridine (**1.52b**). Without the detection of 1-hexene, it appears β -hydride elimination of **1.67** has a lower kinetic barrier than migratory insertion of *n*-butyl. Other ketones containing β -hydrogens (**1.50f–h**) were also shown to form ethyl complex **1.52b** exclusively, except for a cyclopropyl derivative that underwent rearrangement to a π -allyl system (not shown).⁷⁶ Heating **1.52b** at 100 °C or treatment with excess PPh_3 afforded 8-quinolinyll ethyl ketone **1.50b** via reductive elimination (Scheme 18c).

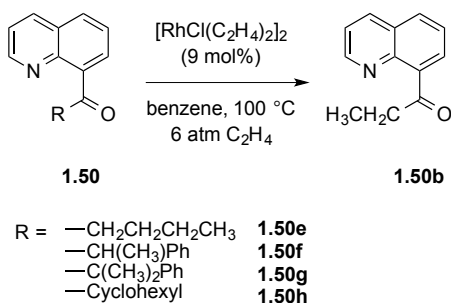


Scheme 18. Stoichiometric alkyl C–C bond exchange to form ethyl ketone **1.50b** a) unexpected complex formation b) ethylation mechanism c) additional alkyl exchange reactions

1.4.2 CATALYTIC C–C BOND ACTIVATION

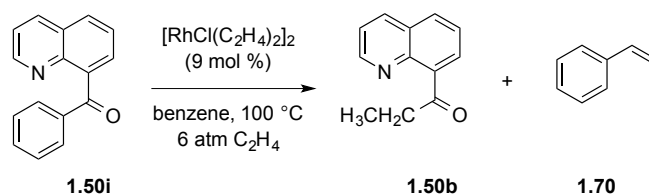
Reactions with compounds **1.50e–h** were made catalytic using higher temperature (100 °C), longer reaction time (48 h), and 6 atm of ethylene pressure (Scheme 19).⁷⁵ Substrate **1.50e** yielded 8-quinolinyl ethyl ketone **1.50b** in 61% yield with the remaining material being unreacted starting material. The insufficient conversion was attributed to catalyst deactivation rather than full equilibration considering the large excess of ethylene employed. Reactions with other alkenes were attempted, but the outcome of these

experiments was not clear. The authors simply stated that “the exchange reaction with alkenes other than ethylene was not efficient,” and that “ β -hydride elimination is too fast to compete with reductive elimination except for ethylene.” It is plausible that the binding of more sterically hindered alkenes promotes reductive elimination. It was found that catalytic C–C bond activation reactions were successful under conditions utilizing $[\text{Rh}(\text{cod})\text{Cl}]_2$, $[\text{Ir}(\text{cod})\text{Cl}]_2$, and even $\text{RhCl}(\text{PPh}_3)_3$, which had been shown to be inactive in related stoichiometric reactions. Complexes that did not catalyze the exchange reaction included $\text{Pd}(\text{PPh}_3)_4$, $\text{Pd}(\text{OAc})_2$, $\text{Pt}(\text{PPh}_3)_4$, $\text{RuCl}_2(\text{PPh}_3)_3$, and $\text{Rh}(\text{Cp})(\text{C}_2\text{H}_4)_2$.



Scheme 19. Catalytic alkyl C–C bond exchange sp^2 – sp^3 substrates with β -hydrogens to ethyl ketone **1.50b**

Although oxidative addition into the sp^2 – sp^2 C–C bond of enone **1.47** did not occur with $\text{RhCl}(\text{PPh}_3)_3$ (Scheme 10), catalytic conversion of 8-quinolinyl phenyl ketone **1.50i** to ethyl ketone **1.50b** with $[\text{RhCl}(\text{C}_2\text{H}_4)_2]_2$ proceeded in quantitative yield (Scheme 20).⁷⁵ The formation of one equivalent of styrene (**1.70**) suggested that the migratory aptitude of phenyl is greater than for alkyl analogs. This difference in reactivity was attributed to the ability of the resulting homobenzylic moiety to coordinate to rhodium through the phenyl π -bond, thus maintaining the electron-count around the metal center post insertion.

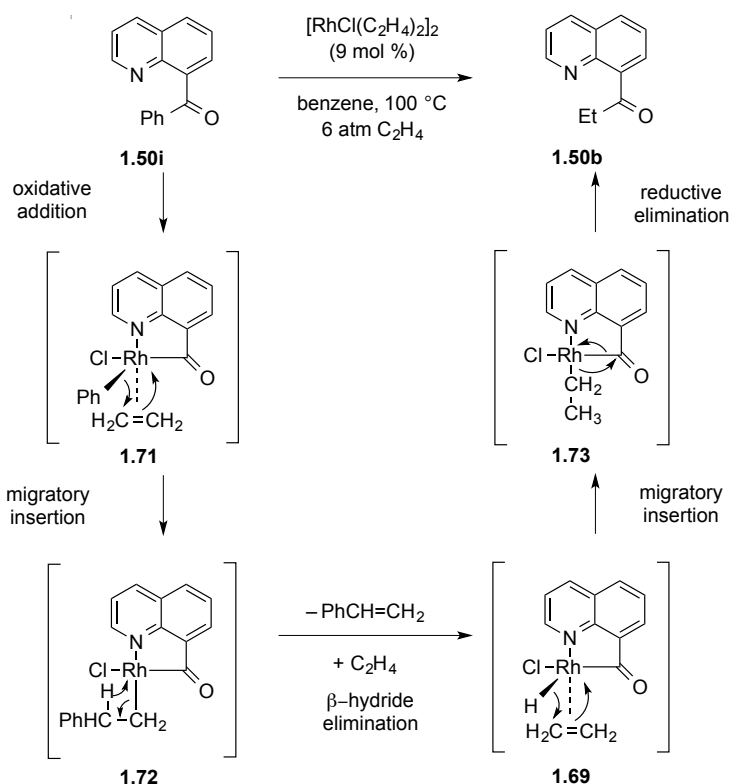


Scheme 20. Catalytic conversion of sp^2 – sp^2 phenyl substrate into ethyl ketone **1.50b** and styrene

A plausible mechanism for the exchange reaction is illustrated in Scheme 21. Following oxidative addition into the acyl C–C bond, the resulting Rh(III)–phenyl complex **1.71** undergoes migratory insertion across ethylene. β -hydride elimination of the homobenzylic intermediate **1.72** and migratory insertion of the subsequent Rh(III)–H **1.69** across another ethylene unit, generates Rh(III)–ethyl species **1.73**. Reductive elimination delivers **1.50b** to complete the net hydroacylation process.

The potential for competitive *ortho* C–H activation was explored through deuterium-label studies. Reaction with penta-deutero phenyl **1.50i** quantitatively yielded **1.50b** with complete deuterium retention in the styrene by-product. While this experiment suggested that *ortho* C–H bond activation was not in competition with C–C bond activation in 8-acylquinolines systems, subsequent work by our group⁶² has identified this as a challenge (see Chapter 2, Section 2.4).

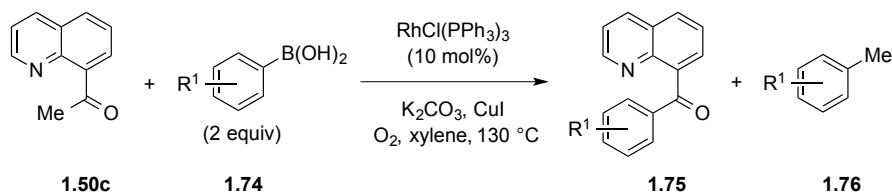
Although many organometallic intermediates have been shown to undergo a wide variety of subsequent functionalization reactions, catalytic C–C bond activation reactions have been relatively limited to additions across π -bonds. With the exception of carbon–nitrile (C–CN) bond activation,⁶³ and β -carbon elimination processes,⁶⁴ examples of direct C–C bond cleavage reactions with successive cross-coupling functionalization are rare.



Scheme 21. Proposed mechanism of phenyl for ethyl exchange

Wang and co-workers embarked on merging the activation of 8-acylquinoline C–C bonds with other known C–C bond-forming reactions, such as the Suzuki-Miyaura coupling.⁸⁰ Methyl ketone **1.50c** was allowed to react with two equivalents of phenylboronic acid ($\text{R} = \text{H}$) **1.74** in the presence of CuI , O_2 , K_2CO_3 , and catalytic $\text{RhCl}(\text{PPh}_3)_3$ in xylene at $130\text{ }^\circ\text{C}$ for 18 h (Scheme 22). The aryl-exchanged product **1.75** was isolated in 93% yield, and toluene ($\text{R} = \text{H}$) **1.76** was detected as the by-product.⁸⁰ Molecular oxygen as a terminal oxidant was critical for the reaction, as no product was formed under anaerobic conditions. Under 1 atm of O_2 , the reaction proceeded in less than 12 h, providing **1.75** in 72% yield along with unidentified side-products. The

increase in reaction rate led to the speculation that O₂ must be involved in the rate-limiting step of catalysis.

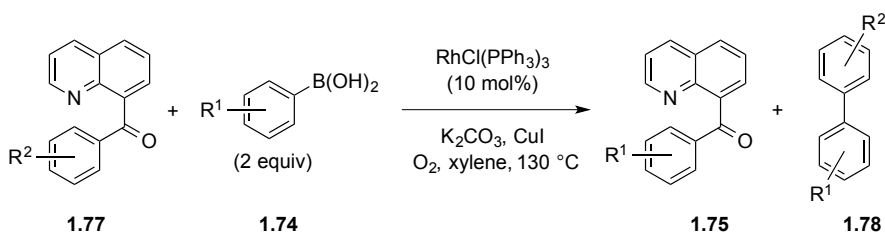


Scheme 22. C–C bond activation/cross coupling methyl-for-aryl exchange reaction

The stereoelectronic effects of the reaction were explored with various arylboronic acids containing electron-donating or electron-withdrawing groups. Although requiring longer reaction times (36 or 48 h), arylboronic acids possessing *meta* and *para* electron-donating groups were well tolerated with yields ranging from 74–90%, whereas those with *ortho* substitution failed to undergo the reaction. Aryl boron species with electron-withdrawing groups requiring extended reaction times and provided products in lower yields (35–57% yields), with the exception of 4-chlorophenylboronic acid which proceeded in 83% yield.

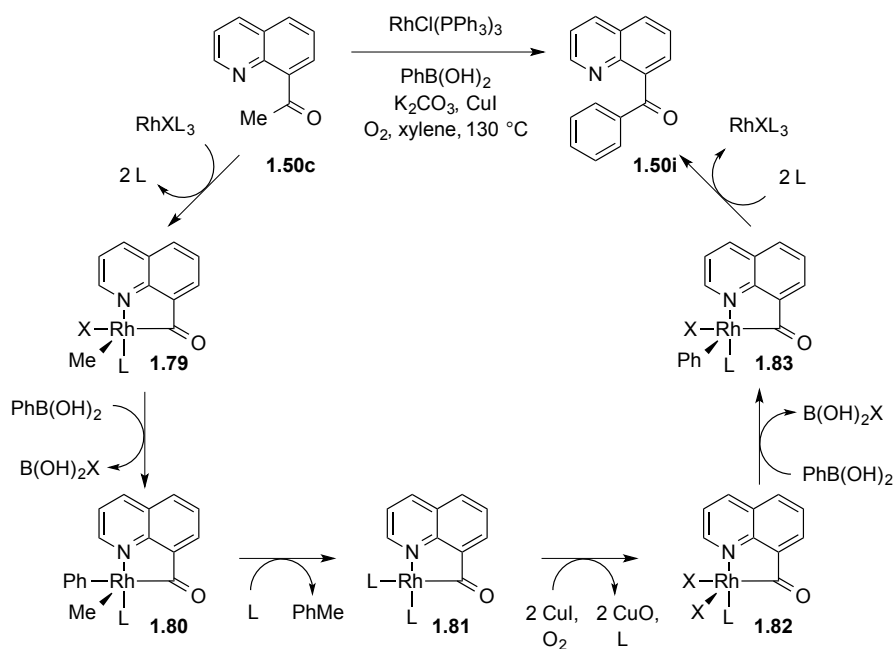
The 8-quinolinylnyl aryl ketones **1.77** and arylboronic acids **1.74** successfully underwent the exchange reaction to yield the corresponding aryl ketones **1.75** and biphenyl by-products **1.78** (Scheme 23). The synergistic stereoelectronic effect between coupling partners significantly impacted the reaction outcomes. Aryl ketone **1.77** with R¹ = H reacted with various electron-rich boronic acids with yields ranging from 45–71%. The combination of electron-donating groups on both **1.77** and **1.74** gave similar results. Optimal conditions employed electron-deficient aryl ketones with

electron-rich boronic acids (61–93%). In all cases, boronic acids with electron-withdrawing groups failed to undergo the reaction.



Scheme 23. C–C bond activation/cross coupling aryl exchange reaction

The authors proposed a catalytic cycle that involves oxidative addition into the acyl C–C bond to form the five-membered Rh(III) metallacycle **1.79** (Scheme 24). Transmetalation with boronic acid generates intermediate **1.80** that undergoes phosphine-promoted reductive elimination. Oxidation of the resulting Rh(I) chelate **1.81** with O_2 in the presence of CuI gives a Rh(III) species **1.82** that participates in a second transmetalation. Reductive elimination of complex **1.83** yields product **1.50i**. With the oxidation of **1.81** suggested to be rate-limiting, it is unclear how the rate is affected by the electronic nature of the boronic acid, and thus further investigation is warranted.



Scheme 24. Proposed mechanism for C–C bond activation/cross coupling reaction

1.5 CONCLUDING REMARKS

Theoretically, the activation of C–C bonds seems impractical from both a thermodynamic and kinetic standpoint. Nevertheless, chemists boldly undertook this challenge and demonstrated that C–C bond activation is not only possible, but can be made favorable and selective over C–H activation. Additional examples of C–C bond activation reactions will be introduced in the following chapters where relevant. A common, underlying feature of the present literature is that C–C bond activation has been limited to stoichiometric reactions and catalytic reactions that are merely fragmentation reactions that reduce molecular complexity.

REFERENCES

- (1) Crabtree, R. H. *Chem. Rev.* **1985**, 85, 245.
- (2) Vaska, L. *Acc. Chem. Res.* **1968**, 1, 335.
- (3) Halpern, J. *Inorg. Chim. Acta* **1985**, 100, 4.
- (4) Labinger, J. A.; Bercaw, J. E. *Organometallics* **1988**, 7, 926.
- (5) Simoes, J. A. M.; Beauchamp, J. L. *Chem. Rev.* **1990**, 90, 629.
- (6) Nolan, S. P.; Hoff, C. D.; Stoutland, P. O.; Newman, L. J.; Buchanan, J. M.; Bergman, R. G.; Yang, G. K.; Peters, K. S. *J. Am. Chem. Soc.* **1987**, 109, 3143.
- (7) Rybtchinski, B.; Milstein, D. *Angew. Chem. Int. Ed.* **1999**, 38, 870.
- (8) Osdene, T. S.; Timmis, G. M.; Maguire, M. H.; Shaw, G.; Goldwhite, H.; Saunders, B. C.; Clark, E. R.; Epstein, P. F.; Lamchen, M.; Stephen, A. M.; Tipper, C. F. H.; Eaborn, C.; Mukerjee, S. K.; Seshadri, T. R.; Willenz, J.; Robinson, R.; Thomas, A. F.; Hickman, J. R.; Kenyon, J.; Crocker, H. P.; Hall, R. H.; Burnell, R. H.; Taylor, W. I.; Watkins, W. M.; Barton, D. H. R.; Ives, D. A. J.; Thomas, B. R. *J. Chem. Soc.* **1955**, 2038.
- (9) Walsh, A. D. *Trans. Faraday Soc.* **1949**, 45, 179.
- (10) Adams, D. M.; Chatt, J.; Guy, R. G.; Sheppard, N. *J. Chem. Soc.* **1961**, 738.
- (11) Keeton, M.; Mason, R.; Russel, D. R. *J. Organomet. Chem.* **1971**, 33, 259.
- (12) Dewar, M. *Bull. Soc. Chim. Fr.* **1951**, 18, C79.
- (13) Chatt, J.; Duncanson, L. A. *J. Chem. Soc.* **1953**, 2939.
- (14) Chatt, J.; Duncanson, L. A.; Venanzi, L. M. *J. Chem. Soc.* **1955**, 4456.
- (15) Murakami, M.; Ito, Y. *Top. Organomet. Chem.* **1999**, 3, 97.
- (16) Ruhland, K. *Eur. J. Org. Chem.* **2012**, 2683.
- (17) Bishop III, K. C. *Chem. Rev.* **1976**, 76, 461.
- (18) Matsuda, T.; Tsuboi, T.; Murakami, M. *J. Am. Chem. Soc.* **2007**, 129, 12596.
- (19) Matsuda, T.; Shigeno, M.; Makino, M.; Murakami, M. *Org. Lett.* **2006**, 8, 3379.
- (20) Seiser, T.; Cramer, N. *J. Am. Chem. Soc.* **2010**, 132, 5340.
- (21) Crépin, D.; Dawick, J.; Aïssa, C. *Angew. Chem. Int. Ed.* **2009**, 49, 620.
- (22) Crépin, D.; Tugny, C.; Murray, J. H.; Aïssa, C. *Chem. Commun.* **2011**, 47, 10957.

- (23) Seiser, T.; Cramer, N. *Angew. Chem. Int. Ed.* **2008**, *47*, 9294.
- (24) Simaan, S.; F G Goldberg, A.; Rosset, S.; Marek, I. *Chem. – Eur. J.* **2009**, *16*, 774.
- (25) Terao, Y.; Wakui, H.; Satoh, T.; Miura, M.; Nomura, M. *J. Am. Chem. Soc.* **2001**, *123*, 10407.
- (26) Souillart, L.; Cramer, N. *Chem. Sci.* **2013**, *5*, 837.
- (27) Murakami, M.; Amii, H.; Ito, Y.; *Nature*. **1994**, *370*, 540.
- (28) Murakami, M.; Tsuruta, T.; Ito, Y. *Angew. Chem. Int. Ed.* **2000**, *39*, 2484
- (29) Murakami, M.; Itahashi, T.; Ito, Y. *J. Am. Chem. Soc.* **2002**, *124*, 13976.
- (30) Parker, E.; Cramer, N. *Organometallics* **2014**, *33*, 780.
- (31) King, R.B.; Efraty, A. *J. Am. Chem. Soc.* **1972**, *94*, 3773.
- (32) Eilbracht, P.; Dahler, P. *J. Organomet. Chem.* **1977**, *135*, C23.
- (33) Eilbracht, P. *Chem. Ber.* **1980**, *113*, 542.
- (34) Halcrow, M. A.; Urbanos, F.; Chaudret, B. *Organometallics* **1993**, *12*, 955.
- (35) Bruce, M. I. *Angew. Chem. Int. Ed.* **1977**, *16*, 73.
- (36) Parshall, G. W. *Acc. Chem. Res.* **1970**, *3*, 139.
- (37) Parshall, G. W. *Acc. Chem. Res.* **1975**, *8*, 113.
- (38) Ryabov, A. D. *Chem. Rev.* **1990**, *90*, 403.
- (39) Trofimenko, S. *Inorg. Chem.* **1973**, *12*, 1215.
- (40) Colby, D.A.; Bergman, R. G.; Ellman, J. A. *Chem. Rev.* **2010**, *110*, 624.
- (41) van der Boom, M. E.; Kraatz, H.-B.; Ben-David, Y.; Milstein, D. *Chem. Commun.* **1996**, 2167.
- (42) Jun, C.-H.; Park, J.-H. *Top. Organomet. Chem.* **2007**, *24*, 117.
- (43) Gozin, M.; Welsman, A.; Ben-David, Y.; Milstein, D. *Nature* **1993**, *364*, 699.
- (44) van der Boom, M. E.; Milstein, D. *Chem. Rev.* **2003**, *103*, 1759.
- (45) McMillen, D. F.; Golden, D. M. *Ann. Rev. Phys. Chem.* **1982**, *33*, 493.
- (46) Liou, S.; Gozin, M.; Milstein, D. *J. Am. Chem. Soc.* **1995**, *117*, 9774.
- (47) van der Boom, M. E.; Liou, S.-Y.; Ben-David, Y.; Gozin, M.; Milstein, D. *J. Am. Chem. Soc.* **1998**, *120*, 13415.
- (48) Liou, S.-Y.; van der Boom, M. E.; Milstein, D. *Chem. Commun.* **1998**, 687.
- (49) Gandelman, M.; Shimon, L. J. W.; Milstein, D. *Chem. – Eur. J.* **2003**, *9*, 4295.

- (50) Salem, H.; Ben-David, Y.; Shimon, L. J. W.; Milstein, D. *Organometallics* **2006**, *25*, 2292.
- (51) van der Boom, M. E.; Liou, S.-Y.; Shimon, L. J. W.; Ben-David, Y.; Milstein, D. *Inorg. Chim. Acta* **2004**, *357*, 4015.
- (52) van der Boom, M. E.; Kraatz, H.-B.; Hassner, L.; Ben-David, Y.; Milstein, D. *Organometallics* **1999**, *18*, 3873.
- (53) Gauvin, R. M.; Rozenberg, H.; Shimon, L. J. W.; Milstein, D. *Organometallics* **2001**, *20*, 1719.
- (54) Gauvin, R. M.; Rozenberg, H.; Shimon, L. J. W.; Ben-David, Y.; Milstein, D. *Chem. – Eur. J.* **2007**, *13*, 1382.
- (55) Cohen, R.; van der Boom, M. E.; Shimon, L. J. W.; Rozenberg, H.; Milstein, D. *J. Am. Chem. Soc.* **2000**, *122*, 7723.
- (56) Cohen, R.; Milstein, D.; Martin, J. M. L. *Organometallics* **2004**, *23*, 2336.
- (57) Müller, E.; Segnitz, A.; Langer, E. *Tetrahedron Lett.* **1969**, *10*, 1129.
- (58) Dermenci, A.; Whittaker, R. E.; Dong, G. *Org. Lett.* **2013**, *15*, 2242.
- (59) Suggs, J. W.; Cox, S. D. *J. Organomet. Chem.* **1981**, *221*, 199.
- (60) Suggs, J. W.; Jun, C. H. *J. Am. Chem. Soc.* **1984**, *106*, 3054
- (61) Suggs, J. W.; Wovkulich, M. J.; Cox, S. D. *Organometallics* **1985**, *4*, 1101.
- (62) Suggs, J. W. *J. Am. Chem. Soc.* **1978**, *100*, 640.
- (63) Cheng, C. H.; Spivack, B. D.; Eisenberg, R. *J. Am. Chem. Soc.* **1977**, *99*, 3003.
- (64) Suggs, J. W.; Wovkulich, M. J.; Cox, S. D. *Organometallics* **1985**, *4*, 1101.
- (65) Adamson, G. W.; Daly, J. J.; Forester, D. *J. Organomet. Chem.* **1974**, *71*, C17.
- (66) Hitchcock, P. B.; Lappert, M. F.; McLaughlin, G. M.; Oliver, A. J. *J. Chem. Soc., Dalton Trans.* **1974**, 68.
- (67) Bombieri, G.; Graziani, R.; Panattoni, C.; Volponi, L. *Chem. Commun.* **1967**, 977a.
- (68) Bruce, M. I. *Angew. Chem. Int. Ed.* **1977**, *16*, 73.
- (69) Milstein, D. *Organometallics* **1982**, *1*, 1549.
- (70) Suggs, J. W.; Jun, C. H. *J. Am. Chem. Soc.* **1986**, *108*, 4679.
- (71) Steenken, S. S.; Schushmann, H. P.; vonSonntag, C. *J. Phys. Chem.* **1975**, *79*, 763.

- (72) Greene, F. D. *J. Am. Chem. Soc.* **1959**, *81*, 2688.
- (73) Ng, F. T.T.; Rempel, G. L.; Halpern, J. *J. Am. Chem. Soc.* **1982**, *104*, 621.
- (74) Finke, R.G.; Hay, B. P. *Inorg. Chem.* **1984**, *23*, 3041.
- (75) Suggs, J. W.; Jun, C.-H. *J. Chem. Soc., Chem. Commun.* **1985**, 92.
- (76) Lee, D. Y.; Jun, C. H. *Bull. Korean Chem. Soc.* **2003**, *24*, 1059.
- (77) Wentzel, M. T.; Reddy, V. J.; Hyster, T. K.; Douglas, C. J. *Angew. Chem. Int. Ed.* **2009**, *48*, 6121.
- (78) Tobisu, M.; Kinuta, H.; Kita, Y.; Rémond, E.; Chatani, N. *J. Am. Chem. Soc.* **2012**, *134*, 115.
- (79) Gribkov, D. V.; Pastine, S. J.; Schnürch, M.; Sames, D. *J. Am. Chem. Soc.* **2007**, *129*, 11750.
- (80) Wang, J.; Chen, W.; Zuo, S.; Liu, L.; Zhang, X.; Wang, J. *Angew. Chem. Int. Ed.* **2012**, *51*, 12334.

CHAPTER TWO

Carboacylation with 8-Acylquinolines

INTRODUCTION

In order to be an effective synthetic strategy, the activation of a C–C bond should result in metal–carbon (M–C) bonds that can be functionalized to produce a more complex product. The term ‘carboacylation’ describes a reaction in which a M–C and M–C_{acyl} bond are added across a unit of unsaturation, such as an alkene or an alkyne (Figure 8a). The term is similar to the prevalent ‘hydroacylation’ reaction, in which a M–H and M–C_{acyl} bond are delivered across an olefin (Figure 8b).

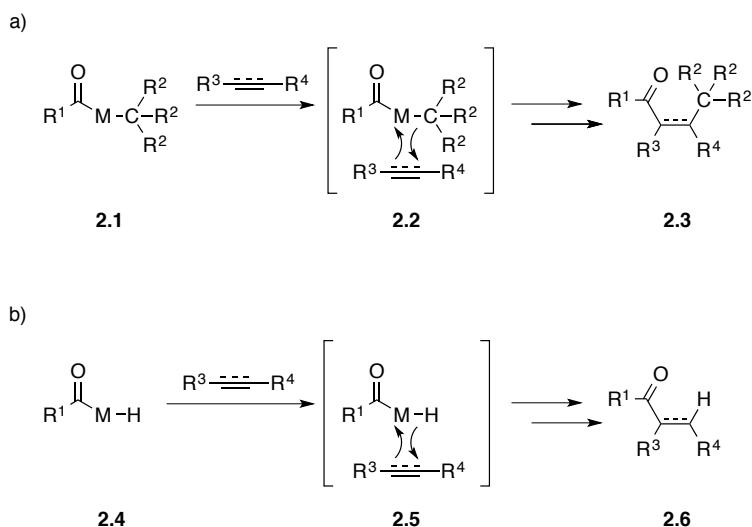


Figure 8. General depiction of a) carboacylation and b) hydroacylation

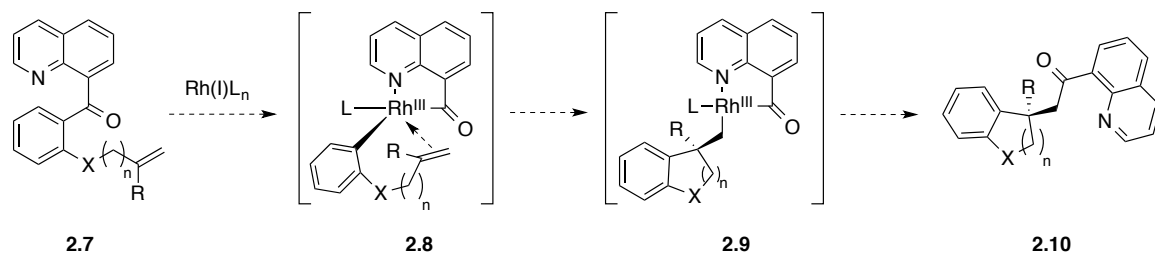
2.1 INTRAMOLECULAR CARBOACYLATION

The C–C bond exchange reactions with 8-acylquinoline that were developed by Suggs and Jun (Section 1.4) rely upon a β -hydride elimination pathway that results in a net hydroacylation process. In addition, this process is limited to reactions with ethylene and therefore the methodology suffers from restricted application. Although this work was influential in the development and fundamental understanding of chelation-assisted C–C bond activation, further exploration was required to exploit the potential synthetic utility. We envisioned that an intramolecular reaction that forgoes β -hydride elimination could overcome the kinetic limitations associated with intermolecular olefin insertions. The proposed intramolecular carboacylation would introduce a synthetic methodology that can rapidly build molecular complexity in a single step.

2.1.1 RESEARCH PROPOSAL

Substrates of the class **2.7** were designed with several features that would render carboacylation feasible (Scheme 25). With C–C_{acyl} bonds weaker than typical C–C bonds, and Rh–C_{aryl} bonds stronger than even some M–H bonds, an aryl ketone was proposed as a thermodynamically desirable bond to activate. Tethering an alkene to the aryl ketone would facilitate carboacylation through forced proximity to the reactive metal center (**2.8**). Cyclization, or migratory insertion, would form two strong C_{alkyl}–C_{alkyl} bonds at the expense of one weaker C_{aryl}–C_{acyl} σ and C=C π bond. The appended olefin was chosen to be 1,1-disubstituted in order to avoid a potential β -hydride elimination pathway from intermediate **2.9**. In addition, the disubstituted nature of the olefin would

allow access to the synthetically elusive all-carbon quaternary stereogenic center^{1,2} as shown in cyclic product **2.10**.

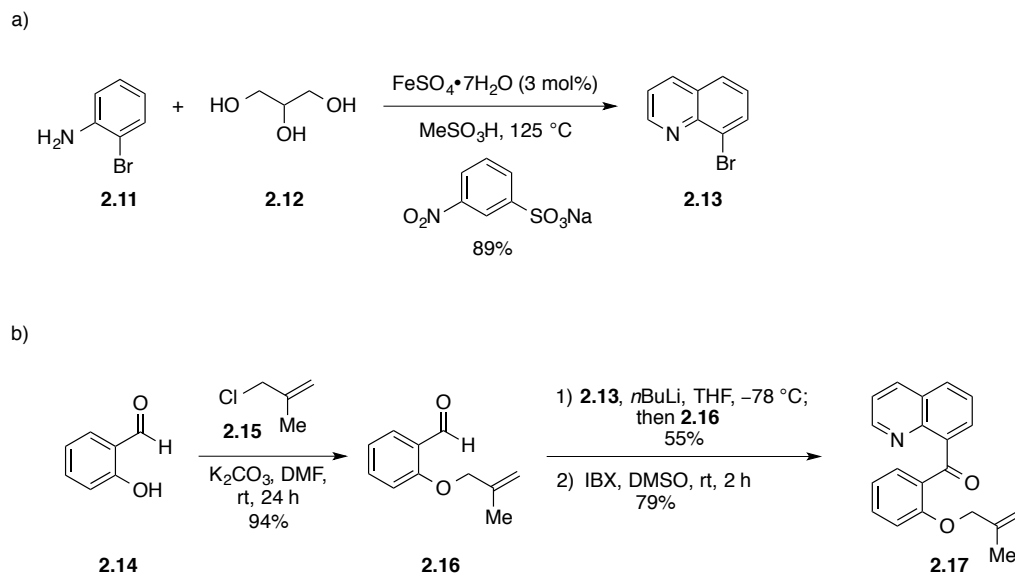


Scheme 25. Proposed intramolecular carboacylation with 8-acylquinolines

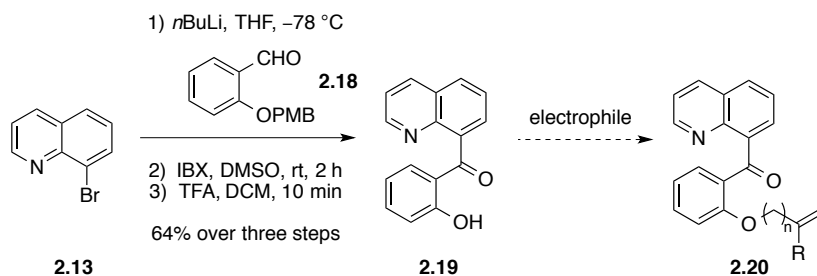
2.1.2 SUBSTRATE SYNTHESSES

The parent substrate **2.17** was prepared in three steps from commercially available material (Scheme 26). 8-bromoquinoline (**2.13**) was readily prepared in 89% yield by an iron sulfate-catalyzed Skraup reaction of 2-bromoaniline (**2.11**) in an acidic solution of glycerol (**2.12**) (Scheme 26a). Alkylation of salicylaldehyde (**2.14**) with 2-methyl chloropropene (**2.15**) provided allylic ether **2.16** in excellent yield. Lithiating 8-bromoquinoline with *n*BuLi, followed by a slow addition into aldehyde **2.16**, provided the corresponding alcohol. The crude alcohol was difficult to purify by column chromatography, however it was found that it could be cleanly precipitated with diethyl ether in 55% yield. An IBX oxidation afforded the parent quinolinyl ketone **2.17** in 79% yield. Due to the inefficiency of the lithium-halogen exchange step, an alternative route was devised in order to divergently prepare allylic ether analogs (Scheme 27). This new synthetic series was carried out with PMB-protected salicylaldehyde **2.18**. Lithium-halogen exchange of 8-bromoquinoline with subsequent addition of **2.18**

delivered the quinolinyl alcohol that was oxidized with IBX to give ketone. Following deprotection, quinolinyl phenol **2.19** was obtained in 64% yield over three steps.



Scheme 26. a) Preparation of 8-bromoquinoline via a Skraup reaction. b) Preparation of quinolinyl ketone **2.17**



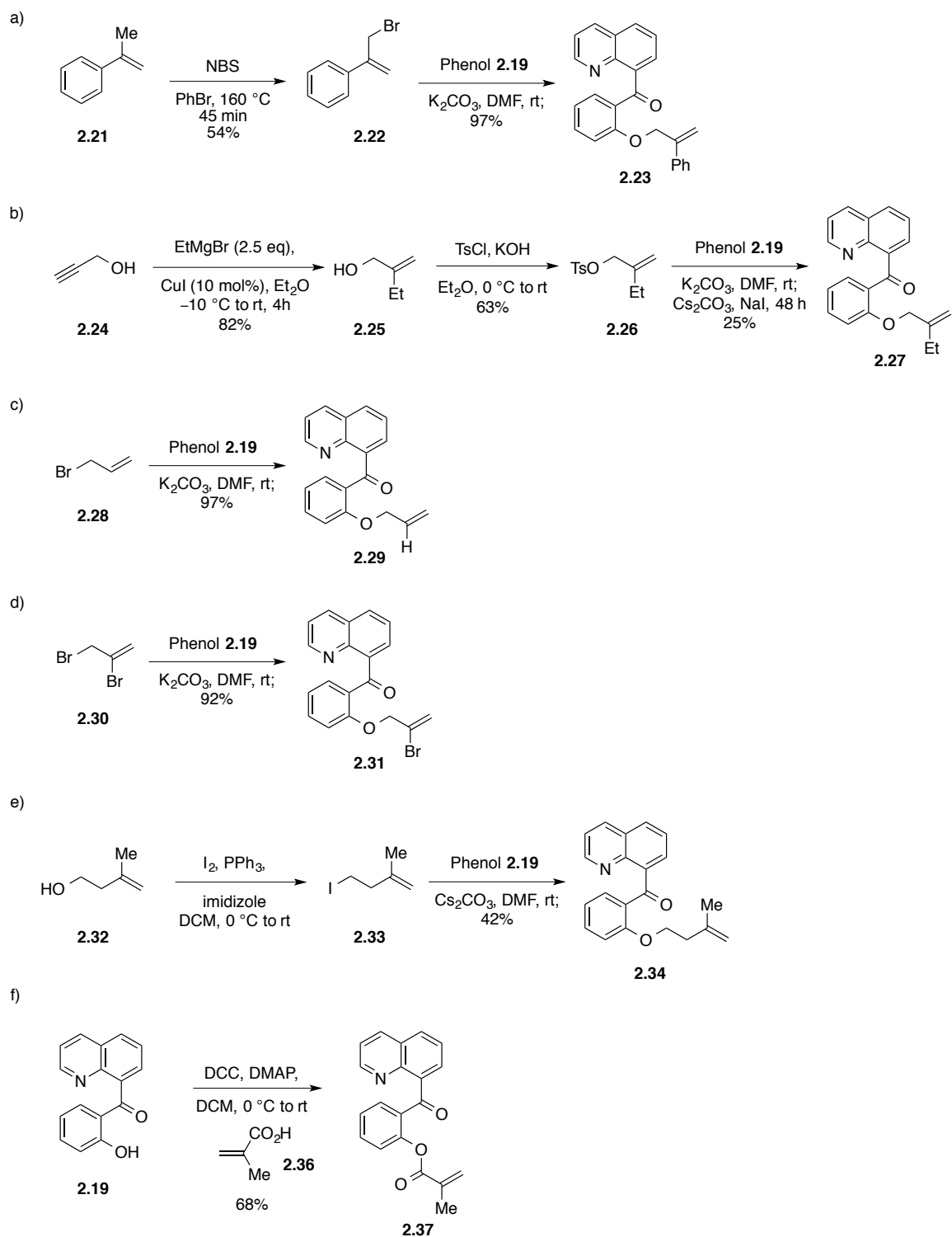
Scheme 27. Re-routed synthetic scheme for the preparation of allylic ether derivatives **2.20**

Substitution reactions between **2.19** and various electrophiles afforded a library of ether-derived substrates (Scheme 28a–f). An allylic bromination of α -methyl styrene (**2.21**) was achieved by heating with NBS to provide bromide **2.22** in 54% yield with the

remaining material being unreacted starting material. Longer reaction times and/or different solvents gave significant vinyl bromide byproducts. Stirring bromide **2.22** in a heterogeneous solution of DMF and K_2CO_3 with phenol **2.19** furnished the styrenyl substrate **2.23** in 97% yield (Scheme 28a).

The ethyl-substituted analog **2.27** was obtained through a sequence beginning with a regioselective Grignard addition into propargyl alcohol (**2.24**), giving allylic alcohol **2.25** (Scheme 28b). This reaction was particularly susceptible to salt formation that inhibited the reaction. A slow addition of Grignard and the use of an overhead stirrer reduced salt aggregation; however, manual scrapping of the sides of the flask with a needle allowed for homogeneity and consumption of starting material. Adding a copious amount of aq. NH_4Cl , and extracting several times (10+) significantly optimized the reaction workup. The tosylate **2.26** was prepared by treating alcohol **2.25** with $TsCl$ and excess KOH in an unoptimized 63% yield. The sluggish alkylation between phenol **2.19** and tosylate **2.26** was enhanced by an *in situ* Finkelstein reaction with the addition of NaI , providing ethyl-substituted substrate **2.27** in 25% yield after 48 h.

The mono-substituted substrate **2.29** was prepared in 97% yield by alkylating phenol **2.19** with allyl bromide (**2.28**) (Scheme 28c). The bromide derivative **2.31** was obtained in 92% yield from phenol **2.19** and dibromide **2.30** (Scheme 28d). Attempts to functionalize the vinyl bromide through Suzuki cross-coupling procedures were unsuccessful.

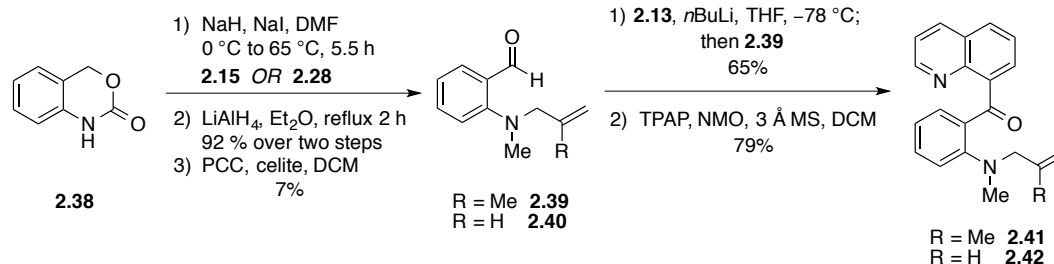


Scheme 28. Syntheses of oxygen-tethered substrates

The homoallylic ether substrate **2.34** was synthesized in 42% yield by alkylating phenol **2.19** with homoallylic iodide **2.23**, which was prepared by iodinating homoallylic alcohol **2.32** under standard conditions (Scheme 28e). Under the reaction conditions, iodide **2.23** was prone to elimination, contributing to the low yield. The analogous reaction with the corresponding tosylate was even less efficient. The methacrylate ester substrate **2.37** was prepared in 68% yield by a DCC coupling of phenol **2.19** and methacrylic acid **2.36** (Scheme 28f). The analogous reaction with trifluoromethacrylic acid was unsuccessful.

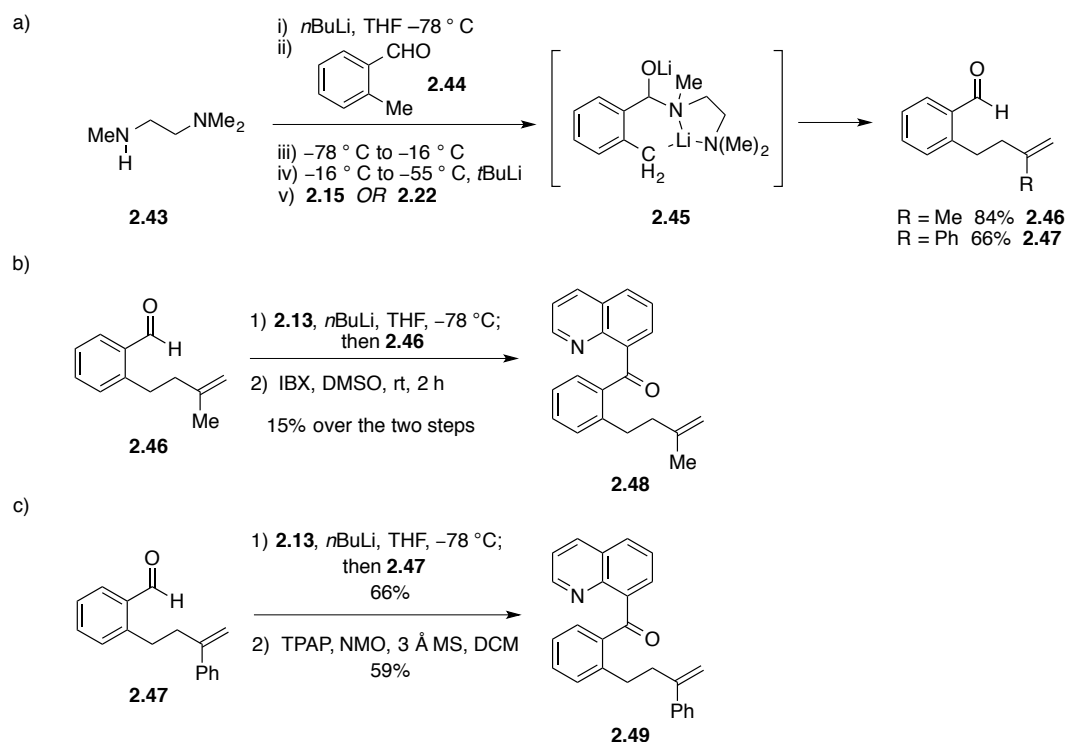
The syntheses of substrates with an olefin tethered by an amine were unexpectedly complicated.ⁱ Several attempts to dialkylate methyl anthranilate were unsuccessful, presumably owing to resonance stabilization of the nitrogen nucleophile. An alternative route was established in which carbamate **2.38** was allylated 2-methyl chloropropene (**2.15**) and then reduced with LAH to give the benzylic alcohol in 92% yield over the two steps (Scheme 29). Oxidation with PCC provided aldehyde **2.39** in a very low yield. Lithium-halogen exchange of 8-bromoquinoline (**2.13**) followed by the addition of aldehyde **2.39** gave the resulting alcohol in 65% yield. Standard IBX oxidation conditions did not afford **2.41**, nor did oxidation with PCC. However, the ketone was obtained with TPAP/NMO to furnish amino substrate **2.41**. The monosubstituted analog **2.42** was prepared under identical conditions.

ⁱ Amino substrates **2.41** and **2.42** were prepared by Christopher J. Douglas, as well as bromide **2.31** and ester **2.37**.



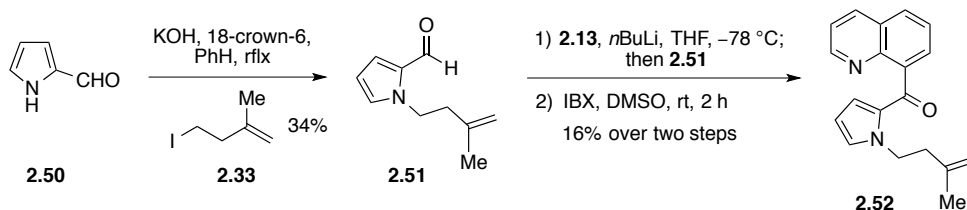
Scheme 29. Syntheses of amino-tethered substrates

Substrates void of a heteroatom linker were prepared by an *in situ* aldehyde protection/directed lithiation strategy. The hemiaminaloxide intermediate **2.45**, obtained from the addition of deprotonated *N,N,N*-trimethylethylene amine (**2.43**) into *o*-tolylaldehyde (**2.44**), directs the deprotonation of the *ortho* methyl group upon treatment with *t*BuLi (Scheme 30a). Addition of either 2-methyl chloropropene (**2.15**) or 2-phenyl bromopropene (**2.22**) afforded the aldehydes **2.46** and **2.47** in 84% and 66% yields, respectively. Aldehydes **2.46** and **2.47** were treated with lithiated quinoline, providing the corresponding secondary alcohols. The methyl derivative contained an inseparable impurity that was carried through the IBX oxidation to give ketone **2.48** in 15% yield over the two steps (Scheme 30b). Attempts to oxidize the alcohol of the phenyl derivative were unsuccessful with IBX, though TPAP/NMO as oxidant effectively gave ketone **2.49** in 59% yield (Scheme 30c).



Scheme 30. Syntheses of methylene-tethered substrates

The pyrrole-derived substrate **2.52** was prepared by *N*-alkylating aldehyde **2.50** with excess iodide **2.33** in refluxing benzene to give product **2.51** in 34% yield, though the reaction did not undergo complete conversion due to the competing elimination pathway. Attempts to avoid the elimination pathway by lowering the temperature completely suppressed all reactivity. Installment of the quinoline directing group, followed by IBX oxidation of the resulting alcohol, gave **2.52** in 16% yield over the two steps.



Scheme 31. Synthesis of pyrrole-linker substrate

2.1.3 RESULTS AND DISCUSSION

Reaction Optimization

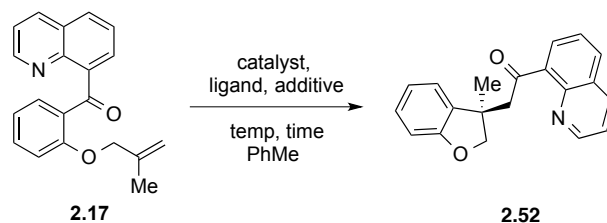
Heating the parent ether substrate **2.17** with various Rh(I) catalysts in toluene (0.1M) at 130 °C for 48 h under nitrogen gave the desired dihydrobenzofuran product **2.52** in good to excellent isolated yields (Table 1).³ Catalysts $[\text{RhCl}(\text{C}_2\text{H}_4)_2]_2$ and $\text{RhCl}(\text{PPh}_3)_3$ were shown to be the most efficient, providing **2.52** in >95% yields (entries 1 and 14) at 10 mol % loading. It was found that the reaction with $[\text{RhCl}(\text{C}_2\text{H}_4)_2]_2$ at 1 mol % catalyst loading was complete in 3 h at 130 °C with a TOF of $1.0 \times 10^{-2} \text{ s}^{-1}$ (entry 4). The $[\text{RhCl}(\text{C}_2\text{H}_4)_2]_2$ catalyst remained active at 100 °C, providing **2.52** at full conversion after an unoptimized 48 h (entry 5). The reaction slowed considerably upon decreasing the temperature to 90 °C, whereby **2.52** was delivered at 30% conversion after 48 h (entry 6). The $\text{RhCl}(\text{PPh}_3)_3$ catalyst proved to be less active in that decreasing the temperature to 100 °C resulted in only 17% conversion (entry 16). Cationic complexes $[\text{Rh}(\text{cod})_2]\text{OTf}$ and $\text{Rh}(\text{cod})_2\text{BF}_4$ were significantly less effective, delivering **2.52** in 62% and 54% yields, respectively (entries 17 and 20).

Attempts to promote the reaction with Lewis acid additives at 80 °C, using $[\text{RhCl}(\text{C}_2\text{H}_4)_2]_2$ as a catalyst were met without success. Reaction with triphenylborane (entry 8) returned unreacted starting material, whereas reactions with aluminum trichloride (entry 9) and zinc chloride (entry 10) gave unidentified decomposition products. Since phosphine ligands have been shown to promote reductive elimination (see Chapter 1, Scheme 14), exogenous phosphine ligand additives were investigated. Isolated yields were obtained when tri-cyclohexyl, -methyl, and -*tert*-butyl phosphine

ligands were added to reactions with $[\text{RhCl}(\text{C}_2\text{H}_4)_2]_2$ as catalyst, though the crude ^1H NMR spectra appeared to be relatively clean (entries 11, 12, and 13). The nature of this discrepancy is unclear. With chiral ligands predominantly used in asymmetric catalysis, bidentate phosphine BINAP was investigated. Unfortunately, the reaction favored alkene isomerization to the corresponding enol ether along with deallylation to give the resulting phenol (entry 19).

With iridium complexes shown to be active catalysts for C–C bond activation (see Chapter 1, Schemes 10 and 19), $[\text{Ir}(\text{coe})_2\text{Cl}]_2$, $[\text{Ir}(\text{cod})_2\text{OMe}]_2$, $\text{Ir}(\text{CO})_2(\text{acac})$, $\text{Ir}(\text{cod})(\text{acac})$ catalysts were explored, but were ineffective toward promoting carboacylation (entries 21–24). In addition, complexes $\text{Pd}(\text{PPh}_3)_4$, Pd_2dba_3 , $\text{Ni}(\text{cod})_2$, $\text{Ni}(\text{PPh}_3)_4$, and $\text{Ru}_3(\text{CO})_{12}$ did not catalyze carboacylation (entries 25–29).

Table 1. Reaction optimization for intramolecular carboacylation with alkenes



entry	catalyst	mol%	ligand/additive	temp	time	yield (%)
1	$[\text{RhCl}(\text{C}_2\text{H}_4)_2]_2$	5	none	130 °C	48 h	95
2	$[\text{RhCl}(\text{C}_2\text{H}_4)_2]_2$	5	none	130 °C	<2 h	100 ^a
3	$[\text{RhCl}(\text{C}_2\text{H}_4)_2]_2$	2.5	none	130 °C	2.5 h	100 ^a
4	$[\text{RhCl}(\text{C}_2\text{H}_4)_2]_2$	1	none	130 °C	3 h	100 ^a
5	$[\text{RhCl}(\text{C}_2\text{H}_4)_2]_2$	5	none	100 °C	48 h	100 ^a
6	$[\text{RhCl}(\text{C}_2\text{H}_4)_2]_2$	5	none	90 °C	48 h	30 ^a
7	$[\text{RhCl}(\text{C}_2\text{H}_4)_2]_2$	5	none	80 °C	48 h	N.R.
8	$[\text{RhCl}(\text{C}_2\text{H}_4)_2]_2$	5	BPh_3	80 °C	48 h	N.R.
9	$[\text{RhCl}(\text{C}_2\text{H}_4)_2]_2$	5	AlCl_3	80 °C	48 h	decomp
10	$[\text{RhCl}(\text{C}_2\text{H}_4)_2]_2$	5	ZnCl_2	80 °C	48 h	decomp
11	$[\text{RhCl}(\text{C}_2\text{H}_4)_2]_2$	5	PCy_3	130 °C	48 h	62
12	$[\text{RhCl}(\text{C}_2\text{H}_4)_2]_2$	5	PMe_3	130 °C	48 h	53
13	$[\text{RhCl}(\text{C}_2\text{H}_4)_2]_2$	5	$\text{P}(t\text{Bu})_3$	130 °C	48 h	54

14	RhCl(PPh ₃) ₃	10	none	130 °C	48 h	96
15	RhCl(PPh ₃) ₃	2	none	130 °C	48 h	90
16	RhCl(PPh ₃) ₃	10	none	100 °C	24 h	17 ^a
17	[Rh(cod) ₂]OTf	5	none	130 °C	48 h	62
18	[Rh(cod) ₂]OTf	5	PMe ₃	130 °C	48 h	72
19	[Rh(cod) ₂]OTf	5	BINAP	130 °C	48 h	<5 ^{a,b}
20	[Rh(cod) ₂]BF ₄	10	none	130 °C	48 h	54
21	[Ir(cod) ₂ OMe] ₂	5	none	130 °C	48 h	0 ^b
22	Ir(CO) ₂ (acac)	10	none	130 °C	48 h	decomp
23	Ir(cod)(acac)	10	none	130 °C	48 h	0 ^b
24	[Ir(coe) ₂ Cl] ₂	5	none	130 °C	48 h	N.R.
25	Ru ₃ (CO) ₁₂	10	none	130 °C	48 h	N.R.
26	Pd ₂ dba ₃	5	none	130 °C	48 h	N.R.
27	Pd ₂ dba ₃	5	PPh ₃	130 °C	48 h	0 ^b
28	Ni(cod) ₂	5	none	130 °C	48 h	N.R.
29	Ni(cod) ₂	5	PPh ₃	130 °C	48 h	N.R.

^a Conversion based on ¹H NMR spectroscopy. ^b Recovered starting material, olefin isomerization, and deallylation

Substrate Scope

With optimal conditions in hand, the substrate scope was explored. The analogues described in Section 2.1.1.1 were reacted with 5 mol % [RhCl(C₂H₄)₂]₂ and heated to 130 °C in toluene for 48 h (Figure 9, Condition A). Dihydrobenzofuran **2.54** (R=Ph) was obtained in a 94% isolated yield, despite forming the sterically-encumbered diaryl all-carbon quaternary center. Interestingly, decreasing the temperature to 110 °C resulted in no reaction. Perhaps even more interesting, no reaction was observed with RhCl(PPh₃)₄, even at 130 °C (Condition C). Although β-hydride elimination was expected to complicate the formation of dihydrobenzofuran **2.55** (R=H), cleavage of the allyl ether was the dominant decomposition pathway with [RhCl(C₂H₄)₂]₂. The less nucleophilic [Rh(cod)₂]OTf catalyst served to limit deallylation, providing **2.55** in 25% yield (Condition B). Although the lack of reactivity with bromine substitution (**2.56**) was

attributed to the inability of the electron-deficient alkene to bind to the metal center, carboacylation with a methacrylate ester successfully gave benzofuranone **2.57** in 81% yield. No coumarin-like byproducts were detected, which would have originated from a 6-*endo* cyclization/ β -hydride elimination pathway. Extending the tether length ($n=2$) allowed for the synthesis of dihydrobenzopyran **2.58** in 80% yield.

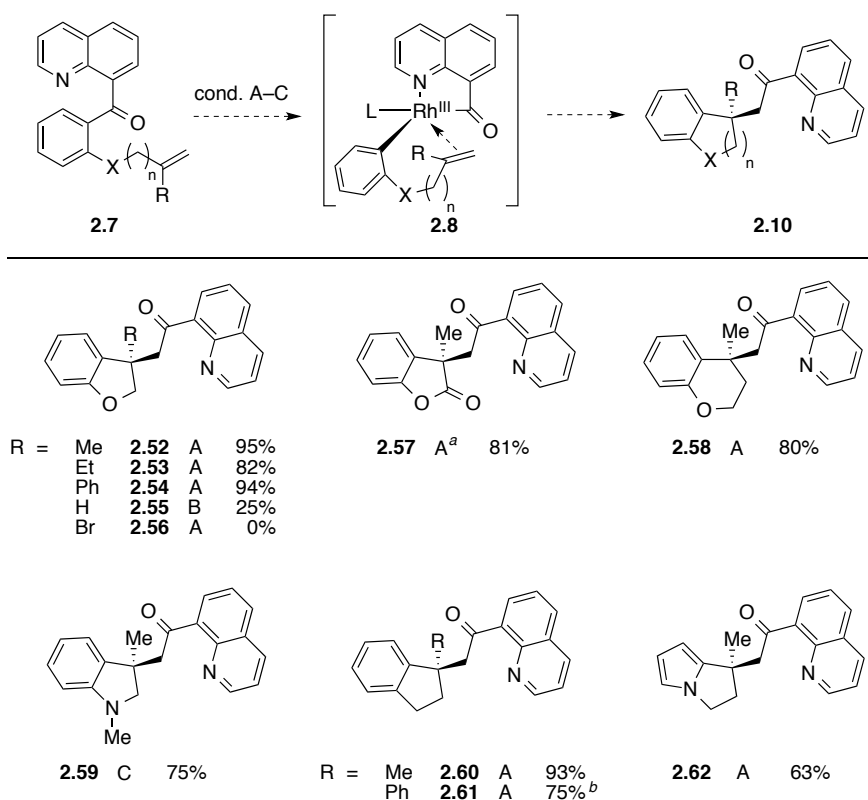
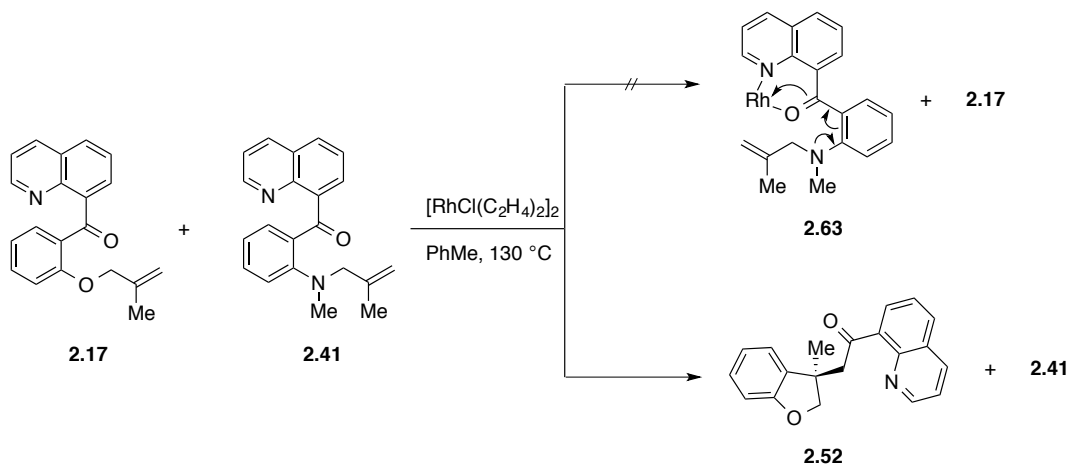


Figure 9. Isolated yields of intramolecular carboacylation products. Condition A: 5 mol % $[\text{RhCl}(\text{C}_2\text{H}_4)_2]_2$, PhMe, 130 °C, 48 h. Condition B: 5 mol % $[\text{Rh}(\text{cod})_2]\text{OTf}$, PhMe, 130 °C, 48 h. Condition C: 10 mol % $\text{RhCl}(\text{PPh}_3)_3$, PhMe, 130 °C, 48 h. ^aRequired 10 mol % hydroquinone; stopped after 24 h. ^bConversion by ^1H NMR spectroscopy.

Exchanging the tethering heteroatom for nitrogen significantly impeded the reaction. Dihydroindole **2.59** was formed at 10% conversion after reacting **2.41** with $[\text{RhCl}(\text{C}_2\text{H}_4)_2]_2$ over 48 h (Figure 9). Running this reaction in the presence of the ether

analogue **2.17**, resulted in complete formation of **2.52**, which disproved the hypothesis that the anthranilic ketone had sequestered the catalyst through non-productive binding (**2.63**) (Scheme 32). Increasing the nucleophilicity of the catalyst ($\text{RhCl}(\text{PPh}_3)_3$) allowed for dihydroindole **2.59** to be obtained in 75% yield. It is therefore likely that electron donation from the 2-amino group simply renders the carbonyl less electrophilic and thus slower in undergoing oxidative addition.

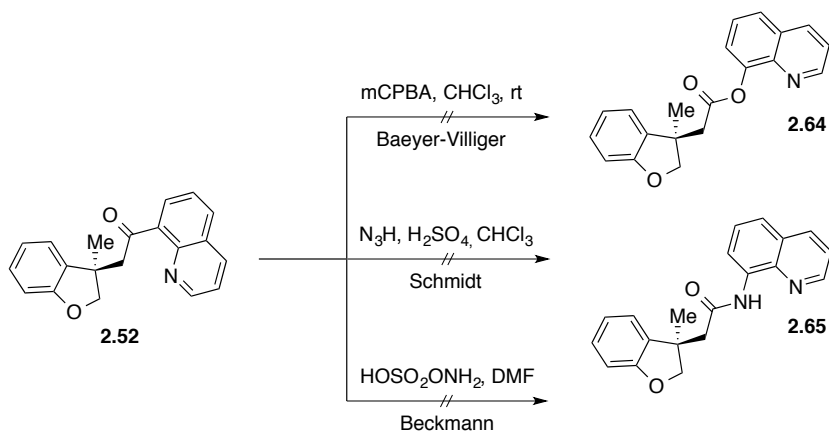


Scheme 32. Competition experiment showing **2.41** does not sequester catalyst

Replacing the tethering heteroatom with a methylene allowed for the preparation of dihydroindenes **2.60** and **2.61** (Figure 9). Comparable to the analogous cyclization to dihydrobenzofuran ($\text{R}=\text{Me}$) **2.52**, dihydroindene **2.60** ($\text{R}=\text{Me}$) was isolated in 93% yield. In contrast, incomplete conversion of the phenyl-substituted derivative **2.49** was observed under all conditions, providing dihydroindene **2.61** ($\text{R}=\text{Ph}$) in 75% yield with $[\text{RhCl}(\text{C}_2\text{H}_4)_2]_2$, 65% yield with $[\text{Rh}(\text{cod})_2]\text{OTf}$, and <10% conversion with $\text{RhCl}(\text{PPh}_3)_3$. The difference in reactivity upon forming dihydrobenzofuran **2.54** and dihydroindene **2.61** is unclear; however, the difference in the bond angles of tetrahydrofuran⁴ ($\theta^{\text{COC}} = 111.8^\circ$, $\theta^{\text{CCO}} = 109.5^\circ$, $\theta^{\text{CCC}} = 112.4^\circ$) and cyclopentane ($\theta = 112.4^\circ$), which

would undoubtedly affect the dihedral angles containing the substituents, may suggest that the diaryl all-carbon quaternary center of a dihydroindene is significantly more hindered. A greater dihedral angle may put the substituents of dihydroindene in closer proximity and thus raise the barrier to migratory insertion and consequently slow the reaction. The substrate with the phenyl backbone replaced with a pyrrole (**2.52**), allowed for the formation of dihydropyrrolizine **2.62**, which proceeded in 63% yield.

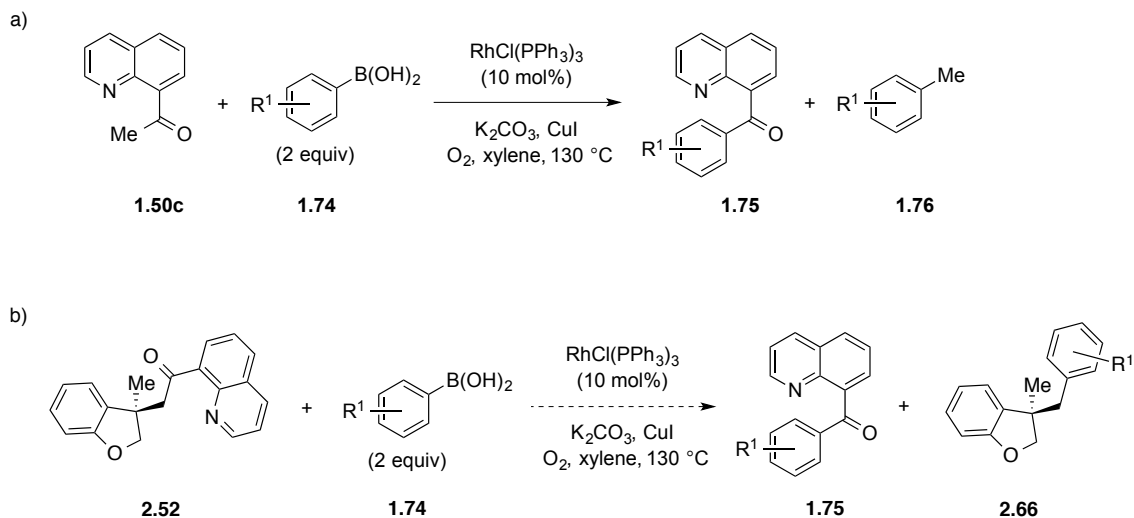
A major limitation to this methodology is the need for a covalently bound directing group. In order to be synthetically viable, an efficient means to remove the quinoline group is necessary. Several attempts to remove the 8-acylquinoline directing group by converting the quinolinyl ketone **2.52** to a more labile ester (**2.64**) or amide (**2.65**) with reactions such as Baeyer-Villiger, Schmidt, and Beckmann were unsuccessful (Scheme 33).



Scheme 33. Attempts to convert quinolinyl ketone to an ester or amide

Efforts toward an alternative method to remove the quinoline directing group are currently underway. Drawing upon the C–C bond activation/cross coupling methodology set forth by Wang⁵ (see Chapter 1, Section 1.4.2), it was envisioned that this strategy

could potentially cleave the 8-acylquinoline directing group. The reaction of a carboacylation product such dihydrobenzofuran **2.52** with two equivalents of an appropriate boronic acid (e.g. **1.74**) may provide products such as dihydrobenzofuran **1.66** and quinolinyl ketone **1.75** (Scheme 34).ⁱⁱ This work is currently ongoing in our laboratory.



Scheme 34. Proposed method for 8-acylquinoline removal by a C–C bond activation cross-coupling strategy. a) Wang’s C–C cross-coupling methodology b) Wang’s method applied to the carboacylation product dihydrobenzofuran **2.52**

2.1.4 CONCLUDING REMARKS

We are pleased to report a highly efficient intramolecular carboacylation methodology with alkenes that produce products of higher molecular complexity.³ In order for such reactions to become useful to the synthetic community, much attention is needed to overcome several prevailing limitations. Developing the reaction enantioselectively may be realized with a thorough ligand screen or perhaps through

ⁱⁱ The idea was proposed by Jason Brethorst, and Dylan Walsh is pursuing the laboratory work.

developing conditions amenable to chiral Lewis acid catalysis. We are currently pursuing methods to remove the quinoline directing group (see Scheme 34) and are making efforts to identify other means to activate C–C bonds, which will be discussed in Chapter 3.

2.1.5 EXPERIMENTAL

Section A

General Details: All reactions were carried out using flame-dried glassware under a nitrogen or argon atmosphere unless aqueous solutions were employed as reagents or dimethyl formamide was used as a solvent. Tetrahydrofuran (THF), dichloromethane (CH_2Cl_2), and toluene (PhMe) were dried according to published procedures.ⁱⁱⁱ Toluene was further degassed by bubbling a stream of argon through the liquid in a Strauss flask and then stored in a nitrogen-filled glovebox. All other commercial reagents were used as received unless otherwise indicated. All rhodium complexes were purchased from Strem and used as received. All other chemicals were purchased from Acros Organics or Sigma-Aldrich and used as received. 3-Bromo-2-phenylpropene was prepared from 2-phenylpropene and *N*-bromosuccinimide according to Kobayashi.^{iv} 1,4-Dihydro-2H-1,3-benzoxazin-2-one was prepared from anthranillic acid in analogy to literature

ⁱⁱⁱ Pangborn, A. B.; Giardello, M. A.; Grubbs, R. H.; Rosen, R. K.; Timmers, F. J. *Organometallics*, **1996**, *15*, 1518.

^{iv} Miyamura, H.; Akiyama, R.; Ishida, T.; Matsubara, R.; Takeuchi, M.; Kobayashi, S. *Tetrahedron* **2005**, *61*, 12177. Residual 2-phenylpropene was removed by column chromatography on silica (hex).

procedures.^v 2-Ethyl-2-propen-1-ol was prepared from propargyl alcohol and ethyl magnesium bromide according to Duboudin and Jousseau; the procedure was modified as described in the text.^{vi} 4-Iodo-2-methyl-1-butene was prepared from the corresponding alcohol according to Hiersemann's report.^{vii} IBX was prepared according to Santagostino.^{viii} All rhodium-catalyzed processes were carried out in a nitrogen-filled glovebox in 1 dram vials with PTFE lined caps and heating was applied by aluminum block heaters.

Analytical thin layer chromatography (TLC) was carried out using 0.25 mm silica plates from E. Merck. Eluted plates were visualized first with UV light and then by staining with ceric sulfate/molybdic acid or potassium permanganate/potassium carbonate. Flash chromatography was performed using 230–400 mesh (particle size 0.04–0.063 mm) silica gel purchased from Merck unless otherwise indicated. ¹H NMR (300 and 500 MHz) and ¹³C NMR (75 and 125 MHz) spectra were obtained on Varian FT NMR instruments. NMR spectra were reported as δ values in ppm relative to chloroform or tetramethylsilane. ¹H NMR coupling constants are reported in Hz; multiplicity was indicated as follows; s (singlet); d (doublet); t (triplet); q (quartet); quint (quintet); m (multiplet); dd (doublet of doublets); ddd (doublet of doublet of doublets); dddd (doublet of doublet of doublet of doublets); dt (doublet of triplets); td (triplet of doublets); ddt (doublet of doublet of triplets); app (apparent); br (broad). Infrared (IR) spectra were obtained as films from CH₂Cl₂ or CDCl₃. Low-resolution mass spectra (LRMS) in EI or CI experiments were performed on a Varian Saturn 2200 GC-MS system, and LRMS and

^v Reduction of anthranillic acid to 2-aminobenzyl alcohol: Nystrom, R. F.; Brown, W. G. *J. Am. Chem. Soc.* **1947**, *69*, 2548; conversion to oxazinanone: Ohno, M.; Sato, H.; Eguchi, S. *Synlett* **1999**, 207.

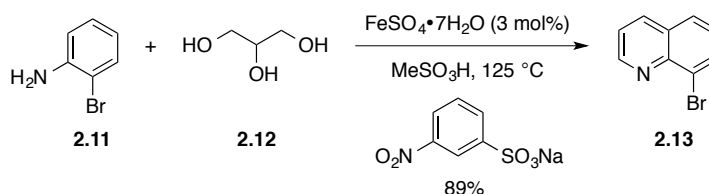
^{vi} Deboudin, J. G.; Jousseau, B. *J. Organomet. Chem.* **1979**, *168*, 1.

^{vii} Helmboldt, H.; Köhler, D.; Hiersemann, M. *Org. Lett.* **2006**, *8*, 1573.

^{viii} Frigerio, M.; Santagostino, M.; Sputore, S. *J. Org. Chem.* **1999**, *64*, 4537.

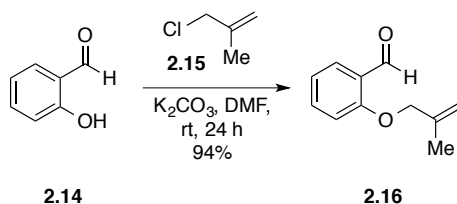
high-resolution mass spectra (HRMS) in electrospray (ESI) experiments were performed on a Bruker BioTOF II.

Section B



8-bromoquinoline 2.13. A 1-L 3-neck round bottom flask was equipped with an overhead mechanical stirrer, an internal temperature thermometer, and a dropping funnel. The flask was charged with methane sulfonic acid (250 mL) and warmed with stirring to an internal temperature of $125\text{ }^\circ\text{C}$. 2-Bromoaniline (**2.11**) (80.55 g, 0.468 mol) was added portion-wise, followed by *meta*-nitrobenzenesulfonic acid sodium salt (66.30 g, 0.293 mol) and $\text{FeSO}_4 \cdot 7\text{H}_2\text{O}$ (3.90 g, 14 mmol). The addition funnel was charged with glycerol (28.3 mL, 0.39 mol) and the glycerol was added drop wise over 15 min. Two additional portions of glycerol ($2 \times 28.3\text{ mL}$, 0.78 mol) were added at three-hour intervals. After the last portion of glycerol was added the brown solution was maintained at $125\text{ }^\circ\text{C}$ for 12 hours. The reaction mixture was allowed to cool to RT and water (250 mL) was added. The resulting brown-black solution was transferred to a 4-L beaker with the aid of 100 mL water. The beaker was placed in an ice bath and an aqueous NaOH solution (50% m/v) was added with stirring until the solution was basified to $\text{pH} \sim 14$. The heterogeneous mixture was extracted with Et_2O ($3 \times 500\text{ mL}$), allowing the emulsion to settle for ~ 10 min each time. The combined organic extracts were washed with brine ($1 \times 400\text{ mL}$), dried over Na_2SO_4 and filtered through Celite. Concentration of

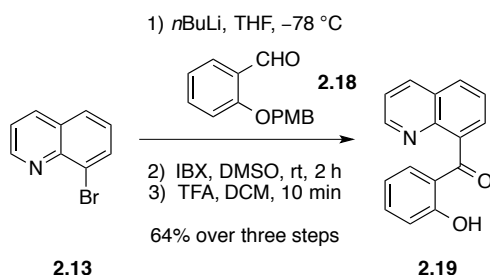
the resulting solution to a viscous brown oil provided the title compound (86.55 g, 0.426 mol, 89%) in ~95% purity as judged by ^1H NMR. The crude product was then purified by kugelrohr distillation (0.14 mm Hg; pot temp, 180–205 °C) to give a yellow oil that solidified on standing (83.69 g, 0.402 mol, 86%): ^1H NMR (300 MHz, CDCl_3) δ 8.98 (dd, J = 4.2, 1.8 Hz, 1H), 8.08 (dd, J = 8.3, 1.7 Hz, 1H), 7.98 (dd, J = 7.4, 1.4 Hz, 1H), 7.72 (dd, J = 8.1, 1.2 Hz, 1H), 7.39 (dd, J = 8.1, 4.2 Hz, 1H), 7.32 (t, J = 8.0 Hz, 1H); ^{13}C NMR (75 MHz, CDCl_3) δ 151.1, 145.0, 136.5, 133.0, 129.4, 127.7, 126.8, 124.5, 121.8. This material identical by NMR to 8-bromoquinoline prepared by other methods.^{ix}



This procedure was adapted from Bashiardes et. al^x: Salicylaldehyde (**2.14**) (2.1 mL, 19.7 mmol), isobutenyl chloride (**2.15**) (2.9 mL, 29.7 mmol), and potassium carbonate (8.29 g, 60 mmol) were combined with DMF (20 mL) and allowed to stir at room temperature for 24 h. Ether (15mL) was added to the mixture, washed with water (30 mL), and the layers were separated. The aqueous portion was extracted with Et_2O (3 \times 15 mL). The combined organic portions were washed with LiCl (2 M, 30 mL), brine; dried over Na_2SO_4 , and concentrated under reduced pressure. Compound **2.16** was purified by silica gel chromatography (5:95 CH_2Cl_2 :Hex) as orange oil (2.85 g, 16.2 mmol, 82%): R_f 0.34 (1:3 CH_2Cl_2 :Hex).

^{ix} Wada, K.; Mizutani, T.; Kitagawa, S. *J. Org. Chem.* **2003**, 68, 5123.

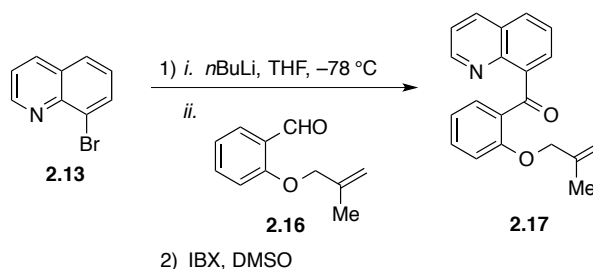
^x Bashiardes, G.; Safir, I.; Mahamed, A. S.; Barbot, F.; Laduranty, J. *Org. Lett.* **2003**, 5, 4915.



To a cooled solution ($-78\text{ }^{\circ}\text{C}$) of 8-bromoquinoline (**2.13**) (2.14 g, 10.3 mmol) in THF (35 mL) in a flame-dried flask under N_2 was added *n*-BuLi (2.5 M in Hex, 8.2 mL, 20.6 mmol) drop-wise. The dark orange mixture was allowed to stir for 10 min. Aldehyde **2.18**^{xi} (5.0 g, 20.6 mmol) was slowly delivered as a solution in THF (36 mL) over a span of 10 min to give a dark red solution. The reaction was stirred at $-78\text{ }^{\circ}\text{C}$ for 10 min, and allowed to warm to room temperature over 30 min. The resulting clear orange solution was quenched with water (40 mL) and the resulting mixture was extracted with EtOAc ($2 \times 75\text{ mL}$). The combined organic portions were washed with brine (75 mL), dried over Na_2SO_4 , and concentrated. The resulting orange crude product was carried on directly dissolving in DMSO (175 mL) and addition of IBX (4.3 g, 15.4 mmol). The solution was maintained at room temperature for 2 h. The reaction was quenched by the addition of isopropanol (10 mL) and stirring for an additional 30 min. Water (400 mL) was added and the mixture was extracted with EtOAc ($3 \times 250\text{ mL}$). The combined organics were washed with brine (250 mL), dried over Na_2SO_4 , filtered through Celite, and concentrated. The crude product was further purified by column chromatography over silica gel (7:1 Hex:EtOAc, then 3:2 Hex:EtOAc) to give the resulting ketone as a viscous yellow oil (2.62 g, 7.1 mmol) which was carried on directly. This ketone was dissolved in CH_2Cl_2 (22 mL) and trifluoroacetic acid (22 mL) was

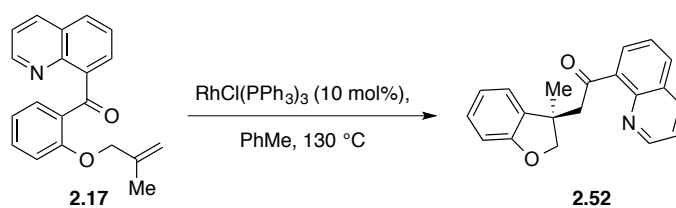
^{xi} Prepared from salicylaldehyde and PMB-Cl in analogy to **2.16**.

added. The solution immediately changed color from light orange to dark brown. After 10 min, the solution was transferred to an Erlenmeyer flask with 100 mL CH₂Cl₂ and sat aq NaHCO₃ was added [Caution: Gas Evolution] until no more gas evolves (pH ~ 8). The phases were separated and the aqueous portion was extracted with CH₂Cl₂ (1 × 100 mL). The combined organic portions were dried over Na₂SO₄ and concentrated. The crude product was further purified by column chromatography on silica (1:99 Et₂O:CH₂Cl₂ then 1:49 Et₂O:CH₂Cl₂) to give **2.19** (1.63 g, 6.57 mmol, 64% over the three steps) as a light yellow powder: ¹H NMR (300 MHz, CDCl₃) δ 12.31 (s, 1H), 8.89 (dd, *J* = 4.2, 1.8 Hz, 1H), 8.24 (dd, *J* = 8.4, 1.8 Hz, 1H), 7.99 (dd, *J* = 8.1, 1.5 Hz, 1H), 7.74–7.62 (m, 2H), 7.50–7.44 (m, 2H), 7.17–7.06 (m, 2H) 6.74–6.68 (m, 1H).

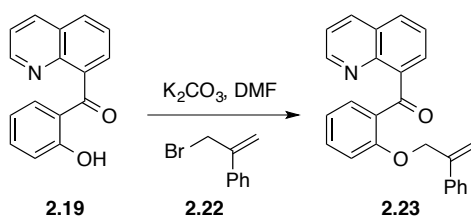


To a cooled solution (-78 °C) of 8-bromoquinoline (**2.13**) (2.25 g, 10.8 mmol) in THF (70 mL) in a flame-dried flask under N₂ was added *n*-BuLi (2.5 M in hex, 6 mL, 15 mmol) drop-wise. The dark orange mixture was allowed to stir for 10 min. Aldehyde **2.16** (2.84 g, 16.2 mmol) was slowly delivered as a solution in THF (3 mL) over a span of 10 min to give a dark cloudy red solution. The reaction was stirred at -78 °C for 20 min, and allowed to warm to room temperature over 2 h. The clear orange solution was quenched with saturated NH₄Cl (60 mL), and the layers were separated. The organic layer was washed with water (10 mL), and the combined aqueous washed were extracted

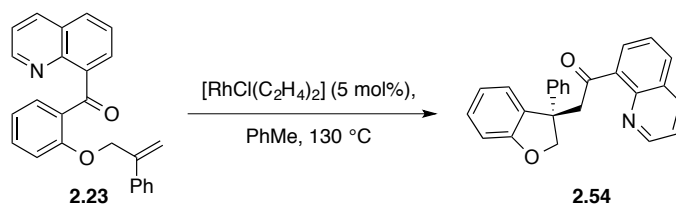
with Et₂O (2 × 50 mL). The combined organic portions were washed with brine (30 mL), dried over Na₂SO₄, and concentrated. The resulting orange-yellow residue was taken up in Et₂O and a colorless precipitate formed. Collection of this precipitate by vacuum filtration gave the alcohol (1.80 g, 5.9 mmol, 55%), which was carried on directly. The intermediate alcohol (1.53 g, 5 mmol) was dissolved in DMSO (33 mL) and allowed to react with IBX (2.92 g, 10 mmol). The solution was maintained at room temperature for 2 h. Ethyl acetate (20 mL) and water (20 mL) were added, and the resulting colorless precipitate was removed by filtration through celite. The layers were separated, and the aqueous portion was extracted with EtOAc (3 × 10 mL). The combined organics were washed with brine (20 mL), dried over Na₂SO₄, and concentrated. The yellow-orange oil was purified by column chromatography over silica gel (1:9 EtOAc:Hex) to give **2.17** as viscous yellow oil (1.20 g, 3.97 mmol, 79%): *R_f* 0.23 (1:4 EtOAc:Hex); ¹H NMR (300 MHz, CDCl₃) δ 8.77 (dd, *J* = 1.8, 4.2 Hz, 1H), 8.13 (dd, *J* = 1.8, 8.4 Hz, 1H), 7.91 (dd, *J* = 1.8, 7.5 Hz, 1H), 7.81 (dd, *J* = 1.5, 8.4 Hz, 1H), 7.78 (dd, *J* = 0.9, 6.6 Hz, 1H), 7.54 (app t, *J* = 7.8 Hz, 1H) 7.47-7.41 (m, 1H), 7.34 (dd, *J* = 4.2, 8.1 Hz, 1H), 7.05 (app t, *J* = 7.5, Hz, 1H), 6.81 (d, *J* = 8.1 Hz, 1H), 4.49-4.36 (m, 2H), 3.97 (s, 2H). 1.16 (s, 3H); ¹³C NMR (75 MHz, CDCl₃) δ 196.8, 158.1, 150.3, 145.9, 141.6, 139.7, 135.7, 133.6, 131.2, 129.8, 129.5, 128.2, 128.0, 125.8, 121.2, 120.5, 112.6, 112.2, 72.0, 18.7; IR (thin film) 3078, 2915, 1645, 1595, 1573, 1485, 1451, 1322, 1294, 1246, 1158, 1109, 1040, 1006, 926, 907, 798, 754, 626; HRMS (ESI) calcd for [C₂₀H₁₇NO₂ + H]⁺ 304.1332, found 304.1329.



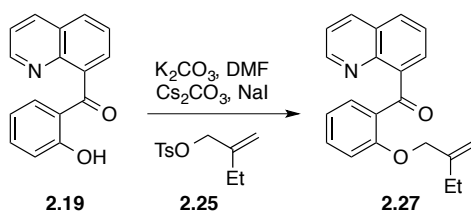
A 0.2 M solution of **1** in PhMe was prepared in a N₂ atmosphere glove box. RhCl(PPh₃)₃ (10 mg, 0.01 mmol) catalyst was carefully weighed into a 1 dram vial, and 0.5 mL **2.17** solution (30 mg, 0.1 mmol) was added followed by toluene (0.5 mL). The resulting yellow-orange solution was maintained at 130 °C for 48 h. The cloudy brown mixture was removed from the glove box and concentrated onto celite. Column chromatography (EtOAc:Hex) gave **2.52** as colorless viscous oil (28.7 mg, 0.095 mmol, 96%): *R_f* 0.31 (1:4 EtOAc:Hex); ¹H NMR (300 MHz, CDCl₃) δ 8.94 (dd, *J* = 2.1, 4.5 Hz, 1H), 8.18 (dd, *J* = 1.8, 8.4 Hz, 1H), 7.91 (dd, *J* = 1.5, 8.4 Hz, 1H), 7.81 (dd, *J* = 1.8, 7.2 Hz, 1H), 7.56 (dd, *J* = 7.2, 8.1 Hz, 1H), 7.44 (dd, *J* = 4.2, 8.4 Hz, 1H), 7.13-7.07 (m, 2H), 6.83-6.78 (m, 2H), 4.72-4.55 (m, 2H), 3.97-3.75 (m, 2H), 1.55 (s, 3H); ¹³C NMR (125 MHz, CDCl₃) δ 204.7, 159.1, 150.5, 145.5, 140.1, 136.3, 135.5, 131.2, 129.0, 128.23, 128.2, 126.1, 122.9, 121.5, 120.4, 109.7, 83.0, 54.2, 44.4, 25.9; IR (thin film), 3045, 2961 1681, 1595, 1568, 1479, 1346, 1247, 1216, 970, 831, 792, 750; HRMS (ESI) calcd for [C₂₀H₁₇NO₂ + H]⁺ 304.1332, found 304.1337. The structure was confirmed by HMQC, COSY, and HMBC.



Phenol **2.19** (200 mg, 0.81 mmol) and potassium carbonate (335 mg, 2.45 mmol) were suspended in DMF (0.8 mL). 3-Bromo-2-phenylpropene (**2.22**) (208 mg, 1.05 mmol) was added in one portion and the resulting suspension was stirred overnight. The reaction mixture was diluted with CH_2Cl_2 (50 mL), washed with a 2 M aqueous solution of LiCl (2×50 mL), and dried over Na_2SO_4 . The resulting solution was concentrated to provide a crude product that was further purified by flash chromatography (gradient, EtOAc:hex) to provide ether **2.23** as a viscous slightly yellow oil (288 mg, 0.79 mmol, 97%): 1H NMR (300 MHz, $CDCl_3$) δ 8.69-8.86 (m, 1H), 8.00 (dd, $J = 1.8, 8.4$ Hz, 1H), 7.86 (dd, $J = 1.5, 7.5$ Hz, 1H), 7.90 (dd, $J = 1.5, 8.4$ Hz, 1H), 7.63-7.60 (m, 1H), 7.44-7.33 (m, 2H), 7.24 (app dd, $J = 4.2, 8.4$ Hz, 1H), 7.16-7.09 (m, 3H), 7.05-6.97 (m, 3H), 6.84 (d, $J = 8.4$ Hz, 1H), 5.03-5.02 (m, 1H), 4.563-4.560 (m, 1H), 4.37 (s, 2H); ^{13}C NMR (75 MHz, $CDCl_3$) δ 196.9, 176.8, 158.0, 150.2, 145.9, 141.54, 141.47, 137.7, 135.8, 133.7, 131.3, 129.7, 128.21, 128.17, 127.9, 127.7, 125.8, 125.5, 121.1, 120.9, 114.1, 112.9, 108.7, 70.0; IR (thin film) 3056, 2924, 1645, 1594, 1572, 1483, 1448, 1320, 1292, 1267, 1157, 1111, 1019, 926, 913, 797, 775, 753, 709, 626; HRMS (ESI) calcd for $[C_{25}H_{19}NO_2 + Na]^+$ 388.1308, found 388.1410.



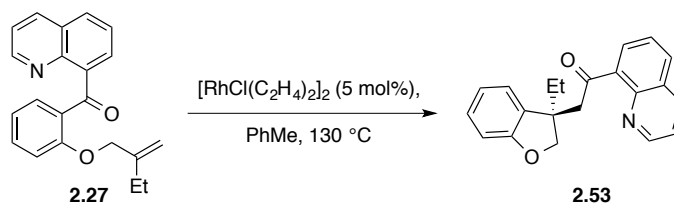
In a nitrogen filled glove box, a 1 dram vial was charged with $[\text{RhCl}(\text{C}_2\text{H}_4)_2]_2$ (2.0 mg, 0.005 mmol). A solution of **2.33** in PhMe (0.99 mL, 0.1 M, 0.099 mmol) was added and the 1 dram vial was capped and the solution was maintain at 130 °C for 48 h. The reaction was removed from the glovebox and concentrated. The resulting yellow-brown residue was purified by flash chromatography (gradient, EtOAc:hex) to provide benzofuran **2.54** as a colorless oil (33.8 mg, 0.093 mmol, 94%): ^1H NMR (300 MHz, CDCl_3) δ 8.97 (dd, $J = 2.1, 4.5$ Hz, 1H), 8.18 (dd, $J = 1.8, 8.1$ Hz, 1H), 7.90 (dd, $J = 1.5, 8.1$ Hz, 1H), 7.72 (dd, $J = 1.2, 6.9$ Hz, 1H), 7.51 (dd, $J = 7.2, 8.1$ Hz, 1H), 7.47-7.42 (m, 3H), 7.29-7.23 (m, 2H), 7.19-7.04 (m, 3H), 6.88-6.85 (m, 1H), 6.76 (ddd, $J = 1.2, 7.5, 7.5$ Hz, 1H), 5.19 (d, $J = 9.6$ Hz, 1H), 4.91 (d, $J = 9.9$ Hz, 1H), 4.75 (d, $J = 18.3$ Hz, 1H), 4.22 (d, $J = 18.3$ Hz, 1H); ^{13}C NMR (75 MHz, CDCl_3) δ 203.3, 159.0, 150.4, 145.4, 139.4, 136.3, 134.4, 131.3, 129.6, 128.4, 128.1, 126.3, 126.1, 125.9, 124.7, 121.4, 120.6, 110.0, 84.5, 53.4, 52.1 (note: two carbon singles are unresolved); IR (thin film) 3056, 2929, 1684, 1596, 1569, 1495, 1479, 1459, 1346, 1236, 1171, 1099, 1020, 9772, 909, 831, 793, 751, 700; HRMS (ESI) calcd for $[\text{C}_{25}\text{H}_{19}\text{NO}_2 + \text{Na}]^+$ 388.1308, found 388.1302.



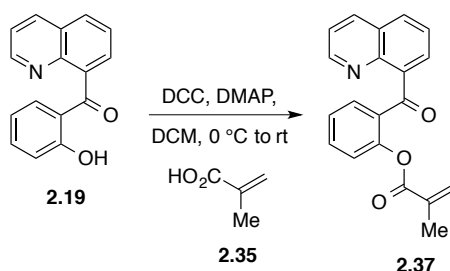
Phenol **2.19** (69 mg, 0.28 mmol), tosylate (**2.25**)^{xii} (100 mg, 0.42 mmol), and potassium carbonate (24 mg, 0.17 mmol) were combined in a 1 dram vial with DMF (0.4 mL) and allowed to stir at room temperature for 8 h. Cesium carbonate (300 mg, 0.92 mmol), and NaI (63 mg, 0.42 mmol) were added and the mixture was stirred for an additional 40 h. It was washed with water and EtOAc (15 mL) was added. The layers were separated, and the aqueous phase was extracted with EtOAc (2 × 15 mL). The combined organic phases were washed with LiCl (2 M, 15 mL), 1.0 M NaOH until aqueous layer was no longer yellow (remove un-reacted phenol), brine, dried over Na₂SO₄, and concentrated. The resulting residue was chromatographed (1:9 EtOAc:Hex) to give compound **2.27** (22.1 mg, 0.069 mmol, 25%): *R_f* 0.44 (1:4 EtOAc:Hex); ¹H NMR (300 MHz, CDCl₃) δ 8.79 (dd, *J* = 1.8, 4.2 Hz, 1H), 8.14 (dd, *J* = 1.8, 8.4 Hz, 1H), 7.92 (dd, *J* = 1.8, 7.8 Hz, 1H), 7.87 (dd, *J* = 1.5, 8.1 Hz, 1H), 7.78 (dd, *J* = 1.8, 7.2 Hz, 1H), 7.55 (dd, *J* = 7.2, 8.4 Hz, 1H), 7.46 (ddd, *J* = 2.1, 7.5, 8.4 Hz, 1H), 7.36 (dd, *J* = 4.2, 8.4 Hz, 1H), 7.07 (dd, *J* = 0.9, 7.5 Hz, 1H), 6.83 (app dd, *J* = 0.9, 8.4 Hz, 1H), 4.49-4.40 (m, 2H), 4.01 (s, 2H), 1.41-1.39 (m, 2H), 0.69 (t, *J* = 7.5 Hz, 3H); ¹³C NMR (75 MHz, CDCl₃) δ 196.9, 158.3, 150.3, 145.9, 145.3, 141.7, 135.8, 133.7, 131.2, 129.8, 129.5, 128.3, 128.0, 125.8, 121.2, 120.6, 112.5, 110.3, 71.3, 24.9, 11.4; IR (thin film) 3078, 2965, 2934, 1649, 1595, 1571,

^{xii} Prepared by reaction of the corresponding alcohol with TsCl and KOH in Et₂O. The alcohol was prepared according to

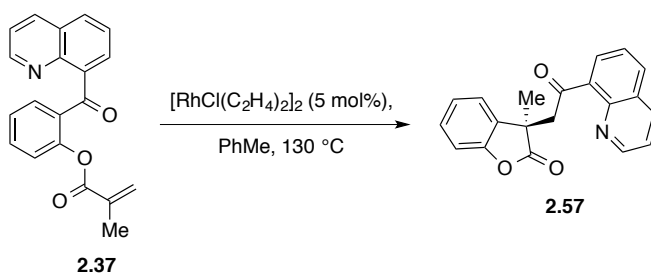
1496, 1485, 1450, 1321, 1295, 1243, 1204, 1162, 1114, 1005, 926, 915, 798, 753, 668, 625; HRMS (ESI) calcd for $[C_{21}H_{19}NO_2 + H]^+$ 318.1489, found 318.1475.



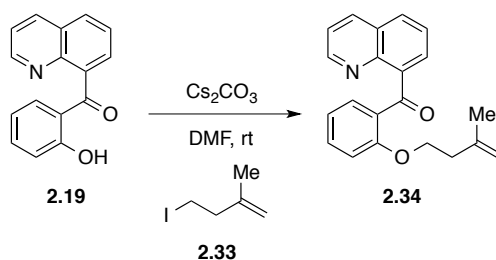
Compound **2.27** (0.65 mL, 20.6 mg, 0.065 mmol) as a 0.1 M solution in toluene was added to $[RhCl(C_2H_4)_2]_2$ (1.2 mg, 0.0032 mmol) catalyst and stirred for 48 h at 130 °C in an N_2 filled glove box. The resulting mixture was removed from the glove box and concentrated onto celite. Column chromatography (EtOAc:Hex) gave **2.53** (16.9 mg, 0.053 mmol, 82%) as pale yellow viscous oil: R_f 0.76 (1:4 EtOAc:Hex); 1H NMR (300 MHz, $CDCl_3$) δ 8.97 (dd, J = 1.8, 4.2 Hz, 1H), 8.21 (dd, J = 1.8, 8.4 Hz, 1H), 7.94 (dd, J = 1.5, 8.1 Hz, 1H), 7.79 (dd, J = 1.5, 7.2 Hz, 1H), 7.57 (dd, J = 7.2, 8.1 Hz, 1H), 7.48 (dd, J = 4.2, 8.4 Hz, 1H), 7.15-7.05 (m, 2H), 6.84-6.78 (m, 2H), 4.75 (d, J = 9.6 Hz, 1H), 4.67 (d, J = 9.6 Hz, 1H), 4.06 (d, J = 17.7 Hz, 1H), 3.82 (d, J = 17.4 Hz, 1H), 2.05 (dddd, J = 7.5, 7.5, 7.5, 13.5 Hz, 1H), 1.86 (dddd, J = 7.5, 7.5, 7.5, 13.8 Hz, 1H), 0.86 (t, J = 7.5 Hz, 3H); ^{13}C NMR (75 MHz, $CDCl_3$) δ 201.9, 159.8, 150.6, 145.5, 140.2, 136.4, 133.1, 131.2, 128.9, 128.3, 126.2, 123.7, 121.6, 120.1, 109.6, 81.4, 52.8, 48.3, 31.3, 8.8; IR (thin film) 2968, 1683, 1595, 1561, 1497, 1481, 1459, 1348, 1230, 1017, 972, 831, 793, 751; HRMS (ESI) calcd for $[C_{21}H_{19}NO_2 + H]^+$ 318.1489, found 318.1477.



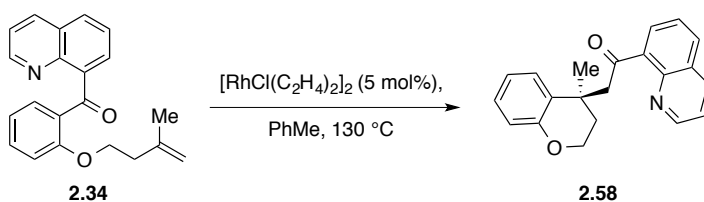
In a flame dry flask, dicyclohexylcarbodiimide (DCC, 250 mg, 1.22 mmol) was combined with *N,N*-dimethyl-4-aminopyridine (DMAP, 49 mg, 0.40 mmol) and phenol **2.19** (200 mg, 0.81 mmol). Dichloromethane (0.8 mL) was added via syringe followed by methacrylic acid (110 mL, 1.3 mmol). A cloudy suspension formed and was stirred overnight. The reaction mixture was diluted with CH₂Cl₂ (50 mL) and washed with saturated aqueous NH₄Cl (2 × 50 mL) followed by saturated aqueous NaHCO₃ (1 × 50 mL). The organic portion was dried over Na₂SO₄ and concentrated. The resulting crude product was further purified by flash chromatography (gradient, EtOAc:hex) to provide methacrylic ester **2.37** (173 mg, 0.55 mmol, 68%) as a yellow oil, characterized as a mixture with EtOAc [NOTE: ester **2.37** readily decomposes when stored neat. Ester **2.37** is best stored as a frozen matrix in benzene or in toluene suspension with 1 % (m/m) hydroquinone added as a stabilizer]: ¹H NMR (300 MHz, CDCl₃) δ 8.84 (dd, *J* = 1.8, 4.2 Hz, 1H), 8.16 (dd, *J* = 1.8, 8.4 Hz, 1H), 7.78 (dd, *J* = 1.5, 8.1 Hz, 1H), 7.85 (dd, *J* = 1.8, 7.8 Hz, 1H), 7.75 (dd, *J* = 1.5, 7.2 Hz, 1H), 7.60-7.51 (m, 2H), 7.40 (dd, *J* = 4.2, 8.4 Hz, 1H), 7.33 (ddd, *J* = 1.2, 7.7, 7.7 Hz, 1H), 7.08 (app dd, *J* = 0.9, 8.1 Hz, 1H), 5.56 (app t, *J* = 1.2 Hz, 1H), 5.25 (app quint, *J* = 1.2 Hz, 1H), 1.61 (app t, *J* = 1.5 Hz, 3H)



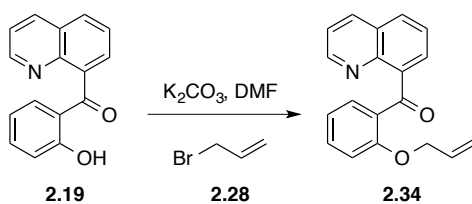
In a nitrogen filled glove box, a 1 dram vial was charged with $[\text{RhCl}(\text{C}_2\text{H}_4)_2]_2$ (2.0 mg, 0.005 mmol). A solution of **2.37** in PhMe (0.99 mL, 0.1 M, 0.099 mmol) was added and the 1 dram vial was capped and the solution was maintain at 130 °C for 24 h. The reaction was removed from the glovebox and concentrated. The resulting brown residue was purified by flash chromatography (gradient, EtOAc:hex) to provide benzofuranone **2.57** as a amorphous solid (25.0 mg, 0.0792 mmol, 80%): ^1H NMR (300 MHz, CDCl_3) δ 9.02 (dd, J = 1.8, 4.2 Hz, 1H), 8.20 (dd, J = 2.1, 8.4 Hz, 1H), 7.94 (app d, J = 8.1 Hz, 1H), 7.86 (dd, J = 0.9, 7.2 Hz, 1H), 7.54-7.46 (m, 2H), 7.31-7.19 (m, 3H), 7.11-7.05 (m, 1H), 4.17 (d, J = 18.9 Hz, 1H), 4.10 (d, J = 18.9 Hz, 1H), 1.58 (m, 3H); ^{13}C NMR (75 MHz, CDCl_3) δ 200.6, 180.7, 153.5, 150.4, 145.7, 136.7, 136.4, 132.3, 131.0, 128.4, 128.2, 126.1, 123.7, 122.4, 121.4, 110.7, 53.1, 44.5, 29.7, 25.5; IR (thin film) 2972, 2930, 1801, 1689, 1619, 1568, 1498, 1478, 1464, 1347, 1293, 1237, 1120, 881, 834, 792, 756; HRMS (ESI) calcd for $[\text{C}_{20}\text{H}_{15}\text{NO}_3 + \text{H}]^+$ 318.1125, found 318.1155.



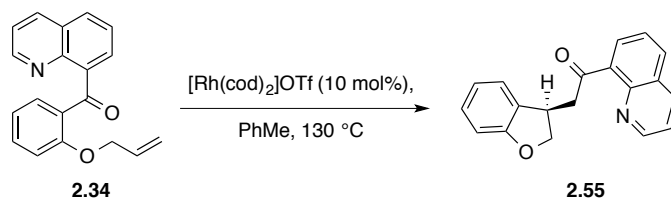
Phenol **2.19** (50 mg, 0.2 mmol), cesium carbonate (200 mg, 0.61 mmol), and 4-iodo-2-methyl-1-butene^{vii} (**2.33**) (500 mg, 2.56 mmol) were combined in a 1 dram vial with DMF (0.2 mL) and stirred at room temperature for 6 d. Water (10 mL) and EtOAc (10 mL) were added and the layers were separated. The aqueous portion was extracted with EtOAc (2 × 10 mL) and the combined organics were repeatedly washed with 1.0 M NaOH until the aqueous phase was no longer yellow (remove un-reacted phenol). The organic phases were washed with brine (15 mL), dried with Na₂SO₄, and concentrated. Column chromatography (1:99 acetone:CH₂Cl₂) yielded **9** (29.4 mg, 0.09 mmol, 42%): *R_f* 0.28 (1:99 Acetone:CH₂Cl₂); ¹H NMR (300 MHz, CDCl₃) δ 8.80 (dd, *J* = 1.5, 4.2 Hz, 1H), 8.17 (dd, *J* = 1.8, 8.1 Hz, 1H), 7.99 (dd, *J* = 1.8, 7.8 Hz, 1H), 7.91 (dd, *J* = 1.5, 9.6 Hz, 1H), 7.75 (dd, *J* = 1.5, 6.8 Hz, 1H), 7.57 (dd, *J* = 7.2, 8.1 Hz, 1H), 7.48 (ddd, *J* = 1.8, 7.5, 8.4 Hz, 1H), 7.38 (dd, *J* = 4.2, 8.1 Hz, 1H), 7.09 (ddd, *J* = 0.9, 7.5, 8.4, Hz, 1H), 6.82 (dd, *J* = 0.6, 8.4 Hz, 1H), 4.49-4.48 (m, 1H), 4.25-4.24 (m, 1H), 3.59 (t, *J* = 7.2 Hz, 2H), 1.41 (s, 3H), 1.36 (t, *J* = 7.2 Hz, 2H); ¹³C NMR (75 MHz, CDCl₃) δ 196.9, 158.5, 150.3, 146.0, 142.2, 141.2, 135.7, 133.9, 131.1, 129.4, 129.2, 127.9, 127.8, 125.9, 121.2, 120.6, 112.5, 111.4, 66.4, 35.9, 22.5; IR (thin film), 3074, 2937, 1649, 1595, 1569, 1452, 1318, 1295, 1242, 1200, 1158, 1113, 1037, 930, 797, 753, 628; HRMS (ESI) calc for [C₂₁H₁₉NO₂ + Na]⁺ 318.1465, found 318.1463.



Compound **2.34** (29.4 mg, 0.093 mmol) as a 0.1 M solution in toluene was transferred to a vial that contained $[\text{RhCl}(\text{C}_2\text{H}_4)_2]_2$ (2 mg, 0.005 mmol) catalyst. The mixture was stirred at 130 °C for 48 h. It was removed from the glove box, concentrated onto celite, and chromatographed over silica gel (EtOAc:Hex) to afford **2.58** (23.9 mg, 0.076 mmol, 81%): R_f 0.29 (1:4 EtOAc:Hex); ^1H NMR (300 MHz, CDCl_3) δ 8.97 (dd, $J = 1.8, 4.2$ Hz, 1H), 8.16 (dd, $J = 1.8, 8.4$ Hz, 1H), 7.87 (dd, $J = 1.5, 8.1$ Hz, 1H), 7.66 (dd, $J = 1.8, 7.2$ Hz, 1H), 7.51 (dd, $J = 7.2, 8.1$ Hz, 1H), 7.44 (dd, $J = 4.2, 8.4$ Hz, 1H), 7.16 (dd, $J = 1.2, 7.5$ Hz, 1H), 6.99 (ddd, $J = 1.5, 6.6, 9.0$ Hz, 1H), 6.76-6.68 (m, 2H), 4.31 (ddd, $J = 3.6, 7.5, 11.1$ Hz, 1H), 4.15 (ddd, $J = 3.3, 8.1, 11.1$ Hz, 1H), 3.86 (d, $J = 15.9$ Hz, 1H), 3.73 (d, $J = 15.9$ Hz, 1H), 2.45 (ddd, $J = 3.3, 7.8, 14.1$ Hz, 1H), 1.99 (ddd, $J = 3.7, 7.2, 14.1$ Hz, 1H), 1.53 (s, 3H); ^{13}C NMR (75 MHz, CDCl_3) δ 205.6, 153.8, 150.4, 145.3, 141.1, 136.2, 130.7, 130.4, 128.5, 128.1, 127.2, 127.0, 126.1, 121.4, 120.1, 116.9, 62.9, 55.1, 34.1, 34.0, 29.7, 28.9; IR (thin film) 2964, 1687, 1573, 1489, 1447, 1348, 1303, 1249, 1223, 1166, 1116, 1059, 987, 835, 793, 755; HRMS (ESI) calcd for $[\text{C}_{21}\text{H}_{19}\text{NO}_2 + \text{Na}]^+$ 318.1489, found 318.1494.

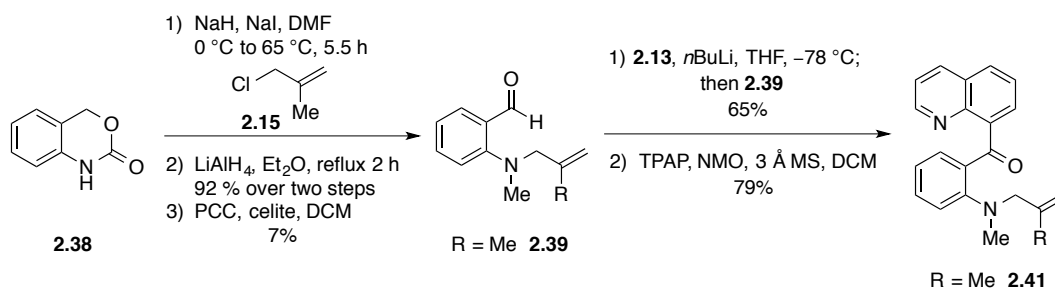


Prepared from **2.19** (0.200 g, 0.81 mmol) in analogy to **2.23**, gave **2.34** as a tan solid (0.229 g, 0.79 mmol, 97%): ^1H NMR (300 MHz, CDCl_3) δ 8.77 (dd, $J = 1.8, 4.2$ Hz, 1H), 8.15 (dd, $J = 1.5, 8.1$ Hz, 1H), 7.94 ($J = 1.5, 7.8$ Hz, 1H), 7.88 (dd, $J = 1.2, 8.1$ Hz, 1H), 7.77 ($J = 1.2, 6.9$ Hz, 1H), 7.56 (app t, $J = 7.5$ Hz, 1H), 7.48-7.43 (m, 1H), 7.36 (dd, $J = 4.2, 8.4$ Hz, 1H), 7.10-7.04 (m, 1H), 6.80 (d, $J = 8.4$ Hz, 1H), 5.12-5.00 (m, 1H), 4.78-4.66 (m, 2H), 4.04-4.02 (m, 2H); ^{13}C NMR (75 MHz, CDCl_3) δ 196.8, 158.1, 150.2, 146.0, 141.9, 135.8, 133.8, 131.8, 131.2, 129.6, 129.4, 128.0, 127.9, 125.9, 121.2, 120.8, 116.8, 112.8, 68.9; IR (thin film) 3070, 1649, 1595, 1574, 1483, 1450, 1421, 1321, 1294, 1241, 1205, 1159, 1114, 1038, 993, 928, 836, 798, 754, 625; HRMS (ESI) calcd for $[\text{C}_{19}\text{H}_{15}\text{NO}_2 + \text{H}]^+$ 290.1176, found 290.1164.



Compound **2.34** (60 mg, 0.207 mmol) was transferred to a vial that contained $[\text{Rh}(\text{cod})_2]\text{OTf}$ (9.7 mg, 0.021 mmol) catalyst. The mixture was stirred at 130 °C for 48 h. It was removed from the glove box and washed with 1 M NaOH until the aqueous layer was no longer yellow (to remove phenol by-product). The resulting solution was washed with brine, dried over Na_2SO_4 , and concentrated onto celite. Chromatography

over silica gel (EtOAc:Hex) afforded **2.55** (14.8 mg, 0.051 mmol, 25%): R_f 0.26 (1:4 EtOAc:Hex); ^1H NMR (300 MHz, CDCl_3) δ 8.88 (dd, $J = 1.8, 6.0$ Hz, 1H), 8.14 (dd, $J = 1.8, 8.4$ Hz, 1H), 7.90-7.87 (m, 2H), 7.54 (app t, $J = 7.7$ Hz, 1H), 7.39 (dd, $J = 4.5, 8.4$ Hz, 1H), 7.18-7.16 (m, 1H), 7.09-7.04 (m, 1H), 6.79 (ddd, $J = 0.9, 7.5, 8.4$ Hz, 1H), 6.74 (app d, $J = 8.1$ Hz, 1H), 4.86 (app t, $J = 9.0$ Hz, 1H), 4.33 (dd, $J = 9.2, 6.8$ Hz, 1H), 4.16-4.08 (m, 1H), 3.86 (dd, $J = 4.5, 18.3$ Hz, 1H), 3.71 (dd, $J = 9.3, 18.3$ Hz, 1H); ^{13}C NMR (125 MHz, CDCl_3) δ 204.5, 160.0, 150.6, 145.6, 139.0, 136.3, 131.5, 130.2, 129.4, 128.3, 126.1, 124.4, 121.5, 120.3, 109.5, 77.4, 50.5, 37.9; IR (thin film) 3052, 2922, 2854, 1679, 1653, 1595, 1559, 1493, 1481, 1459, 1356, 1280, 1232, 1166, 1101, 1014, 970, 911, 830, 792, 751, 658, 630; HRMS (ESI) calcd for $[\text{C}_{19}\text{H}_{15}\text{NO}_2 + \text{H}]^+$ 290.1176, found 290.1179.



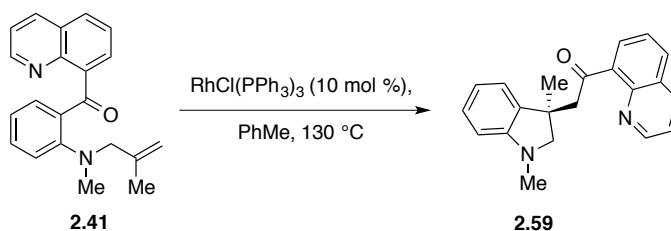
1,4-Dihydro-2H-1,3-benzoxazin-2-one (**2.38**) (4.85 g, 32.5 mmol) and NaI (457 mg, 3.25 mmol) were suspended in anhydrous DMF (120 mL) and cooled to 0 °C. Sodium hydride (1.17 g, 48.7 mmol) was added portion wise [CAUTION: gas evolution] and a colorless precipitate formed. The mixture was stirred at 0 °C for 15 min and 2-methyl-1-chloro-2-propene (**2.15**) (9.5 mL, 97.5 mmol) was added by syringe. The mixture was warmed to 65 °C in an oil bath and the suspension slowly became a cloudy tan solution over 5.5 h. The reaction mixture was allowed to cool to room temperature and then

cautiously poured into water (300 mL). The resulting suspension was extracted with CH_2Cl_2 (3×250 mL), the organic extracts were dried over Na_2SO_4 , and concentrated *in vacuo* to a tan oil which was carried on directly. A 3-neck 500 mL flask was fitted with a reflux condenser, stopper, and pressure equilibrating dropping funnel. The flask was charged with LiAlH_4 (3.1 g, 81.25 mmol) and Et_2O (100 mL). The dropping funnel was charged with a cloudy solution of the tan oil from above in Et_2O (70 mL). The contents of the dropping funnel were added at such a rate that a gentle reflux was initiated and maintained. An additional portion of Et_2O (30 mL) was added via the dropping funnel and external heat was supplied to maintain reflux for an additional 2 h. The grey suspension was allowed to cool to room temperature and then quenched by the sequential addition of water (3.1 mL), 3M aqueous NaOH (3.1 mL), and water (3.1 mL) [CAUTION: gas evolution]. A colorless suspension formed that was filtered through Celite. The filter cake was washed with CH_2Cl_2 (3×100 mL) and the combined washes were combined and concentrated to provide a yellow oil (5.7 g, 29.8 mmol, 92% over the two steps). The yellow oil was taken up in CH_2Cl_2 (20 mL) and added to a suspension of PCC (7.06 g, 32.7 mmol) and Celite (7 g) in CH_2Cl_2 (100 mL).^{xiii,xiv} The resulting brown suspension was stirred at rt overnight and then concentrated. The solid residue was purified by flash column chromatography with a gradient solvent system (5:2 hex: CH_2Cl_2 , 5:3 hex: CH_2Cl_2 , 5:4 hex: CH_2Cl_2 , 1:1 hex: CH_2Cl_2 , 5:3 hex: CH_2Cl_2 , 3:8 hex: CH_2Cl_2) to provide aldehyde **2.39** (0.55 g, 1.90 mmol, 7%). To a cooled solution (-78 °C) of 8-bromoquinoline (250 mg, 1.2 mmol) in THF (4.4 mL) in a flame-dried

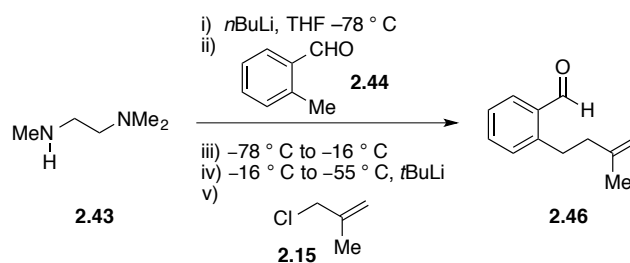
^{xiii} In analogy to the reported oxidation of other 2-amino-benzylalcohol derivatives: Kienzle, F. *Tetrahedron Lett.* **1983**, 24, 2213.

^{xiv} Subsequent work in our labs has shown that TPAP/NMO oxidation is a superior choice to PCC in similar synthetic sequences involving the oxidation of 2-amino-benzylalcohol derivatives.

flask under N₂ was added *n*-BuLi (2.5 M in Hex, 0.53 mL, 1.3 mmol) dropwise. The dark orange mixture was allowed to stir for 10 min. Aldehyde **2.39** (520 mg, 1.8 mmol) was delivered as a solution in THF (3.3 mL) drop wise to give a dark red solution. The reaction was stirred at -78 °C for 30 min, and allowed to warm to room temperature over 30 min. The resulting clear yellow solution was quenched with water (10 mL) and the resulting mixture was extracted with Et₂O (2 × 40 mL). The combined organic portions were washed with brine (40 mL), dried over Na₂SO₄, and concentrated. The resulting yellow oil was purified by column chromatography (gradient, EtOAc:hex) to provide a secondary alcohol (249 mg, 0.78 mmol, 65%). A portion of this alcohol (125 mg, 0.39 mmol) was oxidized by suspending in dry CH₂Cl₂ (7.8 mL) with NMO (91 mg, 0.78 mmol) and 3Å molecular sieves (200 mg). Tetrapropylammonium perruthenate (TPAP, 14 mg, 0.039 mmol) was added and the suspension stirred. Additional TPAP (14 mg) was added after 45 min. Approximately 45 min after the last charge of TPAP was added, the reaction was judged complete by TLC (3:1 hex:EtOAc). The reaction mixture was filtered through silica with the aid of CH₂Cl₂ (130 mL). The yellow solution was concentrated and the resulting residue purified by column chromatography (EtOAc:hex) to provide **2.41** as a yellow oil (97 mg, 79%): ¹H NMR (300 MHz, CDCl₃) δ 8.83 (app dd, *J* = 1.8, 4.2 Hz, 1H), 8.18 (dd, *J* = 1.8, 8.1 Hz, 1H), 7.93 (dd, *J* = 1.5, 8.4 Hz, 1H), 7.85 (dd, *J* = 1.5, 7.2 Hz, 1H), 7.58 (dd, *J* = 7.2, 8.1 Hz, 1H), 7.38 (dd, *J* = 4.2, 8.4 Hz, 1H), 7.35-7.28 (m, 2H), 6.97 (app d, *J* = 8.4 Hz, 1H), 6.73-6.68 (m, 1H), 4.79 (app d, *J* = 1.2 Hz, 2H), 3.76 (s, 2H), 2.82 (s, 3H), 1.56 (s, 3H); IR (thin film) 2916, 2848, 1645, 1593, 1567, 1499, 1440, 1374, 1192, 1106, 1047, 909, 799, 731, 648, 621; HRMS (ESI) calcd for [C₂₁H₂₀N₂O + Na]⁺ 339.1468, found 339.1494.

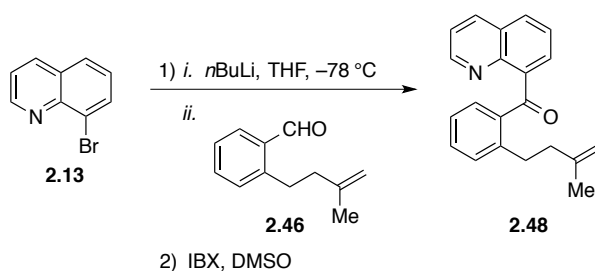


In a glovebox, compound **2.41** was dissolved in toluene to make a 0.1 M solution and a portion of this solution (0.3 mL solution, 9.5 mg **2.41**, 0.03 mmol) was added to RhCl(PPh₃)₃ (2.8 mg, 0.003 mmol) in a 1 dram vial. The vial was capped and stirred for 24 h at 130 °C. The resulting mixture was removed from the glove box and concentrated onto celite. Column chromatography (EtOAc:hex) gave **2.59** as pale yellow oil (7.2 mg, 0.023 mmol, 75%). *R_f* 0.20 (1:4 EtOAc/hex); ¹H NMR (300 MHz, CDCl₃) δ 8.93 (dd, *J* = 1.8, 4.2 Hz, 1H), 8.17 (dd, *J* = 1.8, 8.4 Hz, 1H), 7.89 (dd, *J* = 1.5, 8.1 Hz, 1H), 7.76 (dd, *J* = 1.2, 6.9 Hz, 1H), 7.54 (app t, *J* = 8.1 Hz, 1H), 7.43 (dd, *J* = 4.2, 8.4 Hz, 1H), 7.05 (ddd, *J* = 1.2, 7.8, 7.8 Hz, 1H), 6.98 (dd, *J* = 0.6, 7.5 Hz, 1H), 6.60 (ddd, *J* = 0.6, 7.2, 8.1 Hz, 1H), 6.44 (d, *J* = 7.8 Hz, 1H), 3.81 (d, *J* = 16.8 Hz, 1H), 3.68 (d, *J* = 16.8 Hz, 1H), 3.51 (d, *J* = 9.3 Hz, 1H), 3.35 (d, *J* = 9.0 Hz, 1H), 2.75 (s, 3H), 1.51 (s, 3H); ¹³C NMR (75 MHz, CDCl₃) δ 205.6, 151.9, 150.4, 145.4, 140.8, 137.9, 136.1, 130.7, 128.6, 128.1, 127.7, 126.0, 122.2, 121.4, 117.5, 107.1, 68.0, 53.6, 42.9, 35.6, 25.1; IR (thin film) 3052, 2960, 2865, 2807, 1683, 1654, 1606, 1560, 1495, 1463, 1451, 1300, 1022, 984, 830, 794, 743, 668; HRMS (ESI) calcd for [C₂₁H₂₀N₂O + Na]⁺ 339.1468, found 339.1479.



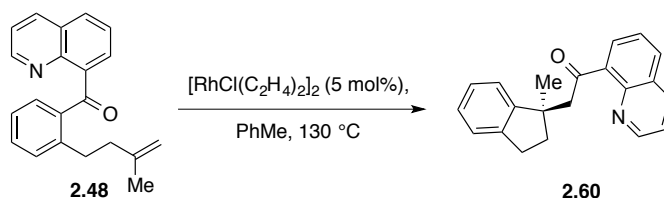
A cooled solution ($-78\text{ }^{\circ}\text{C}$) of *N,N,N*-trimethylethylenediamine (**2.43**) (1.64 mL, 12.8 mmol) in THF (32 mL) was added to a flame-dried flask under argon, and *n*-BuLi (2.5 M in hex, 5.4 mL, 12.4 mmol) was added drop-wise. It was allowed to stir for 30 min, followed by slow addition of 2-methylbenzaldehyde (**2.44**) (1.44 g, 12.0 mmol). The solution was warmed to $-16\text{ }^{\circ}\text{C}$ for 20 min, and re-cooled to $-55\text{ }^{\circ}\text{C}$ for the drop-wise addition of *t*-BuLi (1.7 M in pentane, 21.2 mL, 36 mmol). The resulting deep red solution was stirred at $-55\text{ }^{\circ}\text{C}$ for 2.5 h, and re-cooled to $-78\text{ }^{\circ}\text{C}$. Isobutenyl chloride (**2.15**) (7.0 mL, 72 mmol) was added rapidly, and the pale yellow solution was allowed to come to room temperature and stir for 30 min. The solution was poured onto cold 1 M HCl (75 mL), stirred for 10 min, and the layers were separated. The aqueous layer was extracted with Et_2O ($3 \times 50\text{ mL}$), and the combined organics were washed with brine, dried over Na_2SO_4 , and concentrated. Silica gel chromatography (1:19 EtOAc:Hex) afforded compound **2.46** (1.73 g, 10 mmol, 84%) as pale orange oil: R_f 0.59 (1:4 EtOA:Hex)^{xv}

^{xv} Conditions for this alkylation were adapted from the following: Bailey, W. F.; Wachter-Jurcsak, N. M.; Pineau, M. R.; Ovaska, T. V.; Warren, R. R.; Lewis, C. E.; *J. Org. Chem.* **1996**, *61*, 8216.

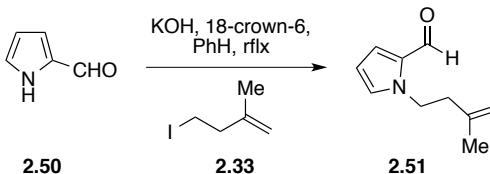


To a cooled (-78°C) solution of 8-bromoquinoline (**2.13**) (500 mg, 2.4 mmol) in THF (29 mL) in a flame-dried flask under N_2 was added $n\text{-BuLi}$ (2.5 M in hex, 2.2 mL, 5.5 mmol) drop-wise. Aldehyde **2.46** (500 mg, 2.9 mmol) was slowly added and the resulting solution was allowed to stir for 30 min at -78°C . It was warmed to room temperature, and stirred for 1 h. The reaction was quenched with saturated NH_4Cl , the mixture washed with water, and the layers separated. The aqueous layer was extracted with EtOAc (3×40 mL), and the combined organics were washed with brine, dried over Na_2SO_4 , and concentrated. The crude alcohol (376 mg) was directly subjected to IBX (1.05 g, 37.5 mmol) in DMSO (8.5 mL) for 3 h. Et_2O (20 mL) was added, and the solution was washed with water. The resulting mixture was filtered through celite to remove the colorless precipitate. The layers were separated and the aqueous portion was extracted Et_2O (2×20 mL). The combined organics were washed with brine, dried over Na_2SO_4 , and concentrated. Silica gel chromatography (1:19 EtOAc:Hex) afforded compound **2.48** as yellow viscous oil (134 mg, 18.5% over two steps): R_f 0.36 (1:4 EtOAc:Hex); ^1H NMR (300 MHz, CDCl_3) δ 8.87 (dd, $J = 1.8, 4.2$ Hz, 1H), 8.19 (dd, $J = 1.8, 8.1$ Hz, 1H), 7.95 (dd, $J = 1.5, 8.1$ Hz, 1H), 7.74 (dd, $J = 1.5, 7.2$ Hz, 1H), 7.57 (dd, $J = 7.2, 8.1$ Hz, 1H), 7.44-7.29 (m, 4H), 7.10 (ddd, $J = 1.5, 7.2, 7.8$ Hz, 1H), 4.712-4.705 (m, 2H), 3.19-3.14 (m, 2H), 2.47-2.42 (m, 2H), 1.78-1.75 (m, 3H); ^{13}C NMR (75 MHz, CDCl_3) δ 199.8, 151.0, 146.0, 145.9, 143.5, 140.3, 138.3, 135.9,

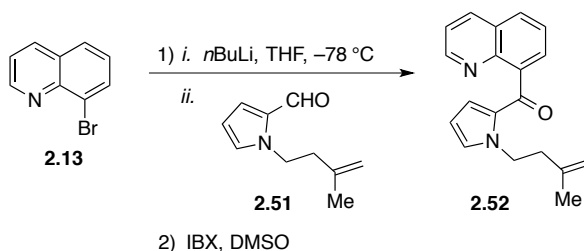
132.0, 131.5, 130.9, 130.3, 129.2, 128.3, 125.6, 125.6, 121.5, 110.0, 39.7, 32.7, 22.4; IR (thin film) 3071, 2934, 1664, 1596, 1571, 1495, 1451, 1319, 1289, 1267, 1208, 929, 887, 801, 749, 668, 627; HRMS (ESI) calcd for $[C_{21}H_{19}NO + H]^+$ 302.1539, found 302.1529.



In a 1 dram vial, compound **2.48** (50 mg, 0.17 mmol) as a 0.1 M solution of in toluene was added to $\{\text{RhCl}(\text{C}_2\text{H}_4)_2\}_2$ (3.3 mg, 0.0085 mmol) in a N_2 atmosphere glove box. The mixture was stirred at 130 $^\circ\text{C}$ for 48 h. It was removed from the glove box and concentrated onto celite. Column chromatography (EtOAc:Hex) gave **2.60** as pale yellow viscous oil (46.5 mg, 0.15 mmol, 93%): R_f 0.26 (1:4 EtOAc:Hex); ^1H NMR (300 MHz, CDCl_3) δ 8.92 (dd, $J = 2.1, 4.2$ Hz, 1H), 8.15 (dd, $J = 1.8, 8.4$ Hz, 1H), 7.86 (dd, $J = 1.5, 8.1$ Hz, 1H), 7.67 (dd, $J = 1.5, 7.2$ Hz, 1H), 7.50 (dd, $J = 7.2, 8.1$ Hz, 1H), 7.41 (dd, $J = 4.2, 8.4$ Hz, 1H), 7.17-7.04 (m, 4H), 3.71 (d, $J = 15.6$ Hz, 1H), 3.65 (d, $J = 15.6$ Hz, 1H), 2.89 (t, $J = 7.2$ Hz, 2H), 2.31 (ddd, $J = 7.2, 7.2, 12.9$ Hz, 1H), 2.01 (ddd, $J = 7.5, 7.5, 12.9$ Hz, 1H), 1.68 (s, 3H); ^{13}C NMR (75 MHz, CDCl_3) δ 206.2, 151.0, 150.3, 145.4, 142.8, 141.3, 136.1, 130.5, 128.5, 128.1, 126.4, 126.1, 126.0, 124.5, 122.6, 121.3, 54.4, 47.0, 38.7, 30.3, 26.7; IR (thin film) 3033, 2953, 2873, 1687, 1595, 1569, 1506, 1497, 1478, 1451, 1348, 1318, 1261, 1170, 1052, 983, 830, 795, 758, 725; HRMS (ESI) calcd for $[C_{21}H_{19}NO + H]^+$ 302.1539, found 302.1538.



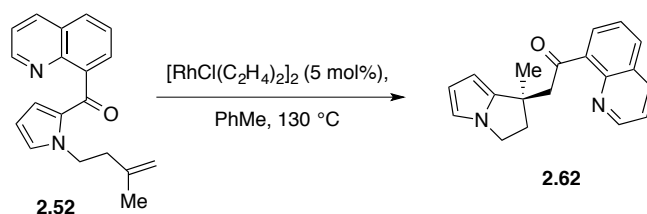
1*H*-pyrrole-2-carbaldehyde (**2.50**) (1.0 g, 10.5 mmol), 18-crown-6 (2.78 g, 10.5 mmol), and powdered KOH (890 mg, 15.9 mmol), were refluxed in benzene (7 mL) for 2 h. 4-Iodo-2-methyl-1-butene (**2.33**) (4.1 g, 21.0 mmol) was added as a solution in benzene (5.3 mL) and reflux was maintained for an additional 4 h. The solution was washed with water, and the layers were separated. The aqueous layer was extracted with Et₂O (3 × 30mL), and the combined organic phases were washed with brine, dried over Na₂SO₄, and concentrated. Silica gel chromatography (1:49 EtOAc:Hex) afforded **2.51** as yellow oil (590 mg, 3.6 mmol, 34%): *R_f* 0.69 (1:4 EtOAc:Hex).^{xvi}



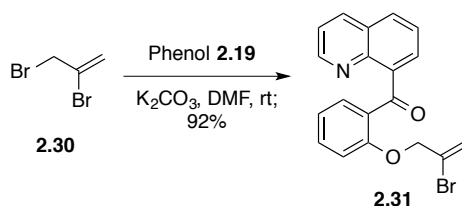
To a cooled solution (−78 °C) of 8-bromoquinoline (**2.13**) (165 mg, 0.59 mmol) in THF (7.9 mL) in a flame-dried flask under N₂ was added 2.5 M *n*-BuLi (0.6 mL, 1.5 mmol) drop-wise. Aldehyde **2.51** (137 mg, 0.84 mmol) was slowly added, and the resulting solution was allowed to stir for 30 min at −78 °C. It was warmed to room temperature, and stirred for 1 h. The reaction was quenched with saturated NH₄Cl, and the mixture

^{xvi} Conditions for pyrrole alkylation adapted from the following: Santaniello, E.; Farachi, C.; Ponti, F.; *Synthesis*, **1979**, 617

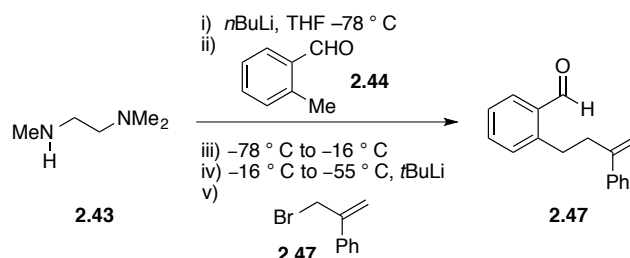
was washed with water, and the layers were separated. The aqueous layer was extracted with EtOAc (3 × 40 mL), and the combined organics were washed with brine, dried over Na₂SO₄, and concentrated. The crude alcohol (284 mg) was subjected to IBX (400 mg, 1.4 mmol) in DMSO (6.5 mL) for 3 h. Et₂O (20 mL) was added, and the solution was washed with water. The resulting mixture was filtered through celite to remove the colorless precipitate. The layers were separated and the aqueous portion was extracted Et₂O (2 × 20mL). The combined organics were washed with brine, dried over Na₂SO₄, and concentrated. Chromatography (1:19 EtOAc:Hex) afforded compound **2.52** as an orange oil (36.6 mg, 0.126 mmol, 16% 2-steps): *R_f* 0.15 (1:4 EtOAc:Hex); ¹H NMR (300 MHz, CDCl₃) δ 8.93 (dd, *J* = 1.8, 4.2 Hz, 1H), 8.18 (dd, *J* = 1.5, 8.1 Hz, 1H), 7.89 (dd, *J* = 1.5, 8.1 Hz, 1H), 7.74 (dd, *J* = 1.5, 6.9 Hz, 1H), 7.56 (dd, *J* = 7.2, 8.1 Hz, 1H), 7.40 (dd, *J* = 4.2, 8.4 Hz, 1H), 6.96 (dd, *J* = 1.8, 2.4 Hz, 1H), 6.39 (dd, *J* = 1.8, 3.9 Hz, 1H), 6.04 (dd, *J* = 3.9, 5.7 Hz, 1H), 4.83-4.81 (m, 1H) 4.79-4.77 (m, 1H), 4.68 (app t, *J* = 7.2 Hz, 2H), 2.65 (app t, *J* = 7.2 Hz, 2H), 1.84-1.83 (m, 3H); ¹³C NMR (75 MHz, CDCl₃) 186.4, 150.9, 146.1, 142.5, 140.0, 135.9, 131.2, 130.0, 129.1, 128.2, 128.1, 125.4, 124.4, 121.3, 112.3, 108.3, 48.7, 39.7, 22.5; IR (thin film) 3074, 2945, 1634, 1575, 1524, 1495, 1471, 1405, 1340, 1258, 1086, 1058, 902, 881, 837, 816, 804, 737, 636; HRMS (ESI) calcd for [C₁₉H₁₈N₂O + H]⁺ 291.1492, found 291.1488



In a 1 dram vial, compound **2.52** (50 mg, 0.17 mmol) as a 0.1 M solution in toluene was added to $\{\text{RhCl}(\text{C}_2\text{H}_4)_2\}_2$ (3.3 mg, 0.0086 mmol) in an N_2 atmosphere glove box. The mixture was stirred at 130 °C for 48 h. It was removed from the glove box and concentrated onto celite. Column chromatography (EtOAc:Hex) gave **2.62** as viscous oil (31.5 mg, 0.11 mmol, 63%): R_f 0.24 (1:4 EtOAc:Hex); ^1H NMR (300 MHz, CDCl_3) δ 8.92 (dd, $J = 1.8, 4.2$ Hz, 1H), 8.16 (dd, $J = 1.8, 8.1$ Hz, 1H), 7.88 (dd, $J = 1.5, 8.1$ Hz, 1H), 7.71 (dd, $J = 1.5, 7.2$ Hz, 1H), 7.53 (dd, $J = 7.2, 8.1$, 1H) 7.42 (dd, $J = 4.2, 8.4$ Hz, 1H), 6.49 (dd, $J = 1.2, 2.4$ Hz, 1H), 6.12 (app t, $J = 3.0$ Hz, 1H), 5.67 (dd, $J = 1.2, 3.3$ Hz, 1H), 4.00 (dd, $J = 2.1, 5.7$ Hz, 1H), 3.97 (dd, $J = 2.7, 6.0$ Hz, 1H), 3.75 (d, $J = 16.5$ Hz, 1H), 3.68 (d, $J = 16.5$ Hz, 1H), 2.76 (ddd, $J = 6.9, 7.8, 12.6$ Hz, 1H), 2.48 (ddd, $J = 6.6, 7.2, 12.9$ Hz, 1H), 1.49 (s, 3H); ^{13}C NMR (75 MHz, CDCl_3) δ 205.6, 150.4, 145.4, 144.7, 140.9, 136.1, 130.6, 128.4, 128.1, 126.0, 121.4, 112.8, 111.7, 97.4, 54.3, 45.0, 42.0, 40.6, 26.4; IR (thin film) 2964, 2880, 1690, 1592, 1569, 1493, 1466, 1348, 1291, 1246, 1170, 1056, 835, 789, 767, 694; HRMS (ESI) calcd for $[\text{C}_{19}\text{H}_{18}\text{N}_2\text{O} + \text{Na}]^+$ 313.1311, found 313.1340.

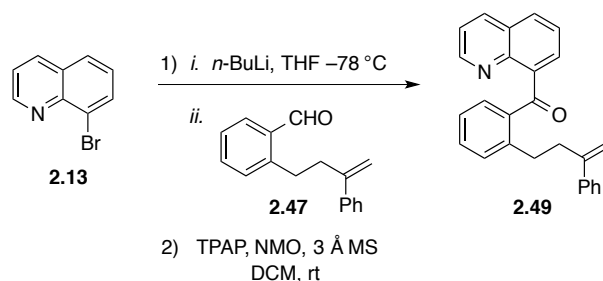


^1H NMR (500 MHz; CDCl_3) δ 8.77 (dd, $J = 4.2, 1.8$ Hz, 1H), 8.16 (dd, $J = 8.3, 1.8$ Hz, 1H), 7.90 (dd, $J = 8.2, 1.4$ Hz, 1H), 7.84 (ddd, $J = 10.4, 7.4, 1.6$ Hz, 2H), 7.58 (dd, $J = 8.1, 7.2$ Hz, 1H), 7.46 (ddd, $J = 8.3, 7.4, 1.8$ Hz, 1H), 7.37 (dd, $J = 8.3, 4.2$ Hz, 1H), 7.09 (td, $J = 7.5, 0.8$ Hz, 1H), 6.81 (d, $J = 8.3$ Hz, 1H), 5.21-5.18 (m, 2H), 4.19 (t, $J = 1.5$ Hz, 2H); ^{13}C NMR (126 MHz; CDCl_3): δ 196.5, 156.9, 150.4, 145.8, 141.0, 135.9, 133.6, 131.4, 130.2, 129.9, 128.7, 128.0, 125.9, 125.3, 121.48, 121.32, 117.0, 113.1, 71.8.



A cooled solution (-78°C) of *N,N,N*-trimethylethylenediamine (**2.43**) (0.54 mL, 4.13 mmol) in THF (10.3 mL) was added to a flame-dried flask under argon, and *n*-BuLi (2.5 M in hex, 1.6 mL, 4.0 mmol) was added drop-wise. It was allowed to stir for 30 min, followed by slow addition of 2-methylbenzaldehyde (**2.44**) (0.45 mL, 3.87 mmol). The solution was warmed to -16°C for 20 min, and re-cooled to -55°C for the drop-wise addition of *t*-BuLi (1.7 M in pentane, 3.0 mL, 5.0 mmol). The resulting deep red solution was stirred at -55°C for 2.5 h, and re-cooled to -78°C . Bromide **2.47** (1.9 g, 9.68 mmol) was added rapidly, and the pale yellow solution was allowed to come to room temperature and stir for 30 min. The solution was poured onto cold 1 M HCl

(75 mL), stirred for 10 min, and the layers were separated. The aqueous layer was extracted with Et₂O (3 × 50mL), and the combined organics were washed with brine, dried over Na₂SO₄, and concentrated. Silica gel chromatography (1:19 EtOAc:Hex) afforded compound **2.47** (602 mg, 2.54 mmol, 66%) as pale yellow oil: *R_f* 0.50 (1:4 EtOAc:Hex)^{xvii}



To a cooled (-78°C) solution of 8-bromoquinoline (**2.13**) (340 mg, 1.6 mmol) in THF (10 mL) in a flame-dried flask under N₂ was added *n*-BuLi (2.5 M in hex, 0.84 mL, 2.09 mmol) drop-wise. Aldehyde **2.47** (570 mg, 2.4 mmol) was slowly added and the resulting solution was allowed to stir for 30 min at -78°C . It was warmed to room temperature, and stirred for 1 h. The reaction was quenched with saturated NH₄Cl, the mixture washed with water, and the layers separated. The aqueous layer was extracted with EtOAc (3 × 40 mL), and the combined organics were washed with brine, dried over Na₂SO₄, and concentrated. The crude mixture was purified by flash chromatography (1:19 EtOAc:Hex) to give the resulting alcohol (354 mg, 0.97 mmol, 59%): *R_f* 0.09 (1:4 EtOAc:Hex). The alcohol (172 mg, 0.47 mmol) was azeotropically dried with benzene and added to a flame-dried flask with *N*-methylmorpholine (110 mg, 0.94 mmol), tetrapropylammonium perruthenate (8.2 mg, 0.02 mmol), 3 Å molecular

^{xvii} Conditions for this alkylation were adapted from the following: Bailey, W. F.; Wachter-Jurcsak, N. M.; Pineau, M. R.; Ovaska, T. V.; Warren, R. R.; Lewis, C. E.; *J. Org. Chem.* **1996**, *61*, 8216.

sieves (250 mg), and dry DCM (9.4 mL). After 45 min of stirring, a second charge of TPAP was added. The resulting mixture was stirred for an additional 3 h. Celite was added to the mixture and filtered through a plug of silica gel and washed with DCM. The residue obtained upon concentration was purified by flash chromatography (1:9 EtOAc:Hex) affording ketone **2.49** (114 mg, 0.31 mmol, 67%): ^1H NMR (300 MHz; CDCl_3): δ 8.67 (dd, $J = 4.2, 1.8$ Hz, 1H), 8.00 (dd, $J = 8.3, 1.8$ Hz, 1H), 7.75 (dd, $J = 8.2, 1.4$ Hz, 1H), 7.55 (dd, $J = 7.1, 1.5$ Hz, 1H), 7.40 (dd, $J = 8.1, 7.2$ Hz, 1H), 7.32 (dt, $J = 8.2, 1.8$ Hz, 2H), 7.23-7.05 (m, 7H), 6.91 (td, $J = 7.4, 1.3$ Hz, 1H), 5.12 (d, $J = 1.3$ Hz, 1H), 4.93 (d, $J = 1.3$ Hz, 1H), 3.03 (t, $J = 9.3, 2\text{H}$), 2.80 (t, $J = 9.5$ Hz, 2H); ^{13}C NMR (75 MHz; CDCl_3): δ 199.9, 150.9, 148.1, 146.0, 143.1, 141.2, 140.3, 138.3, 135.9, 132.0, 131.5, 131.2, 130.2, 129.1, 128.26, 128.22, 127.2, 126.2, 125.6, 125.4, 121.5, 112.5, 36.9, 33.4.

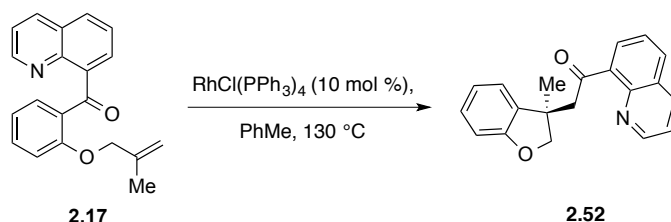
2.2 JOHNSON’S MECHANISM ELUCIDATION

Johnson et al.⁶ reported mechanistic investigations of the intramolecular carboacylation reaction developed by our group (Section 2.3). The rate law, $^{12}\text{C}/^{13}\text{C}$ kinetic isotope effects, and activation parameters were determined for both $\text{RhCl}(\text{PPh}_3)_3$ and $[\text{RhCl}(\text{C}_2\text{H}_4)_2]_2$ complexes and the rate-limiting step of catalysis was identified. The rate laws differed between catalyst systems, and the reaction mechanism was shown to be substrate dependent. In addition, several other substrate derivatives were shown to successfully undergo the reaction.

2.2.1 MECHANISTIC INVESTIGATIONS WITH $\text{RhCl}(\text{PPh}_3)_3$

Traditional kinetic methods revealed a linear consumption of starting material (concentration versus time) through at least 80% conversion when substrate **2.17** was treated with $\text{RhCl}(\text{PPh}_3)_3$ at 130 °C (Scheme 35a). This data indicated a zero-order dependence upon substrate (saturation kinetics) and a first-order dependence upon $\text{RhCl}(\text{PPh}_3)_3$. The overall first-order rate law was determined where $k = 4.98 \times 10^{-2} \text{ s}^{-1}$. Exogenous PPh_3 ligand was introduced to the reaction in concentrations ranging from 0 to 0.108 M. Under these conditions, a change from zero-order to first-order dependence in substrate was observed. An inverse first-order dependence upon PPh_3 was also observed, which indicated reaction inhibition. From these data, it was apparent that $\text{RhCl}(\text{PPh}_3)_3$ must lose one equivalent of PPh_3 prior to C–C bond activation and that PPh_3 disrupts a pre-equilibrium wherein catalyst and substrate are bound in the resting state. The activation parameters were determined; the relatively low change in entropy

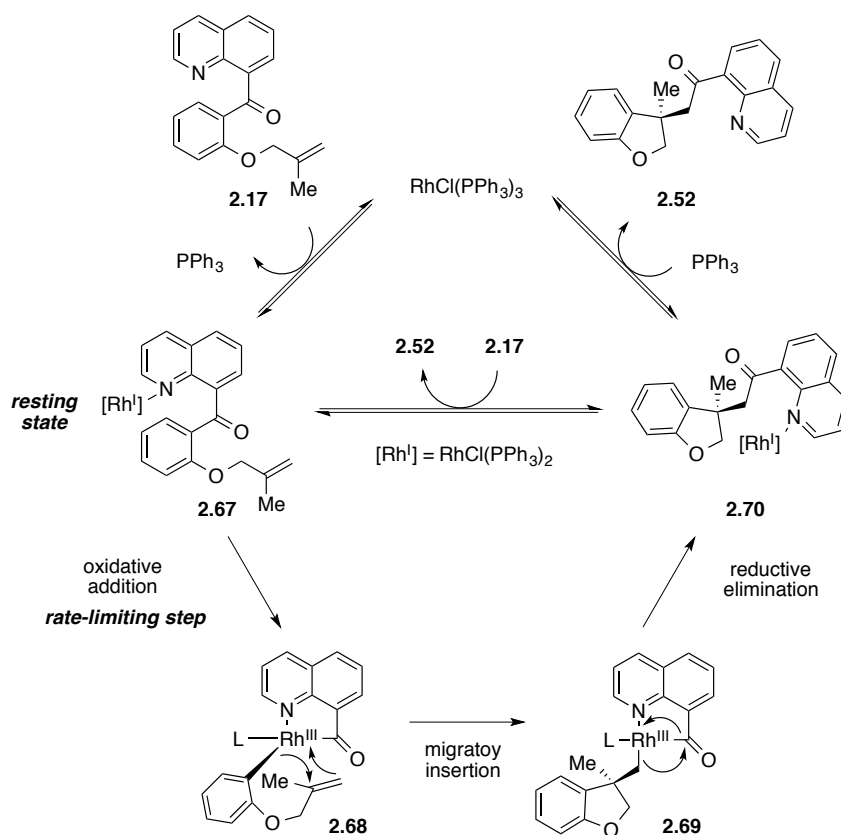
($\Delta S^\ddagger = -4.3 \pm 2.4$ eu) suggested minimal molecular reorganization in the rate-limiting step and the enthalpic change ($\Delta H^\ddagger = 27.8 \pm 1.0$ kcal/mol) quantifies the energy required to cleave this particular C–C bond under transition-metal catalysis.



Scheme 35a. Intramolecular carboacylation with $\text{RhCl(PPh}_3)_4$

Without the ability to probe the relative energies of oxidative addition, migratory insertion, or reductive elimination for intramolecular reactions by traditional kinetic methods, analysis of $^{12}\text{C}/^{13}\text{C}$ kinetic isotope effects by Singleton's method^{7,8} gave insight into the rate-limiting step of the reaction. Negligible isotope effects were seen at both alkene carbons (less than 1.003 ± 0.005) suggesting that neither migratory insertion nor reductive elimination are rate limiting. Conversely, the ketone (1.027 ± 0.005) and α -aryl carbon (1.028 ± 0.004) showed significant isotope effects, which support carbon–carbon bond activation as the slow step in the catalytic cycle.

The combination of kinetic isotope effects, activation parameters, and determined rate law are consistent with the mechanism proposed in Scheme 35b. The nature of intermediates **2.69** and **2.70** are unable to be probed since they occur after the rate-limiting step. Intermediates **2.67** and **2.68** are inferred from the inhibitory effects of product and PPh_3 on the rate of reaction. The relatively low activation entropy is in agreement with intermediate **2.67** as a resting state and oxidative addition being the rate-limiting step in that little change in the overall molecular organization would be expected.

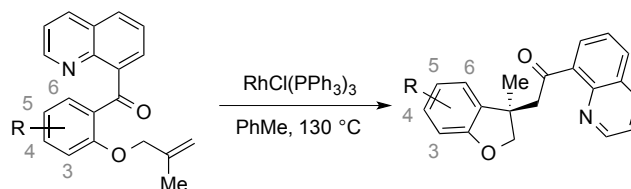


Scheme 35b. Mechanistic proposal for intramolecular carboacylation with $\text{RhCl}(\text{PPh}_3)_3$

The search for additional insight into the reaction mechanism and the nature of the rate-limiting step was continued with a linear free-energy correlation study. Several analogs were prepared containing both electron-withdrawing and electron-donating substituents on the aryl ring (Table 2) and the rates of the reaction were determined with $\text{RhCl}(\text{PPh}_3)_3$ as the catalyst at 130 °C. Electron-donating groups (entries 2–5) accelerated the reaction whereas electron-withdrawing groups (entries 6–7) had an inhibitory effect. Johnson explained this counterintuitive observation by stating that the increased electron density would have a stabilizing effect on the metallacycle intermediate by strengthening the $\text{Rh}-\text{C}_{\text{aryl}}$ bond rather than rendering the ketone less electrophilic. Substrate **2.74** with a 4-diethylamino group underwent the reaction more than twice as fast as the parent

substrate **2.17**. This data seems to conflict with the observation we had made concerning the formation of dihydroindole **2.59** (see Figure 9). Perhaps the nitrogen is either not in conjugation with the aryl ring because the alkene is bound to the metal center during oxidative addition, or that oxidative addition is not the rate-limiting step when an amino group is at the 2-position. It was also observed that the reaction did not tolerate the sterically hindered *tert*-butyl groups (entry 8). Overall, the reaction was shown to be tolerant of several additional functional groups, including aryl chlorides and nitro groups.

Table 2. Linear free-energy relationships with RhCl(PPh₃)₃

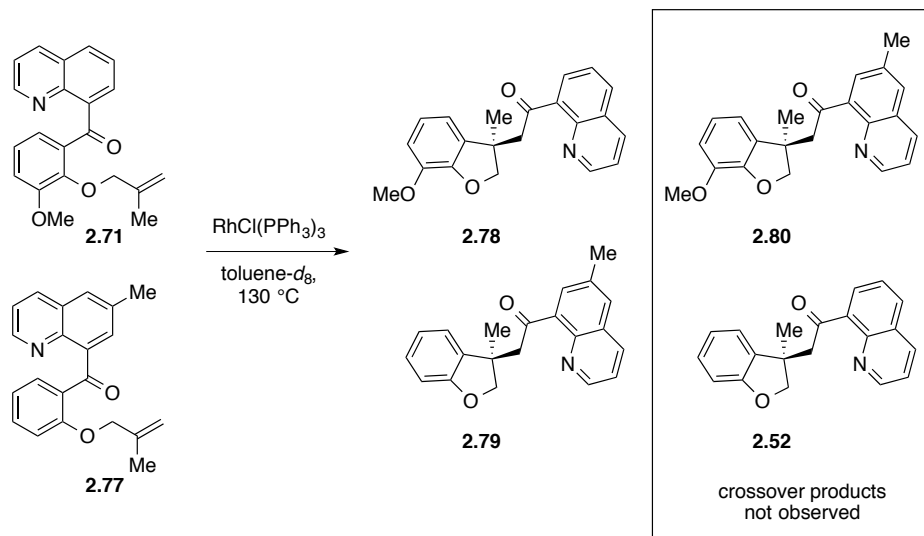


entry	R, substituent	yield (%)	k (s ⁻¹ × 10 ⁻²)
1	H 2.17	97	4.98
2	3-OMe 2.71	95	4.14
3	4-OMe 2.72	93	8.35
4	5-OMe 2.73	97	5.13
5	4-NEt ₂ 2.74	85	12.5
6	5-NO ₂ 2.75	91	2.32
7	5-Cl 2.76	94	3.77
8	3,5-(<i>t</i> Bu) ₂ 2.77	0	n/a

With oxidative addition established as the rate-limiting step for RhCl(PPh₃)₃ catalyzed intramolecular carboacylation of allyl ether substrate **2.17**, it is reasonable to assume that modifications made to the alkene substituent would have no effect on the rate. However, the remaining allylic and homoallylic ether derivatives (see Figure 9) reported to have cyclized with [RhCl(C₂H₄)₂]₂, did not provide product with RhCl(PPh₃)₃. Additional substrates with 1,2-disubstituted alkenes also failed to undergo

the reaction with $\text{RhCl}(\text{PPh}_3)_3$. These results imply a change in mechanism, which will be discussed in Section 2.3.2.

Suggs and Jun had determined that a homolysis-recombination mechanism was operative in the thermolysis of (*S*)-8-quinolinyl α -methoxybenzyl ketone **1.61** (see Chapter 1, Scheme 17). An analogous cage-escape crossover experiment was performed on 3-methoxy-aryl derivative **2.71** with 6-methyl-quinolinyl derivative **2.77** in order to probe the nature of the intermediates (Scheme 36). Both substrates underwent complete conversion to their respective product (**2.78** and **2.79**) without detection of crossover products **2.80** or **2.52**. Therefore it is unlikely that this transformation proceeds through a radical mechanism.



Scheme 36. Radical-recombination crossover experiment

2.2.2 MECHANISTIC INVESTIGATIONS WITH $[\text{RhCl}(\text{C}_2\text{H}_4)_2]_2$

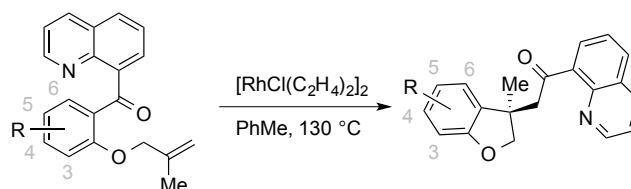
The selective reactivity of $\text{RhCl}(\text{PPh}_3)_3$ prompted Johnson to investigate the mechanism associated with the more active $[\text{RhCl}(\text{C}_2\text{H}_4)_2]_2$ catalyst.⁹ A first-order dependence on both substrate and catalyst led to an overall second-order rate law with a rate constant of $k = 7.59 \times 10^{-2} \text{ M}^{-1}\text{s}^{-1}$. In contrast to the first-order rate law observed with $\text{RhCl}(\text{PPh}_3)_3$, the second-order rate law for catalysis with phosphine-free $[\text{RhCl}(\text{C}_2\text{H}_4)_2]_2$ suggested a lack of a pre-equilibrium coordination of substrate to metal. Additionally, the reaction rate was not subject to product inhibition. The observed rates from reactions at varying temperatures provided a comparable enthalpic value of $\Delta H^\ddagger = 28.4 \pm 1.3 \text{ kcal/mol}$ (in comparison to $\text{RhCl}(\text{PPh}_3)_3$, $\Delta H^\ddagger = 27.8 \pm 1.0 \text{ kcal/mol}$) and a relatively large entropic value of $\Delta S^\ddagger = -26.4 \pm 2.6 \text{ eu}$ (in comparison to $\text{RhCl}(\text{PPh}_3)_3$, $\Delta S^\ddagger = -4.3 \pm 2.4 \text{ eu}$). This supports a bimolecular rate-limiting step which is consistent with $[\text{RhCl}(\text{C}_2\text{H}_4)_2]_2$ as the resting state of catalysis.

The Singleton $^{12}\text{C}/^{13}\text{C}$ kinetic isotope effects were determined for carboacylation catalysis with $[\text{RhCl}(\text{C}_2\text{H}_4)_2]_2$ and parent substrate **2.17**. Similar to catalysis with $\text{RhCl}(\text{PPh}_3)_3$, negligible isotope effects at the alkene carbons (less than 1.002) and significant isotope effects at the ketone carbon (1.1016 ± 0.0005) and the α -aryl carbon (1.1012 ± 0.0004) were discovered for catalysis with $[\text{RhCl}(\text{C}_2\text{H}_4)_2]_2$, thus maintaining oxidative addition as the likely rate-limiting step.

Additional support for oxidative addition as the rate-limiting step for $[\text{RhCl}(\text{C}_2\text{H}_4)_2]_2$ catalysis was demonstrated through linear free-energy correlation studies. As with $\text{RhCl}(\text{PPh}_3)_3$, the rate of the reaction was enhanced with the addition of electron-donating groups on the central aryl ring (Table 4). The magnitude of rate enhancement,

however, was substantially less for $[\text{RhCl}(\text{C}_2\text{H}_4)_2]_2$. For example, 4-diethylamino substrate **2.74** underwent the reaction 1.5 times faster ($k = 11.4 \times 10^{-2} \text{ M}^{-1} \text{ s}^{-1}$) than the parent compound **2.17** ($k = 7.59 \times 10^{-2} \text{ M}^{-1} \text{ s}^{-1}$) with $[\text{RhCl}(\text{C}_2\text{H}_4)_2]_2$, compared to an enhancement factor of 2.5 for $\text{RhCl}(\text{PPh}_3)_3$ (see Table 2).

Table 3. Linear free-energy relationships with $[\text{RhCl}(\text{C}_2\text{H}_4)_2]_2$

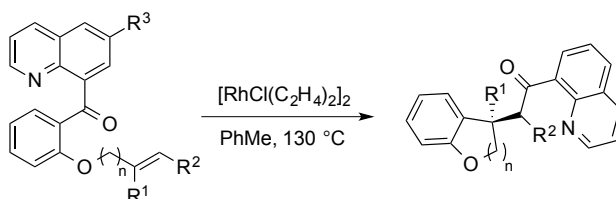


entry	R, substituent	yield (%)	$k (\text{M}^{-1} \text{s}^{-1} \times 10^{-2})$
1	H 2.17	96	7.59
2	3-OMe 2.71	91	7.11
3	4-OMe 2.72	87	9.69
4	4-NEt ₂ 2.74	93	11.4
5	5-NO ₂ 2.75	89	6.39
6	5-Cl 2.76	94	6.72

Mechanistically, $[\text{RhCl}(\text{C}_2\text{H}_4)_2]_2$ and $\text{RhCl}(\text{PPh}_3)_3$ differ only in the resting state of catalysis. The nature of the diminished reactivity of $\text{RhCl}(\text{PPh}_3)_3$ was therefore not apparent. Continued kinetic examination with regard to alkene substitution showed significant rate dependence. Substitution on the quinolinyl 6-position (Table 4, entry 2, **2.81**) with a mild electron-donating group gave rise to a slight increase in reaction rate. The added electron density presumably stabilizes the Rh(III) metallacycle intermediate by enhancing the coordinating ability of the quinoline nitrogen. This observation is in accordance with oxidative addition as the rate-limiting step. Replacing the vinyl methyl group in parent substrate **2.17** (entry 1) with a phenyl group (entry 3, **2.82**) resulted in a three-fold decrease in rate. With literature suggesting that reductive elimination for

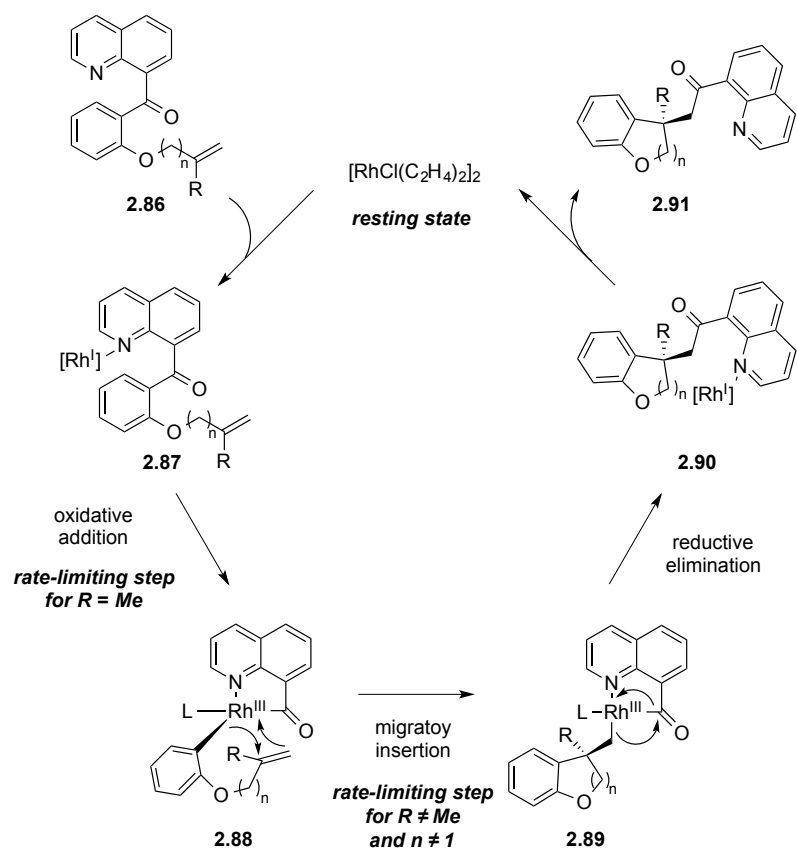
carbon–carbon bonds should be fast relative to oxidative addition and migratory insertion,¹⁰⁻¹² and the assumption that the alkene plays no role in oxidative addition, it was concluded that migratory insertion became rate-limiting for the phenyl substrate. With the general notion that five-membered ring cyclizations are kinetically more facile than six-membered ring cyclizations, the slower rate of homoallylic substrate **2.83** (entry 4) relative to the allylic substrate **2.17** (entry 1) is consistent with migratory insertion as rate-limiting for larger ring-forming reactions.

With 1,1-disubstituted alkenes shown to be optimal, Johnson considered 1,2-disubstituted alkene substrates (Table 4, entries 5 and 6) to target products containing two vicinal stereogenic centers. As mentioned before, these substrates failed to undergo reaction with $\text{RhCl}(\text{PPh}_3)_3$. Under $[\text{RhCl}(\text{C}_2\text{H}_4)_2]_2$ catalysis, substrates **2.84** and **2.85** underwent less than 5% conversion to product, returning mostly starting material as *cis:trans* isomers. The added steric environment (secondary vs. primary Rh–alkyl) post migratory insertion would undoubtedly make the resulting intermediate less stable. These results also imply migratory insertion as the highest energy step of the reaction.

Table 4. Alkene substitution effects on the rates of reaction with $[\text{RhCl}(\text{C}_2\text{H}_4)_2]_2$ 

entry	R ¹	R ²	R ³	n		yield (%)	<i>k</i> (M ⁻¹ s ⁻¹ × 10 ⁻²)
1	Me	H	H	1	2.17	96	7.59
2	Me	H	Me	1	2.81	94	7.90
3	Ph	H	H	1	2.82	91	2.62
4	Me	H	H	2	2.83	89	1.20
5	H	Me	H	1	2.84	<5	n/a
6	H	Ph	H	1	2.85	<5	n/a

The combination of the overall second-order rate law, activation parameters, and Hammett relationships for the intramolecular carboacylation of 2-methyl allylic substrate **2.17** with $[\text{RhCl}(\text{C}_2\text{H}_4)_2]_2$ indicate a free-catalyst resting state and oxidative addition as the rate-limiting step to catalysis (Scheme 37a). The substantial differences in rate based upon alterations made to the alkene appendage suggest a change in mechanism with the assumption that the alkene is not involved in the oxidative addition step. It is likely that migratory insertion becomes rate-limiting for carboacylation reactions producing dihydrobenzofuran **2.54** and dihydrobenzopyran **2.58** (see Figure 9). Unfortunately $^{12}\text{C}/^{13}\text{C}$ kinetic isotope effects were not determined for these derivatives. Observing isotope effects on both alkene carbons would provide further evidence suggesting migratory insertion as rate-limiting, whereas isotope effects on the terminal alkene carbon and ketone carbon would indicate reductive elimination as the slow step.

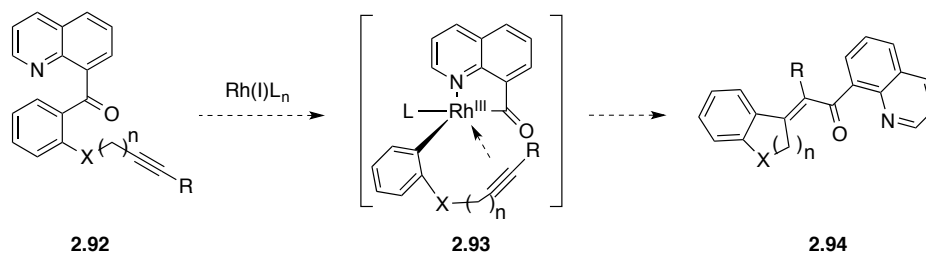


Scheme 37a. Mechanistic proposal for intramolecular carboacylation with $[\text{RhCl}(\text{C}_2\text{H}_4)_2]_2$

2.3 INTRAMOLECULAR CARBOACYLATION WITH ALKYNES

2.3.1 RESEARCH PROPOSAL

The C–C bond activation methodology with 8-acylquinonlines was further investigated to include carboacylation across alkynes. Alkynes typically bind more strongly to metal complexes than do alkenes and thus typically undergo carbometalation reactions faster. It was proposed that cyclization of propargyl substrates **2.92** would produce dihydrobenzofuran **2.94** containing an exocyclic olefin that would likely isomerize into an aromatic benzofuran system (Scheme 37b). With 1,2-disubstituted alkenes shown to be unreactive in carboacylation reactions (see Section 2.3.2, Table 4), the steric nature of internal alkynes may prove problematic.

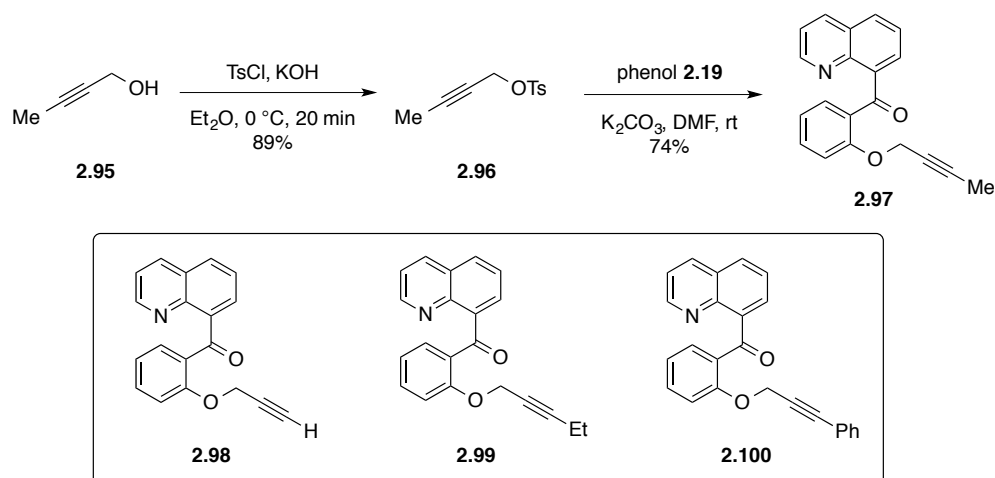


Scheme 37b. Proposed intramolecular carboacylation with alkynes

2.3.2 SUBSTRATE SYNTHESSES

The synthesis of propargyl ether substrate **2.97** was achieved by a straightforward alkylation of phenol **2.19** with tosylate **2.96**, which was prepared from the commercially available alcohol **2.95**. Substrates **2.98–2.100** alkynes were prepared in a similar manner (Scheme 38). The scope of the reaction was initially designed to be analogous to

previous work with alkenes including longer tethers, nitrogen and methylene linkers, and a pyrrole backbone. Attempts to prepare the one-carbon homologated derivatives **2.101** were unsuccessful owing to elimination of the propargylic tosylate electrophile; however, three-carbon analogues **2.102** were readily prepared and would provide 7-membered rings upon cyclization (Figure 10).^{xviii} The amino substrate **2.103** was prepared according to the route described in Section 2.2.1, Scheme 29. Several attempts to alkylate *o*-tolualdehyde (**2.44**) with various propargylic halides and tosylates were unsuccessful in the preparation of methylene-tethered alkyne substrates **2.105** (Scheme 39).



Scheme 38. Preparation of alkynyl substrates **2.97–2.100**

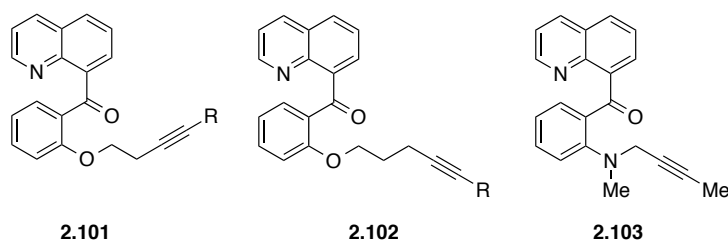
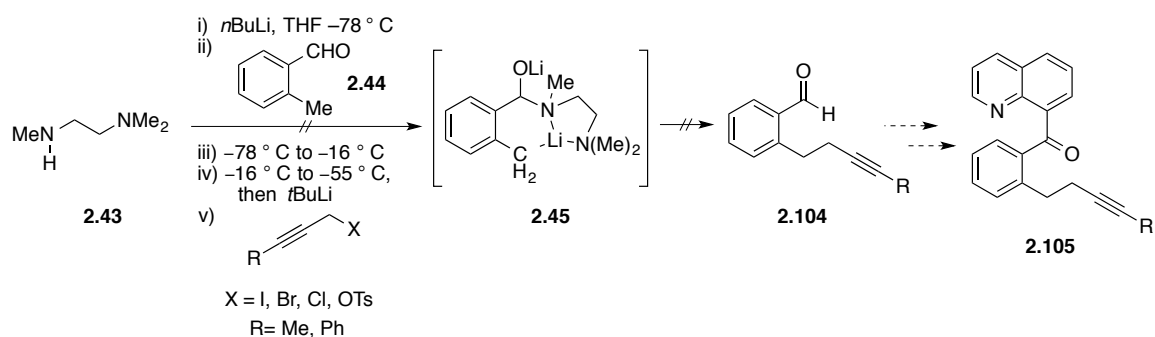


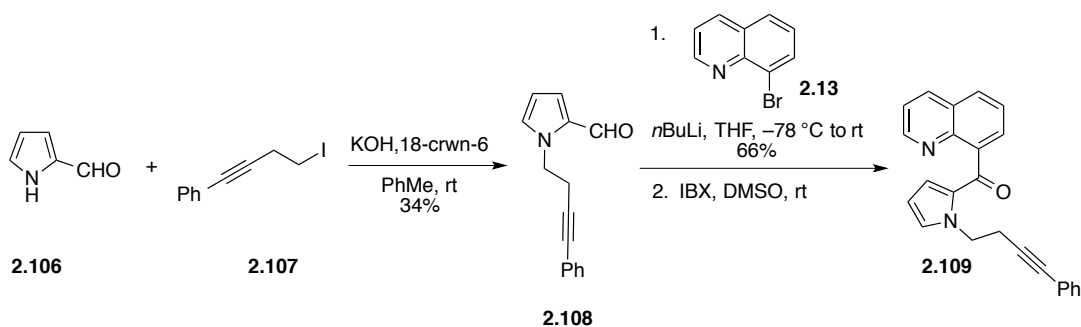
Figure 10. Homologated and amino substrates for carboacylation with alkynes

^{xviii} Substrates prepared by Michael Wentzel



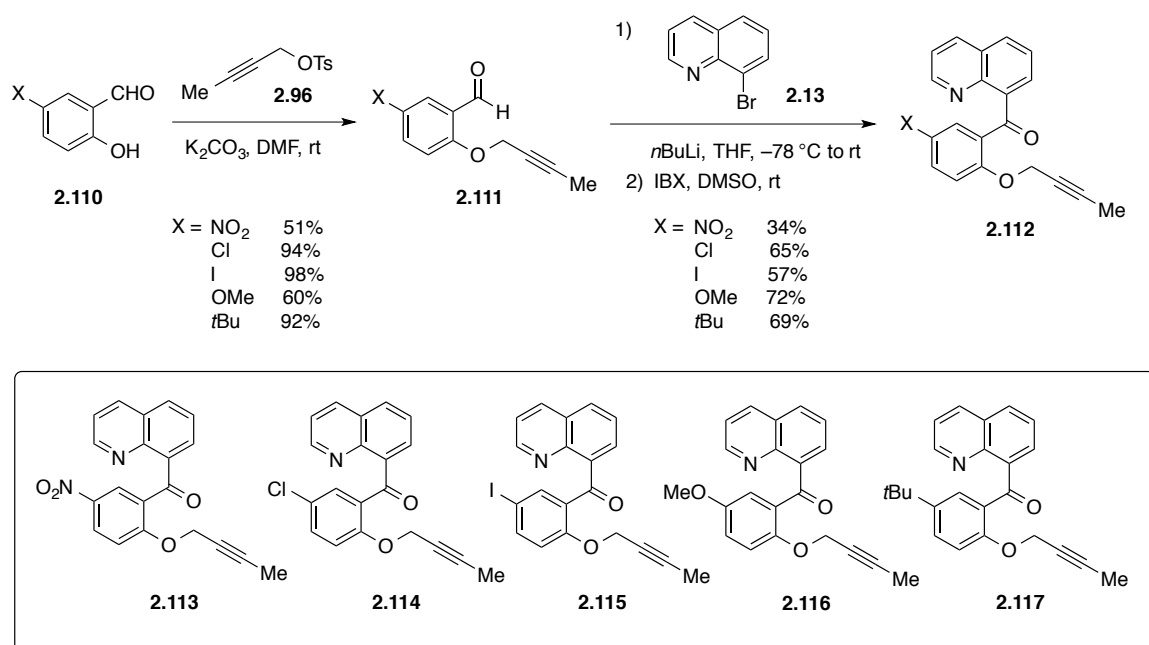
Scheme 39. Attempted synthesis of methylene-tethered alkyne substrates

Several attempts to alkylate 1*H*-pyrrole-2-carbaldehyde (**2.106**) were met with great difficulty owing to the propensity of homopropargylic electrophiles to undergo elimination to afford an enyne. It was found that **2.108** could be obtained in 34% yield by treating **2.106** with iodide **2.107** in a mixture of KOH and 18-crown-6 in toluene at room temperature (Scheme 40). Iodide **2.107** was readily prepared by a Sonogashira reaction between bromobenzene and homopropargyl alcohol, followed by iodination with I_2 , PPh_3 , and imidazole. Aldehyde **2.108** was added to the organolithium of 8-bromoquinoline (**2.13**) to give the corresponding secondary alcohol in 66% yield. The alcohol was oxidized with IBX to furnish the pyrrole substrate **2.109**.



Scheme 40. Preparation of alkyne substrate with a pyrrole backbone

We sought to investigate the electronic nature of the central aryl ring in analogy to Johnson's Hammett studies performed on the alkene derivatives (see Section 2.3, Tables 2 and 3). Substrates **2.113–2.117** were prepared from the commercially available aldehydes **2.110** (Scheme 41). Alkylations with tosylate **2.96** provided aldehydes **2.111** in good to excellent yields. The quinolone directing group was installed by a lithium-halogen exchange of 8-bromoquinoline, and the resulting alcohols were oxidized with IBX to give quinolinyl ketones **2.112** (**2.113–2.117**).



Scheme 41. Preparation of alkynyl substrates **2.113–2.117**

Phenyl alkyne substrates with various electron-donating and electron-withdrawing substituents were also prepared (**2.118–2.123**, Figure 11). Aryl halides **2.124** were cross-coupled (Sonogashira coupling) with propargyl alcohol with $\text{Pd(PPh}_3)_4$ and CuI in DMF at 80°C (Scheme 42a). The corresponding alcohols derived from 4-iodoaniline and 4-iodo-*N,N*-dimethylaniline failed to undergo the Sonogashira coupling reactions under

various conditions. Thus the amino groups were protected as the 2,5-dimethyl pyrrole upon refluxing with hexane-2,5-dione and TsOH in PhMe with a Dean-Stark trap prior to coupling. Tosylation of the alcohols provided compounds **2.125a–f**, which were susceptible to decomposition upon standing or column chromatography. Tosylates with electron-donating groups were especially unstable and were carried through the substitution with salicylaldehyde (**2.14**) crude. The quinoline directing group was installed on aldehydes **2.126a–f**, though an unexpected side reaction routinely complicated the oxidation of the resulting alcohols **2.127a–f**. Although purified alcohols were subjected to reaction with IBX, significant amounts (>40%) of the previous aldehydes **2.126a–f** were obtained! Unfortunately this unprecedented C–C bond cleavage event was not further investigated; however, comparing the ^1H NMR spectra of the IBX employed to that of freshly prepared IBX indicated that the former was contaminated with an unknown compound. Additionally, the amino-substituted alcohols **2.127e–f** were unable to be oxidized by either IBX or TPAP/NMO.

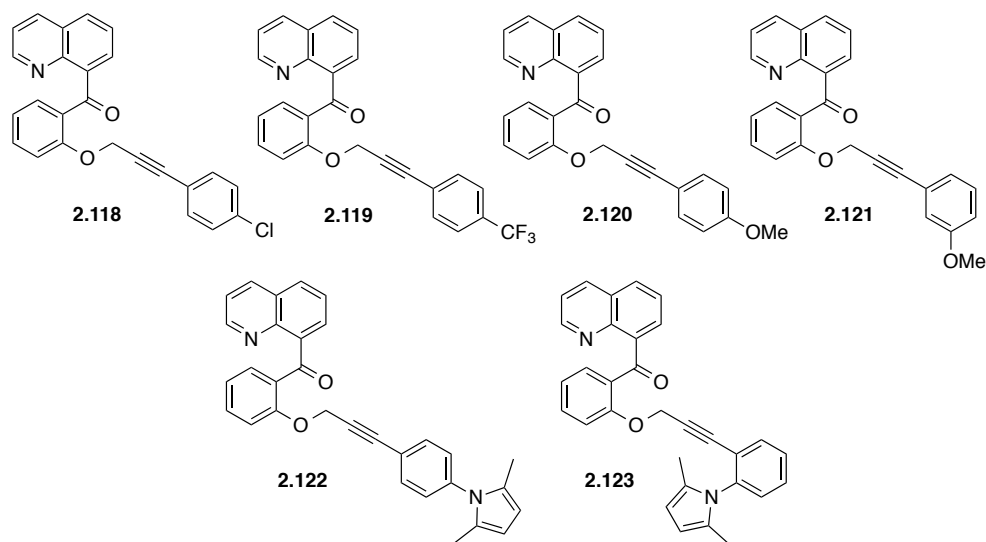
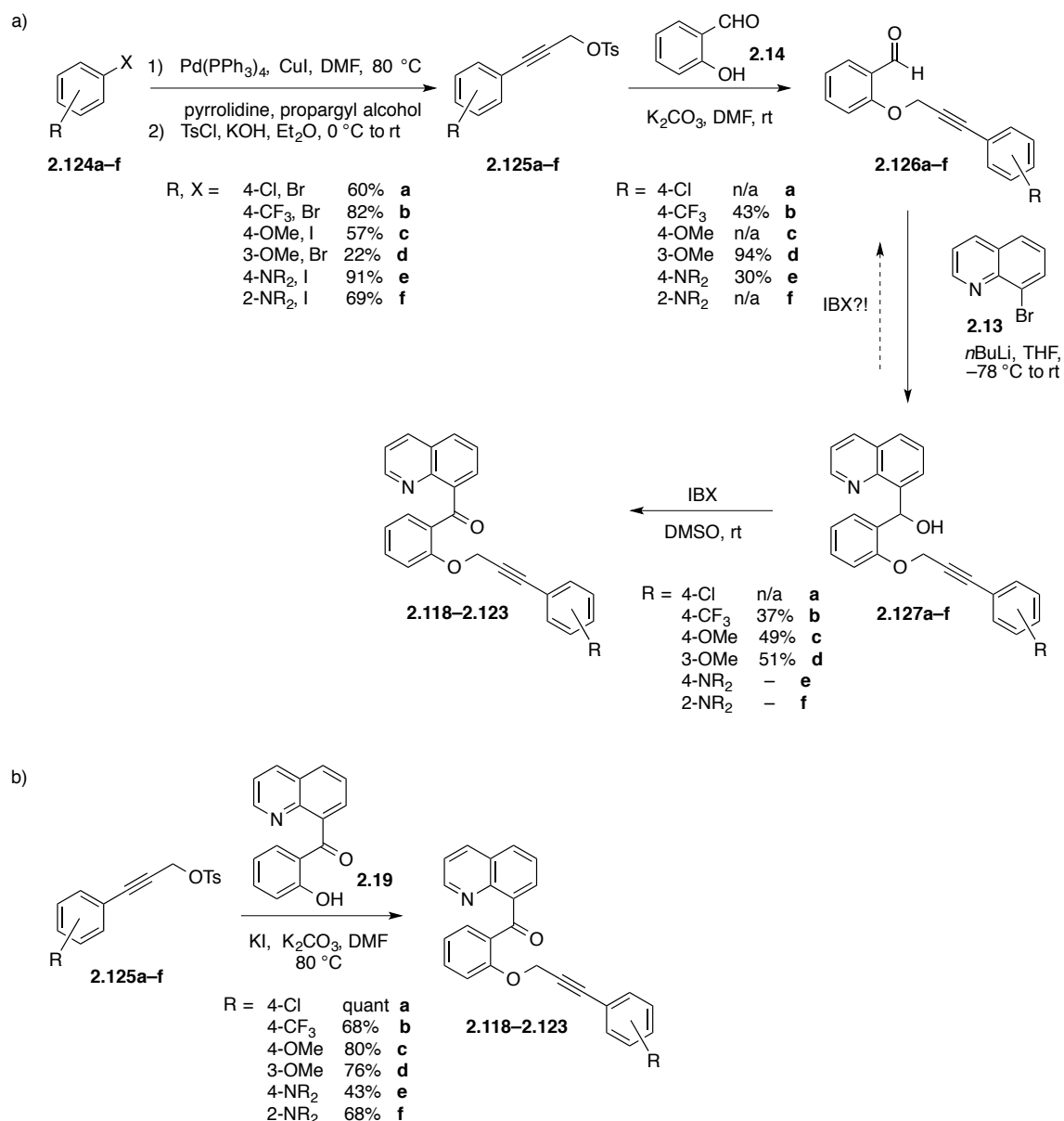


Figure 11. Phenyl alkyne substrate derivatives **2.118–2.123**



Scheme 42. Preparation of phenyl alkyne substrates. a) linear sequence b) divergent syntheses

The linear route to products (Scheme 42a) had been explored rather than the typical divergent phenol **2.19** alkylation route because these reactions were failing under the standard conditions with K_2CO_3 in DMF , even with heating. It was later discovered that an *in situ* Finkelstein reaction with KI at elevated temperatures afforded products in

acceptable yields (Scheme 42b), and thus the problematic oxidation was avoided and allowed for the construction of pyrrole-substituted substrates **2.122** and **2.123**.

2.4.3 RESULTS AND DISCUSSION

Reaction Optimization^{xix}

With optimal conditions determined for carboacylation with alkenes (see Section 2.1.3, Table 1) quinolinyl alkynes **2.97** and **2.98** were treated with $[\text{RhCl}(\text{C}_2\text{H}_4)_2]_2$ in PhMe at 130 °C for 48 h with no indication of product formation (**2.129**, **2.130**, **2.131**) (Table 5, entries 2 and 5). Reactions of **2.97**, **2.98**, and **2.100** with $\text{RhCl}(\text{PPh}_3)_3$ also failed to undergo the desired reaction (entries 1, 4, and 7), though the added steric hinderance of internal alkynes **2.97** and **2.100** limited the de-propargylative side-reaction (to give **2.19**) with this catalyst. Under $\text{Rh}(\text{cod})_2\text{OTf}$ catalysis, terminal alkyne **2.98** gave primarily **2.19** (entry 3), however internal alkyne **2.97** (R = Me) yielded a mixture of benzofuran **2.131**, phenol **2.19**, and unreacted **2.97** in a 45:50:5 ratio, respectively (entry 6). Internal alkyne **2.100** (R = Ph) failed to react with $\text{Rh}(\text{cod})_2\text{OTf}$ (entry 8). The vast differences in reactivity between alkenyl and alkynyl carboacylation reactions may be explained by the added strain in the transition state induced by the linearity of the alkyne moiety. It is plausible that the cationic nature of the $\text{Rh}(\text{cod})_2\text{OTf}$ complex may facilitate alkyne coordination owing to its relatively open coordination site.

With a functional catalyst in hand, optimization ensued with a solvent screening. Reaction of internal alkyne **2.97** with $\text{Rh}(\text{cod})_2\text{OTf}$ in relatively polar solvents PhCF_3 and DCE gave a 15–20% increase in conversion to the desired benzofuran **2.131** (entries 9,

^{xix} Reaction optimization was performed by Michael Wentzel.

10, and 11). Employing THF as solvent at 100 °C allowed for benzofuran **2.131** to be obtained almost exclusively as a 91:4:5 mixture (entry 12).

With optimized solvent and temperature conditions determined, the catalyst choice was re-examined. Both $[\text{RhCl}(\text{C}_2\text{H}_4)_2]_2$ and $\text{RhCl}(\text{PPh}_3)_3$ remained relatively inactive toward carboacylation with alkynes (entries 13 and 14). The cationic $\text{Rh}(\text{cod})_2\text{BF}_4$ complex was less efficient than $\text{Rh}(\text{cod})_2\text{OTf}$, giving product at 75% conversion (entry 15), whereas the analogous norbornadiene complex $\text{Rh}(\text{nbd})_2\text{BF}_4$ returned mostly starting material (entry 16).

Table 5. Reaction optimization for intramolecular carboacylation with alkynes

Entry	R	Catalyst ^c	Solvent	Temp	Pdt : 2.19 : SM ^{xx}
1	H	$\text{RhCl}(\text{PPh}_3)_3$	PhMe	130 °C	0 : 45 : 55
2	H	$[\text{RhCl}(\text{C}_2\text{H}_4)_2]_2$	PhMe	130 °C	0 : 20 : 80
3	H	$\text{Rh}(\text{cod})_2\text{OTf}$	PhMe	130 °C	0 : 90 : 10
4	Me	$\text{RhCl}(\text{PPh}_3)_3$	PhMe	130 °C	N.R.
5	Me	$[\text{RhCl}(\text{C}_2\text{H}_4)_2]_2$	PhMe	130 °C	0 : 15 : 75
6	Me	$\text{Rh}(\text{cod})_2\text{OTf}$	PhMe	130 °C	45 : 50 : 5
7	Ph	$\text{RhCl}(\text{PPh}_3)_3$	PhMe	130 °C	N.R.
8	Ph	$\text{Rh}(\text{cod})_2\text{OTf}$	PhMe	130 °C	N.R.
9	Me	$\text{Rh}(\text{cod})_2\text{OTf}$	PhCF_3	130 °C	60 : 40 : 0
10	Me	$\text{Rh}(\text{cod})_2\text{OTf}$	DCE	130 °C	65 : 35 : 0
11	Me	$\text{Rh}(\text{cod})_2\text{OTf}$	DCE	100 °C	70 : 20 : 10
12	Me	$\text{Rh}(\text{cod})_2\text{OTf}$	THF	100 °C	91 : 5 : 4
13	Me	$\text{RhCl}(\text{PPh}_3)_3$	THF	100 °C	3 : 22 : 75
14	Me	$[\text{RhCl}(\text{C}_2\text{H}_4)_2]_2$	THF	100 °C	5 : 25 : 70
15	Me	$\text{Rh}(\text{cod})_2\text{BF}_4$	THF	100 °C	75 : 8 : 17
16	Me	$\text{Rh}(\text{nbd})_2\text{BF}_4$	THF	100 °C	10 : 10 : 80

^{xx} Relative ratio determined by ^1H NMR spectroscopy. ‘Relative ratio’ is assumed instead of ‘quantitative yield’ as had been reported previously.

Substrate Scope

Before the results for this section are discussed, some ongoing complications with this project should be mentioned. As was alluded to in the preceding section, some unexplained discrepancies in data collection, interpretation, and calculations were encountered that grossly offset the trajectory of this project. Although many of the ^1H NMR of crude product mixtures appeared to contain 1–3 products, the major component being the desired benzofuran, the calculated yields based on an internal standard did not reflect what would have been expected based on product ratios. Isolated yields were in accordance with what was measured in these ^1H NMR yield calculation studies. While it was possible that these compounds could be decomposing during purification by silica gel chromatography, other measures were taken to ensure accuracy. The balances were recalibrated and a de-static ring was introduced. The accuracy of the balances, method of calculation, and general technique were evaluated by weighing known amounts of a chemical into an NMR tube with an internal standard. This exercise was also performed with liquid chemicals based upon volume. Several individuals performed these calibration exercises and also confirmed the calculations. It was speculated that material may not have been completely transferred to the NMR tube, so the reactions were ran in a sealed NMR tube with THF-*d*8. The non-parenthetical values listed in Figure 12 reflect the values I obtained from ^1H NMR spectroscopy with a $d_1=25$ and 4-methoxy acetophenone as an internal standard.

For comparison, entry 12 in Table 5 was repeated, though performed in an NMR tube rather than in a 1-dram vial. Solid **2.97** and $\text{Rh}(\text{cod})_2\text{OTf}$ were weighed directly into the NMR tube and THF-*d*8 was added. The tube was sealed, placed in an oil bath in

the glovebox, and heated for 48 h. The reaction was cooled, and solid 4-methoxy acetophenone was weighed directly into the NMR tube. With a $d1=25$, the ^1H NMR spectrum showed yields of benzofuran **2.131**, phenol **2.19**, and alkyne **2.97** in 39%, 18%, and 22% yield, respectively. Upon closer inspection, it appeared that several additional resonances might be hidden in the baseline.

With optimal conditions in hand, the scope of the reaction was investigated. The more sterically-hindered ethyl alkyne **2.99** underwent the desired reaction to give benzofuran **2.133**. Benzofuran **2.134** ($R=\text{Ph}$) appeared to form less efficiently, though calculations revealed a comparable 34% yield by ^1H NMR spectroscopy with internal standard (isolated yield = 24%). The addition of a *para* electron-withdrawing group ($R^3 = \text{Cl}$ **2.123**, CF_3 **2.124**) did not affect the outcome of the reaction; benzofurans **2.135** ($R^3 = \text{Cl}$) and **2.136** ($R^3 = \text{CF}_3$) were obtained in 32% and 42% yield, respectively. The parenthetical values for **2.135** and **2.136** reflect a ^1H NMR “yield” based upon mole ratio between products, phenol **2.19**, and starting material. The collection of this data used the default delay parameter of $d1=1$, and no internal standard was used. Incorporating a *para* electron-donating methoxy group (**2.125**) unexpectedly inhibited the reaction, giving only trace amount of benzofuran **2.137** and phenol **2.19**. However, a *meta*-methoxy group allowed cyclization to proceed, although in low conversion (**2.138**). An electron-donating *para*-pyrrole group (**2.127**), though less donating due to its aromatic nature, underwent carboacylation to provide **2.139** in 30% yield, whereas the *ortho*-pyrrole **2.128** returned only starting material and phenol.

Substitution on the aryl backbone gave varying results that did not coincide with the analogous reactions with alkenes (see Section 2.3, Tables 2 and 3). Although iodide

substitution (**2.115**) successfully underwent the desired reaction to give benzofuran **2.141**, the corresponding chloride (**2.114**) was inactive toward catalysis. The nitro substituted substrate **2.113** favored depropargylation to provide phenol **2.19** as the major product, which is likely due to the resonance stabilization afforded by the nitro group. In the analogous reactions with alkenes, both chloro- and nitro- substituted substrates underwent carboacylation in excellent yields. Substrates substituted with electron-donating groups ($R^1 = \text{OMe}$ **2.116**, $t\text{Bu}$ **2.117**) however, were better suited for the desired transformation. Benzofuran **2.145** ($R^2 = t\text{Bu}$) was obtained in 41% yield.

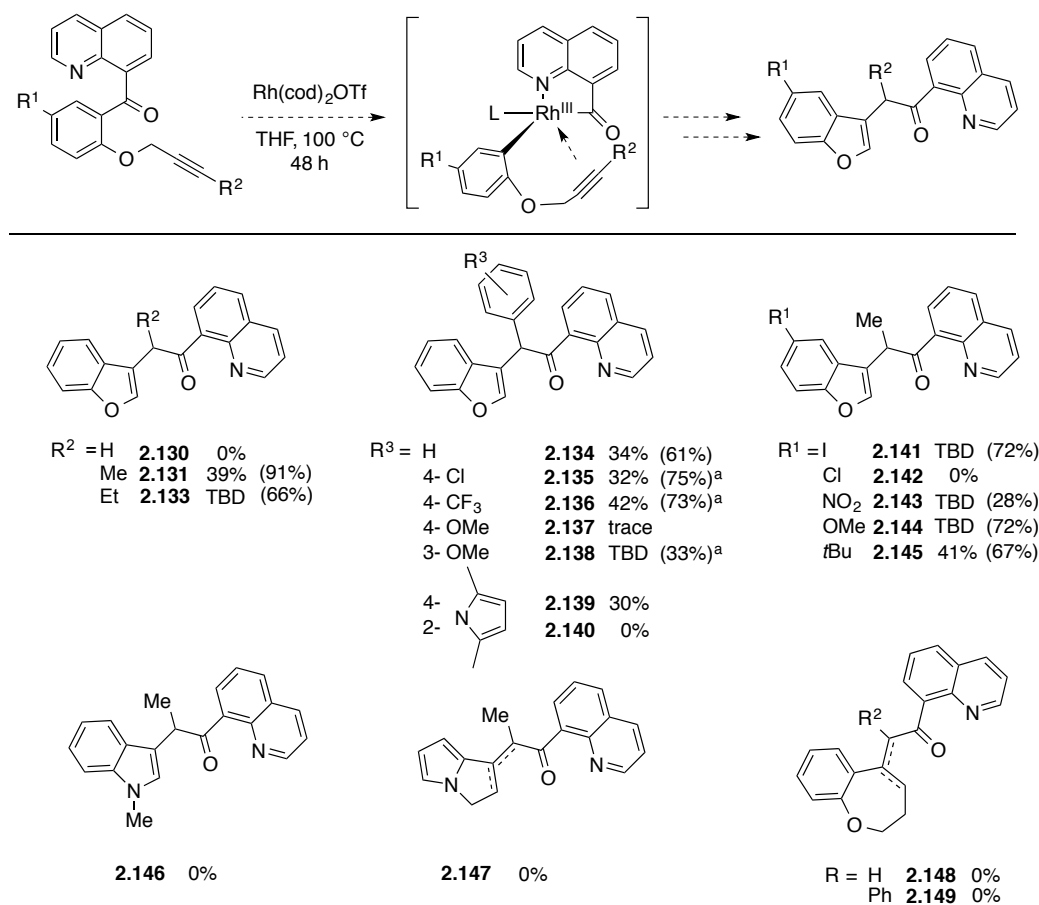


Figure 12. Product yields of intramolecular carboacylation with alkynes by ^1H NMR spectroscopy. Parenthetical values presumed to be based on ^1H NMR product ratios conducted by Michael Wentzel. ^aParenthetical values *known* to be based on ^1H NMR product ratios obtained without determining the longest T_1 value and thus not setting a $d1$ to $5 \times T_1$ – experiments conducted by myself

The anthranilic ketone derivative **2.103** did not provide indole **2.146** upon heating with Rh(cod)₂OTf. This observation was not surprising in that reaction with the analogous alkene required a more nucleophilic catalyst (see Section 2.1.1.2, Figure 9). Pyrrolizine **2.147** and benzoxepine derivatives **2.148–2.149** were also not observed.^{xxi}

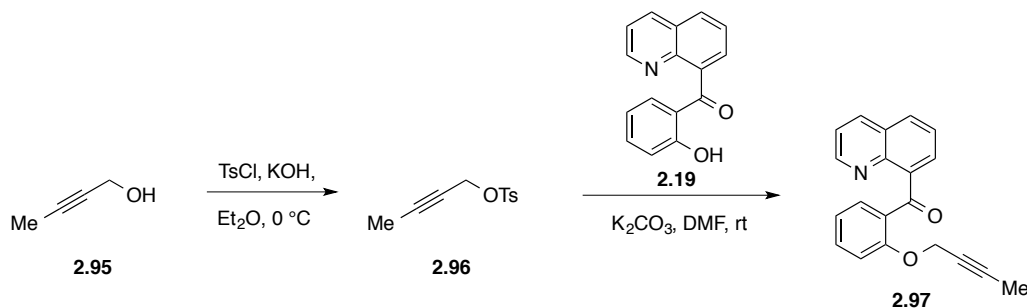
2.3.4 CONCLUDING REMARKS

It is apparent that intramolecular carboacylation with alkynes is less favorable than with alkenes. The nature of the missing mass in these reactions will require evaluation by additional analytical methods in order to generate a complete understanding of the reaction profile. Gaining knowledge about the side-product structure(s) may lead to a better understanding of such decomposition pathways and thus allow for better catalyst and/or ligand design in order to favor carboacylation.

Although alkynes complex more strongly to transition metals and generally undergo carbometallation more readily than alkenes, it is likely that the linearity of the alkyne introduces strain in the ensuing complex for this system. Should this hypothesis be correct, perhaps developing a bimetallic system or complex that could serve to facilitate migratory insertion may be of interest.

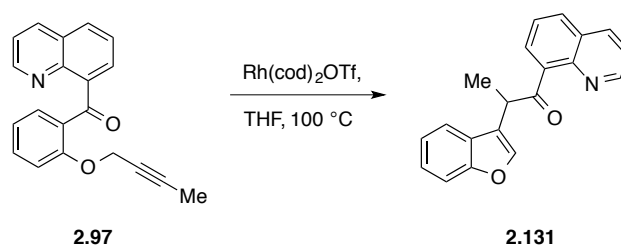
^{xxi} Carboacylation reactions to produce 5-chlorobenzofuran **2.142**, indole **2.146** and benzoxepines **2.148–2.149** were performed by Michael Wentzel.

2.3.5 EXPERIMENTAL

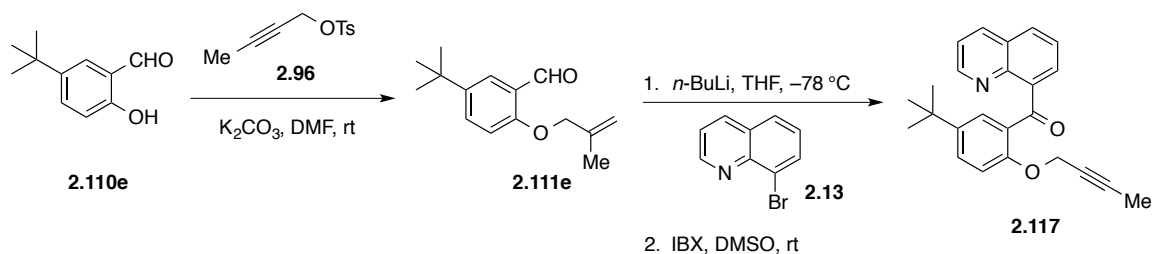


But-2-yn-1-ol (**2.95**) (2.13 mL, 28.53 mmol) and Et₂O (30 mL) were combined in a flask and cooled with an ice bath. Tosyl chloride (5.44 g, 28.53 mmol) and potassium hydroxide (16.0 g, 285.3 mmol), were added and the resulting mixture was stirred at 0 °C for 15 min before removing the ice bath and stirred for 2 h at room temperature. The mixture was transferred to a separatory funnel with Et₂O and water was added (exotherm). The organic layer was washed with water (2 × 100 mL), the aqueous layer was back extracted with Et₂O (2 × 100 mL), and the combined organic layers were washed with brine, dried over Na₂SO₄, filtered, and concentrated. The crude mixture was pure by NMR and the yellow crystalline tosylate **2.96** (5.71 g, 25.46 mmol, 89%) was taken on to the next step. *R_f* 0.35 (1:4 EtOAc:Hex). Phenol **2.19** (300 mg, 1.20 mmol), tosylate **2.96** (269 mg, 1.20 mmol), potassium carbonate (498 mg, 3.60 mmol), and DMF (6 mL) were combined in a flask and stirred at room temperature for 48 h. Water and EtOAc were added to the reaction. The organic layer was washed with water (2 × 100 mL), 2M LiCl, brine, dried over Na₂SO₄, filtered, and concentrated. The crude product was purified by flash chromatography (EtOAc:Hex) to give ketone **2.97** (267 mg, 0.89 mmol, 74%) as a yellow oil: *R_f* 0.14 (1:4 EtOAc:Hex); ¹H NMR (300 MHz, CDCl₃) δ 8.76 (dd, *J* = 4.2, 1.8 Hz, 1H), 8.15 (dd, *J* = 8.3, 1.8 Hz, 1H), 7.90 (app td, *J* = 7.9, 1.6 Hz,

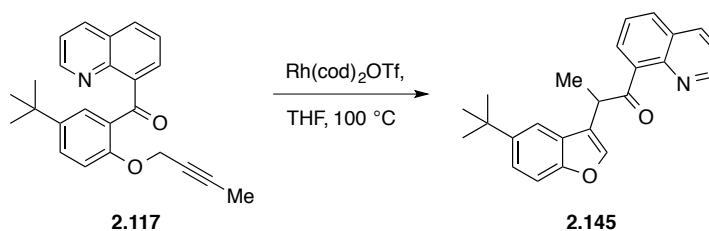
2H), 7.78 (dd, $J = 7.1, 1.5$ Hz, 1H), 7.57 (dd, $J = 8.1, 7.2$ Hz, 1H), 7.47 (ddd, $J = 8.3, 7.3, 1.8$ Hz, 1H), 7.35 (dd, $J = 8.3, 4.2$ Hz, 1H), 7.08 (td, $J = 7.5, 0.8$ Hz, 1H), 6.95-6.92 (m, 1H), 4.08 (q, $J = 2.3$ Hz, 2H), 1.67 (t, $J = 2.3$ Hz, 3H); ^{13}C NMR (75 MHz; CDCl_3) δ 196.8, 157.6, 150.3, 146.1, 141.8, 135.8, 133.7, 131.3, 129.8, 129.7, 128.3, 128.0, 126.0, 121.3, 121.3, 113.7, 83.3, 73.2, 56.9, 3.7; IR (film) 3044, 2919, 2349, 1626, 1251 cm^{-1} ; HRMS (ESI) m/z calcd for $[\text{C}_{20}\text{H}_{15}\text{NO}_2 + \text{Na}]^+$ 324.1000, found 324.1033.



R_f 0.34 (1:4 EtOAc:Hex); ^1H NMR (500 MHz; CDCl_3): δ 8.99 (dd, $J = 4.2, 1.8$ Hz, 1H), 8.17 (dd, $J = 8.3, 1.8$ Hz, 1H), 7.85 (dd, $J = 8.1, 1.4$ Hz, 1H), 7.69 (dd, $J = 7.1, 1.5$ Hz, 1H), 7.57 (d, $J = 7.2$ Hz, 1H), 7.47-7.43 (m, 3H), 7.39 (d, $J = 8.2$ Hz, 1H), 7.23-7.22 (m, 1H), 7.18-7.17 (m, 1H), 5.57 (q, $J = 7.1$ Hz, 1H), 1.71 (d, $J = 7.1$ Hz, 3H). ^{13}C NMR (125 MHz, CDCl_3) δ 206.3, 153.5, 150.6, 124.7, 142.4, 139.3, 136.5, 131.0, 129.9, 128.3, 126.2, 124.3 (2C), 122.5, 121.7, 120.5, 120.4, 111.6, 43.6, 16.9; IR (film) 2983, 2923, 1683, 1453 cm^{-1} ; HRMS (ESI) m/z calcd for $[\text{C}_{20}\text{H}_{15}\text{NO}_2 + \text{Na}]^+$ 324.1000, found 324.1045.

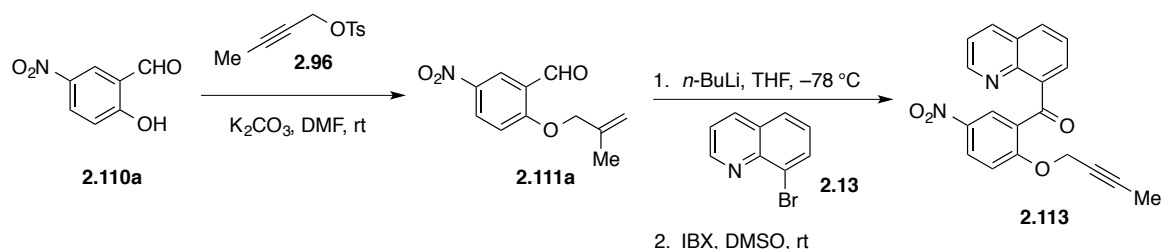


^1H NMR (500 MHz; CDCl_3) δ 8.80 (dd, $J = 4.2, 1.8$ Hz, 1H), 8.16 (dd, $J = 8.3, 1.8$ Hz, 1H), 8.03 (d, $J = 2.6$ Hz, 1H), 7.87 (dd, $J = 8.2, 1.4$ Hz, 1H), 7.72 (dd, $J = 7.1, 1.4$ Hz, 1H), 7.56 (dd, $J = 8.1, 7.1$ Hz, 1H), 7.50 (dd, $J = 8.7, 2.7$ Hz, 1H), 7.37 (dd, $J = 8.3, 4.2$ Hz, 1H), 6.86 (d, $J = 8.7$ Hz, 1H), 4.00 (q, $J = 2.3$ Hz, 2H), 1.67 (t, $J = 2.3$ Hz, 3H), 1.34 (s, 9H); ^{13}C NMR (75 MHz, CDCl_3) δ 196.3, 155.3, 149.7, 145.5, 143.3, 141.9, 135.2, 130.6, 128.7, 127.9, 127.41, 127.4, 127.0, 125.4, 120.6, 112.9, 82.4, 72.8, 59.9, 56.4, 33.8, 30.9, 20.5, 20.5, 13.7; IR (thin film) 3044, 2961, 2866, 2244, 1652, 1495, 1262 cm^{-1} ; HRMS (ESI) m/z calcd for $[\text{C}_{24}\text{H}_{23}\text{NO}_2 + \text{Na}]^+$ 380.1626, found 380.1635.



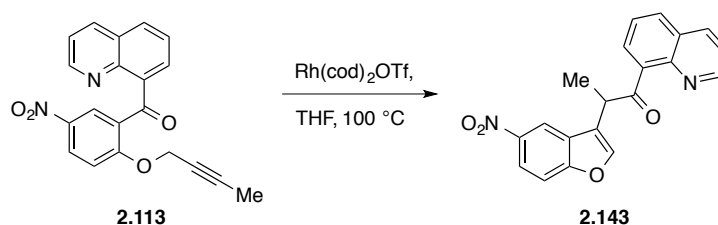
R_f 0.40 (1:4 EtOAc:Hex); ^1H NMR (500 MHz, CDCl_3) δ 9.01 (dd, $J = 4.2, 1.7$ Hz, 1H), 8.18 (dd, $J = 8.3, 1.8$ Hz, 1H), 7.85 (dd, $J = 8.1, 1.4$ Hz, 1H), 7.67 (dd, $J = 7.1, 1.3$ Hz, 1H), 7.48-7.46 (m, 1H), 7.44 (dd, $J = 5.6, 2.3$ Hz, 3H), 7.29-7.28 (m, 2H), 5.54 (q, $J = 7.1$ Hz, 1H), 1.72 (d, $J = 7.1$ Hz, 3H), 1.28 (s, 9H); ^{13}C NMR (75 MHz, CDCl_3) δ 206.8, 153.6, 150.6, 145.68, 145.5, 142.5, 139.5, 136.4, 130.8, 129.8, 128.2, 126.2, 122.2, 121.6,

120.6, 116.4, 110.7, 43.4, 34.8, 31.9 (3C), 16.8; IR (thin film) 2961, 2869, 1699, 1557, 796 cm^{-1} ; HRMS (ESI) m/z calcd for $[\text{C}_{24}\text{H}_{23}\text{NO}_2 + \text{Na}]^+$ 380.1626, found 380.1623.

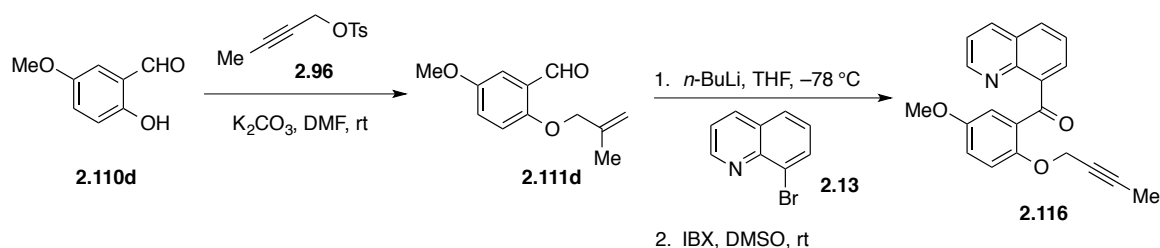


2-hydroxy-5-nitrobenzaldehyde (**2.110a**) (300mg, 1.8 mmol), tosylate (**2.96**) (404 mg, 1.80 mmol), K_2CO_3 (448 mg, 3.24 mmol), and DMF (9 mL) were added to a flask and stirred overnight at room temperature. The reaction mixture was diluted with water and EtOAc was added. The organic layer was washed with water (2×100 mL), LiCl, brine, and dried over Na_2SO_4 , filtered, and concentrated. The crude product was purified by flash chromatography (EtOAc:Hex) to give ether **2.111a** (251 mg, 1.13 mmol, 51%) as a colorless solid: R_f 0.35 (1:4 EtOAc:Hex). 8-bromoquinoline (**2.13**) (290 mg, 1.39 mmol) and THF (8 mL) were added to a flame-dried flask under N_2 and cooled to -78 °C. To the solution was added n -BuLi (2.5M, 0.65 mL, 1.62 mmol) dropwise and the reaction was allowed to stir at -78 °C for 45 min. Aldehyde **2.111a** (251 mg, 1.15 mmol) was added slowly as a solution in THF (10 mL). The reaction was allowed to come to room temperature overnight. The reaction was quenched with sat. NH_4Cl and EtOAc was added. The aqueous layer was back extracted with EtOAc and the combined organic layers were washed with brine, dried over Na_2SO_4 , filtered, and concentrated. The crude product was purified by flash chromatography (EtOAc:Hex) to give the corresponding alcohol (138 mg, 0.39 mmol, 34%): R_f 0.12 (1:4 EtOAc:Hex). A flask

was charged with the alcohol (138 mg, 0.39 mmol), IBX (335 mg, 1.20 mmol), and DMSO (3 mL). The reaction was stirred at room temperature for 3 h. Water and EtOAc were added and was stirred for 10 min. The solids were filtered and the layers separated. The organic layer was washed with water, brine, and dried over Na₂SO₄, filtered, and concentrated. The crude product was purified by flash chromatography to give ketone **2.113**: *R_f* 0.29 (1:4 EtOAc:Hex); ¹H NMR (400 MHz, CDCl₃) δ 8.72 (d, *J* = 2.9, 1H), 8.68 (dd, *J* = 4.3, 1.7 Hz, 1H), 8.37–8.35 (m, 1H), 8.20 (d, *J* = 8.3 Hz, 1H), 7.99–7.95 (m, 2H), 7.65 (d, *J* = 7.3 Hz, 1H), 7.39 (dd, *J* = 8.3, 4.2 Hz, 1H), 7.03 (d, *J* = 9.2 Hz, 1H), 4.20 (app t, *J* = 2.2 Hz, 2H), 1.71 (app t, *J* = 2.3 Hz, 3H); ¹³C NMR (75 MHz, CDCl₃) δ 194.6, 161.4, 150.3, 141.7, 139.7, 136.2, 133.0, 131.7, 131.1, 129.7, 128.4, 128.0, 127.9, 126.8, 121.6, 113.1, 84.8, 71.8, 57.3, 3.7; IR (thin film) 3078, 2922, 2230, 1652, 1339, 1278 cm⁻¹; HRMS (ESI) *m/z* calcd for [C₂₀H₁₄N₂O₄ + Na]⁺ 369.0851, found 369.0834.

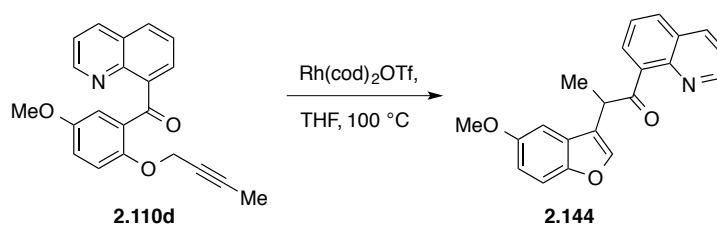


R_f 0.31 (1:4 EtOAc:Hex); ¹H NMR (300 MHz; CDCl₃) δ 9.12 (dd, *J* = 4.2, 1.8 Hz, 1H), 8.86 (d, *J* = 2.4 Hz, 1H), 8.22 (m, 2H), 7.96 (dd, *J* = 8.1, 1.5 Hz, 1H), 7.83 (dd, *J* = 7.1, 1.5 Hz, 1H), 7.74 (s, 1H), 7.59–7.50 (m, 3H), 5.67–5.62 (m, 1H), 1.68 (d, *J* = 7.3 Hz, 3H); ¹³C NMR (75 MHz; CDCl₃) δ 201.2, 153.1, 145.7 (2C), 140.5, 140.3, 133.4, 131.4, 126.3, 124.9, 123.2, 123.1, 121.1, 116.8, 115.1, 112.9, 106.7, 38.1, 24.7, 12.1; IR (thin film) 2934, 2910, 2846, 1699, 1516, 1342 cm⁻¹; HRMS (ESI) *m/z* calcd for [C₂₀H₁₄N₂O₄ + Na]⁺ 369.0851, found 369.0814.

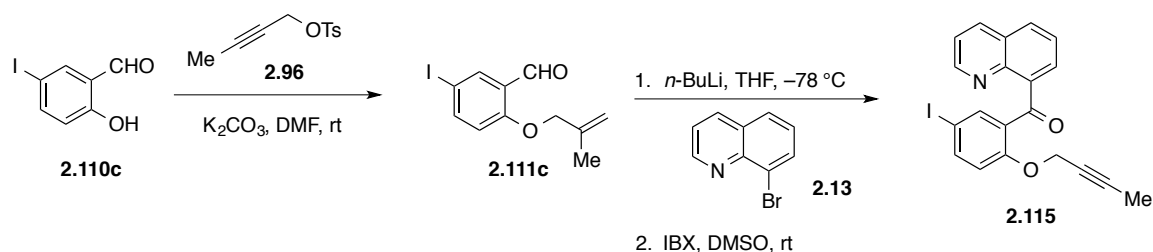


2-hydroxy-5-methoxybenzaldehyde (**2.110d**) (0.25 mL, 1.97 mmol), tosylate (**2.96**) (442 mg, 1.97 mmol), K_2CO_3 (817 mg, 5.19 mmol), and DMF (10 mL) were added to a flask and stirred overnight at room temperature. The reaction mixture was diluted with water and EtOAc was added. The organic layer was washed with water (2×100 mL), LiCl, brine, and dried over Na_2SO_4 , filtered, and concentrated. The crude product was purified by flash chromatography (EtOAc:Hex) to give ether **2.111d** (243 mg, 1.18 mmol, 60%) as an orange solid. R_f 0.41 (1:4 EtOAc:Hex). 8-bromoquinoline (**2.13**) (296 mg, 1.43 mmol) and THF (8 mL) were added to a flame-dried flask under N_2 and cooled to $-78\text{ }^\circ\text{C}$. To the solution was added *n*-BuLi (2.5M, 0.7 mL, 1.66 mmol) dropwise and the reaction was allowed to stir at $-78\text{ }^\circ\text{C}$ for 45 min. Aldehyde **2.111d** (243mg, 1.19 mmol) was added slowly as a solution in THF (10 mL). The reaction was allowed to come to room temperature overnight. The reaction was quenched with sat. NH_4Cl and EtOAc were added. The aqueous layer was back extracted with EtOAc and the combined organic layers were washed with brine, dried over Na_2SO_4 , filtered, and concentrated. The crude product was purified by flash chromatography (EtOAc:Hex) to give the corresponding alcohol (363 mg, 1.10 mmol, 92%): R_f 0.15 (1:4 EtOAc:Hex). A flask was charged with the alcohol (363 mg, 1.10 mmol), IBX (915 mg, 3.27 mmol), and DMSO (7.3 mL). The reaction was stirred at room temperature for 3 h. Water and EtOAc were added and was stirred for 10 min. The solids were filtered and

the layers separated. The organic layer was washed with water, brine, and dried over Na_2SO_4 , filtered, and concentrated. The crude product was purified by flash chromatography to give ketone **2.116**: R_f 0.10 (1:4 EtOAc:Hex); ^1H NMR (300 MHz, CDCl_3) δ 8.64 (dd, $J = 4.2, 1.8$ Hz, 1H), 8.02–7.99 (m, 1H), 7.73 (dd, $J = 8.2, 1.4$ Hz, 1H), 7.61 (dd, $J = 7.1, 1.5$ Hz, 1H), 7.41 (dd, $J = 8.0, 7.2$ Hz, 1H), 7.35 (d, $J = 3.2$ Hz, 1H), 7.21 (dd, $J = 8.3, 4.2$ Hz, 1H), 6.88 (dd, $J = 9.0, 3.2$ Hz, 1H), 6.74 (d, $J = 9.0$ Hz, 1H), 3.79 (q, $J = 2.3$ Hz, 2H), 3.67 (s, 3H), 1.50 (t, $J = 2.3$ Hz, 3H); ^{13}C NMR (75 MHz, CDCl_3): δ 194.1, 151.8, 149.7, 148.0, 143.6, 139.4, 133.6, 128.0, 127.3, 125.8, 125.6, 123.6, 119.0, 118.1, 113.8, 111.9, 80.7, 71.1, 55.6, 53.5, 1.3; IR (thin film) 3010, 2953, 2242, 1652, 1494, 1284, 1216 cm^{-1} ; HRMS (ESI) m/z $[\text{C}_{21}\text{H}_{17}\text{NO}_3 + \text{Na}]^+$ 354.1106, found 354.1111.

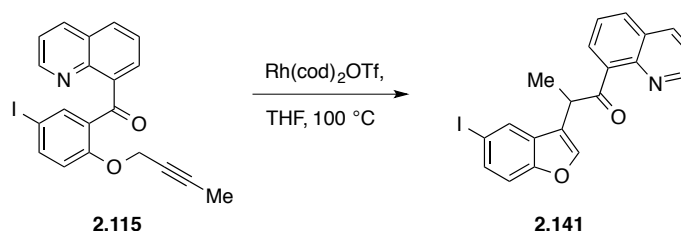


R_f 0.35 (1:4 EtOAc:Hex); ^1H NMR (300 MHz; CDCl_3) δ 9.00 (dd, $J = 4.2, 1.8$ Hz, 1H), 8.19 (dd, $J = 8.3, 1.8$ Hz, 1H), 7.87 (dd, $J = 8.2, 1.5$ Hz, 1H), 7.69 (dd, $J = 7.1, 1.5$ Hz, 1H), 7.49–7.42 (m, 3H), 7.29 (m, 1H), 7.00 (d, $J = 2.6$ Hz, 1H), 6.83 (dd, $J = 8.8, 2.6$ Hz, 1H), 5.56–5.49 (m, 1H), 3.76 (s, 3H), 1.70 (d, $J = 7.1$ Hz, 3H); ^{13}C NMR (75 MHz; CDCl_3): δ 206.1, 155.9, 155.4, 150.5, 143.1, 139.4, 136.4, 131.0, 129.9, 128.2, 127.5, 126.2, 124.2, 122.5, 121.6, 120.6, 118.3, 111.5, 50.7, 24.6, 12.4; IR (thin film) 2957, 2922, 1699, 1474 cm^{-1} ; HRMS (ESI) m/z calcd for $[\text{C}_{21}\text{H}_{17}\text{NO}_3 + \text{Na}]^+$ 354.1106, found 354.1098.

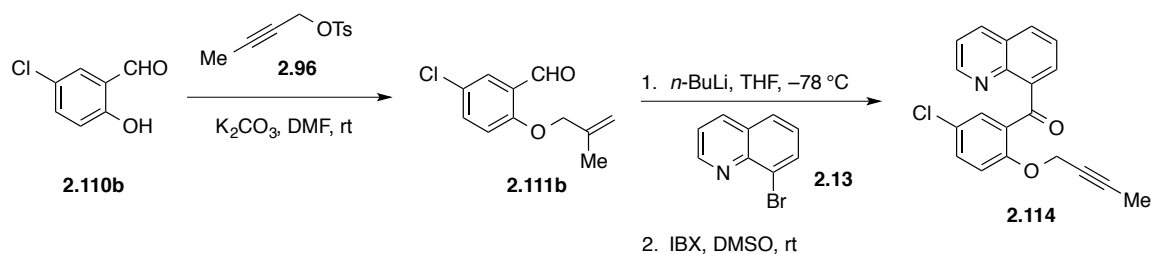


2-hydroxy-5-iodobenzaldehyde (**2.110c**) (300 mg, 1.21 mmol), tosylate (**2.96**) (271 mg, 1.21 mmol), K_2CO_3 (502 mg, 3.63 mmol), and DMF (6 mL) were added to a flask and stirred overnight at room temperature. The reaction mixture was diluted with water and EtOAc was added. The organic layer was washed with water (2×100 mL), LiCl, brine, and dried over Na_2SO_4 , filtered, and concentrated. The NMR of the crude ether **2.111c** was relatively pure and the product was taken on without purification (356 mg, 1.18 mmol, 98%) as a yellow oil: R_f 0.50 (1:4 EtOAc:Hex). 8-bromoquinoline (**2.13**) (296 mg, 1.42 mmol) and THF (8 mL) were added to a flame-dried flask under N_2 and cooled to $-78\text{ }^\circ\text{C}$. To the solution was added $n\text{-BuLi}$ (2.5M, 0.7 mL, 1.66 mmol) dropwise and the reaction was allowed to stir at $-78\text{ }^\circ\text{C}$ for 45 min. Aldehyde **2.111c** (356 mg, 1.19 mmol) was added slowly as a solution in THF (10 mL). The reaction was allowed to come to room temperature overnight. The reaction was quenched with sat. NH_4Cl and EtOAc were added. The aqueous layer was back extracted with EtOAc and the combined organic layers were washed with brine, dried over Na_2SO_4 , filtered, and concentrated. The crude product was purified by flash chromatography (EtOAc:Hex) to give the corresponding alcohol (289 mg, 0.68 mmol, 57%) as an orange film: R_f 0.20 (1:4 EtOAc:Hex). A flask was charged with the alcohol (289 mg, 0.68 mmol), IBX (566 mg, 2.02 mmol), and DMSO (4.5 mL). The reaction was stirred at room temperature for 3 h. Water and EtOAc were added and was stirred for 10 min. The

solids were filtered and the layers separated. The organic layer was washed with water, brine, and dried over Na₂SO₄, filtered, and concentrated. The crude product was purified by flash chromatography to give ketone **2.115**: *R_f* 0.29 (1:4 EtOAc:Hex); ¹H NMR (300 MHz; CDCl₃) δ 8.75 (dd, *J* = 4.2, 1.8 Hz, 1H), 8.17 (dd, *J* = 7.4, 2.1 Hz, 2H), 7.92 (dd, *J* = 8.2, 1.4 Hz, 1H), 7.81 (dd, *J* = 7.1, 1.4 Hz, 1H), 7.73 (dd, *J* = 8.7, 2.3 Hz, 1H), 7.59 (dd, *J* = 8.0, 7.2 Hz, 1H), 7.38 (dd, *J* = 8.3, 4.2 Hz, 1H), 6.71 (d, *J* = 8.7 Hz, 1H), 4.01 (q, *J* = 2.3 Hz, 2H), 1.68 (t, *J* = 2.3 Hz, 3H); ¹³C NMR (75 MHz; CDCl₃) δ 190.8, 152.6, 145.9, 141.5, 137.4, 136.4, 134.8, 131.4 (2C), 127.6, 125.7, 124.3, 123.4, 121.6, 116.9, 111.4, 79.3, 68.2, 52.4, -0.8; IR (thin film) 2957, 1648, 1581, 1475, 1276 cm⁻¹; HRMS (ESI) *m/z* calcd for [C₂₀H₁₄NO₂ + Na]⁺ 449.9967, found 449.9986.

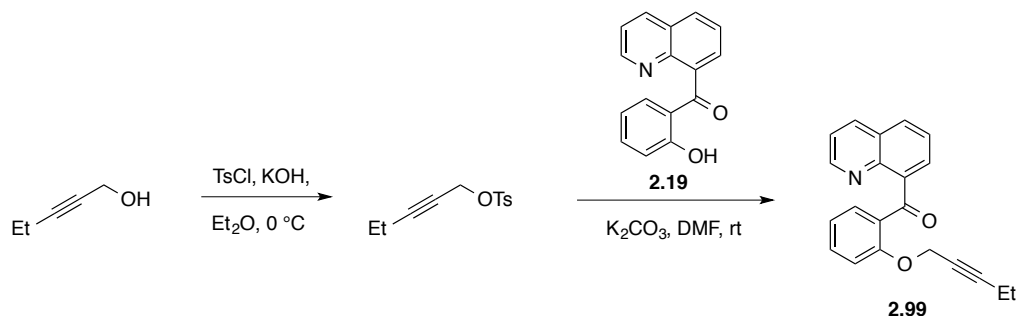


R_f 0.32 (1:4 EtOAc:Hex); ¹H NMR (300 MHz, CDCl₃) δ 9.03 (dd, *J* = 4.2, 1.8 Hz, 1H), 8.21 (dd, *J* = 8.3, 1.7 Hz, 1H), 7.98 (d, *J* = 1.4 Hz, 1H), 7.91 (dd, *J* = 8.2, 1.3 Hz, 1H), 7.74 (dd, *J* = 7.1, 1.4 Hz, 1H), 7.53-7.46 (m, 4H), 7.18 (d, *J* = 8.6 Hz, 1H), 5.55-5.48 (m, 1H), 1.67 (d, *J* = 7.2 Hz, 3H); ¹³C NMR (75 MHz; CDCl₃) δ 206.0, 154.4, 150.2, 145.2, 142.8, 136.1, 132.4, 130.8, 129.8, 129.5, 129.3 (2C), 127.9, 125.8, 121.4, 119.6, 113.1, 85.7, 42.9, 16.6; IR (thin film) 2980, 2942, 2360, 1687, 1449, 797 cm⁻¹; HRMS (ESI) *m/z* calcd for [C₂₀H₁₄INO₂ + Na]⁺ 449.9967, found 449.9974.



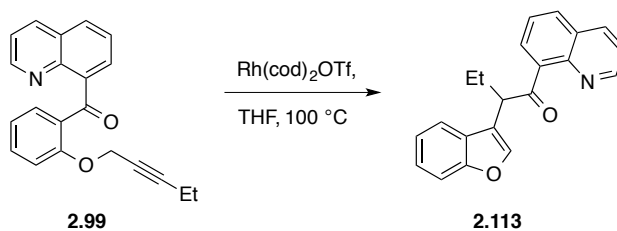
2-hydroxy-5-chlorobenzaldehyde (**2.110b**) (300 mg, 1.92 mmol), tosylate (**2.111b**) (430 mg, 1.92 mmol), K_2CO_3 (796 mg, 5.76 mmol), and DMF (10 mL) were added to a flask and stirred overnight at room temperature. The reaction mixture was diluted with water and EtOAc was added. The organic layer was washed with water (2×100 mL), LiCl, brine, and dried over Na_2SO_4 , filtered, and concentrated. The crude product was purified by flash chromatography (EtOAc:Hex) to give ether **2.111b** (377 mg, 1.79 mmol, 93%) as a yellow solid: R_f 0.48 (1:4 EtOAc:Hex). 8-bromoquinoline (**2.13**) (451 mg, 2.17 mmol) and THF (12 mL) were added to a flame-dried flask under N_2 and cooled to $-78\text{ }^\circ\text{C}$. To the solution was added $n\text{-BuLi}$ (2.5 M, 1.0 mL, 2.53 mmol) dropwise and the reaction was allowed to stir at $-78\text{ }^\circ\text{C}$ for 45 min. Aldehyde **2.111b** (356 mg, 1.19 mmol) was added slowly as a solution in THF (10 mL). The reaction was allowed to come to room temperature overnight. The reaction was quenched with sat. NH_4Cl and EtOAc were added. The aqueous layer was back extracted with EtOAc and the combined organic layers were washed with brine, dried over Na_2SO_4 , filtered, and concentrated. The crude product was unable to be adequately purified by flash chromatography (EtOAc:Hex) to give the corresponding alcohol (134 mg, 0.40 mmol, 22%): R_f 0.17 (1:4 EtOAc:Hex). A flask was charged with the alcohol (134 mg, 0.40 mmol) with impurities, IBX (335mg, 1.20 mmol), and DMSO (3 mL). The reaction was stirred at room temperature for 3 h. Water and EtOAc were added and was stirred

for 10 min. The solids were filtered and the layers separated. The organic layer was washed with water, brine, and dried over Na₂SO₄, filtered, and concentrated. The crude product was purified by flash chromatography to give ketone **2.114**: *R_f* 0.21 (1:4 EtOAc:Hex); ¹H NMR (500 MHz; CDCl₃) δ 8.75 (dd, *J* = 4.2, 1.8 Hz, 1H), 8.17 (dd, *J* = 8.3, 1.7 Hz, 1H), 7.92 (dd, *J* = 8.2, 1.3 Hz, 1H), 7.87 (d, *J* = 2.7 Hz, 1H), 7.83 (dd, *J* = 7.1, 1.4 Hz, 1H), 7.60 (dd, *J* = 8.0, 7.2 Hz, 1H), 7.41 (dd, *J* = 8.8, 2.7 Hz, 1H), 7.38 (dd, *J* = 8.3, 4.2 Hz, 1H), 4.03 (q, *J* = 2.3 Hz, 2H), 1.69 (t, *J* = 2.3 Hz, 3H); ¹³C NMR (75 MHz; CDCl₃) δ 195.2, 155.7, 150.2, 141.7, 135.9, 133.2, 132.9, 131.9, 130.5, 130.0, 128.7, 127.9, 127.8, 126.5, 125.9, 121.3, 115.0, 72.6, 57.0, 3.5; IR (thin film) 3071, 2919, 2230, 1652, 1274 cm⁻¹; HRMS (ESI) *m/z* calcd for [C₂₀H₁₄ClNO₂ + Na]⁺ 358.0611, found 358.0604.



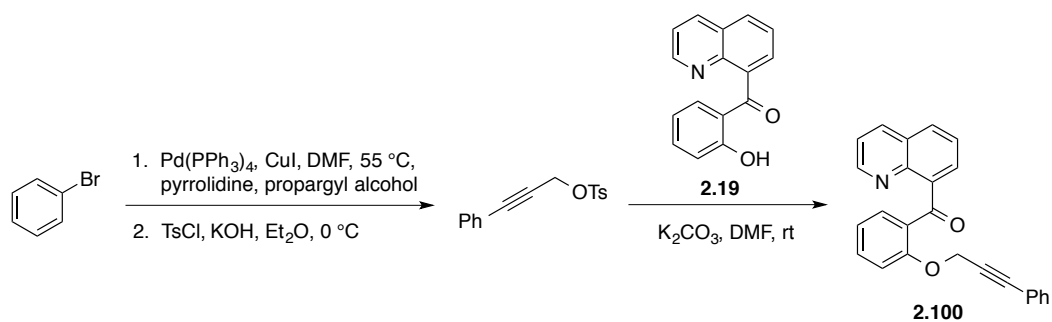
Pent-2-yn-1-ol (0.45 mL, 5.88 mmol) and Et₂O (12 mL) were combined in a flask and cooled with an ice bath. Tosyl chloride (1.12 g, 5.88 mmol) and potassium hydroxide (3.3 g, 58.8 mmol), were added and the resulting mixture was stirred at 0 °C for 15 min before removing the ice bath and stirred for 2 h at room temperature. The mixture was transferred to a separatory funnel with Et₂O and water was added (CAUTION: exotherm). The organic layer was washed with water (2 × 100 mL), the aqueous layer was back extracted with Et₂O × 2, and the combined organic layers were

washed with brine, dried over Na₂SO₄, filtered, and concentrated. The crude mixture was purified by flash chromatography (EtOAc:Hex) to give 2-pentynyl tosylate (918 mg, 3.85 mmol, 66%): *R_f* 0.41 (1:4 EtOAc:Hex). Phenol **2.19** (300 mg, 1.20 mmol), 2-pentynyl tosylate (287 mg, 1.20 mmol), potassium carbonate (498 mg, 3.60 mmol), and DMF (6 mL) were combined in a flask and stirred at room temperature for 48 h. Water and EtOAc were added to the reaction. The organic layer was washed with water (2 × 100 mL), 2 M LiCl, brine, dried of Na₂SO₄, filtered, and concentrated. The crude product was purified by flash chromatography (EtOAc:Hex) to give ketone **2.99** (265 mg, 0.84 mmol, 70%) as a yellow oil: *R_f* 0.16 (1:4 EtOAc:Hex); ¹H NMR (500 MHz; CDCl₃) δ 8.78 (dd, *J* = 4.2, 1.7 Hz, 1H), 8.16 (dd, *J* = 8.3, 1.7 Hz, 1H), 7.92-7.89 (m, 2H), 7.79 (dd, *J* = 7.1, 1.3 Hz, 1H), 7.58 (dd, *J* = 8.0, 7.3 Hz, 1H), 7.47 (d, *J* = 0.6 Hz, 1H), 7.37 (dd, *J* = 8.3, 4.2 Hz, 1H), 7.10 (s, 1H), 6.95 (d, *J* = 8.3 Hz, 1H), 4.10 (d, *J* = 4.1 Hz, 2H), 2.05 (qt, *J* = 7.5, 2.1 Hz, 2H), 1.02 (d, *J* = 15.0 Hz, 3H); ¹³C NMR (75 MHz, CDCl₃) δ 197.3, 158.3, 151.0, 142.2, 136.7, 134.4, 133.5, 132.4, 132.0, 130.4, 129.1, 128.6, 126.6, 122.0, 121.9, 114.4, 89.7, 74.0, 57.6, 14.2, 13.0; IR (thin film) 2976, 2938, 2240, 1652, 1594, 1294 cm⁻¹; HRMS (ESI) *m/z* calcd for [C₂₅H₁₇NO₂ + Na]⁺ 338.1157, found 338.1181.



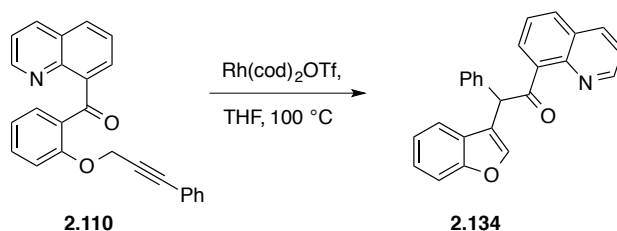
R_f 0.38 (1:4 EtOAc:Hex); ¹H NMR (300 MHz; CDCl₃) δ 8.97 (dd, *J* = 4.2, 1.8 Hz, 1H), 8.17 (dd, *J* = 8.3, 1.8 Hz, 1H), 7.85 (dd, *J* = 8.2, 1.4 Hz, 1H), 7.70–7.67 (m, 1H),

7.62–7.59 (m, 1H), 7.47–7.39 (m, 4H), 7.24–7.16 (m, 2H), 5.39 (q, $J = 8.6$ Hz, 1H), 2.47–1.98 (m, 2H), 1.01 (t, $J = 8.4$ Hz, 3H); ^{13}C NMR (75 MHz; CDCl_3) δ 206.1, 155.4, 150.5, 145.6, 143.1, 139.4, 136.4, 131.0, 129.9, 128.2, 127.5, 126.2, 124.2, 122.5, 121.6, 120.6, 118.3, 111.5, 50.7, 24.6, 12.4; IR (thin film) 2963, 1699, 1558, 1452, 748 cm^{-1} ; HRMS (ESI) m/z calcd for $[\text{C}_{21}\text{H}_{17}\text{NO}_2 + \text{Na}]^+$ 338.1157, found 338.1160.

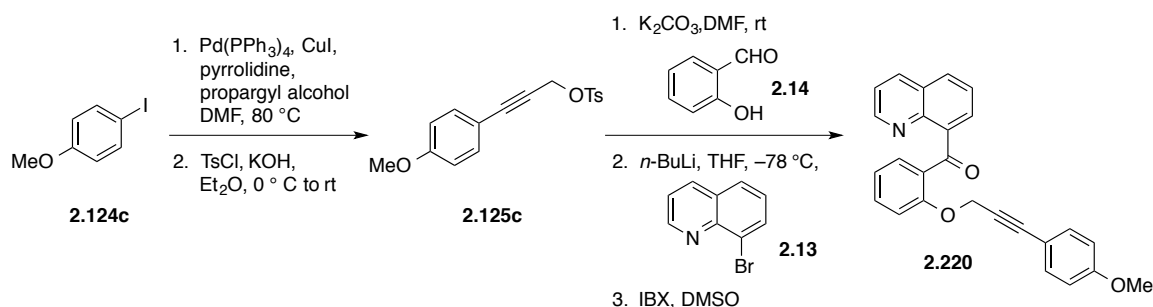


Bromobenzene (2.0 mL, 19.11 mmol), propargyl alcohol (2.26 mL, 38.21 mmol), pyrrolidine (1.88 mL, 38.21 mmol), and DMF (96 mL) were combined in a flame-dried flask. The solution was purged of oxygen by bubbling in N_2 gas. CuI (182 mg, 0.96 mmol) and $\text{Pd}(\text{PPh}_3)_4$ (2.21 g, 1.91 mmol) were added and the resulting mixture was placed under N_2 and heated to 55 $^\circ\text{C}$ overnight. Water and EtOAc were added. The aqueous layer was back extracted with EtOAc and the combined organic layers were washed with 2 M LiCl , brine, dried over Na_2SO_4 , filtered, and concentrated. Flash chromatography ($\text{EtOAc}:\text{Hex}$) provided 3-phenylprop-2-yn-1-ol (680 mg, 5.15 mmol, 27%): R_f 0.20 (1:4 $\text{EtOAc}:\text{Hex}$). 3-phenylprop-2-yn-1-ol (680 mg, 5.15 mmol) and Et_2O (5 mL) were added to a flask and cooled in an ice bath. Tosyl chloride (981 mg, 5.15 mmol) and potassium hydroxide (2.89 g, 51.55 mmol) was added to the reaction and it was allowed to stir at 0 $^\circ\text{C}$ for 15 min before removing the ice bath. The reaction stirred for 2 h at room temperature. The contents were transferred to a separatory funnel

before adding water (CAUTION: exotherm). The aqueous layer was back extracted with Et₂O, and the combined organic layers were washed with brine, dried over Na₂SO₄, filtered, and concentrated. The crude product was passed through a plug of silica gel (EtOAc:Hex) to obtain 3-phenyl-2-propynyl tosylate (1.29 g, 4.51 mmol, 88%) as an orange solid: R_f 0.33 (1:4 EtOAc:Hex). Phenol **2.19** (300 mg, 1.20 mmol), 3-phenyl-2-propynyl tosylate (344 mg, 1.20 mmol), potassium carbonate (498 mg, 3.60 mmol), and DMF (6 mL) were combined in a flask and stirred for 48 h at room temperature. Water and EtOAc were added. The organic layer was washed with water and the combined aqueous layers were back extracted with EtOAc × 2. The combined organic layers were washed with 2 M LiCl, brine, dried over Na₂SO₄, filtered, and concentrated. The crude product was purified by flash chromatography (EtOAc:Hex) to give ketone **2.100** (307 mg, 0.85 mmol, 70%) as a yellow oil: R_f 0.16 (1:4 EtOAc:Hex); ¹H NMR (500 MHz; CDCl₃) δ 8.74 (app s, 1H), 8.05 (d, *J* = 7.9 Hz, 1H), 7.94 (d, *J* = 7.2 Hz, 1H), 7.81-7.79 (m, 2H), 7.54 (app t, *J* = 7.4 Hz, 1H), 7.49 (app t, *J* = 9.8 Hz, 1H), 7.30-7.27 (m, 6H), 7.11 (app t, *J* = 7.2 Hz, 1H), 7.00 (d, *J* = 8.1 Hz, 1H), 4.34 (s, 2H); ¹³C NMR (125 MHz; CDCl₃) δ 196.6, 157.3, 150.2, 145.9, 141.5, 135.7, 133.6, 131.6, 131.2, 129.9, 129.8, 128.6, 128.19, 128.14, 127.8, 125.8, 122.1, 121.5, 121.1, 113.6, 86.6, 82.9, 57.0; IR (thin film) 3054, 2920, 2865, 2238, 1652 cm⁻¹; HRMS (ESI) *m/z* calcd for [C₂₅H₁₇NO₂ + Na]⁺ 386.1157, found 386.1126.



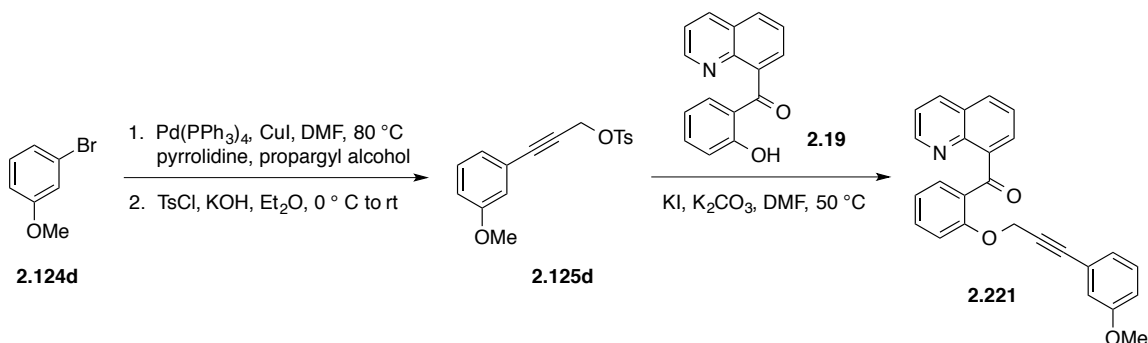
R_f 0.37 (1:4 EtOAc:Hex); ^1H NMR (400 MHz; CDCl_3) δ 9.02 (dd, $J = 4.2, 1.8$ Hz, 1H), 8.19 (dd, $J = 8.3, 1.8$ Hz, 1H), 7.88 (dd, $J = 8.2, 1.4$ Hz, 1H), 7.72 (dd, $J = 7.2, 1.4$ Hz, 1H), 7.67-7.65 (m, 1H), 7.60 (d, $J = 0.9$ Hz, 1H), 7.49-7.34 (m, 2H), 7.39-7.36 (m, 3H), 7.29-7.16 (m, 5H), 7.01 (s, 1H); ^{13}C NMR (126 MHz; CDCl_3) δ 203.6, 155.5, 150.6, 145.8, 144.0, 139.0, 137.6, 136.6, 131.3, 130.9, 129.5, 128.8, 128.3, 127.9, 127.5, 126.3, 124.4, 122.6, 121.7, 121.0, 119.6, 111.6, 55.3; IR (film) 3067, 2923, 1645, 1548, 1450 cm^{-1} ; HRMS (ESI) m/z calcd for $[\text{C}_{25}\text{H}_{17}\text{NO}_2 + \text{Na}]^+$ 386.1157, found 386.1131.



4-iodoanisole (**2.124c**) (2.5 g, 10.68 mmol), propargyl alcohol (1.26 mL, 21.36 mmol), pyrrolidine (1.05 mL, 21.36 mmol), and DMF (11 mL) were combined in a flame-dried flask. The solution was purged of oxygen by bubbling in N_2 gas. CuI (122 mg, 0.64 mmol) and $\text{Pd}(\text{PPh}_3)_4$ (617 mg, 0.53 mmol) were added and the resulting mixture was placed under N_2 and heated to 80 °C overnight. Water and EtOAc were added. The aqueous layer was back extracted with EtOAc and the combined organic layers were washed with 2 M LiCl , brine, dried over Na_2SO_4 , filtered, and concentrated. Flash

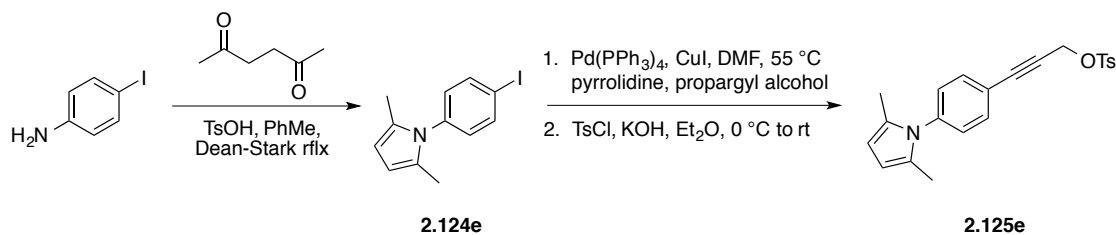
chromatography (EtOAc:Hex) provided 3-(4-methoxyphenyl)prop-2-yn-1-ol (986 mg, 6.08 mmol, 57%): R_f 0.23 (1:4 EtOAc:Hex). 3-(4-methoxyphenyl)prop-2-yn-1-ol (770 mg, 4.75 mmol) and Et₂O (5 mL) were added to a flask and cooled in an ice bath. Tosyl chloride (905 mg, 4.75 mmol) and potassium hydroxide (2.66 g, 47.5 mmol) was added to the reaction and it was allowed to stir at 0 °C for 15 min before removing the ice bath. The reaction stirred for 2 h at room temperature. The contents were transferred to a separatory funnel before adding water (CAUTION: exotherm). The aqueous layer was back extracted with Et₂O, and the combined organic layers were washed with brine, dried over Na₂SO₄, filtered, and concentrated. The crude product decomposes upon standing and silica gel chromatography. Tosylate **2.125c** (1.41 g, 4.46 mmol, 94%) was used in the following step without purification: R_f 0.23 (1:4 EtOAc:Hex). Tosylate **2.125c** (1.41 g, 4.45 mmol), salicylaldehyde (0.47 mL, 4.45 mmol), potassium carbonate (1.84 g, 13.35 mmol), and DMF (5 mL) were combined in a flask and stirred at room temperature overnight. Water and EtOAc were added. The organic layer was washed with water. The aqueous layers were back extracted with EtOAc. The combined organic layers were washed with 2 M LiCl, brine, dried over Na₂SO₄, filtered, and concentrated. The resulting aldehyde was obtained after flash chromatography: R_f 0.45 (1:4 EtOAc:Hex). 8-bromoquinoline (**2.13**) (712 mg, 3.42 mmol) and THF (23 mL) were added to a flame-dried flask under N₂ and cooled to -78 °C. To the solution was added *n*-BuLi (2.5M, 1.8 mL, 4.45 mmol) dropwise and the reaction was allowed to stir at -78 °C for 45 min. Aldehyde (911 mg, 3.42 mmol) was added slowly as a solution in THF (10 mL). The reaction was allowed to come to room temperature overnight. The reaction was quenched with sat. NH₄Cl and EtOAc were added. The aqueous layer was back extracted

with EtOAc and the combined organic layers were washed with brine, dried over Na₂SO₄, filtered, and concentrated. The crude product was purified by flash chromatography (EtOAc:Hex) to give the corresponding alcohol (660 mg, 1.68 mmol, 49%) as an orange-yellow oil: *R*_f 0.18 (1:4 EtOAc:Hex). A flask was charged with the alcohol (660 mg, 1.68 mmol), IBX (935 mg, 3.33 mmol), and DMSO (11 mL). The reaction was stirred at room temperature for 3 h. Water and EtOAc were added and was stirred for 10 min. The solids were filtered and the layers separated. The organic layer was washed with water, brine, and dried over Na₂SO₄, filtered, and concentrated. The crude product was purified by flash chromatography to give ketone **2.220**: ¹H NMR (500 MHz; CDCl₃) δ 8.75 (dd, *J* = 4.2, 1.8 Hz, 1H), 8.08 (dd, *J* = 8.3, 1.7 Hz, 1H), 7.94 (dd, *J* = 7.7, 1.8 Hz, 1H), 7.81 (app td, *J* = 7.7, 1.3 Hz, 2H), 7.55 (t, *J* = 7.6 Hz, 1H), 7.52-7.48 (m, 1H), 7.31 (dd, *J* = 8.3, 4.2 Hz, 1H), 7.23-7.20 (m, 2H), 7.12 (t, *J* = 7.5 Hz, 1H), 7.01 (d, *J* = 8.3 Hz, 1H), 6.84-6.81 (m, 2H), 4.33 (s, 2H), 3.82 (s, 3H); ¹³C NMR (126 MHz; CDCl₃) δ 196.6, 159.8, 157.4, 150.3, 146.0, 141.6, 135.8, 133.6, 133.2, 131.2, 129.9, 129.8, 128.2, 127.8, 125.9, 121.5, 121.2, 114.2, 113.8, 113.7, 86.6, 81.6, 57.1, 55.3 (two overlapping carbons).



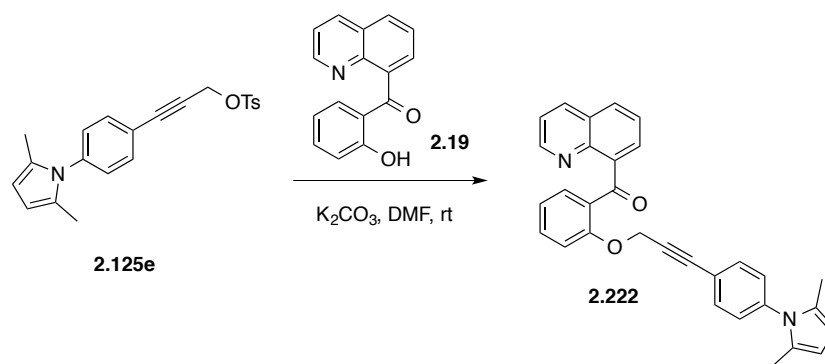
¹H NMR (500 MHz; CDCl₃) δ 8.75 (dd, *J* = 4.2, 1.7 Hz, 1H), 8.09 (dd, *J* = 8.3, 1.7 Hz, 1H), 7.94 (dd, *J* = 7.7, 1.7 Hz, 1H), 7.82 (ddd, *J* = 10.8, 7.7, 1.3 Hz, 2H), 7.56 (dd,

$J = 7.9, 7.3$ Hz, 1H), 7.52-7.48 (m, 1H), 7.31 (dd, $J = 8.3, 4.2$ Hz, 1H), 7.21 (app t, $J = 8.0$ Hz, 1H), 7.13 (app t, $J = 7.5$, 1H), 7.01 (d, $J = 8.3$ Hz, 1H), 6.89-6.86 (m, 2H), 6.81 (dd, $J = 2.3, 1.4$ Hz, 1H), 4.36 (s, 2H), 3.80 (s, 3H); ^{13}C NMR (75 MHz, CDCl_3) δ 196.8, 159.4, 157.6, 150.5, 146.2, 141.8, 136.0, 133.9, 131.5, 130.2, 130.1, 129.5, 128.5, 128.1, 126.1, 124.4, 123.4, 121.8, 121.4, 116.9, 115.2, 113.9, 86.8, 83.0, 57.3, 55.5; IR (thin film) 3078, 2965, 2834, 1654, 1595, 1575, 1497, 1482, 1449, 1320, 1290, 1209, 1164, 1043, 909, 731.

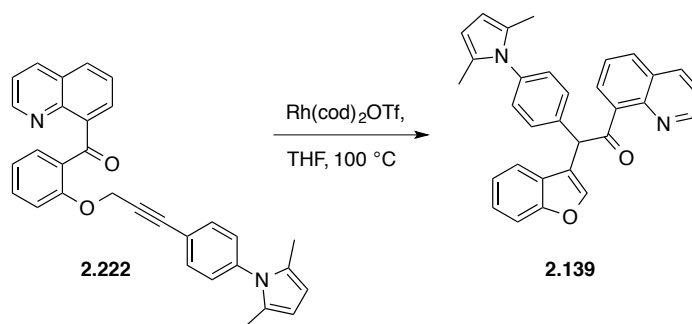


4-iodoaniline (5 g, 22.80 mmol), 2,5-hexanedione (3.2 mL, 27.4 mmol), *p*-toluenesulfonic acid (435 mg, 2.28 mmol), and PhMe (23 mL) were combined in a flask and refluxed with a Dean-Stark trap for 36 h. The mixture was cooled to room temperature, transferred to separatory funnel with EtOAc and acetone (solubilize leftover “goop”), and quenched with sat. NaHCO_3 . The aqueous layer was extracted with EtOAc. The combined organic layers were washed with brine, dried over Na_2SO_4 , filtered, and concentrated. The crude product was purified by column chromatography (EtOAc:Hex) to give pyrrole **2.124e** (5.76 g, 19.38 mmol, 85%) as an orange-red oil: R_f 0.77 (1:4 EtOAc:Hex). Pyrrole **2.124e** (1.09 g, 3.67 mmol), propargyl alcohol (0.43 mL, 7.34 mmol), pyrrolidine (0.36 mL, 7.34 mmol), and DMF (18 mL) were combined in a flask with a rubber septum and N_2 gas was bubbled through the solution. CuI (35 mg, 0.18 mmol) and $\text{Pd(PPh}_3)_4$ (424 mg, 0.37 mmol) were added and the mixture was heated

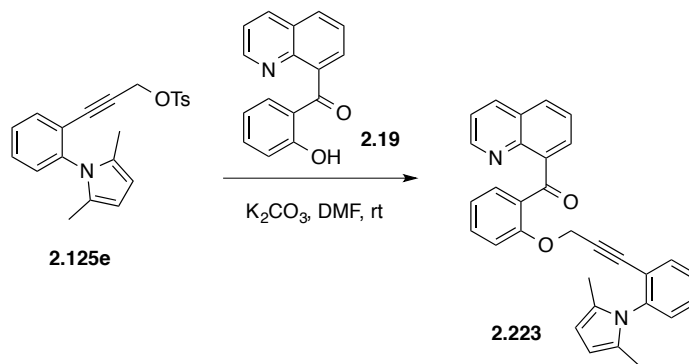
at 55 °C overnight under N₂. The reaction was cooled to room temperature and EtOAc and water were added. The organic layer was washed with water, and the combined aqueous layer was back extracted with EtOAc. The combined organic layers were washed with 2 M LiCl, brine, dried over Na₂SO₄, filtered, and concentrated. The crude product was purified by flash chromatography (EtOAc:Hex) to give the corresponding alcohol (752 mg, 3.34 mmol, 91%) as a dark orange oil: R_f 0.22 (1:4 EtOAc:Hex).



¹H NMR (500 MHz; CDCl₃) δ 9.03 (dd, *J* = 4.2, 1.8 Hz, 1H), 8.22 (dd, *J* = 8.3, 1.7 Hz, 1H), 7.92 (dd, *J* = 8.2, 1.4 Hz, 1H), 7.79 (dd, *J* = 7.1, 1.4 Hz, 1H), 7.68 (d, *J* = 0.5 Hz, 1H), 7.62 (d, *J* = 7.6 Hz, 1H), 7.52-7.47 (m, 5H), 7.29-7.27 (m, 1H), 7.22-7.20 (m, 1H), 7.11 (dd, *J* = 6.5, 1.7 Hz, 3H), 5.87 (s, 2H), 2.01 (d, *J* = 4.3 Hz, 6H); ¹³C NMR (126 MHz; CDCl₃) δ 196.6, 157.3, 150.4, 146.0, 141.5, 139.1, 135.8, 133.6, 132.4, 131.4, 130.1, 129.8, 128.6, 128.4, 128.1, 127.9, 125.9, 125.4, 121.7, 121.6, 121.2, 113.8, 106.1, 85.9, 84.1, 57.1, 13.0.

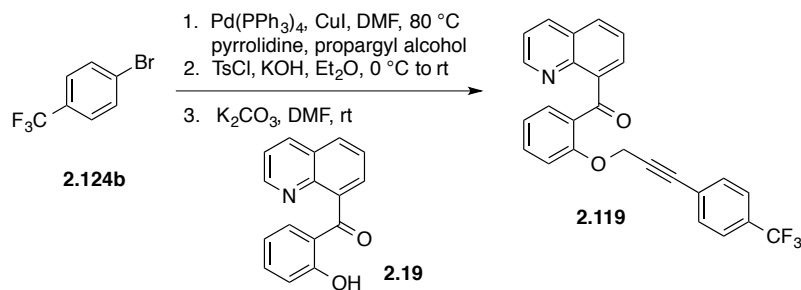


^1H NMR (500 MHz; CDCl_3) δ 9.03 (dd, $J = 4.2, 1.8$ Hz, 1H), 8.22 (dd, $J = 8.3, 1.7$ Hz, 1H), 7.92 (dd, $J = 8.2, 1.4$ Hz, 1H), 7.79 (dd, $J = 7.1, 1.4$ Hz, 1H), 7.68 (d, $J = 0.5$ Hz, 1H), 7.62 (d, $J = 7.6$ Hz, 1H), 7.52-7.47 (m, 5H), 7.31-7.27 (m, 1H), 7.22-7.19 (m, 1H), 7.12-7.10 (m, 3H), 5.87 (s, 2H), 1.98 (s, 6H); ^{13}C NMR (126 MHz; CDCl_3) δ 203.2, 155.3, 150.5, 145.6, 143.8, 138.5, 137.9, 137.2, 136.5, 131.4, 130.7, 129.9, 128.8, 128.2, 127.5, 126.1, 124.4, 122.5, 121.6, 120.5, 118.6, 111.5, 105.5, 54.3, 13.0 (one overlapping carbon).



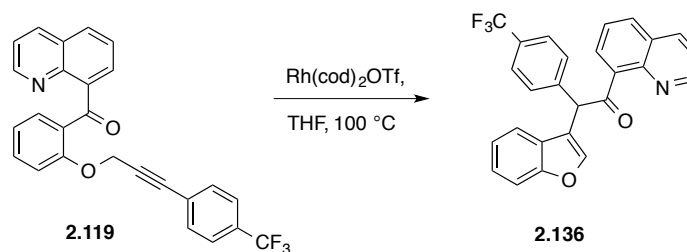
^1H NMR (500 MHz; CDCl_3) δ 8.74 (d, $J = 2.6$ Hz, 1H), 8.14 (d, $J = 8.1$ Hz, 1H), 7.86 (t, $J = 8.9$ Hz, 2H), 7.77 (d, $J = 6.9$ Hz, 1H), 7.56 (t, $J = 7.6$ Hz, 1H), 7.46 (t, $J = 7.3$ Hz, 1H), 7.42 (t, $J = 5.9$ Hz, 2H), 7.34 (td, $J = 9.8, 4.8$ Hz, 2H), 7.19 (d, $J = 7.6$ Hz, 1H), 7.08 (t, $J = 7.5$ Hz, 1H), 6.78 (d, $J = 8.3$ Hz, 1H), 5.86 (s, 2H), 4.16 (s, 2H), 1.87 (s, 6H); ^{13}C NMR (126 MHz; CDCl_3) δ 196.5, 157.2, 150.3, 145.9, 141.5, 141.0, 135.7, 133.8,

133.2, 131.2, 129.7, 129.6, 129.4, 129.1, 128.7, 128.4, 127.9, 127.76, 125.9, 122.5, 121.3, 121.2, 113.8, 105.4, 87.2, 83.0, 56.6, 12.6.



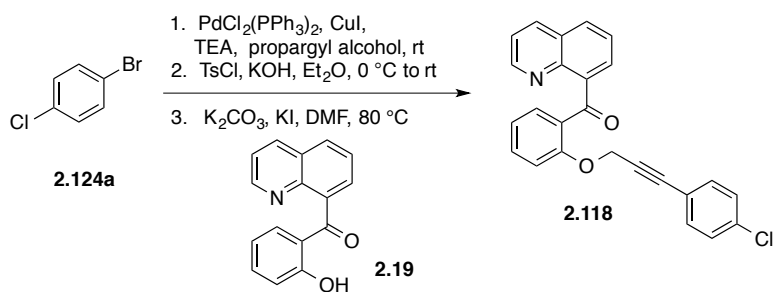
1-bromo-4-(trifluoromethyl)benzene (**2.124b**) (1.56 mL, 11.11 mmol), pyrrolidine (1.10 mL, 22.22 mmol), propargyl alcohol (1.31 mL, 22.22 mmol), and DMF (11 mL) were added to a flame-dried flask. Nitrogen gas was bubbled through the solution and then CuI (127 mg, 0.67 mmol) and $\text{Pd(PPh}_3)_4$ were added. The mixture was heated at $80\text{ }^\circ\text{C}$ for 12 h under N_2 and cooled to room temperature. EtOAc and water were added and the layers separated. The organic layer was washed with water, 2 M LiCl aqueous solution, and brine, then dried over Na_2SO_4 , filtered, and concentrated. The crude mixture was purified by flash chromatography (EtOAc:Hex) to give the alcohol (1.83 g, 9.14 mmol, 82%) as an orange oil: R_f 0.22 (1:4 EtOAc:Hex). The alcohol (1.65 g, 4.66 mmol) and Et_2O (8 mL) were added to a flask and cooled in an ice bath. KOH (2.61 g, 46.6 mmol) and tosyl chloride (1.65 g, 4.66 mmol) were added and the mixture was stirred at $0\text{ }^\circ\text{C}$ for 1 h. The ice bath was removed and the reaction was stirred until starting materials were consumed. The crude product was purified by flash chromatography (EtOAc:Hex) to give the tosylate (741 mg, 2.09 mmol, 45%) as an orange oil: R_f 0.45 (1:4 EtOAc:Hex). NOTE: tosylate decomposes on silica gel column. Tosylate (425 mg, 1.20 mmol), phenol **2.19** (300 mg, 1.20 mmol), K_2CO_3 (498 mg,

3.60 mmol), and DMF (6 mL) were combined in a scintillation vial and stirred overnight at room temperature. The mixture was diluted with EtOAc and washed with water. The aqueous phase was extracted with EtOAc (2 × 25 mL). The combined organic layers were washed with brine, dried over Na₂SO₄, and concentrated. The crude reaction mixture was purified by flash chromatography (EtOAc:Hex) to give the ketone **2.119** (354 mg, 0.82 mmol, 68%): ¹H NMR (300 MHz, CDCl₃) δ 8.74 (dd, *J* = 1.8, 4.2 Hz, 1H), 8.07 (dd, *J* = 1.7, 8.3 Hz, 1H), 7.92 (dd, *J* = 1.8, 7.5 Hz, 1H), 7.83-7.80 (m, 2H), 7.57-7.46 (m, 4H), 7.36 (d, *J* = 8.4 Hz, 2H), 7.32-7.26 (m, 1H), 7.12 (app t, *J* = 7.5 Hz, 1H), 6.99 (app d, *J* = 8.7 Hz, 1H), 4.39 (s, 2H); ¹³C NMR (125 MHz, CDCl₃) δ 196.7, 157.3, 150.5, 146.1, 141.7, 136.0, 133.8, 132.1, 131.5, 130.5 (q, *J* = 32.13) 130.3, 130.1, 128.5, 128.0, 126.2, 126.1, 125.3 (q, *J* = 3.67), 124.3 (q, *J* = 270.8), 121.9, 121.4, 113.9, 85.8, 85.4, 57.2; ¹⁹F (282 MHz, CDCl₃) δ -63.4; IR (thin film) 3080, 2927, 2252, 1656, 1615, 1596, 1575, 1496, 1483, 1453, 1323, 1295, 1217, 1168, 1129, 1106, 1067, 1018, 910, 843; HRMS (ESI) calcd for [C₂₄H₁₆NO₂F₃ + H]⁺ 432.1211, found 432.1199.

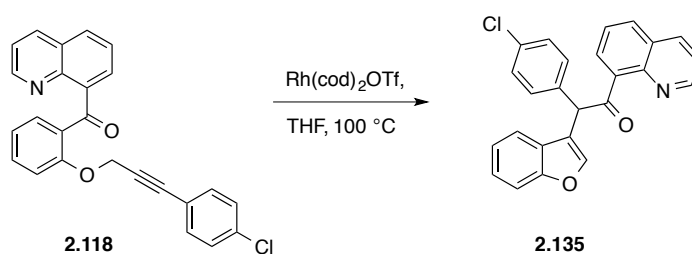


Ketone **2.119** was prepared as a 0.1 M solution in THF in a N₂ atmosphere glove box. Rh(cod)₂OTf (3.2 mg, 0.007 mmol) was carefully weighed into a 1 dram vial, and 0.70 mL **2.119** solution (30 mg, 0.07 mmol) was added. The orange solution was maintained at 100 °C for 48 h. The resulting red solution was removed from the glove box and concentrated onto celite. Column chromatography (EtOAc:Hex) gave **2.136** as a

yellow oil: R_f 0.33 (2:3 EtOAc:Hex); ^1H NMR (300 MHz, CDCl_3) δ 8.95 (dd, $J = 1.8$, 4.2 Hz, 1H), 8.15 (dd, $J = 1.8$, 8.4 Hz, 1H), 7.86 (dd, $J = 1.4$, 8.3 Hz, 1H), 7.76 (dd, $J = 1.5$, 7.2 Hz, 1H), 7.61-7.46 (m, 8H), 7.23-7.18 (m, 2H), 7.13-7.08 (m, 2H); ^{13}C NMR (125 MHz, CDCl_3) δ 202.8, 155.6, 150.7, 145.8, 144.0, 142.1, 138.3, 136.8, 132.0, 131.3, 129.9, 129.6 (q, $J = 35.0$), 128.5, 127.5, 126.4, 125.6 (q, $J = 3.5$), 124.7, 124.3 (q, $J = 271.3$), 122.9, 121.9, 120.6, 118.6, 111.8, 54.6; ^{19}F (282 MHz, CDCl_3) δ -63.1; IR (thin film) 3062, 2929, 2957, 1694, 1614, 1568, 1496, 1450, 1416, 1326, 1165, 1123, 1104, 1070, 1013, 975, 857; HRMS (ESI) calcd for $[\text{C}_{24}\text{H}_{16}\text{NO}_2\text{F}_3 + \text{H}]^+$ 432.1211, found 432.1214.



R_f 0.2 (2:3 EtOAc:Hex); ^1H NMR (300 MHz, CDCl_3) δ 8.74 (dd, $J = 1.7$, 4.4 Hz, 1H), 8.07 (dd, $J = 1.7$, 8.4 Hz, 1H), 7.92 (dd, $J = 1.8$, 7.5 Hz, 1H), 7.83-7.79 (m, 2H), 7.55 (app t, $J = 7.7$ Hz, 1H), 7.50 (ddd, $J = 1.8$, 7.8, 8.3 Hz, 1H), 7.32-7.17 (m, 4H), 7.12 (app t, $J = 7.5$ Hz, 2H), 6.99 (app d, $J = 8.4$ Hz, 1H) 4.36 (s, 2H); ^{13}C NMR (75 MHz, CDCl_3) δ 196.8, 157.5, 150.5, 146.2, 141.7, 136.0, 134.9, 133.8, 133.1, 131.5, 130.2, 130.0, 128.8, 128.5, 128.1, 126.1, 121.8, 121.4, 120.8, 113.9, 85.7, 84.2, 57.2; IR (thin film) 3070, 2925, 1657, 1595, 1576, 1487, 1452, 1373, 1320, 1294, 1269, 1219, 1157, 1091, 1014, 928, 828; HRMS (ESI) calcd for $[\text{C}_{23}\text{H}_{16}\text{NO}_2\text{Cl} + \text{H}]^+$ 398.0948, found 398.0971.



R_f 0.37 (2:3 EtOAc:Hex); ^1H NMR (300 MHz, CDCl_3) δ 9.01 (dd, $J = 1.8, 4.2$ Hz, 1H), 8.21 (dd, $J = 2.1, 8.3$ Hz, 1H), 7.92 (dd, $J = 1.4, 8.3$ Hz, 1H), 7.78 (dd, $J = 1.4, 7.1$ Hz, 1H), 7.60-7.45 (m, 5H), 7.35 (d, $J = 8.7$ Hz, 2H), 7.29 (dd, $J = 1.2, 7.2$ Hz, 1H), 7.24 (d, $J = 8.4$ Hz, 2H), 7.18 (app t, $J = 7.5$ Hz, 1H), 7.05 (s, 1H); ^{13}C NMR (125 MHz, CDCl_3) δ 203.1, 155.6, 150.7, 145.8, 143.9, 138.5, 136.7, 136.4, 133.4, 131.7, 131.1, 130.9, 128.9, 128.4, 127.7, 126.4, 124.6, 122.8, 121.8, 120.8, 119.1, 111.7, 54.4; IR (thin film) 3062, 2929, 2857, 1690, 1591, 1572, 1488, 1454, 1276, 1165, 1101, 1013, 975, 857; HRMS (ESI) calcd for $[\text{C}_{23}\text{H}_{16}\text{NO}_2\text{Cl} + \text{Na}]^+$ 420.0767, found 420.0762.

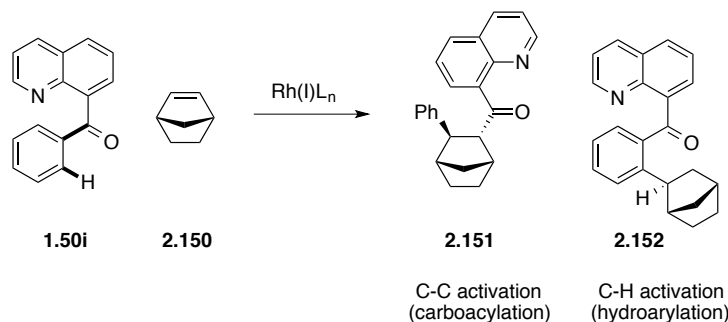
2.5 INTERMOLECULAR CARBOACYLATION

Due to the restriction on alkene reactivity, quinoline-directed intermolecular carboacylation reactions went underdeveloped for a long time. After more than twenty years had passed since Suggs' and Jun's alkyl exchange reactions were developed (see Section 1.3), our group designed a catalytic system that would allow for C–C bond activation to forgo the β -hydride elimination process that leads to fragmentation.¹³ In theory, employing strained [2.2.1]bicycloheptenes would produce intermediates void of accessible *syn* β -hydrogens and thus allow for a complexity-building pathway.

Heating equimolar amounts of 8-quinolinyl phenyl ketone **1.50i** and norbornene (**2.150**) with several Rh(I) catalysts, in a range of solvents and temperatures, gave varying ratios of C–C bond activation (carboacylation) product **2.151** and *ortho* C–H bond activation (hydroarylation) product **2.152** (Table 6). Although Suggs had not reported a competitive C–H bond insertion pathway with ethylene (see Section 1.4.2), advances in C–H bond activation chemistry has shown *ortho*-metalation to occur with carbonyl-like directing groups via five-membered chelates.¹⁴ The relief of ring strain for norbornene (ca. 25 kcal/mol) may lower the barrier for this hydroarylation process. Since migratory insertion is known to proceed in a *syn* fashion, the *anti* stereorelationship in **2.151** likely occurs via epimerization post carboacylation, presumably through an inter- or intramolecular deprotonation by the basic quinoline nitrogen. The possibility for β -hydride elimination to remain a competing pathway through the reverse reaction (metal insertion into the *anti* product) exists.

Reaction between 8-quinoliny phenyl ketone **1.50i**, norbornene (**2.150**), and $[\text{RhCl}(\text{C}_2\text{H}_4)_2]_2$ in toluene at 130 °C for 24 h exclusively gave the hydroarylation product **2.152** in 79% isolated yield (entry 1). Cationic rhodium complexes $[\text{Rh}(\text{cod})_2]\text{BF}_4$ and $[\text{Rh}(\text{cod})_2]\text{OTf}$ allowed for C–C activation to compete with C–H activation, giving a 1:6 (38%, entry 2) and 4:5 (56%, entry 3) product ratio (**2.151**:**2.152**), still favoring C–H activation. The remaining mass in these reactions consisted of unreacted starting material and unidentified side-products. Increasing the alkene loading ten-fold did not improve the conversion. Switching to a more polar solvent and reducing the temperature to 100 °C reversed the chemoselectivity to favor C–C activation, providing products in a 5:3 ratio in acetonitrile (MeCN) (41%, entry 4) and 1:0 in tetrahydrofuran (THF) (50%, entry 5). Reaction with $\text{RhCl}(\text{PPh}_3)_3$ was relatively ineffective (<10%, entry 6).

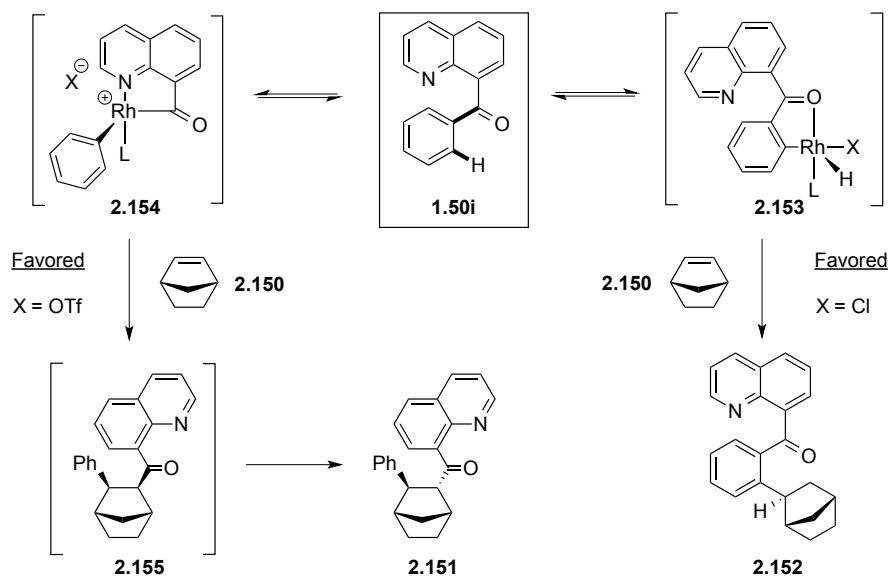
Table 6. Intermolecular carboacylation and hydroarylation



entry	catalyst	solvent	temp	yield (%)	2.151:2.152
1	$[\text{RhCl}(\text{C}_2\text{H}_4)_2]_2$	PhMe	130 °C	79	0:1
2	$[\text{Rh}(\text{cod})_2]\text{BF}_4$	PhMe	130 °C	38	1:6
3	$[\text{Rh}(\text{cod})_2]\text{OTf}$	PhMe	130 °C	56	4:5
4	$[\text{Rh}(\text{cod})_2]\text{OTf}$	MeCN	100 °C	41	5:3
5	$[\text{Rh}(\text{cod})_2]\text{OTf}$	THF	100 °C	50	1:0
6	$\text{RhCl}(\text{PPh}_3)_3$	PhMe	130 °C	<10	–

The nature of the rhodium ligand appears to directly influence the chemoselectivity of the reaction. Assuming that intermediates **2.153** and **2.154** are in equilibrium, it is possible that the coordinating chloride ligand raises the barrier (ΔG^\ddagger) to migratory insertion in **2.154** and thus favors the consumption of **2.153** (Curtin-Hammett kinetics; Scheme 43). The cationic rhodium complex with the less-coordinating triflate ligand in a stabilizing polar solvent, could make the metal center more accessible to olefin complexation, and thus lower the barrier (ΔG^\ddagger) to migratory insertion for intermediate **2.154**.

Alternatively, should there be an equilibrium between **2.151** and epimer **2.155**, and between **2.155** and **2.154** (via β -aryl elimination), it is conceivable that **2.151** and **2.152** would also be in equilibrium. In order to examine this, **2.151** was subjected to the reaction conditions with $[\text{RhCl}(\text{C}_2\text{H}_4)_2]_2$ in toluene without detection of **2.152** by ^1H NMR spectroscopy. Although this proves that **2.151** and **2.152** do not equilibrate, it does not infer anything about the reaction coordinate disposition.



Scheme 43. C–C (carboacylation) vs C–H (hydroarylation) bond activation

The addition of a *para*-CH₃ group on the substrate phenyl ring negatively impacted the reactivity and chemoselectivity of the reaction, producing a 1:1 product mixture in 30% yield (66% brsm) under the optimized reaction conditions ([Rh(cod)₂]OTf, THF, 100 °C) with norbornene. The addition of an electron-withdrawing *para*-CF₃ substituent effectively suppressed the C–H insertion pathway to give the carboacylation product in 24% yield. Exchanging the phenyl group for a methyl group (**1.50c**, see Scheme 22) where C–H activation is not applicable, gave the carboacylation product in 39% yield (60% brsm) under [RhCl(C₂H₄)₂]₂ catalysis.

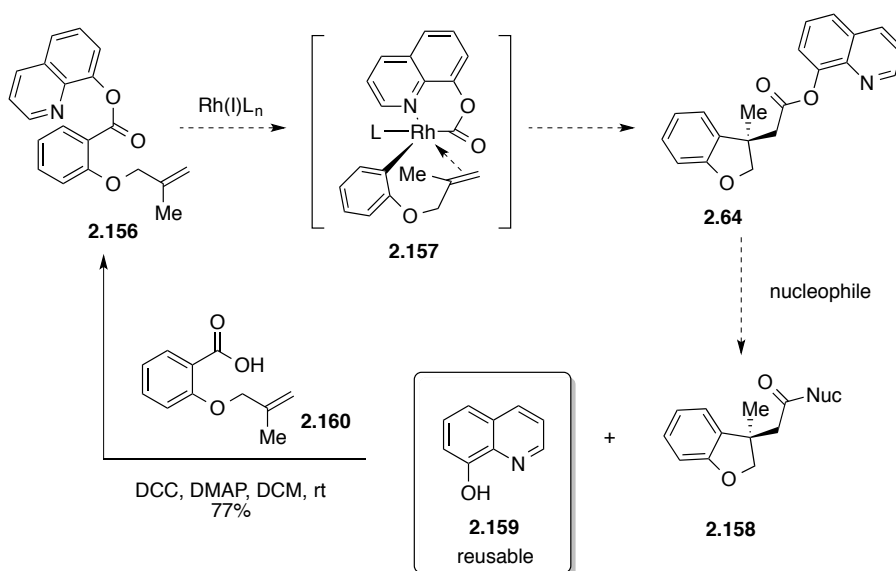
2.6 CARBOACYLATION WITH 8-QUINOLINYL ESTER

An obvious limitation to the carboacylation methodology is the need for a covalently-bound directing group that is difficult to remove post transformation. While attempting to modify the carboacylation products by way of Baeyer-Villiger, Beckmann, and Schmidt reactions in order to subsequently cleave the resulting ester or amide (see Scheme 33), it was envisioned that such an ester or amide may be suitable for C–C bond activation in itself.^{xxii}

2.6.1 RESEARCH PROPOSAL

Ester **2.156**, which could be readily prepared by coupling acid **2.160** with 8-quinolinol **2.159**, was predicted to undergo C–C bond activation through a six-membered metallacycle **2.157**. The resulting dihydrobenzofuran ester **2.64** would be subject to nucleophilic cleavage to generate products of synthetic value (**2.158**). Additionally, the regenerated quinolinol moiety **2.159** would be recyclable.

^{xxii} Idea suggested by Professor Gunda Georg.

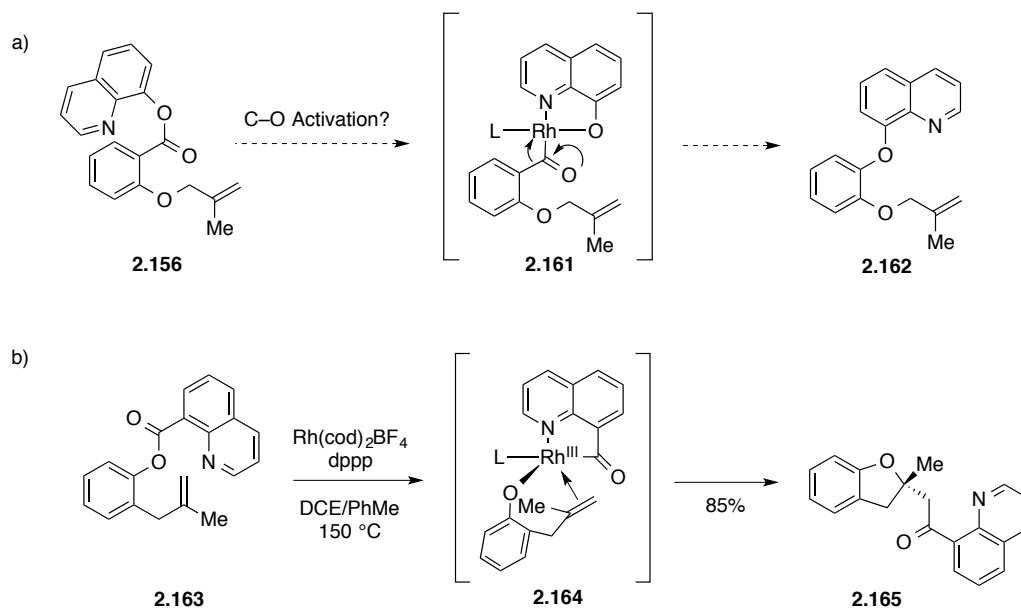


Scheme 44. Proposed intramolecular carboacylation with 8-quinoliny ester

2.6.2 RESULTS AND DISCUSSION

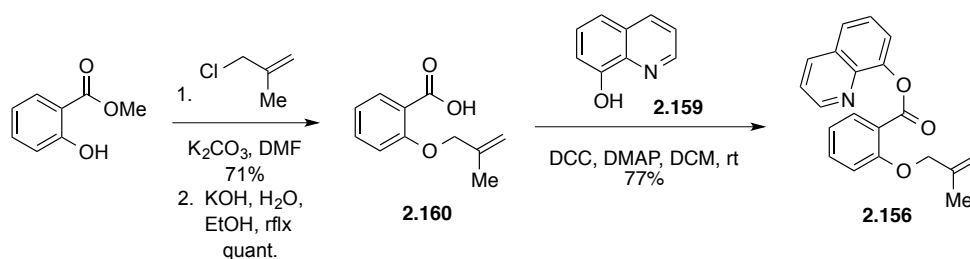
Heating ester **2.156** in PhMe at 130 °C for 48 h with $\text{RhCl}(\text{PPh}_3)_3$, $[\text{RhCl}(\text{C}_2\text{H}_4)_2]_2$, and $\text{Rh}(\text{cod})_2\text{OTf}$ returned only starting material. Ester **2.156** was also inactive toward catalysis in THF at 100 °C. Increasing the temperature to 150 °C in PhMe yielded small quantities of unidentified decomposition product(s) that contained terminal olefins. The inactivity of ester **2.156** may be attributed to the decreased electrophilicity of the ester functionality and/or the reduced stability of the six-membered metallacycle intermediate (**2.157**). The retention of terminal olefins observed in the unidentified byproducts lent to the hypothesis that the catalyst was activating the ester C–O bond through a 5-membered chelate **2.161**, which could undergo decarbonylation to generate **2.162** upon reductive elimination (Scheme 45a). Additionally, our group has developed an oxyacylation

reaction that demonstrates ester C–O bond activation with quinoline directing groups (Scheme 45b).¹⁵



Scheme 45. Ester C–O bond activation with quinoline directing groups. a) Proposed decomposition pathway of ester **2.156**. b) Oxyacylation with 8-acylquinoline

2.5.3 EXPERIMENTAL

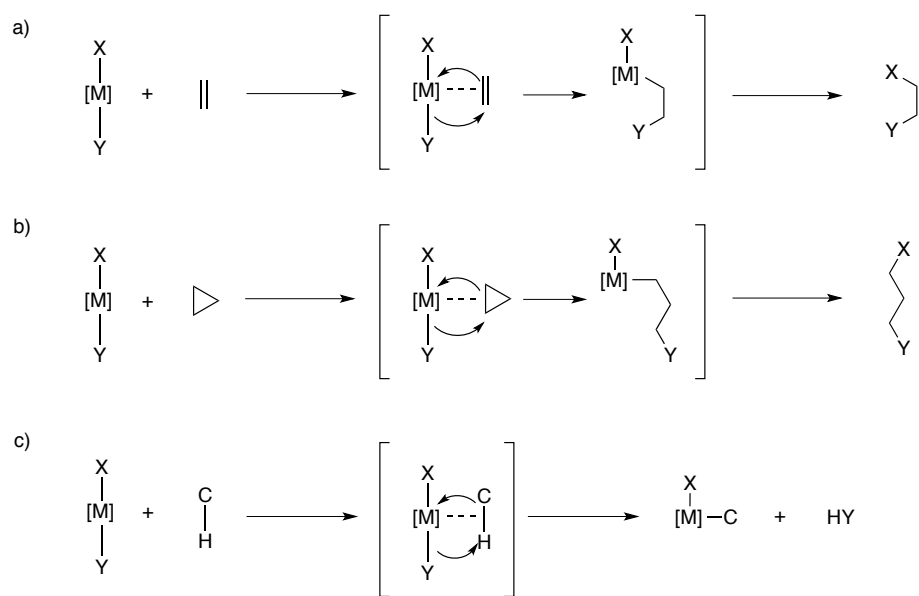


Methylsalicylate (1.3 mL, 10.0 mmol), 3-chloro-2-methylpropene (1.5 mL, 15.0 mmol), K_2CO_3 (4.15 g, 30.0 mmol), and DMF (13 mL) were combined in a flask and stirred at room temperature. After 18 h, an additional charge of 3-chloro-2-methyl-

propene (0.5 mL, 5 mmol) was added. After 24 h, H₂O and EtOAc were added to the reaction and the layers were separated. The organic layer was washed with H₂O and the combined aqueous layers were back extracted with EtOAc. The combined organic layers were washed with 2 M LiCl, brine, dried of Na₂SO₄, and concentrated onto celite. Column chromatography (1:9 EtOAc:Hex) gave the corresponding ether (1.47 g, 7.12 mmol, 71%): *R_f* 0.36 (1:4 EtOAc:Hex). The resulting ester (522 mg, 2.53 mmol), KOH (740 mg 13.2 mmol), and EtOH:H₂O (30:10 mL) were added to a flask and the solution was refluxed for 13 h. EtOAc and H₂O were added and the layers were separated. The aqueous phase was acidified with 1 M HCl and extracted with EtOAc several times. The combined organic layers were washed with brine, dried over Na₂SO₄, filtered, and concentrated to give acid **2.160**. No further purification was necessary. Acid **2.160** (200 mg, 1.04 mmol) was azeotropically dried with PhH and placed under N₂. Dry DCM (3 mL) was added, followed by DCC (325 mg, 1.56 mmol), DMAP (65 mg, 0.52 mmol), and then 8-hydroxyquinoline (**2.159**) (180 mg, 1.25 mmol). The resulting mixture was allowed to stir at room temperature under N₂ overnight. The mixture was diluted with DCM and washed with sat. NaHCO₃, brine, dried over Na₂SO₄, filtered, and concentrated. Chloroform was added and the precipitate was filtered and discarded. Column chromatography (EtOAc:Hex) provided ester **2.156** as a colorless solid (255 mg, 0.8 mmol, 77%): *R_f* 0.17 (1:4 EtOAc:Hex); ¹H NMR (300 MHz; CDCl₃) δ 8.58 (app t, *J* = 2.1 Hz, 1H), 7.98 (dd, *J* = 7.8, 1.8 Hz, 1H), 7.85 (s, 1H), 7.41 (s, 1H), 7.24 (d, *J* = 1.7 Hz, 2H), 7.11 (d, *J* = 4.2 Hz, 1H), 6.77 (s, 1H), 6.72 (d, *J* = 8.4 Hz, 1H), 4.91 (s, 1H), 4.63 (d, *J* = 1.2 Hz, 1H), 4.24 (s, 2H), 1.52 (s, 4H).

2.6 CARBOACYLATION ACROSS CYCLOPROPANE

Insertions of alkenes, alkynes, and allenes into M–C bonds have become common practice in organometallic chemistry. Expanding the scope of such reactions to include migratory insertions across aldehydes,^{16,17} aldimines,^{17,18} ketones,^{17,19} and nitriles^{19,20} with Rh(I) complexes have been realized, despite the added thermodynamic and kinetic challenges. Such challenges are the result of the stronger C–X π bond, the weakness of the resulting M–X bond, and competitive coordination of the lone pair electrons. Coordination of the π system precedes insertion, and since cyclopropane has been shown to have olefin-like character, it was envisioned that a M–C bond could be added across a cyclopropane sigma bond in a manner akin to migratory insertion across olefins (Scheme 46). Alternatively, such a process could be viewed as sigma(σ)-bond metathesis²¹ (a common reactivity mode observed in C–H functionalization).



Scheme 46. a) Mechanism of migratory insertion b) proposed migratory insertion across a cyclopropane C–C sigma bond c) Mechanism of C–H sigma (σ) bond metathesis

2.6.1 BACKGROUND

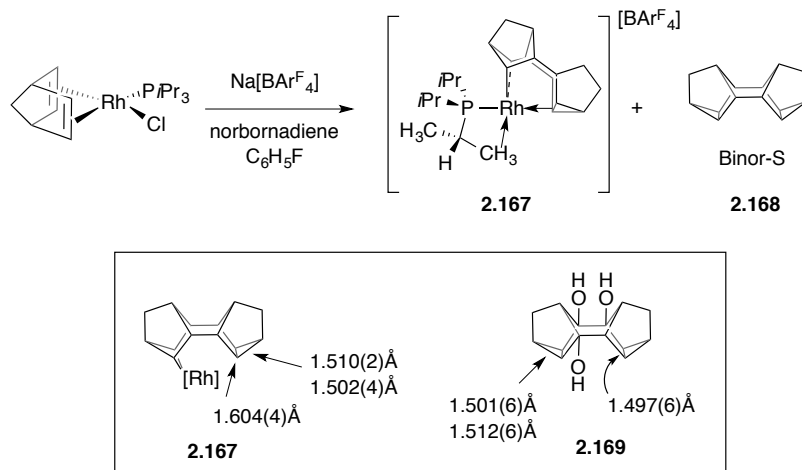
The spectroscopic and conjugative properties between cyclopropane, ethylene, and ethylene oxide as reviewed by Walsh²³ led Tipper²⁴⁻²⁶ to study a host of reactions that examined the relationships between the reactivity of cyclopropane and olefins. With cyclopropane exhibiting significant double bond character, it was anticipated that it could ligate metal complexes similarly to that of olefins. The compound obtained by treating chloroplatinic acid with cyclopropane was presumed to be that of the edge-bound cyclopropane derivative $[\text{PtCl}_2(\text{C}_3\text{H}_6)]_2$ akin to Zeise's dimer $[\text{PtCl}_2(\text{C}_2\text{H}_4)]_2$ (see Chapter 1, Scheme 1). The isolated material was later proven to be the C–C insertion platina(IV)cyclobutane tetramer, which presumably forms through a C–C sigma adduct ($\text{M}\cdots\text{C}-\text{C}$) intermediate or transition state (**2.166**) (Scheme 47).



Scheme 47. Illustration of C–C sigma adduct ($\text{M}\cdots\text{C}-\text{C}$) interaction

Although propositions for such $\text{M}\cdots\text{C}-\text{C}$ interactions preceding C–C activation are prevalent, well-characterized examples of these sigma adducts are rare and limited to intramolecular (agostic) interactions. In order to advance the study of C–C bond activation, a thorough understanding of such fundamental processes are essential. In 2006, Weller²⁷⁻²⁹ described the synthesis of an organometallic complex that not only revealed a well-characterized $\text{Rh}\cdots\text{C}-\text{C}$ agostic interaction, but that also underwent reversible C–C bond activation on the NMR time scale. The dimerization of norbornadiene under reaction with $[\text{RhCl}(\text{nbd})(\text{P}i\text{Pr}_3)]$ and $\text{Na}[\text{BAr}^{\text{F}}_4]$ yielded

[Rh(PiPr₃)(C₁₄H₁₆)] [BAr^F₄] **2.167** and Binor-S **2.168** (Scheme 48). Complex **2.167** exhibits a cationic rhodium center containing one PiPr₃ ligand that shows a weak γ -agostic C–H interaction and a Binor-S ligand in which one of the cyclopropane rings has been activated to form a rhodacyclobutane. The interspatial distance between the metal and the remaining cyclopropane ring (Rh...C1, 2.352(3) Å and Rh...C2, 2.369(3) Å) is well within the Van der Waals radii for rhodium and carbon (3.7 Å), thus suggesting a significant interaction. In comparison to the trishydroxylated Binor-S **2.169**, the proximal C–C bond is elongated by roughly 0.1 Å.



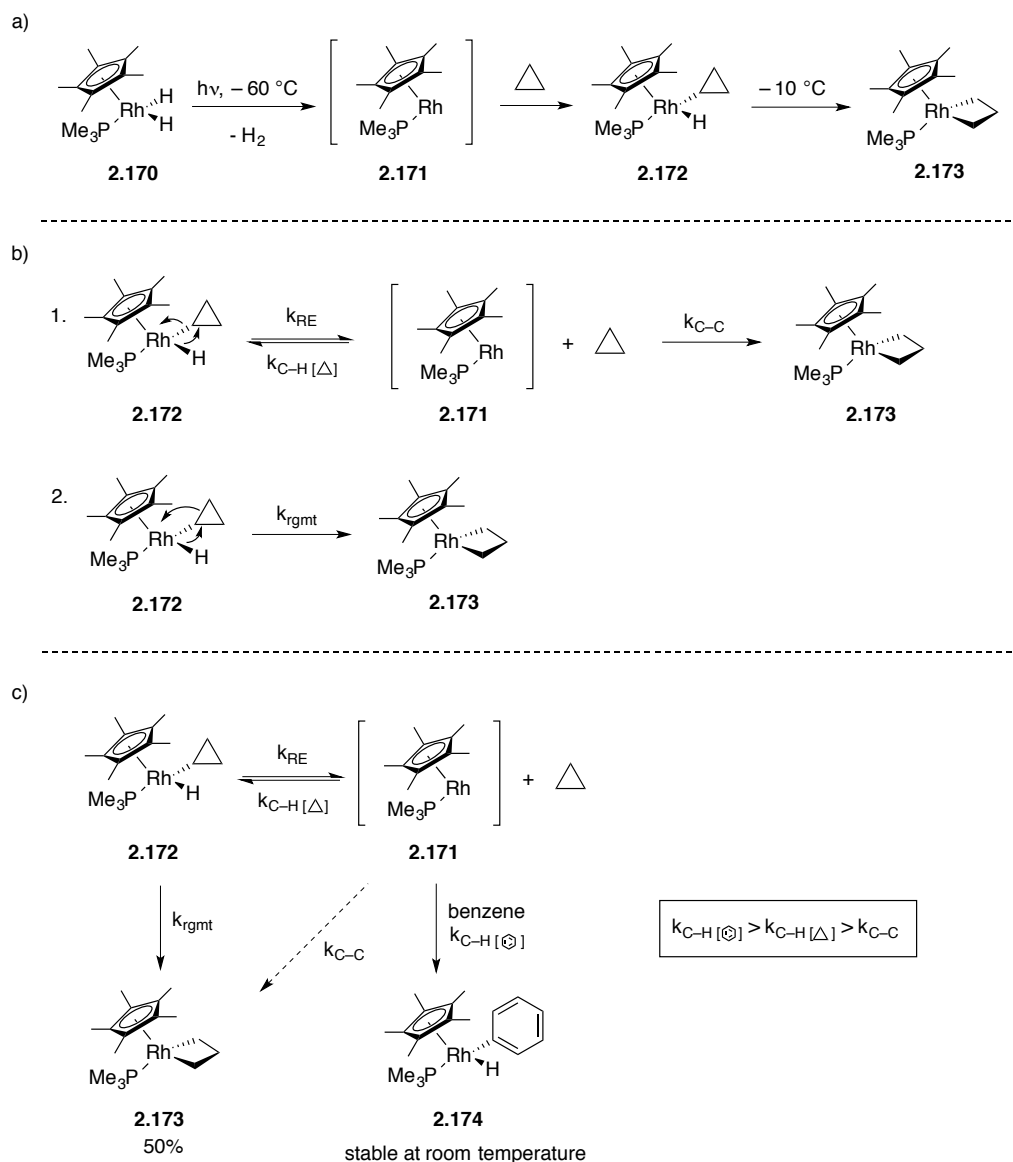
Scheme 48. Rhodacyclobutane-Binor-S complex with M...C–C agostic interaction

At room temperature, the ¹H NMR spectra of **2.167** gave only five resonances, which was indicative of a fluxional process. Upon cooling the sample to –70 °C, ten non-equivalent proton signals were observed. At this temperature, the pairs of cyclopropane carbons each still show coupling to rhodium (¹J_{(Rh,C)metallacycle} = 22 Hz, ¹J_{(Rh,C)cyclopropane} = 9Hz), which lends further support to a Rh...C–C agostic interaction. The stability of this complex was attributed to the C–C sigma orbitals being sufficiently

high in energy to allow bonding with the metal center.

Under less-than-ambient temperatures, hydridoalkylmetal ($\text{C-M}^{n+2}\text{-H}$) complexes are known to undergo rapid reductive elimination to the hydrocarbon ($\text{C-H} + \text{M}^n$). However, in the mid-1980s, Bergman³⁰⁻³² reported an unprecedented rearrangement of hydridocyclopropylrhodium complex **2.172** that yielded the rhodacyclobutane **2.173** rather than simply eliminating cyclopropane (Scheme 49). Mechanistic data for this transformation supports an intramolecular rearrangement, which resembles a migratory insertion process.

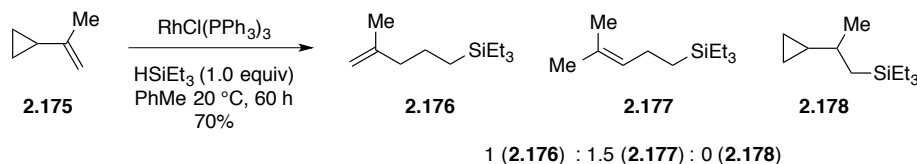
The hydrido cyclopropane complex **2.172** was prepared by ultraviolet irradiation of $\text{Cp}^*(\text{PMe}_3)\text{RhH}_2$ **2.170** in liquid cyclopropane at $-60\text{ }^\circ\text{C}$ (Scheme 49a). Upon warming to $-10\text{ }^\circ\text{C}$, complex **2.172** rearranged to the C–C insertion product **2.173** in quantitative yield. The simplest mechanism to account for this transformation would involve an equilibrium between **2.172** and **2.171**, and irreversible formation of **2.173** (Scheme 49b1). Alternatively, direct intramolecular insertion of the Rh–H bond across cyclopropane could explain the formation of **2.173** (Scheme 49b2). In order to determine whether reductive elimination of the hydrocarbon precedes C–C insertion, hydrido complex **2.172** was warmed in the presence of benzene, which is known to undergo C–H insertion more than twice as fast as cyclopropane C–H insertion (thus much faster than C–C insertion) (Scheme 49c). The incomplete trapping of the putative $[\text{Cp}^*(\text{PMe}_3)\text{Rh}]$ intermediate **2.171** with benzene to generate the hydrido phenyl complex **2.174** suggests that the metallacycle **2.173** is formed primarily through an intramolecular hydride transfer across the cyclopropane C–C bond (Scheme 49b2).



Scheme 49. a) Rearrangement of hydridocyclopropylrhodium complex **2.172** to rhodacyclobutane **2.173**. b) 1. Rearrangement through reductive elimination followed by C–C bond activation. 2. Rearrangement through intramolecular bond insertion. c) Competition experiment with benzene as trapping agent.

In 1995, Beletskaya³³ uncovered an unusual hydrosilylation reaction of vinylcyclopropanes with Wilkinson's catalyst (Scheme 50). Instead of forming the predicted cyclopropylsilane **2.178**, reaction of vinylcyclopropane **2.175** generated ring-opened, silylated pentenes **2.176** and **2.177** in 70% yield as a 1:1.5 mixture. Platinum

catalysts, on the other hand, delivered the expected product **2.178**.



Scheme 50. Hydrosilylation and ring opening of vinylcyclopropane **2.175** with $\text{RhCl(PPh}_3)_3$

Potential mechanistic pathways for the formation of silanes **2.176–2.178** are illustrated in Figure 13. Cycle A represents the predicted pathway that leads to cyclopropyl silane **2.178**. Coordination of the olefin to the metal, followed by oxidative addition into the Si–H bond generates intermediate **2.179**. Regioselective delivery of the hydride across the olefin provides the rhodium-silane complex **2.180**, which undergoes reductive elimination to provide **2.178**. However, the authors did not consider that the unfavorable addition of the hydride to the terminal end of the olefin could generate complex **2.181** that could subsequently undergo β -carbon elimination, followed by reductive elimination to give silylated pentene **2.177**. It is unlikely that this mechanism would also account for the formation of **2.176** in that isomerization of **2.177** to the less substituted olefin would be thermodynamically unfavorable.

Cycle B was proposed to explain the formation of **2.176** and **2.177**. The authors suggested that upon olefin coordination and oxidative addition, the rhodium center is also complexed to the cyclopropane C–C bond (**2.182**). Delivery of the silyl group across cyclopropane would generate a rhodium-hydride π -allyl system (**2.183**) that could reductively eliminate to give either **2.176** or **2.177**.

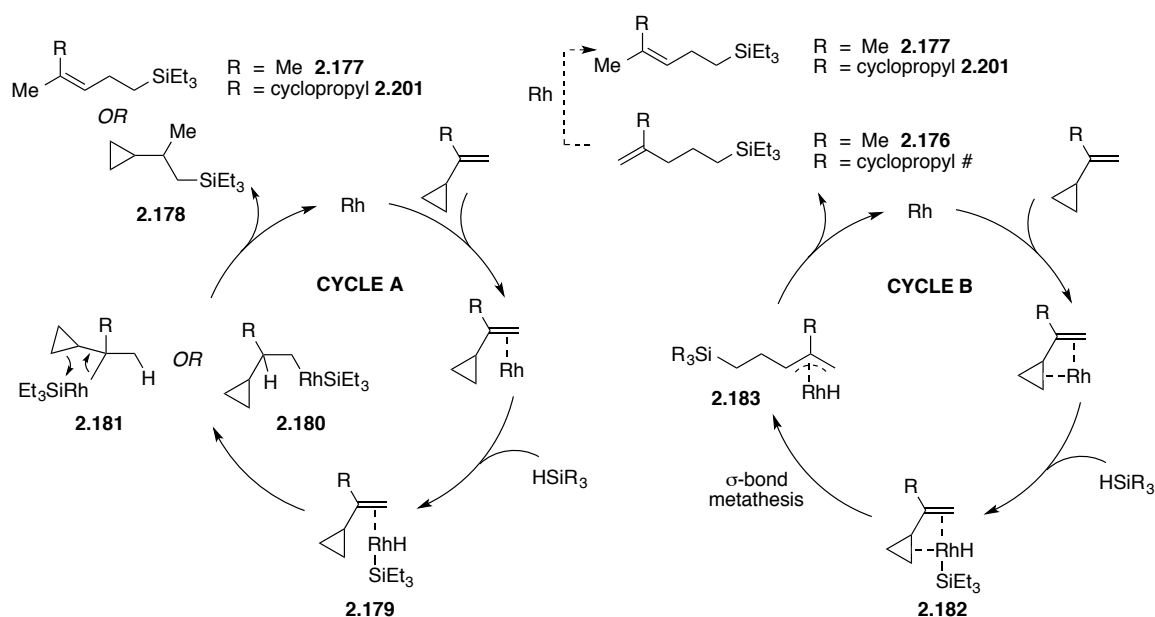
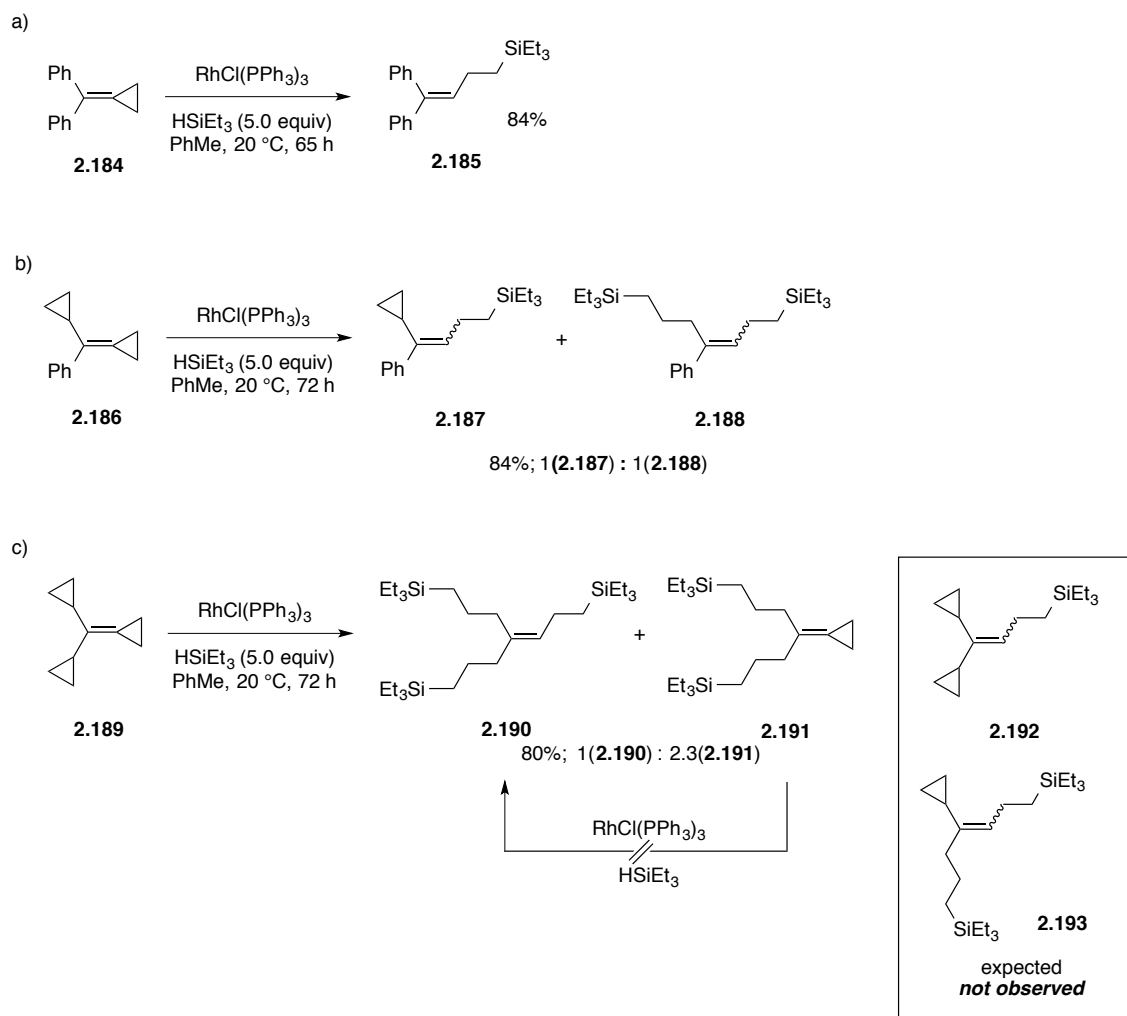


Figure 13. Proposed mechanisms for hydrosilylation of vinylcyclopropanes

Two years later, Beletskaya³⁴ published work on hydrosilylation reactions of methylenecyclopropanes (MCP) (Scheme 51). Under catalysis with $\text{RhCl}(\text{PPh}_3)_3$, MCP **2.184** provided diphenylsilylbutene **2.185** in 84% yield (Scheme 51a). The proposed mechanism for this transformation is illustrated by Cycle C in Figure 14. Olefin coordination and oxidative addition of the silane generates complex **2.194**. Migratory insertion furnishes **2.195** and subsequently goes through a β -carbon elimination and reductive elimination sequence to generate **2.185**. Exchanging one of the aryl groups for a cyclopropane ring (**2.186**) allowed for the formation of the analogous silane **2.187** and the disilylated alkene **2.188** in 84% yield as a 1:1 mixture (Scheme 51b). This second hydrosilylation event occurs through the mechanism proposed in Cycle D of Figure 14. Metal coordination to olefin **2.187** followed by oxidative addition of HSiEt_3 produces intermediate **2.196**. Migratory insertion generates the rhodium complex **2.197**, which undergoes β -carbon elimination followed by reductive elimination to give **2.188**.



Scheme 51. Hydrosilylation reactions of methylenecyclopropanes (MCPs)

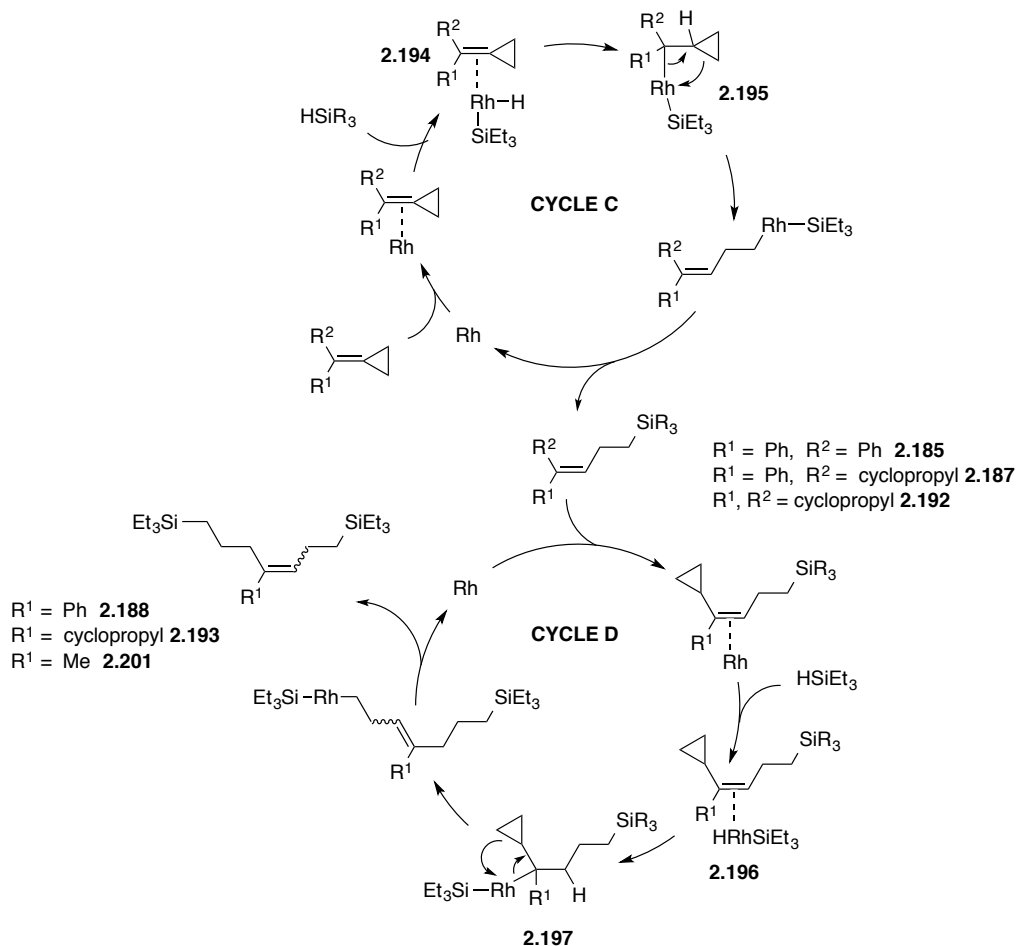
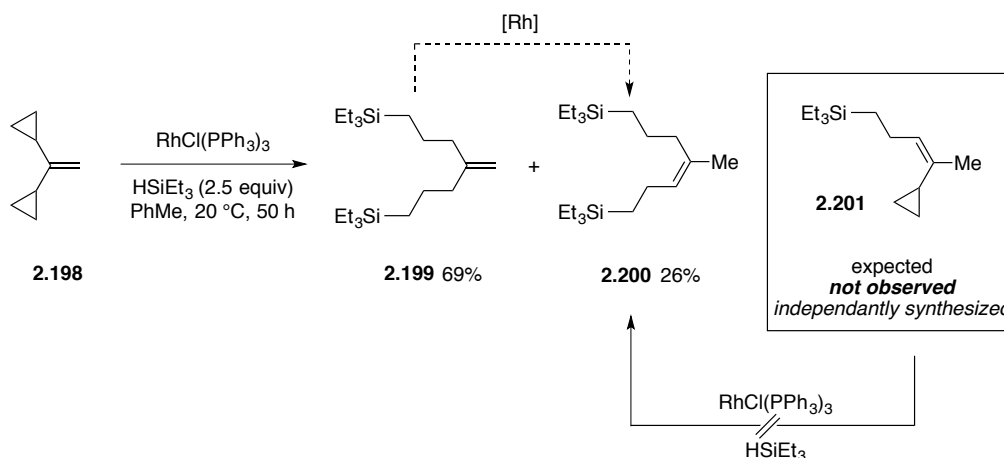


Figure 14. Proposed mechanism for hydrosilylation of methylenecyclopropenes (MCPs)

The reaction of dicyclopropyl MCP **2.189** with RhCl(PPh₃)₃ and triethylsilane gave unusual results (Scheme 51c). Trisilylated alkene **2.190** and disilylated MCP **2.191** were obtained in an 80% yield as a 1:2.3 mixture, respectively. It was anticipated that mono- (**2.192**) or di-silylated olefin **2.193** would have been observed in the reaction mixture rather than the unreacted MCP moiety. Compound **2.191** was isolated and re-subjected to the reaction conditions, and it was observed to be unreactive. It was therefore concluded that **2.191** is not an intermediate to the formation of **2.190**. The formation of **2.190** likely proceeds through disilylated olefin **2.193** by way of the mechanism outlined

in Figure 14. It is apparent, though, that an independent cycle is responsible for the formation of MCP **2.191** and is favored under these conditions.

Returning to the hydrosilylation reaction of vinylcyclopropanes, it appears that the unusual reactivity observed for dicyclopropyl MCP **2.189** (Scheme 51) was also observed for vinylcyclopropane **2.198**. Reaction of **2.198** with $\text{RhCl}(\text{PPh}_3)_3$ and triethylsilane produced a mixture of disilylated olefins **2.199** and **2.200** in 69% and 26% yield, respectively (Scheme 52). Had the mechanism for hydrosilylation that had been proposed in Figure 13 (Cycle A) been operative, the mono-silylated olefin **2.201** would likely have been observed. It is conceivable, however, that **2.201** is merely an intermediate to the formation of **2.200** as depicted by Figure 14, Cycle D. In order to probe whether **2.201** is an intermediate in the reaction, **2.201** was independently synthesized and re-subjected to the reaction conditions but did not afford **2.200**.



Scheme 52. Hydrosilylation of vinylcyclopropane

Drawing upon the mechanism illustrated in Cycle B (Figure 13), it was proposed that **2.199** and **2.200** (and by analogy, MCP **2.191**) could be formed through a mechanism supporting a dual migratory insertion across cyclopropane pathway (Figure 15). A cyclopropane agostic interaction (**2.203**) is assumed to facilitate migration of the

Rh–SiEt₃ bond (**2.204**). Upon reductive elimination (**2.205**) and re-coordination (**2.206**), a second insertion (**2.206**) generates the π -allyl rhodium hydride **2.207**. Reductive elimination of either **2.208** or **2.209** generates the observed products.

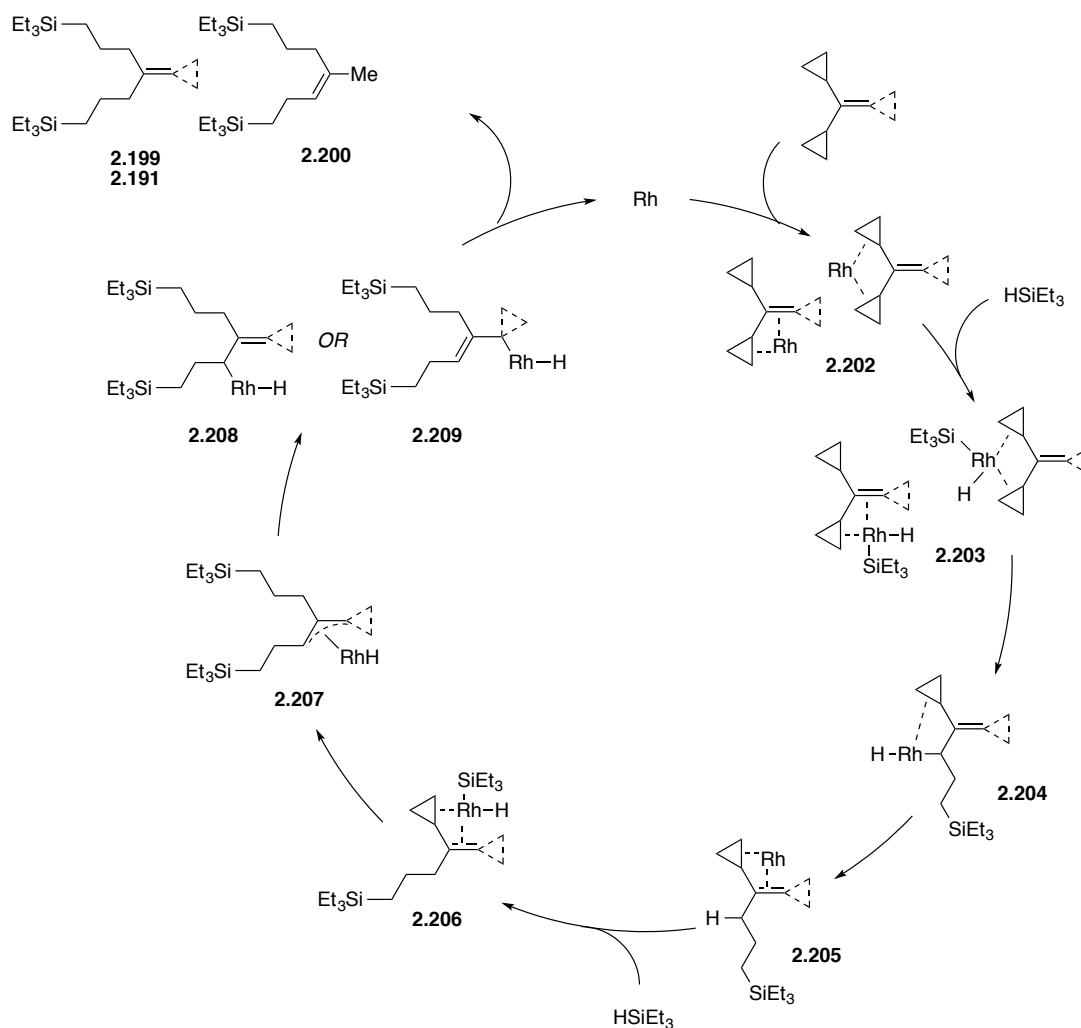
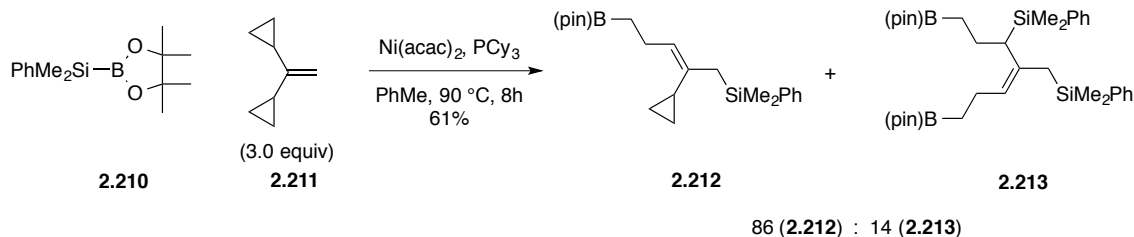


Figure 15. Proposed mechanism for dual migratory insertion across cyclopropane

Nearly two decades later, Ito³⁵ described an analogous C–C sigma-bond metathesis reaction under nickel catalysis with silylborane **2.210** (Scheme 53). Under these conditions, vinylcyclopropanes (**2.211**) were shown to undergo competitive cycloisomerization to cyclopentene, and were thus required in excess. A mixture of the

mono- and di-substituted products **2.212** and **2.13** was obtained in 61% yield, in favor of **2.212** (86:14). The formation of **2.212** and not of **2.201** (Scheme 52) likely is due to the preference for the bulky silyl group to reductively eliminate on the least hindered carbon. Additionally, Ito expanded this work to include reactions with vinylcyclobutanes.

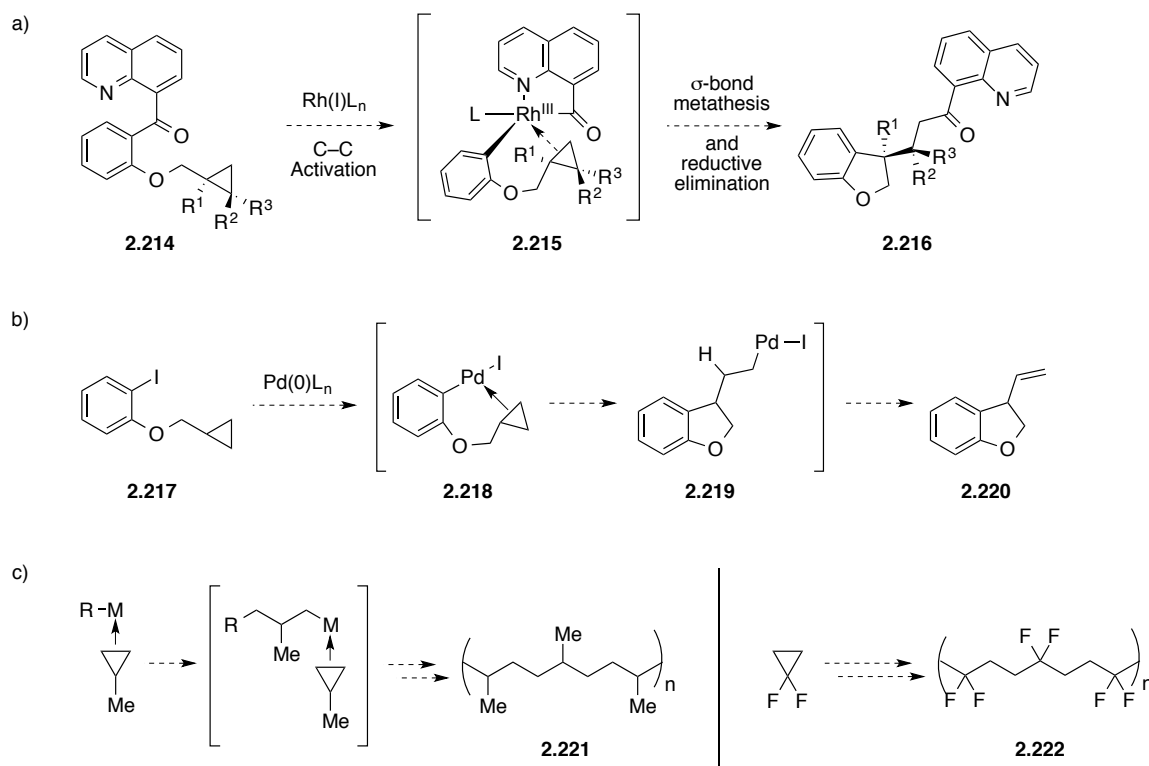


Scheme 53. Silylboration of vinylcyclopropanes

2.6.2 RESEARCH PROPOSAL

With C–C bonds of cyclopropane shown to engage in agostic interactions with transition metals and speculated to participate in σ -bond metathesis-like reactions, it was envisioned that the olefin in our intramolecular carboacylation reaction with 8-acylquinolines could be replaced with a cyclopropane ring (**2.214**) (Scheme 54a). Coupling the C–C bond activation step with a C–C bond cleavage process would produce homologated dihydrobenzofurans **2.216**. Given that many asymmetric cyclopropanation reactions have been developed, functionalized cyclopropane rings could be employed ($\text{R}^1, \text{R}^2, \text{R}^3 \neq \text{H}$) which would allow for the stereospecific construction of adjacent stereocenters. This feature of cyclopropanes addresses the limitation to our current methodology in that 1,2-disubstituted olefins are unreactive (see Section 2.3.2, Table 4).

It was further envisioned that other organometallic transformations with olefins, such as the Mizoroki-Heck reaction, could give homologated products by exploiting cyclopropanes (Scheme 54b). Migratory insertion across cyclopropanes could also be applied in the controlled synthesis of polymers (Scheme 54c). For example, polymer **2.221**, which is essentially a co-polymer of ethylene, propylene, and anti-regio propylene, could conceivably be accessed through a reactivity profile similar to the hydrogenation of cyclopropane.³⁶

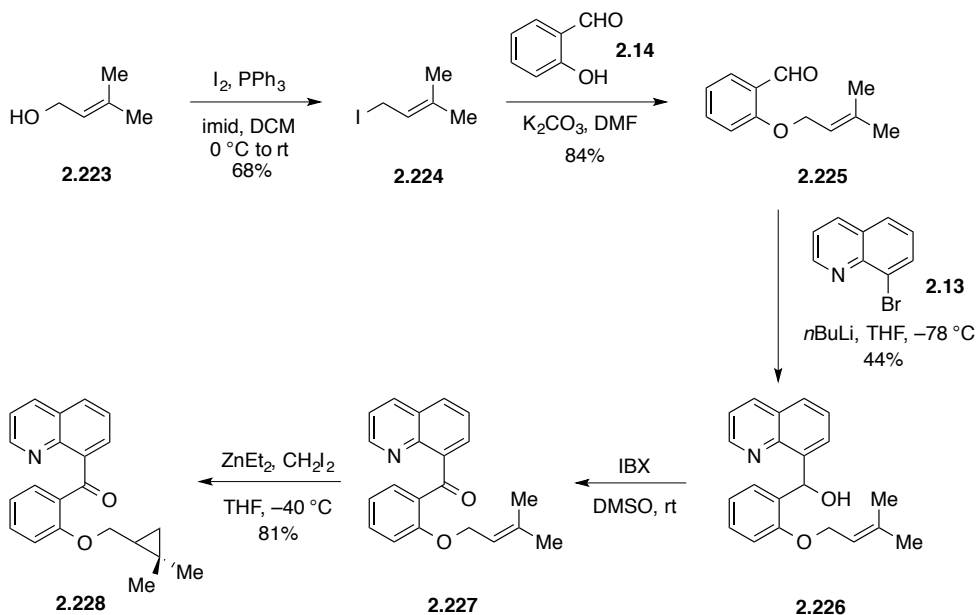


Scheme 54. Proposed sigma bond metathesis reactions with cyclopropane. a) Coupled with C–C bond activation with 8-acylquinolines. b) Homologated Mizoroki-Heck reaction. c) Polymerization of cyclopropane

2.6.3 RESULTS AND DISCUSSION

Substrate Synthesis

The quinolinyl cyclopropane **2.214** was readily prepared in a six-step sequence from commercially available prenol (**2.223**) (Scheme 55). Iodination of **2.223** with I₂ and triphenylphosphine provided iodide **2.224** in 68% yield. Alkylation of salicylaldehyde (**2.14**) and with iodided **2.224** afforded allylic ether **2.225** in 84% yield. The quinoline directing group was installed by traditional means to give alcohol **2.226** in 44% yield, and an IBX oxidation provided ketone **2.227**. Cyclopropanation of the trisubstituted olefin **2.227** with diethylzinc and diiodomethane furnished cyclopropane substrate **2.228** in 81% yield.

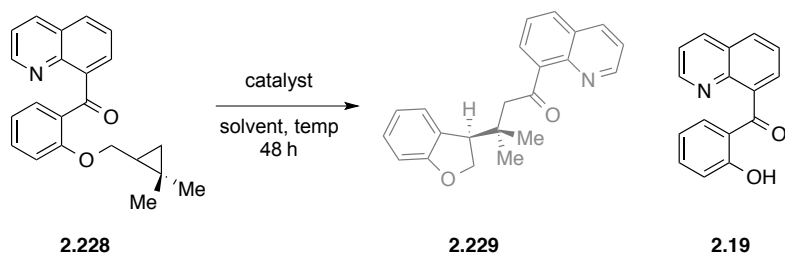


Scheme 55. Synthesis of quinolinyl cyclopropane substrate **2.228**

Reaction Screen

Cyclopropane **2.228** was subjected to a variety of Rh(I) and Ir(I) catalysts in PhMe (130 °C), THF (100 °C), and decalin (200 °C) (Table 7). Under most conditions, the starting material was recovered in full; however, with cationic complexes [Rh(cod)₂]OTf and [Rh(cod)₂]BF₄, phenol **2.19** was formed in 50–100% conversion (entries 2–5). It is speculated that catalyst may act as a Lewis acid and coordinate to the ether oxygen. This forced proximity may facilitate an S_N2'-like attack of the metal onto the cyclopropane ring. The release of 4-methylpenta-1,3-diene (b.p. 76 °C) would accompany such a complex undergoing β-hydride elimination.

Table 7. Carboacylation across cyclopropane reaction screen

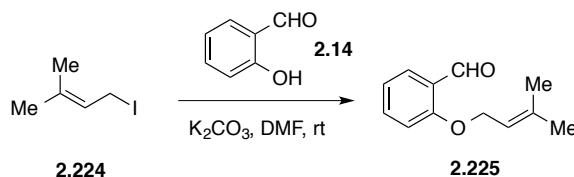


Entry	Catalyst	Solvent	Temperature	2.228:2.19
1	RhCl(PPh ₃) ₃	PhMe	130 °C	1:0
2	Rh(cod) ₂ OTf	PhMe	130 °C	1:1
3	Rh(cod) ₂ OTf	THF	100 °C	1:1
4	Rh(cod) ₂ OTf	decalin	200 °C	0:1
5	Rh(cod) ₂ BF ₄	PhMe	130 °C	2:1
6	[Rh(C ₂ H ₄) ₂ Cl] ₂	PhMe	130 °C	1:0
7	[Rh(C ₂ H ₄) ₂ Cl] ₂	decalin	200 °C	1:0
8	Rh(acac)(cod)	PhMe	130 °C	1:0
9	[Rh(cod)OMe] ₂	PhMe	130 °C	1:0
10	[Rh(cod)OH] ₂	PhMe	130 °C	1:0
11	Rh(nbd) ₂ BF ₄	PhMe	130 °C	1:0
12	Rh(acac)(CO) ₂	PhMe	130 °C	1:0
13	[Rh(coe) ₂ Cl] ₂	PhMe	130 °C	1:0
14	[Ir(coe) ₂ Cl] ₂	PhMe	130 °C	1:0

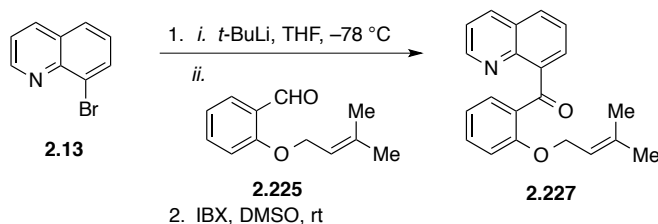
2.6.4 CONCLUDING REMARKS

The preliminary work described in Section 2.6 regarding sigma-bond metathesis across cyclopropane with concurrent C–C bond activation has been less-than promising. It is common for new methodologies to require high-throughput experimentation in order to discover initial reactivity. Without much fundamentally known about the activation and functionalization of C–C bonds, it was perhaps a lofty goal to combine the two methods. Since oxidative addition into C–X bonds is well studied, better understood, and more attuned to a variety of transition metals, combining this elementary step with sigma-bond metathesis across cyclopropane may prove more feasible (see Scheme 54b).

2.6.5 EXPERIMENTAL

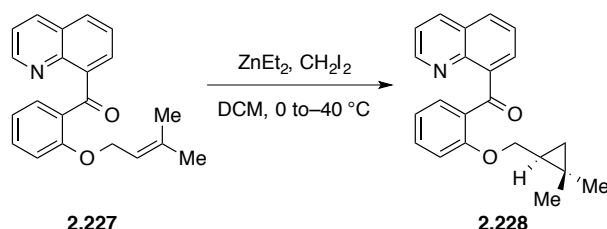


Iodide **2.224** (1.64 g, 8.35 mmol), salicylaldehyde (**2.14**) (0.36 mL, 3.34 mmol), K_2CO_3 (1.38 g, 10.0 mmol), and DMF (22 mL) were added to a flask wrapped in aluminum foil and stirred overnight at rt. Water and EtOAc were added and the layers were separated. The aqueous layer was extracted with EtOAc and the combined organic layers were washed with NaOH (to remove unreacted salicylaldehyde), 2 M LiCl (2×25 mL) and brine; dried over Na_2SO_4 , filtered, and concentrated. Aldehyde **2.225** was obtained as an orange oil (545 mg, 2.86 mmol, 86%).



Dry THF (20 mL) and 8-bromoquinoline (**2.13**) (596 mg, 2.86 mmol) were added to a flame-dried flask under N_2 and cooled to $-78^\circ C$. $t-BuLi$ (1.7 M in pentane, 2.0 mL, 3.43 mmol) was added dropwise and the resulting solution was stirred at $-78^\circ C$ for 1 h. Aldehyde **2.225** (545 mg, 2.86 mmol) was added as a THF solution at $-78^\circ C$ and was allowed to come to room temperature overnight. The reaction was quenched with sat. NH_4Cl and extracted with EtOAc. The combined organic layers were washed with brine, dried over Na_2SO_4 , filtered, and concentrated. Flash chromatography gave the corresponding alcohol (404 mg, 1.26 mmol, 44%) as a yellow solid: R_f 0.20

(1:4 EtOAc:Hex). The alcohol (200 mg, 0.63 mmol) was treated with IBX (353 mg, 1.26 mmol) in DMSO (4 mL) and stirred at room temperature to give ketone **2.227** in quantitative yield.



Diiodomethane (0.87 mL, 3.24 mmol) and dry DCM (2.5 mL) were added to a flame-dried flask and cooled to 0 °C. Diethyl zinc (neat, 0.17 mL, 1.61 mmol) was added dropwise and the resulting solution was stirred at 0 °C for 30 min and then cooled to –40 °C. Ketone **2.227** (256 mg, 0.81 mmol) was added as a cooled (–40 °C) THF solution (5 mL) via cannula and allowed to come to room temperature over night. The solution was cooled to 0 °C and quenched with sat. NH₄Cl. The aqueous layer was extracted with DCM. The combined organic layers were washed with brine, dried over Na₂SO₄, filtered, and concentrated. Flash chromatography provided cyclopropane **2.228** (219 mg, 0.66 mmol, 82%): *R_f* 0.32 (1:4 EtOAc:Hex); ¹H NMR (500 MHz; CDCl₃) δ 8.82 (dd, *J* = 4.2, 1.8 Hz, 1H), 8.16 (dd, *J* = 8.3, 1.8 Hz, 1H), 7.99 (dd, *J* = 7.7, 1.8 Hz, 1H), 7.88 (dd, *J* = 8.2, 1.4 Hz, 1H), 7.76 (dd, *J* = 7.1, 1.4 Hz, 1H), 7.57 (dd, *J* = 8.1, 7.2 Hz, 1H), 7.48–7.44 (m, 1H), 7.38 (dd, *J* = 8.3, 4.2 Hz, 1H), 7.08 (td, *J* = 7.5, 0.8 Hz, 1H), 6.78 (d, *J* = 8.2 Hz, 1H), 3.56 (dd, *J* = 9.9, 6.2 Hz, 1H), 3.41 (dd, *J* = 9.9, 8.6 Hz, 1H), 0.60 (s, 6H), 0.02 (dt, *J* = 8.5, 4.1 Hz, 10H), –0.07–0.13 (m, 1H), –0.31 (t, *J* = 4.9 Hz, 1H); ¹³C NMR (126 MHz; CDCl₃) δ 197.1, 158.7, 150.3, 146.0, 142.3, 135.7, 133.8,

131.0, 129.47, 129.28, 128.0, 127.8, 125.9, 121.2, 120.4, 112.3, 69.4, 26.7, 22.0, 19.2,
17.8, 15.6.

REFERENCES

- (1) Douglas, C. J.; Overman, L. E. *Proc. Natl. Acad. Sci.* **2004**, *101*, 5363.
- (2) Denissova, I.; Barriault, L. *Tetrahedron* **2003**, *59*, 10105.
- (3) Dreis, A. M.; Douglas, C. J. *J. Am. Chem. Soc.* **2009**, *131*, 412.
- (4) Tomimoto, M.; Nobuhiro, G. *J. Phys. Chem.* **1995**, *99*, 563.
- (5) Wang, J.; Chen, W.; Zuo, S.; Liu, L.; Zhang, X.; Wang, J. *Angew. Chem. Int. Ed.* **2012**, *51*, 12334.
- (6) Rathbun, C. M.; Johnson, J. B. *J. Am. Chem. Soc.* **2011**, *133*, 2031.
- (7) Singleton, D. A.; Thomas, A. A. *J. Am. Chem. Soc.* **1995**, *117*, 9357.
- (8) Frantz, D. E.; Singleton, D. A.; Snyder, J. P. *J. Am. Chem. Soc.* **1997**, *119*, 3383.
- (9) Lutz, J. P.; Rathbun, C. M.; Stevenson, S. M.; Powell, B. M.; Boman, T. S.; Baxter, C. E.; Zona, J. M.; Johnson, J. B. *J. Am. Chem. Soc.* **2012**, *134*, 715
- (10) Espinet, P.; Echavarren, A. M. *Angew. Chem. Int. Ed.* **2004**, *43*, 4704.
- (11) Denmark, S. E.; Sweis, R. F. *J. Am. Chem. Soc.* **2004**, *126*, 4876
- (12) Jones, G. D.; Martin, J. L.; McFarland, C.; Allen, O. R.; Hall, R. E.; Haley, A. D.; Brandon, R. J.; Konovalova, T.; Desrochers, P. J.; Pulay, P.; Vicic, D. A. *J. Am. Chem. Soc.* **2006**, *128*, 13175.
- (13) Wentzel, M. T.; Reddy, V. J.; Hyster, T. K.; Douglas, C. J. *Angew. Chem. Int. Ed.* **2009**, *48*, 6121.
- (14) Murai, S.; Kakiuchi, F.; Sekine, S.; Tanaka, Y.; Kamatani, A.; Sonoda, M.; Chatani, N. *Nature*. **1993**, *366*, 529.
- (15) Hoang, G. T.; Reddy, V. J.; Nguyen, H. H. K.; Douglas, C. J. *Angew. Chem. Int. Ed.* **2011**, *123*, 1922.
- (16) Krug, C.; Hartwig, J. F. *J. Am. Chem. Soc.* **2002**, *124*, 1674.
- (17) Krug, C.; Hartwig, J. F. *Organometallics* **2004**, *23*, 4594.
- (18) Krug, C.; Hartwig, J. F. *J. Am. Chem. Soc.* **2004**, *126*, 2694.
- (19) Zhao, P.; Hartwig, J. F. *Organometallics* **2008**, *27*, 4749.
- (20) Murai, M.; Miki, K.; Ohe, K. *Chem. Commun.* **2009**, 3466.
- (21) Waterman, R. *Organometallics* **2013**, *32*, 7249.
- (22) Walsh, A. D. *Trans. Faraday Soc.* **1949**, *45*, 179.

- (24) Tipper, C. F. H.; Lawrence, C. D. *J. Chem. Soc.* **1955**, 713.
- (25) Tipper, C. F. H.; Walker, D. A. *J. Chem. Soc.* **1957**, 1199.
- (26) Tipper, C. F. H.; Walker, D. A. *J. Chem. Soc.* **1959**, 1352.
- (27) Brayshaw, S. K.; Green, J. C.; Kociok-Köhn, G.; Sceats, E. L.; Weller, A. S. *Angewandte Chemie International Edition* **2006**, 45, 452.
- (28) Brayshaw, S. K.; Sceats, E. L.; Green, J. C.; Weller, A. S. *Proc. Nat. Acad. Sci.* **2007**, 104, 6921.
- (29) Chaplin, A. B.; Weller, A. S. *Organometallics* **2010**, 29, 2332.
- (30) Periana, R. A.; Bergman, R. G.; *J. Am. Chem. Soc.* **1984**, 106, 7272.
- (31) Periana, R. A.; Bergman, R. G. *Organometallics* **1984**, 3, 508.
- (32) Periana, R. A.; Bergman, R. G. *J. Am. Chem. Soc.* **1986**, 108, 7346.
- (33) Bessmertnykh, A. G.; Blinov, K. A.; Grishin, Y. K.; Donskaya, N. A.; Beletskaya, I. P. *Tetrahedron Lett.* **1995**, 36, 7901.
- (34) Bessmertnykh, A. G.; Blinov, K. A.; Grishin, Y. K.; Donskaya, N. A.; Tveritinova, E. V.; Yur'eva, N. M.; Beletskaya, I. P. *J. Org. Chem.* **1997**, 62, 6069.
- (35) Suginome, M.; Matsuda, T.; Yoshimoto, T.; Ito, Y. *Organometallics* **2002**, 21, 1537.
- (36) Bond, G. C.; Newham, J. *Trans. Faraday. Soc.* **1960**, 56, 1501.

CHAPTER THREE

A Search for a More Synthetically Viable Method

INTRODUCTION

We have demonstrated that intramolecular carboacylation reactions with 8-acylquinolines can efficiently increase molecular complexity in a single step; however, the methodology is limited by the covalent nature of the directing group. Installation of the quinoline moiety is generally low yielding and purification by column chromatography is often challenging. Moreover, the inability to remove the directing group renders the methodology relatively useless in terms of synthetic applicability. In order to make advancements, we must identify directing groups that can be readily installed and easily removed or functionalized. The focus of this chapter will be on my efforts to design scaffolds that will address the limitations imposed by quinoline as a directing group.

3.1 OTHER HETEROCYCLIC DIRECTING GROUPS

Before beginning the pursuit of an all-encompassing directing group, other covalently-bonded heterocycles were designed in order to study their reactivity toward C–C bond activation. It was anticipated that these studies would provide useful insight

into the fundamental role of the directing group in C–C bond activation. With many biologically relevant molecules containing various heterocyclic manifolds, it was envisioned that obtaining a library of suitable directing groups could prove useful in the synthesis of such compounds. Heterocycles **3.1–3.10** were proposed as substrates for intramolecular carboacylation reactions (Figure 16).

Pyridine **3.4** and pyrimidine **3.5** analogs would probe whether structurally rigid directing groups are required for bond activation. The six-five fused systems of **3.6–3.10** would examine whether the directionality of the nitrogen lone pair affects cyclometalation. It is likely that quinoxaline **3.1**, quinazoline **3.2**, and 1,7-naphthyridine **3.3** will undergo the desired carboacylation reaction in that they closely resemble quinoline in structure. These moieties are prevalent in many cytotoxic drugs. Benzoxazoles (**3.6a**), benzothiazoles (**3.6b**), and benzimidazoles (**3.6c**) exhibit a range of biological activities including antitumor, antimicrobial, anti-inflammatory, antihyperglycaemic, anthelmintic, and CNS activities.¹ [1,2,4]triazolo[1,5-*a*]pyridines (**3.7**) and tetrazolo[1,5-*a*]pyridines (**3.8**) have been shown to inhibit JAK2 receptors which present opportunities for targeted therapy of myeloproliferative diseases.² [1,2,4]triazolo[3,4-*a*]phthalazines (**3.10**) have been known for their anticonvulsive properties.³

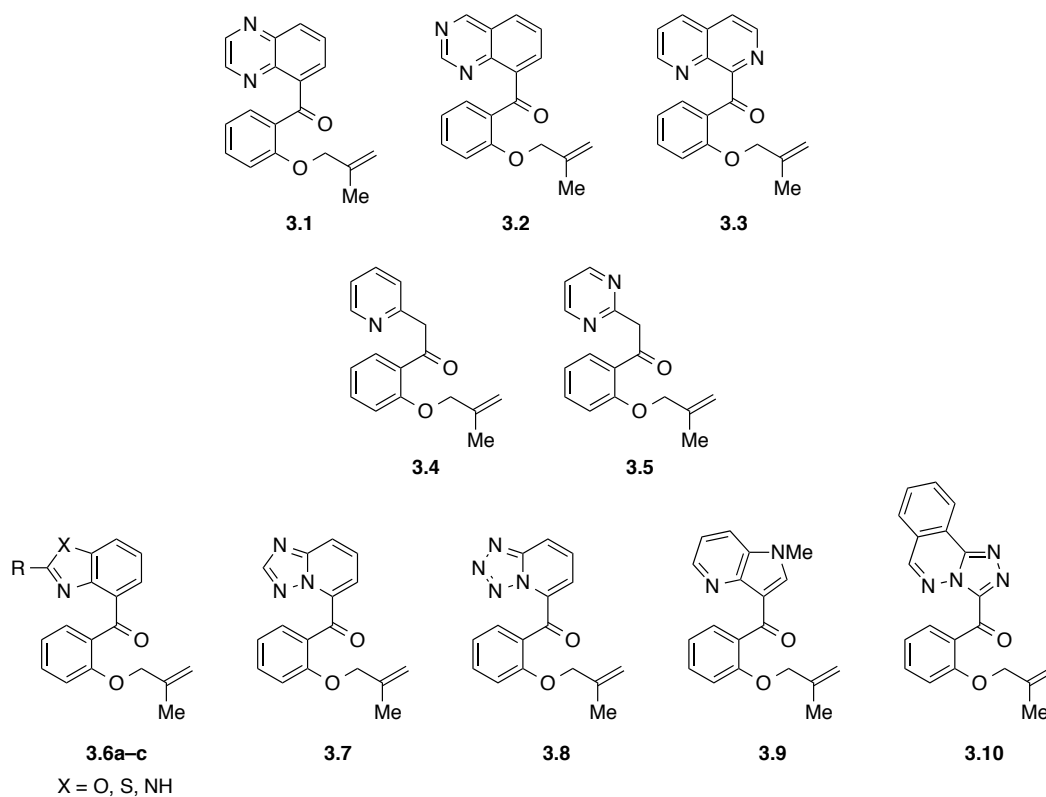
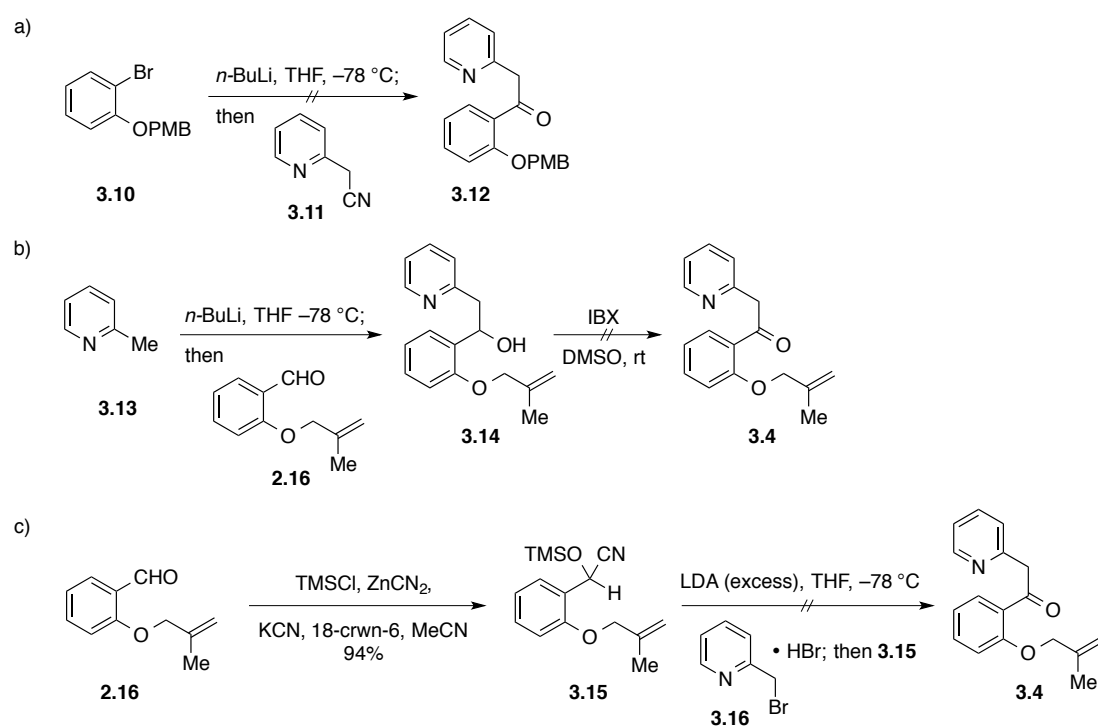


Figure 16. Other heterocyclic directing groups for intramolecular carboacylation reactions

3.1.1 SUBSTRATE SYNTHESSES

Quinoxaline (**3.1**), quinazoline (**3.2**), and 1,7-naphthyridine (**3.3**) closely resemble quinoline and thus compounds **3.4–3.10** were initially chosen to pursue. Three synthetic routes were attempted for the preparation of pyridyl substrate **3.4** (Scheme 56). The addition of lithiated bromide **3.10** into pyridyl nitrile **3.11** did not afford the ketone upon aqueous workup (Scheme 56a). Deprotonation of 2-methyl pyridine (**3.13**) with *n*-BuLi followed by addition into aldehyde **2.16** gave the corresponding alcohol **3.14**; however, oxidation with IBX did not yield **3.4** (Scheme 56b). Unfortunately other oxidation conditions were examined. Cyanohydrin **3.15** was obtained in 94% yield by

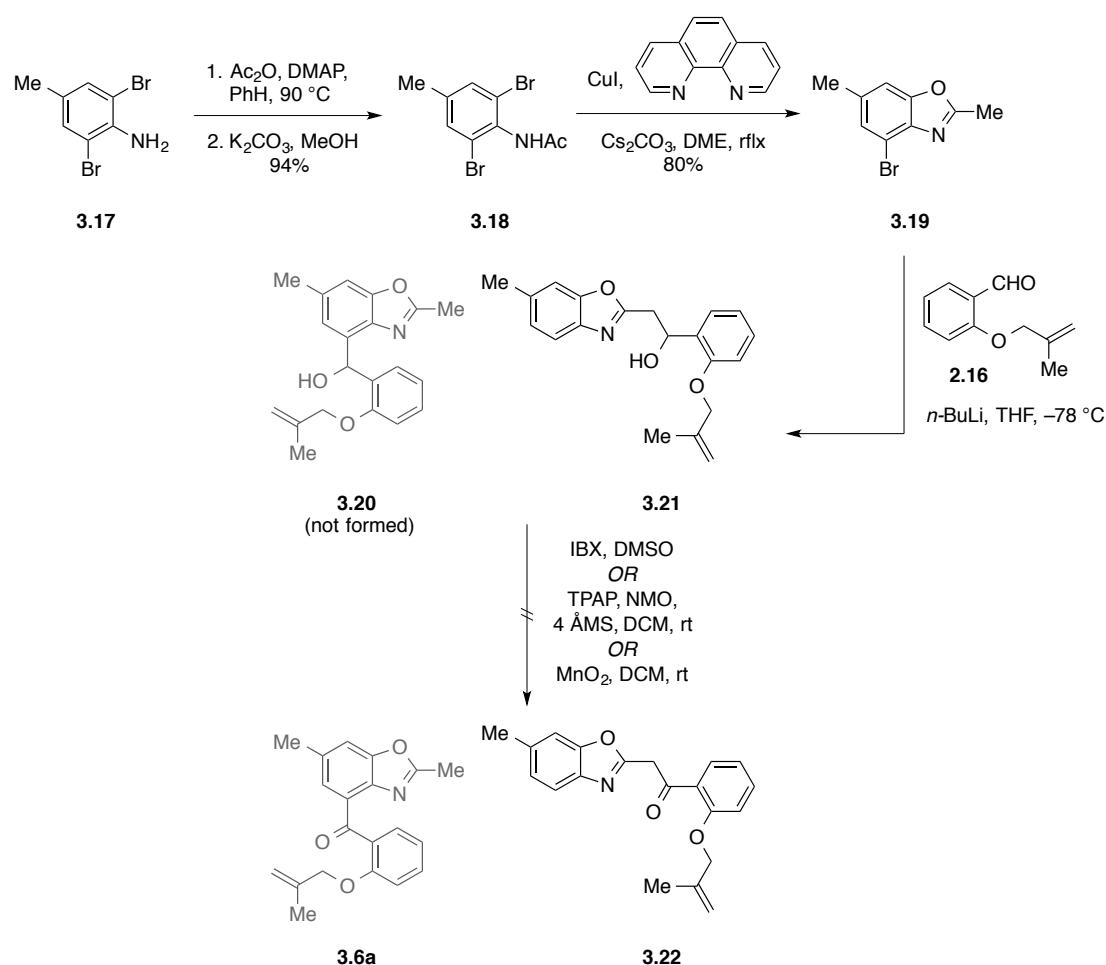
treating aldehyde **2.16** with TMSCl, ZnCN₂, and KCN (Scheme 56c). Several attempts to promote the umpolung substitution of pyridyl bromide **3.16** with deprotonated **3.15** were unsuccessful. The hydrochloride salt of **3.16** was added directly to **3.15** as a solution with excess LDA. In addition, efforts were made to first deprotonate **3.16** and isolate 2-(bromomethyl)pyridine prior to reaction with **3.15**. Upon free-basing **3.16**, the solution turned red in color, which likely indicated that **3.16** readily reacts with itself.



Scheme 56. Attempted syntheses of pyridyl substrate **3.4**

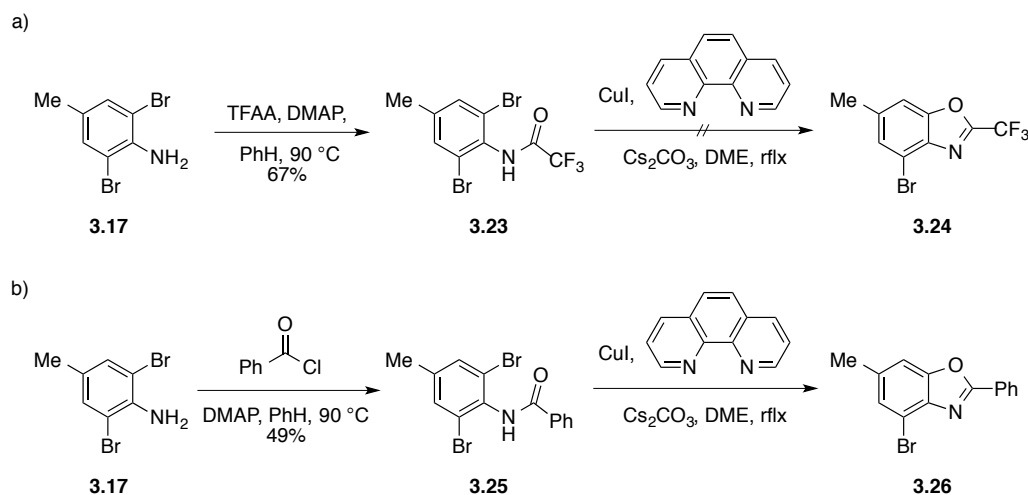
The synthesis of benzoxazole substrate **3.6a** began with an double acylation reaction of 2,6-dibromo-4-methylaniline (**3.17**), followed by cleavage of one of the acyl groups on the resulting imide with K₂CO₃ in MeOH to give amide **3.18** in 94 % yield (Scheme 57). Attempts to monoacylate the aniline were met with surprising difficulty in that a mixture

of starting material, mono- and di-substituted products were obtained. A copper-promoted amide cyclization provided the benzoxazole **3.19** in 80% yield. Lithiation of bromide **3.19** with *n*-BuLi, followed by addition of aldehyde **2.16**, gave a complex mixture wherein the desired alcohol **3.20** was not obtained. The major product was alcohol **3.21**, which likely resulted from initial lithiation of the bromide and subsequent intermolecular deprotonation of the methyl group. Since ketone **3.22** was also properly configured to undergo C_{aryl}–C_{ketone} bond activation, alcohol **3.21** was subjected to oxidation conditions; however, reactions with IBX, TPAP/NMO, and MnO₂ were unsuccessful.



Scheme 57. Attempted synthesis of benzoxazole substrates **3.6a**

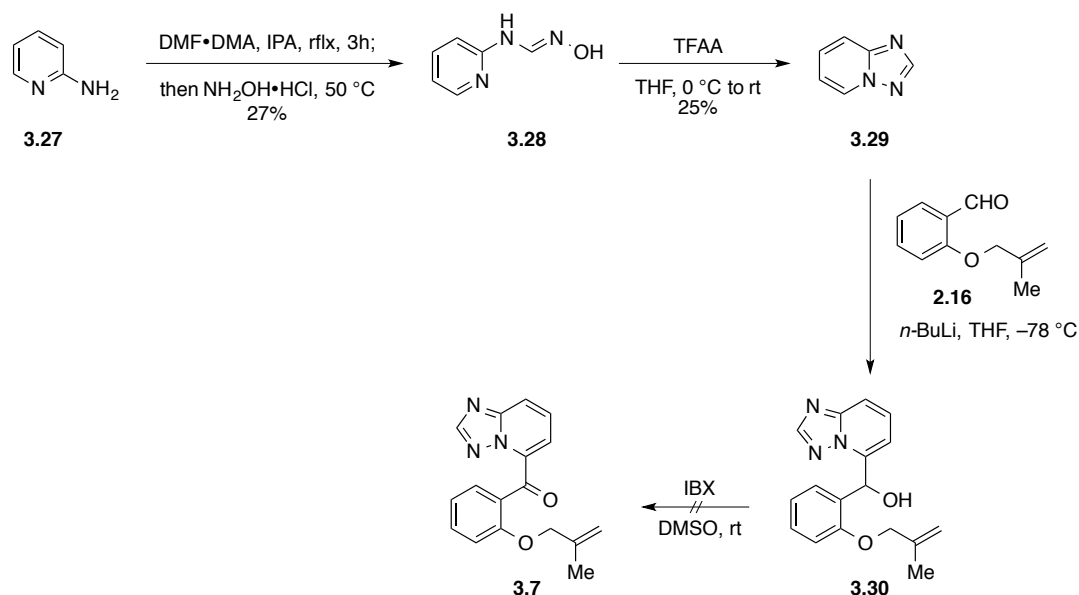
In order to avoid the problematic methyl deprotonation in **3.19**, the synthesis of a CF₃ and Ph derivative were explored. Acylation of **3.17** with trifluoroacetic anhydride delivered the trifluoroacetamide **3.23** in 67% yield. The cyclization of **3.23** under copper catalysis was not effective, likely owing to the decreased basicity of the carbonyl oxygen. Mono-acylation with benzoyl chloride gave amide **3.25** in 49% yield. Phenyl-substituted benzoxazole **3.26** was obtained upon cyclization of amide **3.25** with CuI, 1,10-phenanthroline, and Cs₂CO₃ in refluxing DME. 4-bromo benzoxazole **3.26** has yet to be examined under the lithium-halogen exchange conditions for the addition into salicylaldehyde derivative **2.16**.



Scheme 58. Preparation of 4-bromo benzoxazole derivatives

The [1,2,4]triazolo[1,5-*a*]pyridine heterocycle **3.29** was obtained in two steps from 2-amino pyridine (**3.27**). Treating **3.27** with *N,N*-dimethylformamide dimethyl acetal in refluxing isopropanol, followed by addition of hydroxylamine hydrochloride afforded amide oxime **3.28** in 27% yield. A TFAA-promoted cyclization of **3.28** provided the

heterocycle **3.29** in 25% yield. Regioselective deprotonation with *n*-BuLi, followed by addition of aldehyde **2.16** provided alcohol **3.30**. Oxidation of crude **3.30** with IBX did not provide the desired ketone **3.7**.



Scheme 59. Synthetic efforts toward [1,2,4]triazolo[1,5-*a*]pyridine **3.7**

3.1.2 CONCLUDING REMARKS

The incomplete syntheses of pyridyl ketone **3.4**, benzoxazole ketone **3.6a**, and [1,2,4]triazolo[1,5-*a*]pyridyl ketone **3.7** were due to the unsuccessful oxidation with IBX. During the time of these studies, IBX oxidations of the corresponding quinolinyll alcohols were also problematic. It is possible that the IBX prepared in-house was not of acceptable quality. Furthermore, alternative oxidation conditions should be thoroughly explored. These compounds should be readily obtainable with additional optimization.

At the time, my interest in pursuing other ideas for removable directing groups had

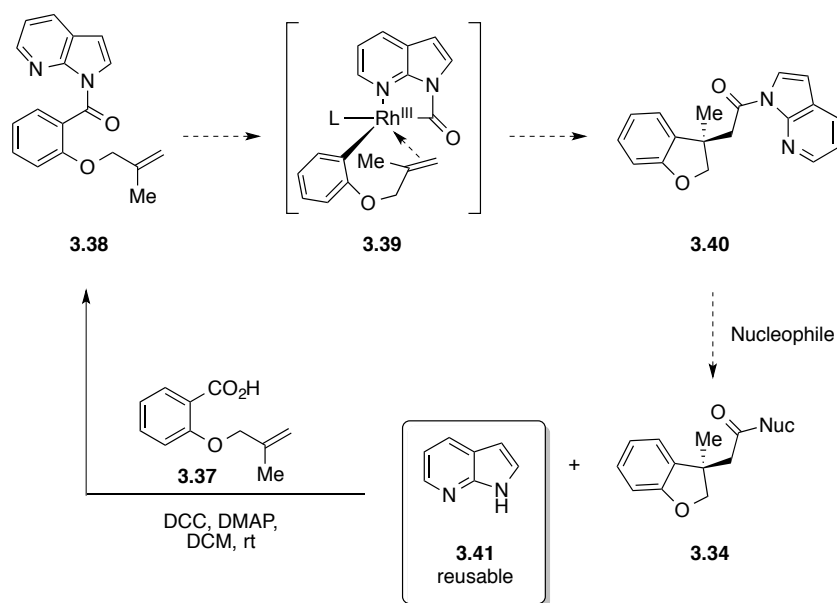
naïvely dissuaded me from continuing efforts toward directing groups that appeared to suffer from the same limitations as quinoline. However, it was not considered that such alternative directing groups, such as those illustrated in Figure 16, may be more electronically conducive to removal and/or exhibit favorable reactivity that otherwise was inaccessible to quinoline-derived carboacylation substrates (such as decreased temperatures, or propensity toward facilitating enantioselective reactions). It is my conjecture that re-investigating alternative covalently-bound directing groups may unveil favorable reactivity despite the perceived limitations.

3.2 CLEAVABLE HETEROCYCLIC DIRECTING GROUPS

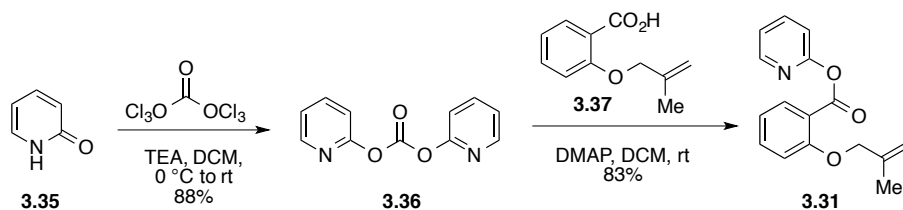
Our attention was turned to heterocyclic directing groups that could readily be removed and/or functionalized. Similar to the idea presented with quinolinyl ester **2.156** (Section 2.6), directing groups that are covalently linked through labile moieties, such as an ester or an amide, were designed. In addition, heterocycles of masked functionality, such as oxadiazoles, tetrazoles, and isoxazoles were envisioned.

3.2.1 RESEARCH PROPOSAL

The lack of reactivity seen with quinolinyl ester **2.156** (Section 2.6) was attributed to the less favored six-membered metallacycle (compared to a five-membered metallacycle) that would be formed. It was imagined that replacing quinoline for pyridine (**3.31**) would allow for the generation of the more stable five-membered metallacycle **3.32** (Scheme 60). The ester of dihydrobenzofuran **3.33** would be susceptible to cleavage by a suitable nucleophile to give a product free of the directing group **3.34** and pyridinone **3.35**, which can be recycled. The preparation of substrate **3.31** begins with the dimerization of pyridinone **3.35** by treatment with triphosgene to give 2-DPC (**3.36**) in 88% yield (Scheme 61). The Yamaguchi-like esterification between **3.36** and acid **3.37** in the presence of DMAP generated pyridyl ester **3.31** in 83% yield.

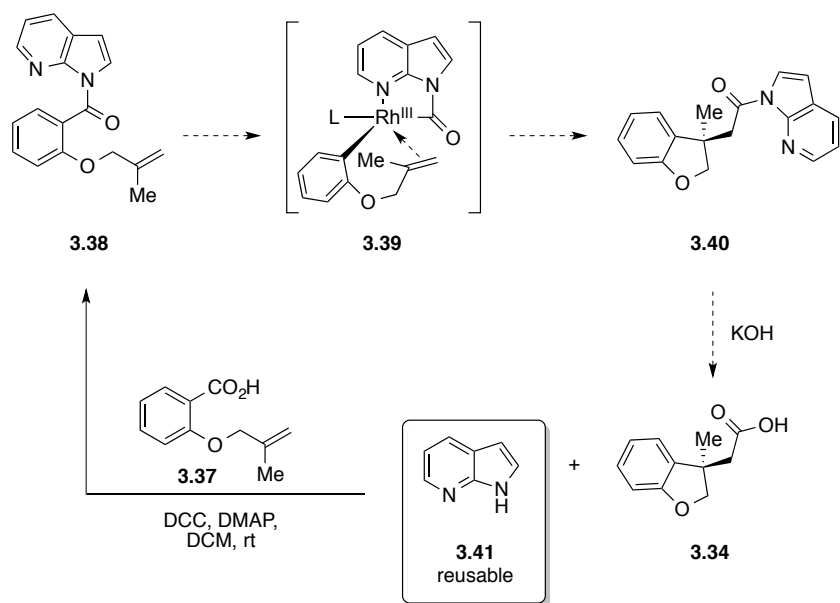


Scheme 60. Proposed intramolecular carboacylation reaction with pyridyl ester directing group



Scheme 61. Synthesis of pyridyl ester **3.31**

Azaindole substrate **3.38** was designed with the idea that the aryl amide bond would be more electrophilic, and thus more prone to nucleophilic cleavage than a typical amide bond. Nucleophilic acyl substitution of dihydrobenzofuran **3.40** would furnish 7-azaindole (**3.41**) that could be reused in the synthesis of **3.38** (Scheme 62). In addition, oxadiazole **3.42**, tetrazole **3.43**, and isoxazole **3.44** were viewed as directing groups of ‘masked functionality.’ After cyclization to dihydrobenzofurans **3.45–3.46**, the heterocycles could reveal synthetically useful groups such as **3.49–3.54** (Figure 17).



Scheme 62. Proposed intramolecular carboacylation reaction with azaindole directing group

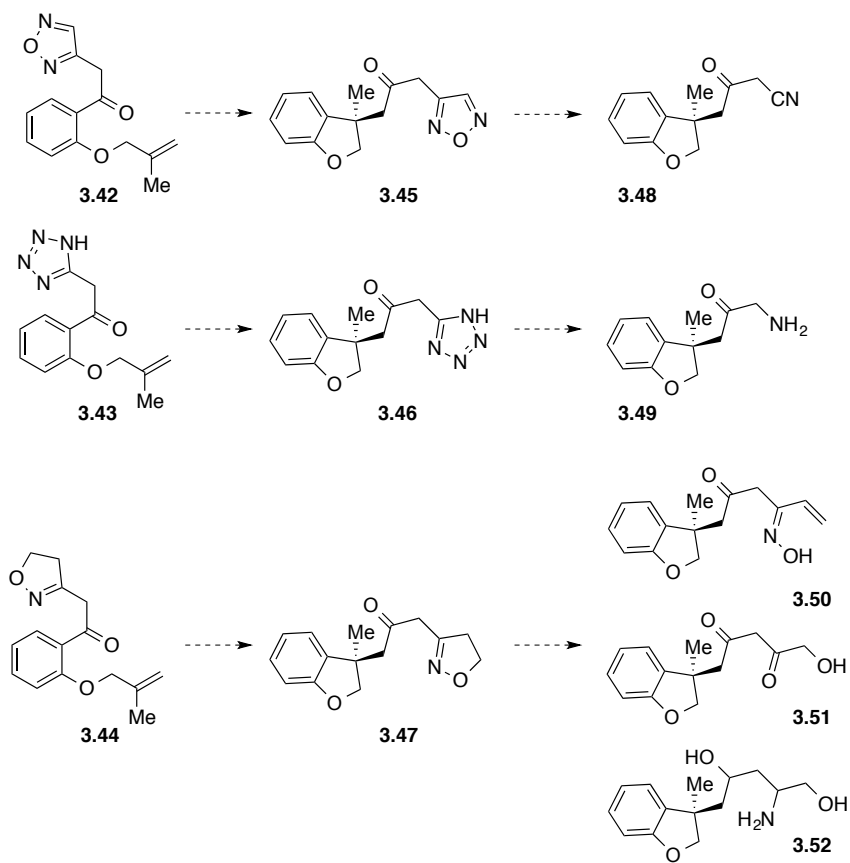
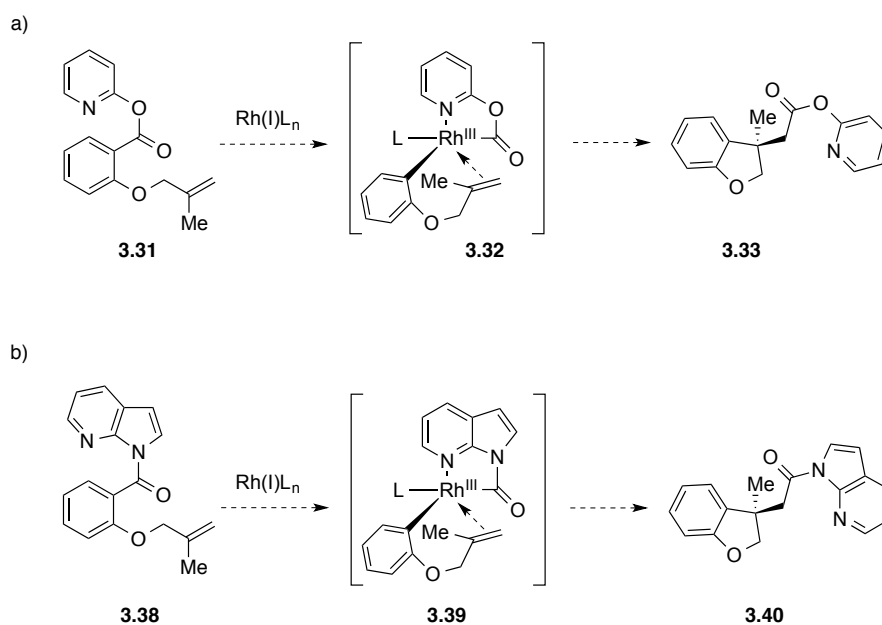


Figure 17. Proposed heterocycles of masked functionality

3.2.2 RESULTS AND DISCUSSION



Scheme 63. Preliminary carboacylation reaction screen with pyridyl ester **3.31** and azaindole **3.38**

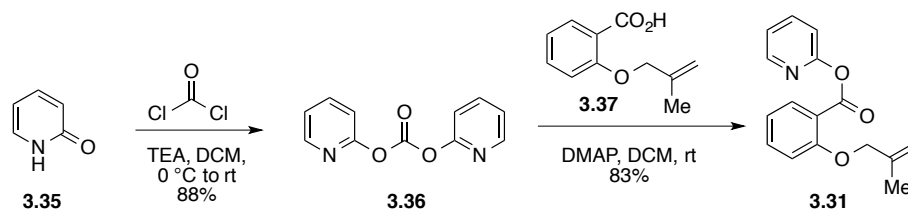
Treating pyridyl ester **3.31** with $\text{RhCl}(\text{PPh}_3)_3$, $[\text{RhCl}(\text{C}_2\text{H}_4)_2]_2$, or $\text{Rh}(\text{cod})_2\text{OTf}$ in PhMe (130 °C), DMF (150 °C), or THF (100 °C) for 48 h gave crude reaction mixtures that showed significant consumption of starting material, though no expected signals attributable to **3.33** were observed. The major product consisted of a terminal olefin reminiscent of the 1,1-disubstituted allylic arrangements, and appeared to contain seven aromatic peaks. Although a phenolic resonance was not apparent, it is presumed that ester **3.31** underwent an aromatic Claisen rearrangement. Interestingly, the reaction in THF (100 °C) with $\text{Rh}(\text{cod})_2\text{OTf}$ exclusively provided acid **3.37** with no resonances observed for the corresponding pyridinone **3.35** moiety after removal of the solvent under reduced pressure. The observed hydrolysis may indicate that the THF was wet.

It was anticipated that the directionality of the nitrogen lone pair imposed by the six-five fused nature of the azaindole heterocycle may complicate cyclometalation. It was found that azaindole **3.38** was unreactive in the presence of $\text{RhCl}(\text{PPh}_3)_3$ or $[\text{RhCl}(\text{C}_2\text{H}_4)_2]_2$ catalysts in PhMe (130 °C) and xylene (150 °C), but was presumably due to the lack of solubility. Though soluble in DCE (100 °C) and THF (100 °C), the reactions with these catalysts also returned starting material. However, running the reaction in THF (100 °C) with $\text{Rh}(\text{cod})_2\text{OTf}$ resulted in decomposition.

3.2.2 CONCLUDING REMARKS

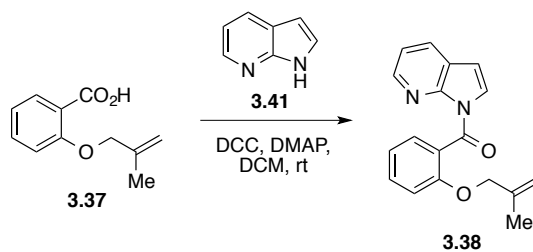
The preliminary investigations toward C–C bond activation reactions with ester- and amide-bound directing groups did not provide promising results. Since the proposed mechanism for $\text{C}_{\text{acyl}}\text{--C}$ bond activation proceeds through a tetrahedral intermediate, in which the transition metal acts as a nucleophile similar to that of all carbonyl substitution reactions, it may be that ester and amide functionalities are not adequately susceptible toward nucleophilic attack by a metal complex. Increasing the electron density around the metal center by introducing electron-rich ligands may facilitate C–C bond activation. In addition, higher temperatures may be required to promote the reaction.

3.2.4 EXPERIMENTAL



2-pyridinone **3.35** (3.0 g, 31.54 mmol), triethylamine (4.4 mL, 31.54 mmol), and dry DCM (30 mL) were added to a flame-dried flask and cooled to 0 °C under N_2 . Phosgene (20% solution in PhMe, 8.3 mL, 15.77 mmol) was added dropwise and the resulting solution was stirred at 0 °C for 1 h and then allowed to come to room temperature. Water was added to the reaction and the layers were separated. The organic layer was washed with brine, dried with Na_2SO_4 , filtered, and concentrated to give 2-di-pyridyl carbonate **3.36** (2.99 g, 1.38 mmol, 88%).ⁱ Acid **3.37** (1.79 g, 9.34 mmol), 2-DPC **3.36** (2.34 g, 9.34 mmol), DMAP (114 mg, 0.93 mmol), and dry DCM (60 mL) were added to a flame-dried flask under N_2 and stirred overnight at room temperature. Celite was added to the reaction mixture and the solvent removed. Flash chromatography provided pyridyl ester **3.31** (2.08 g, 7.72 mmol, 83%) as a colorless oil: ^1H NMR (500 MHz; CDCl_3) δ 8.17 (dd, $J = 7.8, 1.8$ Hz, 1H), 7.55-7.48 (m, 2H), 7.40-7.38 (m, 1H), 7.14-7.11 (m, 1H), 7.04 (d, $J = 8.4$ Hz, 1H), 6.62 (d, $J = 9.2$ Hz, 1H), 6.32 (td, $J = 6.6, 1.0$ Hz, 1H), 5.16 (s, 1H), 5.12 (s, 1H), 4.69 (s, 2H), 1.88 (s, 3H); ^{13}C NMR (126 MHz; CDCl_3): δ 166.3, 165.3, 157.4, 141.9, 138.8, 134.70, 134.51, 133.6, 122.1, 120.3, 118.3, 115.1, 113.0, 107.2, 73.5, 19.4.

ⁱ Procedure: Sunggak, K.; Jae, I. L.; Young, K. K. *Tetrahedron Lett.* **1984**, 25, 4943



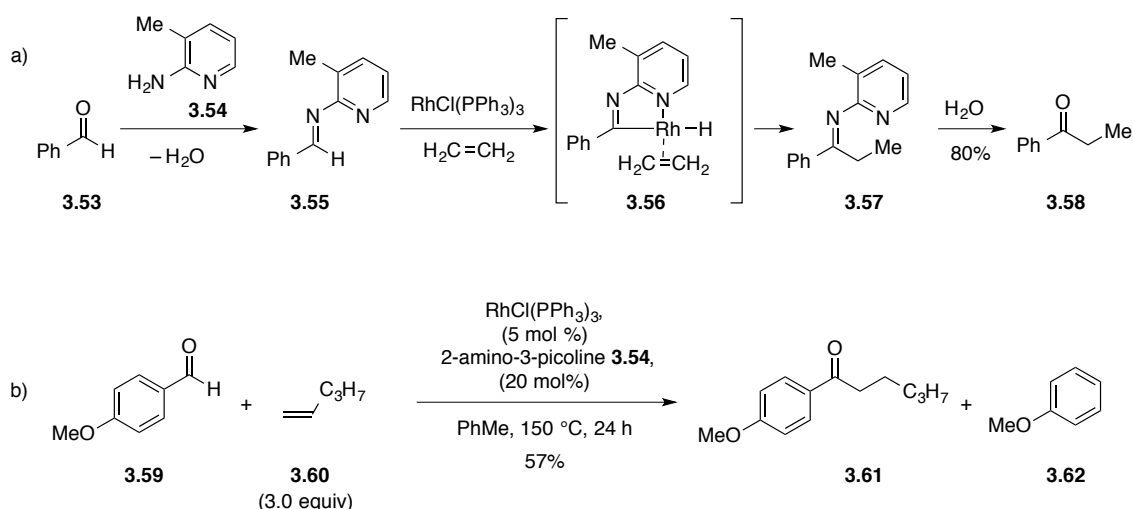
^1H NMR (500 MHz; CDCl_3) δ 8.22 (ddd, $J = 20.0, 6.3, 1.7$ Hz, 1H), 7.84 (dd, $J = 7.8, 1.6$ Hz, 1H), 7.72 (d, $J = 4.1$ Hz, 1H), 7.57-7.48 (m, 2H), 7.14-7.03 (m, 2H), 6.94 (d, $J = 8.3$ Hz, 1H), 4.66 (app s, 1H), 4.63 (app s, 1H), 4.24 (app s, 2H), 1.33-1.31 (m, 3H);

^{13}C NMR (126 MHz; CDCl_3) δ 166.1, 156.4, 148.1, 144.4, 139.9, 132.4, 129.6, 128.9, 126.7, 125.4, 123.4, 120.8, 118.9, 112.2, 105.8, 72.0, 29.7, 18.7.

3.3 METAL-ORGANIC COOPERATIVE CATALYSIS

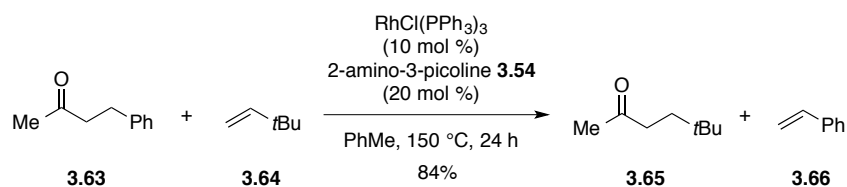
3.3.1 BACKGROUND TO MOCC IN C–C BOND ACTIVATION

The applicability of chelation-assisted bond activation reactions is severely limited by the covalent nature of the directing group. Installment of the directing group can be troublesome, and subsequent removal is often even more challenging. In efforts to suppress decarbonylation in aldehyde C–H bond activation through cyclometalation, Suggs devised a system in which a pyridyl directing group **3.54** is introduced through a condensation reaction with benzaldehyde (**3.53**) to give the aldimine **3.55** (Scheme 64).⁴ Upon treatment with Wilkinson's catalyst, the intermediate metallacycle **3.56** undergoes migratory insertion across ethylene. Reductive elimination affords imine **3.57**, which upon hydrolysis provides the corresponding ketone **3.58** in 80% yield. It was later discovered that 2-amino-3-picoline (**3.54**) could be used catalytically. Without the need to pre-form the aldimine, treating aldehyde **3.59** with 20 mol% 2-amino-3-picoline (**3.54**) and 5 mol% RhCl(PPh₃)₃ gave a 85:15 product ratio of ketone **3.61** and anisole (**3.62**); anisole resulted from the background decarbonylative reaction without chelation assistance.⁵ The rate of reaction was shown to be dependent upon the concentration of co-catalyst **3.54**, which would suggest that imine formation was rate determining. Further evidence for this came about when it was discovered that MOCC hydroacylation reactions were greatly accelerated through a transimination pathway with benzoic acid and aniline additives.⁶



Scheme 64. a) Suggs' C–H bond activation in hydroacylation reactions b) Jun's MOCC C–H bond activation in hydroacylation reactions

In 1999, Jun successfully transitioned into MOCC C–C bond activation with 2-amino-3-picoline co-catalysts.⁷ An alkyl exchange reaction between ketone **3.63** and olefin **3.64** produced ketone **3.65** in 84% yield along with styrene (**3.66**) as the by-product (Scheme 65). The mechanism for this transformation is thought to proceed by a condensation reaction between 2-amino-3-picoline (**3.54**) and ketone **3.64** to produce ketimine **3.67** (Figure 18). The pyridyl nitrogen ligates the catalyst and directs it into the α -iminyl C–C bond to give rhodium complex **3.68**. Upon β -hydride elimination (**3.69** \rightarrow **3.69**) and olefin exchange (**3.69** \rightarrow **3.70**), migratory insertion across the coordination alkene produces rhodium complex **3.71**. Reductive elimination generates ketimine **3.72** and hydrolysis liberates ketone **3.65**. It should be noted that no products resulting from activation of the methyl C–C bond were observed. This observation may indicate that β -hydride elimination is necessary to perturb the equilibrium by means of liberating styrene, which polymerizes under the reaction conditions.



Scheme 65. MOCC C–C bond activation alkyl exchange reaction

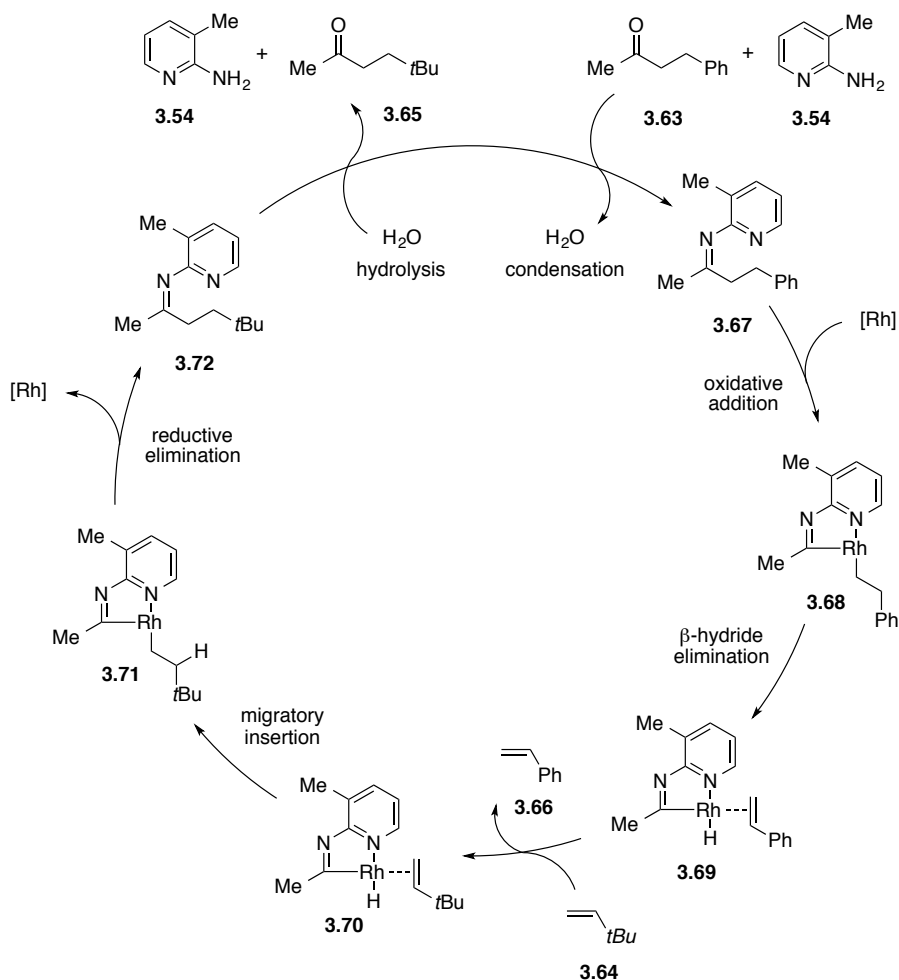
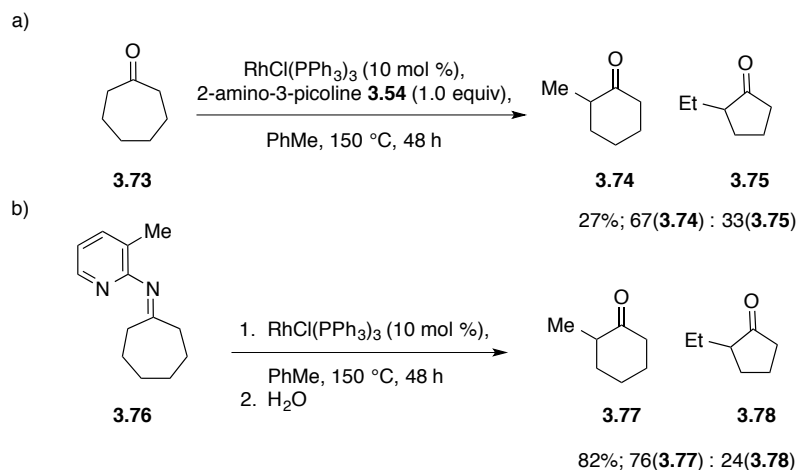


Figure 18. Mechanism for MOCC C–C bond activation alkyl exchange reaction

In 2001, Jun discovered that ring contractions could be promoted by MOCC C–C bond activation with 2-amino-3-picoline.⁵ In the absence of an external olefin, cyclooctanone **3.73** reacts with 2-amino-3-picoline (**3.54**) and RhCl(PPh₃)₃ to give

cyclohexanone **3.74** and cyclopentanone **3.75** in 27% yield as a 67:33 mixture (Scheme 66a). However, subjecting the pre-formed ketimine **3.76** to the reaction conditions increased the efficiency of the reaction to give the respective products in 82% yield (Scheme 66b).



Scheme 66. MOCC C–C bond activation ring contraction reactions. a) Without pre-formed imine b) With pre-formed imine

The ring contraction mechanism involves oxidative addition into the α -iminyl C–C bond of ketimine (**3.76** \rightarrow **3.79a**). The resulting rhodium complex undergoes β -hydride elimination to form the rhodium hydride **3.79b** (Figure 19). Reinsertion of the appended olefin with opposite regioselectivity produces cycloadduct **3.80**, which has the option to either undergo reductive elimination (**3.80** \rightarrow **3.77**), or undergo β -hydride elimination to generate the rhodium hydride **3.81**. Olefin insertion, followed by reductive elimination furnishes the cyclopentimine **3.78**.

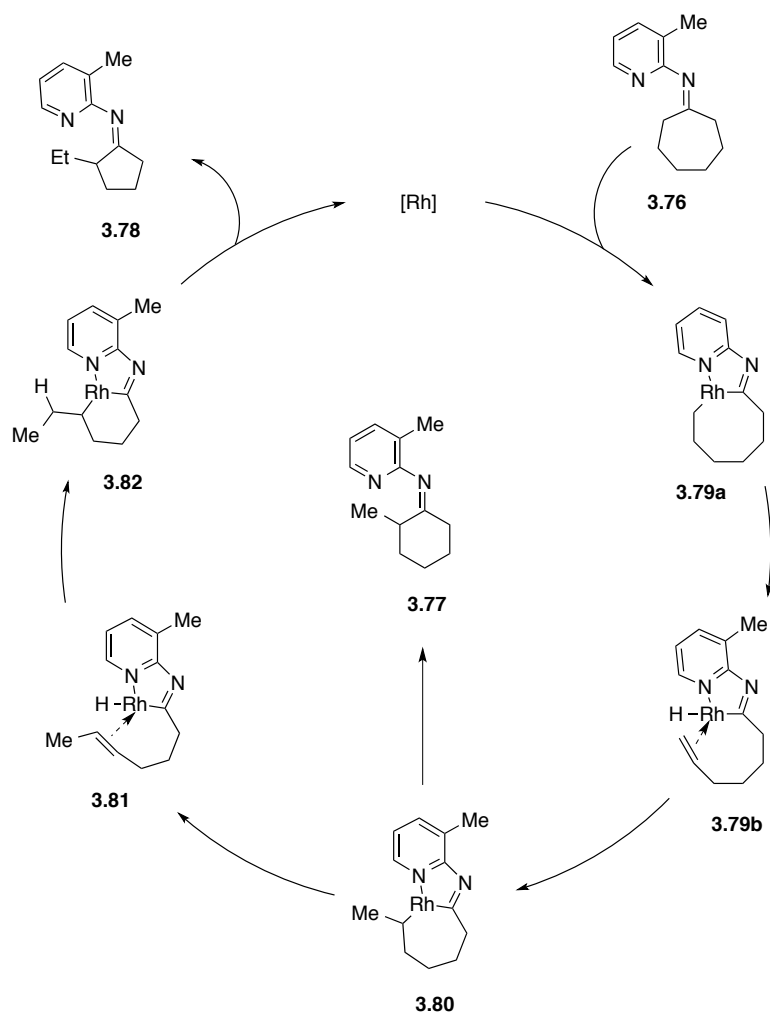


Figure 19. Proposed mechanism for MOCC C–C bond activation ring contraction reactions

In theory, the MOCC work developed by Jun would be applicable to various ketones and thus greatly widen the scope of C–C bond activation. However, the methodology is limited by the need for substrates containing β -hydrogens. This requirement stems from the equilibrium nature of the reaction. The polymerization of styrene in the alkyl exchange reaction works to drive the equilibrium toward products, whereas an excess of olefin was necessary for similar reactions that did not produce styrene as a by-product (Scheme 65). The driving force for the ring contraction reaction is likely the stability gained upon going from a 7-membered ring to either 6- or 5-membered rings. The

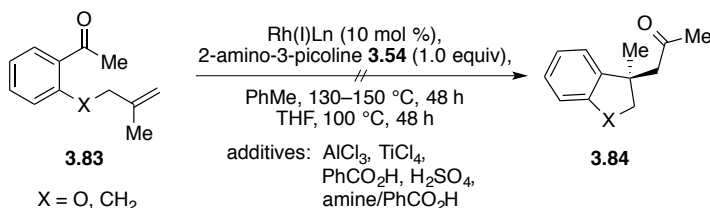
reaction also suffered from an unfavorable equilibrium between ketone and imine, which unfortunately is the rate-limiting step of catalysis.

3.3.2 RESEARCH PROPOSAL

Our group set out to design a system that would bypass the need for substrates to contain β -hydrogens. Drawing upon our previous work in intramolecular carboacylation reactions with 8-acylquinoline (see Section 2.1), we envisioned that a similar strategy would render MOCC as method to build molecular complexity with C–C bond activation while also addressing the limitations of a covalent directing group. Ketone **3.83** was selected as a suitable substrate to investigate the propensity toward intramolecular carboacylation with MOCC (Scheme 67). The driving force for the reaction would be the exchange of a relatively weak C_{acyl}–C bond and C–C π bond for a stronger C–C bond and another C–C σ bond.

Preliminary workⁱⁱ to promote the cyclization of ketones **3.83** to dihydrobenzofurans **3.84** were met without success. Under conditions employing various catalysts with solvent and temperature screens the reaction returned only starting material and, in some cases, a side-product derived from an aromatic Claisen rearrangement. With imine formation suggested to be the rate-limiting step,^{5,6} Lewis and Brønstad acids additives were investigated in order to facilitate the condensation. Unfortunately, no successful conditions were realized, even those involving transimination. Surprisingly, no attempts to subject the pre-formed imine were made.

ⁱⁱ Unpublished results by Michael T. Wenzel



Scheme 67. Unsuccessful attempts at MOCC intramolecular carboacylation with 2-amino-3-picoline

With aryl ketones being less electrophilic than aliphatic ketones, it was imagined that exploiting a more nucleophilic co-catalyst would enable imine formation. Alternative co-catalysts **3.85–3.89** were investigated, though none gave promising results (Figure 20).ⁱⁱⁱ Interestingly though, the pyrrolidine-substituted picoline **3.85** was shown to activate methyl ketones, including acetone, and subsequently undergo intermolecular carboacylation reactions.^{iv} Co-catalysts **3.90–3.91** were also selected for evaluation in MOCC C–C bond activation reactions and will be discussed in the following section.

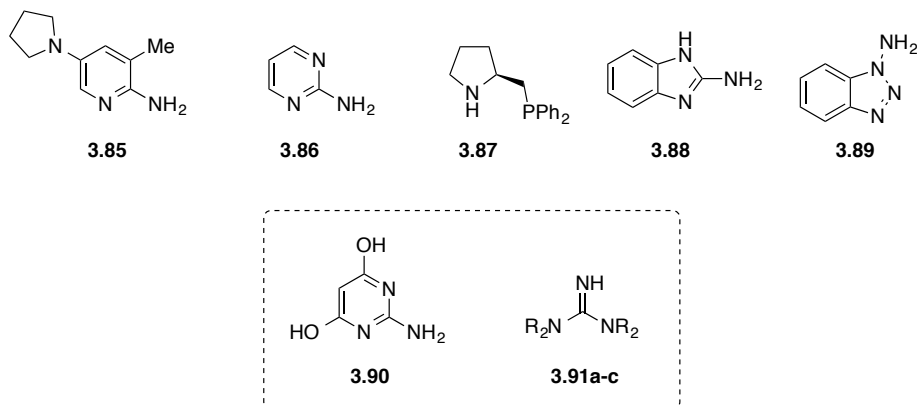


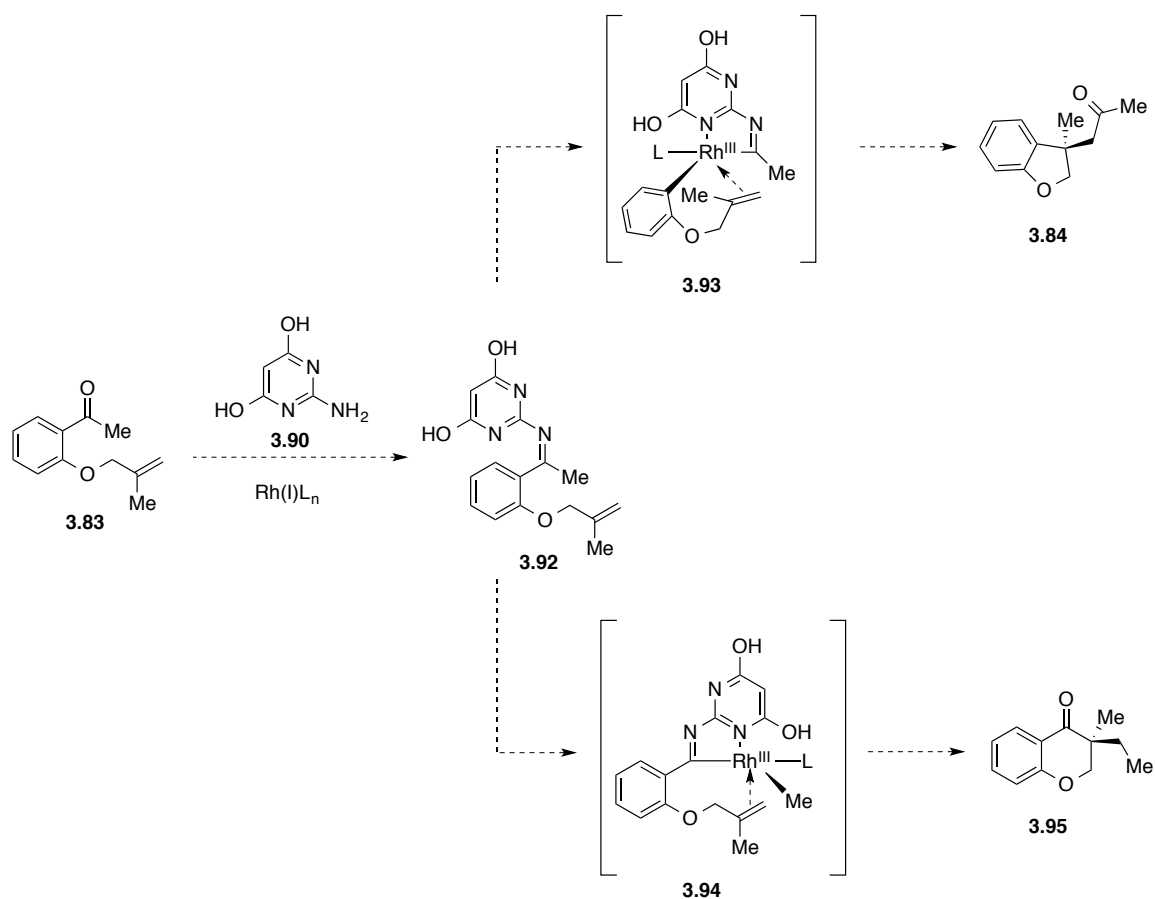
Figure 20. Alternative co-catalyst directing groups for MOCC C–C bond activation

ⁱⁱⁱ Unpublished results by Michael T. Wenzel

^{iv} Unpublished results by Sudheer Chava

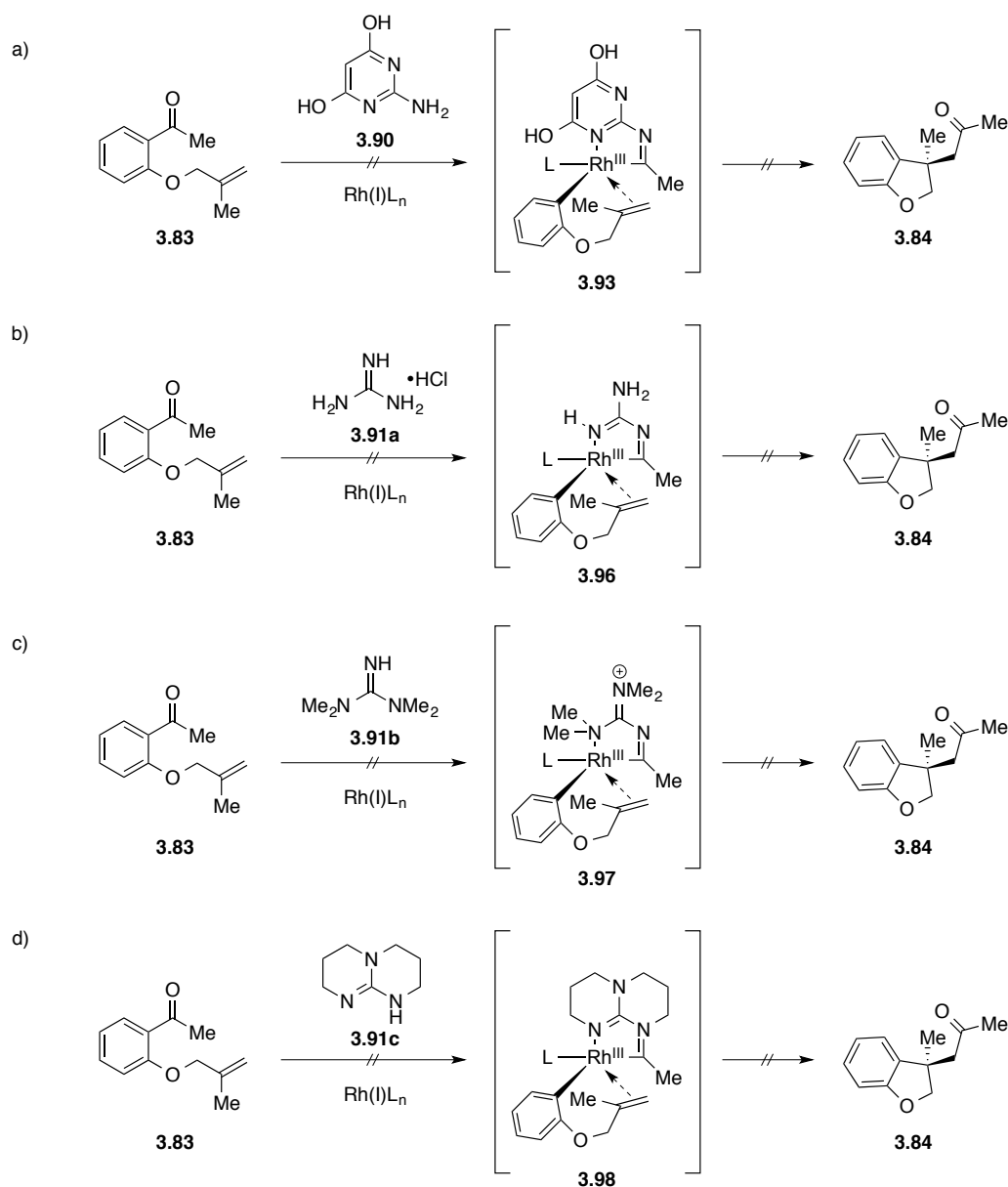
3.3.3 RESULTS AND DISCUSSION

Pyrimidine **3.90** was selected as a potential MOCC directing group with the idea that the added electron density from the hydroxyl groups would render the amino group more nucleophilic and thus more reactive toward condensation with an aromatic ketone (**3.92**) (Scheme 68). Upon oxidative addition of the C_{aryl}–C_{acyl} bond (**3.93**), and subsequent cyclization, a dihydrobenzofuran product **3.84** would be obtained after hydrolysis. Alternatively, since methyl ketones were shown to be reactive with picoline derivative **3.85** (see Figure 20), it was proposed that activation of the C_{methyl}–C_{acyl} bond (**3.94**) could deliver chromanone **3.95**. A preliminary reaction screen with ketone **3.83** and pyrimidine **3.90** was unsuccessful in providing either dihydrobenzofuran **3.83** or chromanone **3.95** (Scheme 69a). Several catalysts were employed, including: RhCl(PPh₃)₃, [Rh(C₂H₄)Cl]₂, Rh(cod)₂BF₄, [Rh(cod)OH]₂, [Rh(coe)₂Cl]₂, Rh(CO)₂(acac), Rh(norb)₂BF₄, [Ir(coe)₂Cl]₂, and [Ir(cod)₂OMe]₂. The reactions were run in toluene at 130 °C for 48 h in sealed vial under a nitrogen atmosphere; DMSO as a solvent was also explored. Product mixtures resulting from unreactive starting material, olefin isomerization, Claisen rearrangement, and deallylation were obtained.



Scheme 68. Proposed MOCC C–C bond activation with 2-aminopyrimidine-4,6-diol (**3.90**)

In pursuit of a transient directing group that is more prone to undergo facile condensation with aromatic ketones, our attention turned to guanidine-type groups **2.91a–c** (Scheme 69b–d). A reaction screen with ketone **2.83** and guanidine HCl (**2.91a**) was conducted with $\text{RhCl}(\text{PPh}_3)_3$, $[\text{Rh}(\text{C}_2\text{H}_4)_2\text{Cl}]_2$, and $\text{Rh}(\text{cod})_2\text{BF}_4$ as catalysts; PhMe, DCE, MeCN, DMSO, and DMF as solvents; with or without K_2CO_3 ; and from temperatures ranging from 100 – 130 °C (Scheme 69b). The reactions gave unreacted starting material with minimal amounts of side-products resulting from deallylation and/or an aromatic Claisen rearrangement. However, reactions with DMF resulted in consumption of starting material, though no identifiable products were isolated.



Scheme 69. Alternative directing groups for MOCC C–C bond activation: a) 2-aminopyrimidine-4,6-diol (**3.90**) b) guanidine (**3.91a**) c) tetramethyl guanidine (**3.91b**) d) triazabicyclodecene (**3.91c**)

Tetramethylguanidine (**3.91b**) was then explored. Treating ketone **2.83** with catalysts $\text{RhCl}(\text{PPh}_3)_3$, $\text{Rh}(\text{CO})\text{acac}$, $\text{Rh}(\text{cod})_2\text{BF}_4$, and $\text{Rh}(\text{cod})_2\text{OH}$ in DMF or PhMe at 130 °C for 48 h resulted in complete conversion to an unidentified major product (Scheme 69c). The isolated product, which appeared blue under UV light on silica gel, delivered a

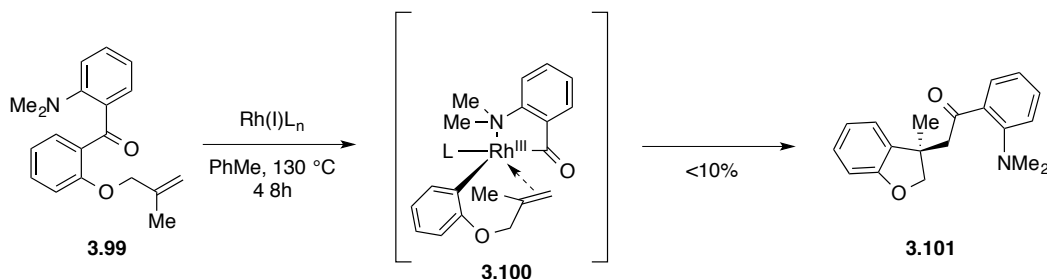
¹H NMR spectrum of the following resonances: (300 MHz; CDCl₃): δ 15.37 (br s, 1H), 7.71 (dd, *J* = 8.0, 1.6 Hz, 1H), 7.28 (ddd, *J* = 8.2, 7.2, 1.7 Hz, 1H), 6.94 (dd, *J* = 8.3, 1.0 Hz, 1H), 6.84 (ddd, *J* = 7.9, 7.2, 1.3 Hz, 1H), 6.23 (s, 1H), 3.17 (s, 6H), 3.13 (s, 6H). The spectrum suggests that ketone **3.83** underwent cleavage of the allyl group and ketone methyl group, while also containing the tetramethylguanidine unit. Additional characterization is required for structural elucidation and to deduce the specified reactivity of this system. In addition, it was discovered that TsOH as an additive inhibited the reaction. A cyclic guanidine derivative was then explored. Treating ketone **3.83** with various rhodium(I) catalysts and triazabicyclodecene (**3.91c**) in DMF and PhMe at 130 °C either returned starting material or resulted in decomposition (Scheme 69d).

3.3.4 CONCLUDING REMARKS

Efforts to incorporate a more nucleophilic co-catalyst to promote amine condensation with aryl ketones in order to afford C–C bond activation through MOCC catalysis were unsuccessful. Although increasing the electrophilicity of the ketone had been attempted by replacing the ether tether with a methylene tether (see Scheme 67; X = O, CH₂), it may prove beneficial to design a substrate containing a suitable electron-withdrawing group in order to facilitate imine formation. In addition, the imines should be pre-formed and subjected to the reaction conditions, which undoubtedly should have preceded efforts to establish carboacylation through MOCC.

3.4 TRIAZENES: A VERSATILE DIRECTING GROUP

The search for alternative directing groups had led our group to pursue 2-acylaniline directing groups. *N,N*-dimethylated aniline **3.99** was shown to participate in rhodium-catalyzed C–C bond activation to give the desired dihydrobenzofuran **3.101** in <10% yield; the major product resulted from demethylation of the aniline nitrogen (Scheme 70).^v It was hypothesized that a more sterically accessible sp^2 hybridized nitrogen (as demonstrated by quinoline) may be required for reaction efficiency. The triazene moiety was considered and a background literature search revealed that this functional group had been employed in C–H bond activation reactions.



Scheme 70. C–C bond activation with 2-acylaniline directing group

3.4.1 BACKGROUND

Triazenes are a versatile class of compounds known as important cytotoxic agents (DNA alkylation), heterocyclic precursors, amine protecting groups, and as latent diazonium ions, which are useful for an array of chemical transformations (Figure 21). The triazene moiety as a directing group is attractive because it serves as a traceless

^v As reported by former graduate student Ross M. Moren

and/or versatile functionality. Triazenes can be “deprotected” to give the free amine,⁹ removed to provide a C–H bond,¹⁰ transformed into halides (including fluorine),¹¹ or converted into azide, nitrile, boronic esters, diazo, carbonyl, or alcohol groups.¹² In addition, triazenes can undergo direct cross-coupling reactions akin to Heck, Sonogashira, Friedel-Crafts, and Suzuki reactions to give alkenes, alkynes, or biaryl systems.¹³ Our interest in pursuing triazenes as a directing group was heightened by the ease of synthesis of these scaffolds, and by the potential to embed chirality within the *N,N*-substituents to impart stereoselectivity.

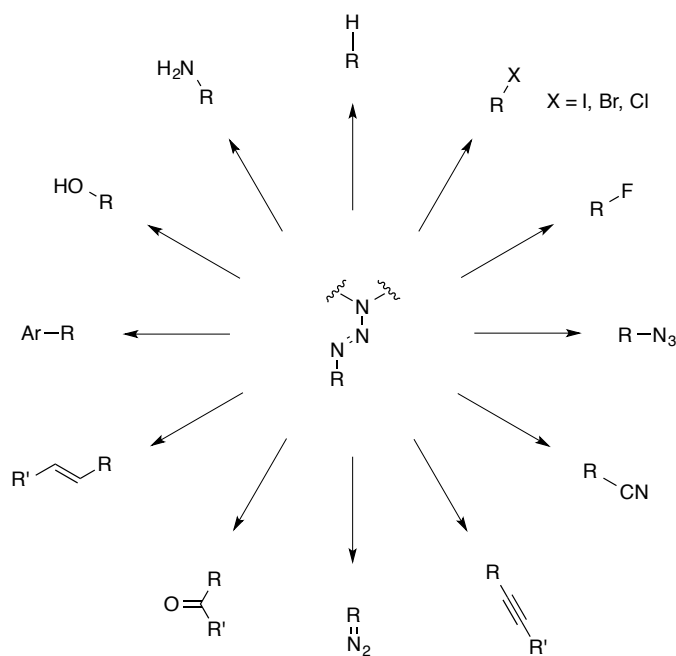
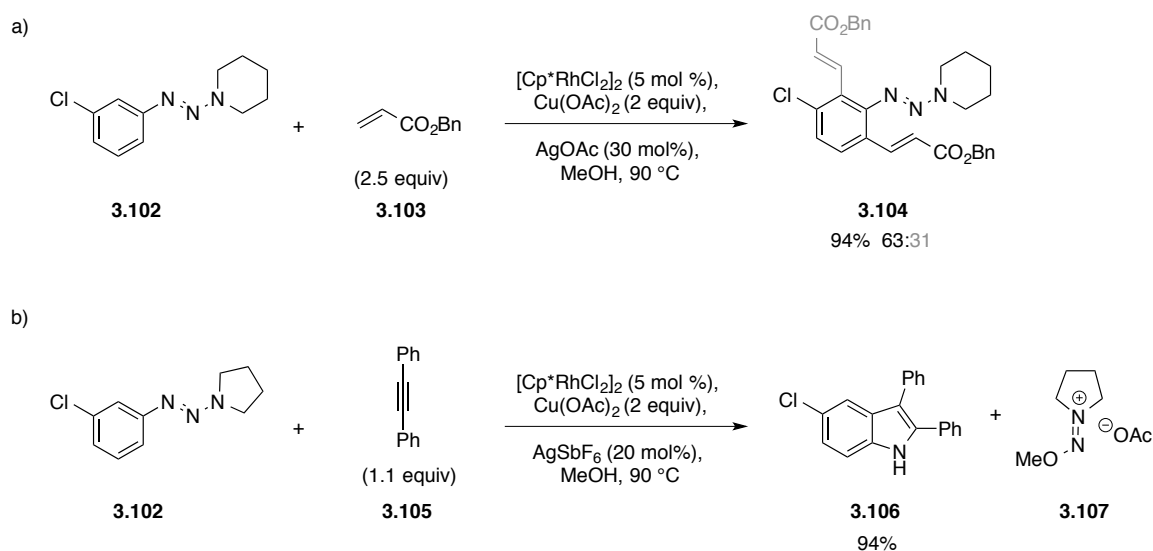


Figure 21. The functional versatility of triazenes

In 2012, Huang¹⁴ reported the use of triazenes as a directing group in a Rh(III)-catalyzed *ortho* C–H functionalization of arenes (Scheme 71). An oxidative Heck-type olefination between triazene **3.102** and acrylate **3.103** was carried out with 5 mol% $[(\text{RhCp}^*\text{Cl}_2)_2]$, $\text{Cu}(\text{OAc})_2$ as an external oxidant, and a substoichiometric amount

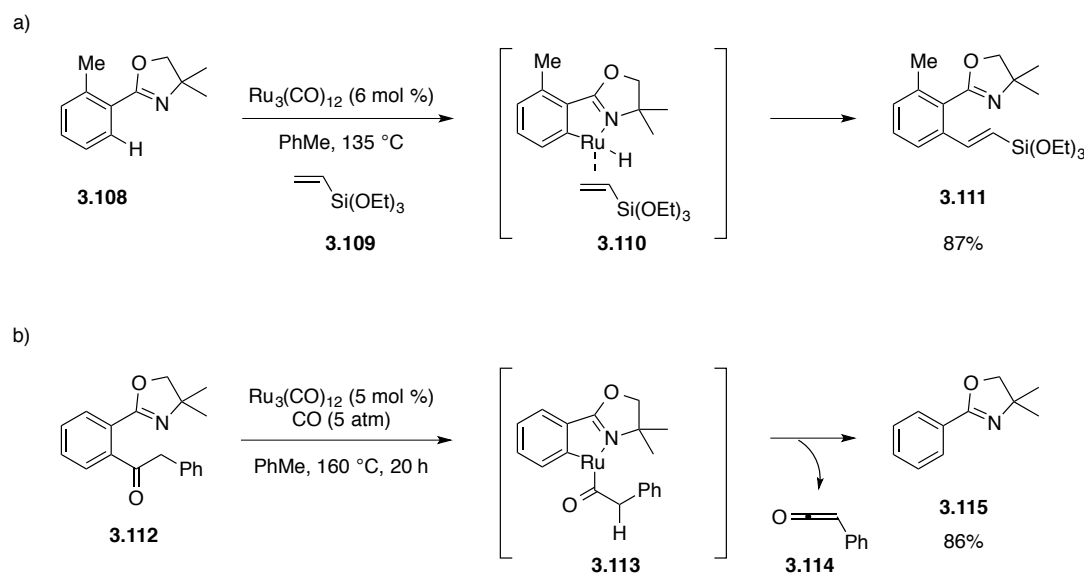
of AgOAc at 90 °C in methanol to give products **3.104** in good to excellent yields (Scheme 71a). The addition of silver acetate was speculated to promote formation of the active $\text{RhCp}^*(\text{OAc})_2$ catalyst. The following year, Huang¹⁵ demonstrated a triazene-directed C–H bond functionalization reaction with alkynes (Scheme 71b). Prior reports had shown that 2-iodo-aryltriazenes underwent cyclization with alkynes under palladium catalysis to provide cinnoline heterocycles. Surprisingly, the analogous C–H bond activation of **3.102** instead provided indole **3.106** in 94% yield.



Scheme 71. Huang’s demonstration of C–H bond activation with triazenes: a) Heck-type coupling b) indole annulation

Direct correlations between cyclometalation reactions of C–H and C–C bonds are rather rare in the literature, perhaps owing to the relatively unexplored field of the latter. Although a number of directing groups such as amines, alcohols, amides, oximes, esters, ketones and carboxylic acids have been shown to afford the C–H activation reaction shown above,¹⁶ the oxazoline group has been one of the only related functionalities reported to undergo both C–H and C–C bond cleavage reactions.¹⁷

In 1999, Murai demonstrated that oxazoline was an effective directing group for both C–H and C–C bond activation reactions with $\text{Ru}_3(\text{CO})_{12}$ as a catalyst. Oxazoline **3.108** underwent a Heck-type reaction with triethoxyvinylsilane (**3.109**) in the presence of $\text{Ru}_3\text{CO}_{12}$ catalyst to give olefin **3.111** by way of C–H activation, carbometallation, and β -hydride elimination (Scheme 72a).¹⁸ Comparatively, ketone **3.112** likely underwent C–C bond activation with $\text{Ru}_3(\text{CO})_{12}$ to produce intermediate **3.113**. The observation of phenylketene (**3.114**) (which was trapped as the methyl ester when the reaction was ran in MeOH) led to the assumption that intermediate **3.113** underwent β -hydride elimination followed by reductive elimination of the Ru–H to generate oxazoline **3.115**, which was obtained in 84% yield.



Scheme 72. Murai's demonstration of C–H and C–C bond activation with oxazoline

The oxazoline and triazene moieties are relatively similar in structure (though most likely quite different electronically), and therefore the comparable reactivity toward C–H and C–C bond activation reactions exhibited by oxazoline directing groups

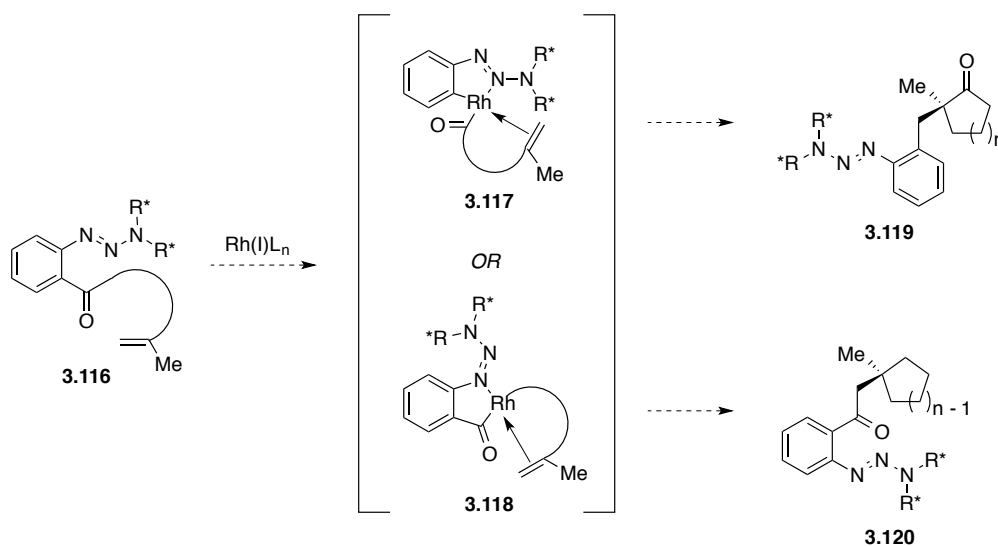
encouraged us to pursue C–C bond activation with triazenes. However, the C–H functionalization reaction with triazenes does *not* go through an oxidative addition pathway, but rather σ -bond metathesis with a Rh(III) catalyst. This subtle difference in reaction profile may render C–C bond activation through Rh(I) catalysis less amenable.

3.4.2 RESEARCH PROPOSAL

The interest in finding a method that addresses the limitations of quinoline-directed carboacylation reactions (see Chapter 2) led to the proposal of triazenes as a potential directing group for C–C bond activation. The triazene moiety can be readily removed or easily converted into synthetically useful functional groups. This utility would allow for a C–C bond activation method that overcomes the unappealing synthetic consequences of a covalently-bound directing group. Employing chiral ligands to the reactions with 8-acylquinoline was not successful in promoting enantioselectivity and was rather detrimental to the efficiency of the reaction. It is conceivable that stereoselectivity may be imparted without the need for chiral ligands by easily introducing chirality onto the sp^3 -hybridized nitrogen atom of the triazene (denoted by R*).

The triazene moiety contains two sp^2 nitrogen atoms that could theoretically participate in metal ligation. Therefore, compounds of the general formula depicted as **3.116** could undergo C–C bond activation one of two ways (Scheme 73). Activation by the less basic medial nitrogen would result in an intermediate (**3.117**) in which the carbonyl is not stabilized within the metallacycle. Although competitive decarbonylation or β -hydride elimination (as seen with Murai's oxazoline C–C bond activation reaction, Scheme 72) could complicate the reaction, it was hypothesized that coordination by a

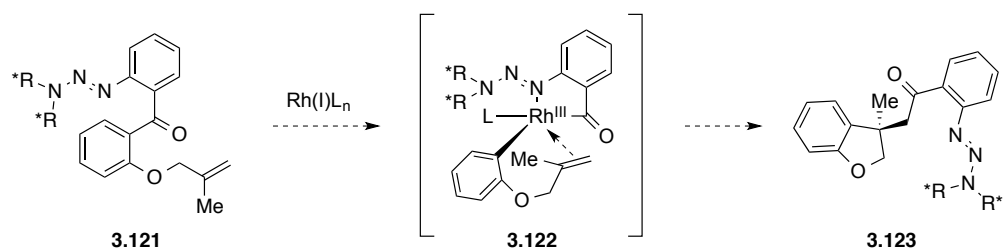
tethered olefin would suppress such side reactions. If successful, the carboacylation of **3.116** would provide α -substituted cyclic ketones (**3.119**). Alternatively, ligation by the more basic proximal nitrogen would generate the intermediate **3.118**. Although complex **3.118** would be more stable toward decarbonylation, β -hydride elimination remains possible. If successful, cycloalkane **3.120** would be generated.



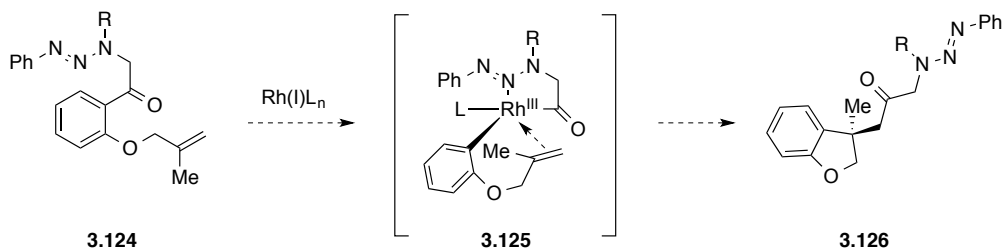
Scheme 73. General illustration of proposed C-C bond activation with triazenes

Three substrates were designed in order to probe the reactivity of triazene as a directing group for intramolecular carboacylation (Schemes 74–76). Triazene **3.121** (Scheme 74) was designed to model the substrates shown to undergo C-C bond activation with quinoline (Chapter 2, Figure 9). Metal coordination with the proximal nitrogen would afford the five-membered metallacycle **3.122** upon oxidative addition. Intramolecular migratory insertion across the appended olefin followed by reductive elimination would generate dihydrobenzofuran **3.123**.

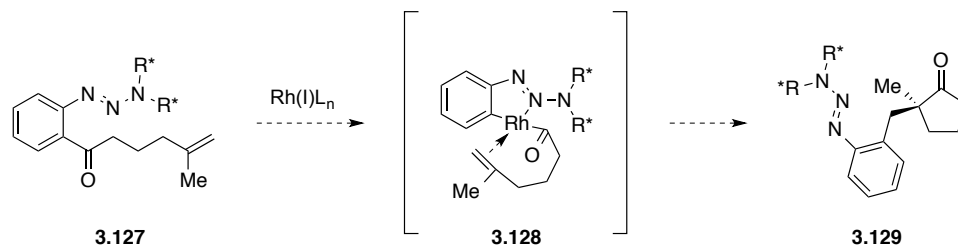
An aliphatic-bound triazene directing group was also imagined as substrate for C–C bond activation (Scheme 75). The α -keto triazene **3.124** would furnish dihydrobenzofuran **3.126** upon reaction with a suitable catalyst. The triazene moiety could readily be removed with acid to reveal an α -amino ketone or converted to the α -diazo compound for further functionalization. Aryl triazene **3.125** was designed with an aliphatic-tethered olefin (Scheme 76). It is likely that activation of the C_{acyl}–C_{aryl} bond (**3.128**) would be favored over the C_{acyl}–C_{alkyl} bond considering that Rh–C_{aryl} bonds are stronger than Rh–C_{alkyl} bonds. Successful carboacylation would afford cyclopentanone **3.129**.



Scheme 74. Proposed aryl triazene substrate with aryl-tethered olefin



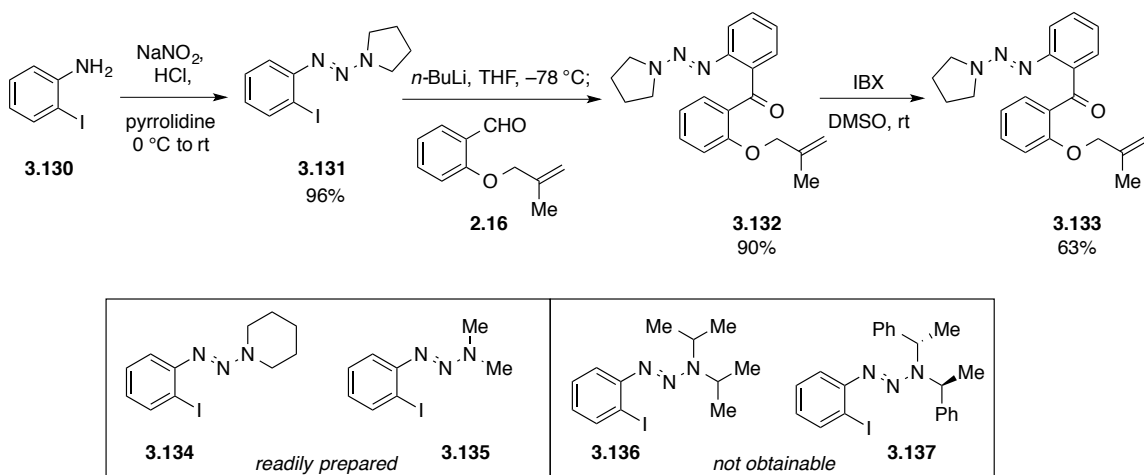
Scheme 75. Proposed aliphatic triazene substrate with aryl-tethered olefin



Scheme 76. Proposed aryl triazene substrate with aliphatic-tethered olefin

3.4.3 SUBSTRATE SYNTHESSES

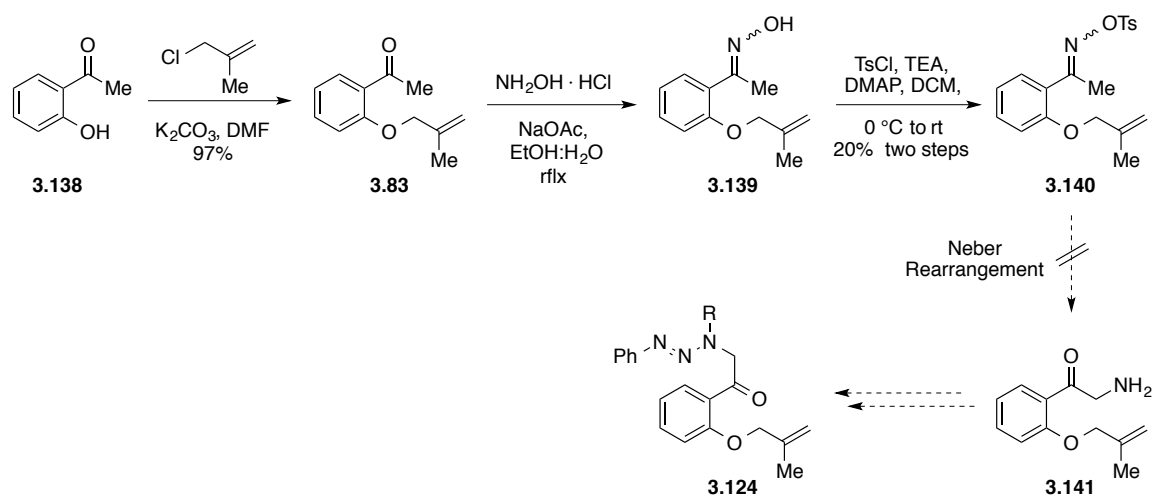
2-Iodo triazene **3.131** was easily prepared in 96% yield by adding sodium nitrite to an acidic solution of 2-iodoaniline (**3.130**) followed by treatment with a large excess of pyrrolidine. Lithiation of the iodide **3.131** with *n*-BuLi followed by slow addition of aldehyde **2.16** provided corresponding alcohol **3.132** in 90% yield. Oxidation of alcohol **3.132** with IBX gave ketone **3.133** in 63% yield. The piperidine (**3.134**) and dimethylamine (**3.135**) triazene derivatives were analogously prepared in good to excellent yields; however, the syntheses of diisopropylamine (**3.136**) and bis-(phenylethyl) amine (**3.137**) triazene derivatives were not successful.



Scheme 77. Preparation of aryl triazene substrate with aryl-tethered olefin

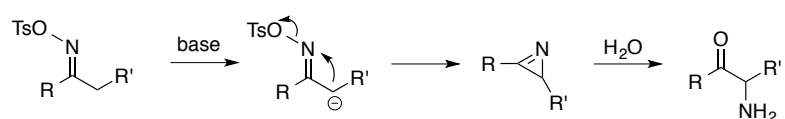
The preparation of the aliphatic triazene substrate **3.124** proved difficult. The synthetic route to α -amino ketone **3.141** began with an alkylation reaction of phenol **3.138** to provide ketone **3.83** in 97% yield. Oxime formation (**3.139**), followed by O-tosylation, afforded the ketoxime tosylate **3.140** in 20% yield over the two steps. The low yield was attributed to the instability of **3.140** upon purification by column

chromatography on alumina. Various conditions were attempted to promote the Neber arrangement of **3.140** in order to obtain α -amino ketone **3.141**; however, the major product in these reactions was the corresponding aryl amide that resulted from a competitive Beckmann rearrangement (Figure 22). An alternative route to **3.141** involved a sequence including α -keto bromination, azide substitution, and a Staudinger reduction; however, the α -keto bromide was unable to be prepared because compound **3.138** favored an EAS reaction to give the aryl bromide and **3.83** resulted olefin bromination.



Scheme 78. Unsuccessful synthesis of aliphatic triazene substrate by way of a Neber rearrangement

Neber Rearrangement



Beckmann Rearrangement

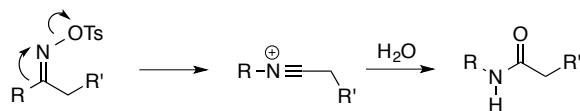
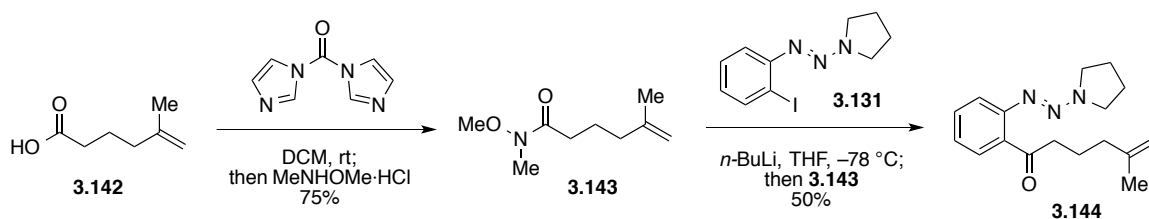


Figure 22. Mechanism of Neber and Beckmann rearrangements

The aryl triazene substrate containing an aliphatic tethered alkene (**3.144**) was readily prepared in three steps (Scheme 79). Acid **3.142** was prepared via a Wittig olefination of 4-acetylbutyric acid in quantitative yield (not shown). The mixed anhydride achieved by treating acid **3.142** with carbonyl diimidazole was converted to the Weinreb amide **3.143** in 75 % yield upon addition of *N,O*-dimethylhydroxylamine hydrochloride. 2-Iodotriazene **3.131** was lithiated with *n*-BuLi and added to a cooled solution containing Weinreb amide **3.143** to furnish the alkyl triazene substrate **3.144** in 50% yield.



Scheme 79. Preparation of aryl triazene substrate with aliphatic-tethered olefin

3.4.4 RESULTS AND DISCUSSION

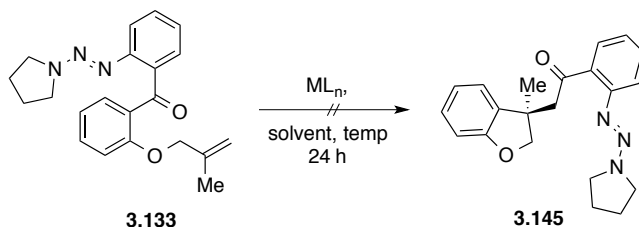
A preliminary reactivity screen was performed on triazenes **3.133** (Table 8) and **3.144** (Table 9) using conditions found to promote intramolecular carboacylation across alkenes with 8-acylquinoline. The ^1H NMR spectra of dihydrobenzofuran **3.145**, cyclopentanone **3.146**, and cyclohexanone **3.147** (arising from a 6-*endo*-trig cyclization) would each show two distinct sets of diastereotopic AB doublets. A quick analysis of the crude ^1H NMR spectra revealed no desired product formation with either triazene substrate. Side-products were not isolated and characterized.

The reactions with triazene **3.133** (Table 8, entries 1–11) returned mostly starting material and were often accompanied by two side-products. Product **B** contains ^1H NMR resonances indicative of a deshielded allylic moiety. Initially this product was assumed to have resulted from an aromatic Claisen rearrangement. Upon further inspection, compound **B** does not appear to contain the triazene moiety. Product **C** shows a resonance above 12 ppm, which likely corresponds to a phenol generated upon allyl ether cleavage.

The reactions with triazene **3.144** (Table 9, entries 1–11) returned mostly starting material, but were also accompanied by two side-products. Product **D** shows ^1H NMR resonances reminiscent of a 1,1-disubstituted olefin and three methylene peaks. The α -keto protons had shifted upfield by approximately 1 ppm, which may suggest that decarbonylation by way of C–C bond activation had occurred. In addition, compound **D**

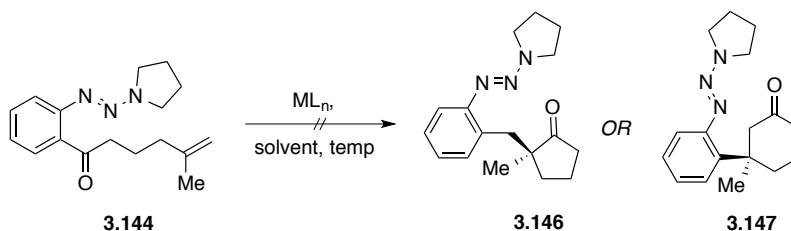
does not appear to have retained the triazene moiety. Compound **E** displays a “tdt”^{vi} at 5.1 ppm ($J = 6.93, 2.97, 1.43$) and is likely the enol ether olefin isomer.

Table 8. C–C bond activation reaction screen of aryl triazene with aryl olefin tether



Entry	Catalyst	Solvent	Temp	Products	Ratio
1	$[RhCl(C_2H_4)_2]_2$	PhMe	130 °C	SM	-
2	$RhCl(PPh_3)_3$	PhMe	130 °C	SM	-
3	$Rh(cod)_2OTf$	PhMe	130 °C	SM + B	2:1
4	$Rh(cod)_2BF_4$	PhMe	130 °C	SM + B	2:1
5	$Rh(acac)(cod)$	PhMe	130 °C	SM	
6	$[Rh(cod)OH]_2$	PhMe	130 °C	SM + B + C	5:1:2
7	$[Rh(cod)_2(OMe)]_2$	PhMe	130 °C	SM + B + C	11:1:1
8	$Rh(CO)_2(acac)$	PhMe	130 °C	SM + B + C	5:1:1
9	$[Ir(coe)_2Cl]_2$	PhMe	130 °C	SM + B + C	7:3:1
10	Ru_3CO_{12}	PhMe	130 °C	decomp	-
11	$Rh(cod)_2OTf$	THF	100 °C	SM + B	2:1

Table 9. C–C bond activation reaction screen of aryl triazene with aliphatic olefin tether



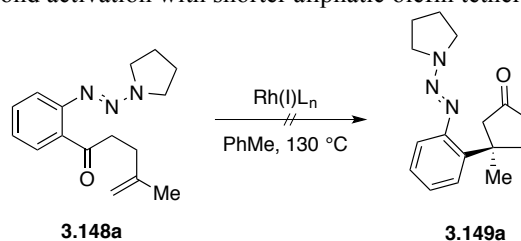
Entry	Catalyst	Solvent	Temp	Products	Ratio
1	$[RhCl(C_2H_4)_2]_2$	PhMe	130 °C	SM + D + E	20:4:1
2	$RhCl(PPh_3)_3$	PhMe	130 °C	SM + E	5:1
3	$Rh(cod)_2OTf$	PhMe	130 °C	SM + D	2:1
4	$Rh(cod)_2BF_4$	PhMe	130 °C	SM + D	2:1
5	$Rh(acac)(cod)$	PhMe	130 °C	SM	--
6	$[Rh(cod)OH]_2$	PhMe	130 °C	SM + E	2:1

^{vi} Interpretation generated by iNMR software.

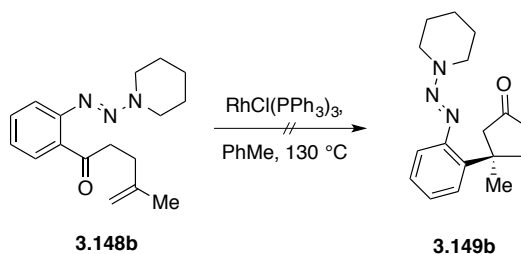
7	$[\text{Rh}(\text{cod})_2(\text{OMe})]_2$	PhMe	130 °C	SM + E	1:1
8	$\text{Rh}(\text{CO})_2(\text{acac})$	PhMe	130 °C	SM	--
9	$[\text{Ir}(\text{coe})_2\text{Cl}]_2$	PhMe	130 °C	SM + D	20:1
10	$\text{Ru}_3\text{CO}_{12}$	PhMe	130 °C	decomp	
11	$\text{Rh}(\text{cod})_2\text{OTf}$	THF	100 °C	SM + D	4:1

Triazenes with a shorter aliphatic tether (pyrrolidine **3.148a** and piperidine **3.148b**) were also prepared with the idea that perhaps a 5-*endo*-trig cyclization (**3.149**) would be favorable (Table 10). Unfortunately the reactions returned starting material, although the presence of a “tdt” at 5.43 ppm ($J = 6.94, 2.81, 1.42$) (**3.148a**) and 5.41 ppm ($J = 6.83, 2.83, 1.41$) (**3.148b**) in the ^1H NMR spectra was observed under $\text{RhCl}(\text{PPh}_3)_3$ catalysis. This resonance is likely indicative of double bond isomerization.

Table 10. Attempted C–C bond activation with shorter aliphatic olefin tethers



Entry	Catalyst	Solvent	Temp	Products	Ratio
1	$[\text{RhCl}(\text{C}_2\text{H}_4)_2]_2$	PhMe	130 °C	SM	--
2	$\text{RhCl}(\text{PPh}_3)_3$	PhMe	130 °C	SM + F	4:1
3	$\text{Rh}(\text{cod})_2\text{OTf}$	PhMe	130 °C	SM	--
4	$\text{Rh}(\text{cod})_2\text{BF}_4$	PhMe	130 °C	SM	--

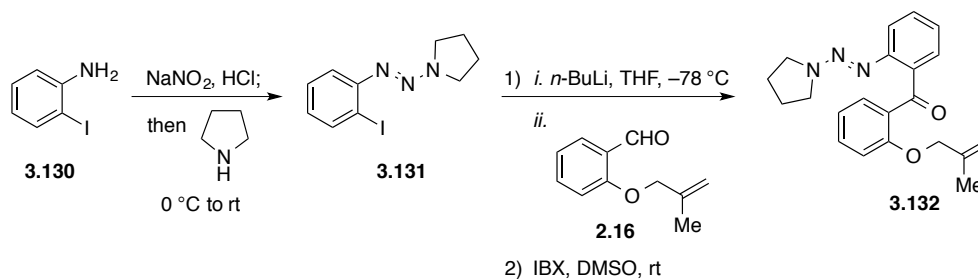


Entry	Catalyst	Solvent	Temp	Products	Ratio
5	$\text{RhCl}(\text{PPh}_3)_3$	PhMe	130 °C	SM + G	3:1

3.4.4. CONCLUDING REMARKS

The desired carboacylation reaction with triazene directing groups was not fruitful under Rh(I) catalysis in PhMe or THF. Starting material was returned in most cases along with products that appeared to result from double bond isomerization and cleavage of the olefin moiety. Additionally, the triazene moiety may not have been stable under the reaction conditions. The broaden proton resonances (^1H NMR) of the pyrrolidine and piperidine moieties made interpretation difficult. The isolation and characterization of these side-reaction products may be helpful in providing insight toward further optimization directions.

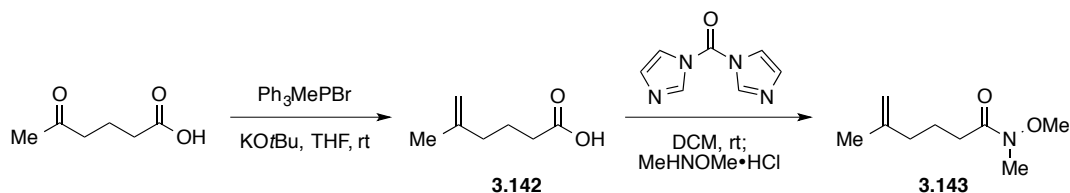
3.4.4 EXPERIMENTAL



To a cooled ($0\text{ }^\circ\text{C}$) solution of 2-iodoaniline (**3.130**) (1.0 g, 4.57 mmol) in 1 M HCl (27 mL) was added NaNO_2 . After the solution was stirred at $0\text{ }^\circ\text{C}$ for 1 h, pyrrolidine (3.75 mL, 45.7 mmol) was added and stirred for an additional 20 min at $0\text{ }^\circ\text{C}$. The ice bath was removed and the resulting orange solution was stirred overnight at room temperature. EtOAc was added to the red-orange reaction mixture and the layers were separated. The red organic layer was washed with $\text{H}_2\text{O} \times 2$, and the combined yellow aqueous layers were extracted with EtOAc. The combined organic layers were washed

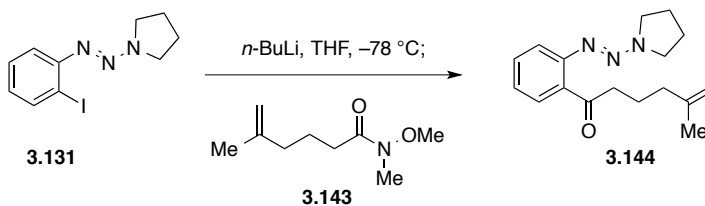
with brine, dried over Na₂SO₄, filtered, and concentrated. The crude mixture was purified by flash chromatography (1:6 EtOAc:Hex) to give triazene **3.131** (1.31 g, 4.35 mmol, 95%) as a red-orange oil: *R_f* 0.52 (1:9 EtOAc:Hex). Triazene **3.131** (596 mg, 1.98 mmol) and dry THF (13.2 mL) were added to a flame-dried flask under N₂ and cooled to -78 °C. *n*-BuLi (2.5M in hexanes, 0.95 mL, 2.38 mmol) was added dropwise and the resulting solution was stirred at -78 °C for 45 min. Aldehyde **2.16** (419mg, 2.38 mmol) was added as a solution in THF (7 mL), stirred at -78 °C for 15 min, and then allowed to warm to room temperature and stirred overnight. The reaction was quenched with sat. NH₄Cl and EtOAc and water were added. The aqueous layer was extracted with EtOAc and the combined organic layers were washed with brine, dried over Na₂SO₄, filtered and concentrated. Flash chromatography (1:6 EtOAc:Hex) provided the corresponding alcohol (665 mg, 1.91mmol, 97% w/ minor aldehyde impurity) as an orange oil: *R_f* 0.31 (1:5 EtOAc:Hex). The resulting alcohol (600 mg, 1.72 mmol) was treated with IBX (1.45 g, 5.17 mmol) in DMSO (11.5 mL) and stirred at room temperature for 18 h. Water was added to the reaction and stirred for 10 min before filtering through celite and washed with EtOAc. The filtrate was separated and the organic layer was washed with water (2 × 25 mL). The organic layer was washed with brine, dried over Na₂SO₄, filtered, and concentrated. The crude product was purified by flash chromatography (1:9 to 1:7 EtOAc:Hex) to give ketone **3.132**: *R_f* 0.38 (1:5 EtOAc:Hex); ¹H NMR (500 MHz; CDCl₃) δ 7.64 (dd, *J* = 7.7, 1.4 Hz, 1H), 7.58 (dd, *J* = 7.6, 1.8 Hz, 1H), 7.39 (td, *J* = 7.7, 1.4 Hz, 1H), 7.33 (ddd, *J* = 8.3, 7.4, 1.7 Hz, 1H), 7.29 (dd, *J* = 8.0, 0.8 Hz, 1H), 7.20 (td, *J* = 7.5, 1.1 Hz, 1H), 6.95 (td, *J* = 7.5, 0.8 Hz, 1H), 6.77 (d, *J* = 8.2 Hz, 1H), 4.71 (d, *J* = 1.2 Hz, 1H), 4.65 (s, 1H), 4.19 (s, 2H),

3.73 (s, 2H), 2.78 (s, 2H), 1.80 (s, 4H), 1.50 (s, 3H); ^{13}C NMR (126 MHz; CDCl_3) δ 197.2, 157.2, 150.3, 140.2, 135.2, 131.97, 131.83, 131.3, 130.7, 129.3, 124.8, 120.2, 118.3, 111.9, 77.2, 72.1, 19.1 (two carbon signals overlapped).

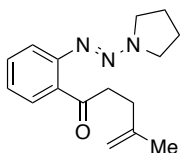


Triphenylmethylphosphonium bromide (5.63 g, 15.75 mmol) was added to a flame-dried flask under N_2 . A solution of potassium *tert*-butoxide in THF (1.0M, 23 mL, 23.0 mmol) was added at room temperature and the resulting mixture was stirred for 30 min. 5-oxohexanoic acid (0.92 mL, 7.68 mmol) was added and reaction was monitored by TLC and allowed to stir for 5 h. EtOAc and 1 M HCl were added to the reaction and the layers were separated. The aqueous layer was acidified with additional HCl and extracted with EtOAc (3 \times 50 mL). The combined organic layers were washed with brine, dried over Na_2SO_4 , filtered, and concentrated. TLC after workup, however, indicated unreacted starting material. Flash chromatography (1:3 EtOAc:Hex) gave alkene **3.142** (315 mg, 2.46 mmol, 32%): R_f 0.47 (2:5 EtOAc:Hex). Acid **3.142** (310 mg, 2.42 mmol) and dry DCM (5 mL) were added to a flame-dried flask under N_2 . Carbonyldiimidazole (471 mg, 2.90 mmol) was added at room temperature and the reaction was allowed to stir for 20 min before the addition of *N,O*-dimethyl hydroxylamine hydrochloride (2.83 g, 2.90 mmol). The reaction was stirred overnight and then was added DCM and 1M HCl. The layers were separated and the organic layer was then washed with NaHCO_3 and brine, dried over Na_2SO_4 , filtered, and concentrated. The

crude product was purified by flash chromatography (1:4 EtOAc:Hex) to give Weinreb amide **3.143** (310 mg, 1.81 mmol, 75%) as a pale yellow oil: R_f 0.35 (2:5 EtOAc:Hex).

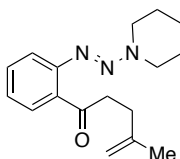


Triazene **3.131** (300 mg, 1.0 mmol) was added to a flame-dried flask, place under N_2 , and cooled to $-78\text{ }^\circ\text{C}$. $n\text{-BuLi}$ (2.5M in hexanes, 0.4 mL, 1.02 mmol) was added dropwise and the resulting solution was stirred at $-78\text{ }^\circ\text{C}$ for 45 min. Weinreb amide **3.143** (210 mg, 1.23 mmol) was added as a THF (5 mL) solution and continued to stir at $-78\text{ }^\circ\text{C}$ for 15 min. The cold bath was removed and the reaction was stirred at room temperature overnight. The reaction was quenched with sat. NH_4Cl and EtOAc were added. The layers were separated and the aqueous phase was extracted with EtOAc. The combined organic layers were washed with brine, dried over Na_2SO_4 , filtered, and concentrated. The crude product was purified by flash chromatography (1:7 EtOAc:Hex) to give ketone **3.144** (226 mg, 0.79 mmol, 50%) as a yellow oil: R_f 0.43 (1:4 EtOAc:Hex): 1H NMR (500 MHz; $CDCl_3$) δ 7.47-7.44 (m, 2H), 7.37 (td, $J = 7.7, 1.5$ Hz, 1H), 7.16-7.13 (m, 1H), 4.69 (app s, 1H), 4.65 (d, $J = 0.8$ Hz, 1H), 3.94 (s, 2H), 3.64 (s, 2H), 2.97 (app t, $J = 7.6$ Hz, 2H), 2.05-2.03 (m, 6H), 1.82 (app quintet, $J = 7.6$ Hz, 2H), 1.70 (s, 3H); ^{13}C NMR (126 MHz; $CDCl_3$) δ 206.9, 149.0, 145.4, 135.1, 131.2, 128.1, 124.9, 117.9, 110.3, 43.9, 37.4, 22.4, 22.2 (two carbon signals overlapped)



3.148a

^1H NMR (500 MHz; CDCl_3) δ 7.48-7.45 (m, 2H), 7.38 (td, $J = 7.7, 1.5$ Hz, 1H), 7.15 (td, $J = 7.4, 1.0$ Hz, 1H), 4.70 (s, 1H), 4.65 (s, 1H), 3.94 (s, 2H), 3.64 (s, 2H), 3.16-3.13 (m, 2H), 2.39 (t, $J = 7.8$ Hz, 2H), 2.04 (s, 4H), 1.73 (s, 3H); ^{13}C NMR (126 MHz; CDCl_3) δ 206.3, 149.1, 145.1, 134.9, 131.3, 128.3, 125.0, 117.8, 109.7, 42.6, 32.3, 22.8 (two carbon signals overlapped).



3.148b

^1H NMR (500 MHz; CDCl_3) δ 7.47-7.45 (m, 2H), 7.40 (td, $J = 7.7, 1.4$ Hz, 1H), 7.18 (td, $J = 7.4, 1.1$ Hz, 1H), 4.70 (s, 1H), 4.65 (s, 1H), 3.80 (app s, 4H), 3.09-3.06 (m, 2H), 2.38 (t, $J = 7.8$ Hz, 2H), 1.72 (s, 3H), 1.71 (app s, 6H).

3.5 HYDROGEN-BOND DIRECTED CATALYSIS

3.5.1 BACKGROUND AND INSPIRATION

Throughout the past five decades, the concept of rate acceleration by decreasing the energy of the lowest unoccupied molecular orbital (LUMO) in electrophiles with the addition of Lewis and Brønsted acid catalysts has led to a host of mild C–C and C–X bond-forming methods. Employing highly tunable chiral ligands and/or structural backbone features within these catalysts to impart asymmetry has begun to revolutionize the way in which chemists construct complex molecules. Traditional Lewis acids are metal-centered (i.e. Al, B), although the proton can be viewed as the smallest member of the Lewis-acid family. As a prominent feature in biocatalysis, hydrogen bonding plays a central role in the acceleration of various reactions including acyl and phosphoryl transfer, carbonyl addition, and pericyclic processes. Throughout the past decade, a bio-inspired approach to enantioselective syntheses of small molecules using hydrogen-bond catalysis has emerged.

In pursuit of synthetically amenable directing groups for C–C bond activation, the idea to use interactions such as hydrogen bonding to “direct the directing group” was envisioned. Inspiration for the idea evolved from Feringa’s work in catalytic asymmetric Michael reactions using molecular motors (Figure 23).¹⁹ The general idea is that the catalyst contains two parts: a thiourea moiety (**B**) to activate a ketone through hydrogen bonding, and a secondary interaction between a basic site (**A**) and the nucleophile. The ‘motor’ aspect of the catalyst serves to bring **A** and **B** together to react. The concept of

guiding the nucleophile into proximity of the electrophile spurred the idea that a transition metal could be directed in a similar fashion for C–C bond activation.

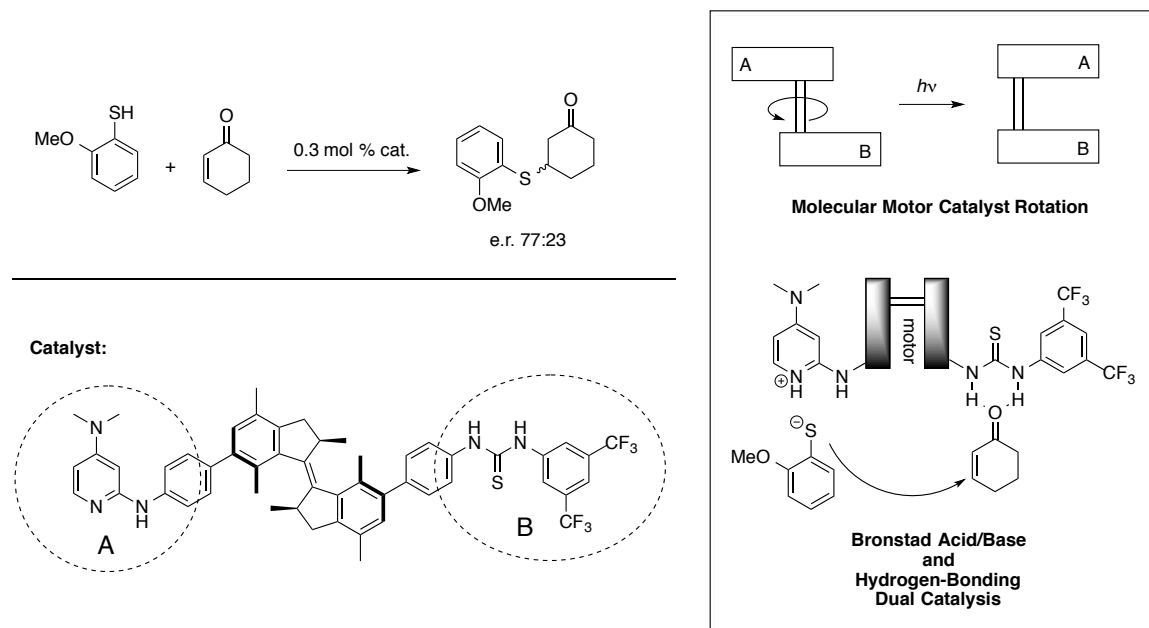


Figure 23. Molecular motors as catalysts for stereoselective Michael addition reactions

Molecular recognition is widely used in nature by enzymes like monooxygenases and fatty acid desaturases; a recognition site tethered to a reactive center binds to a functional group within a substrate through non-covalent interactions such as π -stacking or hydrogen bonding (Figure 24). This structural reorganization allows for preferential approach of the reactive center to ensure selectivity. The implementation of this approach in a synthetic laboratory, however, is very challenging and few successful examples have been reported.

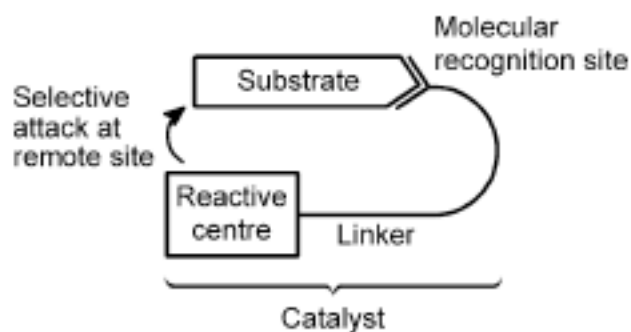


Figure 24. Enzymatic molecular recognition mechanism²⁰

In 2009, Crabtree demonstrated a regioselective benzylic oxidation of ibuprofen using the bio-inspired molecular recognition approach (Figure 25).²⁰ The terpyridine ligand (terpy') contains a "Kemp's triacid" moiety that serves as a hydrogen bond donor/acceptor to bind ibuprofen through its carboxylic acid group. This arrangement orients the distal benzylic C–H bonds near the reactive metal center in order to achieve selectivity. With regards to applying this concept to C–C activation, it was imagined that a "ligand" could be equipped with a moiety capable of hydrogen bonding to the carbonyl in order to bring the C–C_{acyl} bond into proximity of the metal.

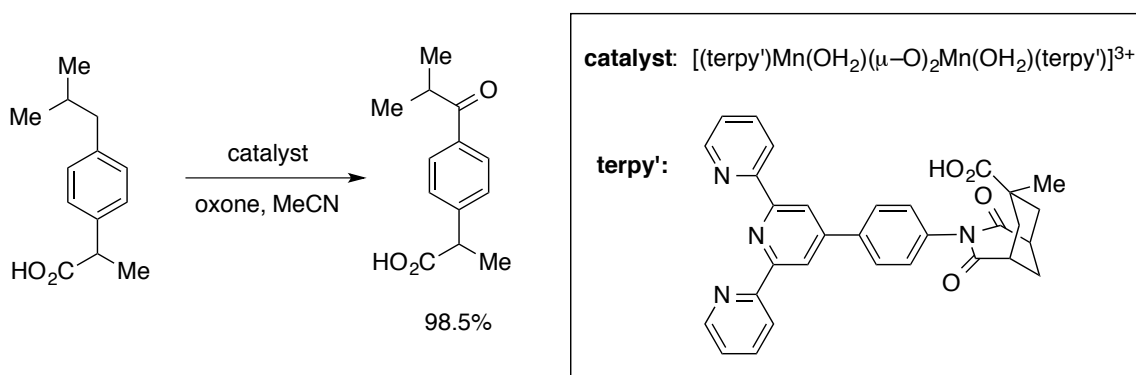


Figure 25a. Hydrogen bond directed regioselective benzylic oxidation of ibuprofen

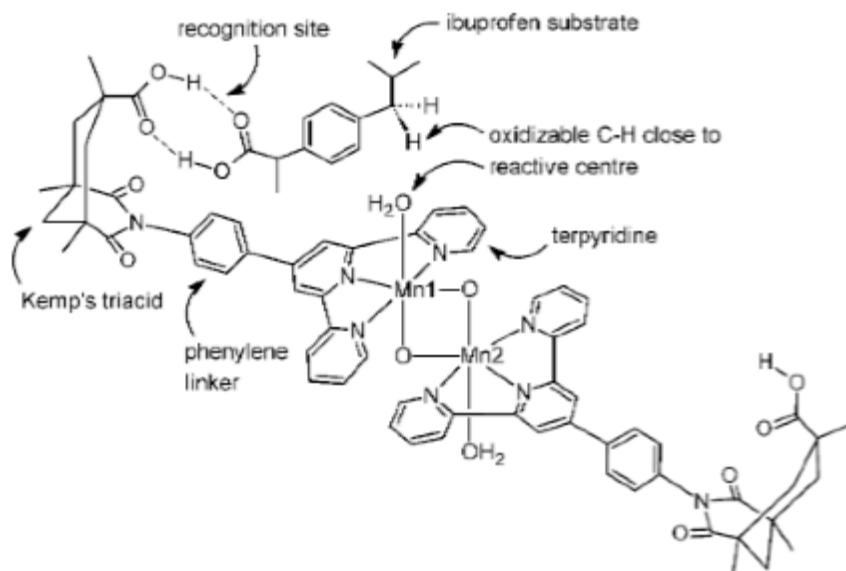
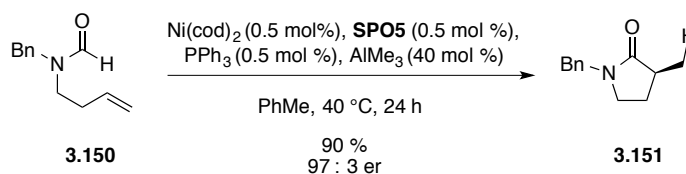


Figure 25b. Hydrogen bond directed regioselective benzylic oxidation of ibuprofen²⁰

After the idea of using Lewis acids/hydrogen bonding as a means to “direct the directing group” had ruminated for some time, Cramer published an elegant report on a nickel-catalyzed asymmetric hydrocarbamoylation reaction using a chiral diaminophosphine oxide (SPO5)-bound Lewis acid as a directing group.²¹ Homoallylic formamide **3.150** was converted into λ -lactam **3.151** in 90% yield and a 97:3 er (Scheme 80).



Scheme 80. Enantioselective hydrocarbamoylation reaction with chiral Lewis acid directing group

The combination of $\text{Ni}(\text{cod})_2$, SPO5 (**3.153**), and AlMe_3 generates a bridged bimetallic system **3.152** with liberation of methane (Figure 26). Secondary phosphine oxides (SPOs) have only recently been acknowledged as air-stable, robust pre-ligands for

transition-metal catalysis. The tautomerism between the pentavalent (P^V) **3.153** and trivalent (P^{III}) **3.154** lends to this stability. Though favoring the P^V form, the strong coordination of phosphorus to late transition metals, such as nickel, causes the equilibrium to shift toward the P^{III} phosphinous acid **3.154**. While oxygen is well known to bind to hard metals such as aluminum, bimetallic catalyst systems such as **3.152** are relatively unexplored. With formamide C–H bonds exceptionally harder to activate (in relation to aldehydes), O–Al coordination (**3.153**) not only serves to direct the metal into the C–H bond, but also to lower the barrier to activation.

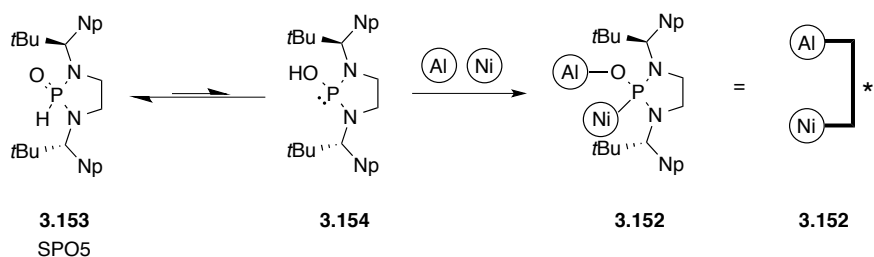


Figure 26. *in situ* generation of the Al–SPO5–Ni bimetallic system for asymmetric intramolecular hydrocarbamoylation

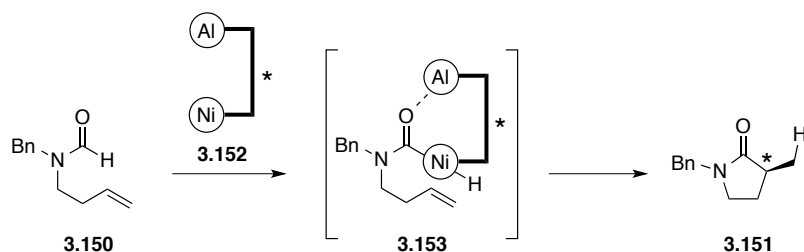


Figure 27. Illustration of Al–SPO5–Ni bimetallic system participating in C–H bond activation

3.5.2 RESEARCH PROPOSAL

Prior to the bimetallic system designed by Cramer for C–H bond activation (Scheme 80, Figures 26–27), a similar bifunctional co-catalyst had been envisioned for the activation of C–C bonds. It was proposed that a hydrogen bond donor (HBD) decorated with a directing group (DG) (**3.154**) could bind a transition metal (M) (**3.155**) and coordinate to the carbonyl of a ketone (**3.156**) (Figure 28). Such an arrangement would facilitate C–C bond activation (**3.157**) by not only lowering the activation barrier with the Lewis acid, but also by guiding the metal into proximity of the C–C bond.

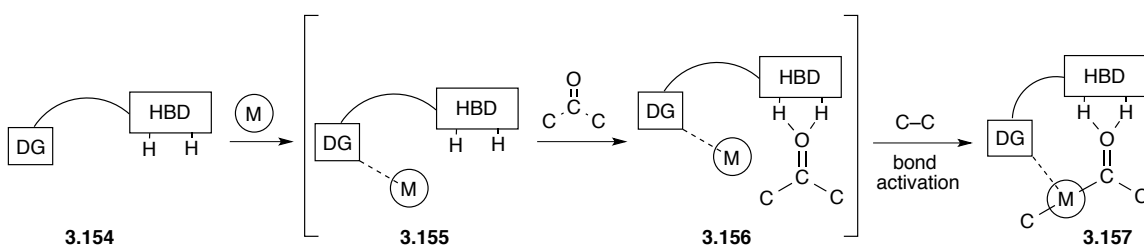


Figure 28. Proposed C–C bond activation through hydrogen-bonded directing group

It is well known that thiourea organocatalysts accelerate a host of reactions by hydrogen bonding to various functional groups including imines, nitroolefins, carbonyls, and even chloride ions. In addition, chiral thiourea catalysts have been effective at promoting asymmetric reactions by containing pendant chiral groups. It was proposed that a thiourea moiety would serve as the source of hydrogen bonding in co-catalyst **3.154**, and the directing group would be a nitrogen-containing heterocycle (Figure 28). Thiosemicarbazones **3.158** were designed with appended pyridyl groups as suitable co-catalysts.

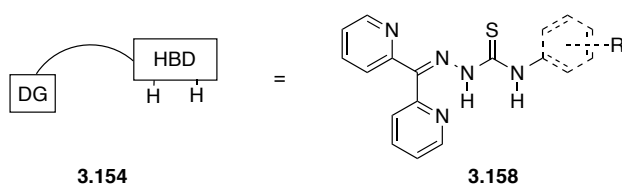
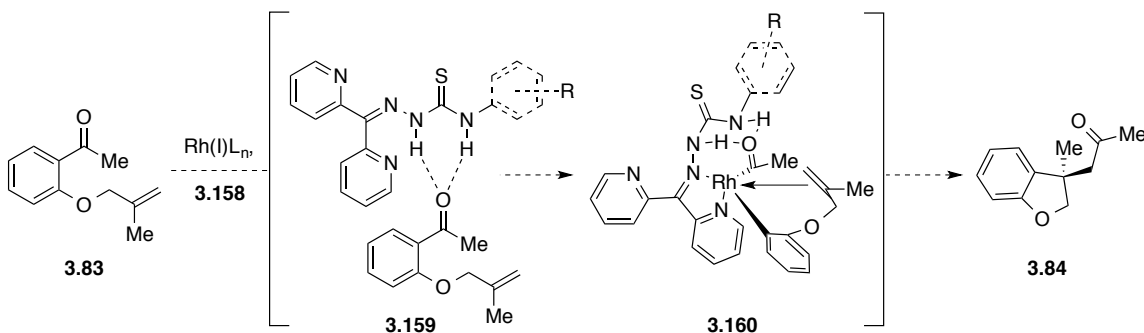


Figure 29. Thiosemicarbazone as a potential directing group for C–C bond activation

Thiosemicarbazone **3.158** was proposed to hydrogen bond with ketone **2.83** to give adduct **3.159** (Scheme 81). The iminyl and pyridyl sp^2 nitrogens of **3.158** would ligate the transition metal and direct it into the $C_{acyl}-C_{aryl}$ bond to form complex **3.160**. It is presumed that the hydrogen bonding interaction(s) in **3.160** could prevent decarbonylation. Migratory insertion across the appended olefin followed by reductive elimination would generate dihydrobenzofuran **3.84**. Although activation of the $C_{acyl}-C_{methyl}$ is plausible, it is likely that the stronger $Rh-C_{aryl}$ would be favored.



Scheme 81. Proposed C–C bond activation with a thiosemicarbazone directing group

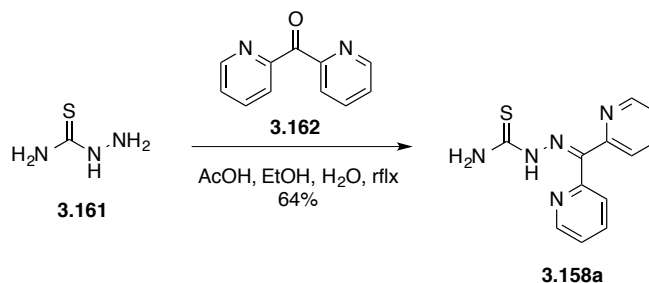
The idea for “directing the directing group” with regards to bond activation is rather unprecedented. Cramer had demonstrated the only related example of such a strategy, as described above (Scheme 80, Figures 26–27). Many unknown factors render this proposal ‘impractical,’ or at least risky. First, hydrogen bonding may not be effective at

elevated temperatures. No examples of hydrogen bonding catalysis above 100 °C have been reported. This may be due, in part, because the reactions employed do not require high temperatures and/or the catalysts serve to lower the activation barrier and thus allow for milder conditions. However, it has been demonstrated that C–C bond activation can take place at room temperature in some cases (see Chapter 1, Scheme 10). Second, hydrogen bonding may not accommodate the cage-like intermediate **3.160**. The maximum hydrogen bond strength is achieved when the X–H---A angle is 180°; however, this preference is considerably relaxed with moderate to weak interactions.²² Nevertheless, I felt the idea was worth pursuing despite these presumably unfavorable factors.

3.5.3 RESULTS AND DISCUSSION

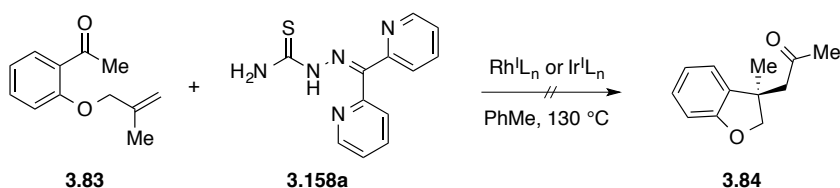
Co-Catalyst Synthesis

Thiosemicarbazone **3.158a** was readily prepared in one step in 64% yield by refluxing commercially available thiocarbazide **3.161** and di(2-pyridyl) ketone **3.162** in acetic acid, ethanol, and water (Scheme 82).



Scheme 82. Preparation of thiosemicarbazone **3.158a**

Reaction Screen



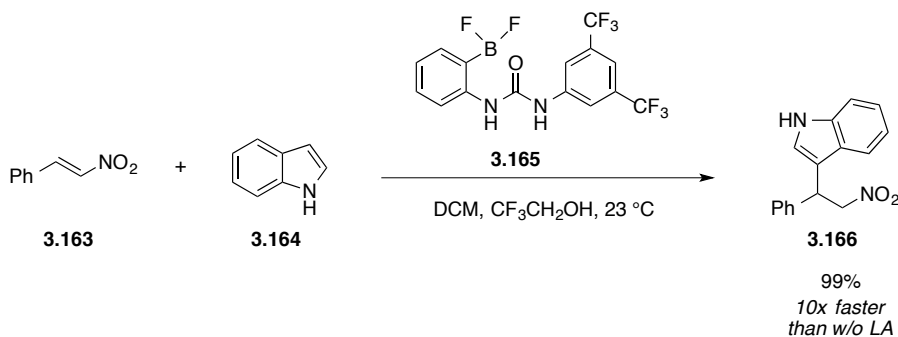
Ketone **3.83** was treated with several rhodium and iridium complexes in the presence of 50 mol% thiosemicarbazone **3.158a**. Upon heating, the formation of a considerable amount of precipitate was observed. Catalysts $\text{RhCl}(\text{PPh}_3)_3$, $[\text{Rh}(\text{C}_2\text{H}_4)_2\text{Cl}]_2$, $\text{Rh}(\text{cod})_2\text{OTf}$, $\text{Rh}(\text{cod})_2\text{BF}_4$, $[\text{Rh}(\text{acac})(\text{cod})]$, $[\text{Rh}(\text{OMe})(\text{cod})_2]_2$, $[\text{Rh}(\text{cod})\text{OH}]_2$, $\text{Rh}(\text{norb})_2\text{BF}_4$, $\text{Rh}(\text{acac})(\text{CO})_2$, $[\text{Rh}(\text{coe})_2\text{Cl}]_2$, and $[\text{Ir}(\text{coe})_2\text{Cl}]_2$ returned starting material, and the crude ^1H NMR spectra indicated that roughly 20% of the thiosemicarbazone was absent (10 mol% rhodium loading). Although the insoluble material formed in the reaction mixture was not characterized, it was assumed that the thiosemicarbazone had sequestered the catalysts. Reactions with 2.5 and 5 mol% loadings of **3.158a** also returned starting material, along with side products resulting from olefin isomerization and deallylation. The absence of all reactivity in the reactions employing 50 mol% **3.158a** further suggested the thiosemicarbazone had inactivated the transition metal.

Literature reports have shown thiosemicarbazone **3.158a** to act as a bi- or tri-dentate ligand to Re ,²³ Ni ,^{24,26,27} Hg ,²⁵ Mn ,^{26,28} Co ,^{24,26} Zn ,^{26,27} V ,²⁷ Cu ,^{24,26} and Fe ^{24,26} complexes. The nature of such binding modes involves coordination through sulfur (and the desired iminyl and pyridyl nitrogens). This led to the idea of using an internal Lewis acid to ‘tie up’ the sulfur atom.

3.5.4 MODIFIED PROPOSAL

Pyridyl thiosemicarbazones (e.g. **3.158a**) have been well documented to form stable metal complexes as bi- and tri-dentate ligands.²³⁻²⁸ Prior to this knowledge, **3.158a** had been designed as a co-catalyst for C–C bond activation (Scheme 81). Preliminary investigations indicated that rhodium and iridium form insoluble complexes with **3.158a**. With thiosemicarbazones known to bind metals through its sulfur, iminyl and pyridyl nitrogen, it was proposed that an internal Lewis acid/base interaction would prevent metal coordination to sulfur. A survey of the literature revealed that the concept of internal Lewis acids in combination with urea catalysts had been investigated.²⁹⁻³¹

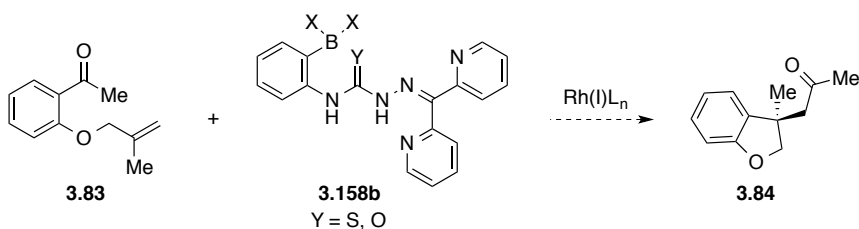
Urea and thiourea organocatalysts are known to facilitate reactions such as Michael additions by hydrogen bonding to the electrophile. In an effort to develop higher yielding and faster reactions, Mattson³¹ theorized that incorporating an internal Lewis acid would increase the reactivity. It was found that boronate catalyst **3.165** accelerated the addition of indole (**3.164**) to β -nitrostyrene (**3.163**) ten times faster than the non-Lewis-acid analogue, and the product was obtained in 99% yield (Scheme 83).



Scheme 83. Michael addition with internal-Lewis-acid-thiourea catalyst

The marked increase in rate was due to the polarizing effect induced by the Lewis acid, which not only elongated the carbonyl bond, but also significantly increased the acidity of the urea protons. Boronate urea **3.165** was found to have a pK_a of 7.5 whereas the conventional bis(3,5-trifluoromethyl-phenyl)urea has a pK_a of 13.8. For comparison, the more reactive bis(3,5-trifluoromethyl-phenyl)thiourea has a pK_a of 8.5. The 6.3 difference in pK_a units attributes to the enhanced rate of reaction.

The modified proposal for hydrogen-bond-directed C–C bond activation (see Scheme 81) with internal Lewis acids would prevent the coordination of sulfur to rhodium ($S \rightarrow Rh$) by creating a Lewis acid/base pair between boron and sulfur ($S \rightarrow B$) (Scheme 84). In addition, the internal Lewis acid would enhance the polarizability of the thionyl group. In turn, this would not only strengthen the degree of hydrogen bonding (and thus directing ability of the co-catalyst), but also lower the LUMO of the substrate carbonyl, therefore making it more susceptible to attack by the metal.

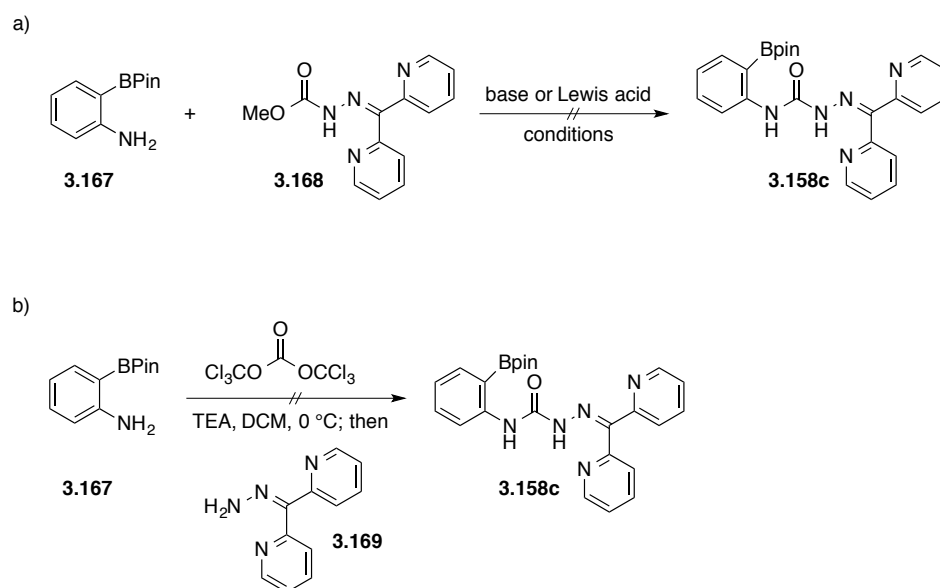


Scheme 84. Proposed internal-Lewis-acid-assisted, hydrogen-bond-directed C–C bond activation

3.5.5 SYNTHETIC EFFORTS TOWARD CO-CATALYST(S)

Efforts to prepare semicarbazone **3.158c**, containing a pinacol boronic ester Lewis acid, began with nucleophilic carbonyl substitution reactions with aniline **3.167**

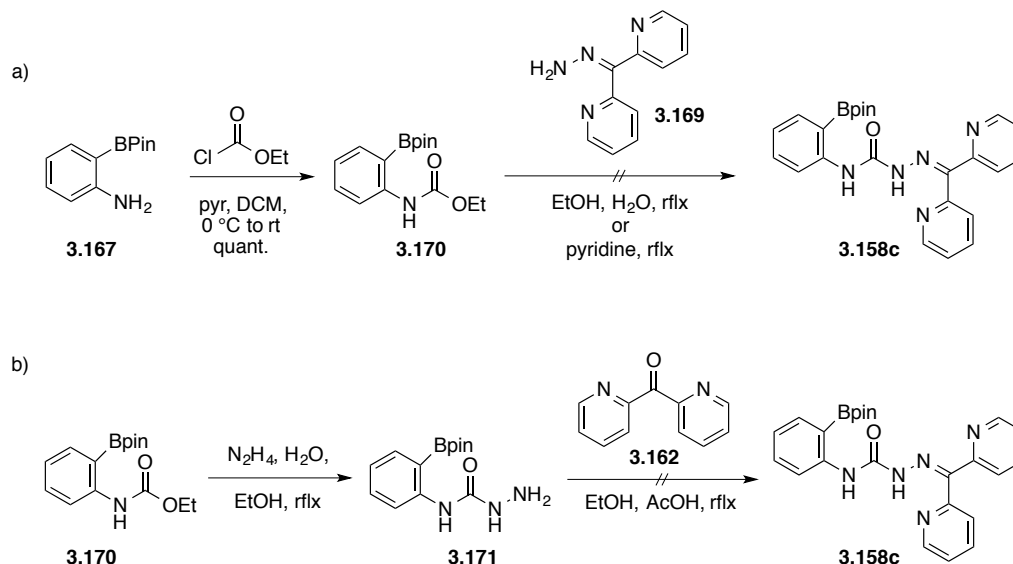
(Scheme 85). Borylated aniline **3.167** was prepared in one step from 2-bromoaniline (not shown). Carbamate **3.168** was prepared in two steps from dimethyl carbonate through a substitution reaction with hydrazine and a condensation of the resulting methyl hydrazinecarboxylate with di-(2-pyridyl) ketone (not shown). Efforts to couple aniline **3.167** and carbamate **3.168** under acidic or basic conditions were not successful in providing **3.158c** (Scheme 85a). An acylation reaction of aniline **3.167** with triphosgene was directly followed by the addition of hydrazone **3.169** (prepared by condensation of hydrazine and the corresponding ketone **3.162**) did not deliver the desired product **3.158c** (Scheme 85b).



Scheme 85. Unsuccessful syntheses of internal-Lewis acid HB co-catalyst

A step-wise approach to **3.158c** was pursued in which borylated aniline **3.167** was successfully acylated with ethyl chloroformate (Scheme 86a). Carbamate **3.170** was heated in the presence of hydrazone **3.169** under neutral and basic conditions, though the reactions returned only starting material. Treating carbamate **3.170** with excess

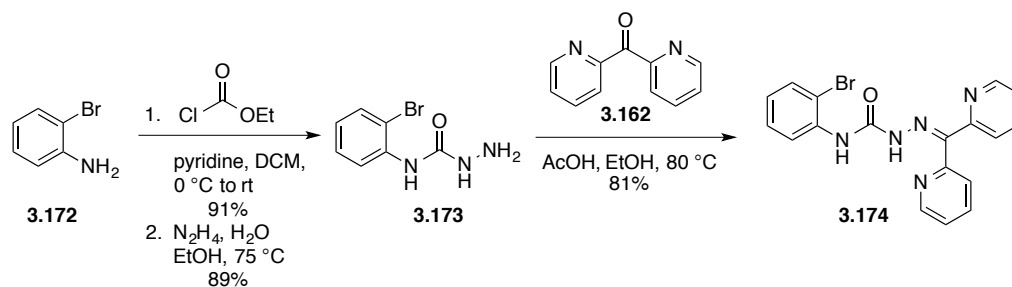
hydrazine, however, afforded the corresponding semicarbazide **3.171** (Scheme 86b). The difference in reactivity between **3.169** and hydrazine could be a result of decreased nucleophilicity due to resonance. An attempt to achieve the desired semicarbazone **3.158c** through a condensation reaction between carbazide **2.171** and di-(2-pyridyl) ketone **3.162** was not successful.



Scheme 86. Unsuccessful syntheses of internal-Lewis-acid HB co-catalyst

Understanding that it is relatively uncommon to successfully carry a boronic ester through multiple synthetic steps, a more logical retrosynthetic disconnection was made in which the borylation reaction would be introduced at a late stage. Acylating 2-bromoaniline (**3.172**) with ethyl chloroformate proceeded in 91% yield and the semicarbazide **3.173** was obtained in 92% yield upon treating the carbamate with excess hydrazine (Scheme 87). Analysis of the crude ^1H NMR spectrum of the subsequent condensation reaction between **3.173** and ketone **3.162** suggested the formation of **3.174** as the major product. However, purification by column chromatography was problematic

due to the extreme polarity of **3.174**; the conditions required for the compound to elute was a 10:20:70 mixture of MeOH:TEA:EtOAc. I then discovered that **3.174** could be crystallized from the reaction mixture and obtained in a 81% yield. The analogous iodo semicarbazone **3.175** was also prepared in this manner.



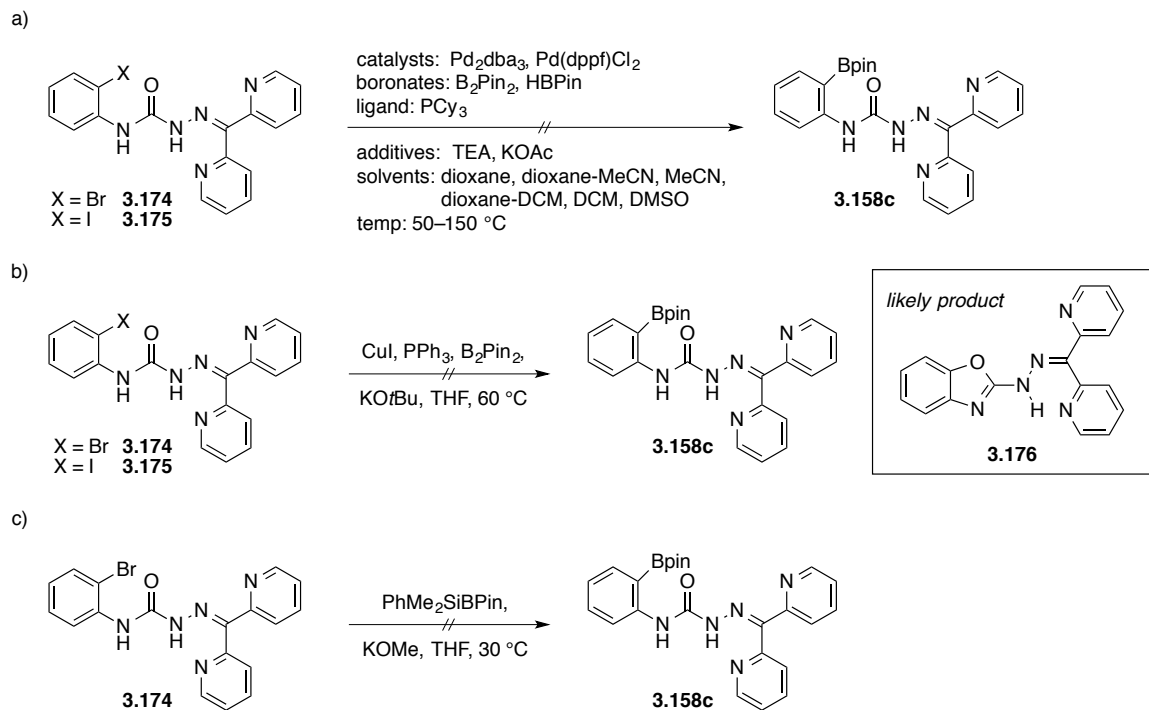
Scheme 87. Preparation of bromosemicarbazone **3.174**

Several attempts to borylate semicarbazones **3.174** and **3.175** with palladium-catalyzed cross-coupling reactions were not met with success (Scheme 88a). All reactions except for those ran in DMSO at 150 °C (decomposition) returned only starting material. While the lack in reactivity was initially attributed to the poor solubility, employing TEA as a co-solvent remedied this matter but failed to promote the reaction. It is likely that the semicarbazones ligate the catalyst (as previously alluded to) and thus prevent oxidative addition.

Under copper-catalyzed borylation conditions,³² semicarbazones **3.174** and **3.175** underwent complete conversion to unidentified products. The major product of these reactions was void of a 12H pinacolyl methyl peak in the ¹H NMR spectrum (Scheme 88b). It is likely that this side-product was the corresponding benzoxazole

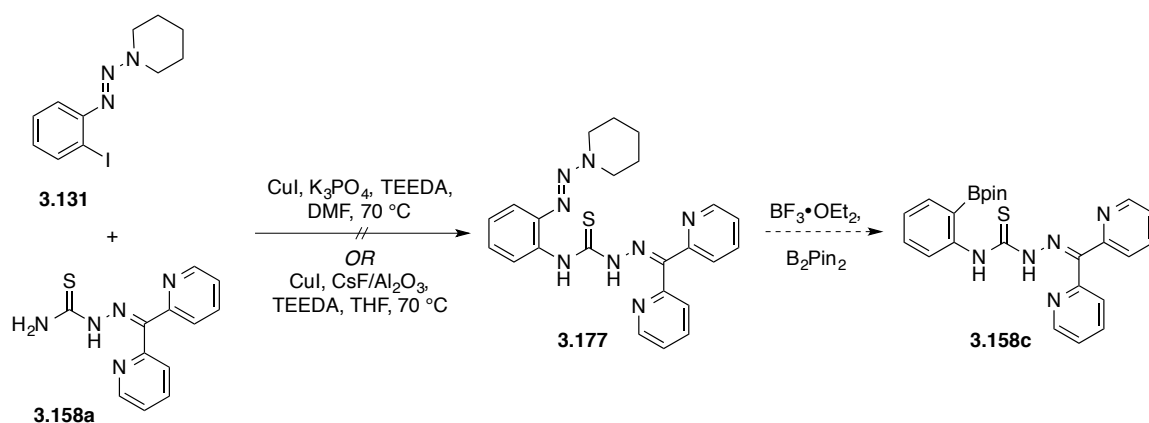
3.176. A metal-free borylation reaction with silylborane had been reported by Ito.³³

Under these conditions, semicarbazone **3.174** was unreactive (Scheme 88c).



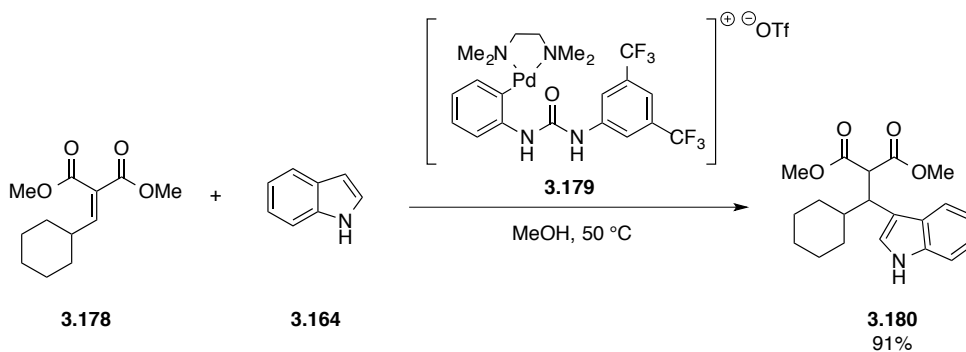
Scheme 88. Unsuccessful borylations of bromo- and iodosemicarbazone

With pyridyl-substituted semicarbazones reluctant to undergo transition-metal catalyzed borylation reactions, it was envisioned that diazonium chemistry might serve as an alternative means to install the desired boronic ester functionality. Yamane³⁴ had demonstrated that subjecting triazenes to strong Lewis acids in the presence of bis(pinacolato)diboron resulted in effective borylation of the transient diazonium ion species (**3.177** to **3.158c**, Scheme 89). Attempts to couple thiosemicarbazone **3.158a** to iodo-aryltriazene **3.131** under copper-mediated conditions^{35,36} resulted in incomplete conversion to unidentified products.



Scheme 89. Unsuccessful coupling of iodo-aryltriazene and thiosemicarbazide

Unlike the di-(2-pyridyl) semicarbazones, *ortho*-halo ureas participate in oxidative addition reactions with palladium catalysts as demonstrated in the preparation of urea catalyst **3.179** (Scheme 90). In addition to boron-based internal Lewis acid urea catalysts, pallado-catalysts have been realized to facilitate similar transformations. Michael addition of alkylidene malonates **3.178**, which are unreactive under conventional urea catalysis, are promoted with urea palladacycle **3.179** (Scheme 90). The preparation of a palladacycle semicarbazone by way of condensation of a pallado-semicarbazide with di-(2-pyridyl) ketone (see Scheme 86b) may be more feasible.

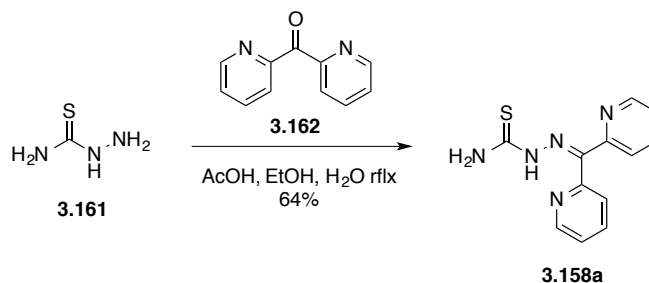


Scheme 90. Michael addition accelerated by pallado-urea catalyst

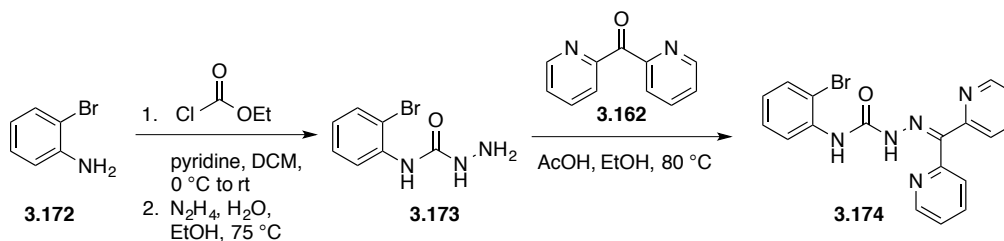
3.5.6 CONCLUDING REMARKS

Attempts to promote carboacylation through hydrogen-bond-directed C–C bond activation were unsuccessful with co-catalyst **3.158a** owing to its propensity to ligate the metal complex unproductively. Unfortunately the idea of incorporating an internal Lewis acid to prevent ligation was unable to be probed. The demonstration that asymmetric hydrocarbamylation can be achieved with a bimetallic catalyst system that plays upon the central idea proposed in this section is encouraging. It is believed that introducing a directing group through such secondary interactions should be further explored for C–C bond activation.

3.5.7 EXPERIMENTAL



To a solution of di-(2-pyridyl) ketone **3.162** (500 mg, 2.50 mmol) in EtOH (4 mL) and H₂O (4 mL) was added thiocarbazide **3.161** (228 mg, 2.5 mmol) and AcOH (5 drops). The resulting solution was refluxed for 3 hr and then cooled in a ~5 °C refrigerator over night. Yellow crystals of thiosemicarbazone **3.158a** (409 mg, 1.59 mmol, 64%) were collected via vacuum filtration: ¹H NMR (500 MHz; CDCl₃) δ 14.39 (s, 1H), 8.82 (ddd, *J* = 4.9, 1.7, 0.8 Hz, 1H), 8.65 (ddd, *J* = 4.8, 1.6, 0.9 Hz, 1H), 7.84 (td, *J* = 7.7, 1.7 Hz, 1H), 7.81-7.78 (m, 2H), 7.54 (app d, *J* = 8.1 Hz, 1H), 7.49 (br s, 1H), 7.40 (ddd, 8.5, 4.5, 1.0, 1H), 7.39 (ddd, 10.0, 5.0, 1.5 Hz, 1H), 6.42 (s, 1H); ¹³C NMR (126 MHz; CDCl₃) δ 180.0, 155.7, 151.5, 148.7, 148.2, 141.7, 137.0, 126.9, 124.4, 124.0, 123.8.



Ethyl chloroformate (0.83 mL, 8.72 mmol) and dry DCM (20 mL) were added to a flame-dried flask and cooled to 0 °C. 2-bromoaniline (**3.172**) (1.5 g, 8.72 mmol) was added and the reaction mixture was brought to room temperature and stirred overnight. The reaction was filtered and the filtrate washed with 1 M HCl. The organic layer was washed with

brine, dried over Na₂SO₄, filtered, and concentrated to give the carbamate (1.93 g, 7.9 mmol, 91%). The resulting carbamate (720 mg, 2.95 mmol) was esterified by treatment with an aqueous solution of hydrazine (2.9 mL, 59.0 mmol) in EtOH (3 mL) at 75 °C (no reaction occurred at room temperature). DCM and water were added to the reaction after 24 h. The organic layer was washed with H₂O and brine, dried over Na₂SO₄, filtered, and concentrated to give semicarbazide **3.173** (625 mg, 2.72 mmol, 92% crude) without the need for further purification: *R_f* 0.16 (1:4 EtOAc:Hex). Semicarbazide **3.173** (400 mg, 1.74 mmol), di-2-pyridyl ketone (**3.162**) (348 mg, 1.74 mmol), acetic acid (7 drops), and EtOH (3 mL) were combined in a scintillation vial and heated at 80 °C for 20 min. The vial was cooled to room temperature and the bromosemicarbazone **3.174** (487 mg, 1.23 mmol, 71%) precipitate was collected by vacuum filtration: *R_f* 0.48 (6:1:3 EtOAc:TEA:Hex); ¹H NMR (500 MHz; CDCl₃) δ 13.35 (s, 1H), 9.24 (s, 1H), 8.78 (ddd, *J* = 4.9, 1.7, 0.8 Hz, 1H), 8.63 (ddd, *J* = 4.8, 1.6, 0.8 Hz, 1H), 8.44 (dd, *J* = 8.3, 1.5 Hz, 1H), 8.03 (d, *J* = 7.9 Hz, 1H), 7.87-7.80 (m, 2H), 7.66 (d, *J* = 8.1 Hz, 1H), 7.54 (dd, *J* = 8.0, 1.4 Hz, 1H), 7.40-7.32 (m, 3H), 6.94 (td, *J* = 7.7, 1.3 Hz, 1H); ¹³C NMR (126 MHz; CDCl₃) δ 156.1, 152.6, 151.7, 148.4, 147.9, 140.5, 137.0, 136.9, 136.2, 132.2, 128.4, 126.6, 124.0, 123.9, 123.67, 123.5, 120.5, 113.0.

REFERENCES

- (1) Lokwani, P.; Nagori, B. P.; Batra, N.; Goyal, A.; Gupta, S.; Singh, N. *J. Chem. Pharm. Res.* **2011**, *3*, 302.
- (2) Siu, M.; Pastor, R.; Liu, W.; Barrett, K.; Berry, M.; Blair, W. S.; Chang, C.; Chen, J. Z.; Eigenbrot, C.; Ghilardi, N.; Gibbons, P.; He, H.; Hurley, C. A.; Kenny, J. R.; Khojasteh, S. C.; Le, H.; Lee, L.; Lyssikatos, J. P.; Magnuson, S.; Pulk, R.; Tsui, V.; Ultsch, M.; Xiao, Y.; Zhu, B.-Y.; Sampath, D. *Bioorg. Med. Chem. Lett.* **2013**, *17*, 5014.
- (3) Zhang, L.; Guan L.-P.; Sun, X.-Y.; Wei, C.-X.; Chai, K.-Y.; Quan, Z.-S. *Chem. Biol. Drug Des.* **2009**, *73*, 313.
- (4) Suggs, J. W. *J. Am. Chem. Soc.* **1979**, *101*, 489.
- (5) Jun, C.-H.; Lee, H.; Hong, J. *J. Org. Chem.* **1997**, *62*, 1200.
- (6) Jun, C.-H.; Lee, H.; Hong, J. *Angew. Chem. Int. Ed.* **2000**, *39*, 3070.
- (7) Jun, C.-H.; Lee, H. *J. Am. Chem. Soc.* **1999**, *121*, 880.
- (8) Jun, C.-H.; Lee, H.; Lim, S.-G. *J. Am. Chem. Soc.* **2001**, *123*, 751.
- (9) Lazny, R.; Sienkiewicz, M.; Bräse, S. *Tetrahedron* **2001**, *57*, 5825; Gross, M. L.; Blank, D. H.; Welch, W. M. *J. Org. Chem.* **1993**, *58*, 2104.
- (10) Lormann, M.; Dahmen, S.; Bräse, S. *Tetrahedron Lett.* **2000**, *41*, 3813.
- (11) Wautelet, P.; Le Moigne, J.; Videva, V.; Turek, P. *J. Org. Chem.* **2003**, *68*, 8025; Patrick, T. B.; Juehne, T.; Reeb, E.; Hennessy, D. *Tetrahedron Lett.* **2001**, *42*, 3353.
- (12) Liu, C.; Knochel, P. *J. Org. Chem.* **2007**, *72*, 7106; Satyamurthy, N.; Barrio, J. R.; Bida, G. T.; Phelps, M. E. *Tetrahedron Lett.* **1990**, *31*, 4409; Zhu, C.; Yamane, M. *Org. Lett.* **2012**, *14*, 4560.
- (13) Kimball, D. B.; Haley, M. M. *Angew. Chem. Int. Ed.* **2002**, *41*, 3338; Zhou, J.; Yang, W.; Wang, B.; Ren, H. *Angew. Chem. Int. Ed.* **2012**, *51*, 12293; Saeki, T.; Son, E.; Tamao, K. *Org. Lett.* **2004**, *6*, 617; Bräse, S.; Schroen, M. *Angew. Chem. Int. Ed.* **1999**, *38*, 1071; Patrick, T. B.; Willaredt, R. P.; DeGonia, D. J. *J. Org. Chem.* **1985**, *50*, 2232; de Meijere, A.; Nüske, H.; Es-Sayed, M.; Labahn, T.; Schroen, M.; Bräse, S. *Angew. Chem. Int. Ed.* **1999**, *38*, 3669.
- (14) Wang, C.; Chen, H.; Wang, Z.; Chen, J.; Huang, Y. *Angew. Chem. Int. Ed.* **2012**,

51, 7242.

- (15) Wang, C.; Sun, H.; Fang, Y.; Huang, Y. *Angew. Chem. Int. Ed.* **2013**, *52*, 5795.
- (16) Murai, S.; Kakiuchi, F.; Sekine, S.; Tanaka, Y.; Kamatani, M.; Sonoda, M.; Chatani, N. *Nature* **1993**, *366*, 529.
- (17) Chatani, N.; Ie, Y.; Kakiuchi, F.; Murai, S. *J. Org. Chem.* **1997**, *62*, 2604.
- (18) Chatani, N.; Ie, Y.; Kakiuchi, F.; Murai, S. *J. Am. Chem. Soc.* **1999**, *121*, 8545.
- (19) Wang, J.; Feringa, B. L. *Science* **2011**, *331*, 1429.
- (20) Balcells, D.; Moles, P.; Blakemore, J. D.; Raynaud, C.; Brudvig, G. W.; Crabtree, R. H.; Eisenstein, O. *Dalton Trans.* **2009**, 5989.
- (21) Donets, P. A.; Cramer, N. *J. Am. Chem. Soc.* **2013**, *135*, 11772.
- (22) Taylor, M. S.; Jacobsen, E. N. *Angew. Chem. Int. Ed.* **2006**, *45*, 1520.
- (23) Bakir, M.; Ordel, B. *J. Mol. Struct.* **2009**, *930*, 65.
- (24) Martinez, M. P.; Valcarcel, M.; Pino, F. *Anal. Chim. Acta* **1976**, *81*, 157.
- (25) Cespedes, G. A.; Perez, B. D.; Valcarcel, M. *Microchem. J.* **1984**, *30*, 105.
- (26) Bernhardt, P. V.; Sharpe, P. C.; Islam, M.; Lovejoy, D. B.; Kalinowski, D. S.; Richardson, D. R. *J. Med. Chem.* **2009**, *52*, 407.
- (27) Sreekanth, A.; Sivakumar, S.; Prathapachandra Kurup, M. R. *J. Mol. Struct.* **2003**, *655*, 47.
- (28) Bakir, M.; Conry, R.; Thomas, D. *J. Coord. Chem.* **2014**, *67*, 249.
- (29) Nickerson, D. M.; Angeles, V. V.; Auvil, T. J.; So, S. S.; Mattson, A. E. *Chem. Commun.* **2013**, *49*, 4289.
- (30) So, S. S.; Auvil, T. J.; Garza, V. J.; Mattson, A. E. *Org. Lett.* **2012**, *14*, 444.
- (31) So, S. S.; Burkett, J. A.; Mattson, A. E. *Org. Lett.* **2011**, *13*, 716.
- (32) Kleeberg, C.; Dang, L.; Lin, Z.; Marder, T. B. *Angew. Chem. Int. Ed.* **2009**, *48*, 5350.
- (33) Yamamoto, E.; Izumi, K.; Horita, Y.; Ito, H. *J. Am. Chem. Soc.* **2012**, *134*, 19997.
- (34) Zhu, C.; Yamane, M. *Org. Lett.* **2012**, *14*, 4560.
- (35) Nandakumar, M. V. *Tetrahedron Lett.* **2004**, *45*, 1989.
- (36) Hosseinzadeh, R.; Sarrafi, Y.; Mohadjerani, M.; Mohammadpourmir, F. *Tetrahedron Lett.* **2008**, *49*, 840.

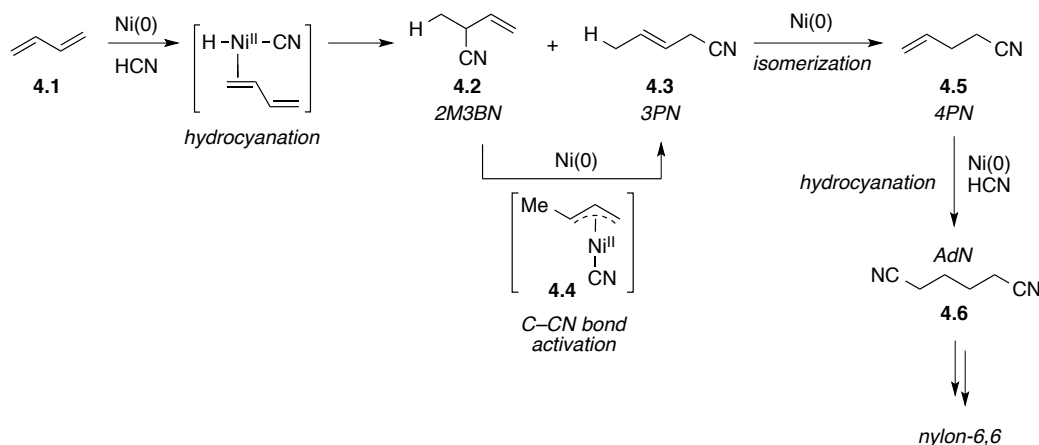
CHAPTER FOUR

An Overview of Carbon–Nitrile Bond Activation

INTRODUCTION

Efforts to advance the field of C–C bond activation have been met with great challenge. The necessity for high-energy starting materials and/or covalently bound directing groups has limited the applicability of the methodology in small molecule synthesis. However, promising work in the area of carbon–nitrile (C–CN) bond activation has avoided both of these limitations. The propensity for nitriles to coordinate to transition metals in a η^1 or η^2 fashion serves to lower the kinetic barriers and thus remove the need for an external directing group. Although carbon–nitrile bonds have high bond dissociation energies (~130 kcal/mol), the formation of strong metal–nitrile (M–CN) bonds help offset the thermodynamics of the reaction. Oxidative addition of low-valent metal complexes into alkyl, vinyl, alkynyl, aryl, and acyl C–CN bonds has been realized, and such processes have been readily applied to catalytic transformations. Arguably the most synthetically important application for C–CN bond activation is the carbocyanation of unactivated olefins, which will be the focus of this chapter. The activation of C–CN bonds with subsequent hydrodecyanation, silylation/borylation, cross-coupling, and cycloaddition events will not be discussed, nor will activation by electron transfer and/or addition/elimination pathways be covered.

Although the activation of C–CN bonds has been known since 1971,¹ its utility in organic synthesis has only begun to emerge within the past 10 years. Metal cyanides have been shown to serve as cyanating agents when reacted with olefins to give nitrile products. An early, notable example of the utility of this methodology is seen in DuPont’s adiponitrile (AdN) process, which is used in the synthesis of nylon-6,6 (Scheme 91).^{2–5} Hydrocyanation of 1,3-butadiene (**4.1**), by *in situ* generation of H–Ni–CN, afforded a mixture of regioisomers: 2-methyl-3-butenenitrile (2M3BN, **4.2**) and 3-pentenitrile (3PN, **4.3**). Catalytic isomerization of 2M3BN is best described as a C–CN bond oxidative addition process to form π -allylnickel intermediate **4.4**.⁶ Since conventional cyanation reactions rely on a stoichiometric amount of highly toxic metal–cyanide and/or hydrogen cyanide, gaining the ability to generate metal–cyanides *in situ* through C–CN bond activation provides a less toxic entry into cyanation chemistries with the potential to build molecular complexity in a single operation.

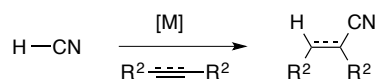


Scheme 91. C–CN bond activation in Dupont’s adiponitrile synthesis

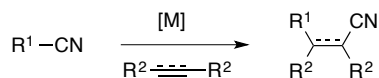
Carbocyanation is a class of reactions that encompasses processes in which an organonitrile is added across an olefin (Figure 30). Cyanoacylation is a term that

describes a subset of carbocyanation reactions that involve a $C_{acyl}-CN$ bond, wherein cyanoamidation, cyanoesterification and cyanothioesterification refer to an amide, ester, or thioester, respectively (Figure 30c). Unlike a typical unstrained C–C bond, which requires a directing group to bring the metal into proximity, the strong coordination of the nitrile π bond serves to direct the metal to the C–CN bond (Figure 30d). The resulting C–M–CN complex coordinates to an olefin, undergoes migratory insertion (carbometallation), and reductively eliminates to generate a product with two new carbon–carbon bonds.

a) HYDROCYANATION



b) CARBOCYANATION



$R^1 = \text{alkyl, alkenyl, alkynyl, aryl}$

c) CYANOACYLATION



$R^1 = C_nH_n, NR_2, OR, SR$

d) GENERAL MECHANISM

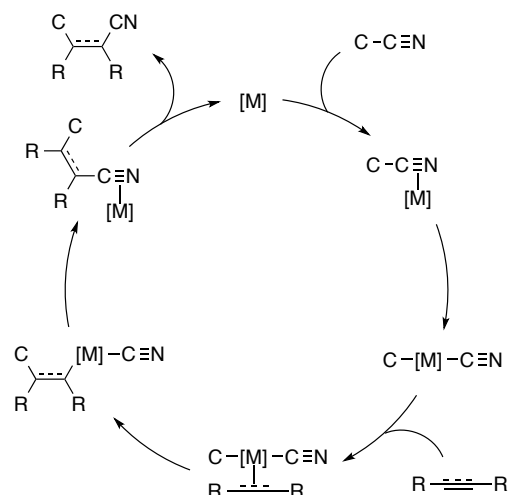


Figure 30. Various additions of organonitriles across olefins: a) hydrocyanation b) carbocyanation c) cyanoacylation (i.e cyanoamidation, cyanoesterification, cyanothioesterification d) accepted mechanism for carbocyanation

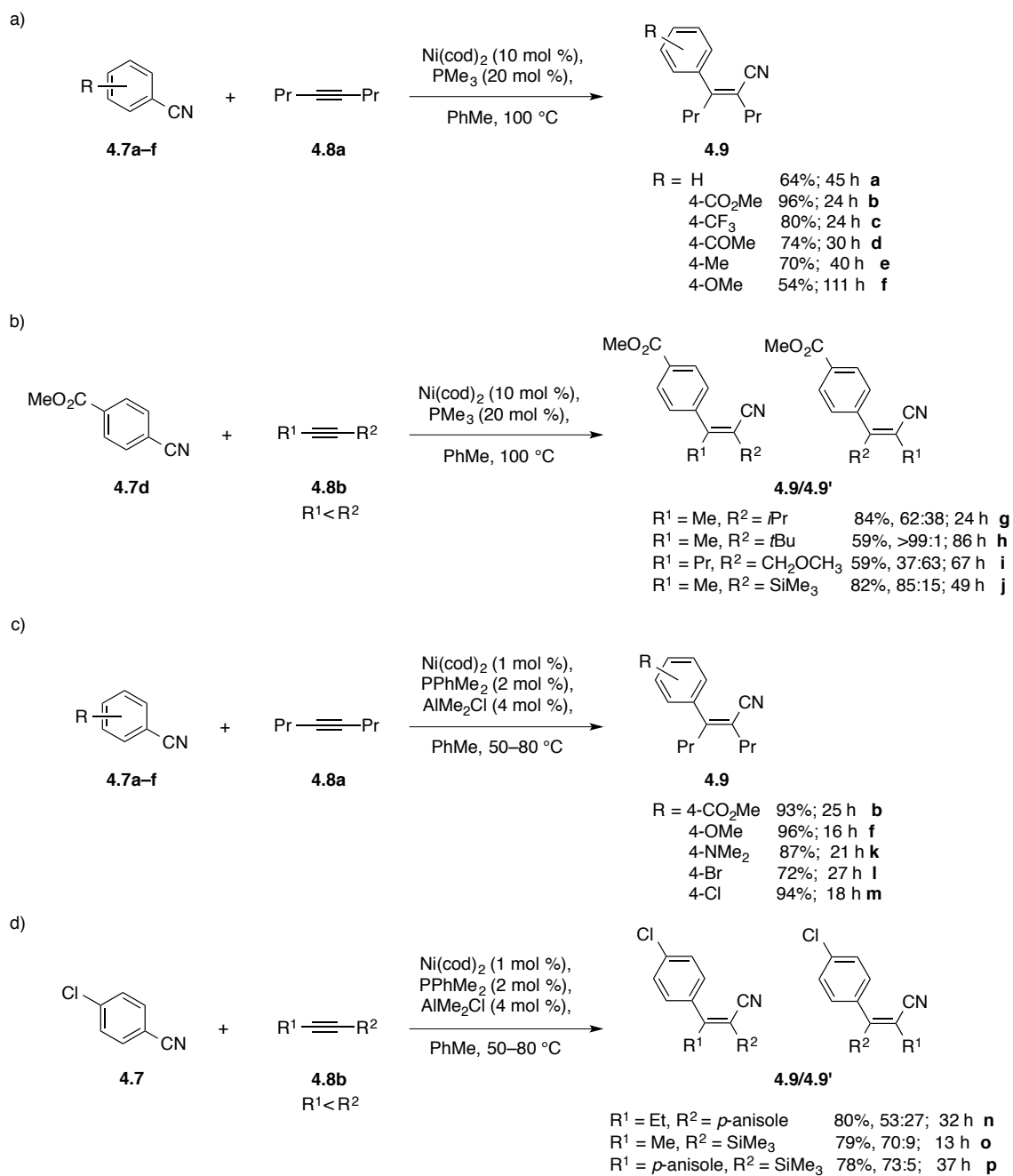
4.1 CARBOCYANATION WITH ALKYNES

In 2004, Nakao and Hiyama were the first to report a nickel-catalyzed arylcyanation reaction in which Ar–CN bonds were efficiently added across alkynes to give tetrasubstituted alkenes.^{7,8} It was found that a 1:2 Ni(cod)₂:PMe₃ system in toluene at 100 °C for 45 h allowed for the addition of benzonitrile (**4.7**) to alkyne **4.8a** to give alkene **4.9a** in 64% yield (Scheme 92a). Introducing electron-withdrawing substituents within the aryl ring greatly enhanced the reaction (R = 4-CO₂Me (**4.9b**), 96%; 4-CF₃ (**4.9c**), 80%; 4-COMe (**4.9d**), 73%) whereas electron-donating substituents suppressed reactivity (R = 4-Me (**4.9e**), 70%; R = 4-OMe (**4.9f**), 54%, *III h*). Upon employing unsymmetrical alkynes, wherein R¹ < R² in size, the regioselectivity of the reaction suggested that the cyano group was delivered first (cyanometalation) in order to reduce the steric environment around the resulting metal center (Scheme 92b). DFT calculations later revealed that carbometalation remained the active pathway and that selectivity was dictated by the repulsion between the aryl and larger R² groups. It was also revealed that oxidative addition is the rate-determining step.⁹

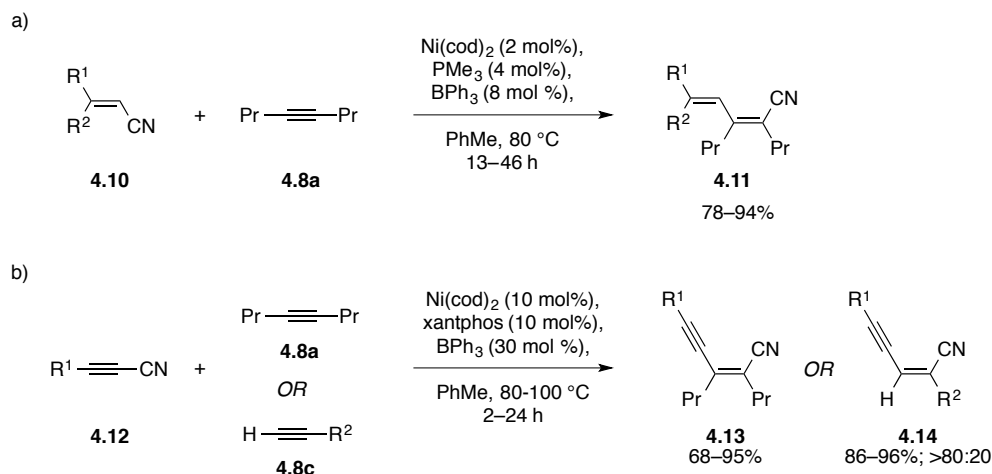
Lewis acids have been shown to facilitate oxidative addition of C–CN bonds by coordinating to the nitrile lone pair.¹⁰ This phenomenon is likely explained by lowering the LUMO of the nitrile, and/or by strengthening the resulting M–CN bond by eliciting increased back donation from the metal center. It was therefore envisioned that a Lewis acid additive would help overcome the electronic limitations of arylcyanation. A dramatic effect was observed when Lewis acids were employed in the reaction. The addition of 4 mol % AlMe₂Cl allowed for a tenfold decrease in Ni-catalyst loading, a substantial reduction in temperature, and it allowed for efficient reactions with

benzonitriles containing electron-donating substituents (R = 4-OMe (**4.9d**), 96%, 16 h; 4-NMe₂ (**4.9k**), 87%)¹¹ while maintaining reactivity with electron-withdrawing substituents (R = CO₂Me (**4.9b**), 93%; Scheme 92c). In addition, the reaction with Lewis acid allowed for remarkable chemoselectivity in the presence of halogenated benzonitriles (R = Br (**4.9l**), 72%; R = Cl (**4.9m**), 94%). The regioselective preference was consistent in the presence of Lewis acid (Scheme 92d). It should be noted that the tetrasubstituted vinyl nitrile products did undergo further reaction.

Nakao and Hiyama expanded the carbocyanation methodology to include the activation of alkenyl and alkynyl C–CN bonds.¹¹ Triphenylborane was found to be the optimal Lewis acid for the reaction with vinyl nitriles **4.10**, though the results of other Lewis acids were not reported for comparison (Scheme 93a). The diene nitrile products **4.11** were obtained in good to excellent yield (78–94%). It was acknowledged that the product C–CN bond could potentially participate in further carbocyanation reactions with **4.8a**, though this was not observed. The authors stated that “catalyst differentiation was based upon steric and/or electronic factors” to explain this observation. Although no examples were reported to support this claim, it has been interpreted to mean that tri- or tetra-substituted cyanoalkenes do not participate in carbocyanation for steric reasons. Since the M–CN intermediate (prior to reductive elimination) does not intercept another alkyne molecule, it may be implied that migratory insertion becomes the rate-limiting step. Alkynyl C–CN bonds (**4.12**) were also shown to undergo the reaction to provide enynes **4.13** in moderate to excellent yields (Scheme 93b).^{12,13} In addition, terminal alkynes **4.11** readily underwent the desired reaction.

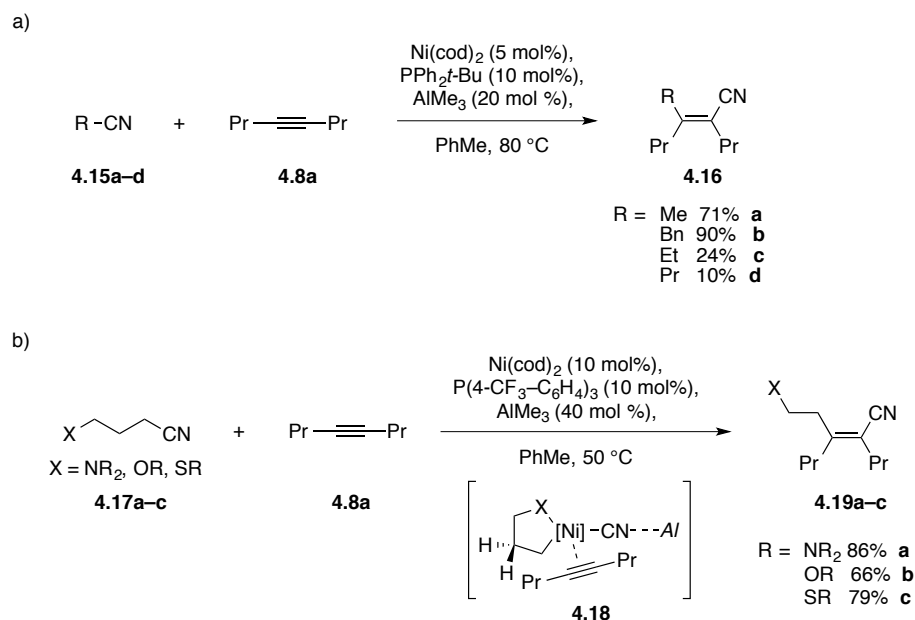


Scheme 92. Intermolecular carbocyanation (arylcyanation) with alkynes: a) without Lewis acid, benzonitrile scope b) without Lewis acid, unsymmetrical alkynes c) with Lewis acid, benzonitrile scope d) with Lewis acid, unsymmetrical alkynes



Scheme 93. Intermolecular carbocyanation with alkynes: a) alkenyl nitriles b) alkynyl nitriles

The activation of alkyl C–CN bonds was successfully demonstrated by the carbocyanation of acetonitrile (**4.15a**) and benzylnitrile (**4.15b**) with alkyne **4.8a** to give alkene **4.16a** and **4.16b** in 71% and 90% yield, respectively (Scheme 94a).^{11,14} However, the utility of such reactions is severely limited to nitriles without β -hydrogens. Substrates with β -hydrogens undergo the reaction in less than 30% yield due to a competitive β -hydride elimination pathway that leads to hydrocyanation of alkyne **4.8a**. Hydrocyanation side-products can be suppressed in alkyl carbocyanation reactions with the addition of a γ -heteroatom (**4.17**) (Scheme 94b). It is assumed that the oxidative addition adducts form a chelated metallacycle **4.18** that retards unwanted β -hydride elimination owing to the lack of available vacant coordination sites on the metal and the fact that the hydrogens are no longer syn-coplanar when the γ -heteroatom is coordinated.¹⁵ Alkenes **4.19a–c** were obtained in 86% (X = NR₂), 66% (X = OR), and 79% (X = SR) yields.

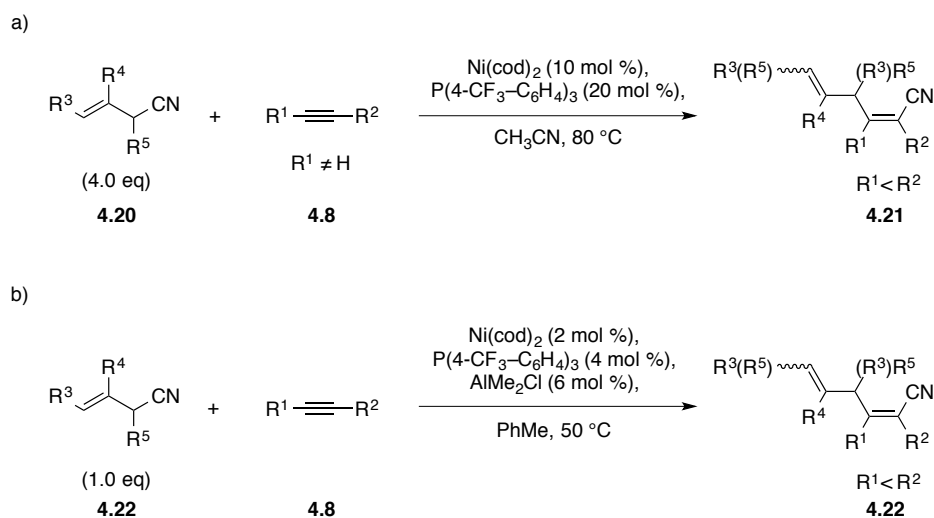


Scheme 94. a) carbocyanation of alkyl nitriles with alkynes b) heteroatom-directed carbocyanation of alkyl nitriles with alkynes

Inspired by Dupont's adiponitrile synthesis (see Scheme 91), Nakao and Hiyama studied the carbocyanation reaction of allylic C–CN bonds. Under Lewis acid-free conditions, allylic nitriles **4.20** did not undergo the desired reaction, nor were the conditions optimized for aryl- and alkenyl–CN bond activation effective (see Schemes 92 and 93). Employing 10 mol % Ni(cod)₂ and an *electron-deficient* phosphine ligand in acetonitrile at 80 °C for 8 hours gave the desired products in yields that varied greatly (Scheme 95).^{16,17} It was found that 4.0 equivalents of allylic nitrile was required to overcome the material lost due to competitive C–H bond activation (olefin isomerization). It is unclear whether such side-products (alkenyl C–CN) resulting from olefin isomerization are active under these reaction conditions. The reaction did not tolerate γ,γ-disubstituted alkenes and terminal alkynes underwent rapid oligomerization.

The reluctance of γ,γ -disubstituted alkenes to participate in the reaction suggests that an SN_2' -type activation is likely the pathway to generate the π -allyl–Ni–CN intermediate.

It was shown that Lewis acid additives increased the rate of the reaction enough to outcompete allylic C–H bond activation.¹⁰ The addition of AlMe_2Cl allowed for an equimolar reaction between **4.22** and **4.8** (Scheme 95b).¹⁷ In addition to lowered catalyst loadings, the decrease in reaction temperature suppressed the oligomerization of terminal alkynes, thus extending the scope of the reaction.



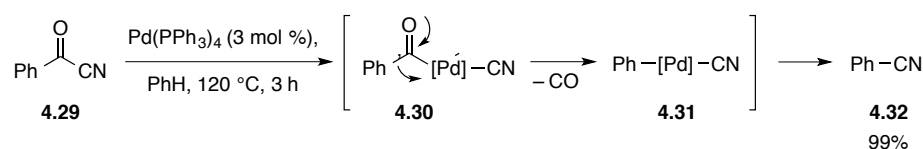
Scheme 95. Intermolecular carbocyanation of alkynes with allylic nitriles: a) without Lewis acid b) with Lewis acid

The synthetic utility of allylcyanation was demonstrated in the total synthesis of plaunotol, an antibacterial natural product active against *Helicobacter pylori* (Scheme 96). The reaction of α -siloxyallyl cyanide **4.23** with terminal alkyne **4.24** provided the silyl enol ether **4.25** on gram scale.¹⁷ Acidic hydrolysis of **4.25** gave aldehyde **4.26** in 64% yield over the two steps.

4.2 CYANOACYLATION WITH ALKYNES

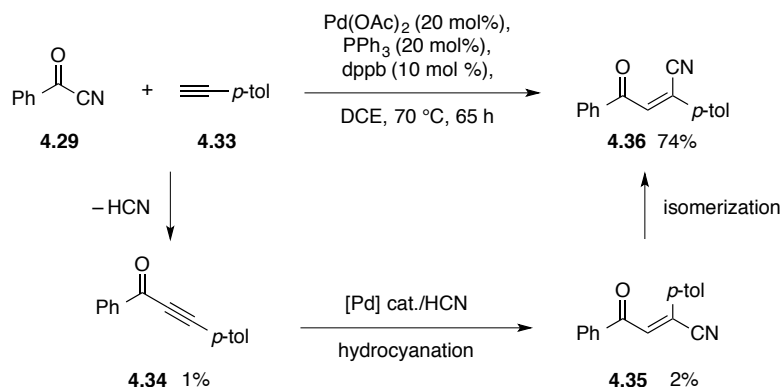
It is known that acyl C–C bonds can be oxidatively cleaved by transition metals more readily than other C–C bonds due to their polarized character and lowered BDE. The activation of acyl C–CN bonds ($103 \text{ kcal mol}^{-1}$),¹⁸ with subsequent addition across olefins (acylmetalation), would provide a mild entry into the preparation of synthetically useful 1,4-dicarbonyl motifs. 1,4-Dicarbonyl compounds are versatile building blocks for the synthesis of various carbocyclic and heterocyclic compounds. Therefore, significant efforts have been directed toward developing methods to access this highly valuable synthon.

In 1967, Bergman had described a rhodium-catalyzed decarbonylation of aryl acyl cyanides, though the reactions required extreme temperatures (300°C).¹⁹ In 1986, Murahashi reported a relatively mild palladium-catalyzed decarbonylation of acyl cyanides (Scheme 98).²⁰ Benzoyl cyanide (**4.29**) was reacted with $\text{Pd}(\text{PPh}_3)_4$ at 120°C in benzene to give benzonitrile (**4.32**) in 99% yield. Oxidative addition into the $\text{C}_{\text{acyl}}\text{--CN}$ bond generates palladium complex **4.30**. Loss of CO (decarbonylation) provides intermediate **4.31** that affords **4.32** upon reductive elimination. The reaction tolerated various functional groups on the phenyl ring, giving products in excellent yields. Reactions with aliphatic acyl cyanides required higher temperature (200°C) and resulted in alkene products (not shown). After decarbonylation, the resulting alkyl–Pd–CN species underwent β -hydride elimination with the release of HCN. Other catalysts, including $\text{Pd}(\text{OAc})_2$ with added 2PPh_3 , $\text{RuCl}_3\cdot\text{H}_2\text{O}$, and $\text{RuCl}_2(\text{PPh}_3)_3$ gave unsatisfactory results, where as well-known catalysts for the decarbonylation of aldehydes, such as $\text{RhCl}(\text{PPh}_3)_3$, $\text{RhCl}(\text{CO})(\text{PPh}_3)_3$, Pd/C , and PdCl_2 , were inactive.



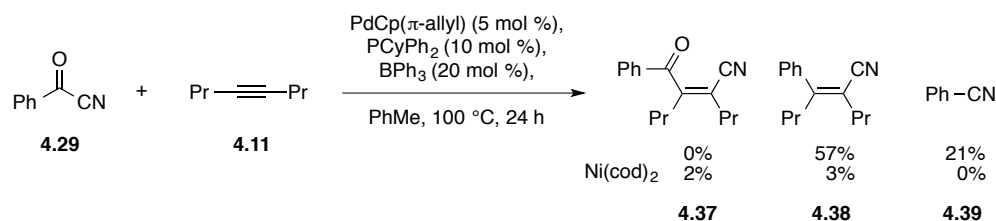
Scheme 98. Decarbonylation of acyl nitriles

In 1994, Nozaki discovered that in the presence of a terminal alkyne **4.33**, $\text{Pd}(\text{OAc})_2$ (with added PPh_3 and dppb ligands) reacts with benzoyl cyanide (**4.29**) to give the product of carboacylation (**4.36**) in 74% yield, along with 2% of (*Z*)-isomer **4.35**, and 1% acetylalkyne **4.34** (Scheme 99).²⁰ The ratios were shown to vary greatly depending upon the catalyst and/or solvent. It was unclear whether the formation of **4.36** was a result of direct addition (carbometalation) or by way of **4.34** and **4.35** as intermediates. Although formation of **4.36** via cyanoacylation cannot be confirmed in this case, additional experiments revealed that the conversion of ketone **4.34** to **4.36** readily occurred under the reaction conditions.²²⁻²⁴ Hydrocyanation of **4.34** yields (*Z*)-**4.35**, and isomerization provides **4.36**. Importantly, no products due to decarbonylation were reported.



Scheme 99. Presumed acylcyanation with terminal alkynes

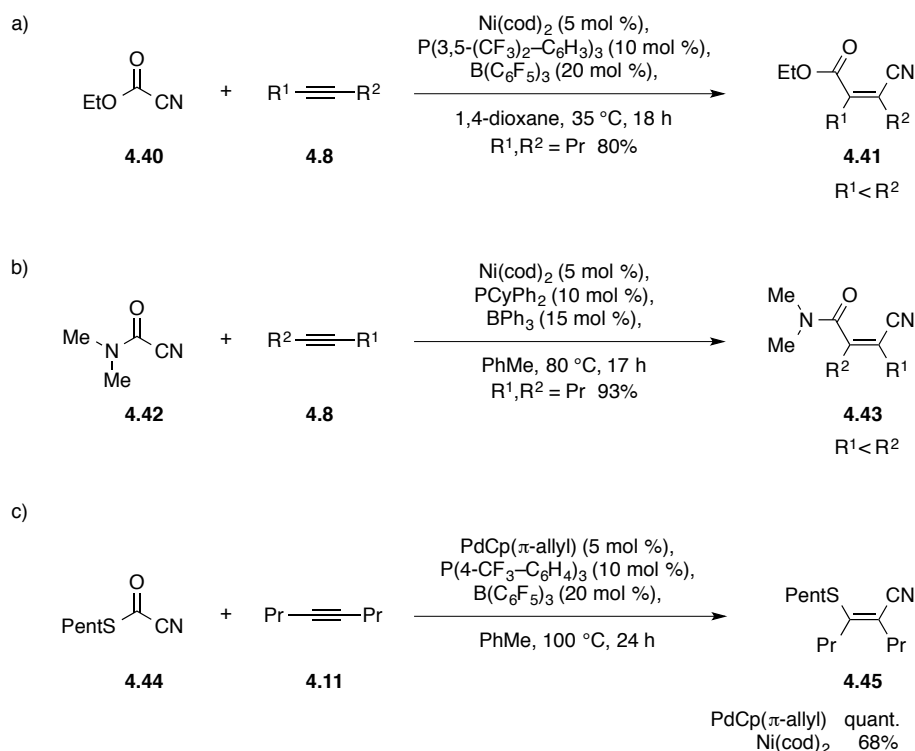
In 2010, Nakao and Hiyama attempted to develop a palladium-catalyzed acyl C–CN activation reaction between benzoyl cyanide (**4.29**) and 4-octyne (**4.11**) with Lewis acid additives (Scheme 100).²⁵ Instead of obtaining acylcyanation product **4.37**, aryl alkene **4.38** and benzonitrile (**4.39**) were formed in 57% and 21%, respectively. Re-subjecting benzonitrile (**4.39**) to the reaction conditions with 4-octyne (**4.11**) did not produce **4.38**, thus indicating that aryl alkene **4.38** is formed directly from **4.29** via decarbonylation. Under catalysis with Ni(cod)₂, 2% of the desired product was obtained.



Scheme 100. Attempted acylcyanation with internal alkynes

Esters and amides are carbonyl moieties that are less prone to undergo decarbonylation due to the stabilization afforded by the electron-donation from the heteroatom. Ethyl cyanoformate **4.40** successfully underwent a cyanoesterification reaction with internal alkyne **4.8** (R¹, R² = Pr) under nickel catalysis to give enoate **4.41** in 80% yield (Scheme 101a).²⁵ Electron-deficient ligands proved optimal (P(3,5-(CF₃)₂-C₆H₃)₃), while electron-neutral or -donating ligands (which were shown to be optimal for arylcyanation reactions) were not effective for cyanoesterification. Triphenylborane showed limited reactivity at 100 °C (35% yield), whereas the more Lewis acidic B(C₆F₅)₃ allowed for the reaction to take place at 35 °C and in sufficiently higher yields. Organoaluminum Lewis acids failed to promote the reaction entirely, as did the absence of any Lewis acid. The regioselectivity of the reactions with unsymmetrical alkynes **4.8**

favoured delivery of the nitrile to the most hindered carbon of the alkyne. This observation was rationalized by minimizing the steric repulsion between the alkyne group and the entering ester.

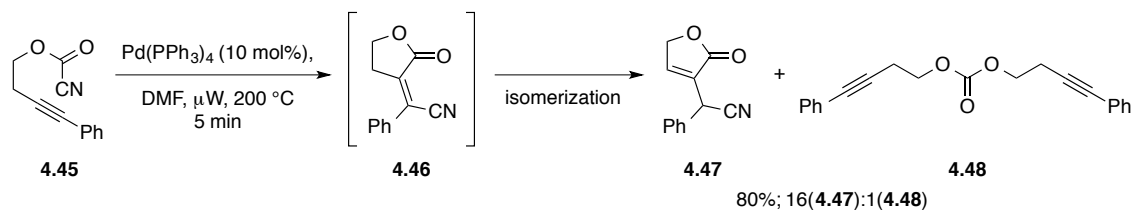


Scheme 101. Heterocarbonyls in acylcyanation reactions: a) cyanoesterification b) cyanoamidation c) thioesterification – decarbonylative thiocyanation

The optimized conditions for cyanoesterification were not suitable for cyanoamidation. The reaction required more electron-rich ligands and a less Lewis-acidic additive to give moderate to excellent yields.²⁵ Cyanoformamide **4.42** was reacted with alkyne **4.8** ($\text{R}^1, \text{R}^2 = \text{Pr}$) in the presence of Ni(cod)_2 , PCyPh_2 , and BPh_3 to give acrylamide **4.43** in 93% yield (Scheme 101b). Interestingly, the reactions with unsymmetrical alkynes resulted in delivery of the nitrile to the least hindered carbon of the alkyne. The change in regioselectivity was speculated to result from the Lewis acid

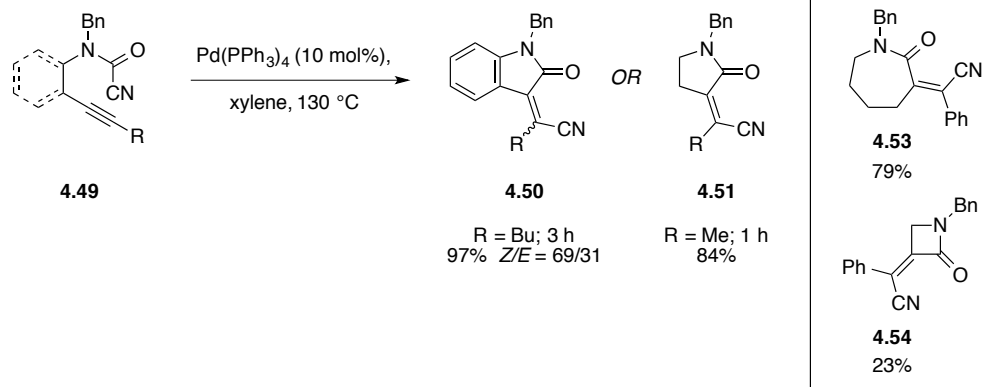
binding to the more basic carbonyl oxygen of the amide. Consequently, the lowered nucleophilicity likely makes the amide–LA adduct reluctant to undergo migration, and therefore the Ni–CN bond is first delivered (to the more sterically accessible carbon). The analogous cyanothioate **4.44**, however, underwent decarbonylation prior to alkyne insertion under both palladium and nickel catalysis (Scheme 101c). This observation may be due to the greater bond strengths observed for M–S bonds relative to M–O and M–N bonds.²⁵

In 2011, our group established a palladium-catalyzed intramolecular cyanoesterification reaction with alkynes (Scheme 102).²⁶ Treating cyanoformate ester **4.45** with Pd(PPh₃)₄ in toluene at 115 °C for 48 h hours, led to a 17% yield of a mixture of butenolide **4.47** and carbonate **4.48**. Carbonate **4.48** likely results from decarbonylation of the ROC(O)–Pd–CN intermediate followed by disproportionation. It was found that Lewis *base* additives reversed the selectivity to favor product **4.47** formation. Shorter reaction times along with increased temperatures were found to provide better yields of **4.47**. Replacing the Lewis base additives with using DMF as a solvent, and heating the reactions to 200 °C in a microwave reactor for 5 min, allowed for **4.47** to be isolated in 80% yield. Considering Lewis acid additives were required to promote the intermolecular cyanoesterification reactions (Scheme 101a), it is somewhat surprising that such conditions were not explored.



Scheme 102. Intramolecular cyanoesterification with alkynes

In 2006, Takemoto developed an intramolecular cyanoamidation reaction involving both alkyl- and aryl-tethered cyanoformamides **4.49** (Scheme 103).²⁷ Without the need for Lewis acid additives (whereas the intermolecular reaction required it), C–CN bond activation with Pd(PPh₃)₄ at 130 °C in xylenes afforded oxindole **4.50** (R = Bu) in 97% yield as a 69:31 mixture of *Z/E* isomers (due to isomerization under the reaction conditions). The corresponding γ -lactam **4.51** (R = Me) was readily prepared in 84% yield. The substrate scope of these reactions tolerated a variety of substitutions upon the alkyne and tether. It was later demonstrated that δ - (**4.52**, 89%), ϵ - (**4.53**, 79%), and even β -lactams (**4.54**, 23%) were prepared by this methodology.²⁸ Unfortunately, catalysis with Ni(cod)₂ was not reported for comparison.

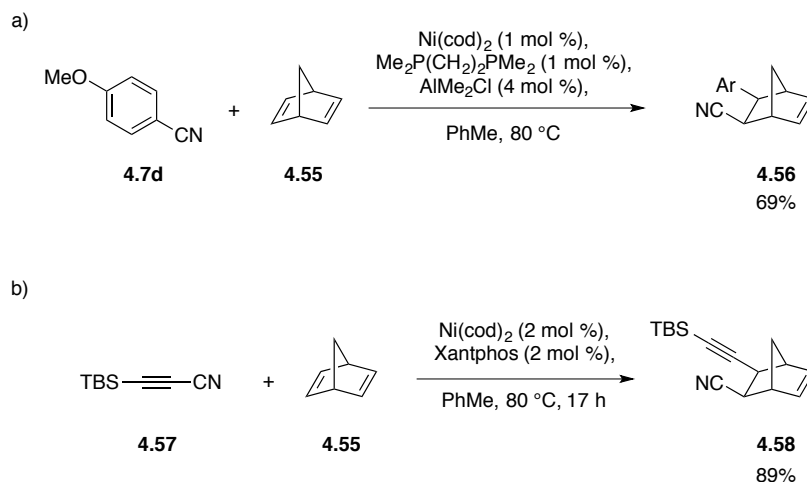


Scheme 103. Intramolecular cyanoamidation with alkynes

4.3 CARBOCYANATION WITH ALKENES

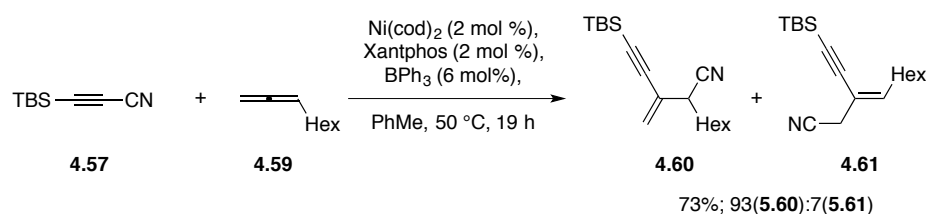
While carbocyanations of alkynes have been demonstrated with broad substrate scope, the analogous reaction with alkenes is much more challenging. This is, in part, due to alkenes less reactive toward insertion processes (carbometalation) than alkynes.²⁹ Moreover, the preference for β -hydride elimination over reductive elimination to give Heck-like products is a major competing pathway.³⁰

Attempted carbocyanation reactions across alkenes (1-octene, styrene, and 1,3-dodecadiene) were not successful under various conditions. However, strained bicyclic alkenes, such as norbornadiene (**4.55**), were capable of undergoing carbocyanation (Scheme 104).³¹ Since migratory insertion and β -hydride elimination fundamentally proceed through *syn* addition/elimination, the latter pathway is not possible in conformationally-restricted alkenes such as norbornadiene (no accessible *syn* β -hydrogens). Additionally, β -hydride elimination of the methine hydrogen of norbornadiene is not favorable due to the resulting *anti*-Bredt olefin. Aryl nitrile **4.7d** selectively underwent arylcyanation across the *exo* face of norbornadiene (**4.55**) to give substituted norbornene **4.56** in 69% yield (Scheme 104a). The corresponding alkynylcyanation with alkyne **4.57** proceeded to give **4.58** in 89% yield (Scheme 104b).



Scheme 104. Intermolecular carbocyanation reactions with norbornadiene: a) arylation b) alkynylation

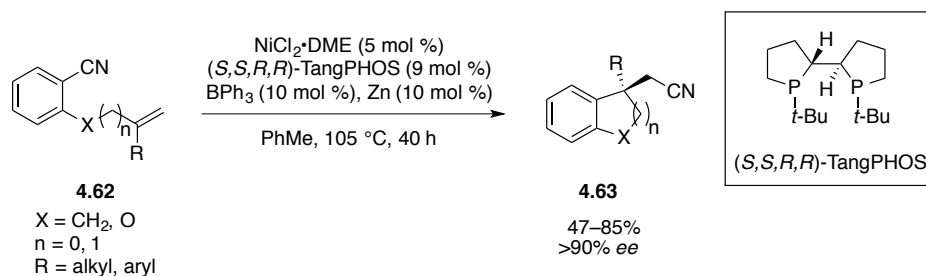
Alkynylation across 1,2-dienes was successful in preparing conjugated enynes (Scheme 105).³¹⁻³³ Under nickel catalysis with a bidentate ligand and BPh_3 , alkyne **4.57b** was reacted with allene **4.59** to give a mixture of enynes **4.60** and **4.61** in 73% yield as a 93:7 mixture, respectively. Mechanistically, the alkyne moiety is transferred to the *sp*-hybrid allenyl carbon to generate a π -allylnickel species. The Ni–CN bond is preferentially delivered to the secondary over the primary carbon presumably due to the steric interaction between the bidentate ligand and hexyl group within the π -allylnickel complex. It should be noted that due to these steric interactions, allenes with 1,1- and 1,4-disubstitution did not participate in the reaction. Nakao and Hiyama attributed the absence of 1,4-diene products to the reluctance of π -allyl complexes to undergo β -hydride elimination.³⁴ Additional carbocyanations of 1,2-dienes, with the exception of cyanoformate esters (Scheme 110), have not been reported.



Scheme 105. Intermolecular carbocyanation reaction with 1,2-dienes

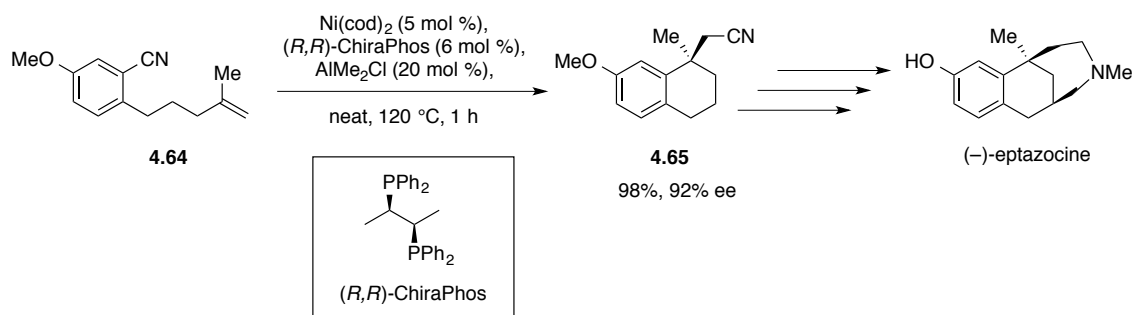
Although intermolecular carbocyanation reactions of norbornadiene and allenes were shown to be effective, the need for highly specific substrates limits the synthetic utility of reactions with alkenes.³³ In 2008, Jacobsen entered the field with a seminal report on an asymmetric, intramolecular carbocyanation with unactivated alkenes (Scheme 106).³⁵ Employing Ni(cod)_2 as a catalyst with achiral phosphine ligands resulted in low yields in the absence of Lewis acid. The addition of Lewis acid greatly enhanced the desired reactivity, providing racemic products in excellent yields. A survey of chiral mono- and bi-dentate phosphine ligands revealed (*S, S, R, R*)-TangPHOS as a promising entry into asymmetric catalysis. TangPHOS provided products in high enantioselectivities, albeit with low yields due to olefin isomerization. This competing pathway was suppressed by the *in situ* reduction of NiCl_2 with Zn to generate the active Ni^0 catalyst. Interestingly, the choice of Lewis acid directly affected the enantioselectivities observed. Of the vast number of boron- and aluminum-based Lewis acids, BPh_3 delivered the highest enantioselectivities. Sterically hindered or electron-deficient alkenes required higher catalyst loadings and extended reaction times. Although dihydroindanes ($\text{X} = \text{CH}_2$; $n = 0$) and dihydrobenzopyrans ($\text{X} = \text{O}$, $n = 1$) were readily prepared in good to excellent yields and enantioselectivities, the analogous allyl ether substrate ($\text{X} = \text{O}$, $n = 0$) did not yield dihydrobenzofurans. Catalyst inhibition by allyl ether substrates was confirmed

through competition experiments in which substrates known to undergo the cyclization failed to react in its presence. With alkene substituents directly influencing the rate of the reaction, it is unlikely that oxidative addition is the rate-limiting step in most cases. It is possible that olefin coordination precedes a rate-determining oxidative addition, or that the activation barriers to oxidative addition and migratory insertion are close in energy as demonstrated by Johnson's mechanistic work in carboacylation with 8-acylquinolines (Section 2.2). Additionally, it is likely that BPh_3 is bound throughout the enantiodetermining step as illustrated by its direct influence on the enantioselectivity.

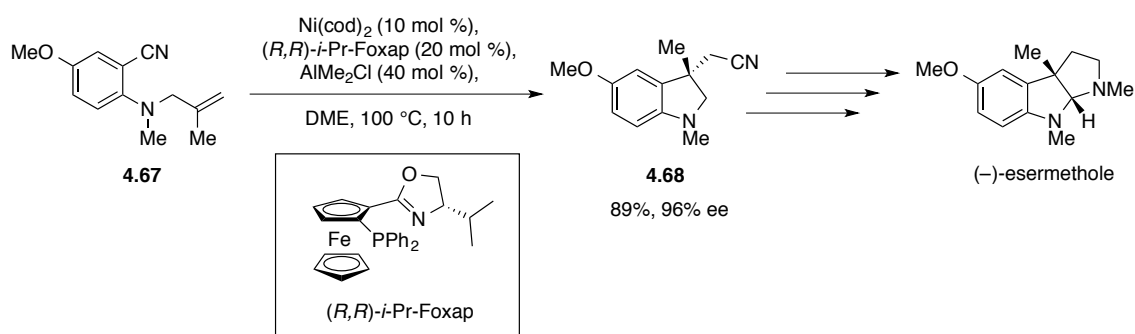


Scheme 106. Enantioselective intramolecular carbocyanation reactions with alkenes

The complexity-building utility of intramolecular carbocyanation was showcased in the asymmetric total syntheses of (–)-eptazocine and (–)-esermethole reported by Nakao and Hiyama later in 2008.³⁶ Similar to the conditions reported by Jacobsen (see Scheme 106), tetrahydronaphthalene **4.65** was prepared in 98% yield and 92% ee (Scheme 107). Many amino-tethered substrates were shown to undergo the reaction to provide dihydroindoles bearing benzylic all-carbon quaternary stereocenters.³⁷ Dihydroindole **4.68** was prepared in 89% yield and 96% ee (Scheme 108).



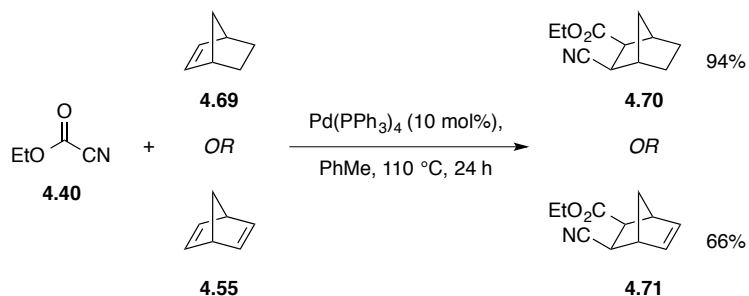
Scheme 107. Synthesis of (–)-eptazocine via enantioselective intramolecular carboacylation



Scheme 108. Synthesis of (–)-esermethole via enantioselective intramolecular carboacylation

4.4 CYANOACYLATION WITH ALKENES

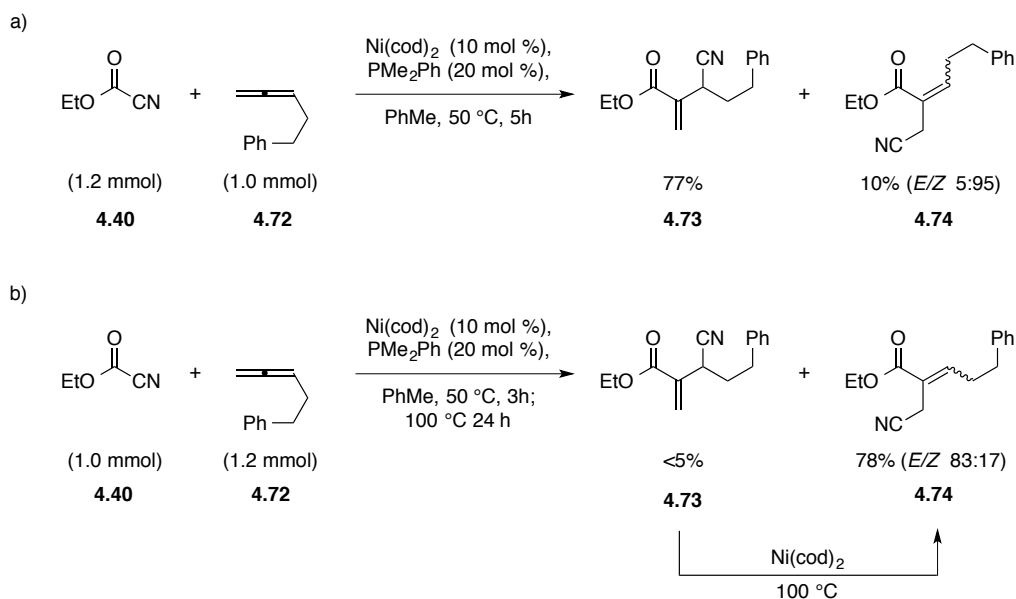
Nishihara was the first to demonstrate intermolecular cyanoesterification reactions with strained alkenes.³⁸⁻⁴⁰ In these reports, cyanoformate ester **4.40** was successfully added across norbornene (**4.69**) and norbornadiene (**4.55**) under palladium catalysis at 110 °C to give β -nitrile esters **4.70** and **4.71** (Scheme 109). Interestingly, a second addition across norbornadiene was never accomplished, even with five equivalents of **4.40**. Cyanoformate ester derivatives were also shown to undergo the reaction, albeit in lower yields. However, phenyl esters failed to undergo the desired reaction. Although C–CN bond activation occurred, the resulting diphenyl carbonate was obtained in quantitative yield. Carbonate side-products were also seen in our lab's work in intramolecular cyanoesterification with alkynes (see Scheme 102).



Scheme 109. Intermolecular cyanoesterification with norbornene and norbornadiene

In 2006, Nakao and Hiyama had introduced the use of 1,2-dienes as surrogates for alkenes in cyanoesterification reactions.^{41,42} Since π -allylmetal complexes are reluctant to undergo β -hydride elimination³⁴ products of increased complexity could be obtained. Surprisingly, the optimal conditions employed for cyanoesterification with $\text{Pd(PPh}_3)_4$ were ineffective at promoting the reaction with 1,2-dienes. However, in the presence of

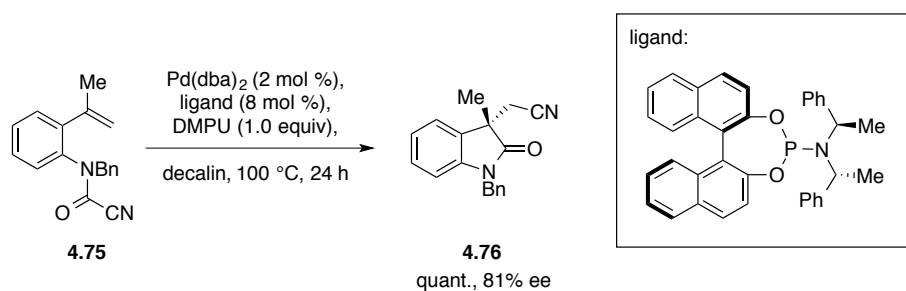
Ni(cod)₂ at 50 °C, cyanoformate ester **4.40** (1.2 mmol) and allene **4.72** (1.00 mmol) gave a mixture of β -cyano enoates **4.73** (77%) and **4.74** (10%, *E/Z* 5:95) (Scheme 110a). Interestingly, the regioselectivity could be reversed by changing the molar ratio of **4.40**:**4.72** to 1.0:1.2 and by running the reaction at 50 °C for 3 h and then at 100 °C for 24 h. Under these conditions, **4.73** was formed in <5% yield and **4.74** was generated in 78% yield as a mixture of *E/Z* isomers (83:17) (Scheme 110b). The mechanistic insights gained from this data revealed the reversibility of reductive elimination and the thermodynamic stabilities of the products. After C–CN oxidative addition, the C–Ni–CN complex coordinates to the terminal alkene and delivers ester moiety to the *sp*-hybrid allenyl carbon. The resulting Ni–CN complex rapidly arranges into a π -allylnickel species. Reductive elimination is more facile at the secondary carbon to generate **4.73**. Considering that the resulting allylic C–CN bond is susceptible toward oxidative addition (see Scheme 95), heating the reaction to 100 °C 24 h after the reaction was complete allowed for **4.73** to isomerize to the thermodynamic product **4.74** (*E/Z* 83:17).



Scheme 110. Intermolecular cyanoesterification with 1,2-dienes: a) reaction at 50 °C – *Z*-**4.74** kinetic product b) reaction at 50 °C, then heated to 100 °C – *E*-**4.74** thermodynamic product

In 2006, Takemoto discovered an intramolecular cyanoamidation with unactivated alkenes to form oxindole products,^{27,43} and in 2008 the reaction was developed asymmetrically (Scheme 111).⁴⁴ Employing $\text{Pd}(\text{dba})_2$ as catalyst, and a BINOL-derived bis[(*R*)-1-phenylethyl]amine phosphoramidite ligand in xylenes at 130 °C, cyanoformamide **4.75** was converted to oxindole **4.76** in 96% yield and 69% ee after 6 h. A solvent screen identified that reaction in decalin gave higher selectivity (74% ee), but lower yield (83%) due to incomplete conversion. After 15 min, reaction in *N*-methyl-2-pyrrolidinone (NMP) as solvent at 130 °C was complete, though the stereoselectivity had diminished to 56% ee. The combination of decalin as the solvent, and Lewis basic NMP (1.0 equiv) as an additive, allowed for the reaction to take place at 100 °C in 24 h to afford **4.76** in 85% yield and 80% ee. Changing the additive to *N,N*-dimethylpropylene urea (DMPU) gave oxindole **4.76** in quantitative yield and 81% ee. Although the effects of Lewis acids on intramolecular cyanoamidation reactions

were not reported in this account, our group has taken initiative in elucidating the mechanism for this transformation, including the roles of both Lewis acids and Lewis bases.ⁱ It has been determined that oxidative addition is the rate-limiting step by way of ¹³C KIE studies. In addition, it has been discovered that both Lewis acids and Lewis bases accelerate the reaction and that under either set of conditions, the nitrile dissociates from the metal, as observed by ¹³CN crossover experiments.



Scheme 111. Enantioselective intramolecular cyanoamidation with alkenes

4.5 CONCLUDING REMARKS

Chapter four has discussed an overview of C–CN bond activation with respect to carbocyanation reactions. The scope of reactions with alkynes is significantly broader than with alkenes owing to competitive β -hydride elimination of the latter. Nevertheless, chemists have found ways to circumvent β -hydride elimination by employing substrates with inaccessible β -hydrogens, 1,1-disubstituted alkenes, and allenes as alkene surrogates. Although a diverse class of transformations has been demonstrated, there is room for the methodology to grow. For instance: intramolecular reactions with vinyl and

ⁱ Laboratory work by Dr. Jodi M. Ogilvie

allylic nitriles have not been explored, nor have reactions with trisubstituted alkenes (either inter- or intramolecular). In addition, there have been no disclosures regarding intramolecular cyanoesterification reactions of alkenes, or intramolecular cyanoamidations of aliphatic-tethered alkenes.

REFERENCES

- (1) Burmeister, J. L.; Edwards, L. M. *J. Chem. Soc., A* **1971**, 1663.
- (2) Tolman, C. A.; McKinney, R. J.; Seidel, W. C.; Druline, J. D.; Stevens, W. R. *Adv. Cat.* **1985**, 33, 1.
- (3) Tolman, C. A. *J. Chem. Ed.* **1986**, 63, 199.
- (4) Backvall, J. E.; Andell, O. S. *Organometallics* **1986**, 5, 2350.
- (5) Druliner, J. D. *Organometallics* **1984**, 3, 205.
- (6) Chaumonnot, A.; Lamy, F.; Sabo-Etienne, S.; Donnadiou, B.; Chaudret, B.; Barthelat, J.-C.; Galland, J.-C. *Organometallics* **2004**, 23, 3363.
- (7) Nakao, Y.; Oda, S.; Hiyama, T. *J. Am. Chem. Soc.* **2004**, 126, 13904.
- (8) Nakao, Y.; Oda, S.; Yada, A.; Hiyama, T. *Tetrahedron* **2006**, 62, 7567.
- (9) Ohnishi, Y.-Y.; Nakao, Y.; Sato, H.; Nakao, Y.; Hiyama, T.; Sakaki, S. *Organometallics* **2009**, 28, 2583.
- (10) Brunkan, N. M.; Brestensky, D. M.; Jones, W. D. *J. Am. Chem. Soc.* **2004**, 126, 3627.
- (11) Nakao, Y.; Yada, A.; Ebata, S.; Hiyama, T. *J. Am. Chem. Soc.* **2007**, 129, 2428.
- (12) Nakao, Y.; Hirata, Y.; Tanaka, M.; Hiyama, T. *Angew. Chem. Int. Ed.* **2008**, 47, 385.
- (13) Hirata, Y.; Tanaka, M.; Yada, A.; Nakao, Y.; Hiyama, T. *Tetrahedron* **2009**, 65, 5037.
- (14) Yada, A.; Yukawa, T.; Nakao, Y.; Hiyama, T. *Chem. Commun.* **2009**, 3931.
- (15) Nakao, Y.; Yada, A.; Hiyama, T. *J. Am. Chem. Soc.* **2010**, 132, 10024.
- (16) Nakao, Y.; Yukawa, T.; Hirata, Y.; Oda, S.; Satoh, J.; Hiyama, T. *J. Am. Chem. Soc.* **2006**, 128, 7116.
- (17) Hirata, Y.; Yukawa, T.; Kashiwara, N.; Nakao, Y.; Hiyama, T. *J. Am. Chem. Soc.* **2009**, 131, 10964.
- (18) Gupta, V. P.; Sharma, A. *Indian Acad. Sci.* **2006**, 67, 487.
- (19) Blum, J.; Oppenheimer, E.; Bergman, E. D. *J. Am. Chem. Soc.* **1967**, 89, 2338.
- (20) Murahashi, S.; Naota, T.; Nakajima, N. *J. Org. Chem.* **1986**, 51, 898.

- (21) Nozaki, K.; Sato, N.; Takaya, H. *J. Org. Chem.* **1994**, *59*, 2679.
- (22) Fu, X.; Zhange, S.; Yin, J.; Schumacher, D. P. *Tetrahedron Lett.* **2002**, *43*, 6673.
- (23) Siegbahn, P. E. M. *Theor. Chim. Acta.* **1994**, *87*, 277.
- (24) Hadi, V.; Yoo, K. S.; Jeong, M.; Jung, K. W. *Tetrahedron Lett.* **2009**, *50*, 2370.
- (25) Hirata, Y.; Yada, A.; Morita, E.; Nakao, Y.; Hiyama, T.; Ohashi, M.; Ogoshi, S. *J. Am. Chem. Soc.* **2010**, *132*, 10070.
- (26) Rondla, N. R.; Levi, S. M.; Ryss, J. M.; Vanden Berg, R. A.; Douglas, C. J. *Org. Lett.* **2011**, *13*, 1940.
- (27) Kobayashi, Y.; Kamisaki, H.; Yanada, R.; Takemoto, Y. *Org. Lett.* **2006**, *8*, 2711.
- (28) Kobayashi, Y.; Kamisaki, H.; Takeda, H.; Yasui, Y.; Yanada, R.; Takemoto, Y. *Tetrahedron* **2007**, *63*, 2978.
- (29) Negishi, E.; Copéret, C.; Ma, S. Liou, S.; Liu, F. *Chem Rev.* **1996**, *96*, 365.
- (30) Nakao, Y. In *Topics in Current Chemistry*; Topics in Current Chemistry; Springer Berlin Heidelberg: Berlin, Heidelberg, 2014.
- (31) Hirata, Y.; Tanaka, M.; Yada, A.; Nakao, Y.; Hiyama, T. *Tetrahedron* **2009**, *65*, 5037.
- (32) Nakao, Y.; Hirata, Y.; Tanaka, M.; Hiyama, T. *Angew. Chem. Int. Ed.* **2008**, *47*, 385.
- (33) Hirata, Y.; Tanaka, M.; Yada, A.; Nakao, Y.; Hiyama, T. *Tetrahedron* **2009**, *65*, 5037.
- (34) Zimmer, R.; Dinesh, C. U.; Nandan, E.; Khan, F. A. *Chem. Rev.* **2000**, *100*, 3067.
- (35) Watson, M. P.; Jacobsen, E. N. *J. Am. Chem. Soc.* **2008**, *130*, 12594.
- (36) Nakao, Y.; Ebata, S.; Yada, A.; Hiyama, T.; Ikawa, M.; Ogoshi, S. *J. Am. Chem. Soc.* **2008**, *130*, 12874.
- (37) Hsieh, J.-C.; Ebata, S.; Nakao, Y.; Hiyama, T. *Synlett* **2010**, *2010*, 1709.
- (38) Nishihara, Y.; Inoue, Y.; Itazaki, M.; Takagi, K. *Org. Lett.* **2005**, *7*, 2639.
- (39) Nishihara, Y.; Inoue, Y.; Izawa, S.; Miyasaka, M.; Tanemura, K.; Nakajima, K.; Takagi, K. *Tetrahedron* **2006**, *62*, 9872.
- (40) Nishihara, Y.; Miyasaka, M.; Inoue, Y.; Yamaguchi, T.; Kojima, M.; Takagi, K.

Organometallics **2007**, *26*, 4054.

- (41) Nakao, Y.; Hirata, Y.; Hiyama, T. *J. Am. Chem. Soc.* **2006**, *128*, 7420.
- (42) Hirata, Y.; Inui, T.; Nakao, T.; Hiyama, T. *J. Am. Chem. Soc.* **2009**, *131*, 6624.
- (43) Yasui, Y.; Takemoto, Y. *Chem. Record* **2008**, *8*, 386.
- (44) Yasui, Y.; Kamisaki, H.; Takemoto, Y. *Org. Lett.* **2008**, *10*, 3303.

CHAPTER FIVE

Intramolecular Cyanoamidation with Alkenes

INTRODUCTION

Ever-changing environmental, economical, and societal demands have increasingly influenced the way chemists approach organic synthesis. Efficiency is an attribute of effective synthetic planning, and it is what drives the pursuit for new synthetic methodologies. The term ‘efficiency’ generally describes the extent to which time, effort, and/or expenses are minimized for the intended task or purpose. It is a term that has widely-varying meanings in different disciplines. For synthetic chemists, time and effort are minimized when reaction sequences to targeted molecules require few steps. In terms of expenses, these ‘tools’ would ideally be free of waste, and thus be atom economical. In order to meet these requirements, we must have available synthetic ‘tools’ that can rapidly build molecular complexity.

Organic synthesis evolves as clever people identify challenges and take the necessary risks to design systems that address current limitations. The following chapter describes the development of a facile approach to 3,3-disubstituted lactams that contain a synthetically elusive all-carbon quaternary stereocenter. This catalytic, asymmetric, and atom-economical methodology is the epitome of ‘efficiency,’ and will likely be of great value as a ‘tool’ for complex alkaloid syntheses.

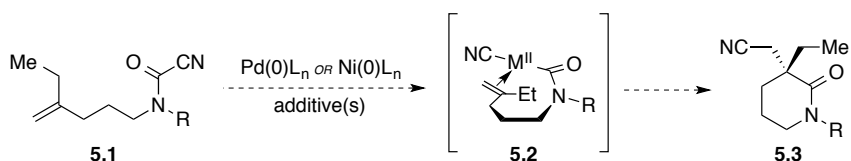
5.1 ENANTIOSELECTIVE CYANOAMIDATION

Important synthetic advances have been made with the development of C–CN bond activation. Intramolecular carbocyanation and cyanoacylation reactions have great potential to expedite the syntheses of complex, cyclic molecules. As described in Chapter 4, such carbocyanation with alkenes has been showcased in the asymmetric synthesis of (–)-eptazocine, a potent opioid analgesic, and (–)-esermethole, a synthetic precursor to acetylcholinesterase inhibitors such as (–)-physostigmine (see Schemes 107 and 108). Enantioselective cyanoamidation with alkenes to produce oxindole frameworks has also been envisioned to access synthetic precursors to pyrroloindoline natural products (see Scheme 111). Such asymmetric reactions, however, have been limited to substrates containing an aryl backbone that separates the nitrile and tethered alkene. However, intramolecular cyanoamidation with *alkynes* has been demonstrated with aliphatic backbones to produce β -, λ -, δ -, and ϵ -lactams containing exocyclic vinyl nitriles (see Scheme 103). The corresponding reaction with aliphatic-tethered alkenes has not yet been developed.

5.1.1 RESEARCH PROPOSAL: 3,3-DISUBSTITUTED LACTAMS

The greatest utility in C–CN bond activation arguably lies in the asymmetric construction of carbo- and heterocyclic ring systems. The prevalence of highly functionalized cyclic amines in biologically active natural products (i.e. alkaloids) and pharmaceutical drugs led to the desire to develop a method to construct lactams containing an all-carbon quaternary stereocenter. It was envisioned that 3,3-disubstituted

lactam scaffolds could readily be prepared by intramolecular cyanoamidation in which the cyanoformamide and alkene are separated by an aliphatic tether (Scheme 112). Oxidative addition into the C–CN bond of **5.1** would produce intermediate **5.2**. Migratory insertion across the tethered olefin, followed by reductive elimination, would generate lactam **5.3**. The stereocenter presented in **5.3** could conceivably be set by the addition of chiral additives, such as ligands or Lewis acids. The resulting aliphatic nitrile leaves a suitable synthetic handle for subsequent transformations.



Scheme 112. Proposed intramolecular cyanoamidation to form 3,3-disubstituted δ -lactams

It is rather surprising that after the discovery of intramolecular cyanoamidation with aliphatic-tethered alkynes (Scheme 103) and aryl-tethered alkenes (Scheme 111) that a follow-up of the proposed research with aliphatic-tethered alkenes (Scheme 112) was not reported. However, Takemoto had suggested that *Aspidosperma*-type terpenoid indole alkaloids (Figure 31) would be attainable through such cyanoamidation methods.^{1,2} It was simply stated that the corresponding chloroformamides were discovered to undergo the desired transformation much more efficiently than the corresponding cyanoformamides. Nevertheless, it was believed that a thorough reaction screen would reveal viable conditions that would allow for streamlined syntheses of such targets (which are currently being pursued in our laboratory).

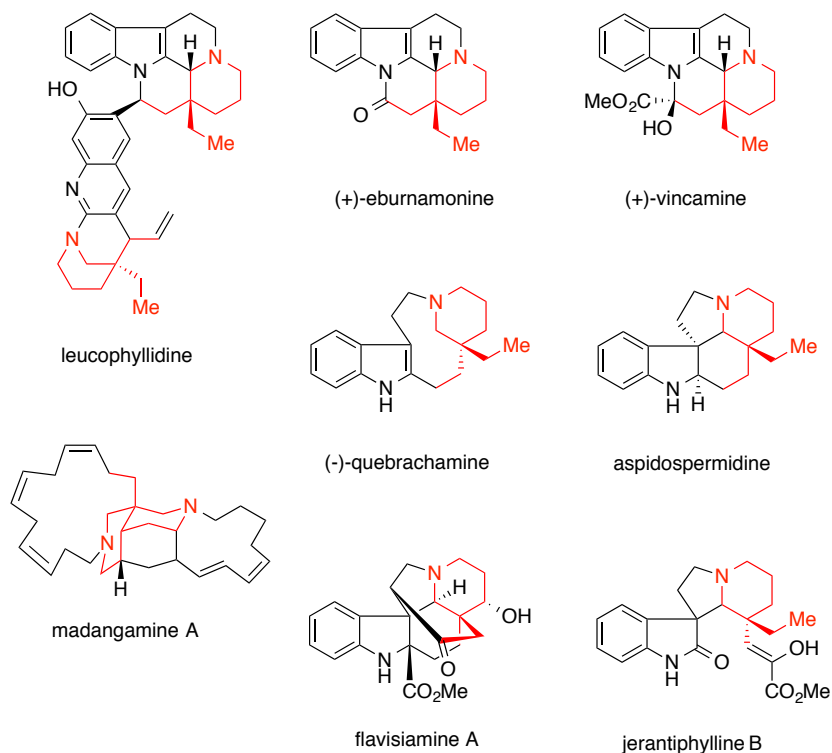
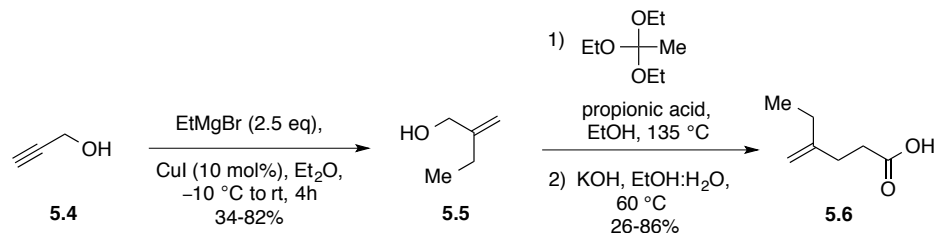


Figure 31. Alkaloid nature products containing 3,3-disubstituted piperidine ring(s)

5.1.2 SUBSTRATE SYNTHESIS

The cyanoformamide substrate **5.1a** was readily prepared in five steps from commercially available materials. A copper-promoted Grignard addition into propargyl alcohol (**5.4**) provided the allylic alcohol **5.5** in widely variable yields (34–82%; Scheme 113). It had been discovered that the accumulation of salts negatively impacted the reaction. Slower Grignard addition with a syringe pump, and the use of an overhead stirrer, reduced the aggregation of these salts. However, it was found that manually scratching the sides of the flask with a long needle inserted through the septum was effective in dissolving the thick salt layer. Upon quenching the reaction with saturated NH_4Cl , excessive salt formation created a thick, green emulsion that complicated work

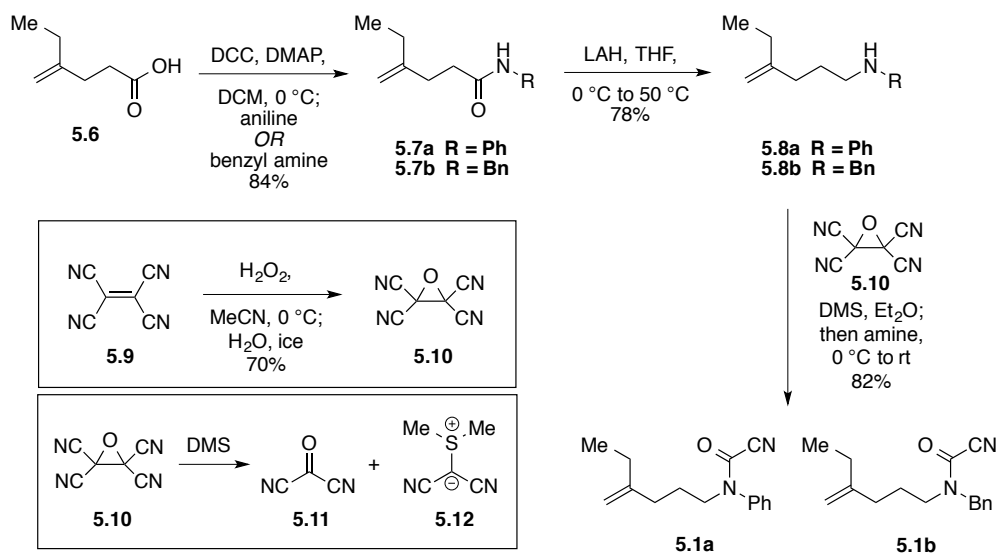
up. Several extractions (>20) were required to obtain appreciable amounts of material from the reaction mixture. It was realized that the emulsion could be remedied by adding a large volume of saturated NH_4Cl and allowed the mixture to stir until the insoluble salts dissolved and the biphasic solution turned blue ($\text{Cu}^{\text{I}} \rightarrow \text{Cu}^{\text{II}}$). A Johnson-Claisen rearrangement between allylic alcohol **5.5** and triethyl orthoacetate with a catalytic amount of acid resulted in the ester, which was then saponified to give acid **5.6**. The rearrangement suffered from irreproducible results, which were never understood. Other researchers have also encountered this problem in the laboratory. Due to the unreliability of the Johnson-Claisen reaction, a more reliable route to acid derivatives was later developed (see Scheme 117).



Scheme 113. Synthesis of cyanoformamide acid precursor **5.6**

A DCC coupling between acid **5.6** and aniline (or benzyl amine) gave amide **5.7** in 84% yield (Scheme 114). Amine **5.8** was obtained in 78% yield by reduction of amide **5.7** with excess lithium aluminum hydride. Dicyano carbonyl (**5.11**) was generated *in situ* by treating tetracyano epoxide (TCEO) **5.10** with dimethyl sulfide (DMS), followed by addition of amine **5.8**, to obtain cyanoformamide **5.1a** in 82% yield. It was discovered that removing the sulfur ylide byproduct **5.12** (prior to subjecting the dicyano carbonyl solution (**5.11**) to amine **5.8**) via syringe filtration significantly improved the yield. TCEO (**5.10**) had been prepared by treating recrystallized (from chlorobenzene)

tetracyanoethylene (TCE, **5.9**) with hydrogen peroxide. The same route was used in the preparation of benzyl-protected cyanoformamide **5.1b**



Scheme 114. Preparation of cyanoformamides **5.1a** and **5.1b**

Based upon Takemoto's success with phosphoramidite ligands in the asymmetric construction of oxindoles (see Scheme 111), we prepared several analogous ligands (Figures 32–35). It was hoped that a 'shotgun' approach would enable us to narrow down particular features within the ligands that were favorable that would subsequently allow us to design new ligands that would enhance the enantioselectivity. The preparation and handling of these ligands were exceptionally troublesome owing to their propensity to oxidize. The order of reagent addition, the use of a Schlenk filter, and alumina chromatography were found to be essential in preparing these ligands.

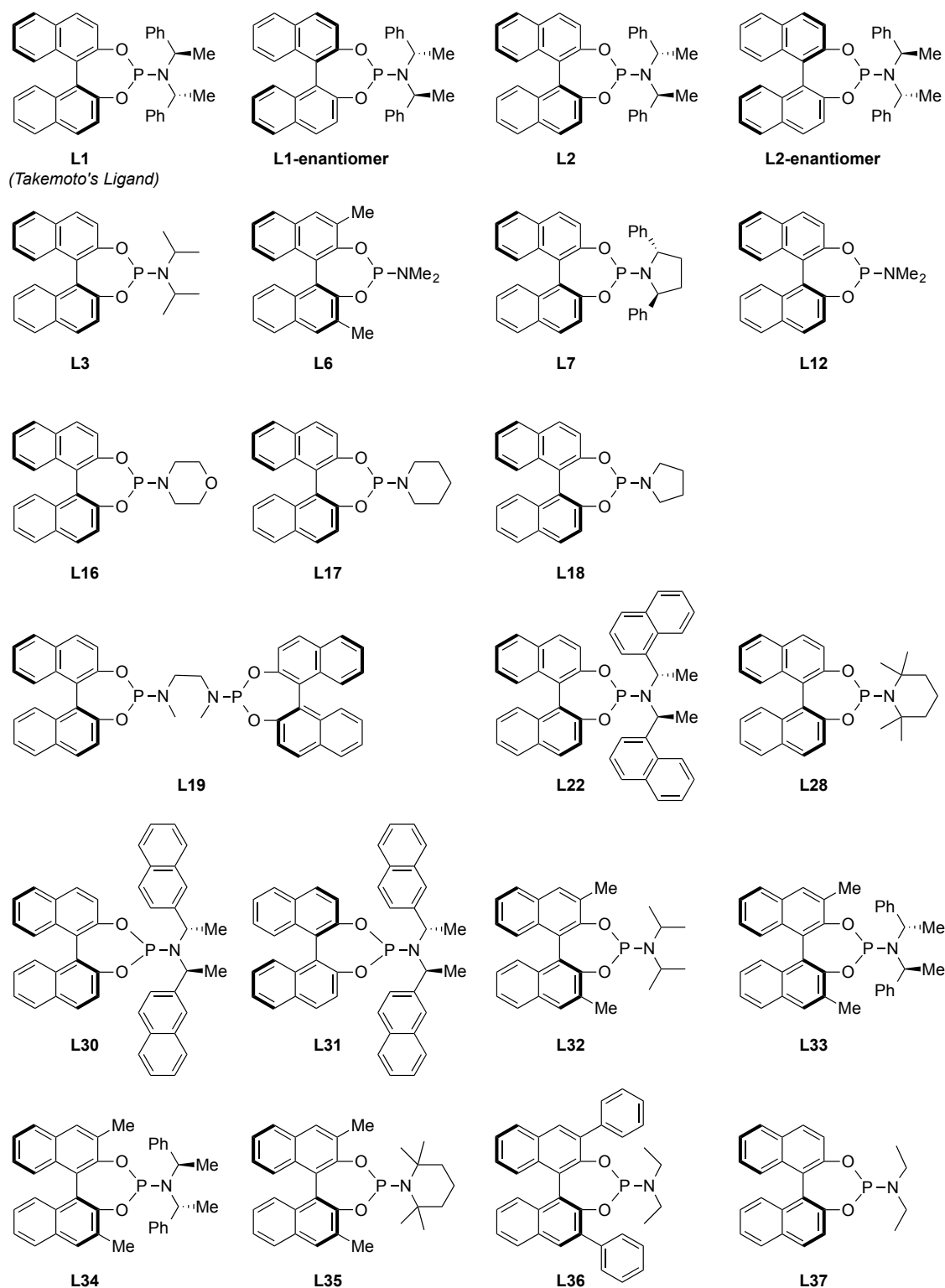


Figure 32. Phosphoramidite ligands with a BINOL backbone

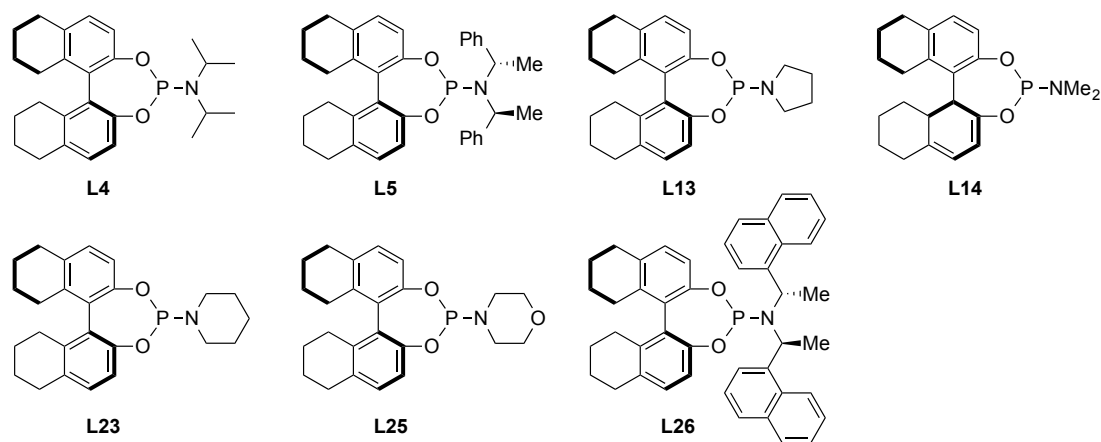


Figure 33. Phosphoramidite ligands with hydrogenated BINOL backbone

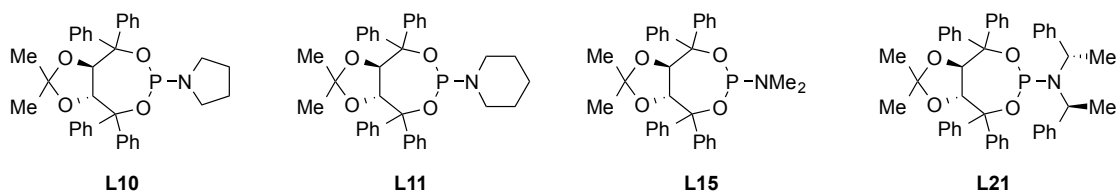


Figure 34. Phosphoramidite ligands with TADDOL backbone

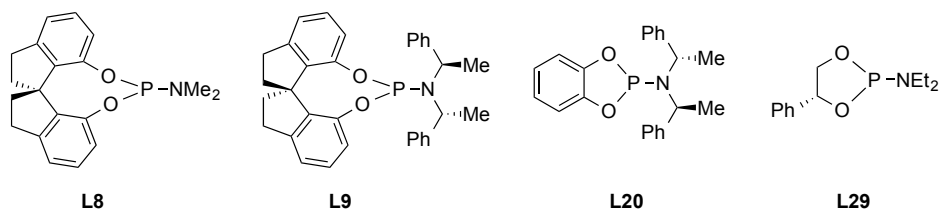


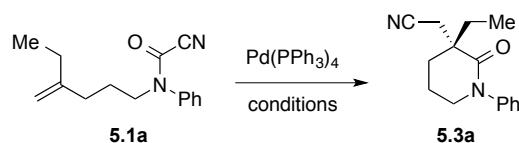
Figure 35. Phosphoramidite ligands with miscellaneous backbones

5.1.3 RESULTS AND DISCUSSION

Under similar conditions reported by Takemoto for the cyclization of aliphatic *alkynyl* cyanoformamides (see Scheme 103), the reaction with the analogous alkenes was

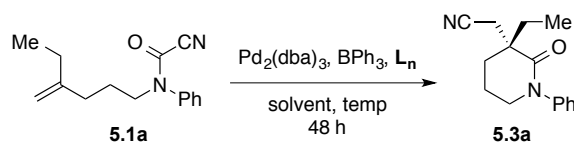
sluggish: treating **5.1a** with Pd(PPh₃)₄ in toluene at 130 °C for 48 h gave the desired lactam **5.3a**, albeit in 12% conversion (entry 1, Table 11). The conditions Takemoto had developed for cyanoamidation of *alkenyl* cyanoformamides to form oxindoles (see Scheme 111) were then employed: treating **5.1a** with Pd(PPh₃)₄ in the presence of 1.0 equivalent of Lewis basic additive DMPU, did not have the same desired effect in that **5.3a** was formed in less than 20% (entry 2). Since it had been demonstrated that *intermolecular* cyanoamidation with alkynes required a Lewis acid additive, these conditions were then explored. The addition of 1.0 equivalent of BPh₃ resulted in a reaction that proceeded at 100% conversion and lactam **5.3a** was isolated in 72% yield (entry 3). The chiral Al-salen ligand [(S,S)-N,N-bis(3,5-di-*tert*-butylsalicylidene)-1,2-cyclohexanediaminoaluminum chloride] was explored, but did not afford product (entry 4). Other aluminum-based Lewis acids were not investigated. Reactions with the more Lewis acidic B(C₆F₅)₃ resulted in decomposition (entry 5). Lowering the temperature to 100 °C in the presence of BPh₃ gave incomplete conversion in both PhMe (52%, entry 6) and THF solvents (12%, entry 7).

Table 11. Cyanoamidation reactivity screen: 3,3-disubstituted δ -lactams



Entry	Ligand	Catalyst	Additive	Solvent	Temp.	Conv. (Yield)	% ee
1	--	Pd(PPh ₃) ₄	--	PhMe	130 °C	12%	--
2	--	Pd(PPh ₃) ₄	DMPU	PhMe	130 °C	19%	--
3	--	Pd(PPh ₃) ₄	BPh ₃	PhMe	130 °C	100% (72%)	--
4	--	Pd(PPh ₃) ₄	Al-salen	PhMe	130 °C	--	--
5	--	Pd(PPh ₃) ₄	B(C ₆ F ₅) ₃	PhMe	130 °C	decomp	--
6	--	Pd(PPh ₃) ₄	BPh ₃	PhMe	100 °C	52% (28%)	--
7	--	Pd(PPh ₃) ₄	BPh ₃	THF	100 °C	12%	--

With BPh₃ identified as an optimal Lewis acid additive, we proceeded to screen chiral phosphoramidite ligands derived from BINOL (see Figure 32). The ligand (**L1**) identified by Takemoto to give high enantioselectivity in forming oxindoles resulted in 100% conversion and 54% ee under Pd₂(dba)₃ catalysis in PhMe at 130 °C (Table 12, entry 1). Lactam **5.3** was isolated in 28% yield owing to difficult separation from ligand decomposition products (upon column chromatography), and removal of BPh₃ (H₂O₂ wash). Lowering the temperature to 100 °C resulted in no product formation in both PhMe and THF as solvents (entries 2 and 3). The reactions in TFT and decalin at 130 °C gave incomplete conversions (entries 4 and 5) and no reaction was observed in DMF (entry 6). Increasing the steric bulk of the amine moiety (**L30**) was well tolerated, but did not improve the ee % (entry 8). The diastereomer of **L1** (**L2**), in which the amino stereochemistry was reversed, provided **5.3** in full conversion in PhMe and TFT solvents, however the mis-matched stereochemistry of **L2** drastically decreased the selectivity (<20 ee %, entries 9 and 10). The reaction in decalin with **L2** did not go to completion (entry 11). Comparatively, the diastereomer of **L30** (**L31**), in which the stereochemistry of the BINOL backbone was reversed, did not provide product (entry 12). Incorporating a chiral cyclic amine (**L7**) negatively impacted the reaction, returning mostly starting material in PhMe and TFT solvents (entries 13 and 14). In decalin, the reaction with **L7** proceeded in 73% conversion, though achieved a 30% ee (entry 15). The best % conversion and % ee with the BINOL-derived phosphoramidite ligands containing a chiral amine was achieved with **L1** (54% ee).

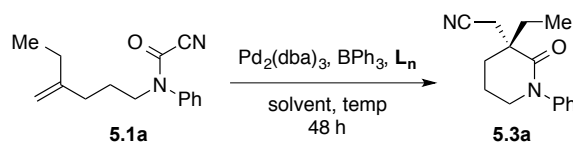
Table 12. Enantioselective cyanoamidation reactivity screen with BINOL-derived ligands

BINOL ligands							
Entry	Ligand	Catalyst	Additive	Solvent	Temp.	Conv. (Yield)	% ee
1	L1	Pd ₂ (dba) ₃	BPh ₃	PhMe	130 °C	100% (28%)	54%
2	L1	Pd ₂ (dba) ₃	BPh ₃	PhMe	100 °C	N.R.	--
3	L1	Pd ₂ (dba) ₃	BPh ₃	THF	100 °C	N.R.	--
4	L1	Pd ₂ (dba) ₃	BPh ₃	TFT	130 °C	7%	n.d.
5	L1	Pd ₂ (dba) ₃	BPh ₃	decalin	130 °C	37%	n.d.
6	L1	Pd ₂ (dba) ₃	BPh ₃	DMF	130 °C	N.R.	--
7	L1	Pd ₂ (dba) ₃	B(C ₆ F ₅) ₃	PhMe	130 °C	decomp	--
8	L30	Pd ₂ (dba) ₃	BPh ₃	PhMe	130 °C	100%	<40%
9	L2	Pd ₂ (dba) ₃	BPh ₃	PhMe	130 °C	100% (76%)	14%
10	L2	Pd ₂ (dba) ₃	BPh ₃	TFT	130 °C	100%	9%
11	L2	Pd ₂ (dba) ₃	BPh ₃	decalin	130 °C	76%	14%
12	L31	Pd ₂ (dba) ₃	BPh ₃	PhMe	130 °C	0%	--
13	L7	Pd ₂ (dba) ₃	BPh ₃	PhMe	130 °C	32% (22%)	24%
14	L7	Pd ₂ (dba) ₃	BPh ₃	TFT	130 °C	21%	13%
15	L7	Pd ₂ (dba) ₃	BPh ₃	decalin	130 °C	73% (61%)	30%
16	L3	Pd ₂ (dba) ₃	BPh ₃	PhMe	130 °C	100% (42%)	19%
17	L3	Pd ₂ (dba) ₃	BPh ₃	TFT	130 °C	3%	n.d.
18	L3	Pd ₂ (dba) ₃	BPh ₃	decalin	130 °C	100% (50%)	41%
19	L12	Pd ₂ (dba) ₃	BPh ₃	PhMe	130 °C	100%	1%
20	L6	Pd ₂ (dba) ₃	BPh ₃	PhMe	130 °C	100% (25%)	7%
21	L6	Pd ₂ (dba) ₃	BPh ₃	TFT	130 °C	100%	12%
22	L6	Pd ₂ (dba) ₃	BPh ₃	decalin	130 °C	100% (15%)	10%
23	L16	Pd ₂ (dba) ₃	BPh ₃	TFT	130 °C	100% ^a	10%
24	L16	Pd ₂ (dba) ₃	BPh ₃	decalin	130 °C	100 % ^a	18%
25	L17	Pd ₂ (dba) ₃	BPh ₃	TFT	130 °C	100% ^a	37%
26	L17	Pd ₂ (dba) ₃	BPh ₃	decalin	130 °C	100 % ^a	33%
27	L18	Pd ₂ (dba) ₃	BPh ₃	TFT	130 °C	70% ^a	46 %
28	L18	Pd ₂ (dba) ₃	BPh ₃	decalin	130 °C	100 % ^a	27%
29	L19	Pd ₂ (dba) ₃	BPh ₃	TFT	130 °C	38% ^a	8%
30	L19	Pd ₂ (dba) ₃	BPh ₃	decalin	130 °C	100 % ^a	10%

^a accompanied by a significant amount of unidentified side-product

We then investigated BINOL-derived phosphoramidite ligands containing achiral amine groups (Table 12). Ligand **L3**, substituted with diisopropyl amine, gave full conversion in PhMe (19% ee) and decalin (41% ee), but was relatively inactive in TFT (entries 16–18). MonoPhos (**L12**) gave complete conversion, though no appreciable selectivity (entry 19). Methylating the BINOL backbone of MonoPhos (**L6**) retained the reaction efficiency, but only mildly improved the selectivity in PhMe, TFT, and decalin (<15% ee, entries 20–22). Ligands **L16–L18**, containing achiral cyclic amines, were effective at promoting the desired reaction, though the crude ^1H NMR spectra indicated formation of an unidentified side-product (entries 23–28). This side-product may have been due to the change in source of BPh_3 Lewis acid, which was visibly colored and ‘tacky.’ Of these ligands, **L18** in TFT gave the highest % ee, though gave incomplete conversion (70% conversion, 46% ee; entry 27). The bidentate BINOL ligand **L19** gave low conversion in TFT, though complete conversion (but low selectivity) in decalin (entries 29 and 30).

We turned to phosphoramidite ligands with hydrogenated BINOL backbones (see Figure 33). Ligand **L5**, which is the hydrogenated form of **L1** was less effective at promoting the reaction though retained comparable selectivity (Table 13, entries 1–4). Surprisingly, all hydrogenated BINOL phosphoramidite ligands containing achiral amine groups (**L4**, **L13**, **L14**, and **L23**) were unsuccessful in promoting the reaction (entries 5–14).

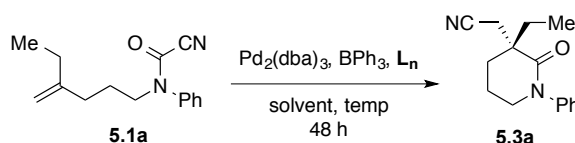
Table 13. Enantioselective cyanoamidation reactivity screen with hydrogenated BINOL-derived ligands

Hydrogenated BINOL ligands							
Entry	Ligand	Catalyst	Additive	Solvent	Temp.	Conv. (Yield)	% ee
1	L5	Pd ₂ (dba) ₃	BPh ₃	PhMe	130 °C	71% (62%)	41%
2	L5	Pd ₂ (dba) ₃	B(C ₆ F ₅) ₃	PhMe	130 °C	decomp	--
3	L5	Pd ₂ (dba) ₃	BPh ₃	TFT	130 °C	34% (15%)	n.d.
4	L5	Pd ₂ (dba) ₃	BPh ₃	decalin	130 °C	59% (34%)	47%
5	L4	Pd ₂ (dba) ₃	BPh ₃	PhMe	130 °C	N.R.	--
6	L4	Pd ₂ (dba) ₃	BPh ₃	TFT	130 °C	N.R.	--
7	L4	Pd ₂ (dba) ₃	BPh ₃	decalin	130 °C	N.R.	--
8	L13	Pd ₂ (dba) ₃	BPh ₃	PhMe	130 °C	N.R.	--
9	L13	Pd ₂ (dba) ₃	BPh ₃	TFT	130 °C	N.R.	--
10	L13	Pd ₂ (dba) ₃	BPh ₃	decalin	130 °C	N.R.	--
11	L14	Pd ₂ (dba) ₃	BPh ₃	PhMe	130 °C	N.R.	--
12	L14	Pd ₂ (dba) ₃	BPh ₃	TFT	130 °C	N.R.	--
13	L14	Pd ₂ (dba) ₃	BPh ₃	decalin	130 °C	N.R.	--
14	L23	Pd ₂ (dba) ₃	BPh ₃	PhMe	130 °C	N.R.	--

The dramatic change in reactivity that was exhibited by the hydrogenated BINOL ligands prompted us to survey the effects of other backbone derivatives. TADDOL-derived phosphoramidite ligands (see Figure 34) demonstrated efficient reactivity toward cyanoamidation (Table 14). Ligand **L10**, which contained a pyrrolidine ring, delivered **5.3a** at full conversion in PhMe, TFT, and decalin, though in low selectivities (<15% ee, entries 1–3). Exchanging the pyrrolidine ring for piperidine (**L11**) maintained high conversions at 130 °C and gave slightly increased selectivities (<30% ee, entries 4 and 8). Attempts to decrease the temperature in order to increase the enantioselectivity were not fruitful. At 100 °C in PhMe, **L11** provided a subtle increase in ee %, though reduced the reaction efficiency (77% conversion, 30% ee, entry 5). The reaction in THF at 100 °C

was relatively ineffective, giving **5.3a** at <25% conversion (entry 7). Introducing chirality into the amine substituents did not effect the outcome of the reaction. Ligand **L21** provided **5.3a** at full conversion with a comparable enantioselectivity to the achiral amine counterparts (<30% ee, entries 10 and 11). The TADDOL-derived ligands appear to be less susceptible to solvent effects than the BINOL-derived ligands.

Table 14. Enantioselective cyanoamidation reactivity screen with TADDOL-derived ligands

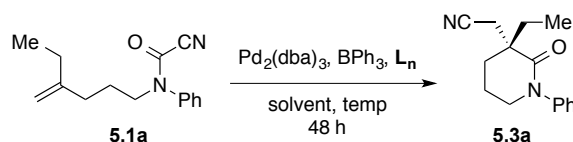


TADDOL ligands							
Entry	Ligand	Catalyst	Additive	Solvent	Temp.	Conv. (Yield)	% ee
1	L10	Pd ₂ (dba) ₃	BPh ₃	PhMe	130 °C	100% (57%)	4%
2	L10	Pd ₂ (dba) ₃	BPh ₃	TFT	130 °C	100% (57%)	14%
3	L10	Pd ₂ (dba) ₃	BPh ₃	decalin	130 °C	100%	9%
4	L11	Pd ₂ (dba) ₃	BPh ₃	PhMe	130 °C	100% (58%)	27 %
5	L11	Pd ₂ (dba) ₃	BPh ₃	PhMe	100 °C	77% (34%)	30 %
6	L11	Pd ₂ (dba) ₃	B(C ₆ F ₅) ₃	PhMe	130 °C	decomp	--
7	L11	Pd ₂ (dba) ₃	BPh ₃	THF	100 °C	24%	n.d.
8	L11	Pd ₂ (dba) ₃	BPh ₃	decalin	130 °C	100% (45%)	24%
9	L11	Pd ₂ (dba) ₃	B(C ₆ F ₅) ₃	decalin	130 °C	decomp	--
10	L21	Pd ₂ (dba) ₃	BPh ₃	TFT	130 °C	100%	20%
11	L21	Pd ₂ (dba) ₃	BPh ₃	decalin	130 °C	100%	27%

We continued our investigation into the effects of the ligand backbone (see Figure 35). Ligand **L20**, which does not contain backbone chirality, provided **5.3a** at full conversion, though was accompanied by an unidentified side-product (Table 15, entries 1 and 2). Again, this result is likely due to the quality of the BPh₃ used. Interestingly, the enantioselectivity obtained with **L20** in decalin was higher than the majority of the more elaborate ligands employed (36% ee). The reaction with spirobi[indene]-derived ligand

L8, which was appended with dimethyl amine, proceeded at 90% conversion in PhMe and gave lactam **5.3a** in 15% ee (entry 3). In TFT and decalin, **L8** gave full conversion, though the % ee was not enhanced (entries 4 and 5). The spirobi[indene] analogue **L9**, which was substituted with (S)-phenyl(ethylene) amine, was less efficient in PhMe and TFT and gave negligible enantioselectivities (entries 6 and 7). In decalin, **L9** gave full conversion with a 6% ee (entry 8). Ligand **L29**, which was derived from a simple phenyl-substituted 1,2-diol, was not efficient in promoting the reaction, providing **5.3a** in 26% conversion.

Table 15. Enantioselective cyanoamidation reactivity screen with miscellaneous ligands



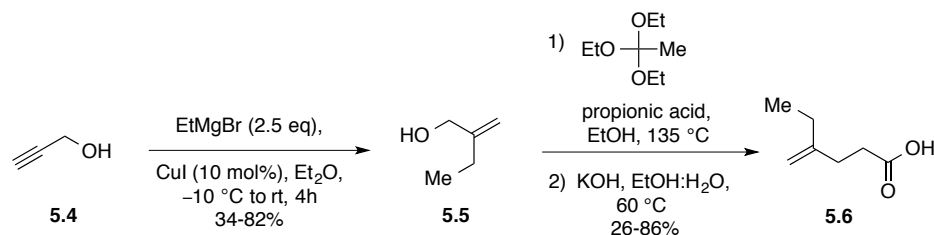
MISCELLANEOUS ligands							
Entry	Ligand	Catalyst	Additive	Solvent	Temp.	Conv. (Yield)	% ee
1	L20	Pd ₂ (dba) ₃	BPh ₃	TFT	130 °C	100% ^a	23%
2	L20	Pd ₂ (dba) ₃	BPh ₃	decalin	130 °C	100% ^a	36%
3	L8	Pd ₂ (dba) ₃	BPh ₃	PhMe	130 °C	90% (80%)	15%
4	L8	Pd ₂ (dba) ₃	BPh ₃	TFT	130 °C	100%	3%
5	L8	Pd ₂ (dba) ₃	BPh ₃	decalin	130 °C	100% (64%)	17%
6	L9	Pd ₂ (dba) ₃	BPh ₃	PhMe	130 °C	69% (27%)	<1%
7	L9	Pd ₂ (dba) ₃	BPh ₃	TFT	130 °C	40%	<1%
8	L9	Pd ₂ (dba) ₃	BPh ₃	decalin	130 °C	100% (28%)	6%
9	L29	Pd ₂ (dba) ₃	BPh ₃	PhMe	130 °C	26%	n.d.

^a accompanied by a significant amount of unidentified side-product

5.1.4 CONCLUDING REMARKS

Intramolecular cyanoamidation with aliphatic tethered alkenes has been successfully demonstrated. Under $\text{Pd}(\text{PPh}_3)_4$ catalysis with BPh_3 as an additive, 3,3-disubstituted δ -lactams are afforded in excellent conversions and obtained in good yields. Efforts to promote the reaction enantioselectively with various chiral phosphoramidite ligands have been met with moderate success. To-date, the best % ee obtained was achieved with (S)-BINOL-(S)-phenyl(ethylene) amine **L1** (54%). The reaction efficiencies were greatly influenced by the choice of solvent (except for TADDOL-derived ligands), though this variable had little effect on enantioselectivity. Without a definitive pattern to design around, the ‘shotgun’ approach was put on hold to pursue an alternative method to achieve selectivity. Additional ligands were afterwards prepared (as illustrated in Figures 32-35) and should be investigated. Moreover, nickel catalysis has not been investigated and should be pursued.

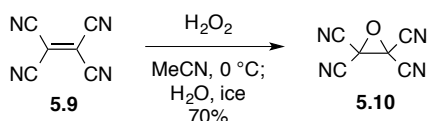
5.1.5 EXPERIMENTAL



ⁱ CuI (387 mg, 2.03 mmol), propargyl alcohol (**5.4**) (1.2 mL, 20.31 mmol), and dry Et_2O (20 mL), were added to a flame-dried flask under N_2 and the solution was cooled to $-10\text{ }^\circ\text{C}$. An ethylmagnesium bromide solution (3.0 M in Et_2O ; 16.9 mL, 190.44 mmol) was added slowly over 30 min at a rate of $0.3 \times 1/10\text{ mL/min}$ with a syringe pump. The solution turned brown and salts accumulated around the sides of the flask making it difficult to stir (with both stir bar and overhead stirrer). A long needle was inserted into the septum and used to scratch the sides of the flask. The layer of salt was disengaged and the reaction became homogenous. The reaction was stirred for an additional 30 min at $-10\text{ }^\circ\text{C}$ and then allowed to stir at room temperature for 4 h. The brown solution was cooled to $0\text{ }^\circ\text{C}$ and quenched with a saturated aq. NH_4Cl solution. An additional 50 mL of aq. NH_4Cl was added and the solution was stirred at $0\text{ }^\circ\text{C}$ for 1 h to effectively dissolve the salts and avoid a significant emulsion. After the solution turned blue and homogenous ($\text{Cu}^{\text{I}} \rightarrow \text{Cu}^{\text{II}}$), Et_2O was added and the layers were separated. The aqueous layer was extracted 8 times due to the water solubility of **5.5**. The combined organic layers were washed with brine, dried over Na_2SO_4 , filtered, and concentrated. The relatively clean alcohol **5.5** was obtained as a pale yellow oil in 82% yield (1.44 g, 16.7 mmol) and was used without further purification. The alcohol can be purified by

ⁱ Duboudin, J. G.; Jousseau, A.S.; *J. Organomet. Chem.* **1979**, 168, 1.

flash chromatography (1:10 acetone:hexanes): R_f 0.64 (1:1 acetone:hexanes). ⁱⁱAllylic alcohol **5.5** (1.57 g, 18.2 mmol), triethyl orthoacetate (6.69 mL, 36.5 mmol), and propionic acid (0.14 mL, 1.82 mmol) were combined into a flask equipped with a pressurized dropping funnel with a condenser on top of it. The reaction was heated to 135 °C and the EtOH formed *in situ* was collected in the dropping funnel. The reaction was monitored by ¹H NMR spectroscopy, and an additional charge of acid (0.14 mL, 1.82 mmol) was used. Upon completion, the reaction was cooled to 100 °C and a 5.75 M aq. solution of KOH (3.0 g, 54.6 mmol) was added. The EtOH was returned to the flask and the reaction was brought to 60 °C and stirred overnight. After cooling the reaction to room temperature, the solution was slowly acidified with 1 M HCl. The reaction was extracted with DCM and the layers were separated. The combined organic layers were washed with brine, dried over Na₂SO₄, filtered, and concentrated. The crude mixture was purified by vacuum distillation to give acid **5.6** in 86% yield (2.0 g, 15.6 mmol): b.p. 87–95 °C at 4 torr. Alternatively, acid **5.6** could be purified by column chromatography (EtOAc:Hex): R_f 0.25 (1:5 EtOAc:Hex).

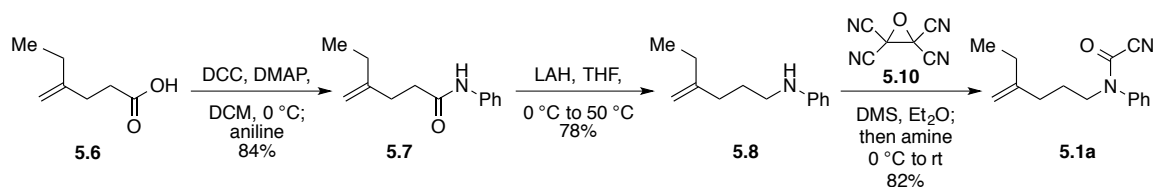


ⁱⁱⁱTetracyanoethylene (TCE) **5.9** was recrystallized from DCE (15 mL/g). TCE (18.9 g, 0.147 mol), MeCN (37 mL; 0.4 M), and a magnetic stir bar were added to an Erlenmeyer flask and cooled to <0 °C with a NaCl/ice bath and stirred. Hydrogen peroxide (30% w/w; 15.5 mL – ratio: 0.2 mol TCE/21 mL H₂O₂ solution) was added dropwise and

ⁱⁱ Yokoshima, S.; Ueda, T.; Satoshi, K.; Sato A.; Kuboyama, T.; Tokuyama, H.; Fukuyama, T. *J. Am. Chem. Soc.* **2002**, *124*, 2137.

ⁱⁱⁱ Linn, W. J. *Org. Syn.* **1973**, *5*, 1007.

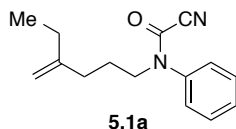
the solution turned purple halfway into the addition; toward the end of the addition the solution returned to yellow. The reaction remained at $< 0\text{ }^{\circ}\text{C}$ for 3 min and was dumped into a large beaker containing a VIGOROUSLY stirring ice/ H_2O mixture (ice: 185 g – ratio 0.2 mol TCE/250 g ice; H_2O : 37 mL – 0.2 mol TCE/500 mL H_2O). The solution was stirred for 30 min without observing precipitation. Two small scoops of ice were added and stirred for an additional 30 minutes – ‘globs’ formed. Two more small scoops of ice were added and the solution turned pink. After 30 min of vigorous stirring, the solution began to foam. One more scoop of ice was added, stirred for 20 minutes, and the resulting colorless solid was separated by vacuum filtration and placed on the hi-vac overnight. Upon standing, the solids turn a light brown color. Tetracyano ethyleneoxide (TCEO) **5.10** was obtained in 70% yield (14.9 g, 0.103 mol).



Acid **5.6** (430 mg, 3.35 mmol) was azeotropically dried with PhH. Dry DCM (4 mL) was added and the solution was cooled to $0\text{ }^{\circ}\text{C}$. DCC (1.04 g, 4.03 mmol) and DMAP (200 mg, 1.68 mmol) were added and the reaction was placed under N_2 and stirred for 10 min. Aniline (0.37 mL, 4.03 mmol) was added and the reaction was allowed to stir for 20 min before warming to room temperature and stirred overnight. DCM and H_2O were added and the layers were separated. The aqueous layer was back extracted with DCM. The combined organic layers were washed with brine, dried over Na_2SO_4 , filtered, and concentrated. The crude mixture was purified by flash chromatography ($\text{EtOAc}:\text{Hex}$) to

give the corresponding amide **5.7** as a yellow oil in 84% yield (570 mg, 2.80 mmol): R_f 0.28 (1:4 EtOAc:Hex). Amide **5.7** (570 mg, 2.80 mmol) was azeotropically dried with PhH and the flask was placed under N_2 . Dry THF (14 mL) was added and the solution was cooled to 0 °C. LAH (215 mg, 5.60 mmol) was slowly added in portions and the resulting mixture was stirred at 0 °C for 15 min. A condenser was assembled onto the flask and the reaction was refluxed overnight. The reaction was cooled to 0 °C and 1 M NaOH was *slowly* added one drop at time (~5 drops) [CAUTION: exotherm], followed by H_2O dropwise (~5 drops), and then alternating 1 M NaOH/ H_2O until the mixture visually ceases to react. The resulting mixture was allowed to stir for an additional 15 min before the aluminum salts were removed by vacuum filtration over celite. Et_2O was added and the layers were separated. The organic layer was washed with H_2O and the combined aqueous layers were back extracted with Et_2O . The combined organic layers were washed with brine, dried over Na_2SO_4 , filtered, and concentrated. The crude product was purified by flash chromatography (EtOAc:Hex) to give amine **5.8** in 71% yield as a yellow oil: R_f 0.74 (1:4 EtOAc:Hex). TCEO (684 mg, 4.75 mmol) and Et_2O (4 mL) were added to a flame-dried flask, placed under N_2 , and cooled to 0 °C. DMS (0.44 mL, 5.94 mmol) was added slowly and the reaction was allowed to stir for 30 min. Amine **5.8** (300 mg, 1.58 mmol) was azeotropically dried with PhH and added as an Et_2O solution and the reaction was allowed to warm to room temperature overnight. The resulting red-orange mixture was diluted with Et_2O , filtered over celite, and concentrated. *Note*: syringe filtering the dicyano carbonyl solution into a flask containing amine and Et_2O reduces the amount of ‘sludge’ formation and increases

yields. After purification by flash chromatography (EtOAc:Hex), cyanoformamide **5.1a** was obtained in 54-82% yield (317 mg, 1.30 mmol): R_f 0.50 (1:4 EtOAc:Hex).

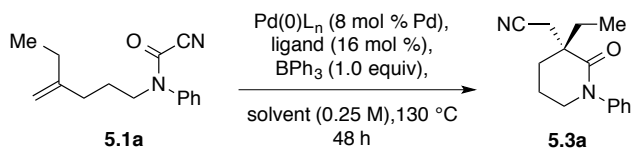


Rotamers 11.5:1

^1H NMR (500 MHz; CDCl_3) δ 7.53-7.49 (m, 3H), 7.30-7.28 (m, 2H), 4.72 (t, $J = 0.7$ Hz, 1H), 4.65 (d, $J = 1.1$ Hz, 1H), 3.77 (m, 2H), 2.03 (app t, $J = 7.6$ Hz, 2H), 1.97 (app quin, $J = 7.4$ Hz, 2H), 1.73-1.67 (m, 2H), 0.99 (t, $J = 7.4$ Hz, 3H);

^1H NMR (500 MHz; CDCl_3) δ 7.53-7.49 (m, 3H), 7.30-7.28 (m, 2H), 4.77 (app t, $J = 0.6$ Hz, 1H), 4.68 (d, $J = 1.1$ Hz, 1H), 3.98 (app t, $J = 7.5$ Hz, 2H), 2.09 (app t, $J = 7.5$ Hz, 2H), 1.76 (app quintet, $J = 7.2$ Hz, 3H) (no ethyl minor rotamer peaks);

^{13}C NMR (126 MHz; CDCl_3): δ 149.5, 144.6, 138.5, 130.0, 129.8, 128.7, 126.4, 110.7, 109.0, 108.6, 52.0, 49.2, 33.1, 32.8, 28.6, 28.5, 26.6, 25.1, 12.3, 12.2 (six signals overlapped for the two rotamers).

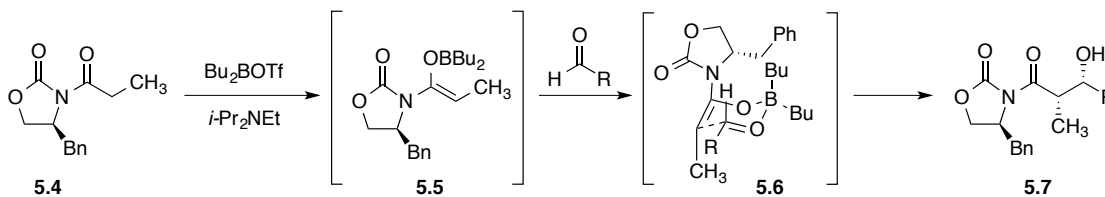


General Procedure: A 0.25 M solution of **5.1a** was prepared in a nitrogen-filled glovebox. $\text{Pd(PPh}_3)_4$ (11.4 mg, 0.01 mmol) or $\text{Pd}_2(\text{dba})_3$ (4.5 mg, 0.0048 mmol), ligand (0.19 mmol), and BPh_3 (29 mg, 0.12 mmol) were weighted into a 1-dram vial, followed the addition of **5.1a** solution (0.5 mL, 30 mg, 0.12 mmol). The vial was equipped with a stir bar, the vial was sealed with a teflon screw cap, and the vessel was placed in an

aluminum block and heated to 130 °C for 48 h. The vial was allowed to cool and the mixture was loaded onto celite and purified by flash chromatography (EtOAc:Hex): R_f 0.10 (1:4 EtOAc:Hex). The product was taken up in EtOAc and washed with 3% H_2O_2 and 1 M NaOH to remove boron by-products. Enantiomeric excess (for enantioselective reactions) was determined using an Agilent Technologies 1200 Series HPLC. 1H NMR (500 MHz; $CDCl_3$) δ 7.41-7.38 (m, 2H), 7.29-7.25 (m, 1H), 7.23-7.21 (m, 2H), 3.75-3.70 (m, 1H), 3.68-3.64 (m, 1H), 2.83 (d, J = 16.6 Hz, 1H), 2.64 (d, J = 16.6 Hz, 1H), 2.10-2.01 (m, 4H), 1.92 (app dq, 14.24, 7.22, 1H), 1.81 (app dq, J = 14.2, 7.2 Hz, 1H), 1.01 (t, J = 7.5 Hz, 3H).

5.2. DIASTEREOSELECTIVE CYANOAMIDATION

A chiral auxiliary is a chemical compound or scaffold that is temporarily incorporated into a synthesis in order to control the stereochemical outcome of a reaction. The chirality present in the auxiliary can bias the stereoselectivity of the transformation, leading to diastereomers, in which one is favored over another. The diastereomers can be separated (in theory) and the auxiliary can then be cleaved from the substrate to reveal enantiopure products. Ideally the auxiliary can be recovered and reused. E. J. Corey first introduced the concept of chiral auxiliaries ((-)-8-phenylmenthol) in his 1978 synthesis of prostaglandins. Since then, several auxiliaries have been realized. Oxazolidinones, popularized by David Evans, have been applied to many stereoselective transformations, including aldol,⁴ alkylation,⁵ and Diels-Alder reactions⁶ (Scheme 115). Other prevalent auxiliaries include Myers' pseudoephedrine^{7,8} (or pseudoephedrine)⁹, Enders' SAMP/RAMP,^{10,11} and Ellman's *tert*-butanesulfinamide.¹²⁻¹⁴

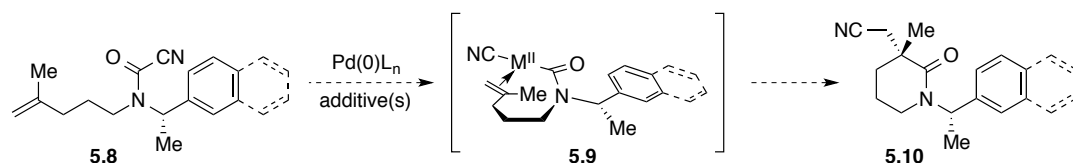


Scheme 115. Evan's oxazolidinone auxiliary in an asymmetric aldol reaction

5.2.1 RESEARCH PROPOSAL: 3,3-DISUBSTITUTED LACTAMS

During a meeting, in which we aimed to discuss a QSAR (quantitative structure-activity relationship) molecular modeling approach to help guide our ligand-based

enantioselective inquiries, the idea of using a chiral auxiliary to aid or perhaps even alleviate the dependency upon ligand design was proposed. It was initially presumed that a chiral sulfinamide could serve as a suitable unit to impart selectivity. Considering that the benzyl cyanoformamide derivative **5.1b** was successful in undergoing cyanoamidation (not shown), it was suggested that a chiral benzyl (or naphthyl) group could be readily prepared and tested (Scheme 116). Cyanoformamide(s) **5.8** were envisioned to undergo oxidative addition to provide intermediate(s) **5.9**. Although **5.9** is not suggestively illustrated, rotation about the N–C_{benzyl} bond may impart facial selectivity upon migratory insertion. Reductive elimination would afford 3,3-disubstituted δ -lactam(s) **5.10**. The resulting benzylic moiety could then be removed by either hydrogenation or a Birch reduction.

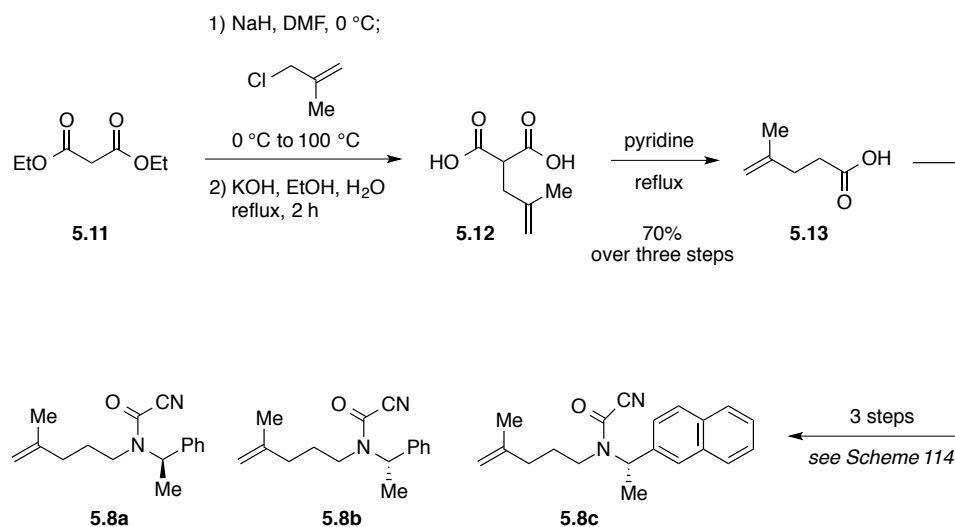


Scheme 116. Proposed diastereoselective cyanoamidation with chiral auxiliaries

5.2.2 SUBSTRATE SYNTHESIS

The unreliability of the Johnson-Claisen rearrangement previously used to access 4-pentenoic acids (see Scheme 114) was cause for redirection in substrate preparation. Acid **5.13** was prepared in 70% yield over three steps without the need for intermediate purification (Scheme 117). Diethyl malonate **5.11** was alkylated with 3-chloro-2-methylpropene and the resulting diester was saponified to give diacid **5.12**.

Decarboxylation of diacid **5.12** was accomplished by refluxing in pyridine to give acid **5.13**. Acid **5.13** was coupled with amines (*R*)- or (*S*)-phenyl(ethyl)amine and (*S*)-naphthyl(ethyl)amine, which provided the respective amides that were then reduced with LAH and acylated with TCEO to give cyanoformamides **5.8a–c** (see Scheme 114).



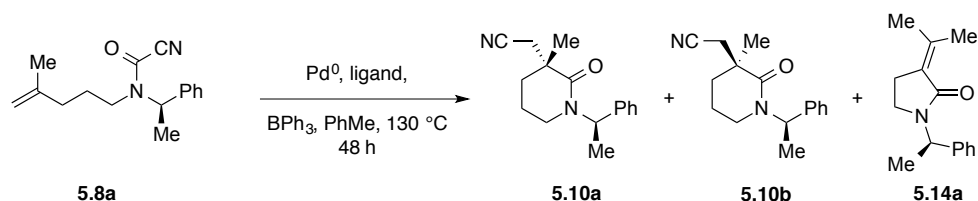
Scheme 117. Re-routed synthesis of 4-pentenoic acid derivatives **5.8a–c**

5.2.3 RESULTS AND DISCUSSION

Heating cyanoformamide **5.8a** with Pd(PPh₃)₄ and BPh₃ in toluene for 48 h resulted in full conversion to **5.10** as a 3.8:1 mixture of diastereomers (Table 16; 58% de, entry 1). We were encouraged with the observation that the chiral auxiliary alone was achieving higher selectivities than any of the enantioselective reactions with phosphoramidite ligands (Table 12, entry 1; **L1**, 54% ee). An attempt to increase the selectivity by decreasing the temperature was not successful. Although the reaction was complete after 48 h at 100 °C, no change in selectivity was observed (entry 2). We next examined additional achiral phosphine ligands in order to gain insight into stereoelectronic effects

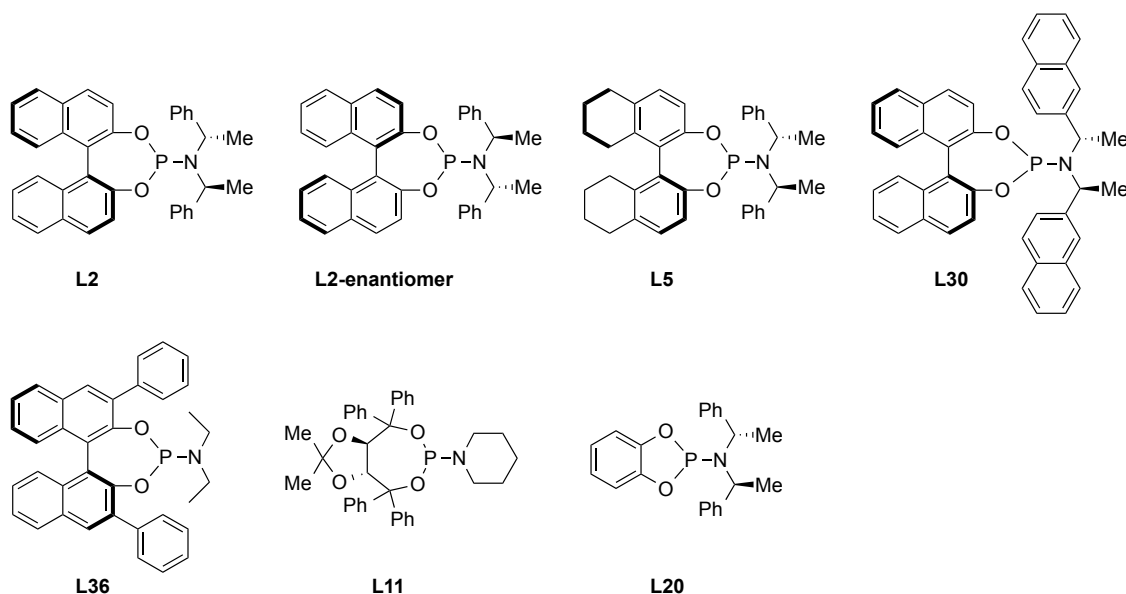
of the ligands. Subtle differences in cone angle and electron-donating ability of the ligands did not appear to have much influence on the reaction outcomes and no correlations could be made (entries 1, 3–5); [cone angle: $\text{P}(o\text{-tol})_3 > \text{PCy}_3 > \text{PPh}_3 > \text{PPh}_2\text{Me}$; electron density: $\text{PCy}_3 > \text{PPh}_2\text{Me} > \text{P}(o\text{-tol})_3 > \text{PPh}_3$; diastereoselectivity: $\text{PPh}_3 > \text{PCy}_3 > \text{PPh}_2\text{Me} > \text{P}(o\text{-tol})_3$]. Decreasing the temperature to 110 °C (from 130 °C) had an unusual substantial effect on the selectivity with PPh_2Me (51% de \rightarrow 17% de, entry 6), whereas relatively little change was observed for PCy_3 (55% de \rightarrow 46% de, entry 7). Moreover, neither ligand promoted the reaction to proceed to completion at reduced temperatures.

Table 16. Diastereoselective cyanoamidation [*R*-phenyl(ethyl)amine]: 3,3-disubstituted δ -lactams



Entry	Ligand	Catalyst	Temp.	Convers.	Products 5.10:5.14	d.r. (de%) 5.10a:5.10b ^a
1	--	$\text{Pd}(\text{PPh}_3)_4$	130 °C	100%	1:0	3.8:1 (58%)
2	--	$\text{Pd}(\text{PPh}_3)_4$	100 °C	100%	1:0	3.8:1 (58%)
3	$\text{P}(o\text{-tol})_3$	Pd_2dba_3	130 °C	100%	1:0	2.6:1 (44%)
4	PPh_2Me	Pd_2dba_3	130 °C	100%	1:0	3.1:1 (51%)
5	PCy_3	Pd_2dba_3	130 °C	100%	1:0	3.4:1 (55%)
6	PPh_2Me	Pd_2dba_3	110 °C	43%	1:0	1.4:1 (17%)
7	PCy_3	Pd_2dba_3	110 °C	67%	1:0	3.4:1 (46%)
8	L2	Pd_2dba_3	130 °C	100%	1.5:1	1:1.6 (22%)
9	L5	Pd_2dba_3	130 °C	100%	1:1	1:1.6 (23%)
10	L2-ent	Pd_2dba_3	130 °C	100%	7.2:1	6.3:1 (73%)
11	L2-ent	Pd_2dba_3	110 °C	4%	n.d.	n.d.
12	L30	Pd_2dba_3	130 °C	100%	1:0	1.1:1 (5%)
13	L36	Pd_2dba_3	130 °C	100%	16:1	3.4:1 (55%)
14	L11	Pd_2dba_3	130 °C	100%	1:0	4.1:1 (61%)
15	L20	Pd_2dba_3	130 °C	100%	1:0	2.6:1 (44%)

^a absolute configuration of **5.10a** and **5.10b** not determined



We then investigated the compounding effects of adding chiral phosphoramidite ligands. Reacting ligand **L2** ((*S*)-BINOL, (*S*, *S*)-amine) with (*R*)-cyanoformamide **5.8a** resulted in the formation of **5.10** as a 1:1.6 diastereomeric ratio, favoring **5.10b** (Table 16, entry 8). In addition, another product was formed in 40%. This side-product was initially proposed to be the 7-membered lactam arising from a 7-*endo-trig* rather than the desired 6-*exo-trig* cyclization, owing to the small coupling constants observed (< 2 Hz) in the ^1H NMR spectrum. Additional spectroscopic evidence, primarily by ^{13}C DEPT NMR and IR, determined this side-product to be the 5-membered lactam **5.14** containing an exocyclic olefin. The formation of **5.14** would result from initial olefin isomerization of **5.8a** to the tri-substituted olefin **5.15** (Figure 36). Oxidative addition into the $\text{C}_{\text{acyl}}\text{--CN}$ bond, followed by migratory insertion would give intermediate **5.17**. β -hydride elimination from **5.17** would generate **5.14** and one equivalent of HCN. Upon opening the sealed vial, a noticeable pressure release had been observed. The analogous reaction with the hydrogenated **L2** ligand (**L5**) gave comparable results (entry 9).

Unfortunately the diastereomer(s) of **L2** (**L1**; (*R*)-BINOL, (*S,S*)-amine) had not available for comparison, though these experiments would be ideal considering **L1** had been found to give the best enantioselectivity in previous studies.

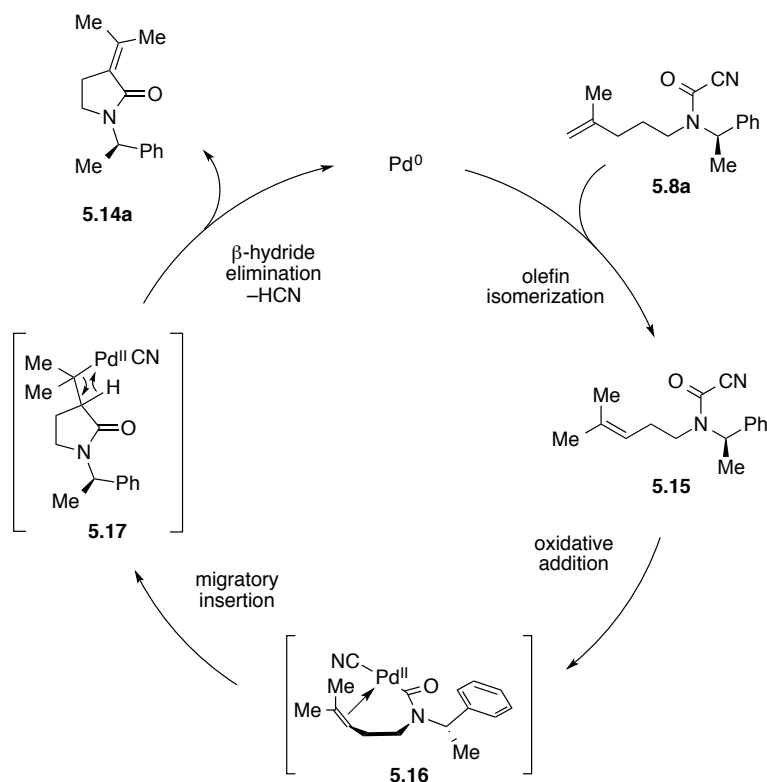
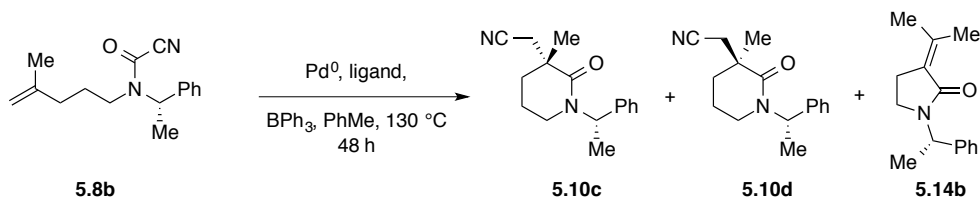


Figure 36. Proposed mechanism for the formation of side-product **5.14a**

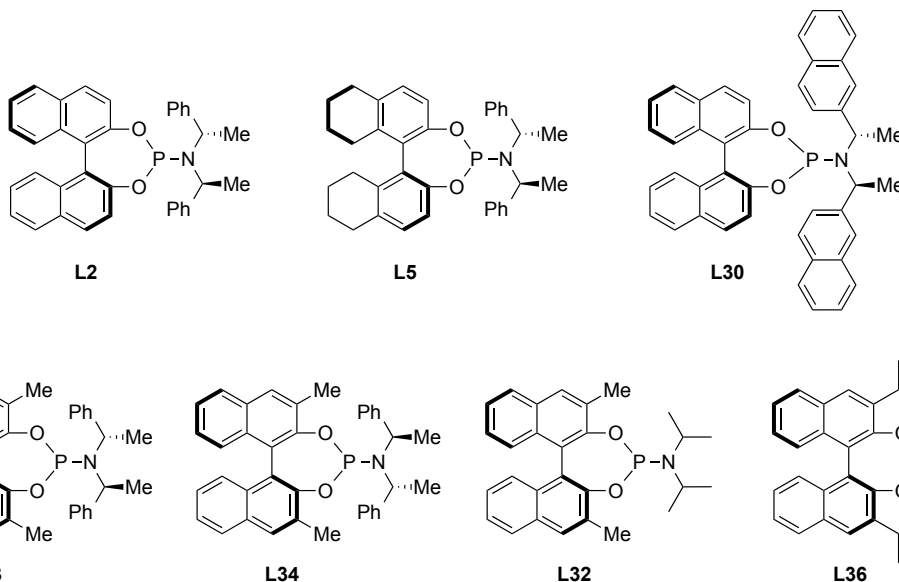
It was hypothesized that an auxiliary-ligand stereochemical mismatch with **L2** may be responsible for the observed change in diastereoselectivity and chemoselectivity. Reacting (*R*)-cyanoformamide **5.8a** with **L2-enantiomer** ((*R*)-BINOL, (*R,R*)-amine) returned to the selectivity in favor of **5.10a** as a 6.3:1 mixture (Table 16, entry 10). However, 12% of the material remained as **5.14**. Reducing the temperature to 110 °C with **L2-enantiomer** resulted in less than 5% conversion (entry 11). Returning to the (*S*)-BINOL backbone, we investigated the effects of the bulkier

(*S, S*)-bis[naphthyl(ethyl)] amine (**L30**). Surprisingly, formation of **5.14** was not observed and very little selectivity was obtained (5% de, entry 12). Substituting the (*S*)-BINOL backbone with phenyl groups (**L36**) led to the formation of **5.10** as a 3.4:1 diastereomeric mixture in favor of **5.10a**; λ -lactam **5.14** was formed in less than 6%. TADDOL-derived ligand **L11** gave full conversion to **5.10** with 61% de and no formation of **5.14** (entry 13). The catechol-derived ligand **L20** provided lactams **5.10** in a 44% de (entry 14).

In order to further probe the significance of the match/mis-matched discrepancies between the auxiliary and BINOL ligands, (*S*)-cyanoformamide **5.8b** was prepared. Entry 1 with **L2** was inferred from Table 16 (Table 17). The hydrogenated backbone of **L2** (**L5**) gave comparable diastereoselectivity, though **5.14** made up 40% of the mixture (entry 2). In the matched case, the bis[naphthyl(ethyl)] amine ligand **L30** delivered **5.10** in a 77% de and suppressed the formation of **5.14** (entry 3). Introducing methyl substituents on the BINOL backbone of **L2** (**L33**) increased the diastereo- and chemoselectivity (78% de, entry 4). The diastereomer **L34** gave a comparable selectivity and no observed formation of **5.14** (79% de, entry 5). Having no stereochemistry in the amino group of the ligand, ligand **L32** gave an appreciable diastereoselectivity (71% de), however 36% of the material was **5.14** (entry 6). In comparison, the phenyl-substituted BINOL ligand **L36** containing an achiral amine, greatly reduced the stereoselectivity (38% de) but increased the chemoselectivity (entry 7).

Table 17. Diastereoselective cyanoamidation [*S*-phenyl(ethyl)amine]: 3,3-disubstituted δ -lactams

Entry	Ligand	Catalyst	Temp.	Convers.	Products 5.10:5.14	d.r. (de%) 5.10c:5.10d
1	L2	$\text{Pd}_2(\text{dba})_3$	130°C	100%	7.2:1	6.3:1 (73%)
2	L5	$\text{Pd}_2(\text{dba})_3$	130°C	100%	1.4:1	5.7:1 (70%)
3	L30	$\text{Pd}_2(\text{dba})_3$	130°C	100%	1:0	7.8:1 (77%)
4	L33	$\text{Pd}_2(\text{dba})_3$	130°C	100%	14.6:1	8.1:1 (78%)
5	L34	$\text{Pd}_2(\text{dba})_3$	130°C	100%	1:0	8.7:1 (79%)
6	L32	$\text{Pd}_2(\text{dba})_3$	130°C	100%	1.8:1	5.9:1 (71%)
7	L36	$\text{Pd}_2(\text{dba})_3$	130°C	100%	5.3:1	2.2:1 (38%)

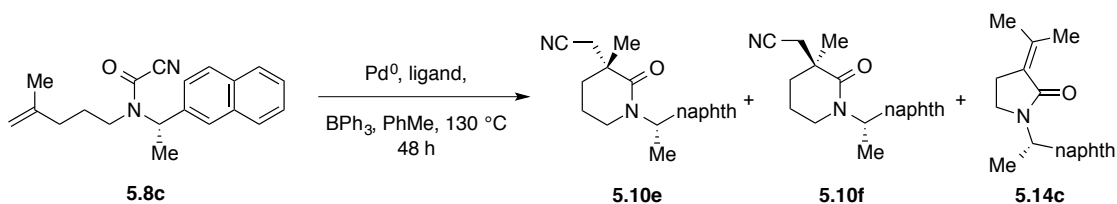


We next investigated the bulkier (*S*)-naphthyl(ethyl) auxiliary **5.8c** under the cyanoamidation conditions. Heating cyanoformamide **5.8c** with $\text{Pd}(\text{PPh}_3)_4$ with BPh_3 in toluene for 48 h resulted in full conversion to **5.10** in a 4.1:1 diastereomeric ratio (Table 18, entry 1). The selectivity for this auxiliary (61% de) was only slightly higher than the phenyl(ethyl) analogue (58% de), though the reaction with $\text{Pd}_2(\text{dba})_3$ and

exogenous PPh₃ gave a comparable 59% de (entry 2). The ligand P(*p*-OMePh)₃ had the same outcome as PPh₃ (59% de, entry 3), whereas the reaction did not go to completion with ligands with larger cone angles (P(*o*-tol)₃ and PCy₃; entries 4 and 5). The decreased reactivity of P(*o*-tol)₃ and PCy₃ likely results from the added steric hindrance imposed by the naphthyl auxiliary since the analogous phenyl auxiliary was well tolerated with these ligands.

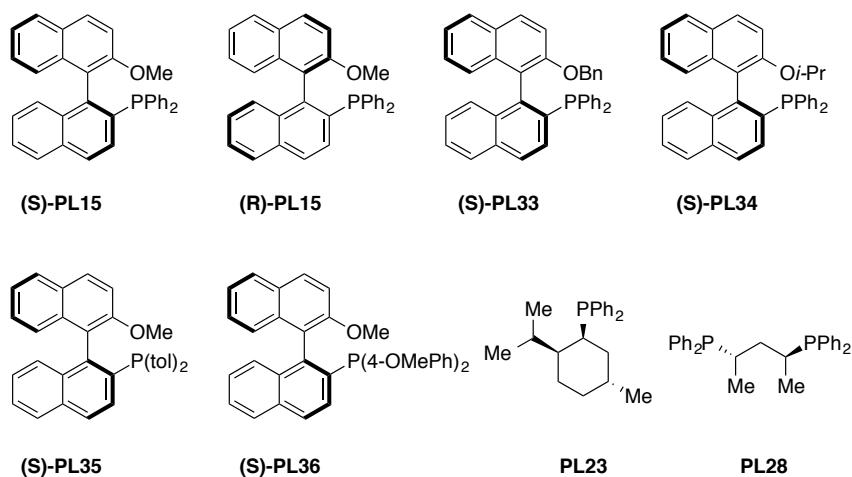
Chiral binaphthyl-based mono-phosphine ligands were also surveyed. The “matched” **PL15(S)** gave approximately 10% higher selectivity than the “mismatched” **PL15(R)** ligand (67% de, 58% de, entries 6 and 7). In comparison, exchanging the methoxy group for either a benzyloxy (**PL33**) or isopropoxy group (**PL34**) had no effect on the reaction (entries 8 and 9). Adding electron density to the phosphine (**PL35** and **PL36**) slightly increased the selectivity (71% de, entries 10 and 11). A menthol-derived phosphine ligand **PL23** showed no improvement over the achiral phosphine ligands (60% de, entry 12). The 1,3-dimethyl dppp bidentate ligand **PL28** afforded product **5.10** in less than 5% conversion (entry 13).

Table 18. Diastereoselective cyanoamidation [*S*-naphthyl(ethyl)amine]: 3,3-disubstituted δ -lactams



Entry	Ligand	Catalyst	Temp.	Convers.	Products 5.10:5.14	d.r. (de%) 5.10e:5.10f
1	--	Pd(PPh ₃) ₃	130 °C	100 %	1:0	4.1:1 (61%)
2	PPh ₃	Pd ₂ (dba) ₃	130 °C	100%	1:0	3.9:1 (59%)
3	P(<i>p</i> -OMePh) ₃	Pd ₂ (dba) ₃	130 °C	100%	1:0	3.9:1 (59%)
4	P(<i>o</i> -tol) ₃	Pd ₂ (dba) ₃	130 °C	82%	1:0	2.9:1 (49%)

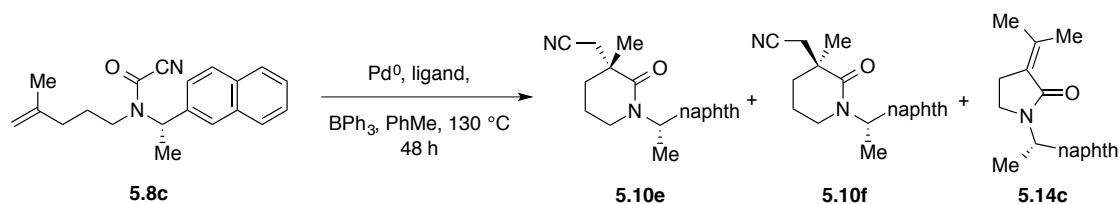
5	PCy ₃	Pd ₂ (dba) ₃	130 °C	65%	1:0	3.6:1 (57%)
6	PL15(S)	Pd ₂ (dba) ₃	130 °C	100%	1:0	5.1:1 (67%)
7	PL15(R)	Pd ₂ (dba) ₃	130 °C	100%	1:0	3.8:1 (58%)
8	PL33(S)	Pd ₂ (dba) ₃	130 °C	100%	1:0	5:1 (67%)
9	PL34(S)	Pd ₂ (dba) ₃	130 °C	100%	1:0	4.9:1 (66%)
10	PL35(S)	Pd ₂ (dba) ₃	130 °C	100%	1:0	6:1 (71%)
11	PL36(S)	Pd ₂ (dba) ₃	130 °C	100%	1:0	5.9:1 (71%)
12	PL23	Pd ₂ (dba) ₃	130 °C	100%	1:0	4.0:1 (60%)
13	PL28	Pd ₂ (dba) ₃	130 °C	4%	1:0	n.d.



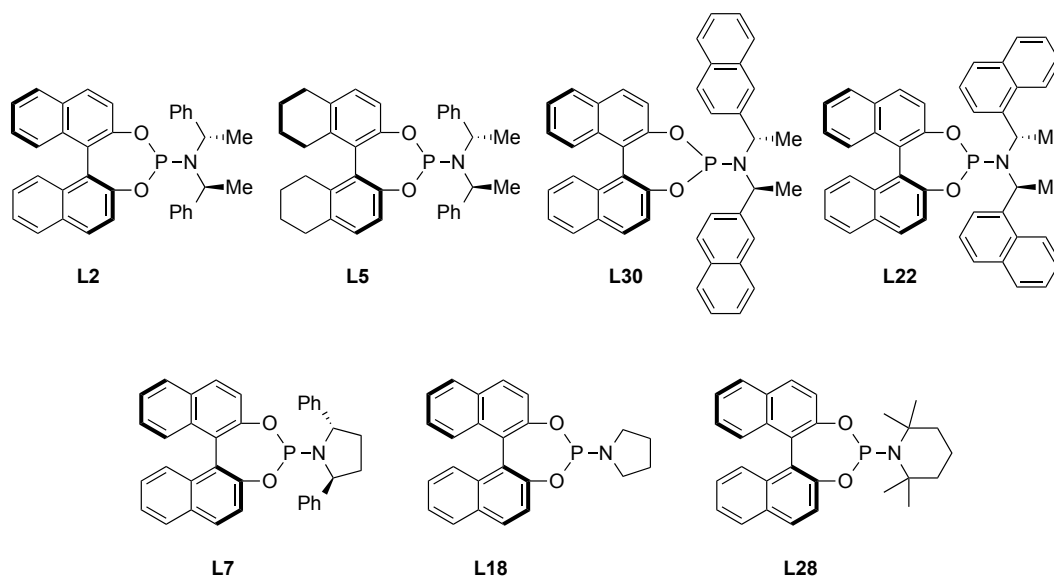
Comparing the reactions of cyanoformamide **5.8b** (phenyl auxiliary, Table 17) with chiral phosphoramidite ligands with the reactions of cyanoformamide **5.8c** and phosphoramidite ligands (Table 18), it appears that the added steric bulk of the naphthyl auxiliary contributes to a decrease in chemoselectivity. Reaction with ligand **L2** produced a mixture of **5.10** diastereomers in a 10.2:1 ratio (82% de); however, the reaction suffered with 40% of the material resulting from the formation of **5.14** (entry 14). The enantiomer of **L2** (**L2-ent**) gave a significantly lowered selectivity, though still in favor of **5.10a**; however, the chemoselectivity *increased* with 30% of the material resulting from the formation of **5.14** (entry 15). The reaction of **5.8c** with hydrogenated backbone **L5** increased in diastereoselectivity relative to the reaction with **5.8b**, though

the chemoselectivity decreased (entry 16). Increasing the steric bulk on the amine (**L30**) was not effective in the cyanoamidation with **5.8c**, providing **5.10** in 62% de with a product ratio of 4.5:1 (compared to the analogous reaction with **5.8b**, which was completely selective for **5.10** with a 77% de) (entry 17). Interestingly, the configurational isomer of **L30** (**L22**) gave complete selectivity for **5.10** and a comparable lactam ratio (58% de, entry 18). The cyclic amine analogue of **L2** (**L7**) gave improved chemoselectivity, though reduced the stereoselectivity (entry 19). The achiral cyclic amine ligand **L18** demonstrated complete conversion to the δ -lactam and slight reduction in stereoselectivity (53% de, entry 20). The sterically more hindered TMP ligand **L28** gave excellent chemoselectivity, but the reaction did not go to completion in 48 h (57% de, entry 21).

Table 18. Continued



Entry	Ligand	Catalyst	Temp.	Convers.	Products 5.10:5.14	d.r. (de%) 5.10e:5.10f
14	L2	$\text{Pd}_2(\text{dba})_3$	$130\text{ }^\circ\text{C}$	100%	1.5:1	10.2:1 (82%)
15	L2-ent	$\text{Pd}_2(\text{dba})_3$	$130\text{ }^\circ\text{C}$	100%	2.3:1	2.3:1 (39%)
16	L5	$\text{Pd}_2(\text{dba})_3$	$130\text{ }^\circ\text{C}$	100%	1:1	7.8:1 (77%)
17	L30	$\text{Pd}_2(\text{dba})_3$	$130\text{ }^\circ\text{C}$	100%	4.5:1	4.3:1 (62%)
18	L22	$\text{Pd}_2(\text{dba})_3$	$130\text{ }^\circ\text{C}$	100%	1:0	3.8:1 (58%)
19	L7	$\text{Pd}_2(\text{dba})_3$	$130\text{ }^\circ\text{C}$	100%	13:1	3.7:1 (57%)
20	L18	$\text{Pd}_2(\text{dba})_3$	$130\text{ }^\circ\text{C}$	100%	1:0	3.3:1 (53%)
21	L28	$\text{Pd}_2(\text{dba})_3$	$130\text{ }^\circ\text{C}$	48%	1:0	3.7:1 (57%)



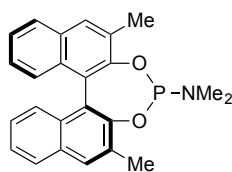
Cyanoamidation reactions of **5.8c** and BINOL-based ligands gave varied results (Table 18 continued, page 281). Ligand **L6**, containing the simplest amine (NMe_2), gave **5.10c** in full conversion and chemoselectivity, though occurred with lower diastereoselectivity (43% de, entry 21). Increasing the sterics on the amine (**L32**) led to an increase in % de, though allowed for 29% conversion to the undesired λ lactam **5.14** (76% de, entry 22). Surprisingly, by changing to the (*S*)-bis[phenyl(ethyl)] amine ligand **L33**, complete selectivity for **5.10** was achieved and the higher diastereoselectivity was maintained; however, the reaction suffered from incomplete conversion, leaving 30% starting material (entry 23). Increasing the concentration from 0.25 M to 0.5 M allowed for the reaction to proceed to completion, though both selectivities suffered as a result (entry 24). Even more surprising, switching to the (*R*)-bis[phenyl(ethyl)] amine ligand **L34** resulted in a reaction that produced δ -lactam **5.10** exclusively and in 78% de (entry 25). The phenyl-substituted BINOL containing diethylamine **L36** was less reactive, giving **5.10** at 57% conversion, and much less stereoselective (26% de, entry 26). TADDOL-based ligands **L11** and **L21** promoted the reaction to completion, though the

reactions suffered from lowered diastereoselectivity (51% and 41% de, respectively) and were accompanied by $\leq 10\%$ formation of **5.14** (entries 27 and 28). The catechol-derived phosphoramidite ligand **L20** performed well to give **5.10** exclusively with full conversion and in moderate stereoselectivity (61% de, entry 29). The bisphosphoramidite **L19** proceeded at 72% conversion to give **5.10** in 60% de (entry 30).

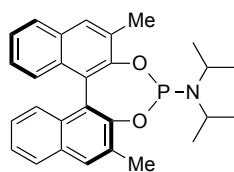
Table 18. Continued

Entry	Ligand	Catalyst	Temp.	Convers	Products 5.10:5.14	d.r. (de%) 5.10e:5.10f
21	L6	$\text{Pd}_2(\text{dba})_3$	130 °C	100%	1:0	2.5:1 (43%)
22	L32	$\text{Pd}_2(\text{dba})_3$	130 °C	100%	2.4:1	7.3:1 (76%)
23	L33	$\text{Pd}_2(\text{dba})_3$	130 °C	70%	1:0	6.55:1 (74%)
24 ^a	L33	$\text{Pd}_2(\text{dba})_3$	130 °C	100%	2.6:1	4.9:1 (66%)
25	L34	$\text{Pd}_2(\text{dba})_3$	130 °C	100%	1:0	8.3:1 (78%)
26	L36	$\text{Pd}_2(\text{dba})_3$	130 °C	57%	1:0	1.7:1 (26%)
27	L11	$\text{Pd}_2(\text{dba})_3$	130 °C	100%	16:1	3.1:1 (51%)
28	L21	$\text{Pd}_2(\text{dba})_3$	130 °C	100%	9:1	2.4:1 (41%)
29	L20	$\text{Pd}_2(\text{dba})_3$	130 °C	100%	1:0	4.1:1 (61%)
30	L19	$\text{Pd}_2(\text{dba})_3$	130 °C	72%	1:0	4.0:1 (60%)

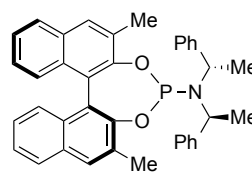
^a Reaction run at 0.5 M rather than 0.25 M



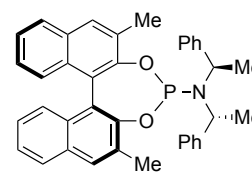
L6



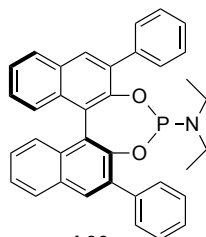
L32



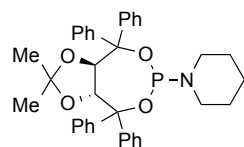
L33



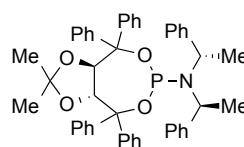
L34



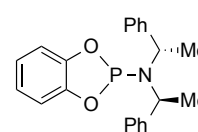
L36



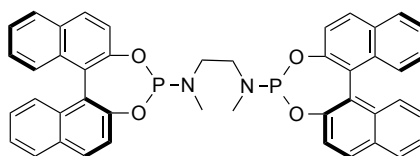
L11



L21



L20



L19

Substrate Scope

In order to probe the scope of the reaction, substrates containing different alkene appendages (**5.8d–5.8g**) were prepared (Figure 37). The new synthetic route developed in Scheme 117 was efficient in preparing the acid intermediates (as opposed to the Johnson-Claisen route in Scheme 113). Unfortunately, these substrates have yet to be subjected to the reaction conditions.

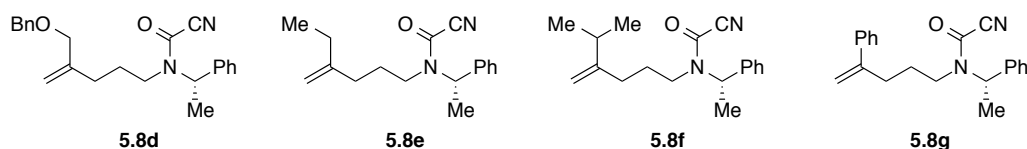
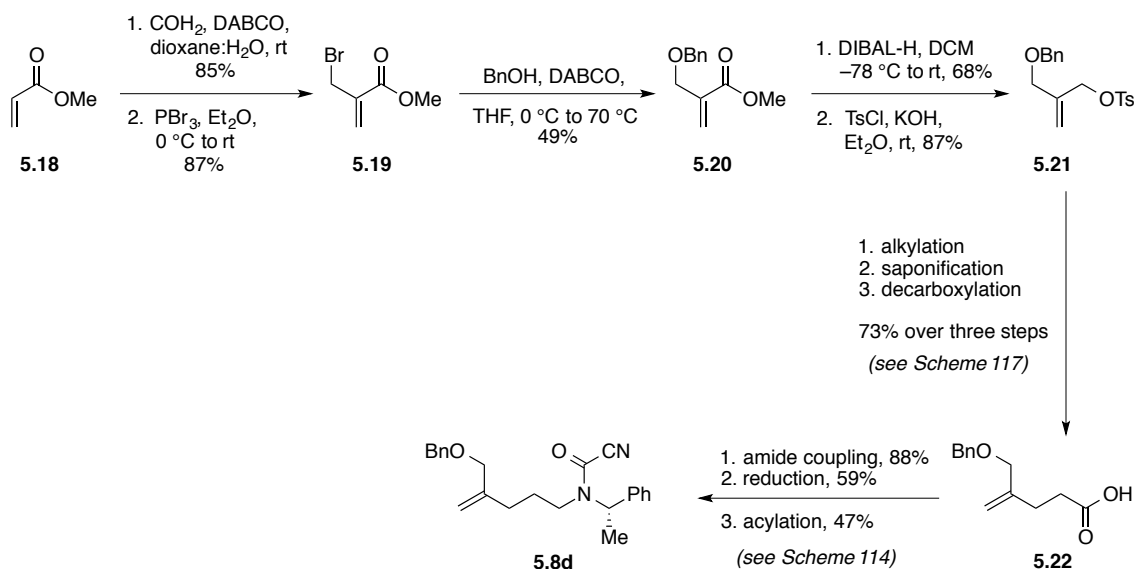


Figure 37. Additional substrates prepared for intramolecular cyanoamidation

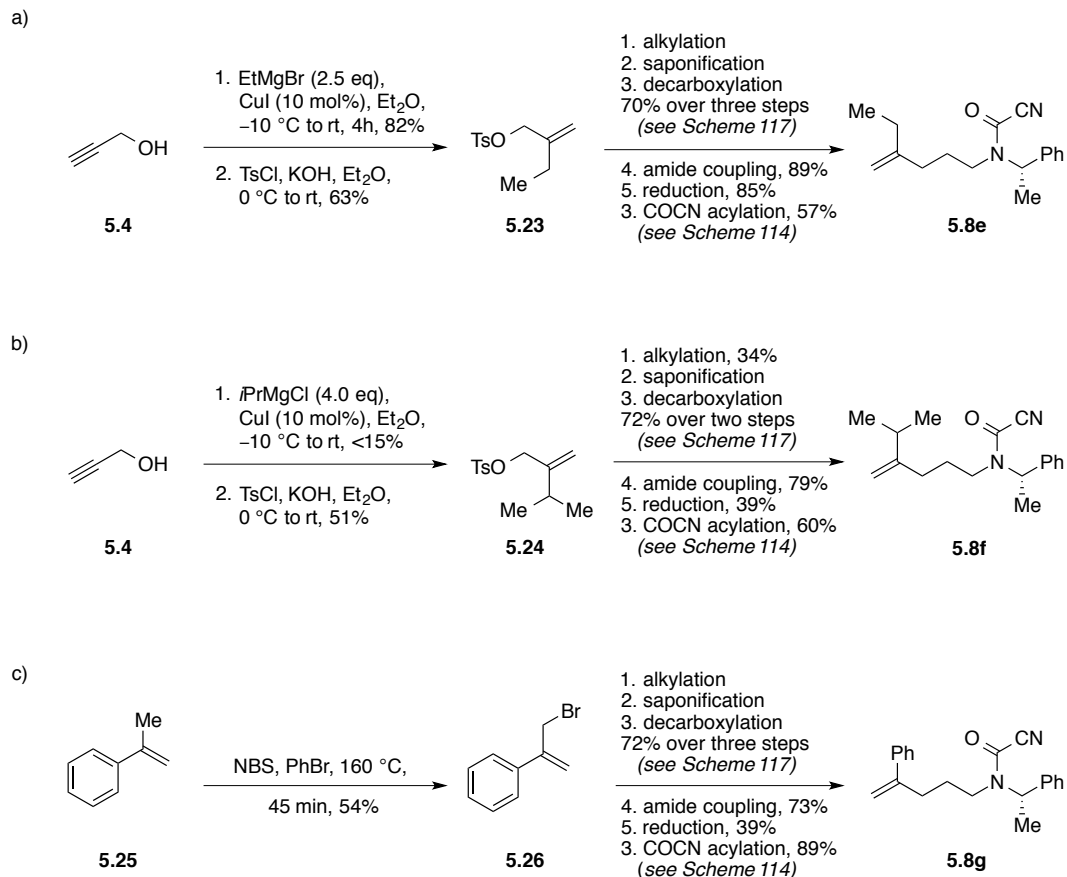
Benzyloxy cyanoformamide **5.8d** was prepared through an eleven-step sequence beginning with a Baylis-Hillman reaction of methacrylate **5.18** and formaldehyde that proceeded in 85% yield (Scheme 118). The resulting alcohol was then brominated upon treatment with PBr_3 to give the bromide **5.19** in 87% yield. Substitution with benzyl alcohol afforded ester **5.20** with DABCO as the optimal base. Reduction of ester **5.20** with DIBAL-H to the primary allylic alcohol (68% yield), followed by tosylation, gave tosylate **5.21** (87% yield). The three-step sequence to acid **5.22** by way of alkylation with diethyl malonate, saponification, and decarboxylation (see Scheme 117) proceeded in 73% yield over the three steps without need for intermediate purification. Coupling acid **5.22** to (*S*)-phenyl(ethyl)amine (88% yield) with subsequent reduction of the amide with LAH (59% yield) gave the corresponding amine that was then acylated with dicyano carbonyl to give cyanoformamide **5.8** (47% yield).



Scheme 118. Preparation of cyanoformamide **5.8d**

The preparation of cyanoformamides **5.8e–5.8g** were prepared in seven to eight steps that followed the same sequence as previously described (Scheme 119). The synthesis of the corresponding tosylates **5.23** (see Scheme 117) and **5.24** were prepared by a copper-promoted Grignard addition into propargyl alcohol **5.4**. Although the procedure for this addition had been well optimized to obtain the ethyl-substituted alcohol (82% yield, Scheme 119a), the analogous reaction with *i*PrMgCl was inefficient even upon using excess Grignard and allowing the reaction to run overnight (<15% yield, Scheme 119b). The alkylation of isopropyl tosylate **5.24** with diethyl malonate was also less effective. Attempts to carry the resulting crude diester through the proceeding two steps were met with limited success. The malonate ester was therefore isolated in 34% yield before continuing with the synthesis to obtain **5.8f**. The analogous phenyl-substituted cyanoformamide **5.8g** was prepared through the same six-step sequence with bromide **5.26**, which was prepared by brominating α -methylstyrene **5.25** with NBS

(Scheme 119c). It is anticipated that the preparation of additional allylic electrophiles could readily broaden substrate scope through this six-step route to cyanoformamides.



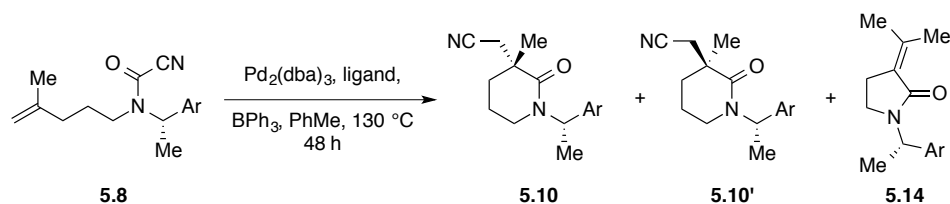
Scheme 119. Preparation of cyanoformamide derivatives **5.8e–g**

5.2.4 CONCLUDING REMARKS

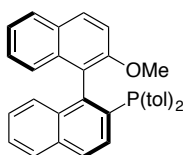
The diastereoselective formation of δ -lactams through the use of chiral auxiliaries was found to be more effective than the enantioselective reactions previously discussed. Table 19 compares the outcomes of the best performing ligands under the diastereoselective conditions with either **5.8a/b** (phenyl auxiliary; a = (*R*), b = (*S*)) or **5.8c**

(naphthyl auxiliary). Cyanoformamides **5.8a** and **5.8c** performed similarly with achiral phosphine ligands (58% and 61% de, entries 1 and 2). These selectivities were higher than the best enantioselectivity (54% ee) achieved with **L1**. An increase in selectivity was achieved by introducing chiral phosphine ligands (71% de, entry 3). It should be noted that *all* reactions with phosphine ligands (non-phosphoramidite) did *not* give rise to the formation of λ -lactam sideproducts **5.14a–c**. This observation is likely due to the more facile nature of the reaction with less-hindered ligands, thus preventing the slower olefin isomerization pathway to compete. In addition, the reactions with phosphine ligands could be run at lowered temperatures (100 °C) whereas phosphoramidite ligands required higher temperatures.

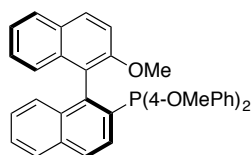
Table 19. Comparing ligand performance between chiral auxiliaries



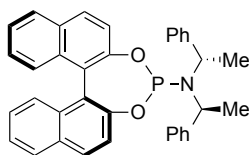
Entry	Substrate	Ligand	Conversion	5.10:5.14	% de
1	5.8a	PPh ₃	100%	1:0	58%
2	5.8c	PPh ₃	100%	1:0	61%
3	5.8c	PL35 or PL36	100%	1:0	71%
4	5.8a	L2	100%	1.5:1	22%
5	5.8a (5.8b)	L2-ent (L2)	100%	7.2:1	73%
6	5.8c	L2	100%	1.5:1	82%
7	5.8b	L33	100%	14.6:1	78%
8	5.8c	L33	70%	1:0	74%
9	5.8b	L34	100%	1:0	79%
10	5.8c	L34	100%	1:0	78%
11	5.8a	L30	100%	1:0	5%
12	5.8b	L30	100%	1:0	77%
13	5.8c	L30	100%	4.5:1	62%



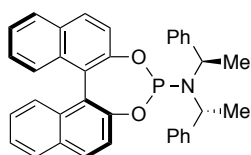
(S)-PL35



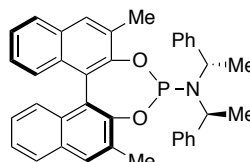
(S)-PL36



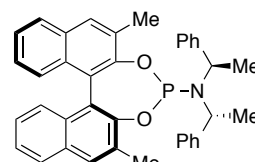
L2



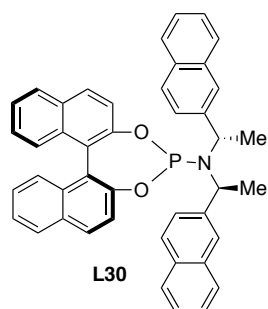
L1



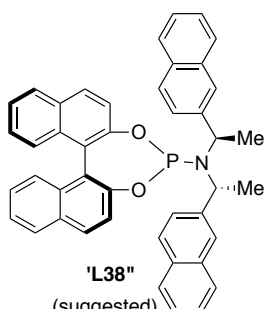
L33



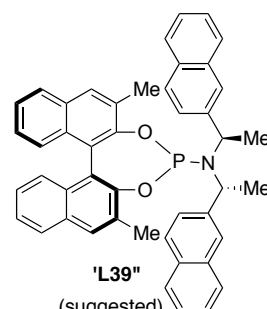
L34



L30



'L38'
(suggested)



'L39'
(suggested)

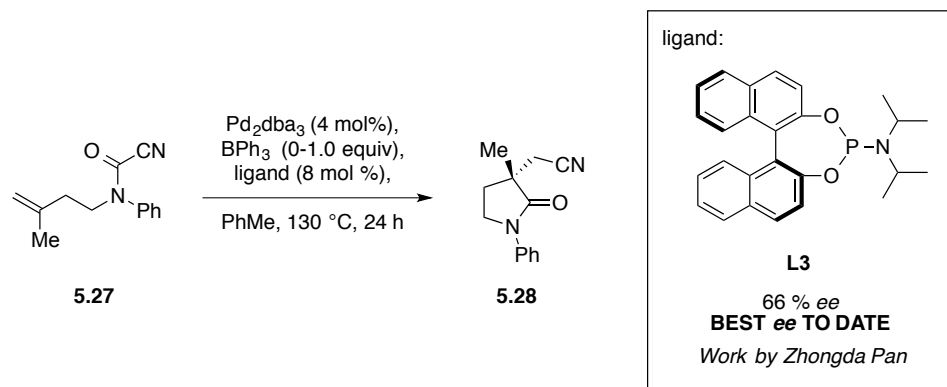
Phosphoramidite ligands without a BINOL backbone did not surpass the selectivity obtained with achiral phosphine ligands, nor did those with BINOL backbones containing achiral amines. The effects of matched vs. mismatched ligand stereochemistries were compounded with the chiral auxiliaries. For example, the enantioselective reaction with **L2** (*S*-BINOL, *S,S*-bisphenyl(ethyl)amine) gave a 14% ee whereas the diastereomeric ligand **L1** (*S*-BINOL, *R,R*-bisphenyl(ethyl)amine) gave a 54% ee. The (*R*)-**5.8a** cyanoformamide with **L2** gave a 22% de, along with a significant amount of material owing to the formation of λ -lactam side-product **5.14** (Table 16, entry 4). The corresponding (*S*)-**5.8b** cyanoformamide with **L2** gave a substantial increase in both diastereo- and chemoselectivity (73% de, entry 5). The reaction with **L2** and the larger auxiliary (*S*)-**5.8c** further increased the diastereoselectivity, but negatively affected the

chemoselectivity (82% de, entry 6). Unfortunately the diastereomer of **L2** (**L1**) had not been available for investigation. This follow-up experiment should be run considering the sizable difference observed in the enantioselective reaction between **L1** vs. **L2**. The diastereomeric ligand trend was less pronounced in comparing the reactivities of **L33** and **L34** (entries 7-10). Both **L33** and **L34** ligands gave relatively superior chemo- and diastereoselectivities for both **5.8b** and **5.8c**. In relation to **L2**, increasing the sterics upon the amine (**L30**) likely had a favorable conformational effect that allowed for exclusive formation of the desired product for both **5.8a** (5% de) and **5.8b** (77% de), though it was evident that **5.8b** was better-matched stereochemically. However, the increased sterics impaired both chemo- and stereoselectivities with cyanoformamide **5.8c**. From these observations, the diastereomer of **L30** (**L38**) and the methylated diastereomer (**L39**) are proposed for further studies with **5.8a** and **5.8b**.

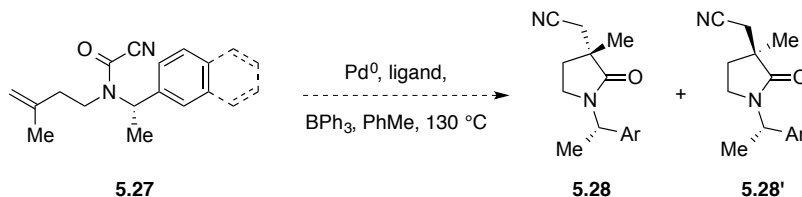
In summary, the use of chiral auxiliaries in metal-catalyzed transformations has been shown to be a promising strategy into achieving greater stereoselectivities. Making predictions about transition state conformations by recognizing reactivity patterns amongst ligand performance is extremely difficult. Employing computational methods would undoubtedly make this daunting challenge more efficient and focused and therefore better enable researchers to design more effective ligands.

5.2.5 RESEARCH PROPOSAL: 3,3-DISUBSTITUED γ -LACTAMS

An extensive enantioselectivity screen had been undertaken for the intramolecular cyanoamidation to form 3,3-disubstituted λ -lactams, though the highest selectivity obtained was 66% ee with phosphoramidite **L3** (Scheme 120). In addition, it had been found that the 5-membered ring formation did not require a Lewis acid additive; however, the selectivities were enhanced in its presence. This likely suggests that the Lewis acid plays a significant role in the migratory insertion step since very little reaction is observed without Lewis acid in analogous δ -lactam-forming reactions. The enhanced selectivity obtained in the cyanoamidation reaction to form δ -lactams by the addition of an *N*-chiral auxiliary prompted the investigation of its effectiveness in λ -lactam formation (Scheme 121).



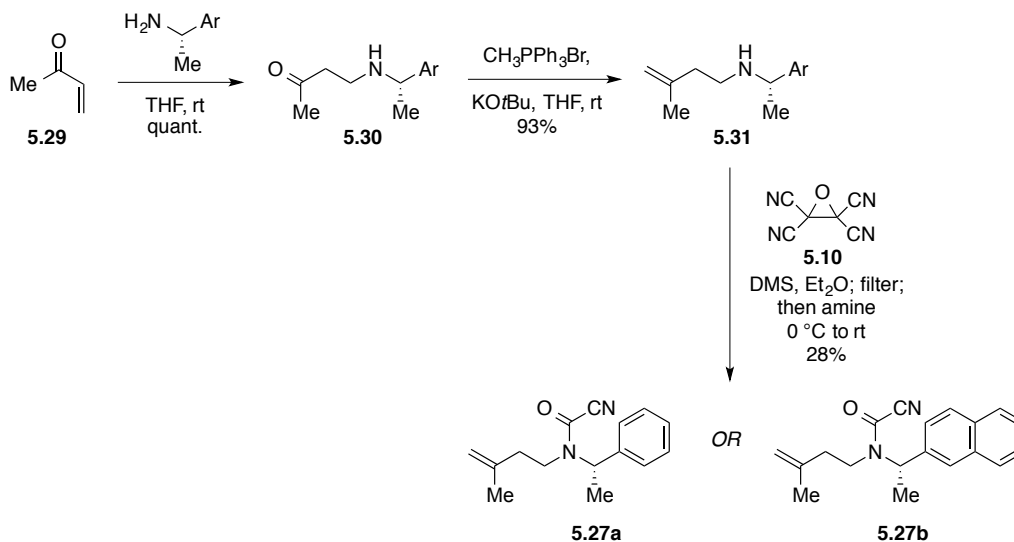
Scheme 120. Enantioselective cyanoamidation to form 3,3-disubstituted λ -lactams



Scheme 121. Proposed diastereoselective cyanoamidation to form 3,3-disubstituted λ -lactams

5.2.6 SUBSTRATE SYNTHESSES

Cyanoformamides **5.27a–b** were readily prepared in three steps. An aza-Michael addition between (*S*)-phenyl(ethyl)amine and MVK gave β -aminoketone **5.30** in quantitative yield. Ketone **5.30** underwent a Wittig olefination with methyltriphenyl phosphonium ylide to provide alkene **5.31** in 93% yield. Acylation of amine **5.31** with dicyano carbonyl (formed *in situ* upon treating TCEO **5.10** with dimethyl sulfide) resulted in cyanoformamides **5.27a** and **5.27b**.



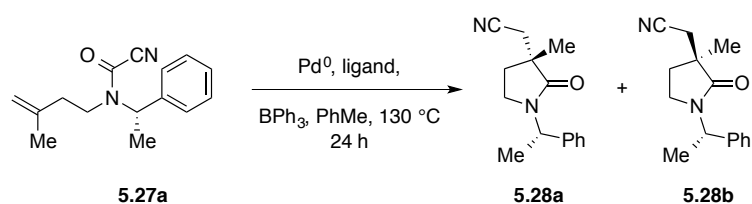
Scheme 122. Preparation of cyanoformamides **5.27a–b**

5.2.7 RESULTS AND DISCUSSION

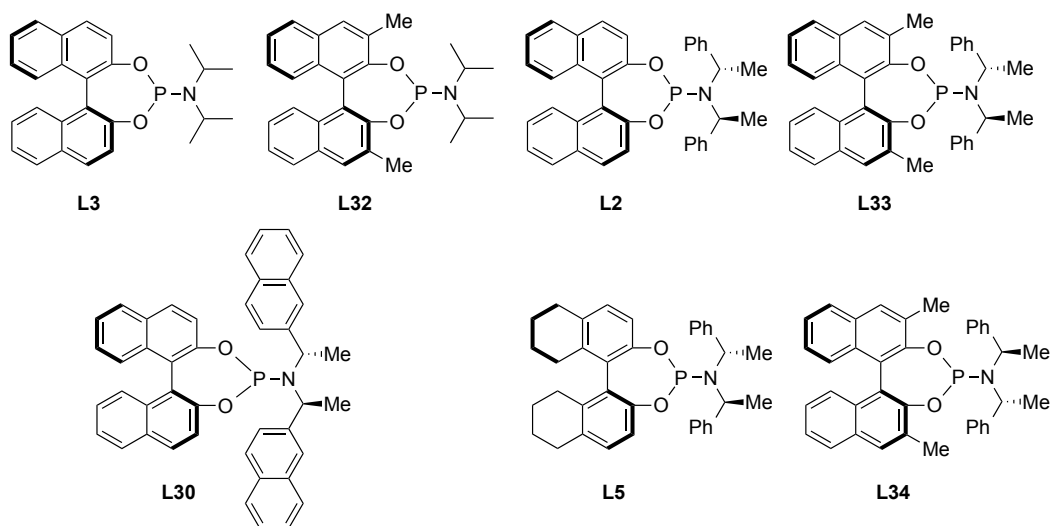
Subjecting cyanoformamide **5.27a** to $\text{Pd}(\text{PPh}_3)_4$ catalysis in the presence of BPh_3 (and absence of chiral ligand) yielded γ -lactam diastereomers **5.28** as a 2:1 mixture (33% de, Table 20, entry 1). Introducing ligand **L3**, which had been shown to give the

highest enantioselectivity in forming γ -lactams (66% ee), surprisingly gave negligible selectivity with the chiral auxiliary cyanoformamide (entry 2, see below table for ligand depictions). The analogous **L32** ligand, containing a methylated BINOL backbone, slightly increased the selectivity (17% de, entry 3). Introducing chirality onto the amine (**L2**) improved the selectivity (26% de), though remained lower than the outcome of the reaction with no chiral additive (entry 4). Substituting the BINOL backbone (**L33**) further increased the diastereoselectivity to match that of reaction with PPh_3 as ligand (33% de, entry 6). The diastereomer of **L33** (**L34**), did not significantly impact the reaction, giving a comparable 29% de (entry 7). The hydrogenated derivative of **L2** (**L5**) also gave a diastereomeric mixture in a 2:1 ratio (entry 8). Increasing the steric bulk on the amine was not favorable (**L30**) and lowered the selectivity (17% de, entry 9). All reactions proceeded with full conversion.

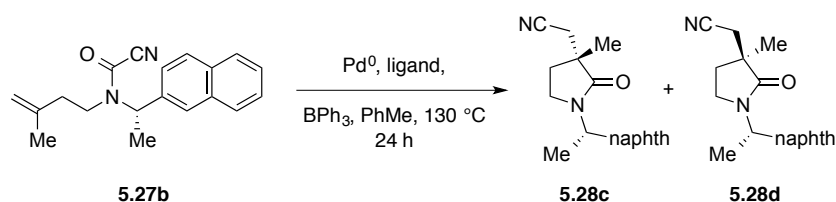
Table 20. Diastereoselective cyanoamidation [*S*-phenyl(ethyl)amine]: 3,3-disubstituted γ -lactams



entry	Ligand	Catalyst	Additive	Solvent	Temp.	Conv.	d.r. (de%)
1	--	$\text{Pd}(\text{PPh}_3)_4$	BPh_3	PhMe	130 °C	100%	2:1 (33%)
2	L3	Pd_2dba_3	BPh_3	PhMe	130 °C	100%	1:1.1 (4%)
3	L32	Pd_2dba_3	BPh_3	PhMe	130 °C	100%	1.4:1 (17%)
4	L2	Pd_2dba_3	BPh_3	PhMe	130 °C	100%	1.7:1 (26%)
5	L2-ent	Pd_2dba_3	BPh_3	PhMe	130 °C	100%	1.3:1 (13%)
6	L33	Pd_2dba_3	BPh_3	PhMe	130 °C	100%	2:1 (33%)
7	L34	Pd_2dba_3	BPh_3	PhMe	130 °C	100%	1.8:1 (29%)
8	L5	Pd_2dba_3	BPh_3	PhMe	130 °C	100%	2:1 (33%)
9	L30	Pd_2dba_3	BPh_3	PhMe	130 °C	100%	1.4:1 (17%)



The added steric bulk of the naphthyl analogue **5.27b** did not improve the selectivity (Table 21). In the absence of ligand, **5.27b** underwent the reaction with $\text{Pd}(\text{PPh}_3)_4$ and BPh_3 to give a mixture of γ -lactams **5.28** in a 1.9:1 ratio (31% de, entry 1). In the absence of Lewis acid, negligible selectivity was obtained (entry 2). This observation was consistent with the enantioselective dependence upon the Lewis acid. Ligand **L3** gave a 26% de with Lewis acid and no selectivity without Lewis acid (entries 3 and 4). The addition of BINOL backbone substituents (**L32**) diminished the selectivity (13% de), though adding chirality to the amine (**L33**) overrode the substituent effect (26% de, entries 5 and 6). Again it was observed that the opposite amine configuration (**L34**) in comparison to **L33** did not affect the outcome of the reaction (26% de, entry 7). Hydrogenating the backbone (**L5**) had no effect in relation to **L2** (26% de, entry 8), and increasing the bulk of the amine (**L30**) was not beneficial (17% de, entry 9). All reactions proceeded in full conversion.

Table 21. Diastereoselective cyanoamidation [*S*-naphthyl(ethyl)amine]: 3,3-disubstituted γ -lactams

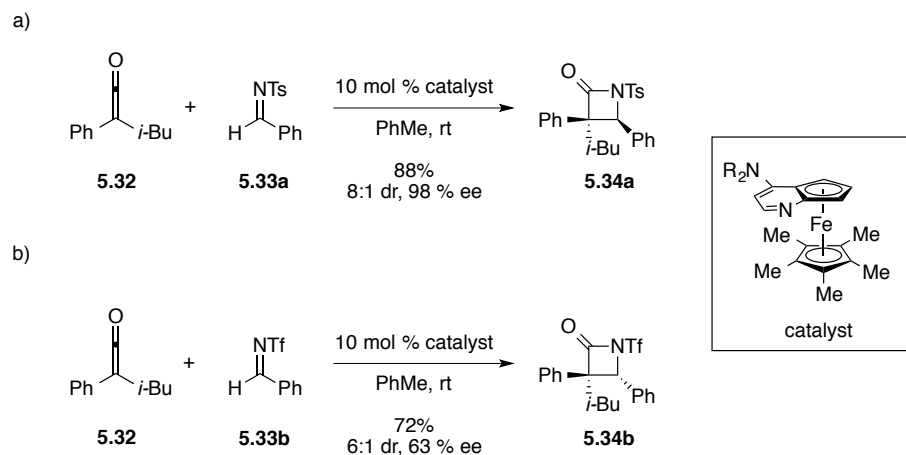
Entry	Ligand	Catalyst	Additive	Solvent	Temp.	Conv.	d.r. (de%)
1	--	$\text{Pd}(\text{PPh}_3)_4$	BPh_3	PhMe	130°C	100%	1.9:1 (31%)
2	--	$\text{Pd}(\text{PPh}_3)_4$	--	PhMe	130°C	100%	1.1:1 (4%)
3	L3	$\text{Pd}(\text{PPh}_3)_4$	BPh_3	PhMe	130°C	100%	1.7:1 (26%)
4	L3	$\text{Pd}(\text{PPh}_3)_4$	--	PhMe	130°C	100%	1:1
5	L32	Pd_2dba_3	BPh_3	PhMe	130°C	100%	1.3:1 (13%)
6	L33	Pd_2dba_3	BPh_3	PhMe	130°C	100%	1.7:1 (26%)
7	L34	Pd_2dba_3	BPh_3	PhMe	130°C	100%	1.7:1 (26%)
8	L5	Pd_2dba_3	BPh_3	PhMe	130°C	100%	1.7:1 (26%)
9	L30	Pd_2dba_3	BPh_3	PhMe	130°C	100%	1.4:1 (17%)

5.2.8 CONCLUDING REMARKS

In summary, cyanoamidation to produce 3,3-disubstituted λ -lactams with aryl(ethyl)amine chiral auxiliaries was not effective at imparting high levels of stereoselectivity. With such auxiliaries, the selectivities were markedly reduced in comparison to the corresponding enantioselective conditions (66% ee, **L3**). The best outcome for the chiral cyanoformamides was without any chiral additive (31–33% de). What was most interesting, was that reactions without Lewis acid gave no diastereoselectivity. Based upon this observation, perhaps we want to revisit the idea of chiral Lewis acids, or at least think about surveying the effects of different Lewis acid additives from a synergistic standpoint.

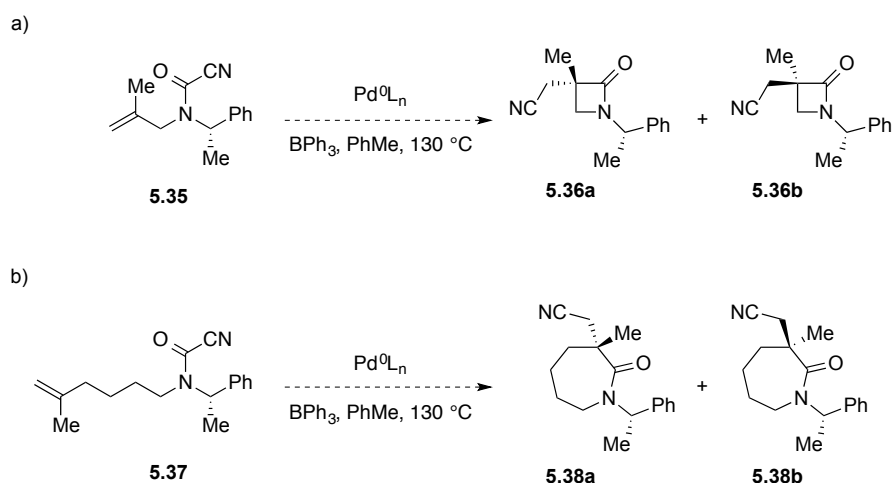
5.2.9 RESEARCH PROPOSAL: β - and ϵ -LACTAMS

The development of efficient methods for the stereoselective construction of β -lactams is becoming increasingly important due to the emergence of bacteria strains that are becoming resistant to existing drugs. The β -lactam antibiotics are the largest and most widely used class of bacterial cell wall synthesis inhibitors. They inhibit the transpeptidase enzymes that mediate peptide cross-linking by mimicking a residue. The susceptibility for attack at the amide carbonyl not only is the mechanism for this inhibition, but is also responsible for their increased resistance in that bacteria have developed lactamases that preferentially attack the lactam before the drug can interact with the desired transpeptidases. Developing methods to produce asymmetrically functionalized β -lactams may lead to compounds with increased selectivity. In particular, α,α -disubstituted lactams may slow the attack by the lactamases, and suitable substitution patterns may serve as secondary binding sights selective for the transpeptidases. In 2002, Fu elegantly demonstrated the stereoselective generation of β -lactams **5.34** containing all-carbon α -stereocenters through a formal [2 + 2] Staudinger cycloaddition with ketenes **5.32** and aldimines **5.33** (Scheme 122a).¹⁵ In 2005, he found that the diastereoselectivity of the reaction was dependent upon the nitrogen substituent (**5.33a** vs **5.33b**) (Scheme 122b).¹⁶ In addition, the reactivity of β -lactams make them versatile synthons for a variety of protein and non-protein amino acids, peptides, peptide turn mimetics, peptidomimetics, taxoid antitumor agents, heterocycles, and other types of compounds of biological and medicinal interest.¹⁷



Scheme 123. Fu's stereoselective synthesis of β -lactams containing all-carbon quaternary stereocenters: a) *cis* selectivity b) *trans* selectivity

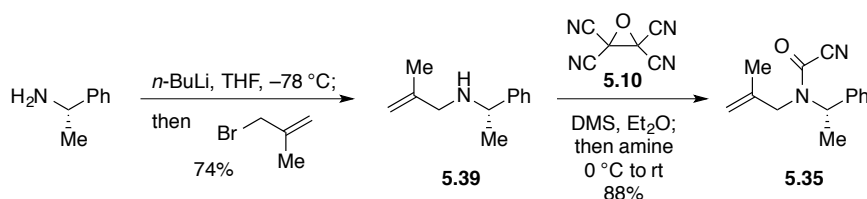
Takemoto had demonstrated that β - and even ϵ -lactams could be accessed through intramolecular cyanoamidation with alkynes in 23% and 79% yield, respectively (see Scheme 103). It was envisioned that both 4- and 7-membered rings (5.36 and 5.38, respectively) containing all-carbon quaternary stereocenters could be accessed via intramolecular cyanoamidation with alkenes (Scheme 123).



Scheme 124. Proposed intramolecular cyanoamidations: a) β -lactams b) ϵ -lactams

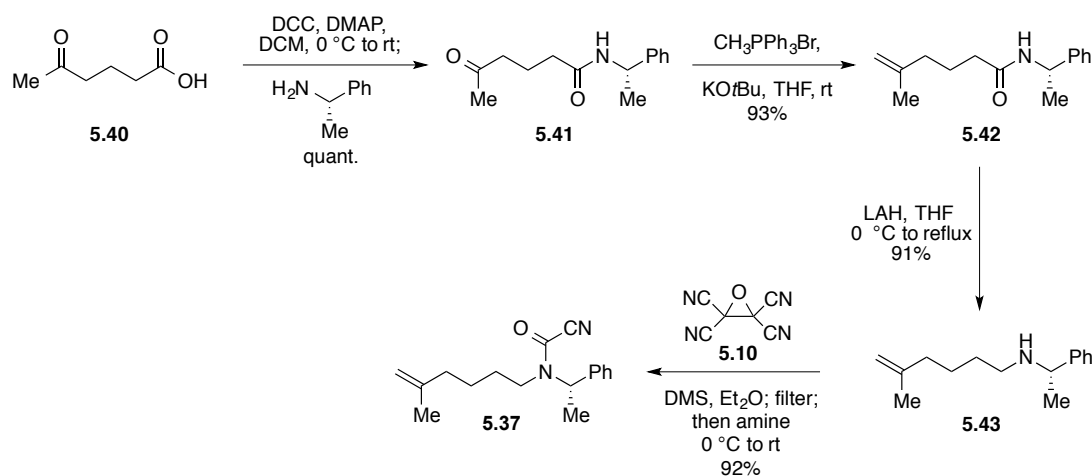
5.2.10 SUBSTRATE SYNTHESSES

The allylic cyanoformamide **5.35** was prepared in two steps from commercially available (*S*)-phenyl(ethyl)amine. Amino alkylation with 3-bromo-2-methylpropene delivered the secondary amine **5.39** in 74% yield (Scheme 125). Installation of the cyanoformamide functionality was accomplished by treating amine **5.39** with TCEO (**5.10**) and DMS to give **5.35** in 88% yield.



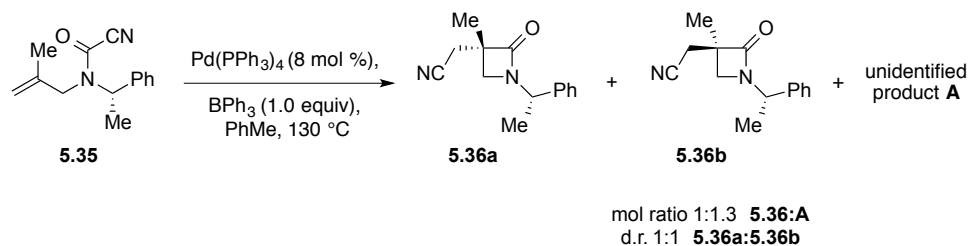
Scheme 125. Synthesis of allylic cyanoformamide **5.35**

The ϵ -lactam cyanoformamide substrate **5.37** was prepared in three steps from commercially-available 5-oxohexanoic acid (**5.40**). A DCC coupling with (*S*)-phenyl(ethyl)amine gave amide **5.41** in quantitative yield (Scheme 126). Ketone **5.41** was olefinated to give alkene **5.42** in 93% yield. Amide reduction with LAH proceeded to give amine **5.43** in 91% yield, and the cyanoformamide **5.37** was obtained in 92% yield upon treatment with TCEO (**5.10**) and DMS.



Scheme 126. Synthesis of cyanoformamide **5.37**

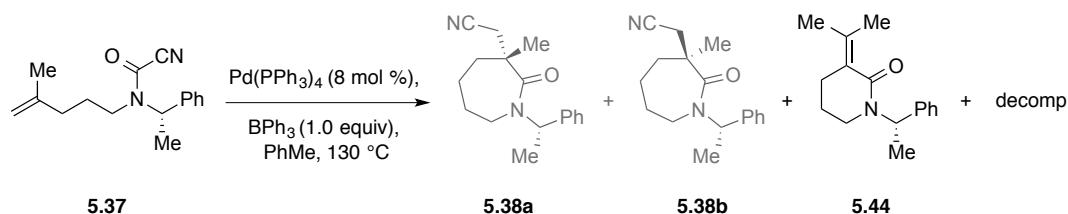
5.2.11 RESULTS AND DISCUSSION



Scheme 127. Cyanoamidation to form β -lactams

Subjecting allylic cyanoformamide **5.35** to $\text{Pd}(\text{PPh}_3)_4$ catalysis with BPh_3 in toluene at 130 °C for 48 h resulted in complete consumption of starting material (Scheme 127). Analysis of the crude ^1H NMR spectrum indicated the formation three distinct products, none of which contained olefinic resonances. The major product, which contains a quintet at 5.33 ppm and a doublet at 1.59 ppm, had been assumed to result from competitive deallylation to provide the secondary cyanoformamide; however, this compound had been independently prepared and the spectra did not match. Unfortunately this product

was not isolated. The ^1H NMR spectrum showed two sets of AB doublets with coupling constants on the order of geminal coupling observed in β -lactams: 3.09 (d, $J = 10.0$ Hz, 1H), 3.08 (d, $J = 10.5$ Hz, 1H); and 2.69 (d, $J = 17.5$, 1H), 2.62 (d, $J = 17.0$ Hz, 1H). The β -lactam diastereomers **5.36** were isolated as a 1:1 mixture, though the material obtained was impure. Assuming the quintet resonance in the unidentified product **A** corresponds to one proton, a 1:1.3 molar ratio between **5.36** and **A** was produced. All attempts to employ phosphoramidite ligands returned only unreacted starting material. Further optimization with additional phosphine ligands should be pursued.



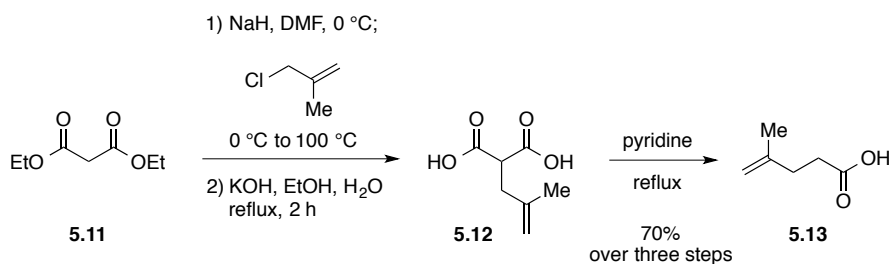
Scheme 128. Unsuccessful cyanoamidation to form ϵ -lactams

Heating cyanoformamide **5.37** with $\text{Pd(PPh}_3)_4$ and BPh_3 in toluene for 48 h resulted in complete consumption of starting material (Scheme 128). Analysis of the ^1H NMR spectra was not definitive: many resonances were broad and relatively unsplit, which may indicate oligomerization. Alternatively, these broadened peaks could be due to interchange between ring conformations of the 7-membered ring. Cooling the NMR probe may resolve these peaks and allow for characterization. A very minor product was isolated which was likely δ -lactam **5.44**, though could not be sufficiently purified. Lactam **5.44** would arise from olefin isomerization prior to cyanoamidation (similar to that of **5.19**; see Figure 36). A lack of reactivity was observed with phosphoramidite ligands. Future work should include a thorough screening of phosphine ligands.

5.2.12 CONCLUDING REMARKS

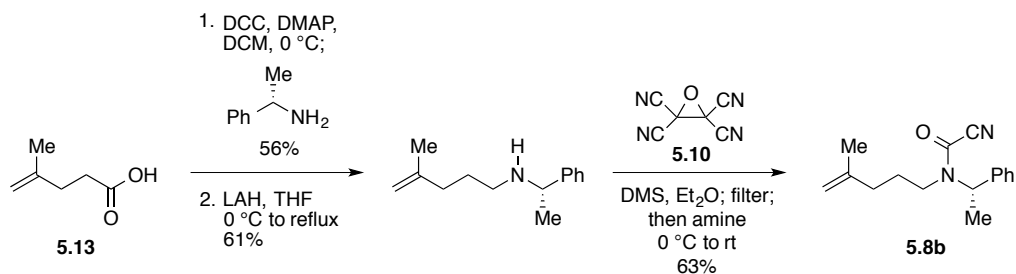
It has been demonstrated that 3,3-disubstituted β -lactams can be prepared via cyanoamidation under $\text{Pd(PPh}_3)_4$ catalysis in the presence of BPh_3 in PhMe at 130 °C. However, under these conditions, the reaction favored formation of an unidentified side product (1.3:1 molar ratio). Although the reaction showed no diastereoselectivity and the substrate was inactive toward phosphoramidite ligands, a thorough optimization screen with chiral phosphine ligands may show enhanced chemo- and stereoselectivity. Attempts to obtain ϵ -lactams via cyanoamidation were inconclusive. The product was unidentifiable by ^1H NMR at room temperature. Further characterization is warranted to elucidate the structure of the material obtained.

5.2.13 EXPERIMENTAL

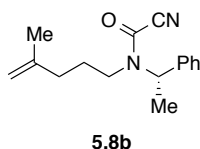


Diethyl malonate (**5.11**) (5.0 g, 30.01 mmol) and DMF (43 mL) were added to a flame-dried flask under N₂ and cooled to 0 °C. NaH (903 mg, 37.62 mmol) was slowly added in portions. After H₂ cessation (30 min), the reaction was warmed to room temperature and 3-chloro-2-methylpropene (1.9 mL, 18.81 mmol) was added. The reaction was heated to 100 °C overnight and then cooled to room temperature before quenching with saturated aq. NH₄Cl. EtOAc was added and the layers were separated. The organic layer was washed with H₂O and the combined aqueous layers were back extracted with EtOAc. The combined organic layers were washed with an aq. 2 M LiCl solution, brine, dried over Na₂SO₄, filtered, and concentrated. The crude diester underwent saponification without further purification: R_f 0.65 (1:4 EtOAc:Hex). Crude diester (6.23 g, 29.07 mmol), KOH (16.3 g, 290 mmol), EtOH (41.5 mL), and H₂O (10 mL) were combined and refluxed overnight (does not afford decarboxylation; saponification done in 2 h). The reaction was cooled to room temperature and EtOAc was added. The layers were separated and the organic phase was washed with water. The organic layer was discarded. The combined aqueous layers were acidified with 1 M HCl and extracted with EtOAc, washed with brine, dried over Na₂SO₄, filtered, and concentrated. The resulting diacid **5.12** was used without further purification: R_f 0.07 (1:4 EtOAc:Hex). Crude

diacid **5.12** (5.48 g, 34.65 mmol) was treated with pyridine (14 mL) and refluxed overnight. The resulting orange solution was cooled to room temperature and EtOAc and 1 M HCl was added. The organic phase was washed with additional 1 M HCl, and the combined aqueous layers were back extracted with EtOAc. The combined organic layers were washed with brine, dried over Na₂SO₄, filtered, and concentrated to give relatively pure acid **5.13** (2.32 g, 20.33 mmol) as a yellow-orange oil. Column chromatography with EtOAc:Hex gave acid **5.13** (2.32 g, 20.33 mmol, 70% over three steps) as a yellow oil: *R_f* 0.20 (1:4 EtOAc:Hex).



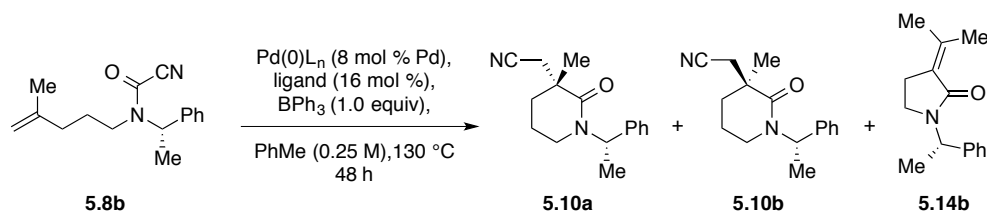
Cyanoformamide **5.8b** was prepared analogously to cyanoformamide **5.1**. Amide (1.24 g, 5.71 mmol, 56%): *R_f* 0.48 (1:1 EtOAc:Hex). *N*-(*S*)-phenyl(ethyl)-4-methyl-4-pentanamine (757 mg, 3.48 mmol, 61%): *R_f* 0.5 (2:3 EtOAc:Hex + 1% TEA). Cyanoformamide **5.8b** (559 mg, 2.18 mmol, 63%): *R_f* 0.75 (1.5:3.5 EtOAc:Hex).



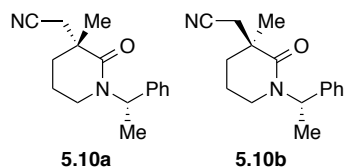
Rotamers 1.2:1

¹H NMR (500 MHz; CDCl₃) δ 7.43-7.32 (m, 5H), 5.74 (q, *J* = 7.1 Hz, 1H), 4.69 (s, 1H), 4.57 (d, *J* = 0.7 Hz, 1H), 3.29 (ddd, *J* = 14.7, 10.9, 5.6 Hz, 1H), 3.36-3.23 (m, 1H), 1.90

(app t, $J = 7.4$ Hz, 2H), 1.60 (d, $J = 7.2$ Hz, 3H), 1.59 (s, 3H), 1.39-1.29 (m, 2H); ^1H NMR (500 MHz; CDCl_3) δ 7.43-7.32 (m, 5H), 5.57 (q, $J = 6.9$ Hz, 1H), 4.65 (s, 1H), 4.54 (d, $J = 0.8$ Hz, 1H), 3.07 (ddd, $J = 16.5, 11.0, 5.0$ Hz, 1H), 3.07 (ddd, $J = 16.5, 11.0, 5.0$ Hz, 1H), 1.84 (app t, $J = 7.4$ Hz, 2H), 1.72 (d, $J = 7.0$ Hz, 3H), 1.67-1.49 (m, 2H), 1.57 (s, 3H); ^{13}C NMR (126 MHz; CDCl_3): δ 145.4, 144.5, 144.0, 143.5, 138.1, 137.5, 129.0, 128.8, 128.7, 128.5, 127.7, 127.1, 111.1, 111.0, 110.9, 110.7, 57.6, 52.8, 45.3, 42.7, 35.0, 34.9, 28.5, 25.2, 22.0, 17.9, 16.5 (one carbon signal overlapped for the two rotamers).

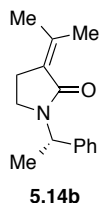


General Procedure: A 0.25 M solution of **5.8** was prepared in a nitrogen-filled glovebox. $\text{Pd(PPh}_3)_4$ (11.4 mg, 0.01 mmol) or $\text{Pd}_2(\text{dba})_3$ (4.5 mg, 0.0048 mmol), ligand (0.19 mmol), and BPh_3 (29 mg, 0.12 mmol) were weighted into a 1-dram vial, followed the addition of **5.8** solution (0.5 mL, 30 mg, 0.12 mmol). The vial was equipped with a stir bar, the vial was sealed with a teflon screw cap, and the vessel was placed in an aluminum block and heated to 130 $^\circ\text{C}$ for 48 h. The vial was allowed to cool to room temperature and the mixture was concentrated. The diastereomeric ratio was determined by ^1H NMR integration. Prep TLC was unable to separate the diastereomers: **5.10** R_f 0.10 (1:4 EtOAc:Hex); **5.14b** R_f 0.44 (1:4 EtOAc:Hex).



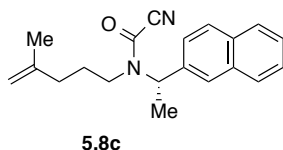
^1H NMR (500 MHz; CDCl_3) δ 7.36-7.33 (m, 2H), 7.29-7.27 (m, 1H), 7.26-7.24 (m, 2H), 6.07 (q, $J = 7.1$ Hz, 1H), 3.18 (ddd, $J = 12.2, 10.4, 4.8$ Hz, 1H), 2.87 (app dddd, $J = 12.2, 5.1, 3.7, 1.6$ Hz, 1H), 2.81 (d, $J = 16.5$ Hz, 1H), 2.68 (d, $J = 16.5$ Hz, 1H), 1.97 (ddd, $J = 13.4, 11.8, 3.7$ Hz, 1H), 1.84 (app dddd, $J = 13.4, 5.1, 3.4, 1.7$ Hz, 1H), 1.81-1.70 (m, 2H), 1.52 (d, $J = 7.1$ Hz, 3H), 1.41 (s, 3H);

^1H NMR (500 MHz; CDCl_3) δ 7.36-7.33 (m, 2H), 7.30-7.27 (m, 1H), 7.26-7.24 (m, 2H), 6.08 (q, $J = 7.1$ Hz, 1H), 3.09 (dtd, $J = 12.5, 4.8, 1.4$ Hz, 1H), 2.83 (d, $J = 16.6$ Hz, 1H), 2.79-2.73 (m, 1H), 2.65 (d, $J = 16.5$ Hz, 1H), 1.81-1.78 (m, 2H), 1.73-1.68 (m, 2H), 1.50 (d, $J = 7.1$ Hz, 3H), 1.38 (s, 3H).



^1H NMR (500 MHz; CDCl_3) δ 7.33-7.30 (m, 5H), 5.59 (q, $J = 7.1$ Hz, 1H), 3.28 (td, $J = 9.4, 5.1$ Hz, 1H), 2.93 (td, $J = 9.5, 4.4$ Hz, 1H), 2.64-2.58 (m, 1H), 2.56-2.49 (m, 1H), 2.31 (app t, $J = 2.0$ Hz, 3H), 1.76 (s, 3H), 1.53 (d, $J = 7.1$ Hz, 3H); ^{13}C NMR DEPT (126 MHz; CDCl_3) δ 168.5, 141.4, 140.4, 128.4, 127.3, 127.2, 124.3, 48.8 (CH), 38.5 (CH_2), 23.9 (CH_2), 23.5 (CH_3), 19.0 (CH_3), 16.0 (CH_3); IR (thin film): 3086, 3061,

2972, 2938, 2871, 1629, 1493, 1485, 1465, 1434, 1377, 1355, 1299, 1201, 1175, 1056, 1042, 753, 675, 663, 654, 651, 642, 630, 618, 606.

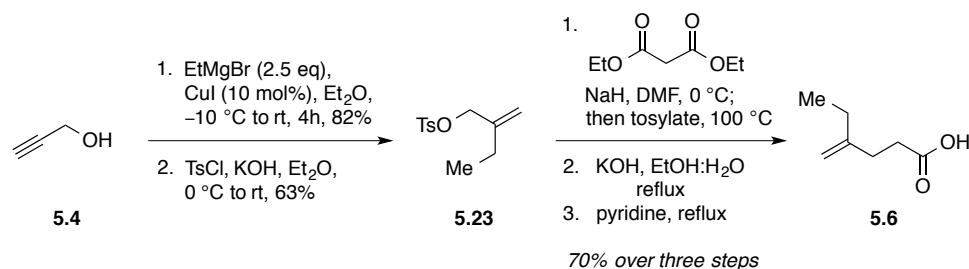


Rotamers 1:1.24

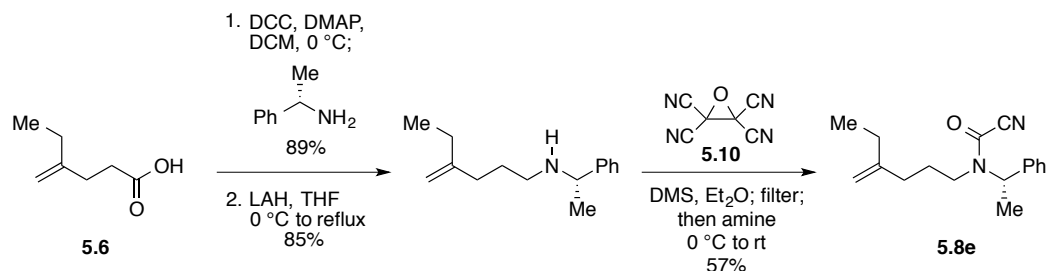
^1H NMR (500 MHz; CDCl_3) δ 7.89-7.84 (m, 3H), 7.78 (d, $J = 3.7$ Hz, 1H), 7.56-7.52 (m, 2H), 7.38 (ddd, $J = 8.5, 6.7, 1.8$ Hz, 1H), 5.91 (q, $J = 7.1$ Hz, 1H), 4.63 (app s, 1H), 4.51 (app s, 1H), 3.36 (ddd, $J = 15.6, 11.0, 5.0$ Hz, 1H), 3.26 (ddd, $J = 15.6, 10.9, 5.0$ Hz, 1H), 1.87 (app t, $J = 7.4$ Hz, 2H), 1.84 (d, $J = 6.9$ Hz, 3H), 1.69-1.57 (m, 2H), 1.48 (s, 3H);

^1H NMR (500 MHz; CDCl_3) δ 7.89-7.84 (m, 4H), 7.78 (d, $J = 3.7$ Hz, 1H), 7.56-7.52 (m, 2H), 7.38 (ddd, $J = 8.5, 6.7, 1.8$ Hz, 1H), 5.72 (q, $J = 6.9$ Hz, 1H), 4.60 (app s, 1H), 4.48 (app s, 1H), 3.16 (ddd, $J = 13.5, 11.4, 5.0$ Hz, 1H), 3.03 (ddd, $J = 13.5, 11.3, 5.1$ Hz, 1H), 1.80 (app t, $J = 7.4$ Hz, 2H), 1.72 (d, $J = 7.1$ Hz, 3H), 1.46 (s, 3H), 1.44-1.31 (m, 2H);

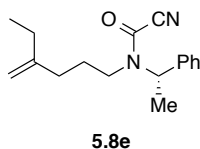
^{13}C NMR (126 MHz; CDCl_3) δ 145.6, 144.6, 143.9, 143.4, 135.5, 134.8, 133.1, 133.1, 128.9, 128.8, 128.1, 128.0, 127.99, 127.7, 126.9, 126.8, 126.7, 126.3, 125.9, 125.8, 125.1, 111.2, 111.04, 110.98, 110.7, 57.8, 52.8, 45.3, 42.8, 35.0, 34.9, 28.6, 25.3, 21.86, 21.84, 18.0, 16.6 (one carbon signal overlapped for the two rotamers).



2-ethyl-2-propenol (**5.23**) was prepared according to the procedure in Experimental 5.1.5. The crude 2-ethyl-2-propenol (**5.23**) (400 mg, 4.64 mmol) was combined with Et₂O (9.3 mL) and cooled to 0 °C. TsCl (930 mg, 4.88 mmol) and KOH (2.6 g, 46.4 mmol) were added and the mixture was stirred at 0 °C for 1 h. The reaction was allowed to come to room temperature and stirred for an additional 1 h and monitored by TLC. The resulting tan mixture was added to a separatory funnel before diluting with H₂O (CAUTION: exotherm). EtOAc was added and the layers separated. The organic layer was washed with H₂O and the combined aqueous layers were back extracted with EtOAc. The combined organic layers were washed with brine, dried over Na₂SO₄, filtered, and concentrated. Incomplete conversion was discovered due to difficult visualization of TLC stained with KMnO₄. The crude product was purified by flash chromatography (DCM:Hex) to give tosylate **5.23** (700 mg, 2.90 mmol, 63%) as a yellow oil: R_f 0.24 (1.5:3.5 DCM:Hex). Acid **5.6** was prepared analogously to acid **5.13**. Alkylated malonate ester (2.91 mmol theoretical yield): R_f 0.64 (1.5:3.5 EtOAc:Hex). Diacid: R_f 0.05 (1:4 EtOAc:Hex). Acid **5.6** (260 mg, 2.03 mmol, 70% over three steps): R_f 0.55 (1:1 EtOAc:Hex).



Cyanoformamide **5.8e** was prepared analogously to cyanoformamide **5.8b**. Amide (420 mg, 1.82 mmol, 89%, pale yellow oil): R_f 0.39 (2:3 EtOAc:Hex). (*S*)-*N*-phenyl(ethyl)-4-ethyl-4-pentenamine (240 mg, 1.10 mmol, 85%, colorless oil): R_f 0.15 (2:3 EtOAc:Hex). Cyanoformamide **5.8e** (239 mg, 0.88 mmol, 57%, pale yellow oil): R_f 0.63 (1:4 EtOAc:Hex).

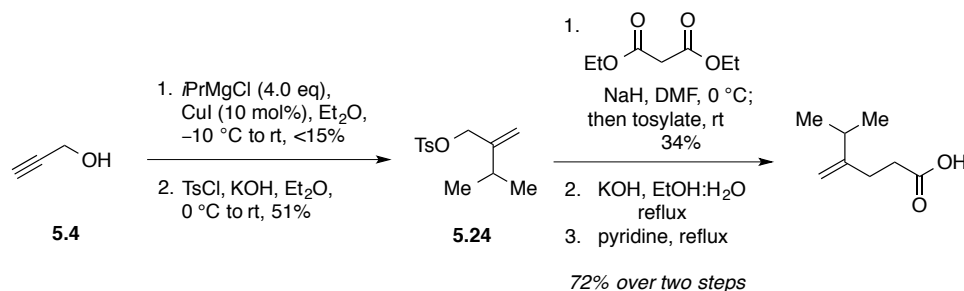


Rotamers 1.2:1

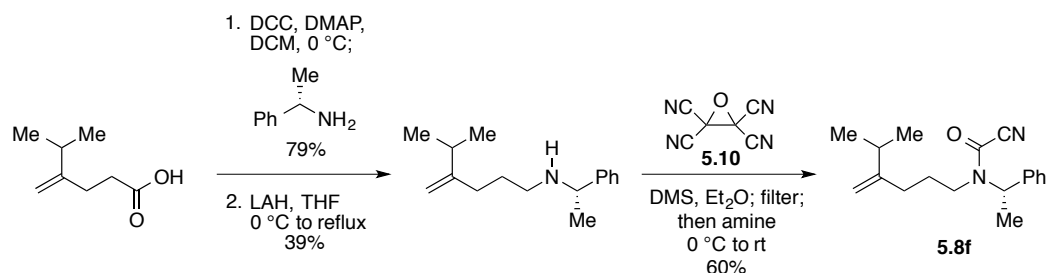
¹H NMR (500 MHz; CDCl₃) δ 7.43-7.31 (m, 5H), 5.73 (q, J = 7.1 Hz, 1H), 4.70 (d, J = 1.2 Hz, 1H), 4.58 (d, J = 0.6 Hz, 1H), 3.35-3.23 (m, 2H), 1.91 (app t, J = 7.6 Hz, 2H), 1.88-1.83 (m, 2H overlap), 1.72 (d, J = 7.0 Hz, 3H), 1.67-1.49 (m, 2H), 0.96 (t, J = 7.5, 3H);

¹H NMR (500 MHz; CDCl₃) δ 7.43-7.31 (m, 5H), 5.57 (q, J = 6.9 Hz, 1H), 4.66 (s, 1H), 4.55 (s, 1H), 3.07 (ddd, J = 16.5 11.5, 5.0 Hz, 1H), 3.07 (ddd, J = 16.5, 11.0, 5.0 Hz, 1H), 1.88-1.83 (m, 4H overlap), 1.60 (d, J = 7.1 Hz, 3H), 1.42-1.25 (m, 2H), 0.94 (t, J = 7.0 Hz, 3H); ¹³C NMR (126 MHz; CDCl₃): δ 149.5, 149.0, 145.4, 144.5, 138.1, 137.5, 129.0, 128.8, 128.7, 128.5, 127.7, 127.1, 111.0, 110.9, 108.8, 108.4, 57.6, 52.8,

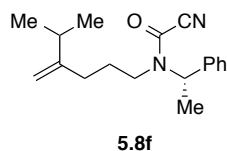
45.4, 42.9, 33.5, 33.4, 28.8, 28.3, 25.5, 17.9, 16.5, 12.16, 12.13 (one carbon signal overlapped for the two rotamers).



2-isopropyl-2-propenol was prepared according to Experimental 5.1.5 and was purified by column chromatography. The isopropylmagnesium chloride (2.0 M THF) was not titrated, though 1.5 equiv. excess was used. 2-isopropyl-2-propenol (588 mg, 5.87 mmol, 15%, yellow oil): R_f 0.64 (1.5:3.5 acetone:Hex). Tosylate **5.24** was prepared analogously to tosylate **5.23**. Tosylate **5.24** (333mg, 1.31 mmol, 51%, pale yellow oil): R_f 0.63 (1:4 EtOAc:Hex). 4-isopropyl-4-pentenoic acid was prepared analogously to acid **5.6**. Alkylation of dimethyl malonate with tosylate **5.24** was performed at room temperature (rather than heating to $100\text{ }^\circ\text{C}$) and purified by flash chromatography (EtOAc:Hex) to give the alkylated malonate ester as a colorless oil (263 mg, 1.09 mmol, 34%): R_f 0.68 (1:4 EtOAc:Hex). Diacid: R_f 0.07 (1:1 EtOAc:Hex). 4-isopropyl-4-pentenoic acid (110 mg, 0.77 mmol, 72% over two steps, yellow oil): R_f 0.33 (1:1 EtOAc:Hex).



Cyanoformamide **5.8f** was prepared analogously to cyanofomamide **5.8b**. (*S*)-*N*-phenyl(ethyl)-4-isopropyl-4-pentenamide (149 mg, 0.65 mmol, 79%, viscous yellow liquid): *R_f* 0.20 (1:4 EtOAc:Hex). (*S*)-*N*-phenyl(ethyl)-4-isopropyl-4-pentenamine (61mg, 0.26 mmol, 39%): *R_f* 0.13 (2:3 EtOAc:Hex). Cyanoformamide **5.8f** (44 mg, 1.55 mmol, 60%, pale yellow oil): *R_f* 0.57 (1:4 EtOAc:Hex).



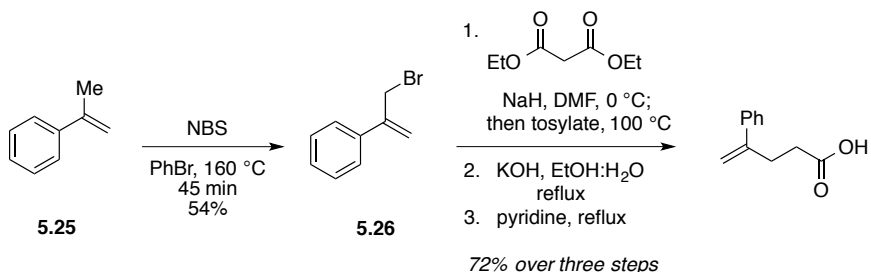
Rotamers 1.2:1

¹H NMR (500 MHz; CDCl₃) δ 7.43-7.31 (m, 5H), 5.73 (q, *J* = 7.2 Hz, 1H), 4.72 (s, 1H), 4.53 (d, *J* = 1.0 Hz, 1H), 3.37-3.24 (m, 2H), 2.05 (sept, *J* = 7.0 Hz, 1H overlap), 1.91 (app t, *J* = 7.5 Hz, 2H), 1.72 (d, *J* = 7.0 Hz, 3H), 1.66-1.50 (m, 2H), 0.96 (d, *J* = 6.8 Hz, 6H).

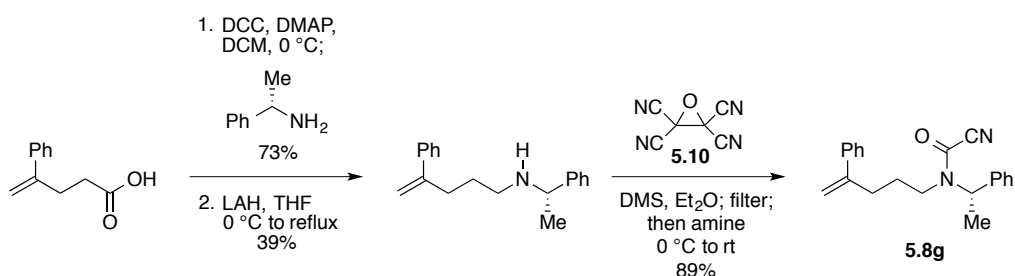
¹H NMR (500 MHz; CDCl₃) δ 7.43-7.31 (m, 5H), 5.57 (q, *J* = 6.9 Hz, 1H), 4.68 (s, 1H), 4.51 (d, *J* = 1.1 Hz, 1H), 3.08 (ddd, *J* = 16.0, 11.0, 5.0 Hz, 1H), 3.08 (ddd, *J* = 16.0, 11.0, 5.0 Hz, 1H), 2.05 (sept, *J* = 7.0 Hz, 1H overlap), 1.85 (app t, *J* = 7.6 Hz, 2H), 1.61 (d, *J* = 7.1 Hz, 3H), 1.45-1.30 (m, 2H), 0.94 (d, *J* = 6.8 Hz, 6H);

¹³C NMR (126 MHz; CDCl₃) δ 154.0, 153.6, 145.4, 144.5, 138.1, 137.5, 129.0, 128.8,

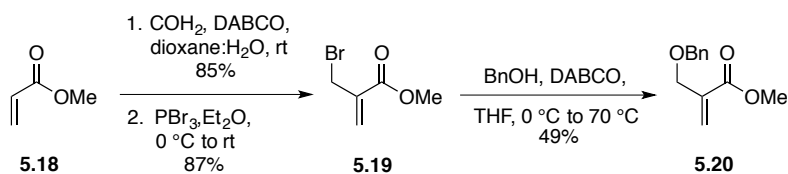
128.7, 128.5, 127.7, 127.1, 111.0, 110.9, 107.4, 107.0, 57.7, 52.8, 45.5, 43.0, 33.35, 33.34, 31.6, 31.5, 29.3, 25.9, 21.67, 21.66, 17.9, 16.5 (two rotamers).



4-phenyl-4-pentenoic acid was prepared analogously to acid **5.6**. Alkylated malonate ester: R_f 0.43 (1:4 EtOAc:Hex). Diacid: R_f 0.1 (1:1 EtOAc:Hex). 4-phenyl-4-pentenoic acid (358 mg, 0.77 mmol, 72% over three steps, yellow oil): R_f 0.38 (1:1 EtOAc:Hex).



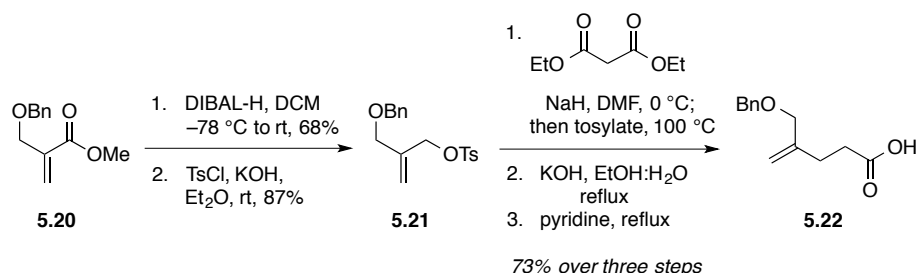
Cyanoformamide **5.8g** was prepared analogously to cyanoformamide **5.8b**. (*S*)-*N*-phenyl(ethyl)-4-phenyl-4-pentenamide (443 mg, 1.59 mmol, 73%, colorless solid): R_f 0.38 (1:4 EtOAc:Hex). (*S*)-*N*-phenyl(ethyl)-4-phenyl-4-pentenamine (163mg, 0.61 mmol, 39%): R_f 0.1 (1:1:10 EtOAc:TEA:Hex). Cyanoformamide **5.8g** (172 mg, 0.54 mmol, <89%, yellow-orange oil): R_f 0.46 (1:4 EtOAc:Hex). See spectra (contains impurities).



Methacrylate (**5.18**) (3.1 mL, 34.85 mmol), formaldehyde (37% in H₂O; 0.9 mL, 11.62 mmol), DABCO (1.3 g, 11.62 mmol), dioxane (12 mL) and H₂O (12 mL) were combined in a flask and stirred at room temperature for 22 h. Et₂O was added and the layers were separated. The organic layer was washed with water and the combined aqueous layers were back extracted with Et₂O. The combined organic layers were washed with brine, dried over Na₂SO₄, filtered, and concentrated. The crude mixture^{iv} was purified by flash chromatography: R_f 0.2 (1:4 EtOAc:Hex). Methyl 2-(bromomethyl)acrylate was obtained as a colorless oil (1.14 g, 9.8 mmol, 85%): R_f 0.25 (2:3 Et₂O:Hex). Methyl 2-(bromomethyl)acrylate (1.14 g, 10.14 mmol) was added to a flame-dried flask with Et₂O (11 mL) under N₂ and cooled to 0 °C. PBr₃ (0.95 mL, 10.14 mmol) was slowly added and the reaction was allowed to come to room temperature overnight. The resulting orange solution was cooled to 0 °C and quenched with cold H₂O (turned colorless). The solution was diluted with Et₂O and the layers were separated. The organic layer was washed with H₂O and the combined aqueous layers were back extracted with Et₂O. The combined organic layers were washed with brine, dried over Na₂SO₄, filtered, and concentrated. The relatively pure bromide **5.19** was obtained without further purification (1.58 g, 8.83 mmol, 87%, pale yellow oil): R_f 0.85 (2:3 EtOAc:Hex). Bromide **5.19** (777 mg, 4.34 mmol), benzyl alcohol (0.9 mL, 8.68 mmol), and THF (9.3 mL) were combined in a scintillation vial. Upon addition of

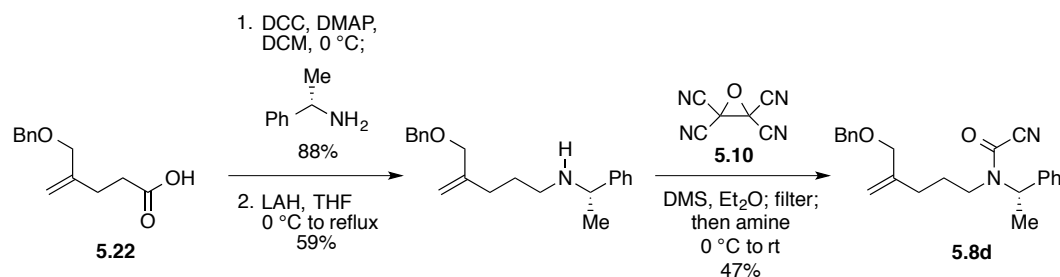
^{iv} Methyl 2-(bromomethyl)acrylate readily polymerizes in rotavap basin upon removal of EtOAc. Chromatography with Et₂O:Hex is optimal.

DABCO (731 mg, 6.51 mmol), a colorless precipitate formed. Heating the reaction to 70 °C overnight resulted in loss of solvent. The mixture was cooled to room temperature and filtered into a separatory funnel and the precipitate was washed with Et₂O. The filtrate was washed with 1 M HCl and brine, dried over Na₂SO₄, filtered, and concentrated. The crude product was purified by flash chromatography (Et₂O:Hex) and the benzyl ether **5.20** was obtained as a colorless oil (439 mg, 2.13 mmol, 49%): *R_f* 0.48 (1:4 Et₂O:Hex).

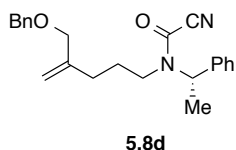


Enoate **5.20** (439 mg, 2.13 mmol) was added to a flame-dried flask with DCM (7 mL) under N₂ and cooled to -78 °C. DIBAL-H (1.0 M in PhMe; 6.4 mL, 6.39 mmol) was added dropwise over 25 min. The solution was stirred at -78 °C for 2 h then allowed to come to room temperature and stirred for 24 h. The reaction was cooled to 0 °C and 30 mL of MeOH was added and allowed to stir overnight. The resulting precipitate was filtered and washed with EtOAc. The filtrate was concentrated onto celite and purified by flash chromatography (EtOAc:Hex) to give the corresponding allylic alcohol as a colorless oil (315 mg, 1.77 mmol, 68%): *R_f* 0.19 (1:4 EtOAc:Hex). 2-((benzyloxy)methyl)-2-propenol (310 mg, 1.74 mmol) was treated with TsCl (332 mg, 1.74 mmol), KOH (976 mg, 17.40 mmol) and Et₂O (3.5 mL) in a scintillation vial and stirred for 20 h at room temperature. The reaction mixture was dumped into a separatory

prior to adding H₂O [CAUTION: exotherm] and EtOAc. The layers were separated and the organic layer was washed with H₂O. The combined aqueous layers were back extracted with EtOAc. The combined organic layers were washed with brine, dried over Na₂SO₄, filtered and concentrated. The crude product was purified by flash chromatography (1:9 EtOAc:Hex) to give tosylate **5.21** as a colorless oil (503 mg, 1.51 mmol, 87%): *R_f* 0.44 (1:4 EtOAc:Hex). Acid **5.22** was prepared analogously to acid **5.6**. Alkylated malonate ester (2.42 mmol scale): *R_f* 0.46 (1:4 EtOAc:Hex). Diacid: *R_f* 0.02 (1:4 EtOAc:Hex). Acid **5.22** (242 mg, 1.10 mmol, 73% over three steps): *R_f* 0.54 (3:2 EtOAc:Hex).



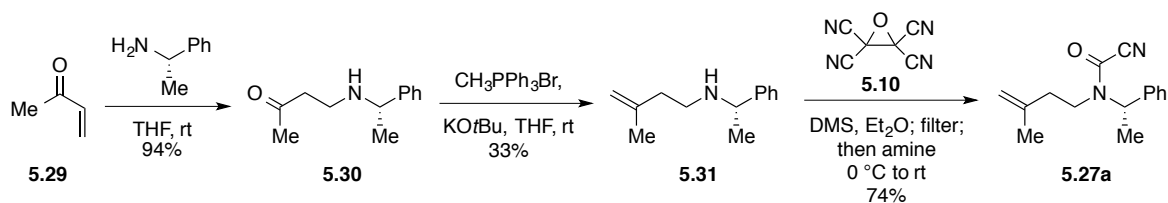
Cyanoformamide **5.8d** was prepared analogously to cyanoformamide **5.8b**. (*S*)-*N*-phenyl(ethyl)-4-((benzyloxyl)methyl)-4-pentenamide (347 mg, 1.03 mmol, 88%): *R_f* 0.21 (1.5:3.5 EtOAc:Hex). (*S*)-*N*-phenyl(ethyl)-4-((benzyloxyl)methyl)-4-pentenamine (196 mg, 0.63 mmol, 59%): *R_f* 0.05 (1.5:3.5 EtOAc:Hex). Cyanoformamide **5.8d** [complete after 2 h] (107 mg, 0.30 mmol, 47%, pale yellow oil): *R_f* 0.34 (1:4 EtOAc:Hex).



Rotamers 1.3:1

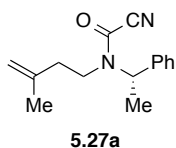
^1H NMR (500 MHz; CDCl_3) δ 7.41-7.28 (m, 10H), 5.71 (q, J = 7.1 Hz, 1H), 5.03 (s, 1H), 4.81 (s, 1H), 4.44 (s, 2H), 3.83 (s, 2H), 3.30 (ddd, J = 16.5, 11.0, 4.0, 1H), 3.37-3.236 (m, 1H), 1.99 (app t, J = 7.5 Hz, 2H), 1.69-1.53 (m, 2H), 1.57 (d, J = 7.1 Hz, 3H);

^1H NMR (500 MHz; CDCl_3) δ 7.32 (s, 10H), 5.55 (q, J = 6.9 Hz, 1H), 5.00 (s, 1H), 4.79 (s, 1H), 4.43 (s, 2H), 3.81 (s, 2H), 3.09 (ddd, J = 16.5, 11.0, 5.0 Hz, 1H), 3.09 (ddd, J = 16.5, 11.5, 5.0 Hz, 1H), 1.92 (app q, J = 6.9 Hz, 3H), 1.69 (d, J = 7.0 Hz, 3H), 1.46-1.31 (m, 2H); ^{13}C NMR (126 MHz; CDCl_3) δ 145.4, 144.5, 144.3, 143.9, 138.2, 138.1, 138.06, 137.5, 129.0, 128.9, 128.7, 128.5, 128.39, 128.36, 127.7, 127.6, 127.1, 113.0, 112.5, 111.0, 110.9, 72.8, 72.7, 72.1, 72.0, 57.6, 52.8, 45.4, 42.8, 30.4, 30.3, 28.7, 25.4, 17.9, 16.5 (two rotamers).



(*S*)-phenyl(ethyl) amine (2.2 mL, 17.1 mmol), methyl vinyl ketone (**5.29**) (1.4 mg, 17.1 mmol), and THF (17 mL) were combined under N_2 and stirred at room temperature for 12 h. The solution was concentrated to provide the relatively pure crude amino ketone in 94% yield as a yellow-orange oil (3.08 g, 15.15 mmol): R_f 0.46 (3:7:1 EtOAc:Hex:TEA). Methyltriphenylphosphonium bromide (11.2 g, 31.14 mmol)

and potassium *tert*-butoxide (1.0 M in THF; 31.1 mL, 31.1 mmol) were added to a flame-dried flask under N₂ at room temperature. The yellow mixture was stirred for 1 h before amino ketone **5.30** (3.0 g, 14.6 mmol) was added as a solution in THF (5 mL). The resulting mixture was stirred at room temperature overnight. Saturated aq. NH₄Cl was added and the mixture turned from yellow to a homogenous orange solution. Et₂O and H₂O were added and the layers were separated. The organic layer was washed with H₂O, and the combined aqueous layers were back extracted with Et₂O. The combined organic layers were washed with brine, dried over Na₂SO₄, filtered, and concentrated. The crude product was purified by flash chromatography (3:1:1 EtOAc:Hex:MeOH) to provide amino alkene **5.31** as an orange oil (922 mg, 4.87 mmol): R_f 0.40 (3:1:1 EtOAc:Hex:MeOH). TCEO (2.1 g, 14.6 mmol) and Et₂O (6.1 mL, 33%) were added to a flame-dried flask under N₂ and cooled to 0 °C. DMS (1.1 mL, 15.1 mmol) was added slowly and the resulting solution was stirred at 0 °C for 45 min. The resulting orange dicyano carbonyl solution was syringe-filtered into a cooled (0 °C) solution of azeotropically dried amine **5.31** (920 mg, 4.86 mmol) and Et₂O (5 mL). *Note:* use purple-tipped needles upon filtering to avoid clogging. The reaction was allowed to come to room temperature and stirred for 48 h. The reaction was concentrated onto celite and purified by flash chromatography (EtOAc:Hex) to afford cyanoformamide **5.27a** as a pale yellow oil (875 mg, 3.61 mmol, 74%): R_f 0.69 (1.5:3.5 EtOAc:Hex).

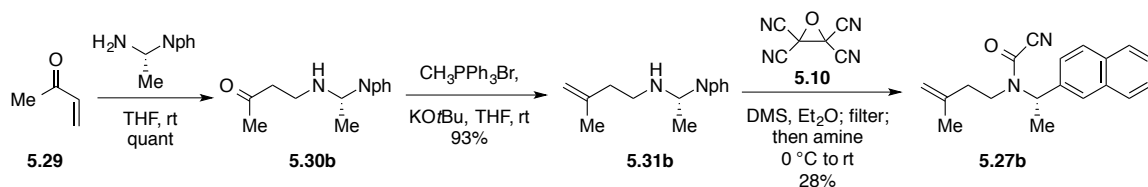


Rotamers 1.2:1

^1H NMR (500 MHz; CDCl_3) δ 7.44-7.33 (m, 5H), 5.75 (q, J = 7.1 Hz, 1H), 4.76 (app t, J = 1.5 Hz, 1H), 4.57 (app d, J = 0.7 Hz, 1H), 3.40 (ddd, J = 10.3, 6.5, 4.2 Hz, 1H), 3.40 (m, 1H), 1.63 (s, 3H), 1.62 (d, J = 7.1 Hz, 3H);

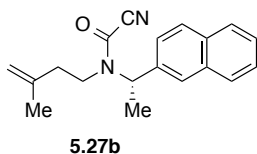
^1H NMR (500 MHz; CDCl_3) δ 7.44-7.33 (m, 5H), 5.58 (q, J = 7.0 Hz, 1H), 4.68 (app t, J = 1.4 Hz, 1H), 4.51 (app d, J = 0.7 Hz, 1H), 3.21 (ddd, J = 16.3, 11.0, 5.4 Hz, 1H), 3.21 (ddd, J = 16.5, 11.5, 5.5 Hz, 1H), 1.73 (d, J = 7.0 Hz, 4H), 1.59 (s, 3H);

^{13}C NMR (126 MHz; CDCl_3): δ 145.4, 144.4, 142.0, 141.0, 138.0, 137.4, 129.0, 128.9, 128.8, 128.6, 127.8, 127.2, 113.3, 112.1, 111.0, 110.9, 57.7, 52.9, 44.4, 41.9, 38.9, 35.5, 22.23, 22.15, 17.9, 16.5 (two rotamers).



Cyanoformamide **5.27b** was prepared analogously to cyanoformamide **5.27a**. Amino ketone **5.30b** (4.28 mmol, quantitative yield, yellow oil): R_f 0.15 (1.5:3.5 EtOAc:Hex). Amino alkene **5.31b** (950 mg, 3.93 mmol, 93%, pale yellow oil): R_f 0.83 (1:4 EtOAc:Hex + 10% TEA). *Note:* pentane was added after concentration and the solution was cooled; triphenyl phosphine was removed from the mixture by filtration over celite. Cyanoformamide **5.27b** (328 mg, 1.12 mmol, 28%, pale yellow oil):

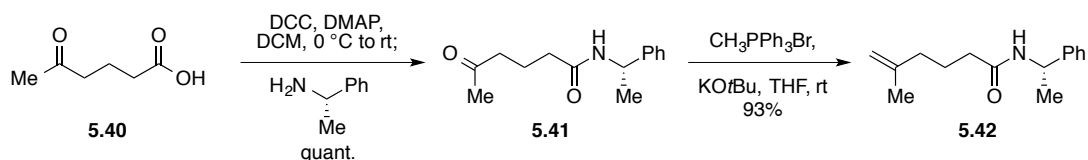
R_f 0.61 (3:7 EtOAc:Hex). Low yield was due to 1.5 equiv of TCEO instead of 3.0 equiv; recovered starting material.



Rotamers 1.2:1

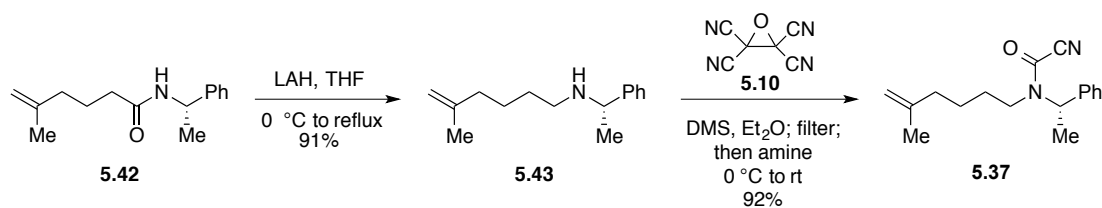
^1H NMR (500 MHz; CDCl_3) δ 7.59-7.54 (m, 5H), 7.43-7.41 (m, 2H), 5.95 (q, $J = 7.1$ Hz, 1H), 4.74 (app t, $J = 1.5$ Hz, 1H), 4.54 (app d, $J = 0.5$ Hz, 1H), 3.50 (ddd, $J = 15.2, 11.1, 5.5$ Hz, 1H), 3.41 (ddd, $J = 15.2, 11.0, 5.5$ Hz, 1H), 2.22 (ddd, $J = 13.2, 11.5, 5.4$ Hz, 1H), 1.95-1.90 (m, 1H), 1.76 (d, $J = 7.1$ Hz, 3H);

^1H NMR (500 MHz; CDCl_3) δ 7.91-7.87 (m, 5H), 7.83-7.82 (m, 2H), 5.76 (q, $J = 6.9$ Hz, 1H), 4.66 (app t, $J = 1.4$ Hz, 1H), 4.48 (app d, $J = 0.6$ Hz, 1H), 3.33 (ddd, $J = 13.4, 11.3, 5.1$ Hz, 1H), 3.20 (ddd, $J = 13.4, 11.2, 5.3$ Hz, 1H), 2.14 (td, $J = 12.4, 5.1$ Hz, 1H), 1.90-1.85 (m, 4H), 1.56 (s, 3H); ^{13}C NMR (126 MHz; CDCl_3) δ 145.5, 144.5, 141.9, 140.9, 135.4, 134.7, 133.06, 133.05, 133.03, 129.0, 128.8, 128.06, 127.98, 127.71, 127.67, 126.87, 126.84, 126.7, 126.4, 126.0, 125.8, 125.0, 113.3, 112.1, 111.0, 110.93, 57.9, 52.9, 44.4, 42.0, 39.0, 35.6, 22.2, 22.12, 18.0, 16.7 (two carbon signals overlapped for two rotamers).

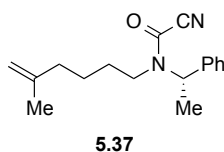


To a flame-dried flask was added DCC (5.95 g, 28.82 mmol), DMAP (1.2 g, 9.61), and dry DCM (28 mL). The solution was cooled to 0 °C and 4-acetylbutyric acid (**5.40**)

(2.5 g, 19.21 mmol) was added. The reaction was allowed to stir for 45 min at 0 °C before (*S*)-phenyl(ethyl) amine (2.5 mL, 19.21 mmol) was added. The resulting mixture was allowed to warm to room temperature overnight. The precipitate was filtered into a separatory funnel and the solids were washed with DCM. The filtrate was washed with H₂O. The combined aqueous layers were back extracted with DCM. The combined organic layers were washed with brine, dried over Na₂SO₄, filtered, and concentrated. The crude product was purified by flash chromatography (EtOAc:Hex) to give the corresponding amide **5.41** as a colorless solid (quant.): *R_f* 0.49 (EtOAc). Methyltriphenylphosphonium bromide (3.14 g, 8.80 mmol) and potassium *tert*-butoxide (1.0 M in THF; 8.8 mL, 8.80 mmol) were added to a flame-dried flask under N₂. The resulting mixture was stirred at room temperature for 25 min before amide **5.41** (1.0 g, 4.29 mmol) was added. The yellow mixture was stirred overnight. Saturated aq. NH₄Cl was added and the mixture diluted with EtOAc. The layers were separated and the organic layer was washed with H₂O. The combined aqueous layers were back extracted with EtOAc. The combined organic layers were washed with brine, dried over Na₂SO₄, filtered, and concentrated. The crude product was purified by flash chromatography (EtOAc:Hex) to afford alkene **5.42** as a colorless oil (927 mg, 4.00 mmol, 93%): *R_f* 0.39 (1.5:3.5 EtOAc:Hex).

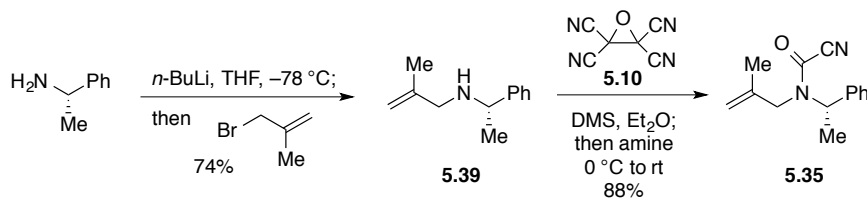


Azeotropically dried amide **5.42** (927 mg, 4.01 mmol) was added to a flame-dried flask with THF (20 mL) and cooled to 0 °C under N₂. Lithium aluminum hydride (760 mg, 20.04 mmol) was added slowly, portion-wise. The reaction was allowed to stir until H₂ release had ceased before heating to reflux overnight. The mixture was diluted with THF and cooled to 0 °C. 1 M NaOH was added drop-wise followed by a similar addition of H₂O and then an alternating drop addition of 1 M NaOH and H₂O. The mixture was filtered into a separatory funnel and the precipitate was washed with EtOAc. The layers were separated and the aqueous layer was extracted with EtOAc. The combined organic layers were washed with brine, dried over Na₂SO₄, filtered, and concentrated. Amine **5.43** was obtained as a yellow oil without need for further purification (792 mg, 3.64 mmol, 91%): *R_f* 0.12 (1.5:3.5 EtOAc:Hex). TCEO (1.38 g, 9.58 mmol) and Et₂O (12 mL) were added to a flame-dried flask under N₂ and cooled to 0 °C. DMS (0.7 mL, 9.90 mmol) was added dropwise. The resulting orange solution was stirred at 0 °C for 1 h. The dicyano carbonyl solution was syringe-filtered into a solution of amine **5.43** (790 mg, 3.19 mmol) and Et₂O (5 mL). The reaction was allowed to come to room temperature overnight. The solution was concentrated onto celite and purified by flash chromatography (EtOAc:Hex) to give cyanoformamide **5.37** as a yellow-orange oil (797 mg, 2.95 mmol, 92%): *R_f* 0.5 (1:4 EtOAc:Hex).



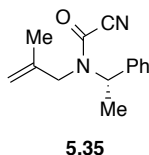
Rotamers 1.1:1

^1H NMR (500 MHz; CDCl_3) δ 7.43-7.31 (m, 10H), 5.72 (q, $J = 7.1$ Hz, 1H), 5.56 (q, $J = 7.0$ Hz, 1H), 4.68 (d, $J = 0.4$ Hz, 1H), 4.65 (d, $J = 0.4$ Hz, 1H), 4.59 (d, $J = 0.9$ Hz, 1H), 4.56 (d, $J = 0.9$ Hz, 1H), 3.39-3.24 (m, 2H), 3.19-3.00 (m, 2H), 1.91-1.85 (m, 4H), 1.72 (d, $J = 7.0$ Hz, 3H), 1.64 (s, 3H), 1.62 (s, 3H), 1.60 (d, $J = 7.2$ Hz, 3H), 1.51-1.44 (m, 1H), 1.41-1.20 (m, 7H) (two rotamers); ^{13}C NMR (126 MHz; CDCl_3) δ 145.3, 145.0, 144.6, 144.4, 138.1, 137.5, 128.91, 128.8, 128.6, 128.4, 127.6, 127.0, 111.0, 110.9, 110.4, 110.1, 57.6, 52.8, 45.6, 43.0, 36.9, 36.8, 30.4, 27.4, 24.8, 24.5, 22.11, 22.07, 17.9, 16.5 (two rotamers).



(*S*)-phenyl(ethyl) amine (2.1 mL, 16.50 mmol) and dry THF (63 mL) were added to a flame-dried flask under N_2 and was cooled to -78 °C. $n\text{-BuLi}$ (1.7 M in hexanes; 9.7 mL, 16.50 mmol) was added dropwise and the solution turned a pale yellow color. The reaction stirred at -78 °C for 30 min before 3-bromo-2-methylpropene (1.8 mL, 18.15 mmol) was added. The resulting orange solution was allowed to warm to room temperature overnight. It was quenched with saturated aq. NH_4Cl , turning the solution yellow in color. EtOAc was added and the layers were separated. The organic layer was washed with H_2O and the combined aqueous layers were back extracted with EtOAc .

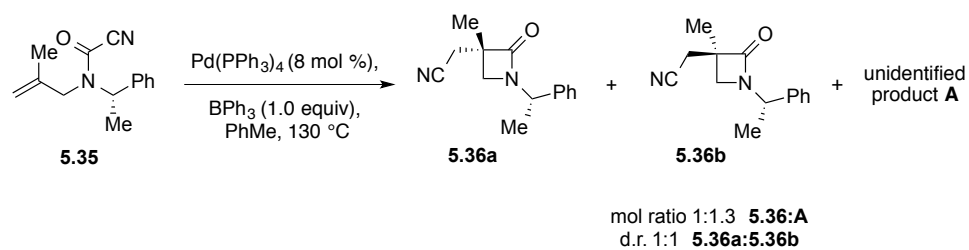
The combined organic layers were washed with brine, dried over Na₂SO₄, filtered, and concentrated. The crude product was purified by flash chromatography (EtOAc:Hex, then EtOAc:MeOH; fractions cut) to obtain amine **5.39** in 57% yield as a yellow oil (1.61 g, 9.19 mmol) *R_f* 0.44 (1:1 EtOAc:Hex). TCEO (3.9 g, 27.4 mmol) and Et₂O (11.5 mL) were added to a flame-dried flask under N₂ and cooled to 0 °C. DMS (2.1 mL, 28.3 mmol) was added to the heterogeneous mixture and it was allowed to stir at 0 °C for 45 min. The resulting orange mixture was syringe filtered into a flame-dried flask containing azeotropically dried amine **5.39** (1.6 g, 9.14 mmol) and Et₂O (10 mL) at 0 °C. The reaction was allowed to warm to room temperature overnight and was then filtered through celite and concentrated. The crude product was purified by flash chromatography (EtOAc:Hex) to give cyanoformamide **5.35** in 88% yield as a yellow-orange oil (1.83 g, 8.02 mmol): *R_f* 0.54 (1:4 EtOAc:Hex).



Rotamers 1.7:1

¹H NMR (500 MHz; CDCl₃): δ 7.43-7.29 (m, 5H), 5.68 (q, *J* = 7.2 Hz, 1H), 4.96 (s, 1H), 4.79 (s, 1H), 4.02 (t, *J* = 8.0 Hz, 1H), 3.72 (d, *J* = 17.5 Hz, 1H), 1.71 (s, 3H *overlapped*), 1.60 (d, *J* = 7.2 Hz, 3H);

¹H NMR (500 MHz; CDCl₃): δ 7.43-7.29 (m, 5H), 5.63 (q, *J* = 7.0 Hz, 1H), 4.82 (t, *J* = 1.2 Hz, 1H), 4.64 (s, 1H), 3.98 (s, 1H), 3.41 (d, *J* = 16.1 Hz, 1H), 1.72 (d, 7.0 HZ, 3H *overlapped*), 1.63 (s, 3H); ¹³C NMR (126 MHz; CDCl₃) δ 146.0, 144.9, 140.1, 139.2, 138.1, 137.6, 129.0, 128.8, 128.7, 128.4, 127.7, 127.1, 113.5, 112.2, 110.92, 110.87, 58.2, 53.8, 51.1, 47.7, 20.3, 20.0, 17.9, 16.5 (two rotamers).



^1H NMR (500 MHz; CDCl_3) δ Aryl peaks undefined, 4.96 (q, $J = 7.0$ Hz, 1H), 3.28 (d, $J = 6.0$ Hz, 1H), 3.09 (d, $J = 10.0$ Hz, 1H), 3.08 (d, $J = 10.5$ Hz, 1H), 2.91 (d, $J = 6.0$ Hz, 1H), 1.63 (d, $J = 7.0$ Hz, 3H), 1.46 (s, 3H);

^1H NMR (500 MHz; CDCl_3) δ Aryl peaks undefined, 4.91 (q, $J = 7.0$ Hz, 1H), 2.69 (d, $J = 17.5$, 1H), 2.62 (d, $J = 17.0$ Hz, 1H), 2.59 (app s, 1H), 2.18 (app s, 1H), 1.62 (d, $J = 7.5$ Hz, 3H), 1.38 (s, 3H).

REFERENCES

- (1) Yasui, Y.; Takemoto, Y. *Chem. Record* **2008**, 8, 386.
- (2) Yasui, Y.; Takeda, H.; Takemoto, Y. *Chem. Pharm. Bull.* **2008**, 56, 1567
- (3) Corey, E. J.; Ensley, H. E. *J. Am. Chem. Soc.* **1975**, 97, 6908.
- (4) Evans, D. A.; Bartroli, J.; Shih, T. L. *J. Am. Chem. Soc.* **1981**, 103, 2127.
- (5) Evans, D. A.; Ennis, M. D.; Mathre, D. J. *J. Am. Chem. Soc.* **1982**, 104, 1737.
- (6) Evans, D. A.; Chapman, K. T.; Bisaha, J. *J. Am. Chem. Soc.* **1984**, 106, 4261.
- (7) Myers, A. G.; Yang, B. H.; McKinstry, L.; Kopecky, D. J.; Gleason, J. L. *J. Am. Chem. Soc.* **1997**, 119, 6496.
- (8) Kummar, D. A.; Chain, W. J.; Morales, M. R.; Quiroga, O.; Myers, A. G. *J. Am. Chem. Soc.* **2008**, 130, 13231.
- (9) Myers, A. G.; Morales, M. R.; Mellem, K. T. *Angew. Chem. Int. Ed.* **2012**, 124, 4646.
- (10) Corey, E. J.; Enders, D. *Tetrahedron Letters* **1976**, 17, 3.
- (11) Job, A.; Janeck, C. F.; Bettray, W.; Peters, R.; Enders, D. *Tetrahedron* **2002**, 58, 2253.
- (12) Liu, G.; Cogan, D. A.; Ellman, J. A. *J. Am. Chem. Soc.* **1997**, 119, 9913.
- (13) Ellman, J. A. *Pur. App. Chem.* **2003**, 75, 39.
- (14) Robak, M. T.; Herbage, M. A.; Ellman, J. A. *Chem. Rev.* **2010**, 110, 3600.
- (15) Hodous, B. L.; Fu, G. C. *J. Am. Chem. Soc.* **2002**, 124, 1578.
- (16) Lee, E.C.; Hodous, B. L.; Bergin, E.; Shih, C.; Fu, G. C. *J. Am. Chem. Soc.* **2005**, 127, 11586.
- (17) Ojima, I.; Delalogue, F. *Chem. Soc. Rev.* **1997**, 26, 377.

BIBLIOGRAPHY

- Adams, D. M.; Chatt, J.; Guy, R. G.; Sheppard, N. "The Structure of Cyclopropane Platinous Chloride" *Journal of the Chemical Society* **1961**, 738-742.
- Adamson, G. W.; Daly, J. J.; Forester, D. "Reaction of Iodocarbonylrhodium Ions with Methyl Iodide. Structure of the Rhodium Acetyl Complex: $[\text{Me}_3\text{PhN}^+]_2[\text{Rh}_2\text{I}_6(\text{MeCO})_2(\text{CO})_2]^{2-}$ " *Journal of Organometallic Chemistry* **1974**, 71, C17-C19.
- Backvall, J. E.; Andell, O. S. "Stereochemistry and Mechanism of Nickel-Catalyzed Hydrocyanation of Olefins and Conjugated Dienes" *Organometallics* **1986**, 5, 2350-2355
- Bakir, M.; Conry, R.; Thomas, D. "Synthesis, Solution Properties, and Solid-State Structure Analysis of $[\text{Mn}(\kappa^4\text{-}N,N,S,N\text{-dpktsc})\text{Br}]_2 \cdot n\text{CH}_3\text{CN}$ ($n = 1$ or 0 , and dpktsc = Di-2-pyridyl thiosemicarbazone" *Journal of Coordination Chemistry* **2014**, 67, 249-264.
- Bakir, M.; Ordel, B. "Synthesis, Characterization and Molecular Sensing Capability of fac- $[\text{Re}(\text{CO})_3(\kappa^2\text{-}N,N\text{-dpktsc})\text{Cl}]$ where dpktsc = Di-2-pyridyl thiosemicarbazone" *Journal of Molecular Structure* **2009**, 930, 65-71.
- Balcells, D.; Moles, P.; Blakemore, J. D.; Raynaud, C.; Brudvig, G. W.; Crabtree, R. H.; Eisenstein, O. "The Synergy Between Theory and Experiment" *Dalton Transactions* **2009**, 5989-6000.
- Bernhardt, P. V.; Sharpe, P. C.; Islam, M.; Lovejoy, D. B.; Kalinowski, D. S.; Richardson, D. R. "Iron Chelators of the Dipyridyl Thiosemicarbazone Class: Precomplexation and Transmetalation Effects on Anticancer Activity" *Journal of Medicinal Chemistry* **2009**, 52, 407-415
- Bessmertnykh, A. G.; Blinov, K. A.; Grishin, Y. K.; Donskaya, N. A.; Tveritinova, E. V.; Yur'eva, N. M.; Beletskaya, I. P. "Synthesis of Mono-, Di-, and Trisilyl-Substituted Alkenes via the Hydrosilylation of Methylene-cyclopropanes Catalyzed by Rh(I) Complexes" *Journal of Organic Chemistry* **1997**, 62, 6069-6076.
- Bessmertnykh, A. G.; Blinov, K. A.; Grishin, Y. K.; Donskaya, N. A.; Beletskaya, I. P. "C-C Bond Activation of Cyclopropane Ring in a Hydrosilylation Catalyzed by Wilkinson Complex" *Tetrahedron Letters* **1995**, 36, 7901-7904.
- Bishop III, K. C. "Transition Metal Catalyzed Rearrangements of Small Ring Organic Molecules" *Chemical Reviews* **1976**, 76, 461-486.

- Blum, J.; Oppenheimer, E.; Bergman, E. D. "Decarbonylation of Aromatic Carbonyl Compounds Catalyzed by Rhodium Complexes" *Journal of the American Chemical Society* **1967**, *89*, 2338-2341.
- Bombieri, G.; Graziani, R.; Panattoni, C.; Volponi, L. "Crystal Structure of the Complex 1,2,6-Trichlorobis-(*o*-phenyl-enedimethylaminodimethylarsine)rhodium(III)" *Chemical Communications* **1967**, 977.
- Bond, G. C.; Newham, J. "Catalysis on Metals of Group 8. Part 5. – The Kinetics of the Hydrogenation of Cyclopropane and of Methylcyclopropane" *Transactions of the Faraday Society* **1960**, *56*, 1501-1514.
- Bräse, S.; Schroen, M. "Efficient Cleavage–Cross-Coupling Strategy for Solid-Phase Synthesis. A Modular Building System for Combinatorial Chemistry" *Angewandte Chemie International Edition* **1999**, *38*, 1071-1073.
- Brayshaw, S. K.; Green, J. C.; Kociok-Köhn, G.; Sceats, E. L.; Weller, A. S. "A Rhodium Complex with One Rh···C–C and One Rh···H–C Agostic Bond" *Angewandte Chemie International Edition* **2006**, *45*, 452-456.
- Bruce, M. I. "Cyclometalation Reactions" *Angewandte Chemie International Edition* **1977**, *16*, 73-86.
- Brunkan, N. M.; Brestensky, D. M.; Jones, W. D. "Kinetics, Thermodynamics, and Effect of BPh₃ on Competitive C–C and C–H Bond Activation Reactions in the Interconversion of Allyl Cyanide by [Ni(dippe)]" *Journal of the American Chemical Society* **2004**, *126*, 3627-3641.
- Burmeister, J. L.; Edwards, L. M. "Carbon–Carbon Bond Cleavage via Oxidative Addition: Reaction of Tetrakis(triphenylphosphine)platinum(0) with 1,1,1-Tricyanoethane" *Journal of the Chemical Society, A* **1971**, 1663-1666.
- Céspedes, G. A.; Perez, B. D.; Valcarcel, M. "Spectrophotometric Study of Complexes of Mercury(II) with Mono- and Dithiosemicarbazones" *Microchemical Journal* **1984**, *30*, 105-113
- Chatani, N.; Ie, Y.; Kakiuchi, F.; Murai, S. "Ru₃(CO)₁₂-Catalyzed Reaction of Pyridylbenzenes with Carbon Monoxide and Olefins. Carbonylation at a C–H Bond in the Benzene Ring" *Journal of Organic Chemistry* **1997**, *62*, 2604-2610.
- Chatani, N.; Ie, Y.; Kakiuchi, F.; Murai, S. "Ru₃(CO)₁₂-Catalyzed Decarbonylative Cleavage of a C–C Bond of Alkyl Phenyl Ketones" *Journal of the American Chemical Society* **1999**, *121*, 8545-8646.
- Chatt, J.; Duncanson, L. A. "Olefin Co-ordination Compounds. Part III.* Infra-red Spectra and Structure: Attempted Preparation of Acetylene Complexes" *Journal of the Chemical Society* **1953**, 2939-2947.

- Chatt, J.; Duncanson, L. A.; Venanzi, L. M. "Directing Effects in Inorganic Substitution Reactions. Part 1. A Hypothesis to Explain the Trans-Effect" *Journal of the Chemical Society* **1955**, 4456-4460.
- Chaplin, A. B.; Weller, A. S. "C–C Bond Activation of a Cyclopropyl Phosphine: Isolation and Reactivity of a Tetrameric Rhodacyclobutane" *Organometallics* **2010**, 29, 2332-2342.
- Chaumonnot, A.; Lamy, F.; Sabo-Etienne, S.; Donnadieu, B.; Chaudret, B.; Barthelat, J.-C.; Galland, J.-C. "Catalytic Isomerization of Cyanoolefins Involved in the Adiponitrile Process. C–CN Bond Cleavage and Structure of the Nickel π -Allyl Cyanide Complex $\text{Ni}(\eta^3\text{-1-Me-C}_3\text{H}_4)(\text{CN})(\text{dppb})$ " *Organometallics* **2004**, 23, 3363-3365.
- Cheng, C. H.; Spivack, B. D.; Eisenberg, R. "The Addition of Alkyl Halides to Rhodium(I) Dithiolene Complexes. The Synthesis, Structure, and Chemical Properties of Rhodium(III) Acyl Species" *Journal of the American Chemical Society* **1977**, 99, 3003-3011.
- Cohen, R.; van der Boom, M. E.; Shimon, L. J. W.; Rozenberg, H.; Milstein, D. "The Methylene-Transfer Reaction: Synthetic and Mechanistic Aspects of a Unique C–C Coupling and C–C Bond Activation Sequence" *Journal of the American Chemical Society*. **2000**, 122, 7723-7734.
- Cohen, R.; Milstein, D.; Martin, J. M. L. "Mechanism of the Methylene Transfer Reaction. C–C Activation and Reductive Elimination in One System. A DFT Study" *Organometallics* **2004**, 23, 2336-2342.
- Colby, D. A.; Bergman, R. G.; Ellman, J. A. "Rhodium-Catalyzed C–C Bond Formation via Heteroatom-Directed C–H Bond Activation" *Chemical Reviews* **2010**, 110, 624-655.
- Corey, E. J.; Ensley, H. E. "Preparation of an Optically Active Prostaglandin Intermediate via Asymmetric Induction" *Journal of the American Chemical Society* **1975**, 97, 6908-6909.
- Corey, E. J.; Enders, D. "Applications of *N,N*-dimethylhydrazones to Synthesis. Use in Efficient, Positionally and Stereochemically Selective C–C Bond Formation; Oxidative Hydrolysis to Carbonyl Compounds" *Tetrahedron Letters* **1976**, 17, 3-6.
- Crabtree, R. H. "The Organometallic Chemistry of Alkanes" *Chemical Reviews* **1985**, 85, 245-269.

- Crépin, D.; Dawick, J.; Aïssa, C. "Combined Rhodium-Catalyzed Carbon-Hydrogen Activation and β -Carbon Elimination to Access Eight-Membered Rings" *Angewandte Chemie International Edition* **2009**, 49, 620-623.
- Crépin, D.; Tugny, C.; Murray, J. H.; Aïssa, C. "Facile and Chemoselective Rhodium-Catalyzed Intramolecular Hydroacylation of α,α -Disubstituted 4-Alkylidenecyclopropanals" *Chemical Communications* **2011**, 47, 10957-10959.
- de Meijere, A.; Nüske, H.; Es-Sayed, M.; Labahn, T.; Schroen, M.; Bräse, S. "New Efficient Multicomponent Reactions with C–C Coupling for Combinatorial Application in Liquid and on Solid Phase" *Angewandte Chemie International Edition* **1999**, 38, 3669-3672.
- Denissova, I.; Barriault, L. "Stereoselective Formation of Quaternary Carbon Centers and Related Functions" *Tetrahedron* **2003**, 59, 10105-10146.
- Denmark, S. E.; Sweis, R. F. "Cross-Coupling Reactions of Alkenylsilanolates. Investigation of the Mechanism and Identification of Key Intermediates Through Kinetic Analysis" *Journal of the American Chemical Society* **2004**, 126, 4876-4882.
- Dermenci, A.; Whittaker, R. E.; Dong, G. "Rh(I)-Catalyzed Decarbonylation of Diynones via C–C Activation: Orthogonal Synthesis of Conjugated Diynes" *Organic Letters* **2013**, 15, 2242-2245.
- Dewar, M. "A Review of π Complex Theory" *Bulletin de la Société Chimique de France. Mémoires* **1951**, 18, C79.
- Donets, P. A.; Cramer, N. "Diaminophosphine Oxide Ligand Enabled Asymmetric Nickel-Catalyzed Hydrocarbonylations of Alkenes" *Journal of the American Chemical Society* **2013**, 135, 11772-11775.
- Douglas, C. J.; Overman, L. E. "Catalytic Asymmetric Synthesis of All-Carbon Quaternary Stereocenters" *Proceedings of the National Academy of Sciences* **2004**, 101, 5363-5367.
- Dreis, A. M.; Douglas, C. J. "Catalytic Carbon–Carbon σ Bond Activation: An Intramolecular Carbo-Acylation Reaction with Acylquinolines" *Journal of the American Chemical Society* **2009**, 131, 412-413.
- Druliner, J. D. "Mechanistic Studies of Nickel-Catalyzed Addition of DCN and $H^{13}CN$ to Pentenenitriles" *Organometallics* **1984**, 3, 205-208.
- Eilbracht, P.; Dahler, P. "C–C-Einfachbindungsspaltung 1,1-Dialkylsubstituierter Cyclopentadiene Durch $Fe_2(CO)_9$ Unter Ausbildung Von π -Cyclopentadienyl- σ -alkyl-eisen-komplexen" *Journal of Organometallic Chemistry* **1977**, 135, C23.

- Eilbracht, P.; Dahler, P. "Die Spaltung nichtgespannter CC-Einfachbindungen in Tricarbonyleisenkomplexen 5,5-dialkylsubstituierter Cyclopentadiene" *Chemische Berichte* **1980**, *113*, 542-554.
- Ellman, J. A. "Applications of *tert*-Butanesulfinamide in the Asymmetric Synthesis of Amines" *Pure and Applied Chemistry* **2003**, *75*, 39-46.
- Espinet, P.; Echavarren, A. M. "The Mechanism of the Stille Reaction" *Angewandte Chemie International Edition* **2004**, *43*, 4704-4734.
- Evans, D. A.; Bartroli, J.; Shih, T. L. "Enantioselective Aldol Condensations: Erythro-Selective Chiral Aldol Condensations via Boron Enolates" *Journal of the American Chemical Society* **1981**, *103*, 2127-2129.
- Evans, D. A.; Ennis, M. D.; Mathre, D. J. "Asymmetric Alkylation Reactions of Chiral Imide Enolates. A Practical Approach to the Enantioselective Synthesis of α -Substituted Carboxylic Acid Derivatives" *Journal of the American Chemical Society* **1982**, *104*, 1737-1739.
- Evans, D. A.; Chapman, K. T.; Bisaha, J. "New Asymmetric Diels-Alder Cycloaddition Reactions. Chiral α,β -Unsaturated Carboximides as Practical Chiral Acrylate and Crotonate Dienophile Synthons" *Journal of the American Chemical Society* **1984**, *106*, 4261-4263.
- Finke, R.G.; Hay, B. P. "Thermolysis of Adenosylcobalamin: A Product, Kinetic, and Co-C5' Bond Dissociation Energy Study" *Inorganic Chemistry* **1984**, *23*, 3041-3043.
- Frantz, D. E.; Singleton, D. A.; Snyder, J. P. "¹³C Kinetic Isotope Effects for the Addition of Lithium Dibutylcuprate to Cyclohexenone. Reductive Elimination is Rate-Determining" *Journal of the American Chemical Society* **1997**, *119*, 3383-3384.
- Fu, X.; Zhange, S.; Yin, J.; Schumacher, D. P. "A Copper-Free Palladium Catalyzed Cross-Coupling Reaction of Vinyl Tosylates with Terminal Acetylenes" *Tetrahedron Letters* **2002**, *43*, 6673-6676.
- Gandelman, M.; Shimon, L. J. W.; Milstein, D. "C-C versus C-H Activation and versus Agostic C-C Interaction Controlled by Electron Density at the Metal Center" *Chemistry - A European Journal* **2003**, *9*, 4295-4300.
- Gandelman, M.; Vigalok, A.; Shimon, L. J. W.; Milstein, D. "A PCN Ligand System. Exclusive C-C Activation with Rhodium(I) and C-H Activation with Platinum(II)" *Organometallics* **1997**, *16*, 3891-3986.

- Gauvin, R. M.; Rozenberg, H.; Shimon, L. J. W.; Milstein, D. "Synthesis and Structure of New Osmium-PCP Complexes. Osmium-Mediated C–C Bond Activation" *Organometallics* **2001**, *20*, 1719-1724.
- Gauvin, R. M.; Rozenberg, H.; Shimon, L. J. W.; Ben-David, Y.; Milstein, D. "Osmium-Mediated C–H and C–C Bond Cleavage of a Phenolic Substrate: *p*-Quinone Methide and Methylene Arenium Pincer Complexes" *Chemistry - A European Journal* **2007**, *13*, 1382-1393.
- Gozin, M.; Welsman, A.; Ben-David, Y.; Milstein, D. "Activation of a Carbon–Carbon Bond in Solution by Transition-Metal Insertion" *Nature* **1993**, *364*, 699-701.
- Greene, F. D. "Mechanism of Hypochlorite Decompositions. The Thermal Decomposition of L-(+)-2-Methyl-3-phenyl-2-butyl Hypochlorite" *Journal of the American Chemical Society* **1959**, *81*, 2688-2691.
- Gribkov, D. V.; Pastine, S. J.; Schnürch, M.; Sames, D. "Ruthenium Catalyzed Decarbonylative Arylation at sp^3 Carbon Centers in Pyrrolidine and Piperidine Heterocycles" *Journal of the American Chemical Society* **2007**, *129*, 11750-11755.
- Gross, M. L.; Blank, D. H.; Welch, W. M. "The Triazene Moiety as a Protecting Group for Aromatic Amines" *Journal of Organic Chemistry* **1993**, *58*, 2104-2109.
- Gupta, V. P.; Sharma, A. "Quantum Chemical Study of Mechanisms of Dissociation and Isomerization Reactions in Some Molecules and Radicals of Astrophysical Significance: Cyanides and Related Molecules" *Indian Academy of Sciences* **2006**, *67*, 487-501.
- Hadi, V.; Yoo, K. S.; Jeong, M.; Jung, K. W. "Expeditious Enyne Construction from Alkynes via Oxidative Pd(II)-Catalyzed Heck-type Coupling" *Tetrahedron Letters* **2009**, *50*, 2370-2373.
- Halcrow, M. A.; Urbanos, F.; Chaudret, B. "Aromatization of the B-Ring of 5,7-Dienyl Steroids by the Electrophilic Ruthenium Fragment "[Cp*Ru]⁺" *Organometallics* **1993**, *12*, 955-957.
- Halpern, J. "Activation of Carbon–Hydrogen Bonds by Metal Complexes: Mechanistic, Kinetic and Thermodynamic Considerations" *Inorganica Chimica Acta* **1985**, *100*, 41-48.
- Hirata, Y.; Tanaka, M.; Yada, A.; Nakao, Y.; Hiyama, T. "Alkynylcyanation of Alkynes and Dienes Catalyzed by Nickel" *Tetrahedron* **2009**, *65*, 5037-5050.

- Hirata, Y.; Yukawa, T.; Kashiwara, N.; Nakao, Y.; Hiyama, T. "Nickel-Catalyzed Carbocyanation of Alkynes with Allyl Cyanides" *Journal of the American Chemical Society* **2009**, *131*, 10964-10973.
- Hirata, Y.; Yada, A.; Morita, E.; Nakao, Y.; Hiyama, T.; Ohashi, M.; Ogoshi, S. "Nickel/Lewis Acid-Catalyzed Cyanoesterification and Cyanocarbamoylation of Alkynes" *Journal of the American Chemical Society* **2010**, *132*, 10070-10077.
- Hirata, Y.; Tanaka, M.; Yada, A.; Nakao, Y.; Hiyama, T. "Alkynylcyanation of Alkynes and Dienes Catalyzed by Nickel" *Tetrahedron* **2009**, *65*, 5037-5050.
- Hirata, Y.; Inui, T.; Nakao, T.; Hiyama, T. "Cyanoesterification of 1,2-Dienes Catalyzed by Nickel" *Journal of the American Chemical Society* **2009**, *131*, 6624-6631.
- Hitchcock, P. B.; Lappert, M. F.; McLaughlin, G. M.; Oliver, A. J. "Carbene Complexes. Part VI. Complexes from Imidoyl Chloride and Rhodium(I) Precursors, and the Crystal and Molecular Structure of Carbonyltri-iodo-[α -(*N*-methyl- α -methyliminobenzylamino)benzylidene-*N*,*C*]rhodium, $\text{I}(\text{OC})\text{Rh}-\text{CPh}(\text{NMe})\text{CPh}:\text{NMe}$ " *Journal of the Chemical Society, Dalton Transactions* **1974**, 68-74.
- Hoang, G. T.; Reddy, V. J.; Nguyen, H. H. K.; Douglas, C. J. "Insertion of an Alkene into an Ester: Intramolecular Oxyacylation Reaction of Alkenes Through Acyl C–O Bond Activation" *Angewandte Chemie International Edition* **2011**, *123*, 1922-1924.
- Hodous, B. L.; Fu, G. C. "Enantioselective Staudinger Synthesis of β -Lactams Catalyzed by a Planar-Chiral Nucleophile" *Journal of the American Chemical Society* **2002**, *124*, 1578-1579.
- Hosseinzadeh, R.; Sarrafi, Y.; Mohadjerani, M.; Mohammadpourmir, F. "Copper-Catalyzed arylation of Phenylurea using $\text{KF}/\text{Al}_2\text{O}_3$ " *Tetrahedron Letters* **2008**, *49*, 840-843.
- Hsieh, J.-C.; Ebata, S.; Nakao, Y.; Hiyama, T. "Asymmetric Synthesis of Indolines Bearing a Benzylic Quaternary Stereocenter Through Intramolecular Arylcyanation of Alkenes" *Synlett* **2010**, *2010*, 1709-1711.
- Job, A.; Janeck, C. F.; Bettray, W.; Peters, R.; Enders, D. "The SAMP/RAMP-Hydrazone Methodology in Asymmetric Synthesis" *Tetrahedron* **2002**, *58*, 2253-2329.
- Jones, G. D.; Martin, J. L.; McFarland, C.; Allen, O. R.; Hall, R. E.; Haley, A. D.; Brandon, R. J.; Konovalova, T.; Desrochers, P. J.; Pulay, P.; Vivic, D. A. "Ligand Redox Effects in the Synthesis, Electronic Structure, and Reactivity of an Alkyl–Alkyl Cross-Coupling Catalyst" *Journal of the American Chemical Society* **2006**, *128*, 13175-13183.

- Jun, C.-H.; Lee, H.; Lim, S.-G. "The C–C Bond Activation and Skeletal Rearrangement of Cycloalkanone Imine by Rh(I) Catalysts" *Journal of the American Chemical Society* **2001**, *123*, 751-752.
- Jun, C.-H.; Lee, H. "Catalytic Carbon–Carbon Bond Activation of Unstrained Ketone by Soluble Transition-Metal Complex" *Journal of the American Chemical Society*. **1999**, *121*, 880-881.
- Jun, C.-H.; Lee, H.; Hong, J. "A Highly Active Catalyst System for Intermolecular Hydroacylation" *Angewandte Chemie International Edition* **2000**, *39*, 3070-3072.
- Jun, C.-H.; Lee, H.; Hong, J. "Chelation-Assisted Intermolecular Hydroacylation: Direct Synthesis of Ketone from Aldehyde and 1-Alkene" *Journal of Organic Chemistry* **1997**, *62*, 1200-1201.
- Jun, C.-H.; Park, J.-H. In *Directed C–C Bond Activation by Transition Metal Complexes*; Chatani, N., Ed.; Topics in Organometallic Chemistry; Springer-Verlag: Berlin Heidelberg, 2007; pp 117-143.
- Keeton, M.; Mason, R.; Russel, D. R. "The Crystal and Molecular Structure of Two Pyridinium Propylide Complexes of Platinum(II) and Platinum(IV)" *Journal of Organometallic Chemistry* **1971**, *33*, 259-266.
- Kimball, D. B.; Haley, M. M. "Triazenes: A Versatile Tool in Organic Synthesis" *Angewandte Chemie International Edition* **2002**, *41*, 3338-3351.
- King, R.B.; Efraty, A. "Pentamethylcyclopentadienyl Derivatives of Transition Metals. II. Synthesis of Pentamethylcyclopentadienyl Metal Carbonyls from 5-Acetyl-1,2,3,4,5-pentamethylcyclopentadiene" *Journal of the American Chemical Society*. **1972**, *94*, 3773-3779.
- Kleeberg, C.; Dang, L.; Lin, Z.; Marder, T. B. "A Facile Route to Aryl Boronates: Room Temperature, Copper-Catalyzed Borylation of Aryl Halides with Alkoxy Diboron Reagents" *Angewandte Chemie International Edition* **2009**, *48*, 5350-5354.
- Kobayashi, Y.; Kamisaki, H.; Yanada, R.; Takemoto, Y. "Palladium-Catalyzed Intramolecular Cyanoamidation of Alkynyl and Alkenyl Cyanoformamides" *Organic Letters* **2006**, *8*, 2711-2713.
- Kobayashi, Y.; Kamisaki, H.; Takeda, H.; Yasui, Y.; Yanada, R.; Takemoto, Y. "Intramolecular Cyanoamidation of Unsaturated Cyanoformamides Catalyzed by Palladium: An Efficient Synthesis of Multi-Functionalized Lactams" *Tetrahedron* **2007**, *63*, 2978-2989.

- Krug, C.; Hartwig, J. F. "Direct Observation of Aldehyde Insertion into Rhodium–Aryl and –Alkoxide Complexes" *Journal of the American Chemical Society* **2002**, *124*, 1674-1679.
- Krug, C.; Hartwig, J. F. "Reactions of an Arylrhodium Complex with Aldehydes, Imines, Ketones, and Alkynones. New Classes of Insertion Reactions" *Organometallics* **2004**, *23*, 4594-4607.
- Krug, C.; Hartwig, J. F. "Imine Insertion into a Late Metal–Carbon Bond to Form a Stable Amido Complex" *Journal of the American Chemical Society* **2004**, *126*, 2694-2695.
- Kummar, D. A.; Chain, W. J.; Morales, M. R.; Quiroga, O.; Myers, A. G. "Stereocontrolled Alkylative Construction of Quaternary Carbon Centers" *Journal of the American Chemical Society* **2008**, *130*, 13231-13233.
- Labinger, J. A.; Bercaw, J. E. "Metal–Hydride and Metal–Alkyl Bond Strengths: The Influence of Electronegativity Differences" *Organometallics* **1988**, *7*, 926-928.
- Lazny, R.; Sienkiewicz, M.; Bräse, S. "Application of Triazenes for Protection of Secondary Amines" *Tetrahedron* **2001**, *57*, 5825-5832.
- Lee, D. Y.; Jun, C. H. "A Double Carbon–Carbon Bond Activation of 8-Quinolinyll Cyclopropyl Ketone by Chlorobis(ethylene)rhodium(I) Dimer" *Bulletin of the Korean Chemical Society* **2003**, *24*, 1059-1060.
- Lee, E. C.; Hodous, B. L.; Bergin, E.; Shih, C.; Fu, G. C. "Catalytic Asymmetric Staudinger Reactions to Form β -Lactams: An Unanticipated Dependence of Diastereoselectivity on the Choice of the Nitrogen Substituent" *Journal of the American Chemical Society* **2005**, *127*, 11586-11587.
- Liou, S.; Gozin, M.; Milstein, D. "Directly Observed Oxidative Addition of a Strong Carbon–Carbon Bond to a Soluble Metal Complex" *Journal of the American Chemical Society* **1995**, *117*, 9774-9775.
- Liou, S.-Y.; van der Boom, M. E.; Milstein, D. "Catalytic Selective Cleavage of a Strong C–C Single Bond by Rhodium in Solution" *Chemical Communications* **1998**, 687-688.
- Liu, C.; Knochel, P. "Preparation of Polyfunctional Aryl Azides from Aryl Triazenes. A New Synthesis of Ellipticine, 9-Methoxyellipticine, Isoellipticine, and 7-Carboxyisoellipticine" *Journal of Organic Chemistry* **2007**, *72*, 7106-7115.
- Liu, G.; Cogan, D. A.; Ellman, J. A. "Catalytic Asymmetric Synthesis of tert-Butanesulfinamide. Application to the Asymmetric Synthesis of Amines" *Journal of the American Chemical Society* **1997**, *119*, 9913-9914.

- Lokwani, P.; Nagori, B. P.; Batra, N.; Goyal, A.; Gupta, S.; Singh, N. "Benzoxazole: The Molecule of Diverse Biological Activities" *Journal of Chemical and Pharmaceutical Research* **2011**, *3*, 302-311
- Lormann, M.; Dahmen, S.; Bräse, S. "Hydro-dediazoniatioⁿ of Diazonium Salts Using Trichlorosilane: New Cleavage Conditions for the T₁ Traceless Linker" *Tetrahedron Letters* **2000**, *41*, 3813-3816.
- Lutz, J. P.; Rathbun, C. M.; Stevenson, S. M.; Powell, B. M.; Boman, T. S.; Baxter, C. E.; Zona, J. M.; Johnson, J. B. "Rate-Limiting Step of the Rh-Catalyzed Carboacylation of Alkenes: C–C Bond Activation or Migratory Insertion?" *Journal of the American Chemical Society* **2012**, *134*, 715-722.
- Martinez, M. P.; Valcarcel, M.; Pino, F. "Di-2-pyridyl Ketone Thiosemicarbazone as an Analytical Reagent" *Analytica Chimica Acta* **1976**, *81*, 157-165.
- Matsuda, T.; Tsuboi, T.; Murakami, M. "Rhodium-Catalyzed Carbonylation of Spiropentanes" *Journal of the American Chemical Society* **2007**, *129*, 12596-12597.
- Matsuda, T.; Shigeno, M.; Murakami, M. "Asymmetric Synthesis of 3,4-Dihydrocoumarins by Rhodium-Catalyzed Reaction of 3-(2-Hydroxyphenyl)cyclobutanones" *Journal of the American Chemical Society* **2007**, *129*, 12086-12087.
- Matsuda, T.; Shigeno, M.; Makino, M.; Murakami, M. "Enantioselective C–C Bond Cleavage Creating Chiral Quaternary Carbon Centers" *Organic Letters* **2006**, *8*, 3379-3381.
- McMillen, D. F.; Golden, D. M. "Hydrocarbon Bond Dissociation Energies" *Annual Review of Physical Chemistry* **1982**, *33*, 493-532.
- Milstein, D. "*cis*-Hydridoacylrhodium(III) Complexes not Stabilized by Chelation. Reductive Elimination and Decarbonylation" *Organometallics* **1982**, *1*, 1549-1551.
- Müller, E.; Segnitz, A.; Langer, E. "Komplexbildung und Decarbonylierung von Mono- und Diacetylen-Ketonen mit Tris-(Triphenylphosphin)-Rhodium(I)-Chlorid" *Tetrahedron Letters* **1969**, *10*, 1129-1132.
- Murahashi, S.; Naota, T.; Nakajima, N. "Palladium-Catalyzed Decarbonylation of Acyl Cyanides" *Journal of Organic Chemistry* **1986**, *51*, 898-901.

- Murai, S.; Kakiuchi, F.; Sekine, S.; Tanaka, Y.; Kamatani, A.; Sonoda, M.; Chatani, N. "Efficient Catalytic Addition of Aromatic Carbon–Hydrogen Bonds to Olefins" *Nature*. **1993**, *366*, 529-531.
- Murai, M.; Miki, K.; Ohe, K. "A New Route to 3-Acyl-2-Aminobenzofurans: Palladium-Catalysed Cycloisomerisation of 2-(Cyanomethyl)phenyl Esters" *Chemical Communications* **2009**, 34663468.
- Murakami, M.; Amii, H.; Ito, Y. "Selective Activation of Carbon–Carbon Bonds Next to a Carbonyl Group" *Nature*. **1994**, *370*, 540-541.
- Murakami, M.; Tsuruta, T.; Ito, Y. "Lactone Formation by Rhodium-Catalyzed C–C Bond Cleavage of Cyclobutanone" *Angewandte Chemie International Edition* **2000**, *39*, 2484-2486.
- Murakami, M.; Itahashi, T.; Ito, Y. "Catalyzed Intramolecular Olefin Insertion into a Carbon–Carbon Single Bond" *Journal of the American Chemical Society* **2002**, *124*, 13976-13977.
- Murakami, M.; Ito, Y. "Cleavage of Carbon–Carbon Single Bonds by Transition Metals" In *Activation of Unreactive Bonds and Organic Synthesis*; Murai, S., Ed.; Topics in Organometallic Chemistry; Springer-Verlag: Berlin Heidelberg, 1999; pp 97-129.
- Myers, A. G.; Morales, M. R.; Mellem, K. T. "Pseudoephedrine: A Practical Chiral Auxiliary for Asymmetric Synthesis" *Angewandte Chemie International Edition* **2012**, *124*, 4646-4649.
- Myers, A. G.; Yang, B. H.; McKinstry, L.; Kopecky, D. J.; Gleason, J. L. "Pseudoephedrine as a Practical Chiral Auxiliary for the Synthesis of Highly Enantiomerically Enriched Carboxylic Acids, Alcohols, Aldehydes, and Ketones" *Journal of the American Chemical Society* **1997**, *119*, 6496-6511.
- Nakao, Y.; Yada, A.; Ebata, S.; Hiyama, T. "A Dramatic Effect of Lewis-Acid Catalysts on Nickel-Catalyzed Carbocyanation of Alkynes" *Journal of the American Chemical Society* **2007**, *129*, 2428-2429.
- Nakao, Y.; Hirata, Y.; Tanaka, M.; Hiyama, T. "Nickel/BPh₃-Catalyzed Alkynylcyanation of Alkynes and 1,2-Dienes: An Efficient Route to Highly Functionalized Conjugated Enynes" *Angewandte Chemie International Edition* **2008**, *47*, 385-387.
- Nakao, Y.; Yukawa, T.; Hirata, Y.; Oda, S.; Satoh, J.; Hiyama, T. "Allylcyanation of Alkynes: Regio- and Stereoselective Access to Functionalized Di- or Trisubstituted Acrylonitriles" *Journal of the American Chemical Society* **2006**, *128*, 7116-7117.

- Nakao, Y.; Ebata, S.; Yada, A.; Hiyama, T.; Ikawa, M.; Ogoshi, S. "Intramolecular Arylcyanation of Alkenes Catalyzed by Nickel/ AlMe_2Cl " *Journal of the American Chemical Society* **2008**, *130*, 12874-12875.
- Nakao, Y.; Hirata, Y.; Hiyama, T. "Cyanoesterification of 1,2-Dienes: Synthesis and Transformations of Highly Functionalized α -Cyanomethylacrylate Esters" *Journal of the American Chemical Society* **2006**, *128*, 7420-7421.
- Nakao, Y.; Oda, S.; Hiyama, T. "Nickel-Catalyzed Arylcyanation of Alkynes" *Journal of the American Chemical Society* **2004**, *126*, 13904-13905.
- Nakao, Y.; Oda, S.; Yada, A.; Hiyama, T. "Arylcyanation of Alkynes Catalyzed by Nickel" *Tetrahedron* **2006**, *62*, 7567-7576.
- Nakao, Y.; Yada, A.; Hiyama, T. "Heteroatom-Directed Alkylcyanation of Alkynes" *Journal of the American Chemical Society* **2010**, *132*, 10024-10026.
- Nakao, Y. "Catalytic C–CN Bond Activation" In *Topics in Current Chemistry*; Topics in Current Chemistry; Springer Berlin Heidelberg: Berlin, Heidelberg, 2014.
- Nandakumar, M. V. "Copper Catalyzed Arylation of Urea" *Tetrahedron Letters* **2004**, *45*, 1989-1990.
- Negishi, E.; Copéret, C.; Ma, S. Liou, S.; Liu, F. "Cyclic Carbopalladation. A Versatile Synthetic Methodology for the Construction of Cyclic Organic Compounds" *Chemical Reviews* **1996**, *96*, 365-393.
- Ng, F. T. T.; Rempel, G. L.; Halpern, J. "Ligand Effects on Transition-Metal-Alkyl Bond Dissociation Energies" *Journal of the American Chemical Society* **1982**, *104*, 621-623.
- Nickerson, D. M.; Angeles, V. V.; Auvil, T. J.; So, S. S.; Mattson, A. E. "Internal Lewis Acid Assisted Ureas: Tunable Hydrogen Bond Donor Catalysts" *Chemical Communications* **2013**, *49*, 4289-4291.
- Nishihara, Y.; Inoue, Y.; Itazaki, M.; Takagi, K. "Palladium-Catalyzed Cyanoesterification of Norbornenes with Cyanoformates via the NC–Pd–COOR (R = Me and Et) Intermediate" *Organic Letters* **2005**, *7*, 2639-2641.
- Nishihara, Y.; Inoue, Y.; Izawa, S.; Miyasaka, M.; Tanemura, K.; Nakajima, K.; Takagi, K. "Cyanoesterification of Norbornenes Catalyzed by Palladium: Facile Synthetic Methodology to Introduce Cyano and Ester Functionalities via Direct Carbon–Carbon Bond Cleavage of Cyanoformates" *Tetrahedron* **2006**, *62*, 9872-9882.

- Nishihara, Y.; Miyasaka, M.; Inoue, Y.; Yamaguchi, T.; Kojima, M.; Takagi, K. "Preparation, Structures, and Thermal Reactivity of Alkoxy carbonyl(cyano)palladium(II) Complexes *trans*-Pd(COOR)(CN)(PPh₃)₂ (R = Me, Et, ⁿPr, ⁱPr, ⁿBu, ⁱBu, and Bn) as Intermediates of the Palladium-Catalyzed Cyanoesterification of Norbornene Derivatives" *Organometallics* **2007**, *26*, 4054-4060.
- Nolan, S. P.; Hoff, C. D.; Stoutland, P. O.; Newman, L. J.; Buchanan, J. M.; Bergman, R. G.; Yang, G. K.; Peters, K. S. "Heats of Reaction of Cp(PMe₃)Ir(R)(H) (R = C₆H₅, C₆H₁₁, H) with HCl, CCl₄, CBr₄, and MeI. A Solution Thermochemical Study of C–H Insertion Reaction" *Journal of the American Chemical Society* **1987**, *109*, 3143-3145.
- Nozaki, K.; Sato, N.; Takaya, H. "Acylcyanation of Terminal Acetylenes: Palladium-Catalyzed Addition of Aryloyl Cyanides to Arylacetylenes" *Journal of Organic Chemistry* **1994**, *59*, 2679-2681.
- Ohnishi, Y.-Y.; Nakao, Y.; Sato, H.; Nakao, Y.; Hiyama, T.; Sakaki, S. "A Theoretical Study of Nickel(0)-Catalyzed Phenylcyanation of Alkynes. Reaction Mechanism and Regioselectivity" *Organometallics* **2009**, *28*, 2583-2594.
- Ojima, I.; Delalogue, F. "Asymmetric Synthesis of Building-Blocks for Peptides and Peptidomimetics by Means of the β-Lactam Synthon Method" *Chemical Society Reviews* **1997**, *26*, 377-386.
- Parker, E.; Cramer, N. "Asymmetric Rhodium(I)-Catalyzed C–C Activations with Zwitterionic Bis-phospholane Ligands" *Organometallics* **2014**, *33*, 780-787.
- Parshall, G. W. "Intramolecular Aromatic Substitution in Transition Metal Complexes" *Accounts of Chemical Research* **1970**, *3*, 139-144.
- Parshall, G. W. "Homogenous Catalytic Activation of Carbon–Hydrogen Bonds" *Accounts of Chemical Research* **1975**, *8*, 113-117.
- Patrick, T. B.; Juehne, T.; Reeb, E.; Hennessy, D. "Zinc(II) Promoted Conversion of Aryltriazenes to Aryl Iodides and Aryl Nitriles" *Tetrahedron Letters* **2001**, *42*, 3353-3554.
- Patrick, T. B.; Willaredt, R. P.; DeGonia, D. J. "Synthesis of Biaryls from Aryltriazenes" *Journal of Organic Chemistry* **1985**, *50*, 2232-2235.
- Periana, R. A.; Bergman, R. G. "Rapid Intramolecular Rearrangement of a Hydridocyclopropylrhodium Complex to a Rhodacyclobutane. Independent Synthesis of the Metallacycle by Addition of Hydride to the Central Carbon Atom of a Cationic Rhodium π-Allyl Complex" *Journal of the American Chemical Society* **1984**, *106*, 7272-7273.

- Periana, R. A.; Bergman, R. G. "Oxidative Addition of Rhodium to Alkane C–H Bonds: Enhancement in Selectivity and Alkyl Group Functionalization" *Organometallics* **1984**, *3*, 508-510.
- Periana, R. A.; Bergman, R. G. "C–C Activation of Organic Small Ring Compounds by Rearrangement of Cycloalkylhydridorhodium Complexes to Rhodacycloalkanes. Synthesis of Metallacyclobutanes, Including One with a Tertiary M–C Bond, by Nucleophilic Addition to π -Allyl Complexes" *Journal of the American Chemical Society* **1986**, *108*, 7346-7355.
- Rathbun, C. M.; Johnson, J. B. "Rhodium-Catalyzed Acylation with Quinolinyl Ketones: Carbon–Carbon Single Bond Activation as the Turnover-Limiting Step of Catalysis" *Journal of the American Chemical Society* **2011**, *133*, 2031-2033.
- Robak, M. T.; Herbage, M. A.; Ellman, J. A. "Synthesis and Applications of tert-Butanesulfinamide" *Chemical Reviews* **2010**, *110*, 3600-3740.
- Rondla, N. R.; Levi, S. M.; Ryss, J. M.; Vanden Berg, R. A.; Douglas, C. J. "Palladium-Catalyzed C–CN Activation for Intramolecular Cyanoesterification of Alkynes" *Organic Letters* **2011**, *13*, 1940-1943.
- Ruhland, K. "Transition-Metal-Mediated Cleavage and Activation of C–C Single Bonds" *European Journal of Organic Chemistry* **2012**, *2012*, 2683-2706.
- Ryabov, A. D. "Mechanisms of Intramolecular Activation of Carbon–Hydrogen Bonds in Transition-Metal Complexes" *Chemical Reviews* **1990**, *90*, 403-424.
- Rybtchinski, B.; Milstein, D. "Metal Insertion into C–C Bonds in Solution" *Angewandte Chemie International Edition* **1999**, *38*, 870-883.
- Rybtchinski, B.; Vigalok, A.; Ben-David, Y.; Milstein, D. "A Room Temperature Direct Metal Insertion into a Nonstrained Carbon–Carbon Bond in Solution. C–C vs C–H Bond Activation" *Journal of the American Chemical Society* **1996**, *118*, 12406-12415.
- Saeki, T.; Son, E.; Tamao, K. "Boron Trifluoride Induced Palladium-Catalyzed Cross-Coupling Reaction of 1-Aryltriazenes with Areneboronic Acids" *Organic Letters* **2004**, *6*, 617-619.
- Salem, H.; Ben-David, Y.; Shimon, L. J. W.; Milstein, D. "Exclusive C–C Activation and an Apparent α -H Elimination with a Rhodium Phosphinite Pincer Complex" *Organometallics* **2006**, *25*, 2292-2300.
- Satyamurthy, N.; Barrio, J. R.; Bida, G. T.; Phelps, M. E. "Efficient Conversion of 1-Aryl-3,3-Dialkyltriazenes to Phenols and Oxygen-18 Labeled Phenols" *Tetrahedron Letters* **190**, *31*, 4409-4412.

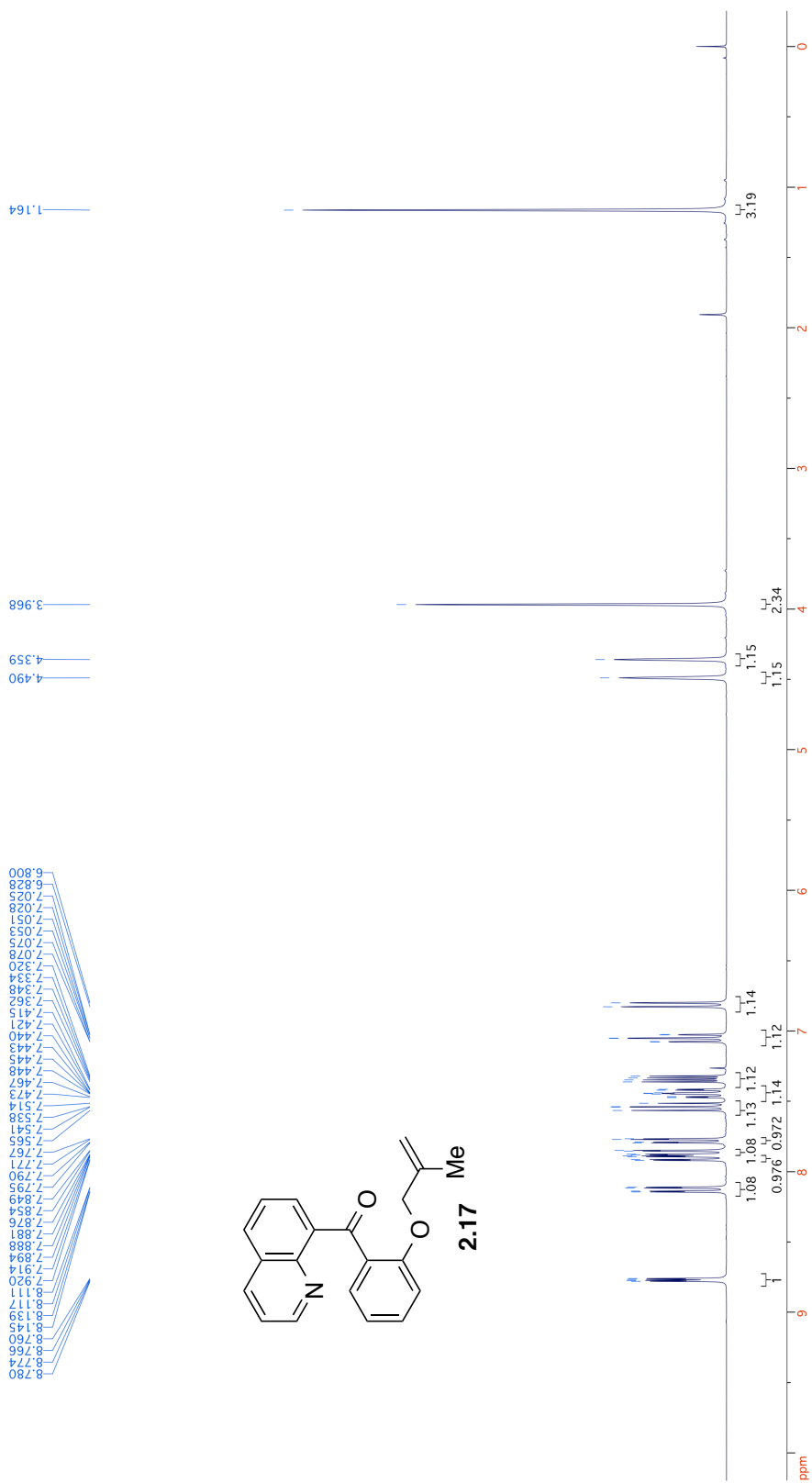
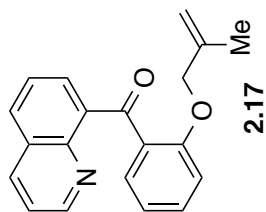
- Seiser, T.; Cramer, N. "Rhodium-Catalyzed C–C Bond Cleavage: Construction of Acyclic Methyl Substituted Quaternary Stereogenic Centers" *Journal of the American Chemical Society* **2010**, *132*, 5340-5341.
- Seiser, T.; Cramer, N. "Enantioselective C–C Bond Activation of Allenyl Cyclobutanes: Access to Cyclohexenones with Quaternary Stereogenic Centers" *Angewandte Chemie International Edition* **2008**, *47*, 9294.
- Siegbahn, P. E. M. "The Activation of the C–H Bond in acetylene by Second Row Transition Metal Atoms" *Theoretica Chimica Acta*. **1994**, *87*, 277-292.
- Simaan, S.; F G Goldberg, A.; Rosset, S.; Marek, I. "Metal-Catalyzed Ring-Opening of Alkydenecyclopropanes: New Access to Building Blocks with an Acyclic Quaternary Stereogenic Center" *Chemistry - A European Journal* **2009**, *16*, 774-778.
- Simoes, J. A. M.; Beauchamp, J. L. "Transition Metal–Hydrogen and Metal–Carbon Bond Strengths: The Keys to Catalysis" *Chemical Reviews* **1990**, *90*, 629-688.
- Singleton, D. A.; Thomas, A. A. "High Precision Simultaneous Determination of Multiple Small Kinetic Isotope Effects at Natural Abundance" *Journal of the American Chemical Society* **1995**, *117*, 9357-9358.
- Siu, M.; Pastor, R.; Liu, W.; Barrett, K.; Berry, M.; Blair, W. S.; Chang, C.; Chen, J. Z.; Eigenbrot, C.; Ghilardi, N.; Gibbons, P.; He, H.; Hurley, C. A.; Kenny, J. R.; Khojasteh, S. C.; Le, H.; Lee, L.; Lyssikatos, J. P.; Magnuson, S.; Pulk, R.; Tsui, V.; Ultsch, M.; Xiao, Y.; Zhu, B.-Y.; Sampath, D. "2-Amino-[1,2,4]triazolo[1,5-a]pyridines as JAK2 inhibitors" *Bioorganic & Medicinal Chemistry Letters* **2013**, *17*, 5014.
- So, S. S.; Auvil, T. J.; Garza, V. J.; Mattson, A. E. "Boronate Urea Activation of Nitrocyclopropane Carboxylates" *Organic Letters* **2012**, *14*, 444-447.
- So, S. S.; Burkett, J. A.; Mattson, A. E. "Internal Lewis Acid Assisted Hydrogen Bond Donor Catalysis" *Organic Letters* **2011**, *13*, 716-719.
- Souillart, L.; Cramer, N. "Exploitation of Rh(I)–Rh(III) Cycles in Enantioselective C–C Bond Cleavages: Access to β -Tetralones and Benzobicyclo[2.2.2]octanones" *Chemical Science* **2013**, *5*, 837-840.
- Sreekanth, A.; Sivakumar, S.; Prathapachandra Kurup, M. R. "Structural Studies of Six and Four Coordinate Zinc(II), Nickel(II) and Dioioxovanadium(V) Complexes with Thiosemicarbazones" *Journal of Molecular Structure* **2003**, *655*, 47-58.

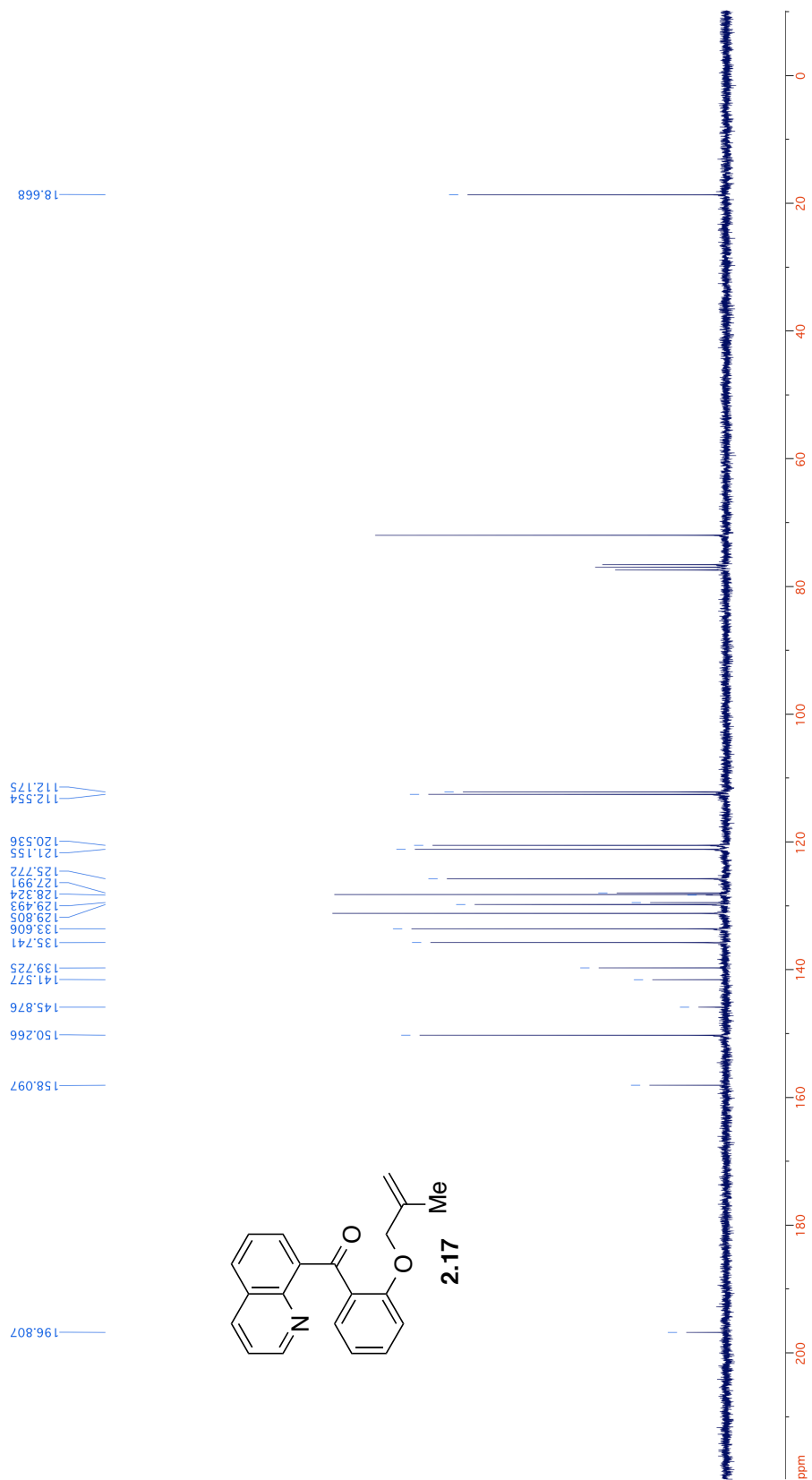
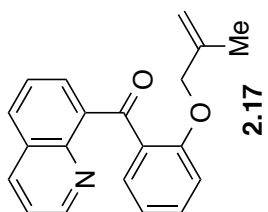
- Steenken, S. S.; Schushmann, H. P.; vonSonntag, C. "Fragmentation of α -Alkoxyalkyl Radicals. An Electron Paramagnetic Resonance Study" *The Journal of Physical Chemistry* **1975**, *79*, 763-764.
- Suggs, J. W. "Isolation of a Stable Acylrhodium(III) hydride Intermediate Formed During Aldehyde Decarbonylation. Hydroacylation" *Journal of the American Chemical Society* **1978**, *100*, 640-641.
- Suggs, J. W.; Cox, S. D. "Directed Cleavage of sp^2 - sp Carbon-Carbon Bonds" *Journal of Organometallic Chemistry* **1981**, *221*, 199-201.
- Suggs, J. W.; Jun, C.-H. "Directed Cleavage of Carbon-Carbon Bonds by Transition Metals: The α -Bonds of Ketones" *Journal of the American Chemical Society* **1984**, *106*, 3054-3056.
- Suggs, J. W.; Wovkulich, M. J.; Cox, S. D. "Synthesis, Structure, and Ligand-Promoted Reductive Elimination in an Acylrhodium Ethyl Complex" *Organometallics* **1985**, *4*, 1101-1107.
- Suggs, J. W. "Activation of Aldehyde C-H Bonds to Oxidative Addition via Formation of 3-Methyl-2-Aminopyridyl Aldimines and Related Compounds: Rhodium Based Catalytic Hydroacylation" *Journal of the American Chemical Society* **1979**, *101*, 489.
- Suggs, J. W.; Jun, C.-H. "Synthesis of a Chiral Rhodium Alkyl via Metal Insertion into an Unstrained C-C Bond and Use of the Rate of Racemization at Carbon to Obtain a Rhodium-Carbon Bond Dissociation Energy" *Journal of the American Chemical Society* **1986**, *108*, 4679-4681.
- Suggs, J. W.; Jun, C.-H. "Metal-Catalyzed Alkyl Ketone to Ethyl Ketone Conversions in Chelating Ketones via Carbon-Carbon Bond Cleavage" *Journal of the Chemical Society Chemical Communications* **1985**, 92-93.
- Suginome, M.; Matsuda, T.; Yoshimoto, T.; Ito, Y. "Nickel-Catalyzed Silaboration of Small-Ring Vinylcycloalkanes: Regio- and Stereoselective (*E*)-Allylsilane Formation via C-C Bond Cleavage" *Organometallics* **2002**, *21*, 1537-1539.
- Taylor, M. S.; Jacobsen, E. N. "Asymmetric Catalysis by Chiral Hydrogen-Bond Donors" *Angewandte Chemie International Edition* **2006**, *45*, 1520-1543.
- Terao, Y.; Wakui, H.; Satoh, T.; Miura, M.; Nomura, M. "Palladium-Catalyzed Arylative Carbon-Carbon Bond Cleavage of α,α -Disubstituted Arylmethanols" *Journal of the American Chemical Society* **2001**, *123*, 10407-10408.

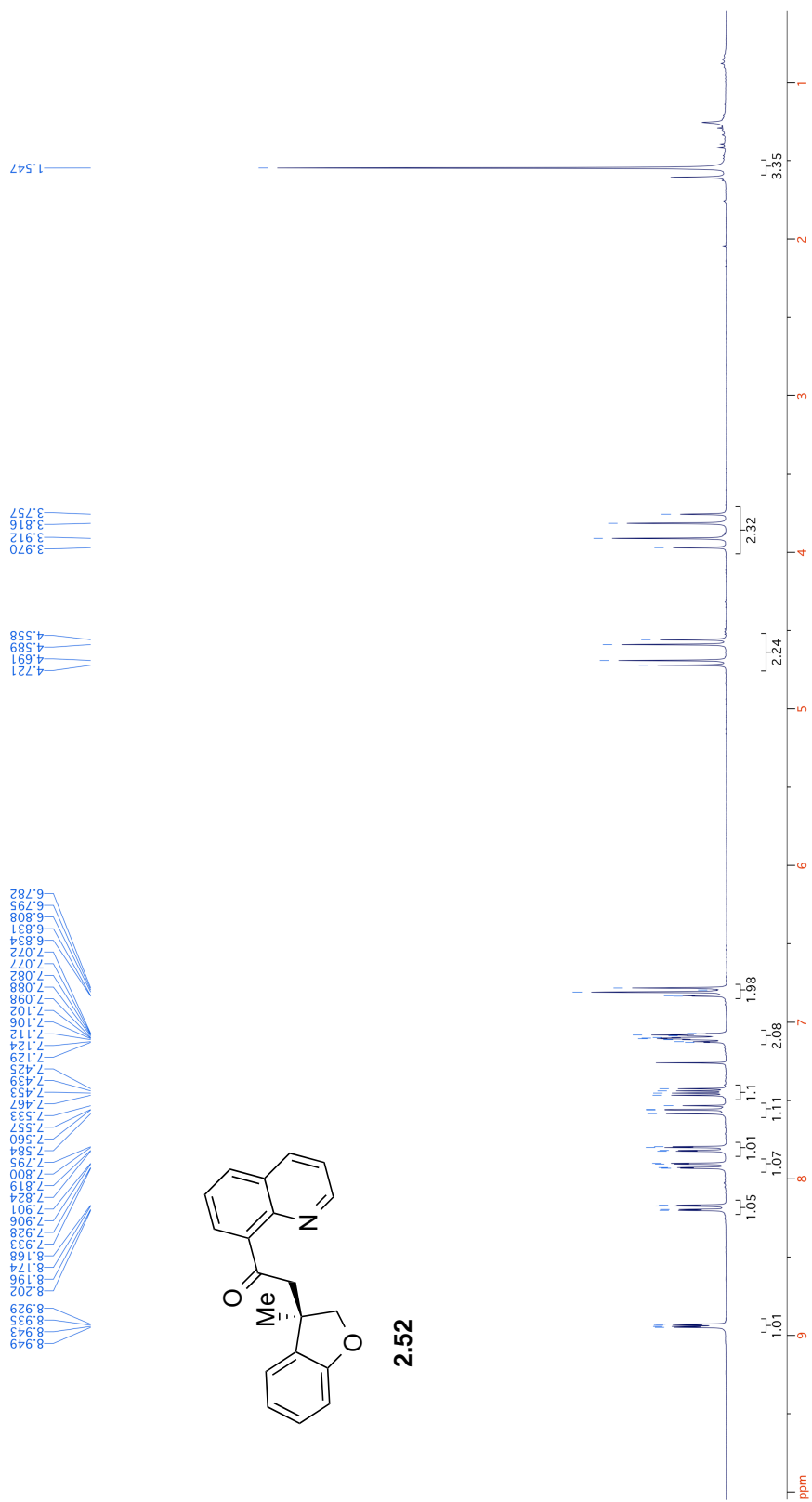
- Tipper, C. F. H.; Lawrence, C. D. "Some Reactions of Cyclopropane and a Comparison with the Lower Olefins. Part I. Introduction, and Reaction with Strong Acids" *Journal of the Chemical Society* **1955**, 713-716.
- Tipper, C. F. H. "Some Reactions of Cyclopropane, and a Comparison with the Lower Olefins. Part II.* Some Platinous-Cyclopropane Complexes" *Journal of the Chemical Society* **1955**, 2038-2056. (article of interest begins on pp 2045)
- Tipper, C. F. H.; Walker, D. A. "Some Reactions of Cyclopropane and a Comparison with the Lower Olefins. Part III.* The Friedel-Crafts Reaction" *Journal of the Chemical Society* **1957**, 1199-1206.
- Tipper, C. F. H.; Walker, D. A. "Some Reactions of Cyclopropane and a Comparison with the Lower Olefins. Part IV.* Friedel-Crafts Polymerization" *Journal of the Chemical Society* **1959**, 1352-1359.
- Tobisu, M.; Kinuta, H.; Kita, Y.; Rémond, E.; Chatani, N. "Rhodium(I)-Catalyzed Borylation of Nitriles through the Cleavage of Carbon–Cyano Bonds" *Journal of the American Chemical Society* **2012**, *134*, 115-118.
- Tolman, C. A. "Steric and Electronic Effects in Olefin Hydrocyanation at Du Pont: A Scientific and Industrial Success Story" *Journal of Chemical Education* **1986**, *63*, 199-201.
- Tolman, C. A.; McKinney, R. J.; Seidel, W. C.; Druline, J. D.; Stevens, W. R. "Homogenous Nickel-Catalyzed Olefin Hydrocyanation" *Advances in Catalysis* **1985**, *33*, 1-46.
- Tomimoto, M.; Gō, N. "Analytical Theory of Pseudorotation in Five-Membered Rings. Cyclopentane, Tetrahydrofuran, Ribose, and Deoxyribose" *The Journal of Physical Chemistry* **1995**, *99*, 563-577.
- Trofimenko, S. "Cyclopalladation Reaction" *Inorganic Chemistry* **1973**, *12*, 1215-1221.
- van der Boom, M. E.; Kraatz, H.-B.; Ben-David, Y.; Milstein, D. "Activation of a non-strained C–C Bond with Platinum(II)" *Chemical Communications* **1996**, 2167-2168.
- van der Boom, M. E.; Kraatz, H.-B.; Hassner, L.; Ben-David, Y.; Milstein, D. "Carbon–Carbon vs Carbon–Hydrogen Bond Activation by Ruthenium(II) and Platinum(II) in Solution" *Organometallics* **1999**, *18*, 3873-3884.
- van der Boom, M. E.; Liou, S.-Y.; Ben-David, Y.; Gozin, M.; Milstein, D. "Carbon–Carbon Bond Activation by Rhodium(I) in Solution. Comparison of sp^2 – sp^2 vs sp^3 – sp^3 C–C, C–H vs C–C, and Ar–CH₃ vs Ar–CH₂CH₃ Activation" *Journal of the American Chemical Society* **1998**, *120*, 13415-13421.

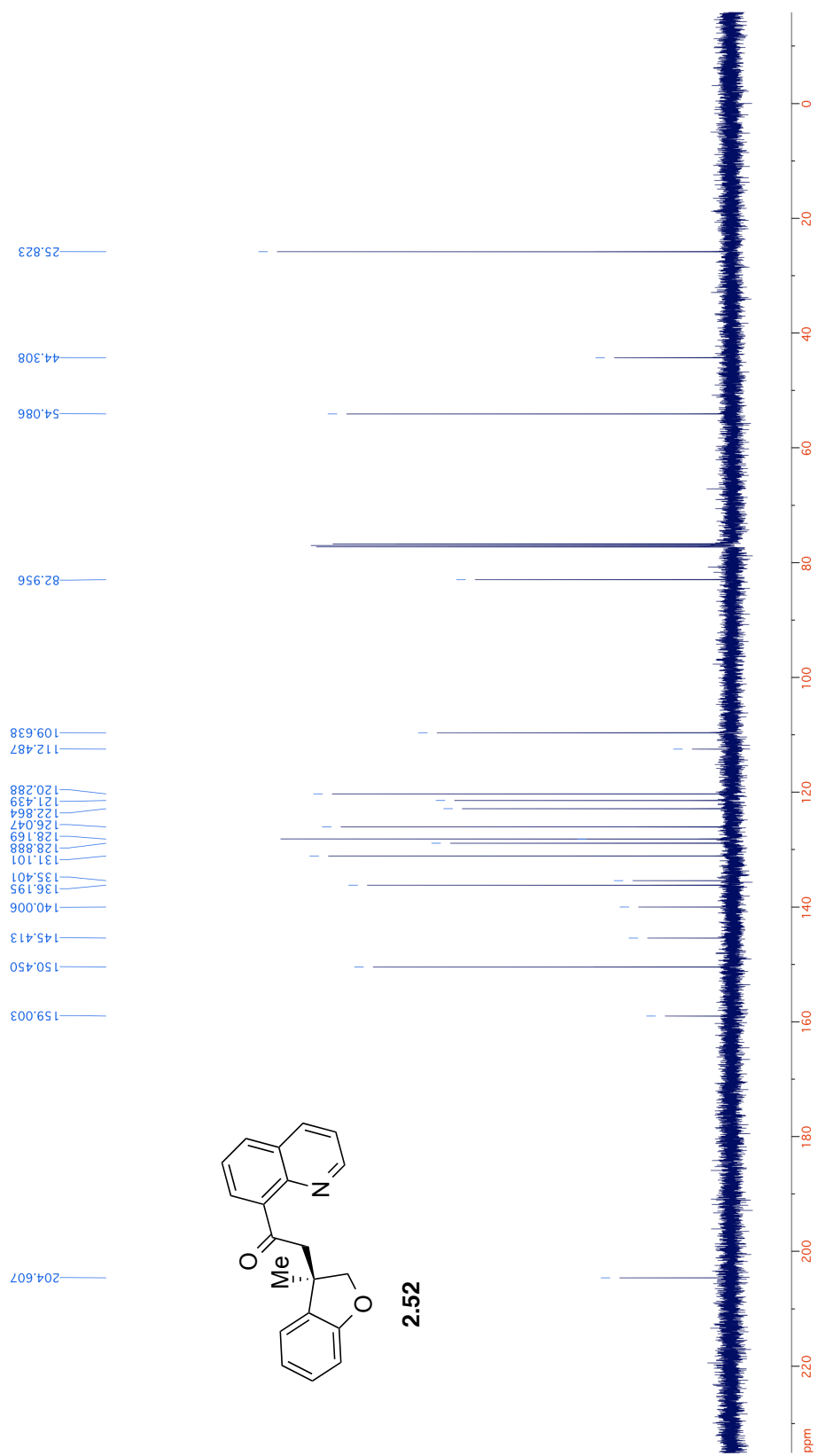
- van der Boom, M. E.; Liou, S.-Y.; Shimon, J. W.; Ben-David, Y.; Milstein, D. "Nickel promoted C–H, C–C and C–O Bond Activation in Solution" *Inorganica Chimica Acta* **2004**, 357, 4015-4023.
- van der Boom, M. E.; Milstein, D. "Cyclometalated Phosphine-Based Pincer Complexes: Mechanistic Insight into Catalysis, Coordination, and Bond Activation" *Chemical Reviews* **2003**, 103, 1759-1792.
- Vaska, L. "Reversible Activation of Covalent Molecules by Transition Metal Complexes. The Role of the Covalent Molecule" *Accounts of Chemical Research* **1968**, 1, 335-244.
- Walsh, A. D. "The Structures of Ethylene Oxide, Cyclopropane, and Related Molecules" *Transactions of the Faraday Society* **1949**, 45, 179-190.
- Wang, J.; Chen, W.; Zuo, S.; Liu, L.; Zhang, X.; Wang, J. "Direct Exchange of a Ketone Methyl or Aryl Group to Another Aryl Group through C–C Bond Activation Assisted by Rhodium Chelation" *Angewandte Chemie International Edition* **2012**, 51, 12334-12338.
- Wang, C.; Sun, H.; Fang, Y.; Huang, Y. "General and Efficient Synthesis of Indoles Through Triazene-Directed C–H Annulation" *Angewandte Chemie International Edition* **2013**, 52, 5795.
- Wang, J.; Feringa, B. L. "Dynamic Control of Chiral Space in a Catalytic Asymmetric Reaction" *Science* **2011**, 331, 1429-1432.
- Waterman, R. "σ-Bond Metathesis: A 30-Year Retrospective" *Organometallics* **2013**, 32, 7249-7263.
- Watson, M. P.; Jacobsen, E. N. "Asymmetric Intramolecular Arylcyanation of Unactivated Olefins via C–CN Bond Activation" *Journal of the American Chemical Society* **2008**, 130, 12594-12595.
- Wautelet, P.; Le Moigne, J.; Videva, V.; Turek, P. "Spin Exchange Interaction Through Phenylene-Ethynylene Bridge in Diradicals Based on Iminonitroxide and Nitronylnitroxide Radical Derivatives. 1. Experimental Investigation of the Through-Bond Spin Exchange Coupling" *Journal of Organic Chemistry* **2003**, 68, 8025-8036.
- Wentzel, M. T.; Reddy, V. J.; Hyster, T. K.; Douglas, C. J. "Chemoselectivity in Catalytic C–C and C–H Bond Activation: Controlling Intermolecular Carboacylation and Hydroarylation of Alkenes" *Angewandte Chemie International Edition* **2009**, 48, 6121-6123.

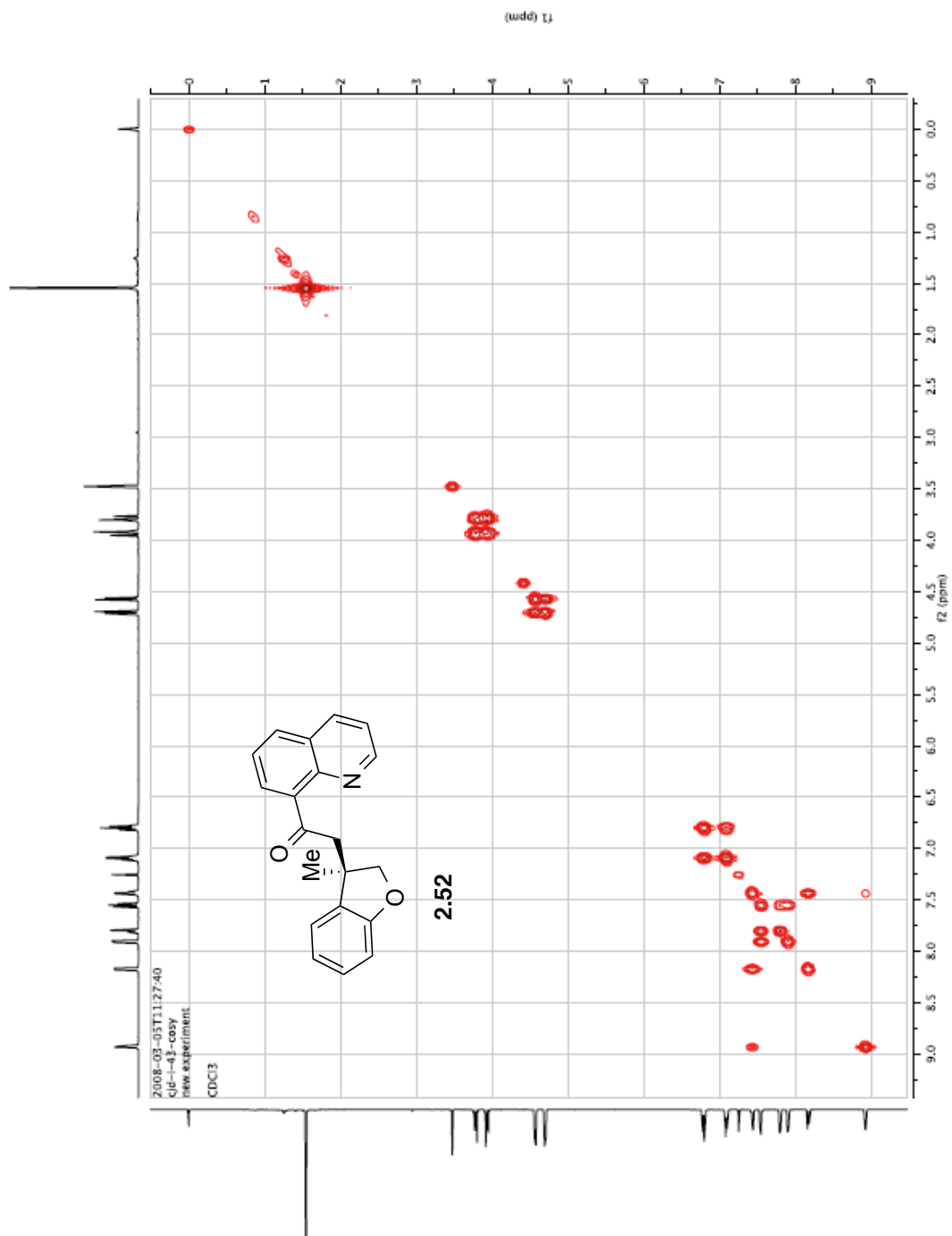
- Yada, A.; Yukawa, T.; Nakao, Y.; Hiyama, T. "Nickel/ AlMe_2Cl -Catalysed Carbocyanation of Alkynes Using Arylacetonitriles" *Chemical Communications* **2009**, 3931-3933.
- Yamamoto, E.; Izumi, K.; Horita, Y.; Ito, H. "Anomalous Reactivity of Silylborane: Transition-Metal-Free Boryl Substitution of Aryl, Alkenyl, and Alkyl Halides with Silylborane/Alkoxy Base Systems" *Journal of the American Chemical Society* **2012**, 134, 19997-20000.
- Yasui, Y.; Takemoto, Y. "Intra- and Intermolecular Amidation of C–C Unsaturated Bonds Through Palladium-Catalyzed Reactions of Carbamoyl Derivatives" *The Chemical Record* **2008**, 8, 386-394.
- Yasui, Y.; Kamisaki, H.; Takemoto, Y. "Enantioselective Synthesis of 3,3-Disubstituted Oxindoles Through Pd-Catalyzed Cyanoamidation" *Organic Letters* **2008**, 10, 3303-3306.
- Yasui, Y.; Takeda, H.; Takemoto, Y. "Toward General Access to the *Aspidosperma*-Type Terpenoid Indole Alkaloids: Synthesis of the Key 3,3-Disubstituted Piperidones through Enantioselective Intramolecular Heck-Type Reaction of Chloroformamides" *Chemical and Pharmacy Bulletin* **2008**, 56, 1567-1574.
- Zhang, L.; Guan L.-P.; Sun, X.-Y.; Wei, C.-X.; Chai, K.-Y.; Quan, Z.-S. "Synthesis and Anticonvulsant Activity of 6-Alkoxy-[1,2,4]Triazolo[3,4-a]Phthalazines" *Chemical Biology & Drug Design* **2009**, 73, 313-319.
- Zhao, P.; Hartwig, J. F. "Insertions of Ketones and Nitriles into Organorhodium(I) Complexes and β -Hydrocarbyl Eliminations from Rhodium(I) Alkoxo and Iminyl Complexes" *Organometallics* **2008**, 27, 4749-4757.
- Zhou, J.; Yang, W.; Wang, B.; Ren, H. "Friedel-Crafts Arylation for the Formation of C- sp^2 –C sp^2 Bonds: A Route to Unsymmetrical and Functionalized Polycyclic Aromatic Hydrocarbons from Aryl Triazenes" *Angewandte Chemie International Edition* **2012**, 51, 12293-12297.
- Zhu, C.; Yamane, M. "Transition-Metal-Free Borylation of Aryltriazene Mediated by $\text{BF}_3 \cdot \text{OEt}_2$ " *Organic Letters* **2012**, 14, 4560-4563.
- Zimmer, R.; Dinesh, C. U.; Nandanan, E.; Khan, F. A. "Palladium-Catalyzed Reactions of Allenes" *Chemical Reviews* **2000**, 100, 3067-3126.

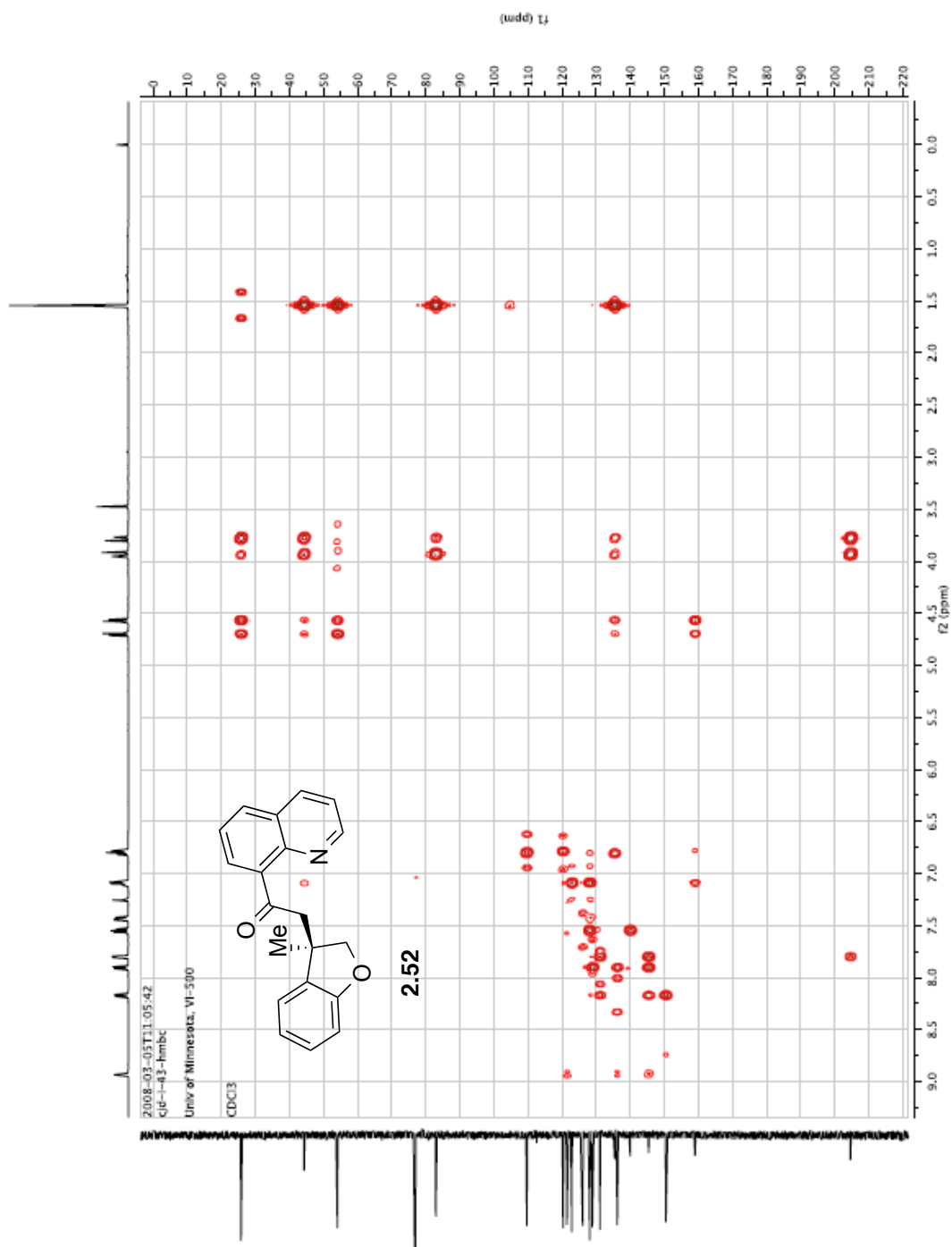


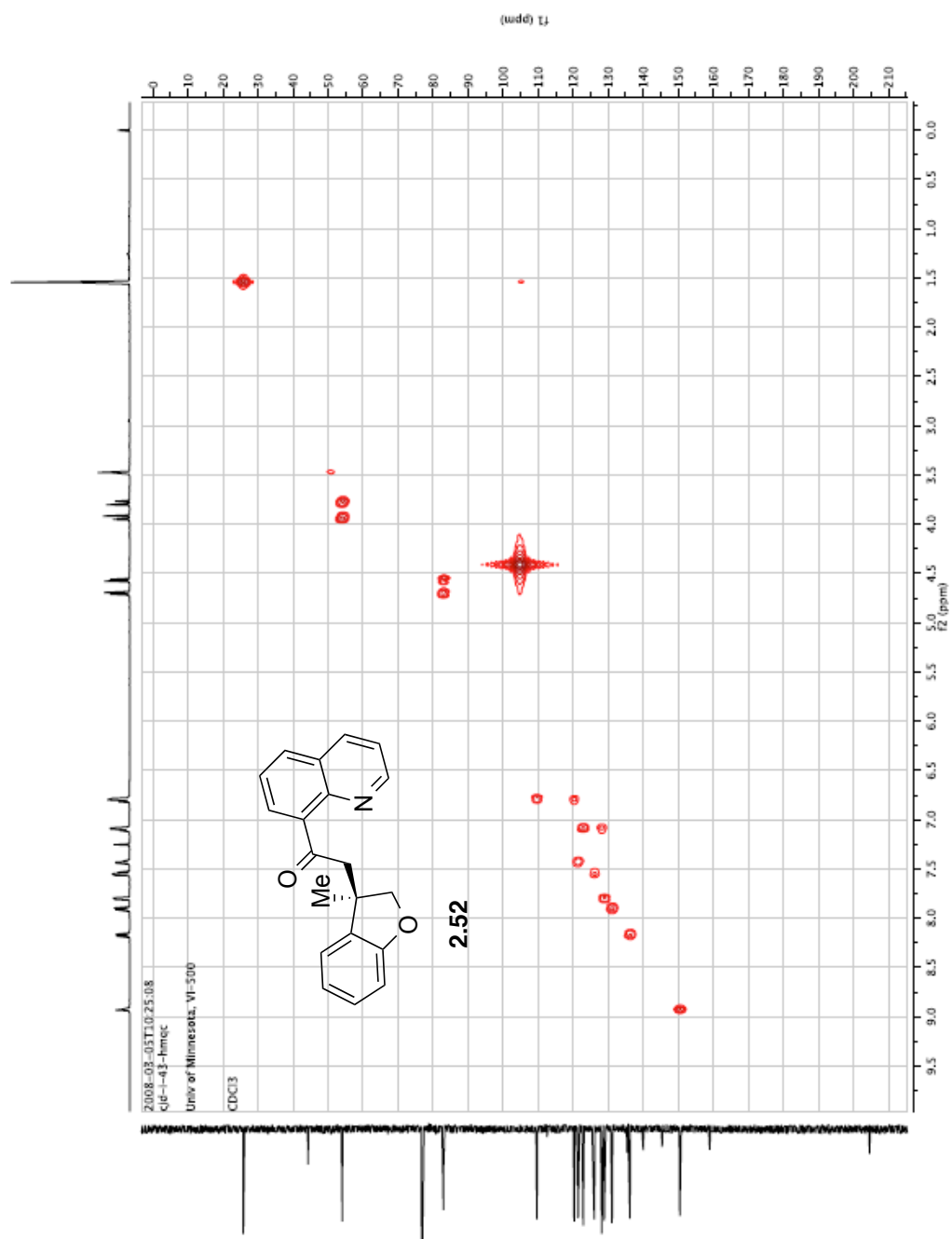


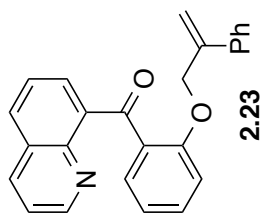


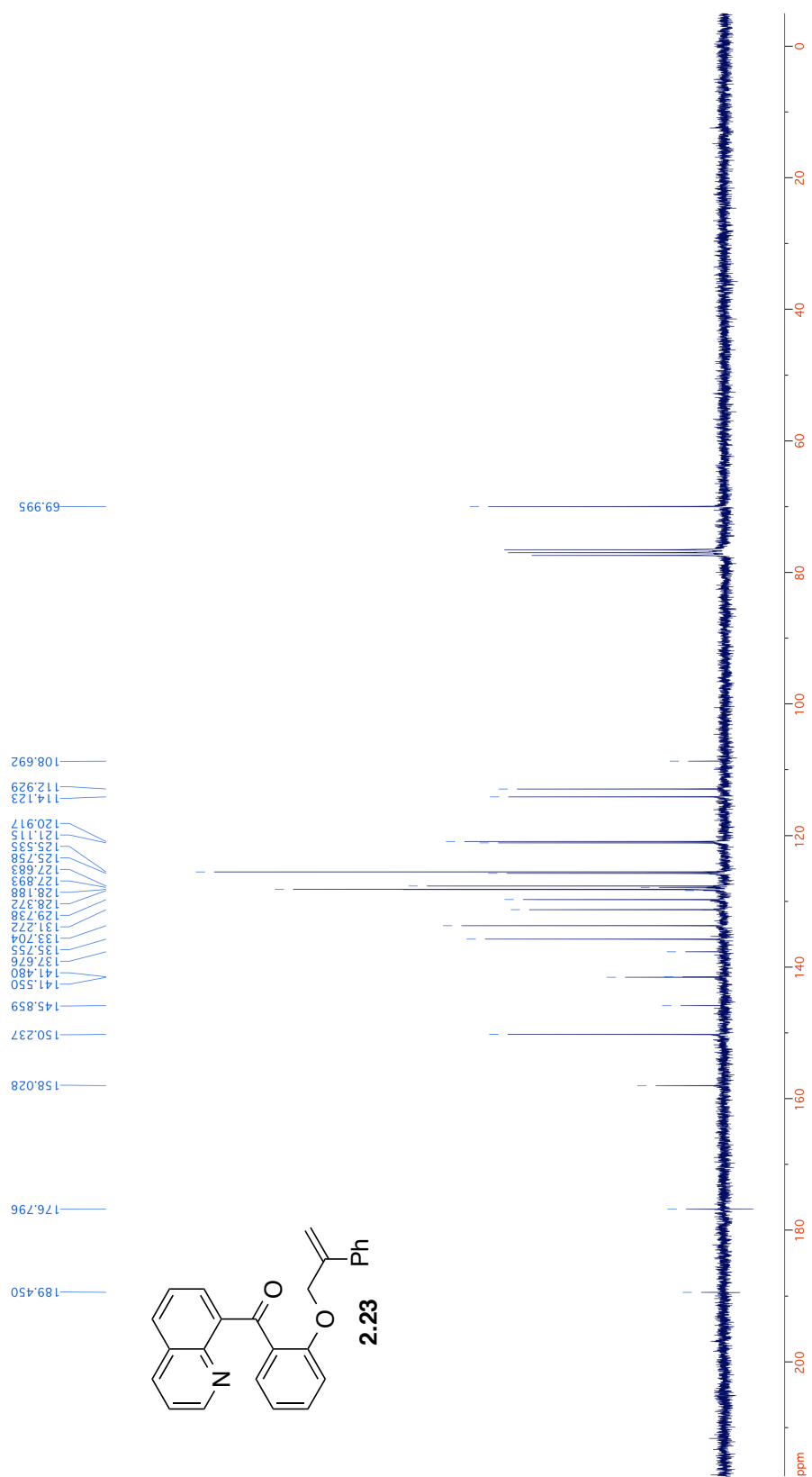


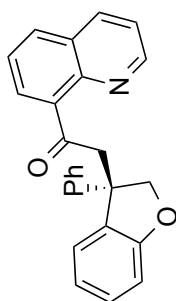
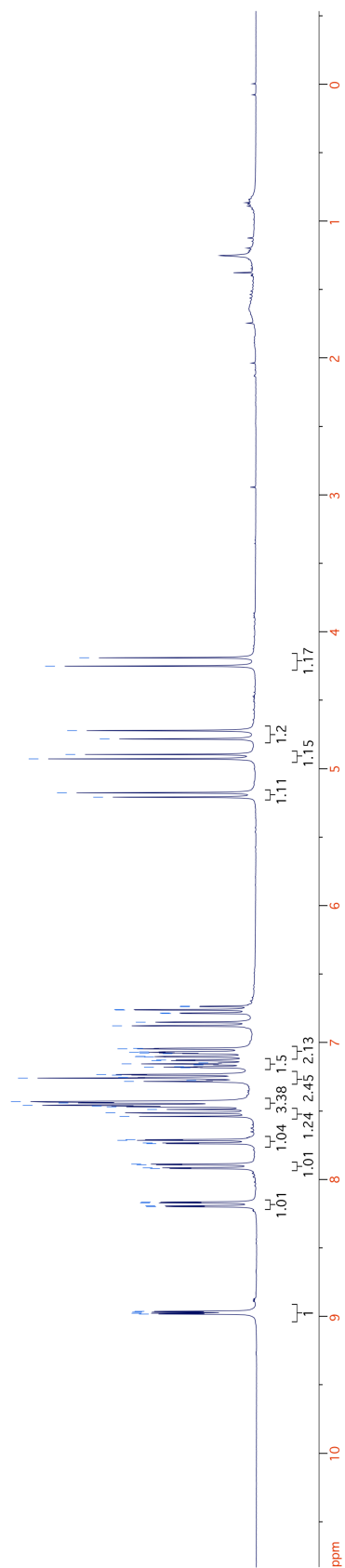




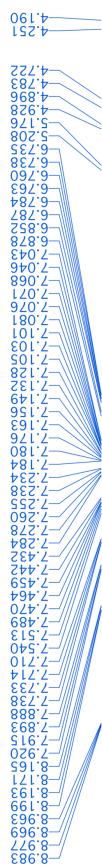


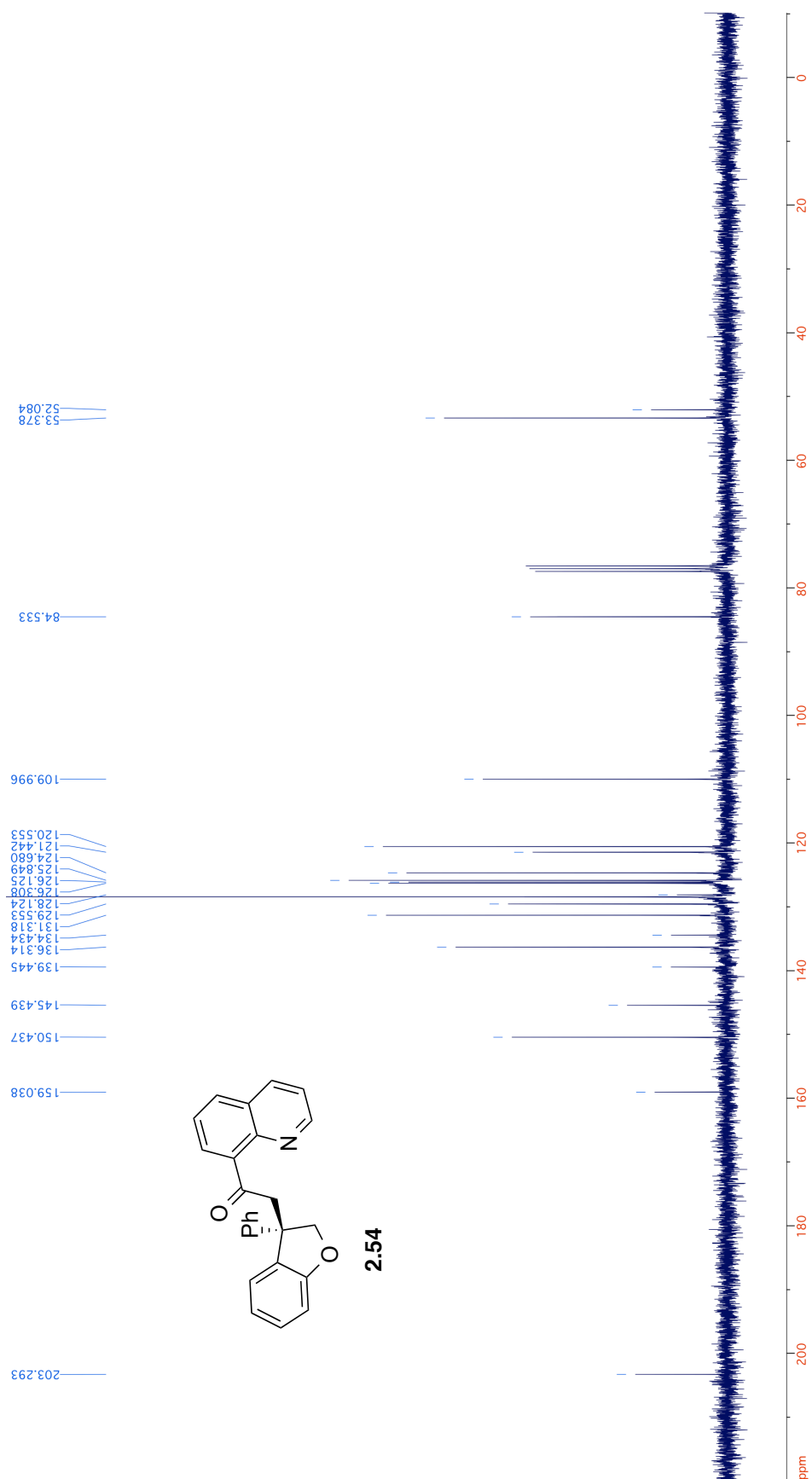


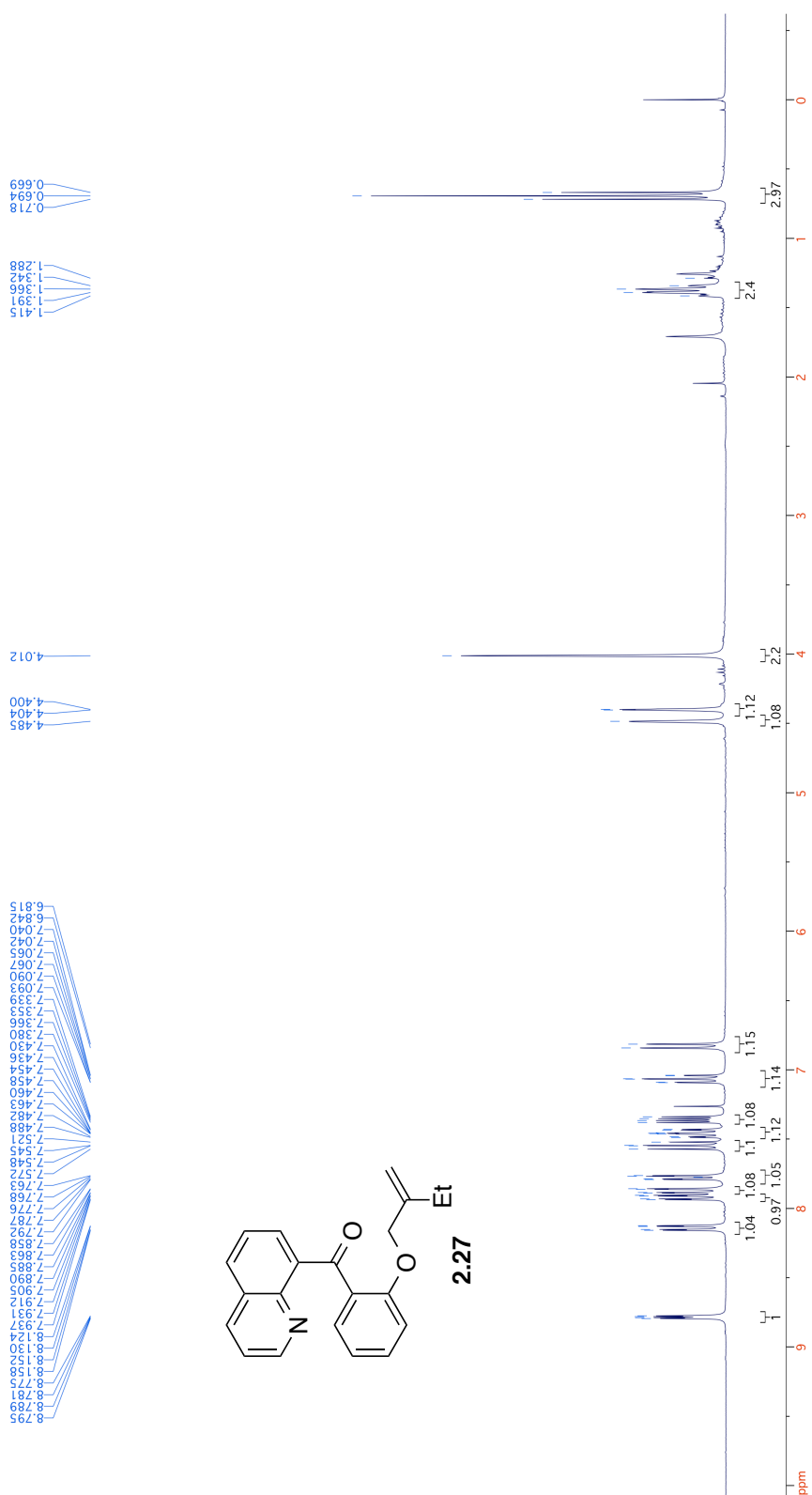
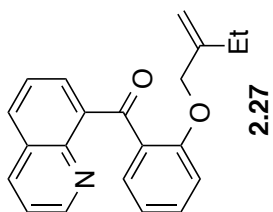


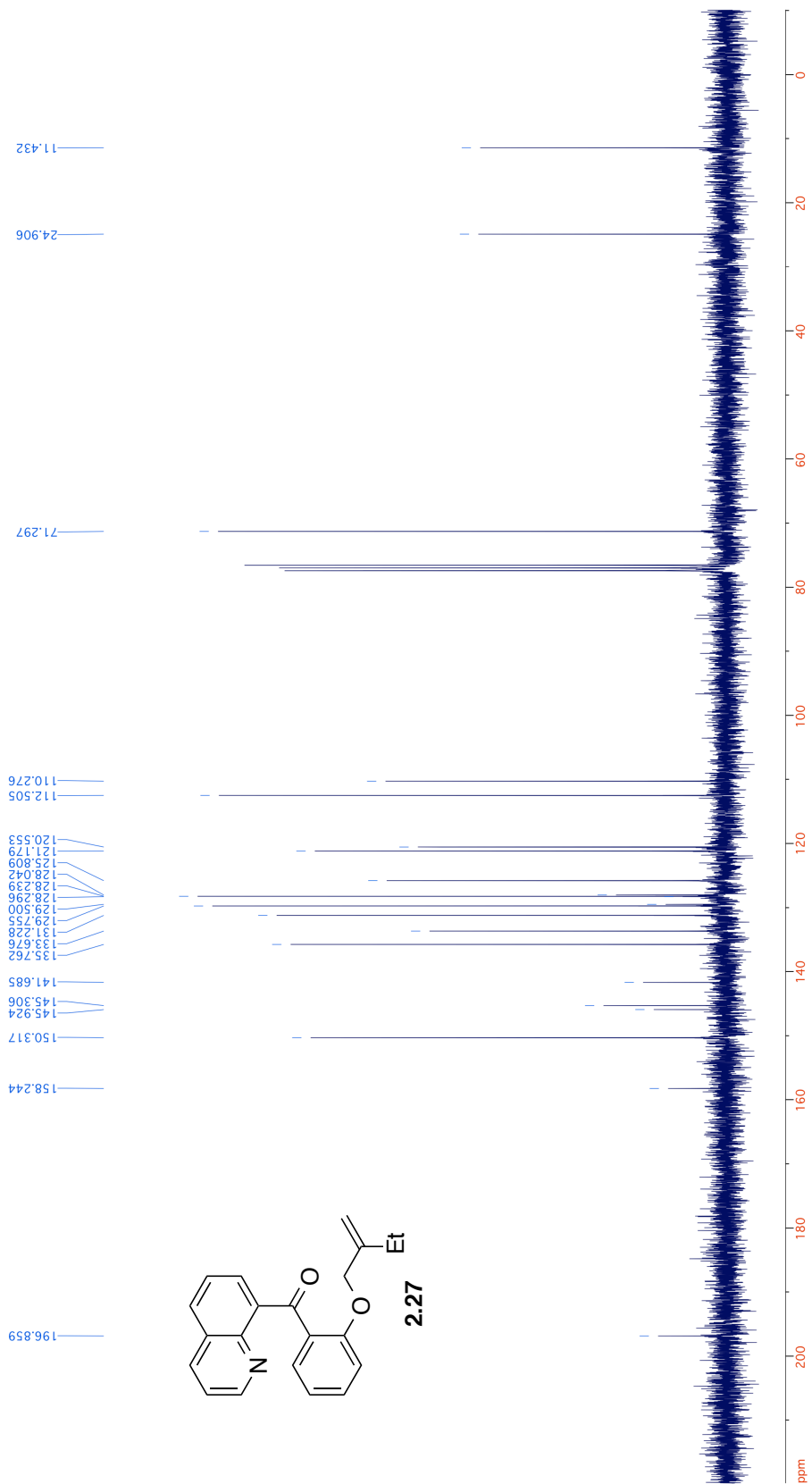


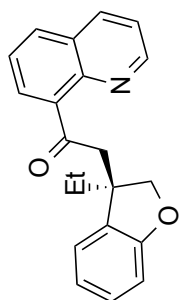
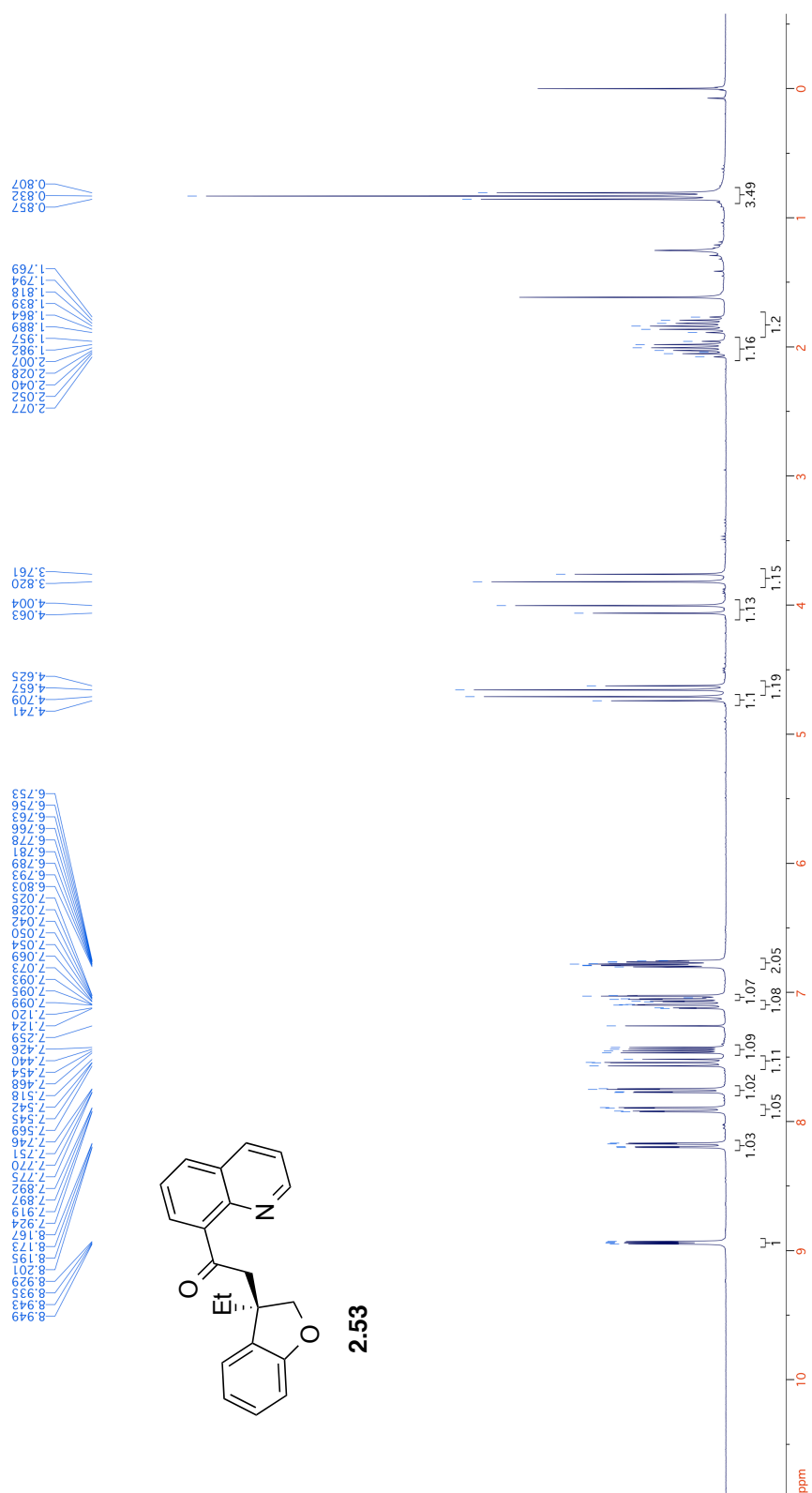
2.54



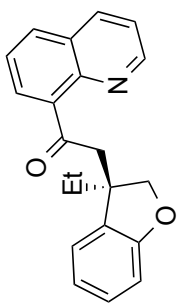
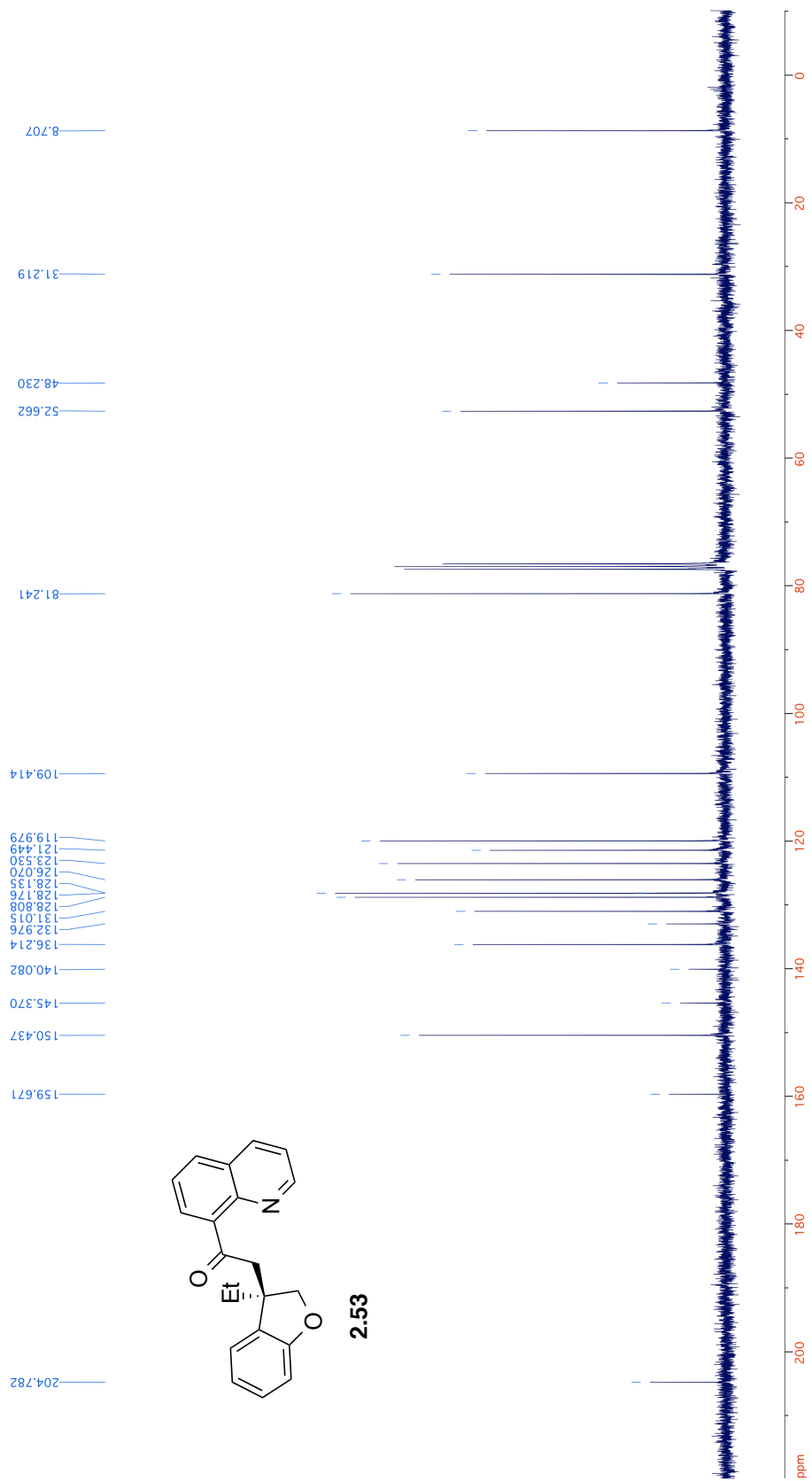




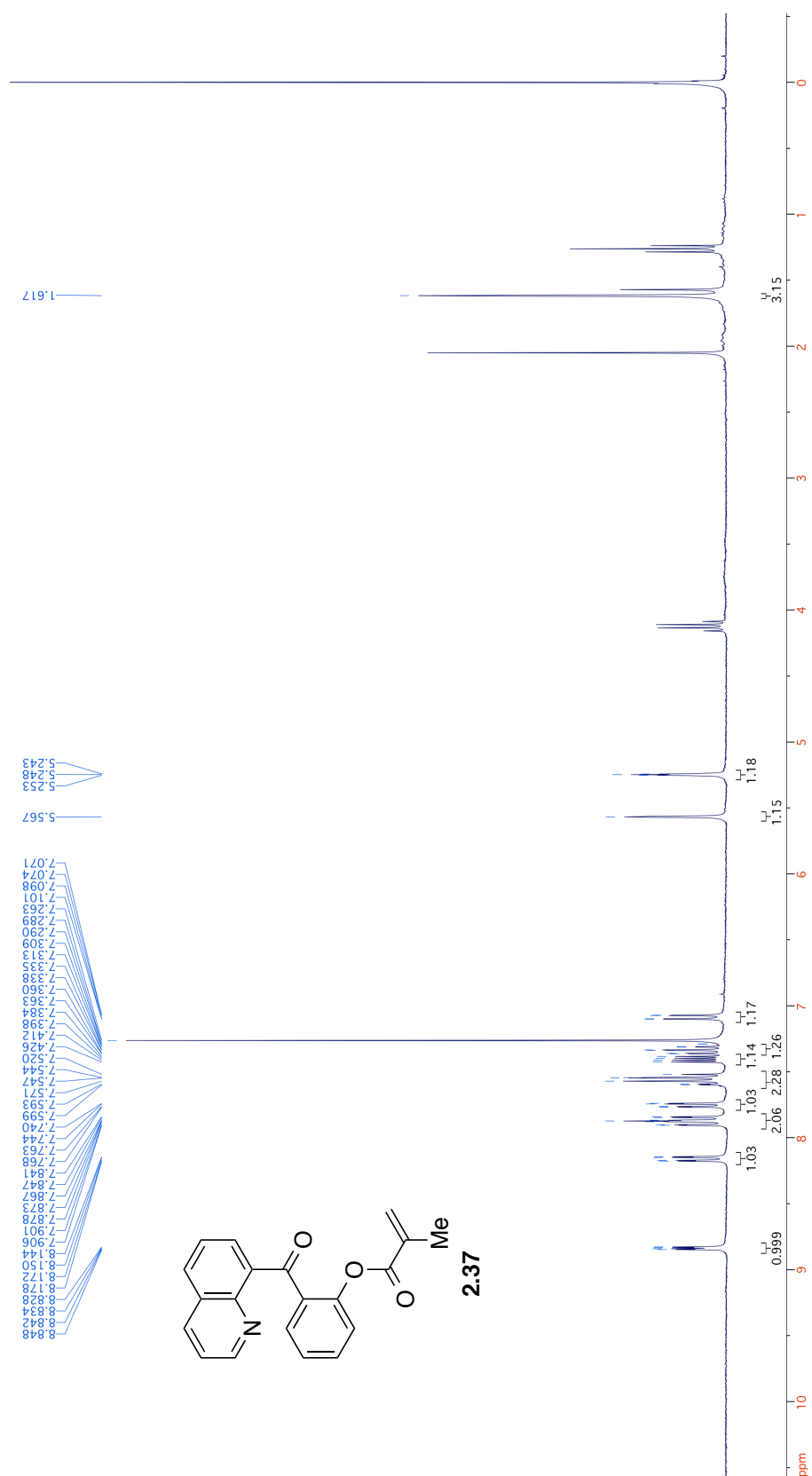


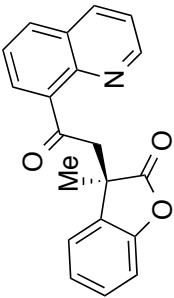


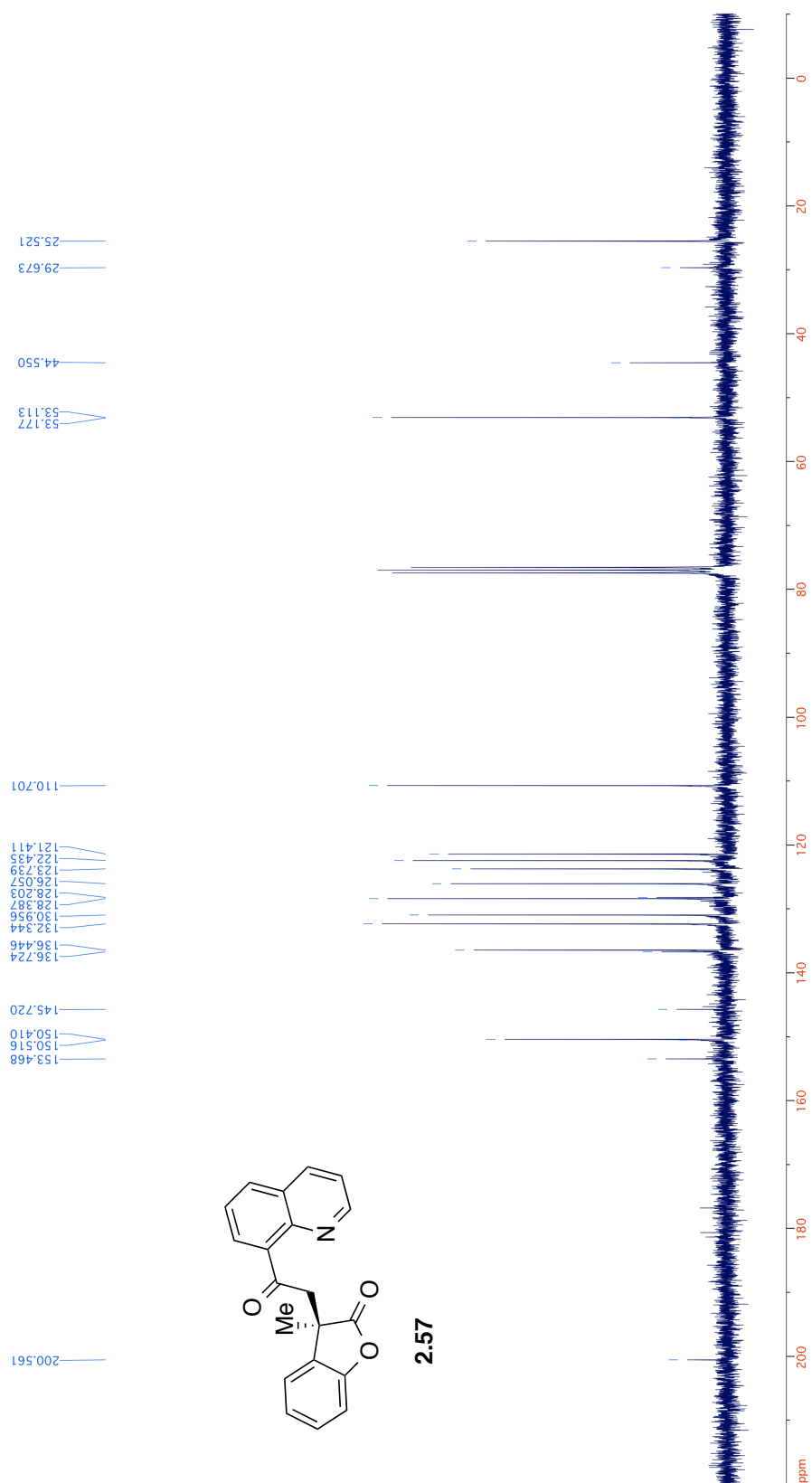
2.53

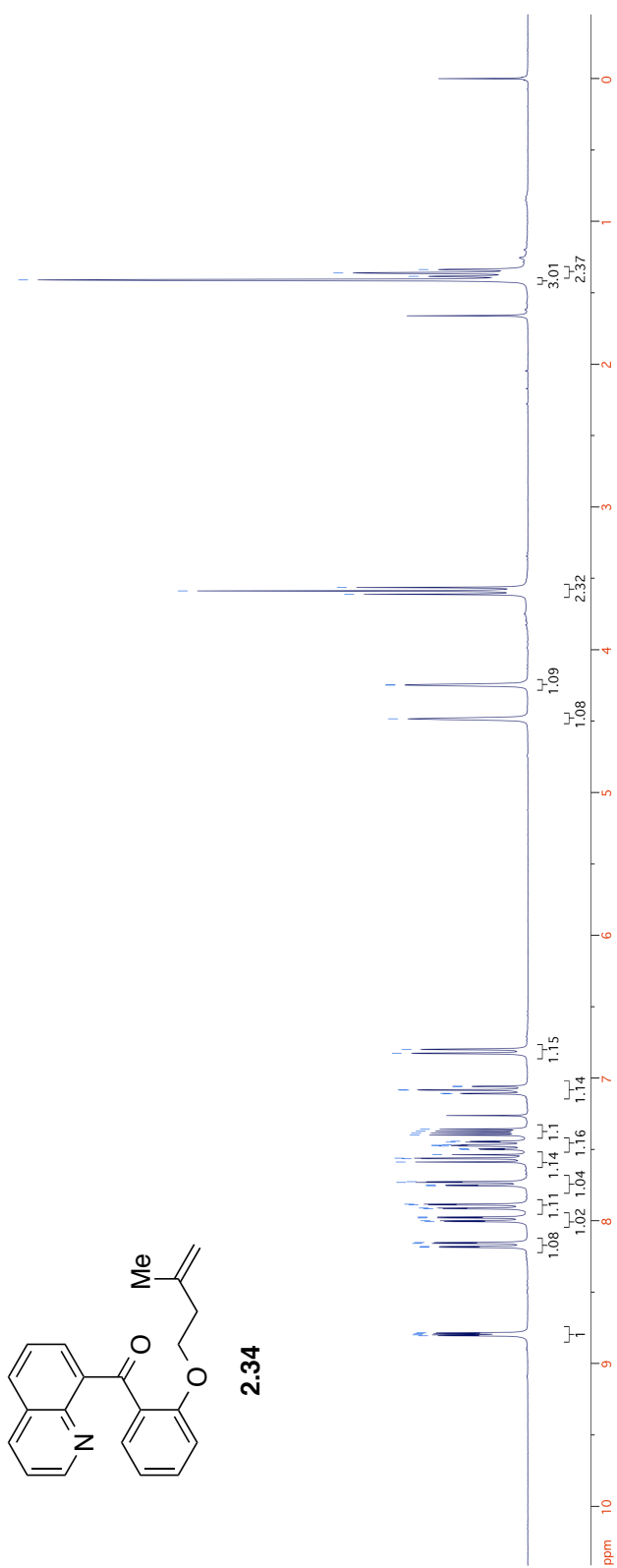


2.53







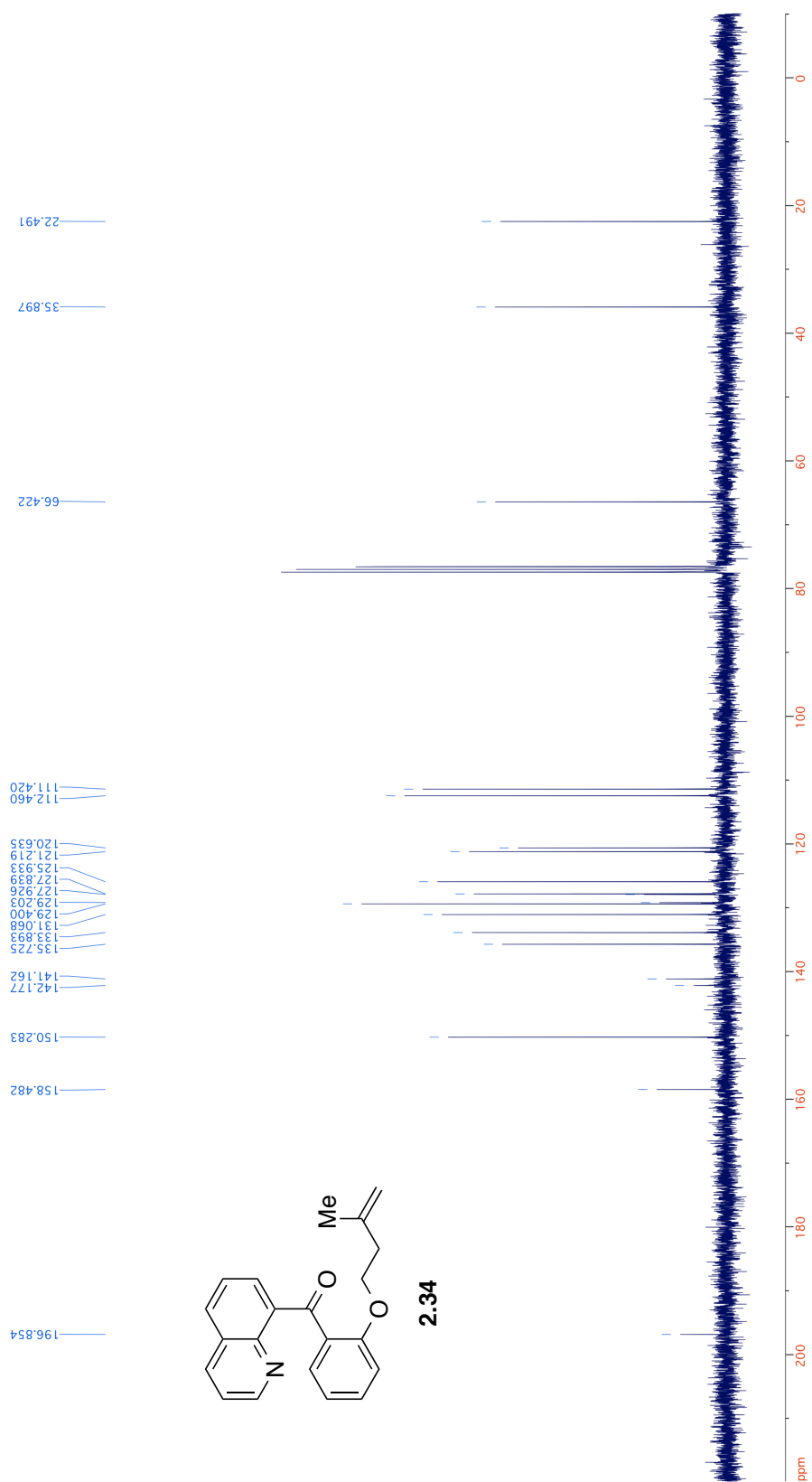


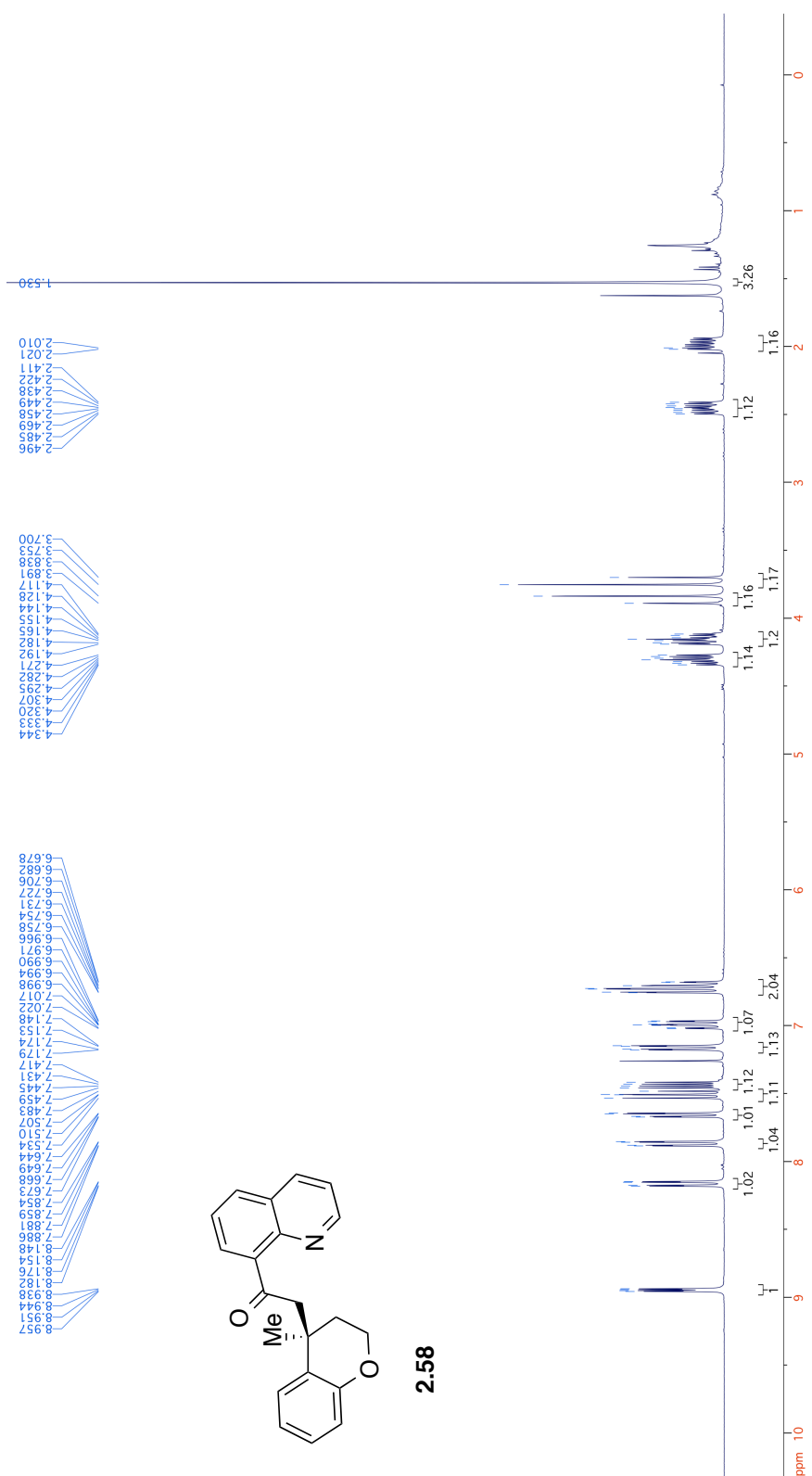
1.410
1.385
1.361
1.338

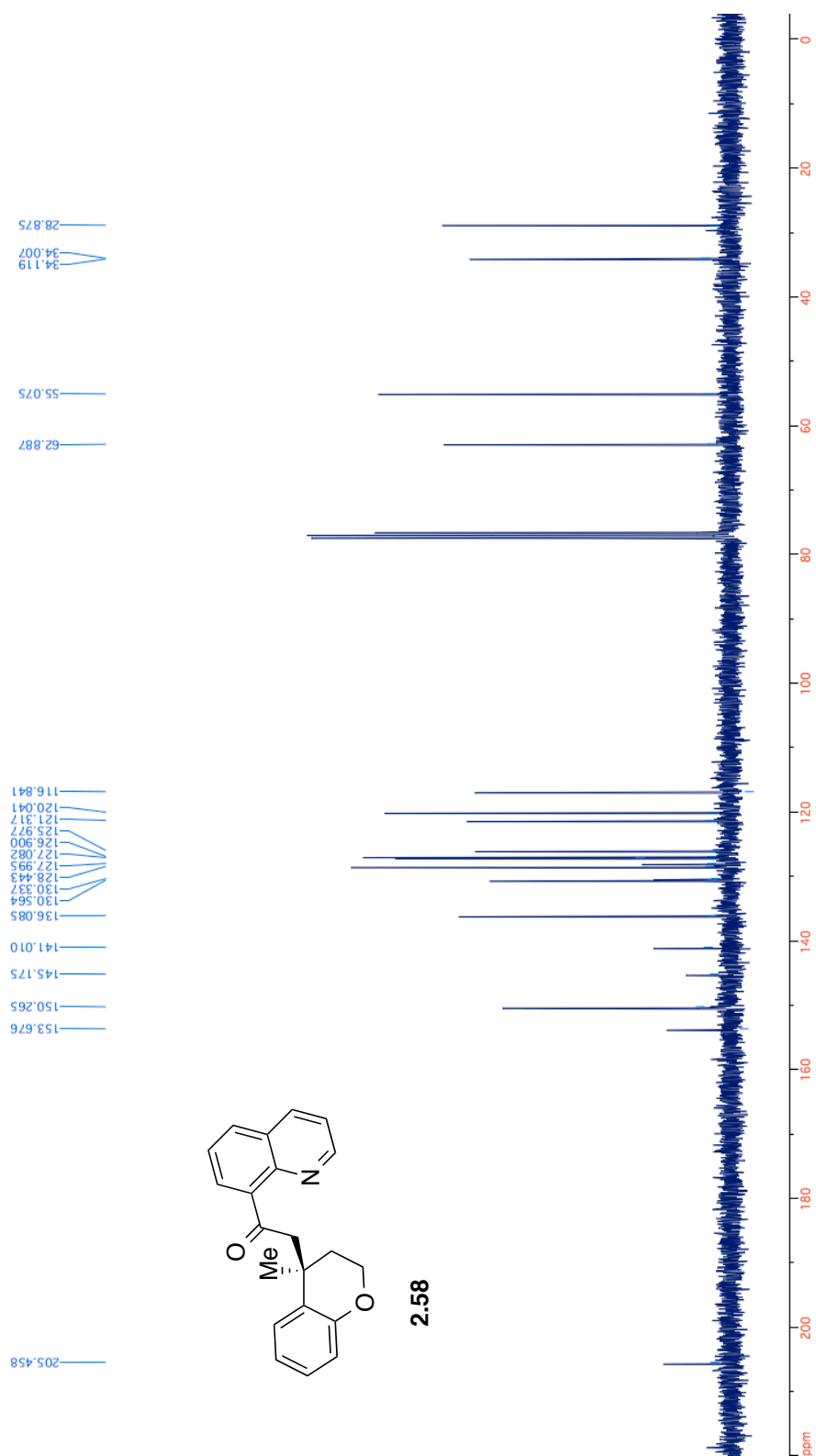
3.612
3.588
3.565

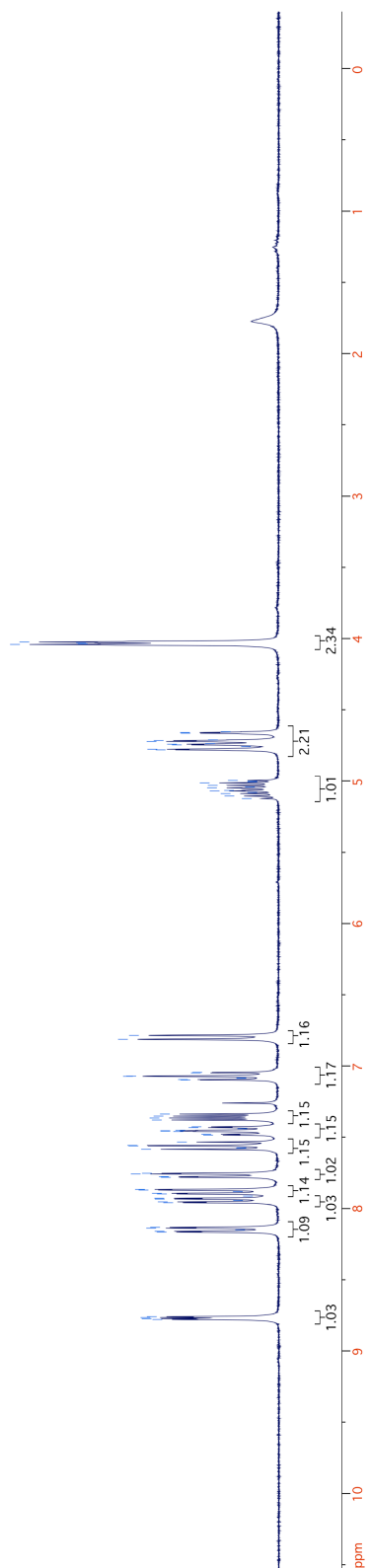
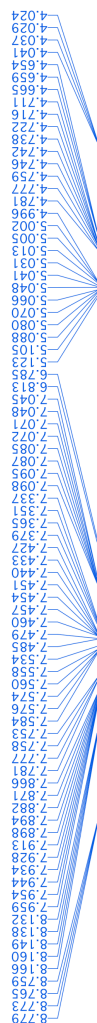
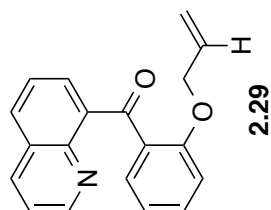
4.246
4.248
4.484

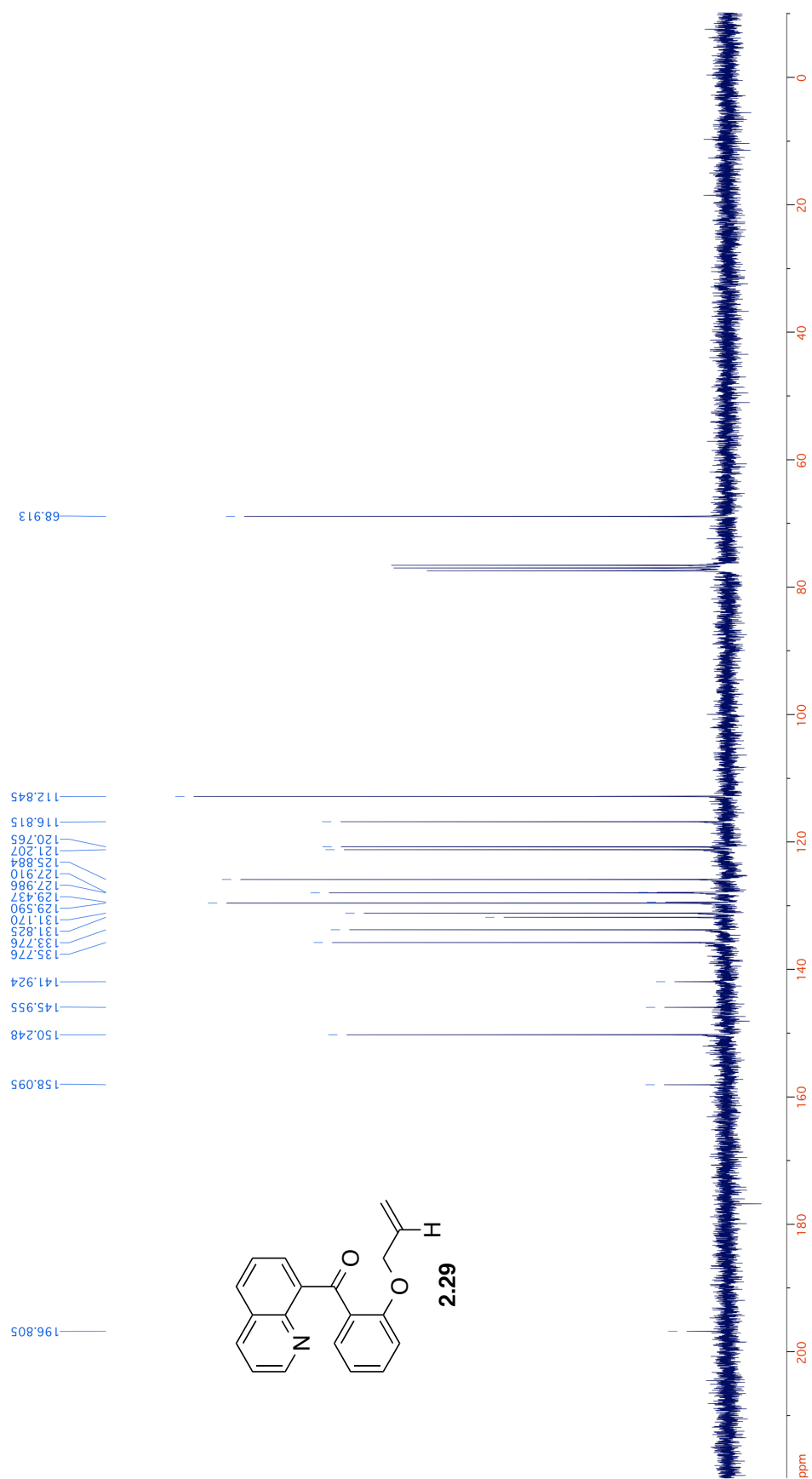
8.805
8.799
8.791
8.785
8.180
8.158
8.132
8.005
7.999
7.980
7.974
7.916
7.884
7.880
7.888
7.884
7.755
7.731
7.726
7.588
7.564
7.538
7.501
7.495
7.477
7.473
7.471
7.468
7.443
7.400
7.386
7.372
7.358
7.110
7.107
7.085
7.083
7.060
7.057
6.827
6.800

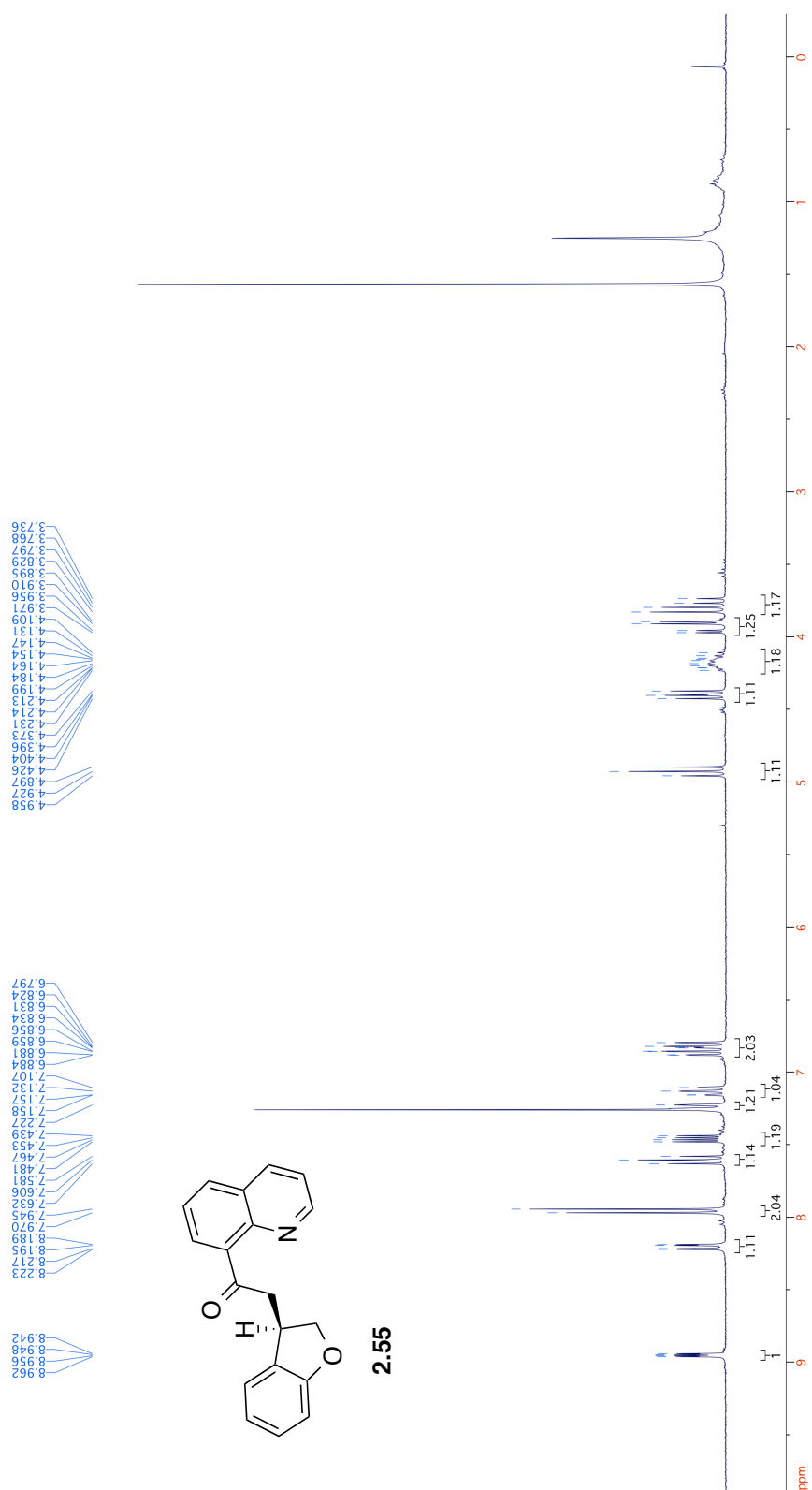






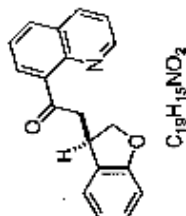


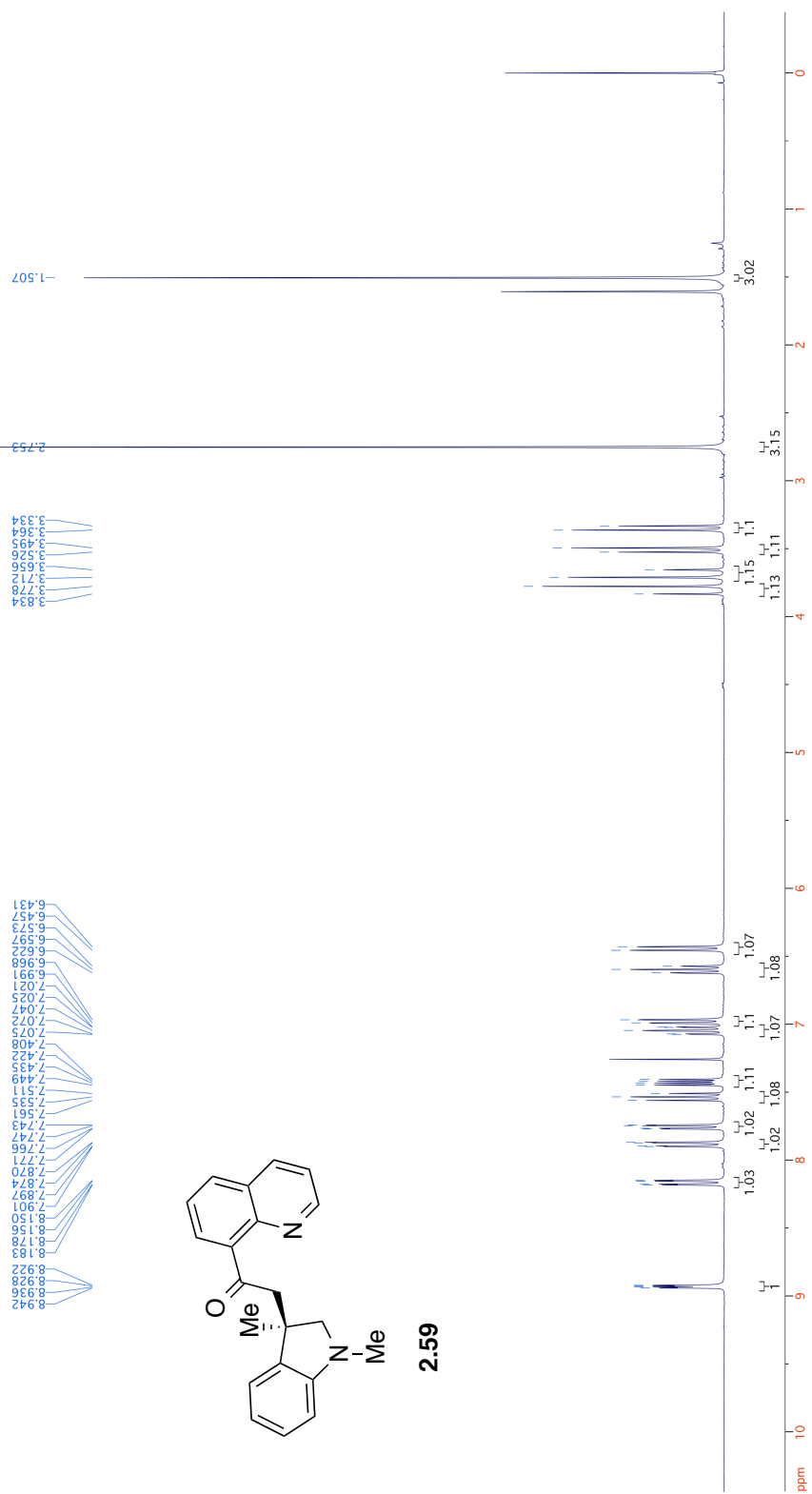


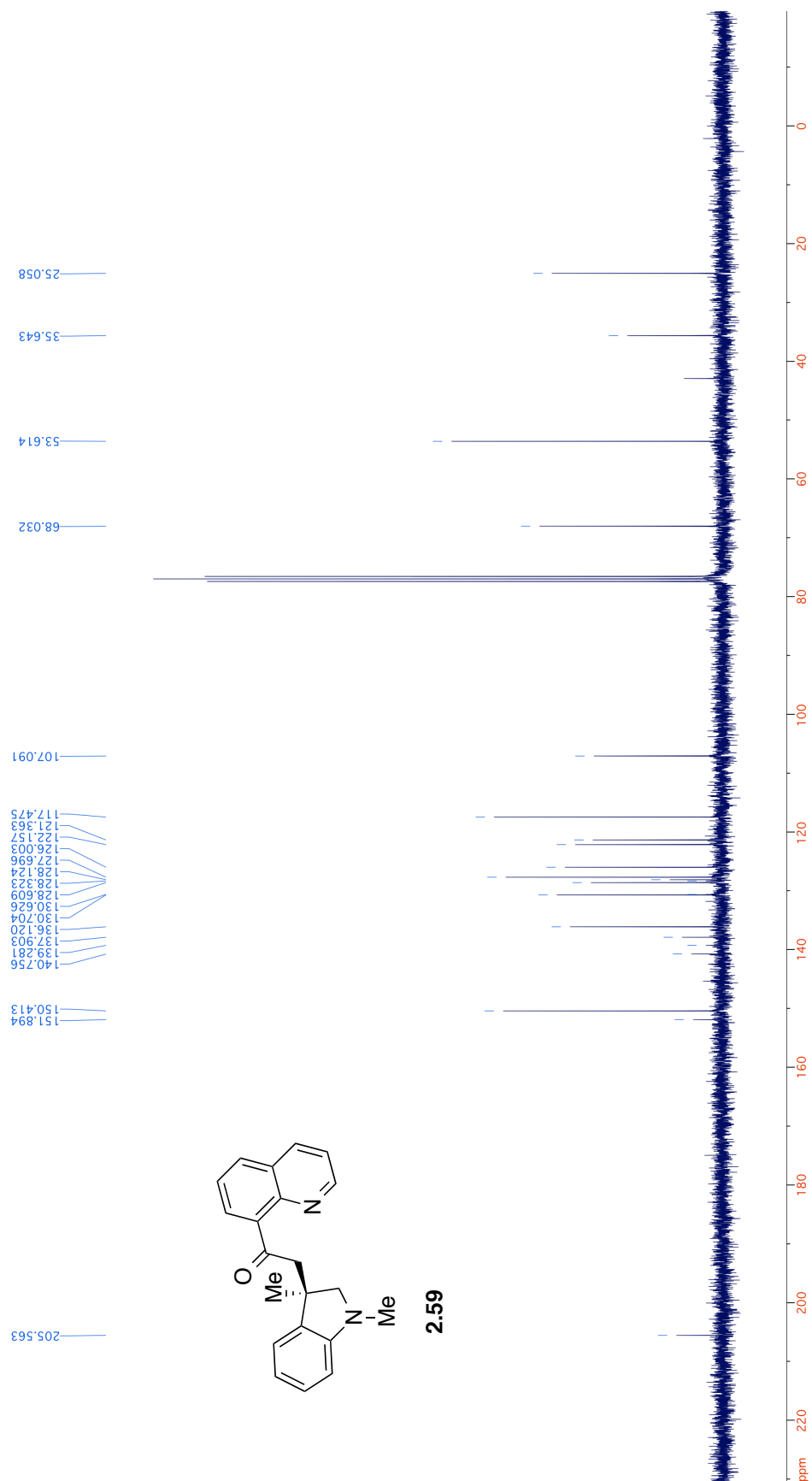


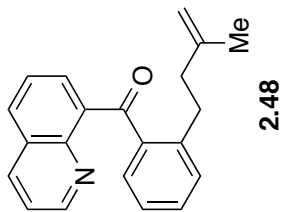
O=C(C1=CC=CC2=C1N=CC=CC2)C1OC(C1)C
 $C_{19}H_{15}NO_2$

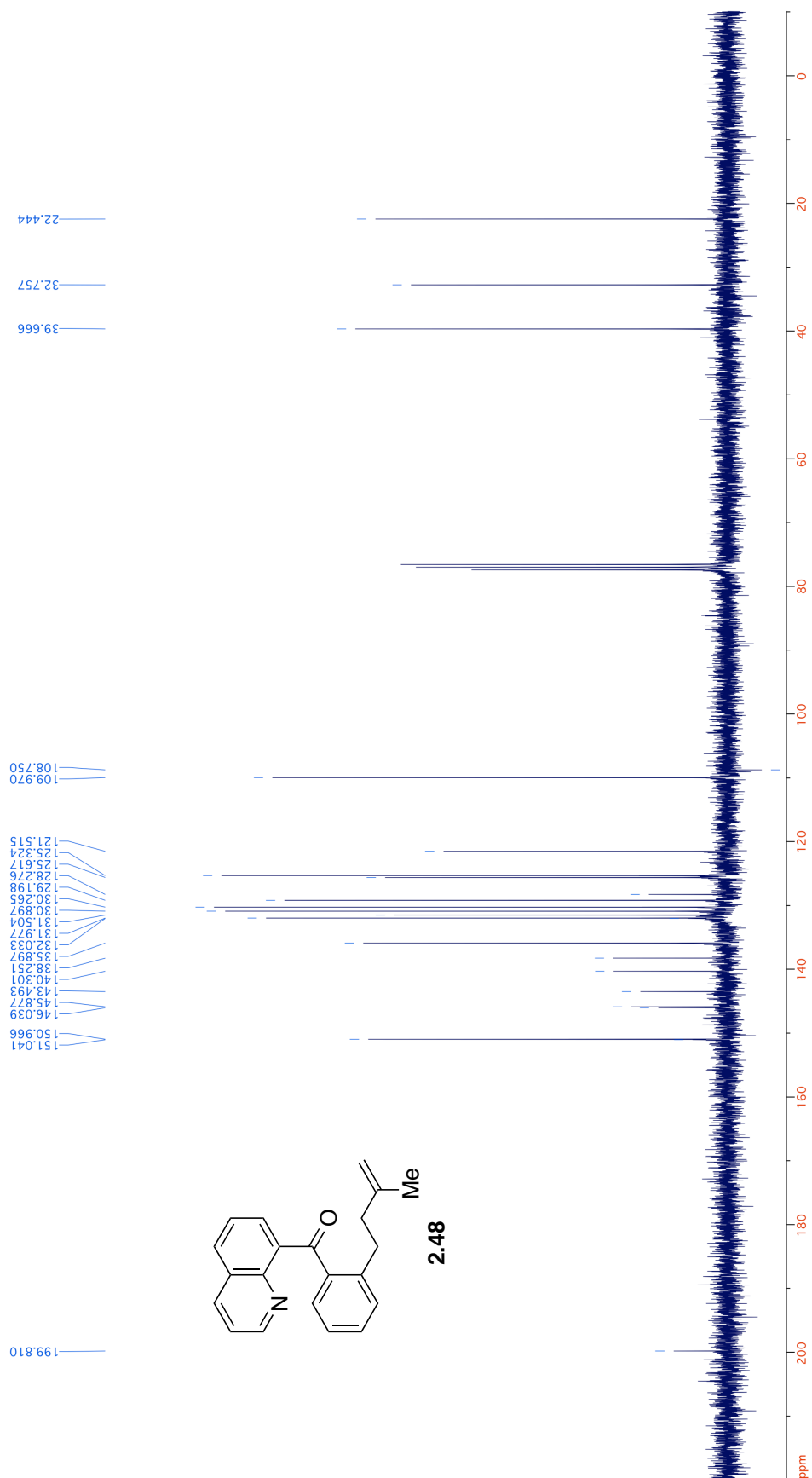
Only of Minnesota VT-500
 Pulse Sequence: *zgpg30
 Date: 1-15-87
 Solvent: CDCl3
 Acquisition: 4000 MHz, 8.18
 Processing: 4000 MHz, 8.18
 Total acq. time: 0:35:24
 Total acq. time: 1:7 hours
 Ambient temperature: 25.00
 PULSE SEQUENCE: zgpg30
 Pulse delay: 1.000 sec
 Pulse: 67.5 degrees
 Acq. time: 0.980 sec
 Width: 22108.7 Hz
 100% repetition
 OBSERVE: D13, 125.00 MHz
 DECOUPLE: 13, 400.00 MHz
 on during acq: :on
 off during delay
 WALTZ-16 modulated
 DATA PROCESSING
 Line broadening: 1.0 Hz
 FI size: 6536

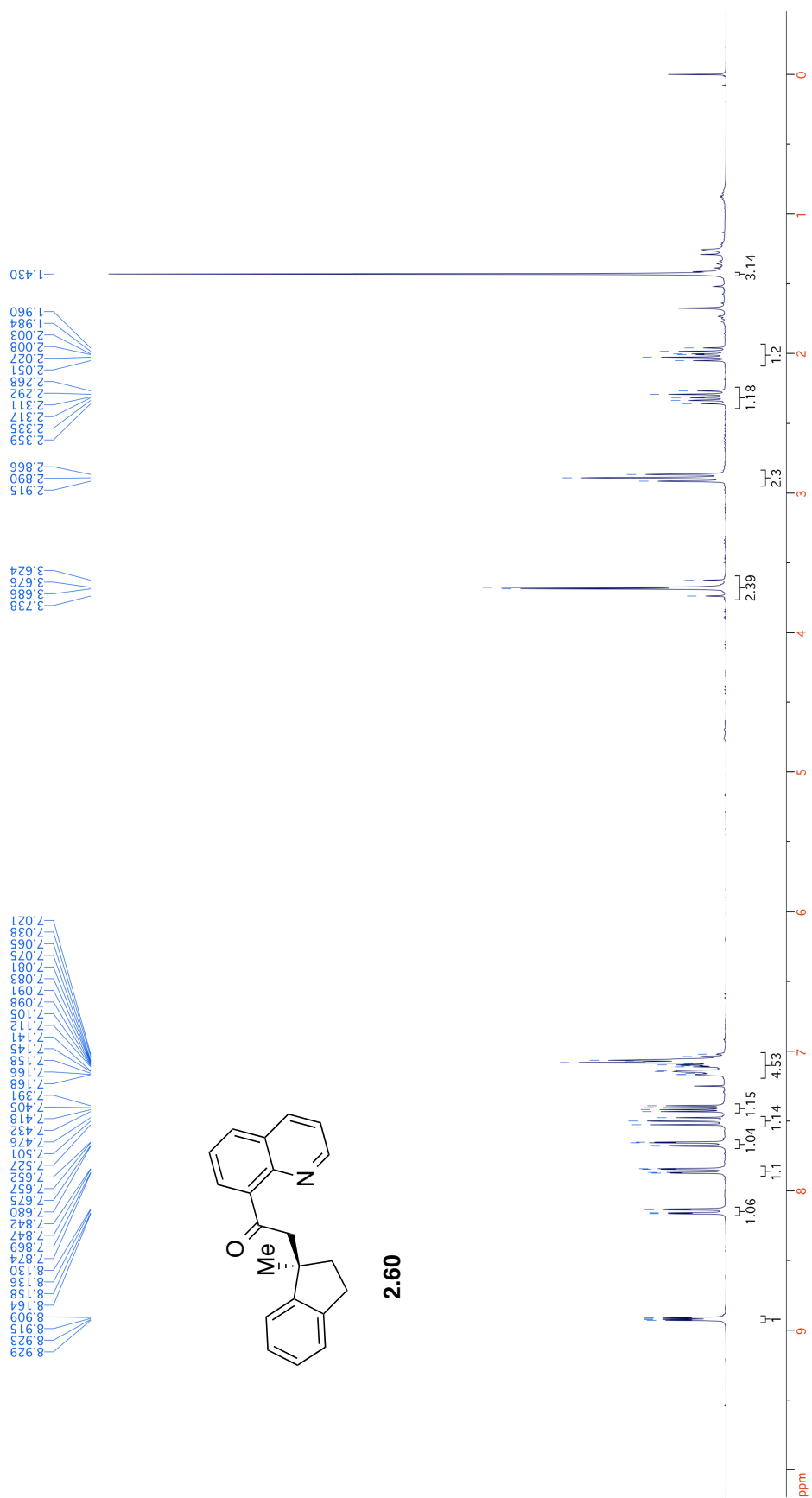


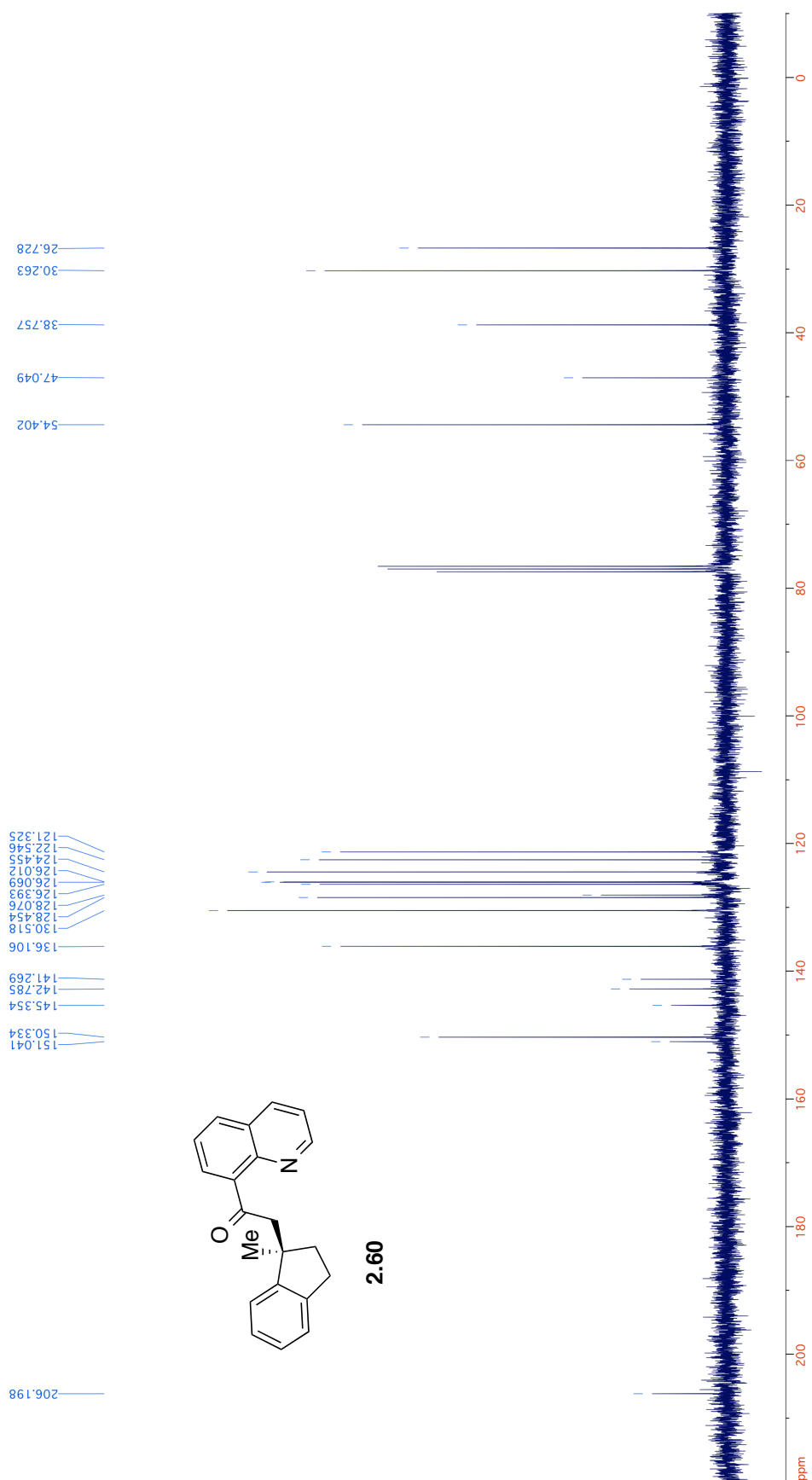


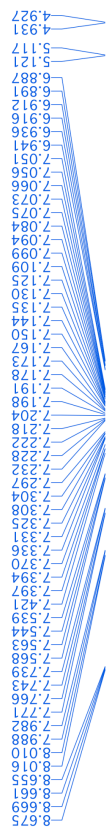


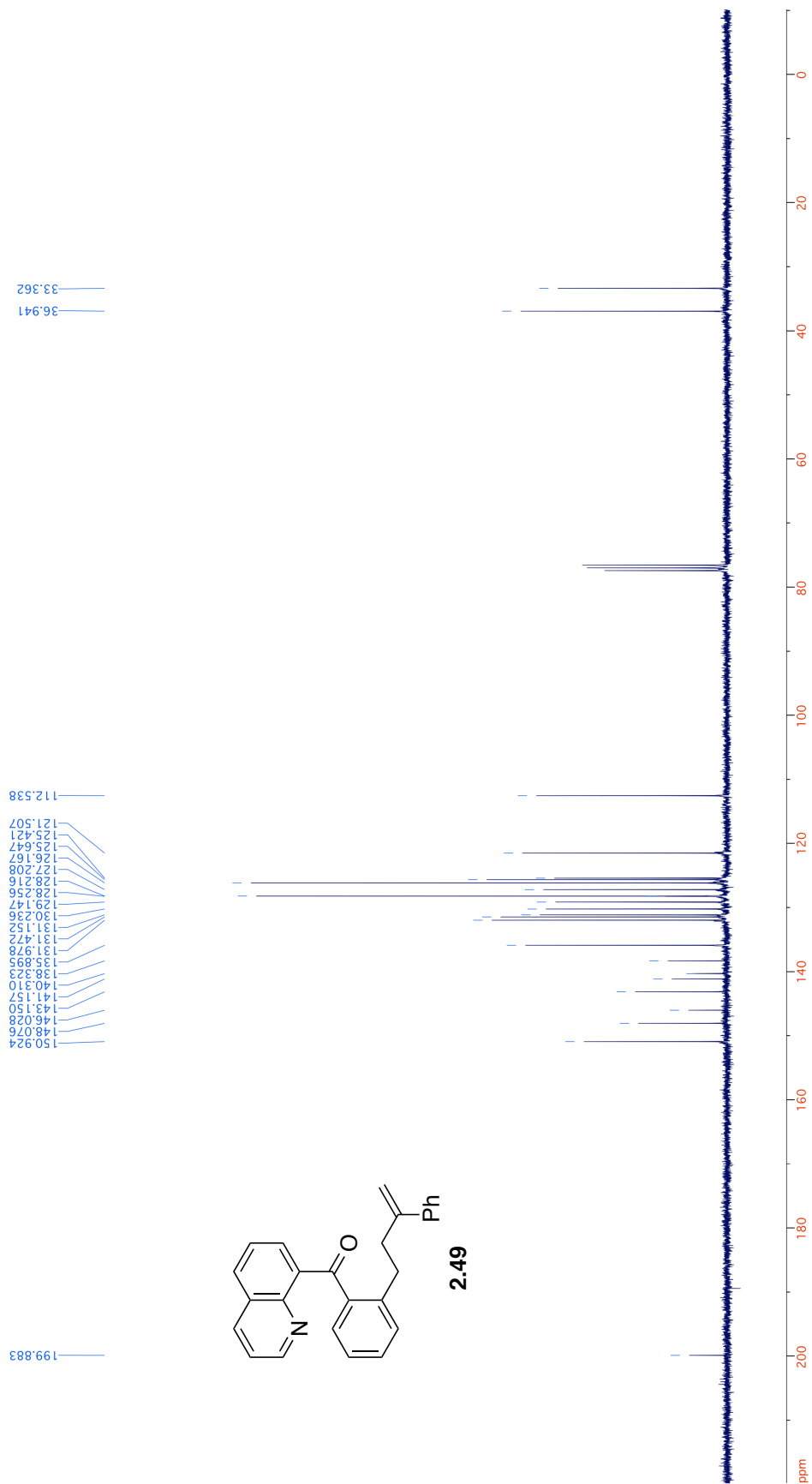
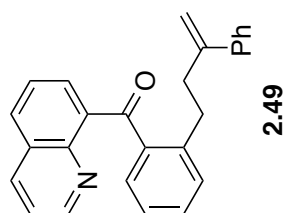


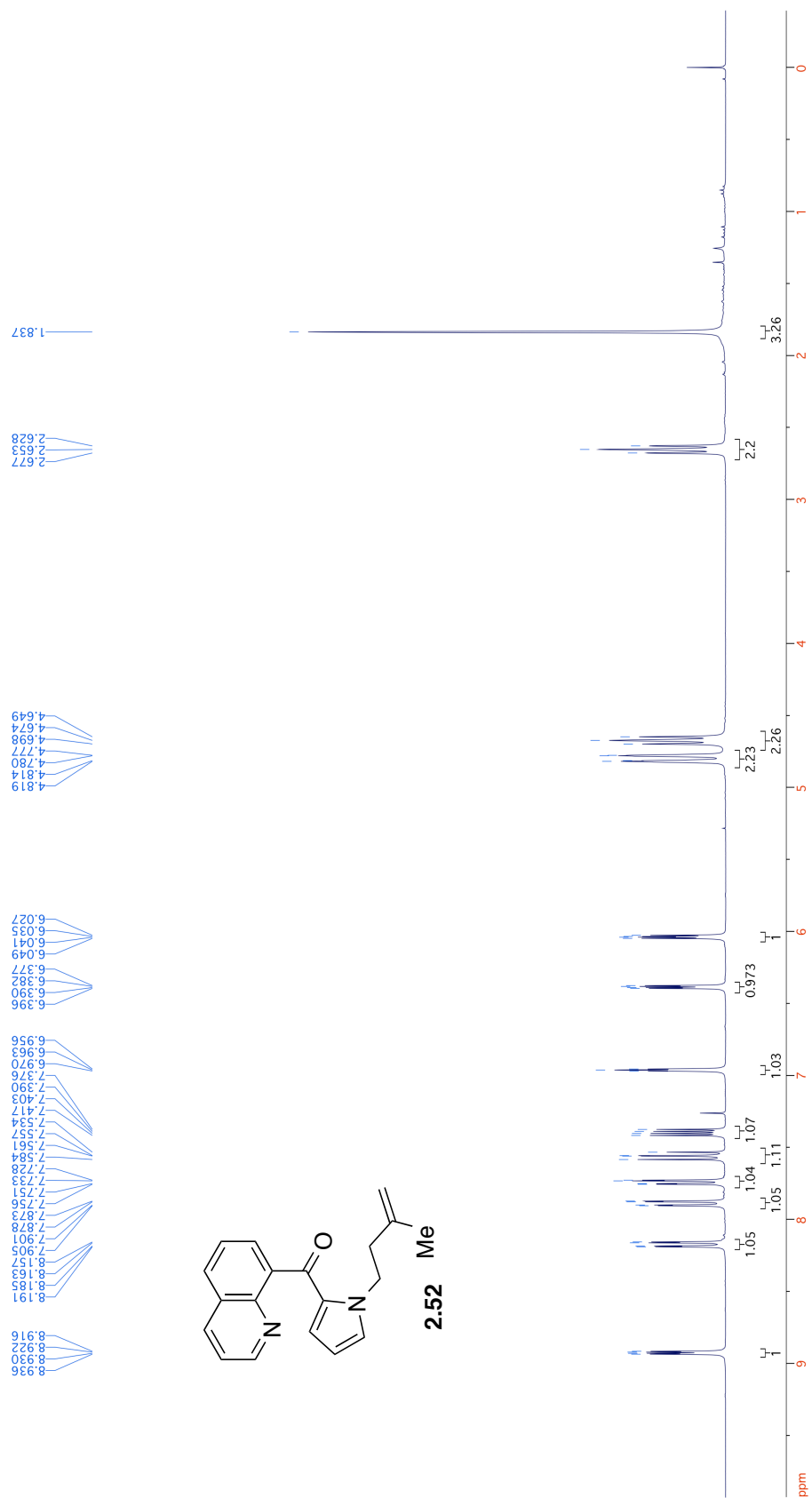
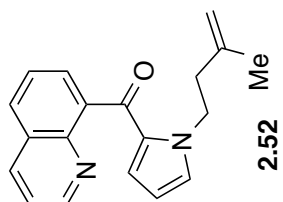


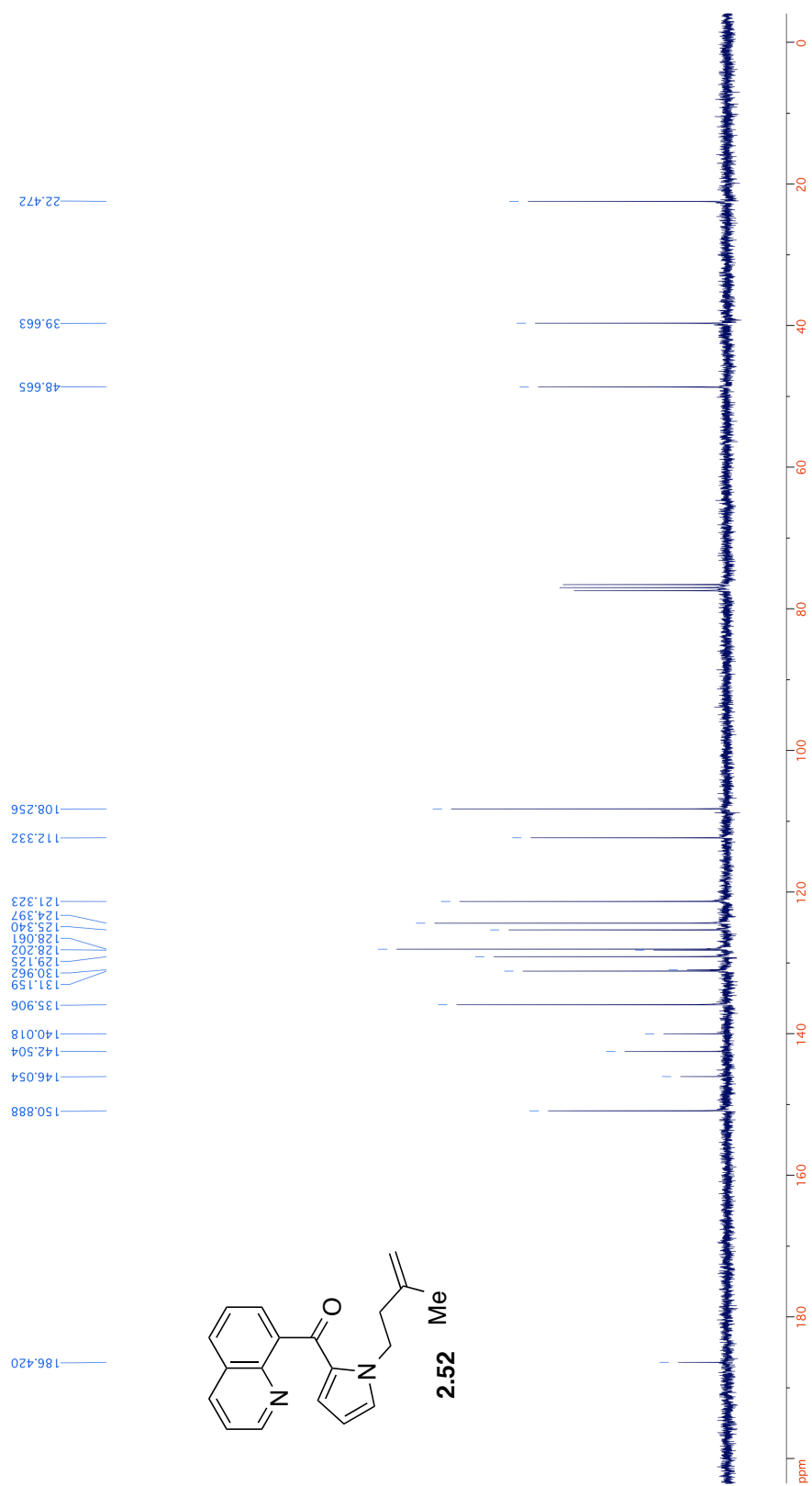


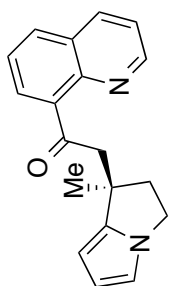
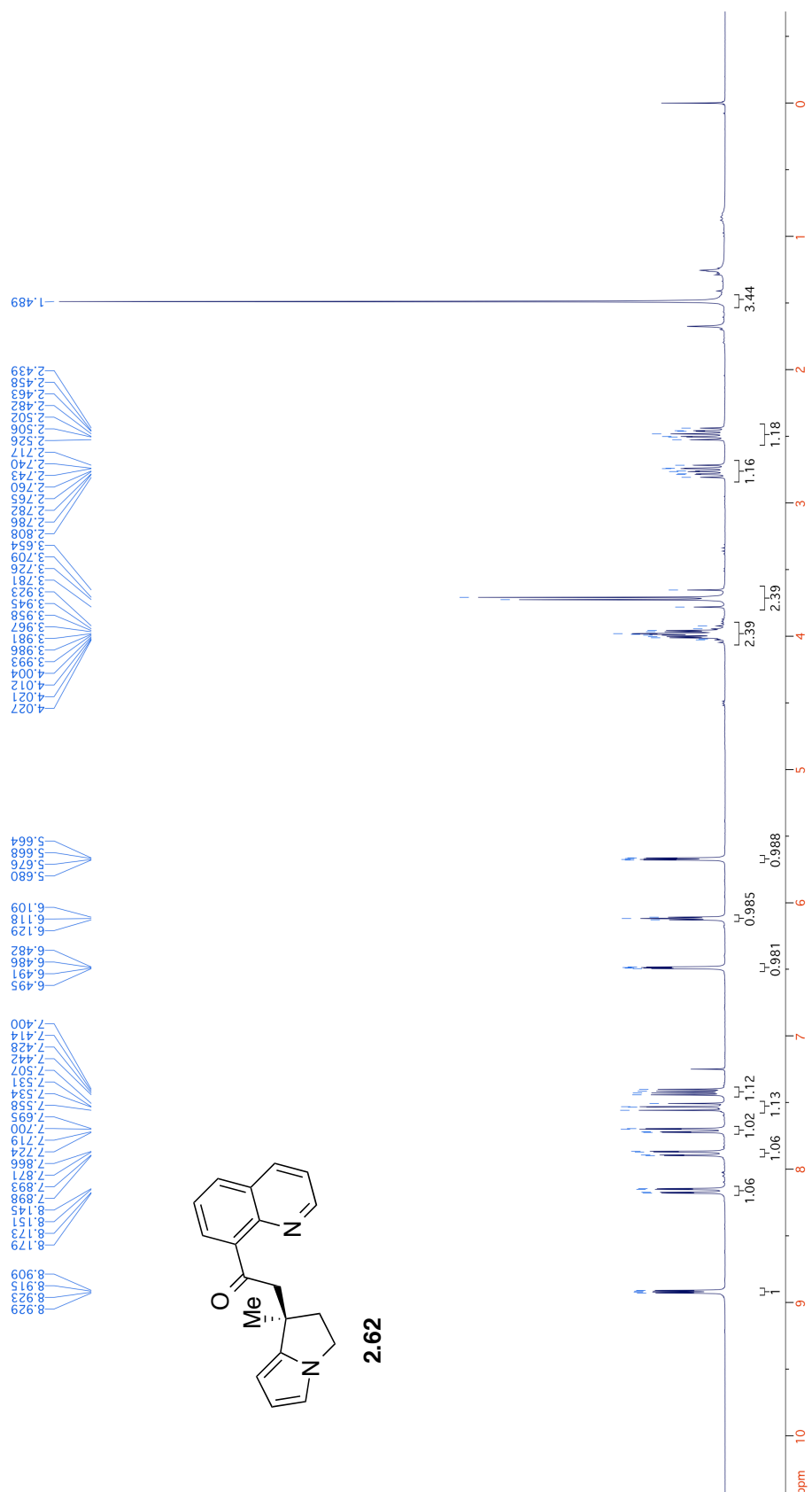




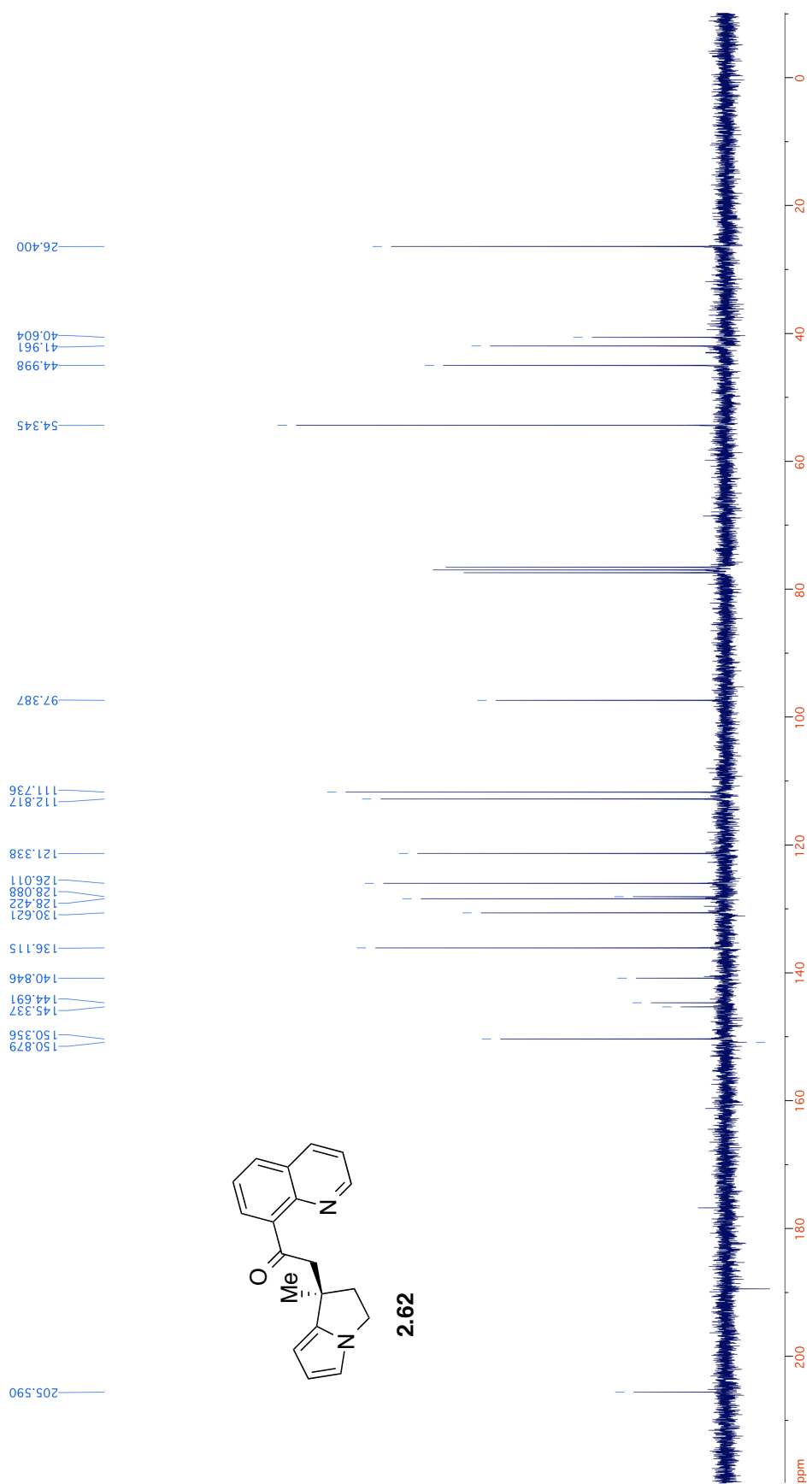


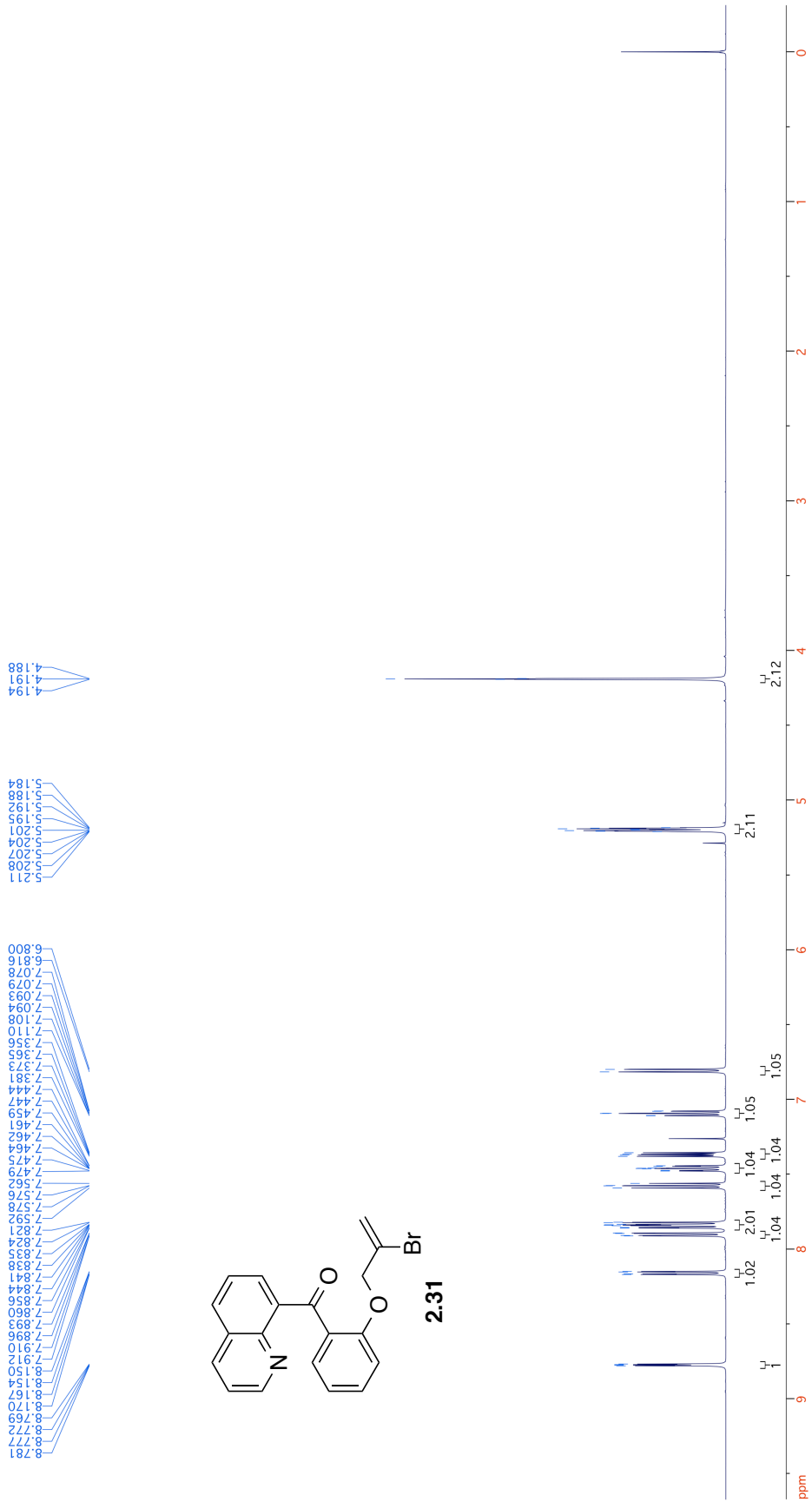
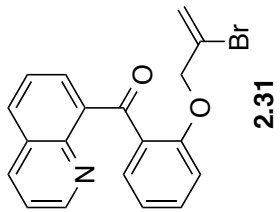


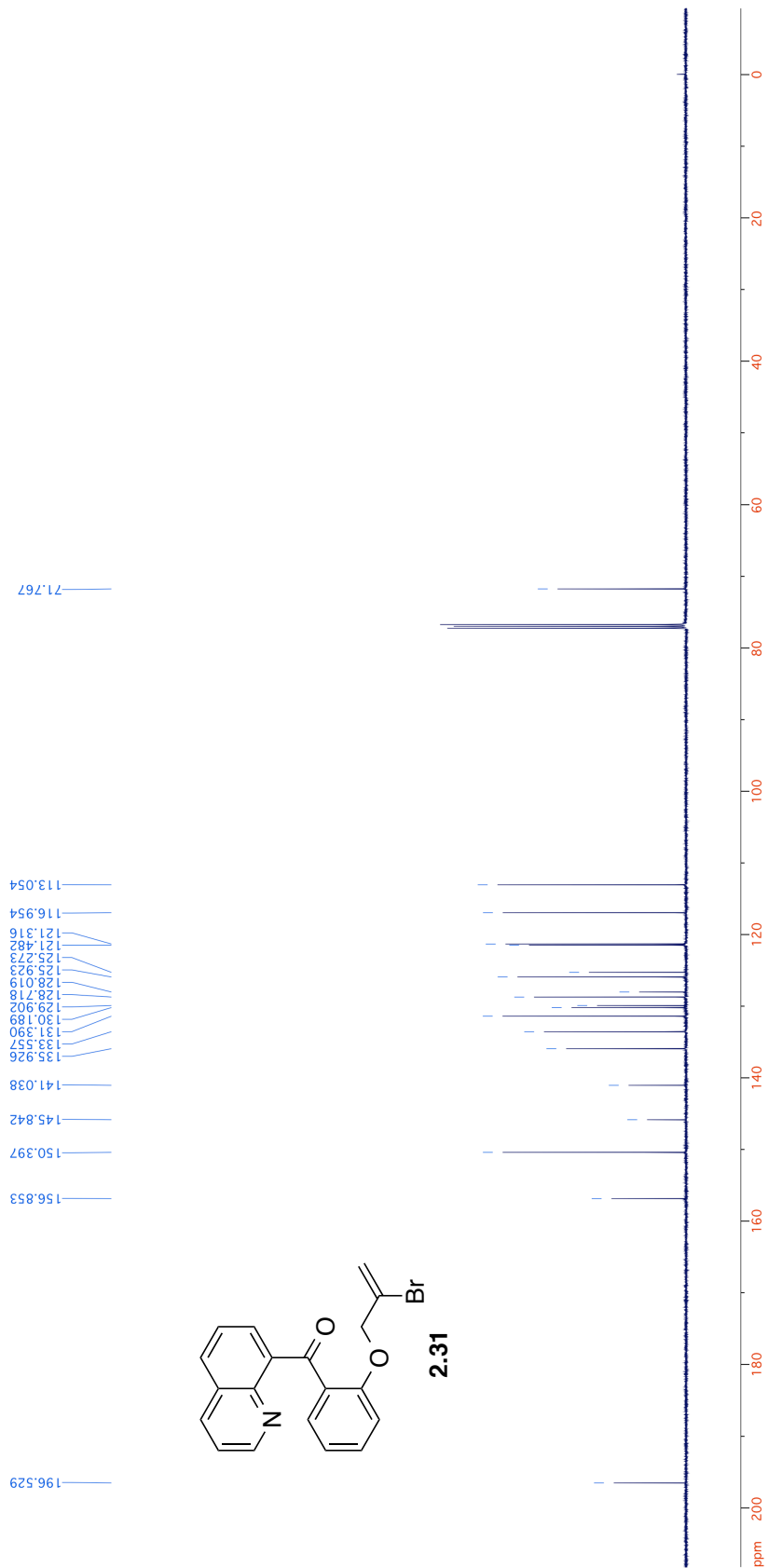
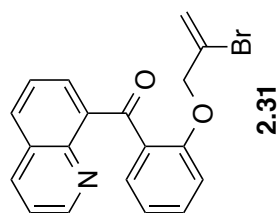


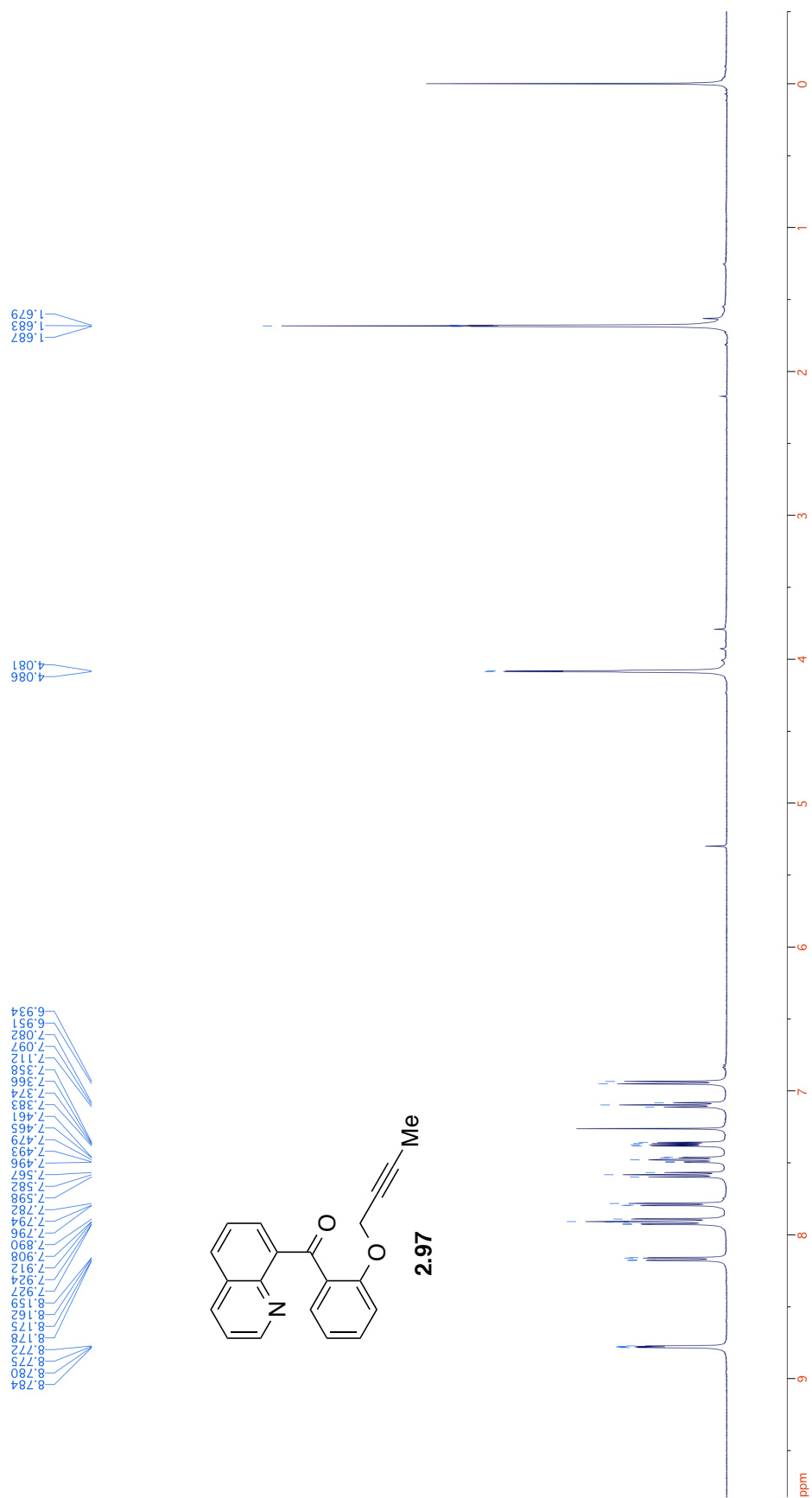


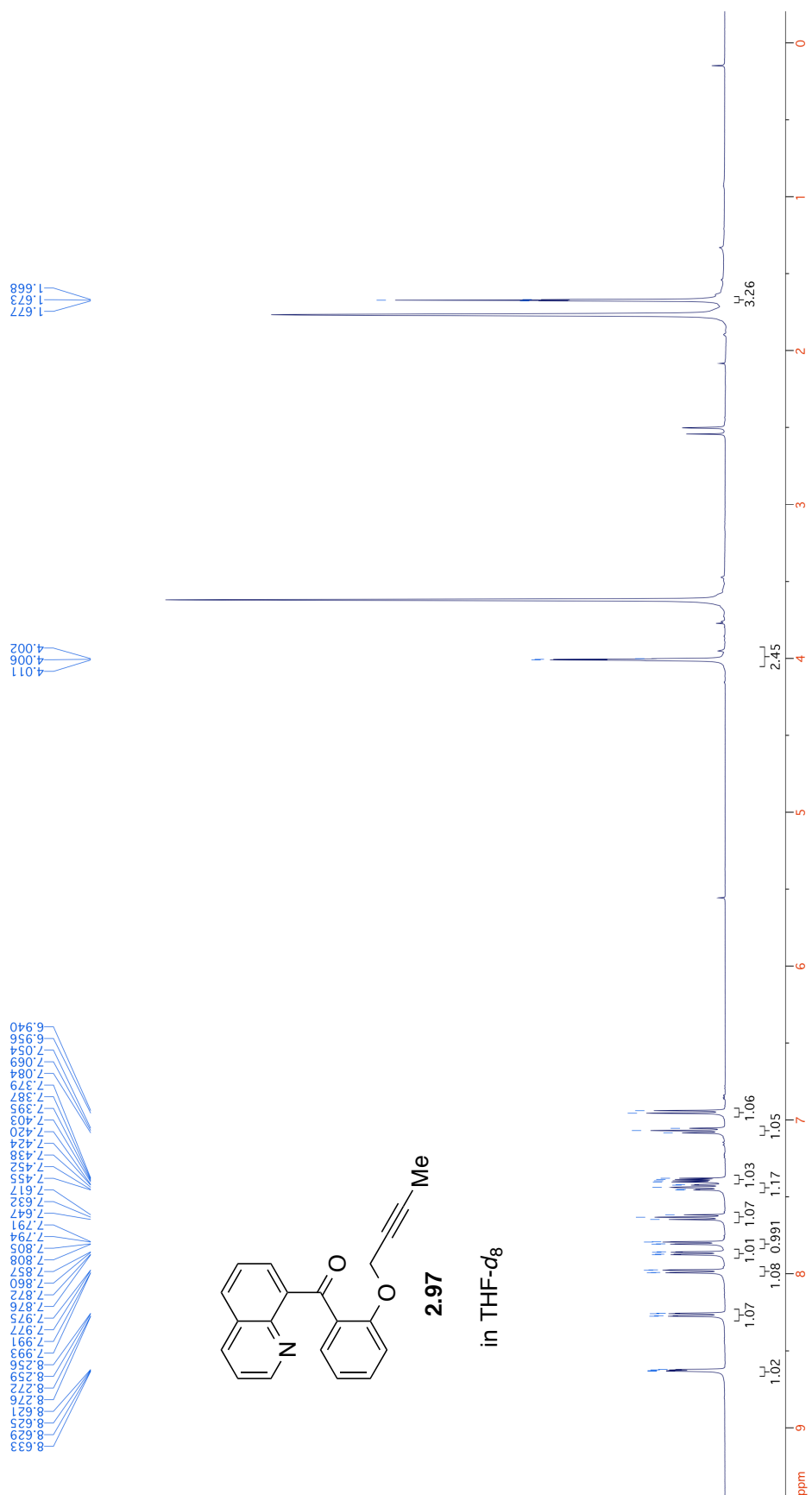
2.62

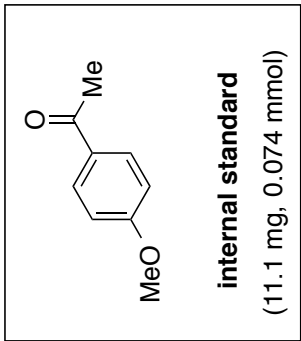
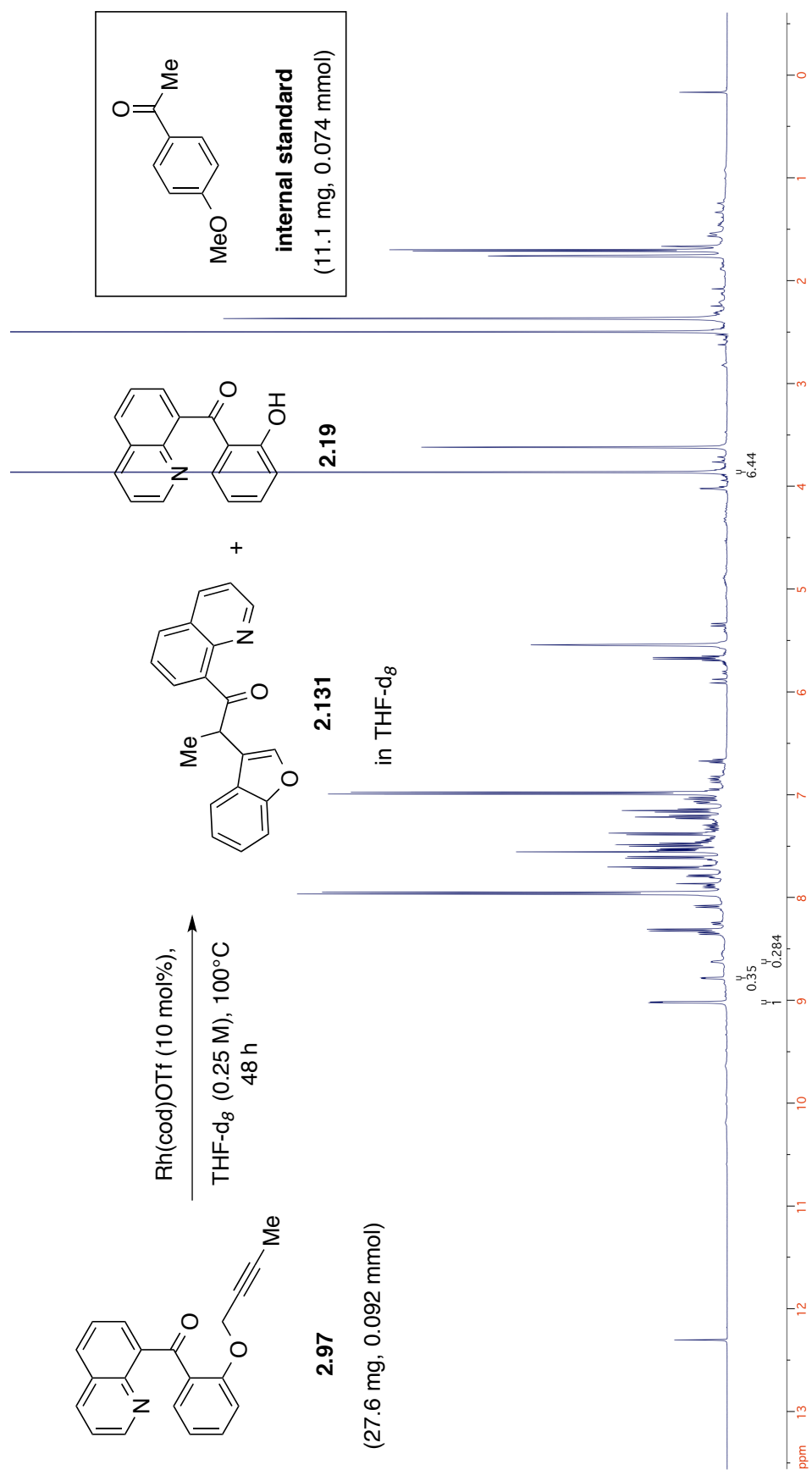


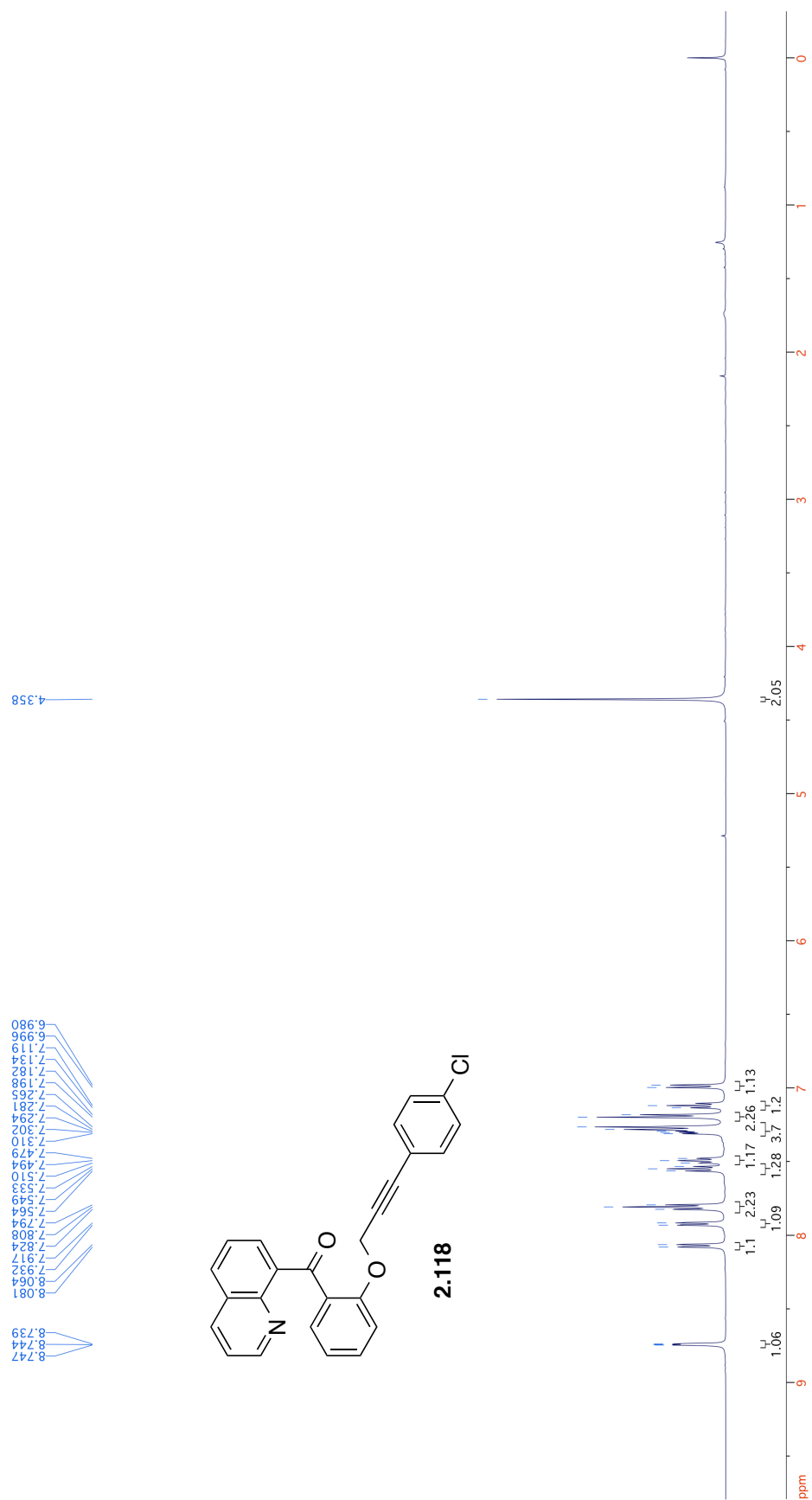


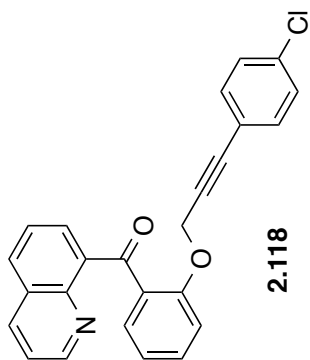




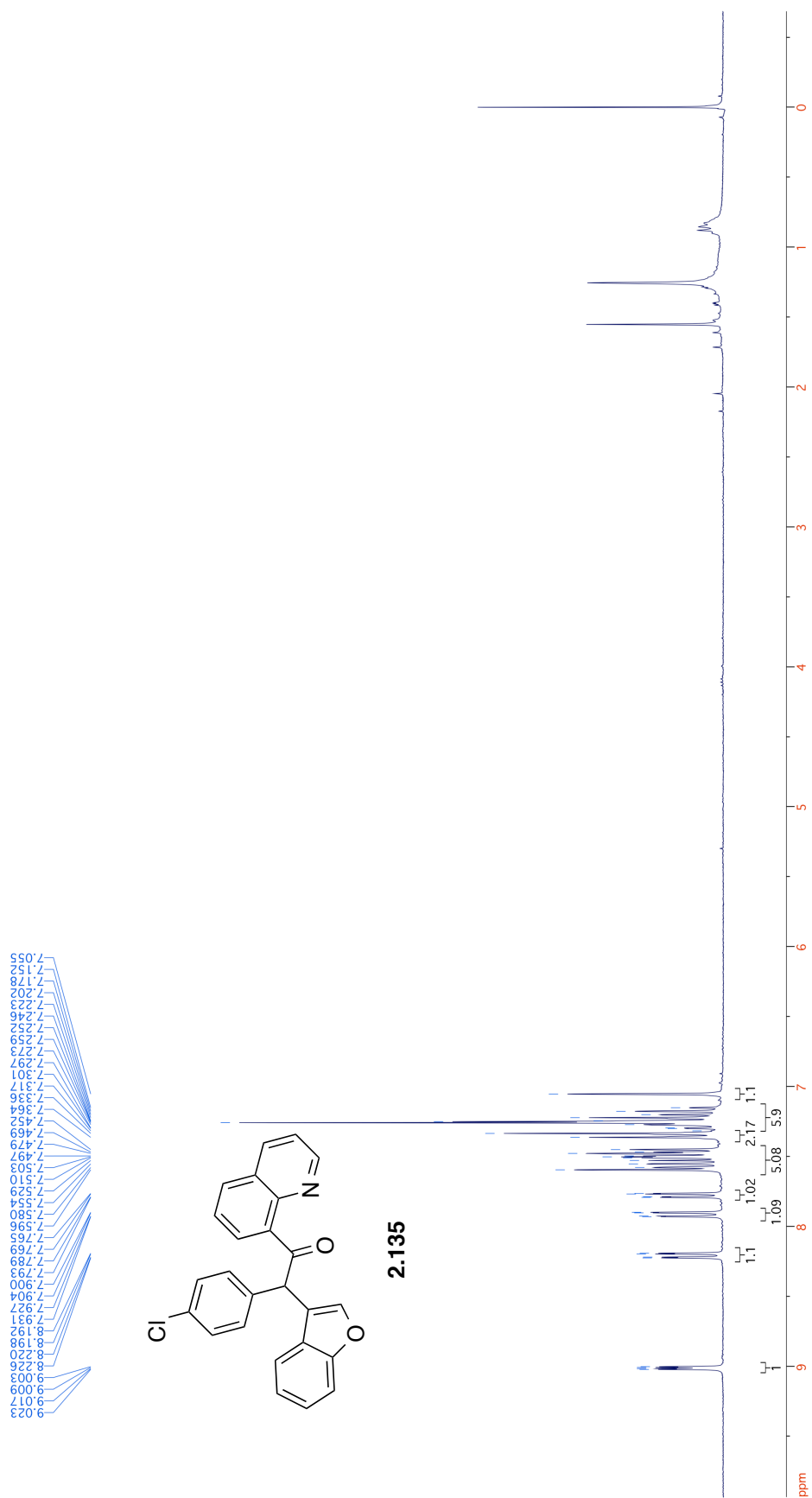




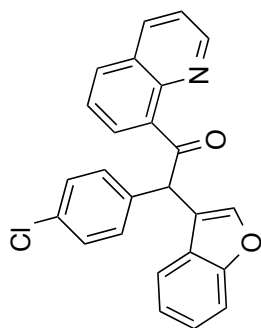




196.538
157.215
150.284
145.934
141.508
135.745
134.660
133.607
132.842
131.303
129.990
129.809
128.544
128.279
127.816
125.845
121.605
121.191
120.602
113.641
85.491
83.988
56.974

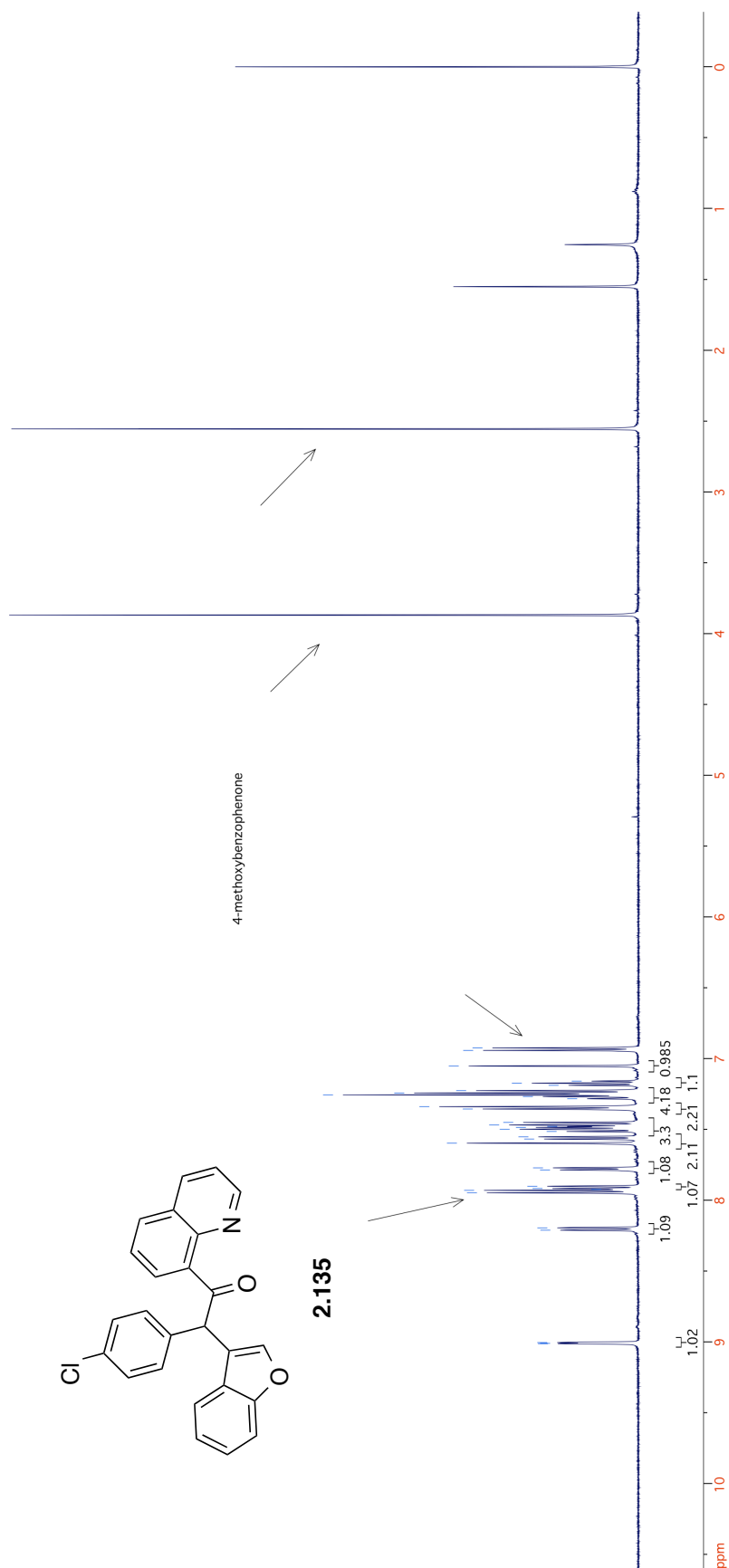


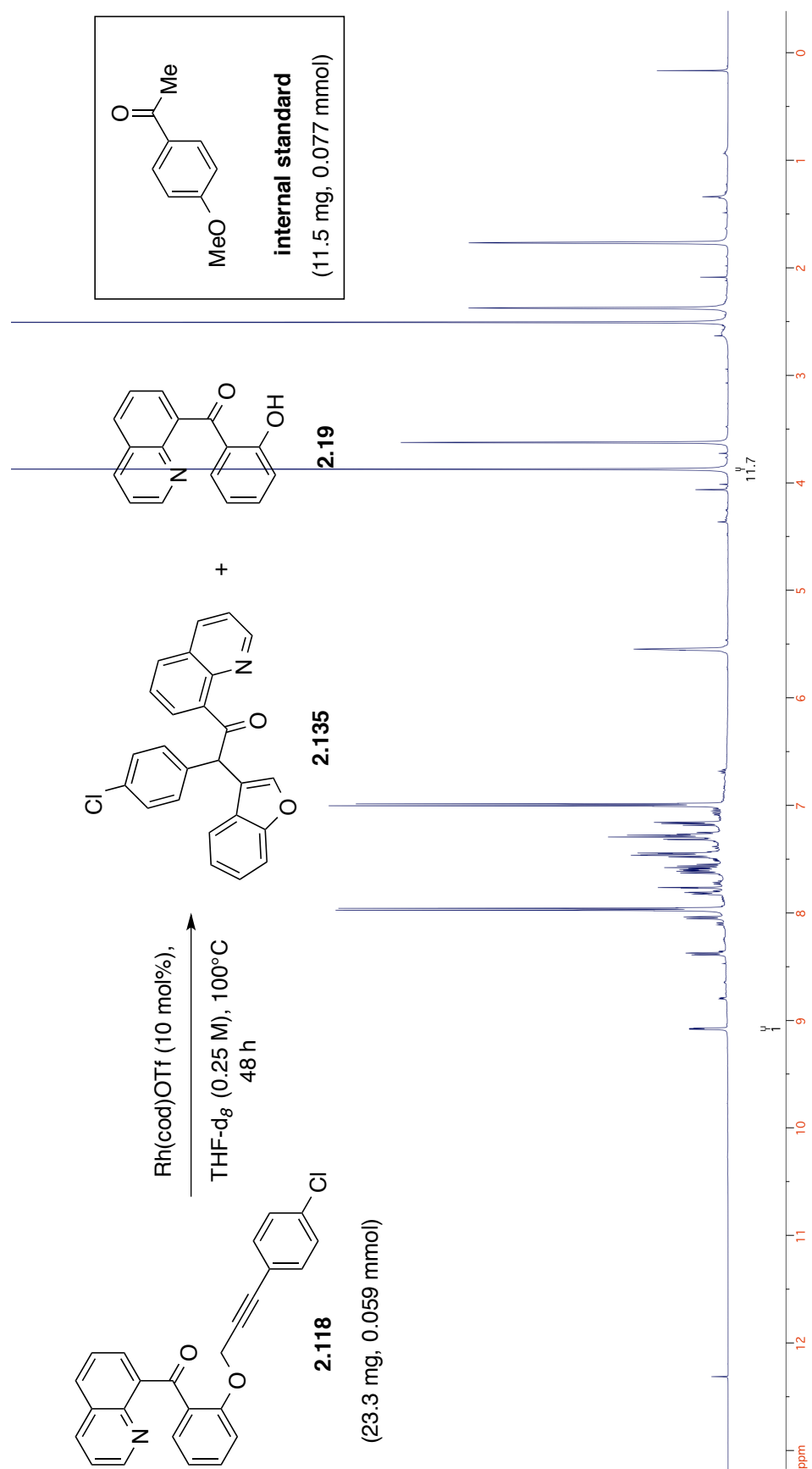
9.013
9.010
9.005
8.212
8.195
7.948
7.930
7.924
7.901
7.786
7.772
7.597
7.582
7.515
7.499
7.486
7.479
7.469
7.451
7.356
7.339
7.283
7.268
7.256
7.243
7.226
7.189
7.174
7.159
7.053
6.942
6.925

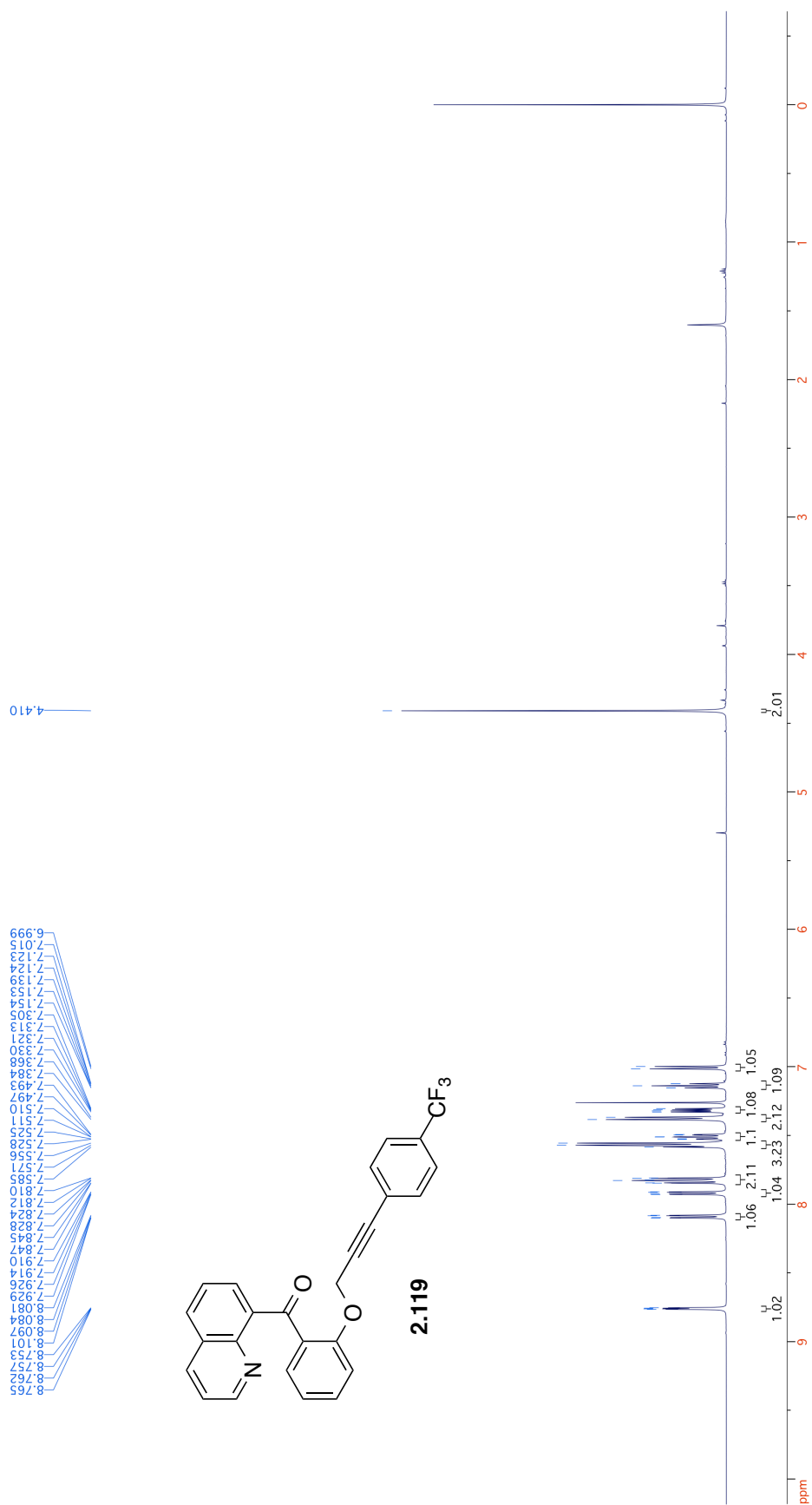


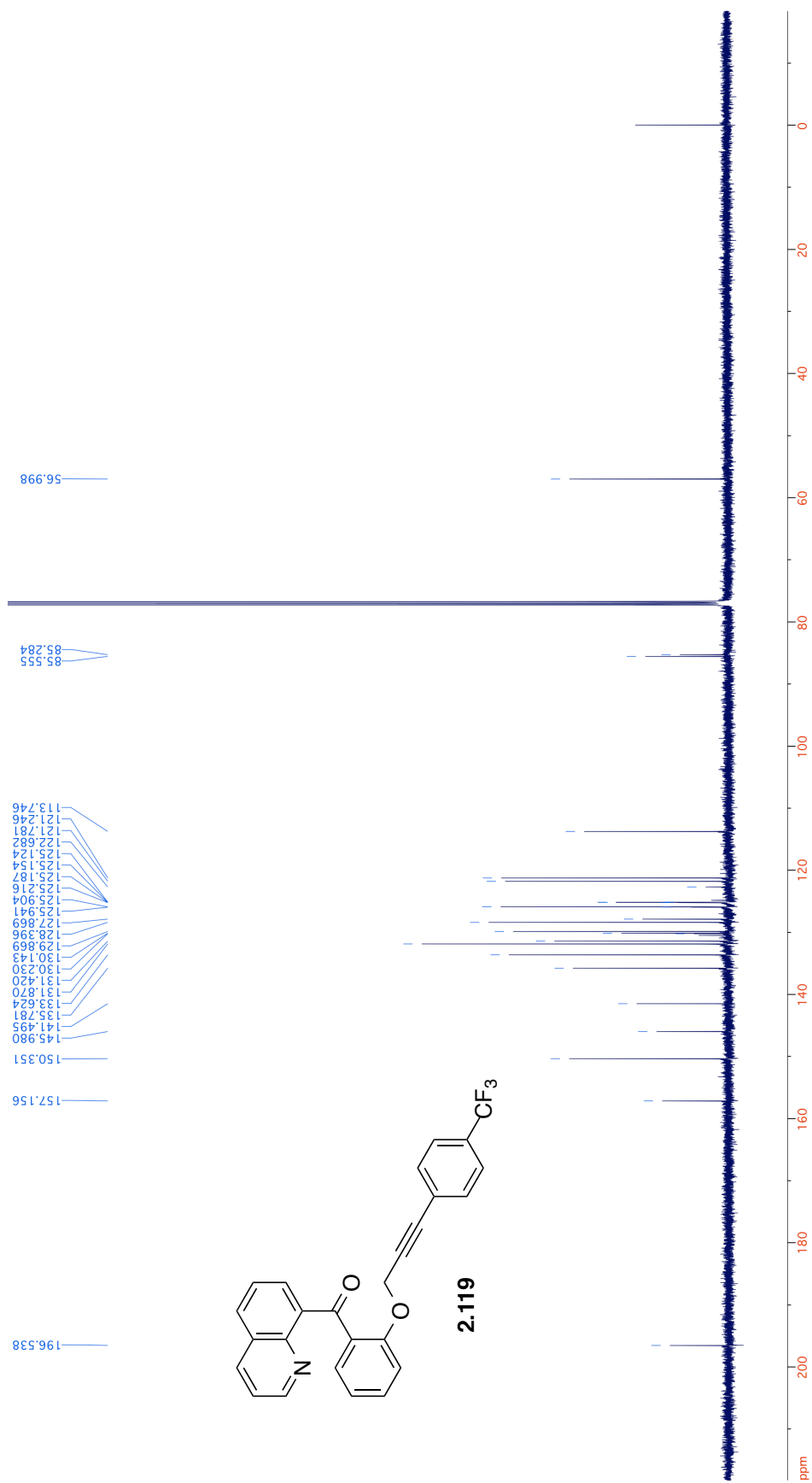
2.135

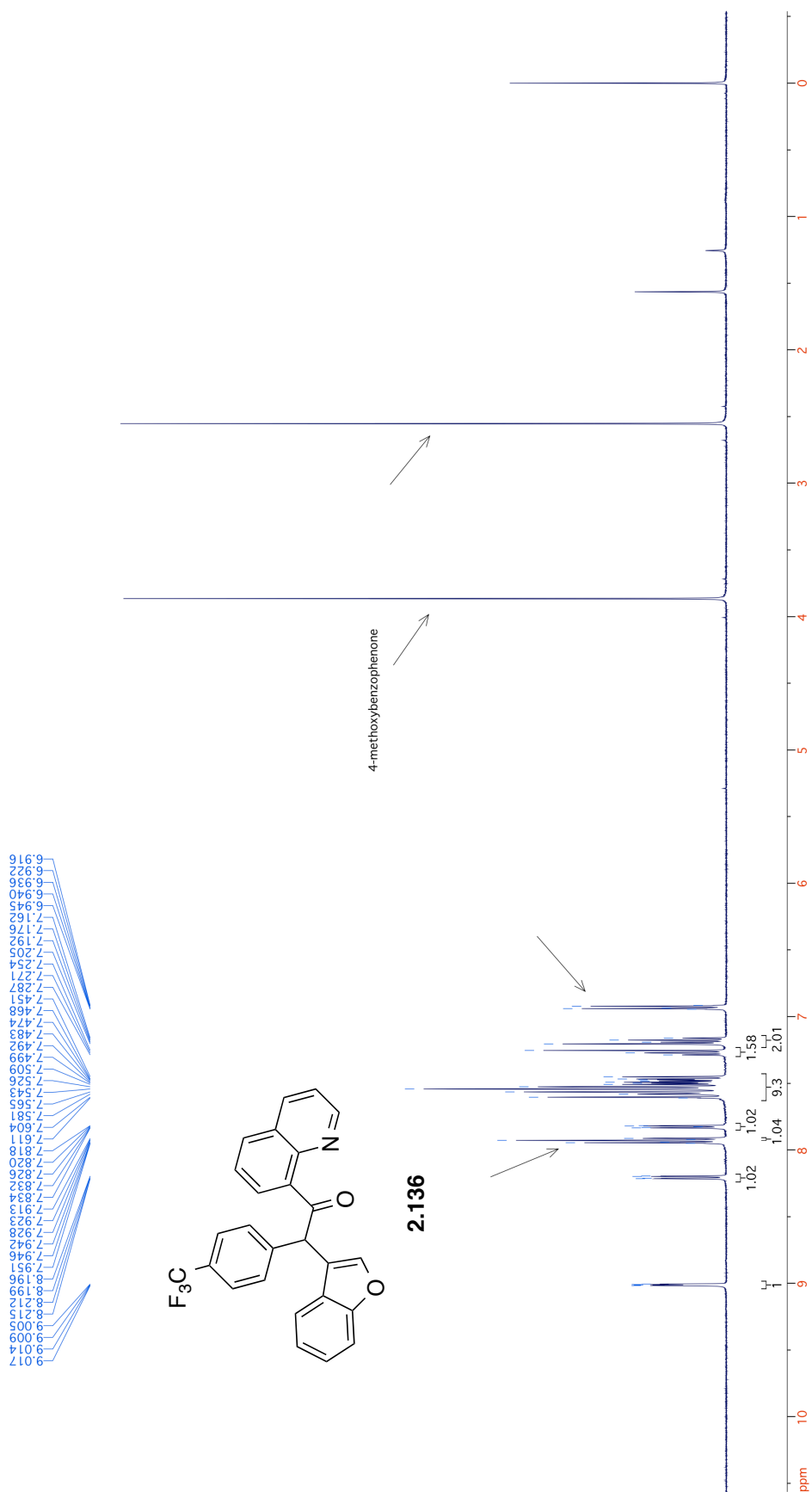
4-methoxybenzophenone

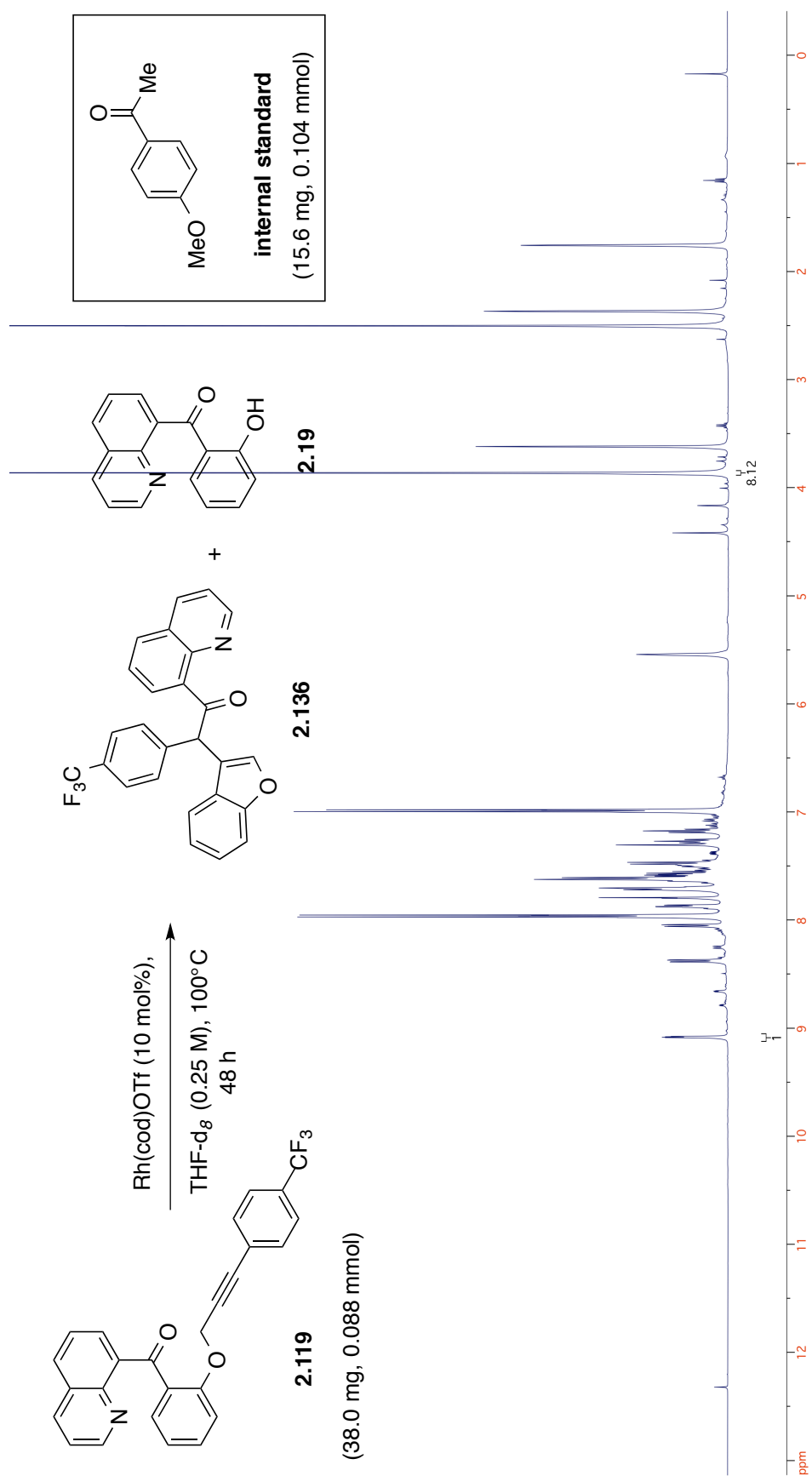


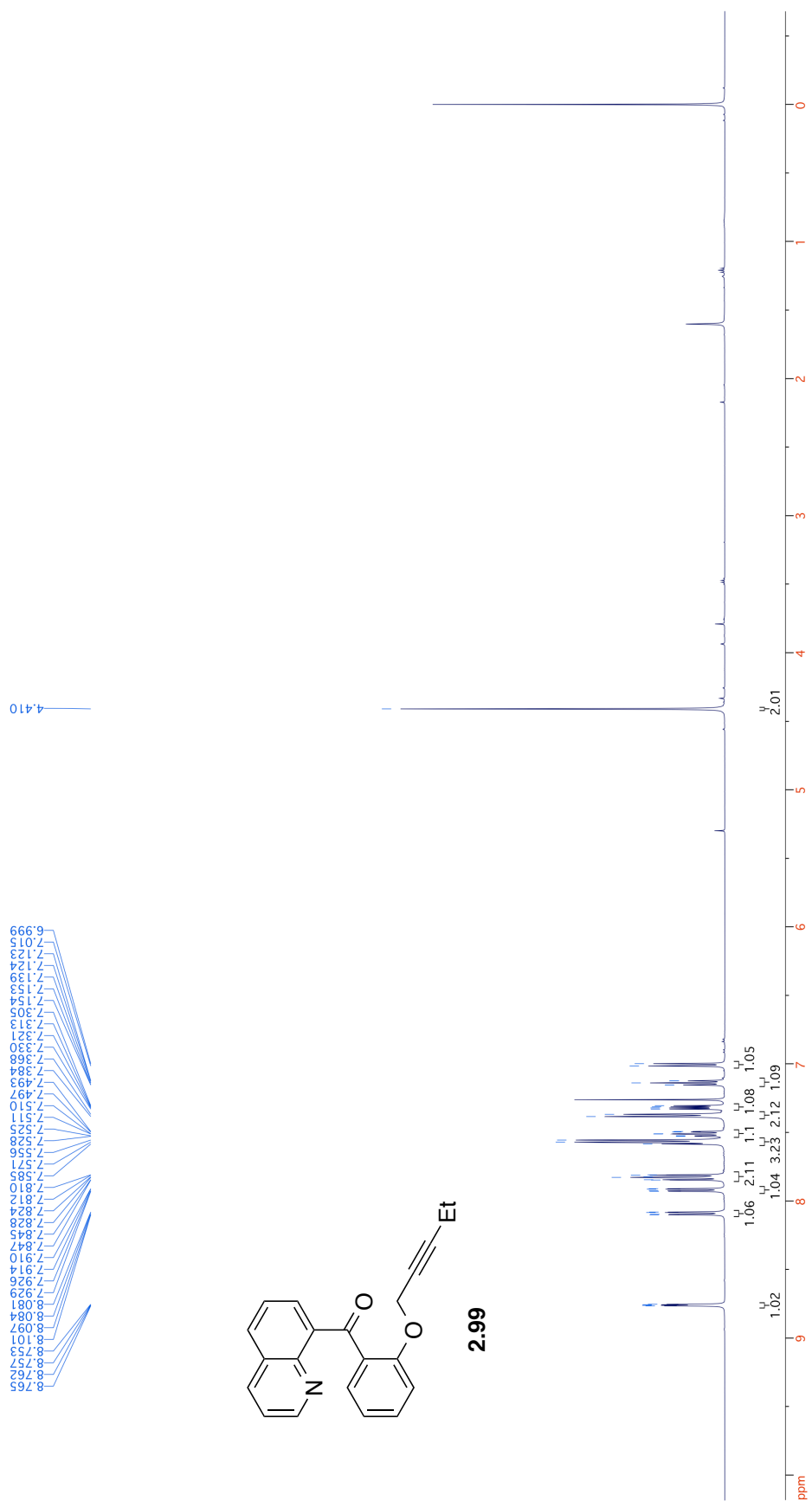


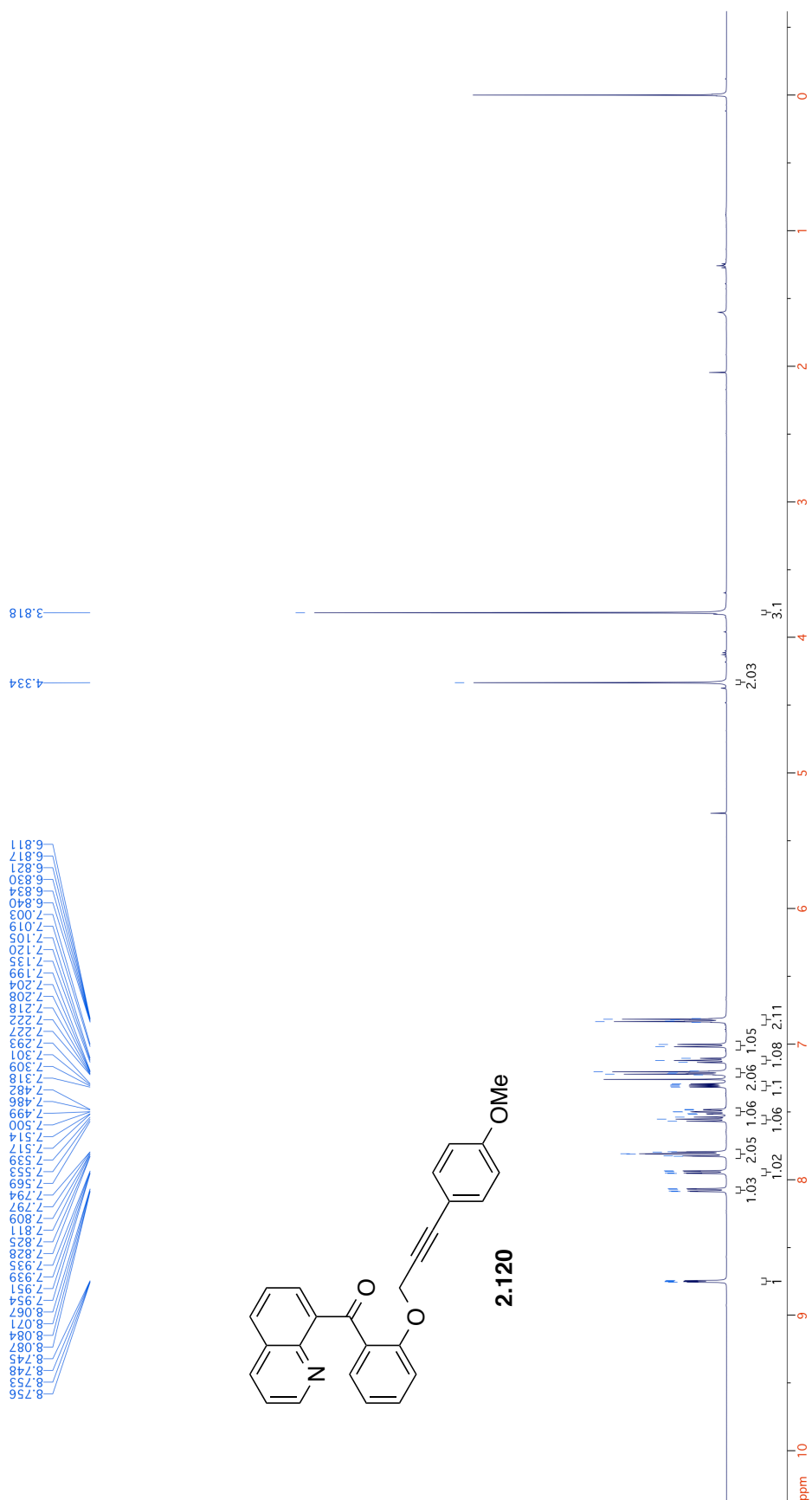
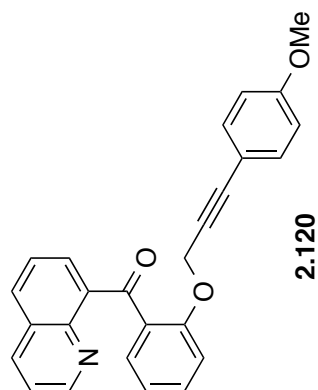


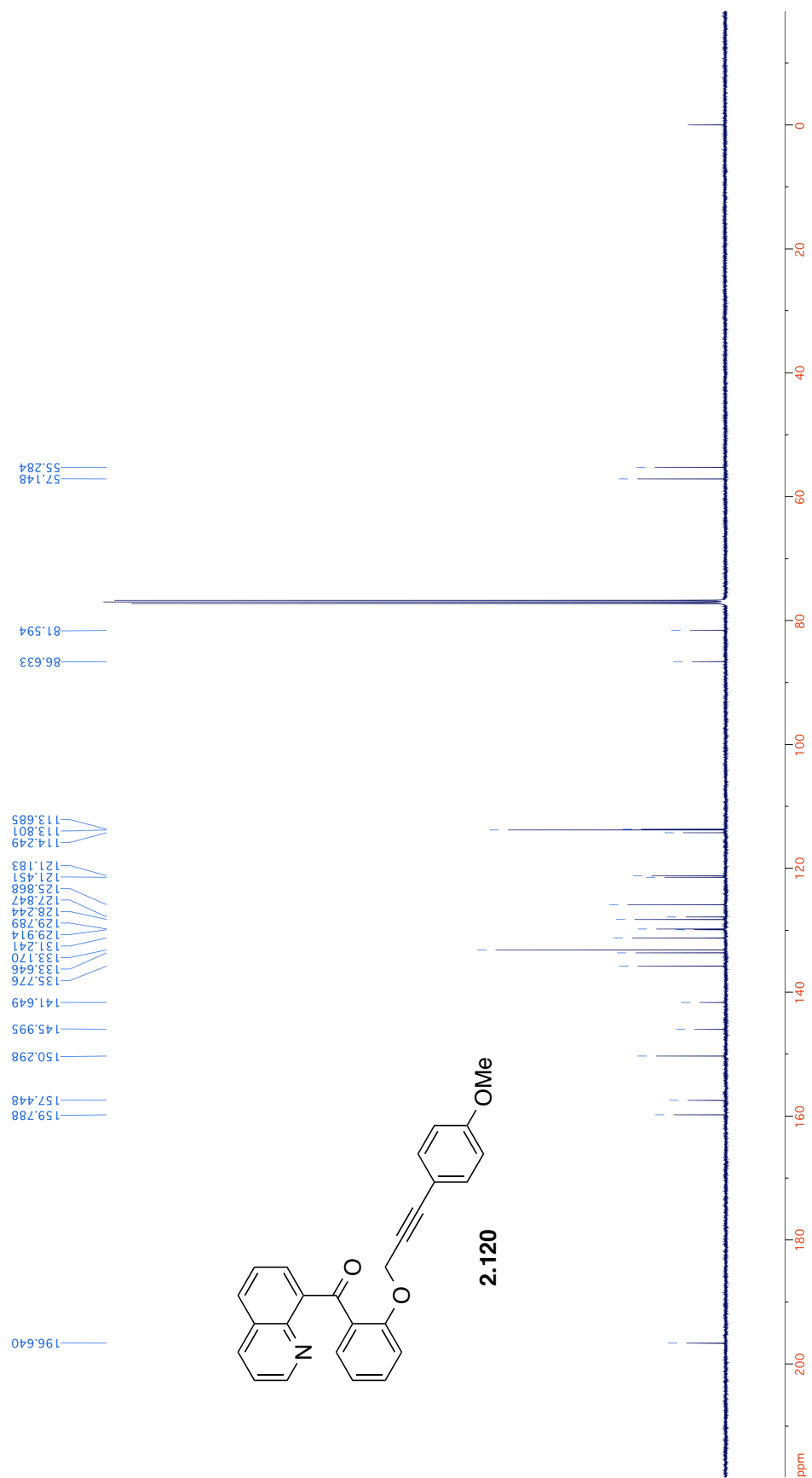


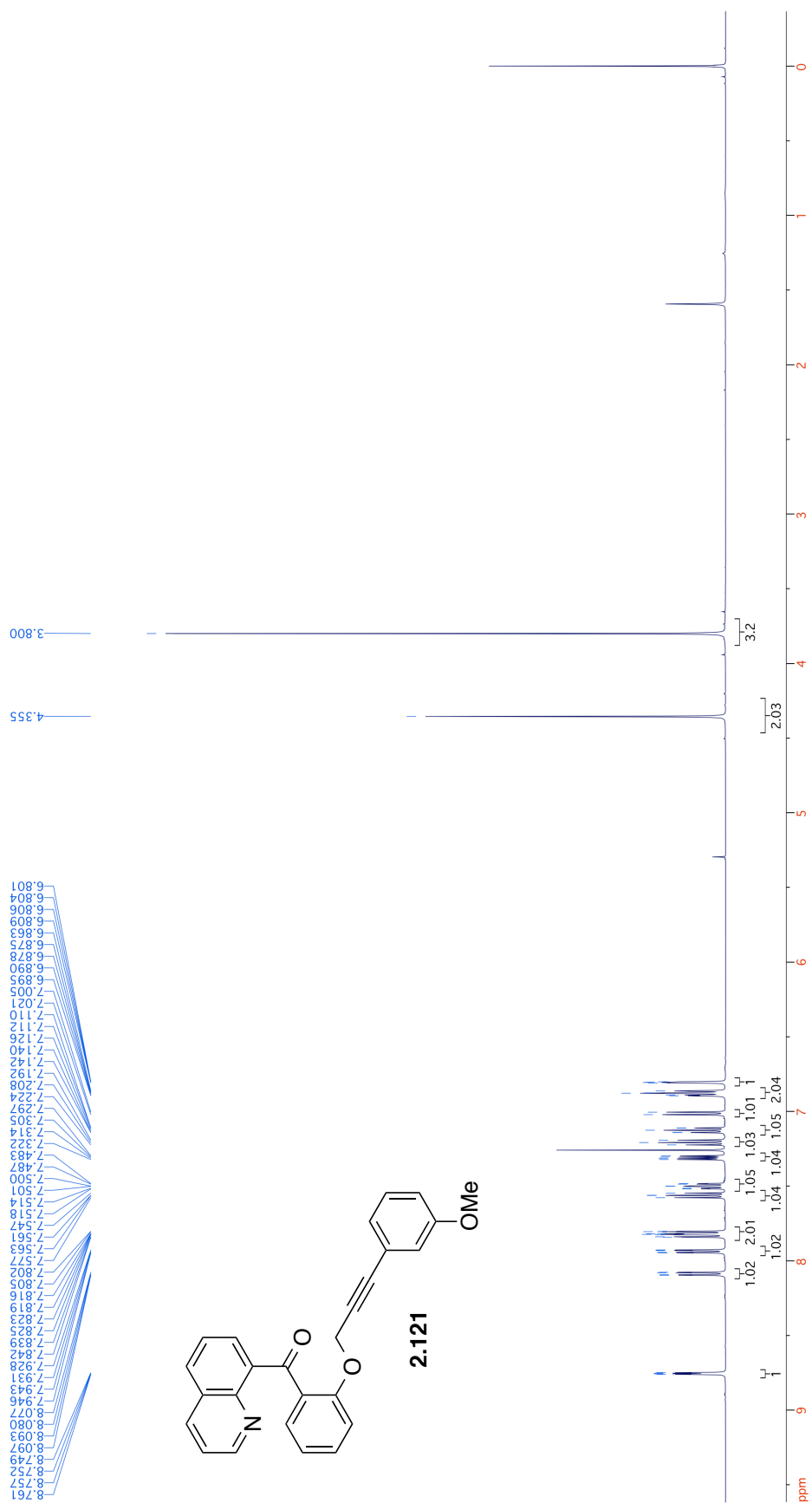


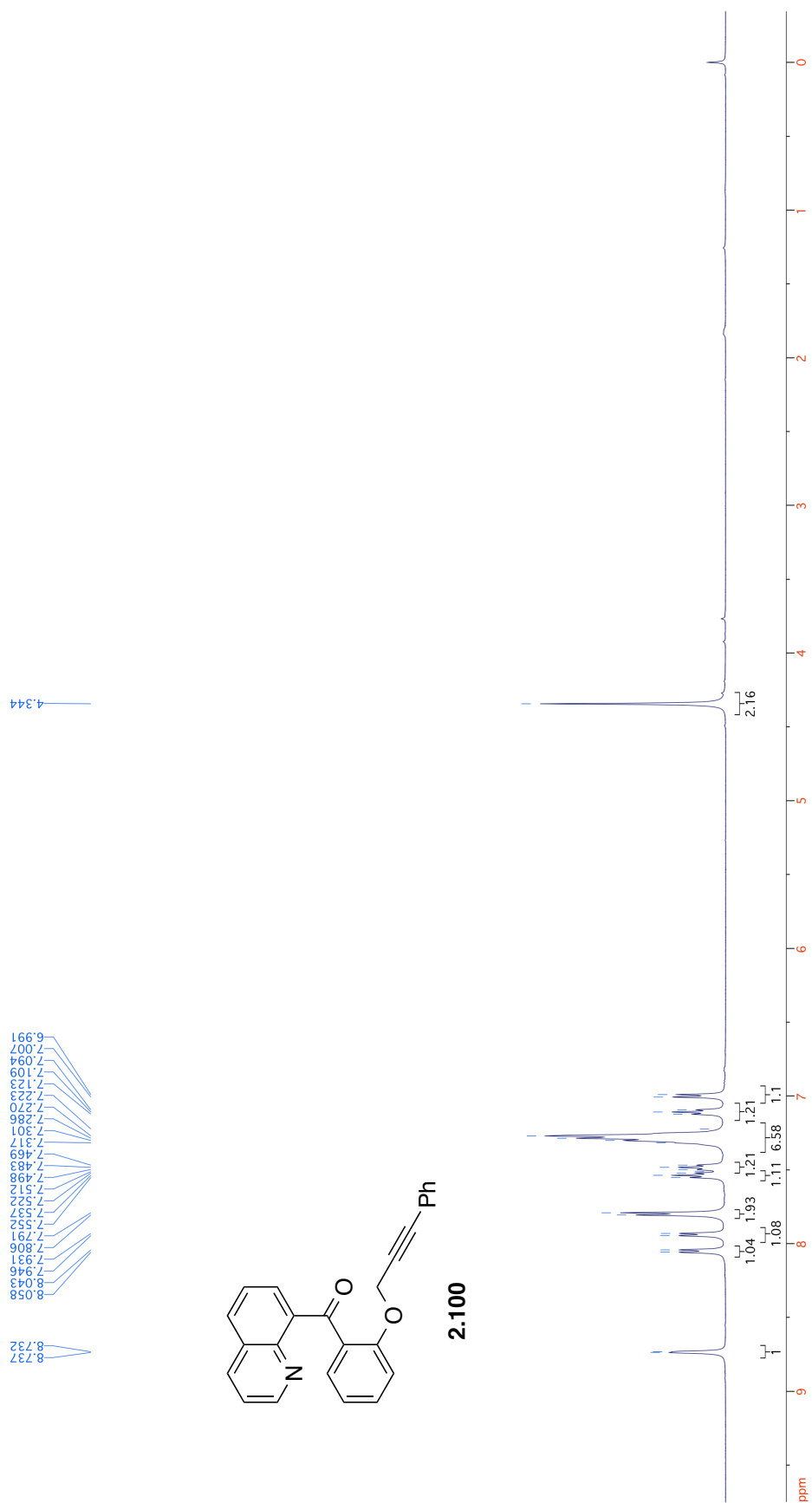


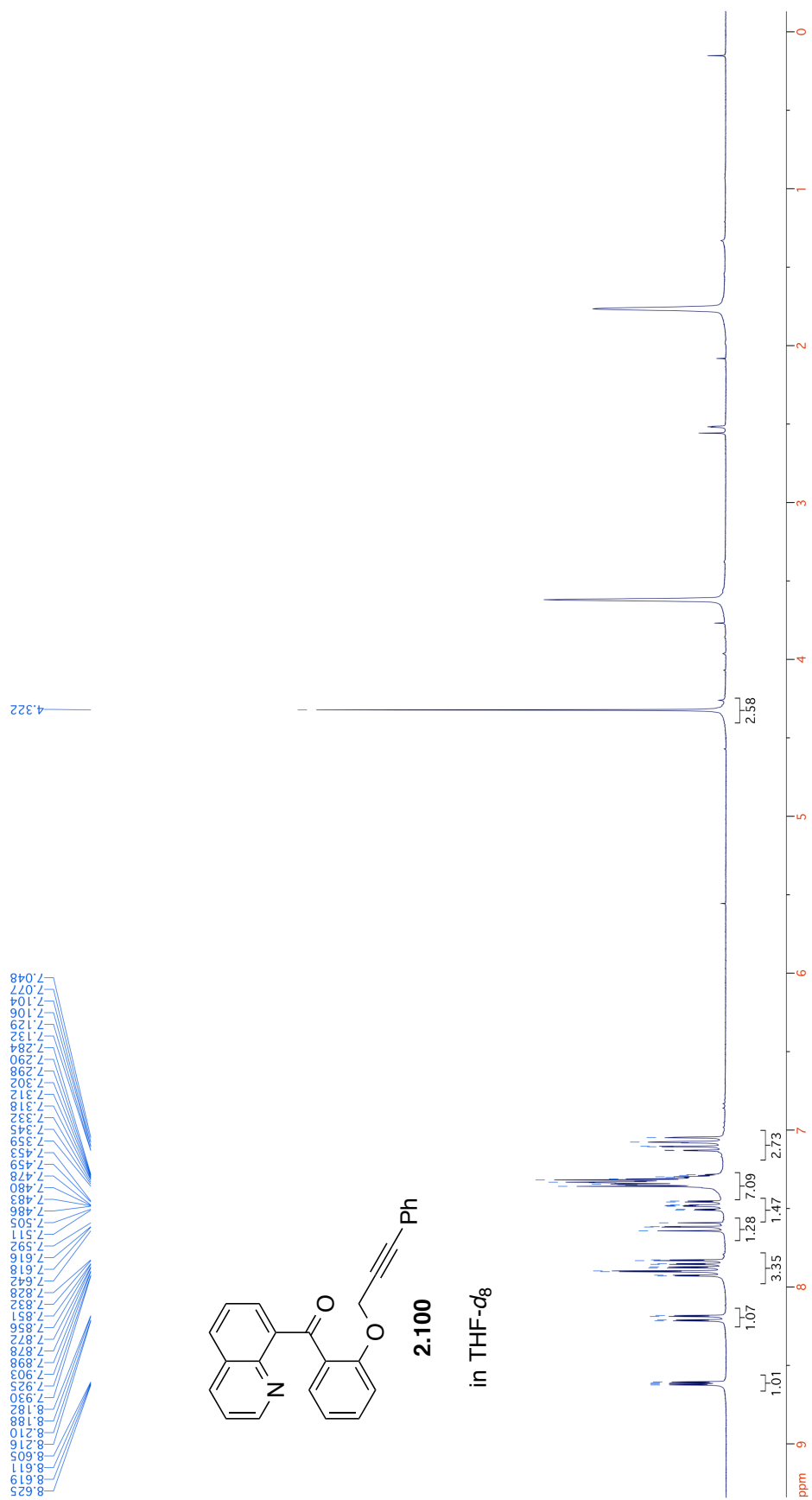


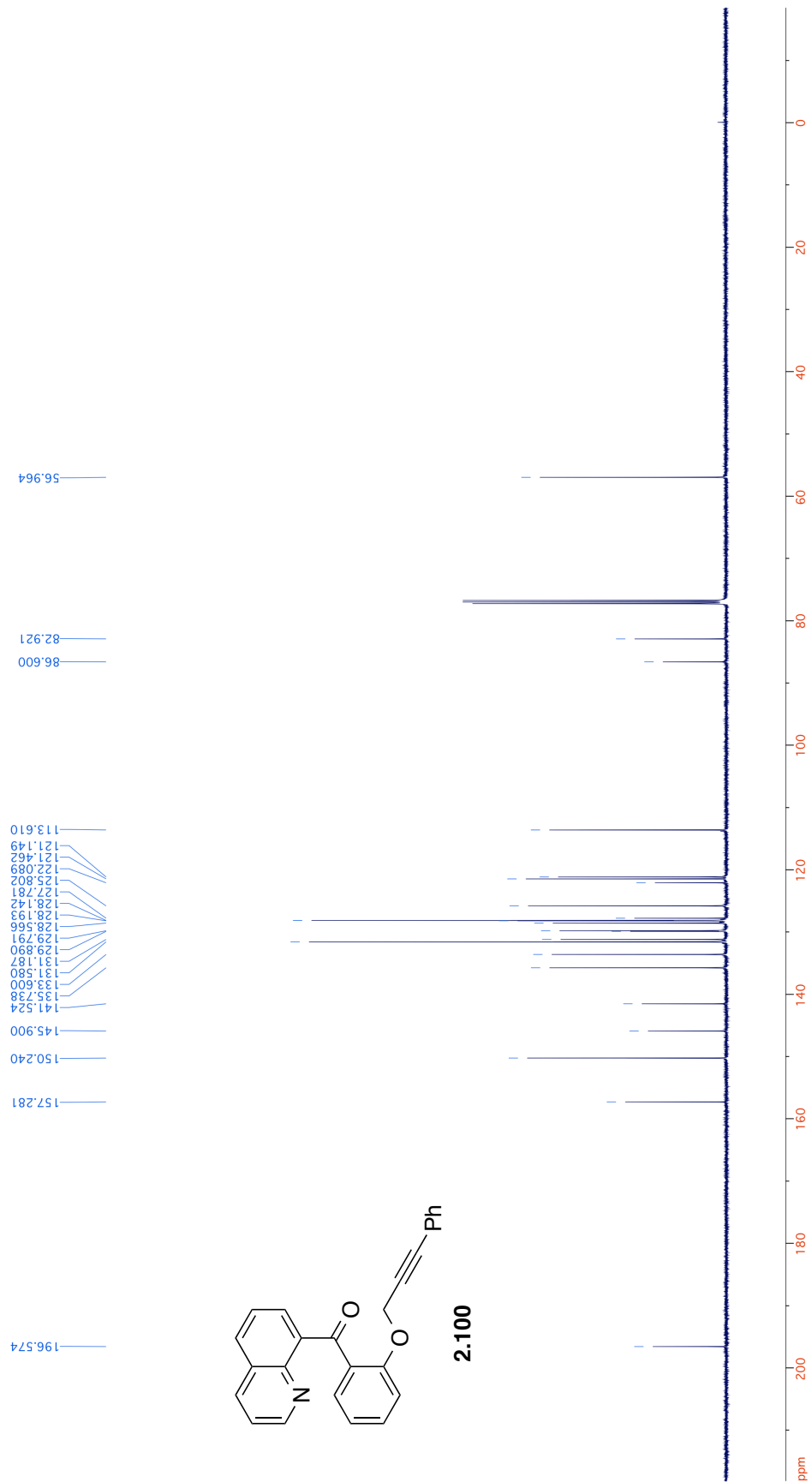


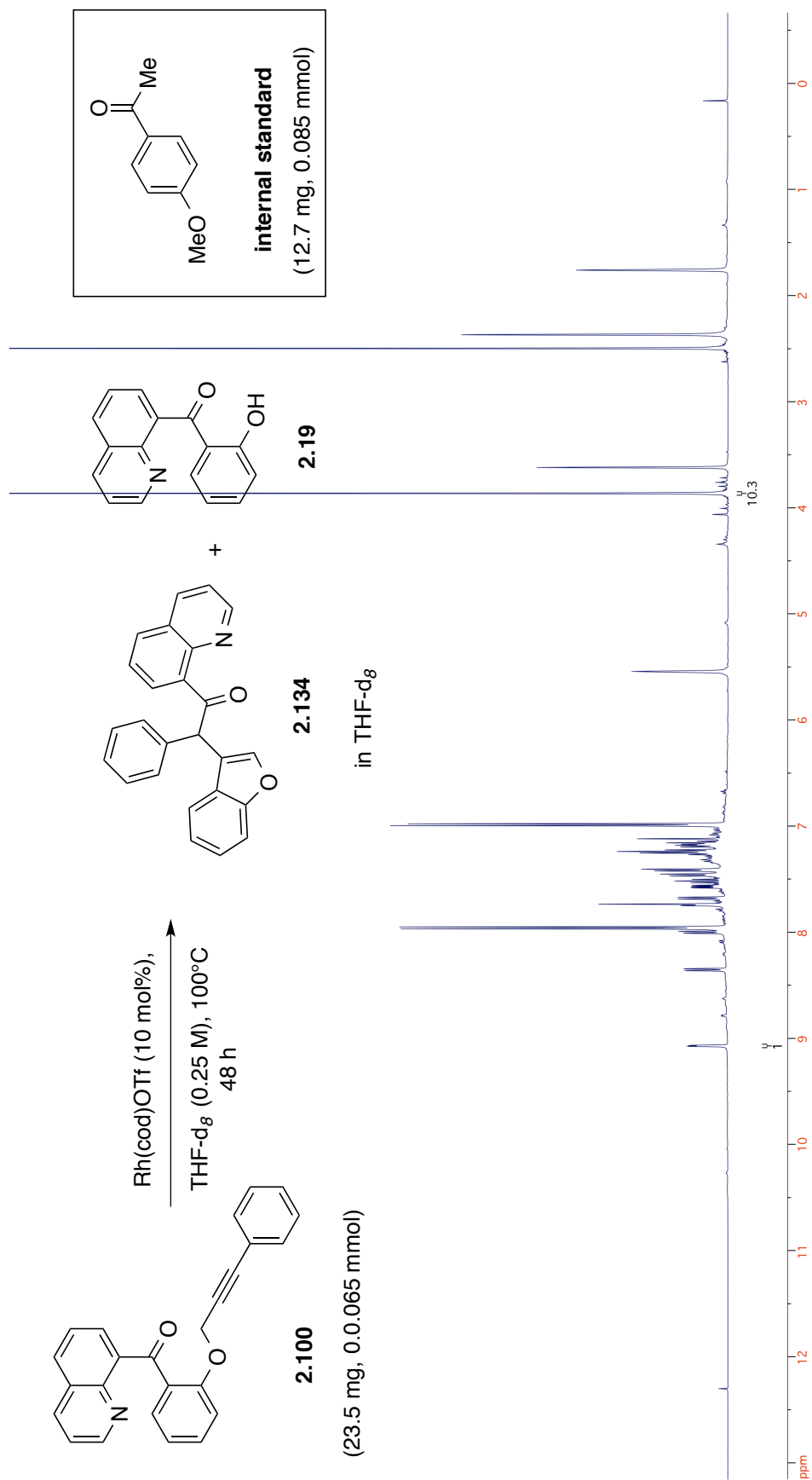


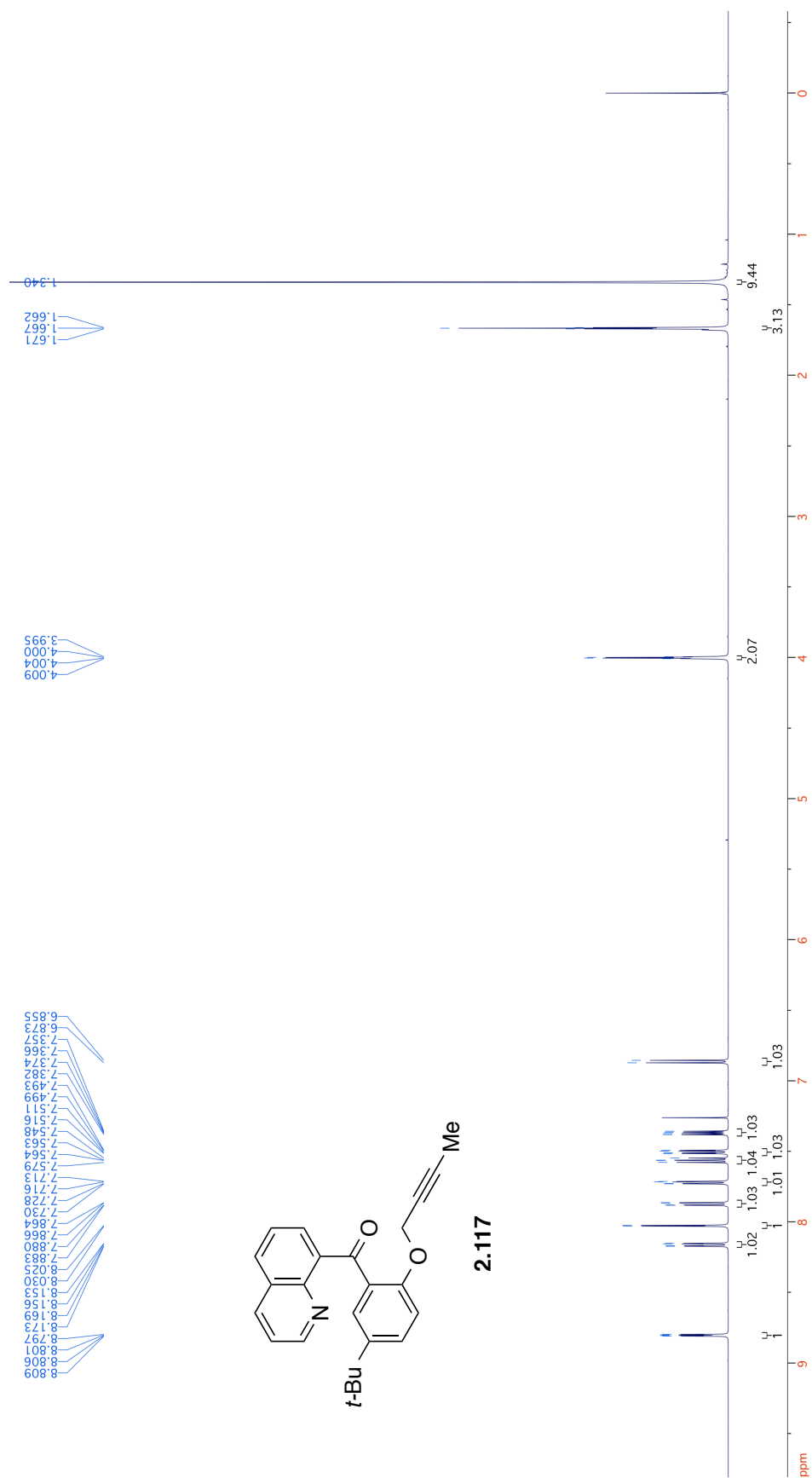


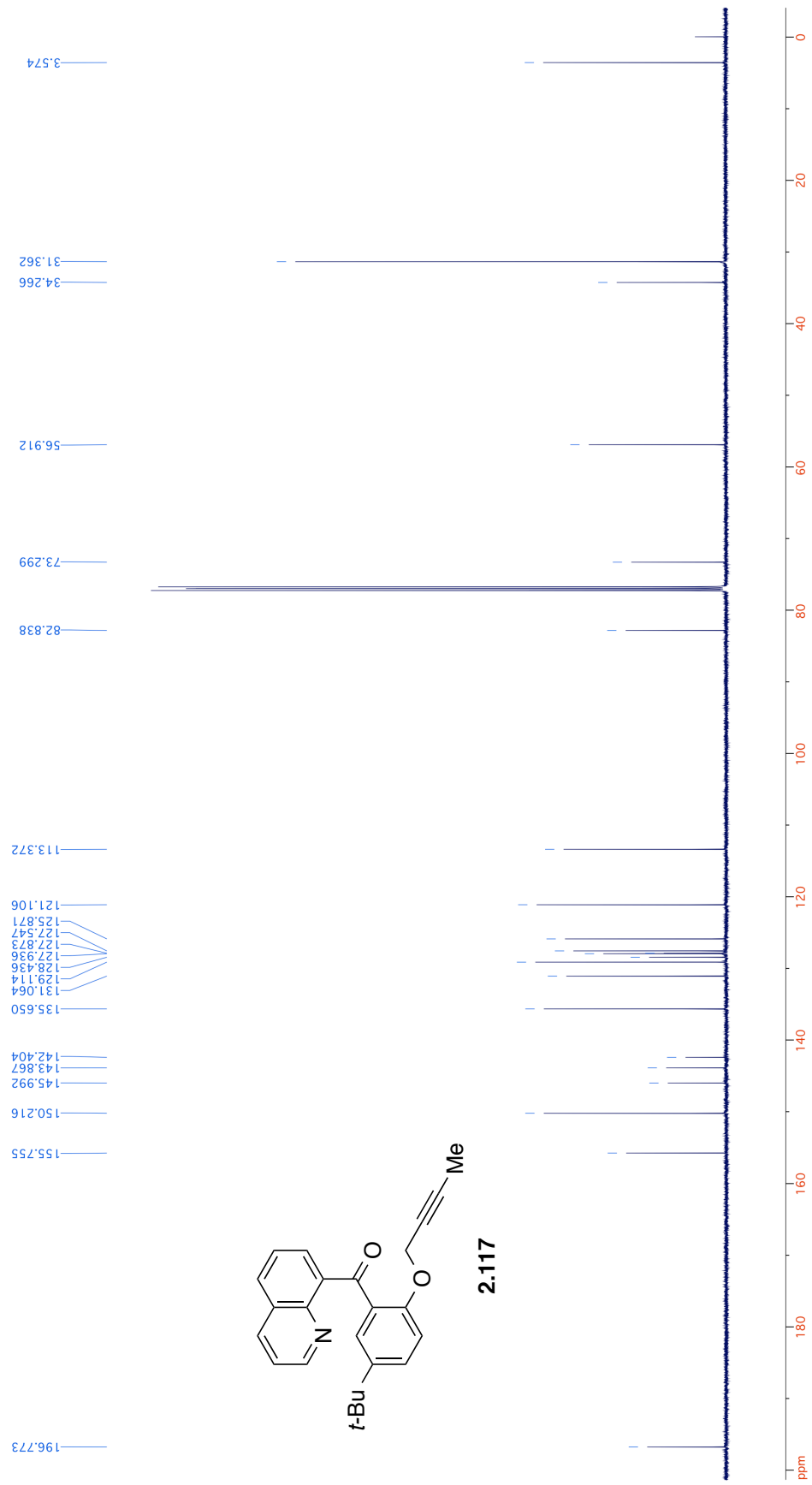


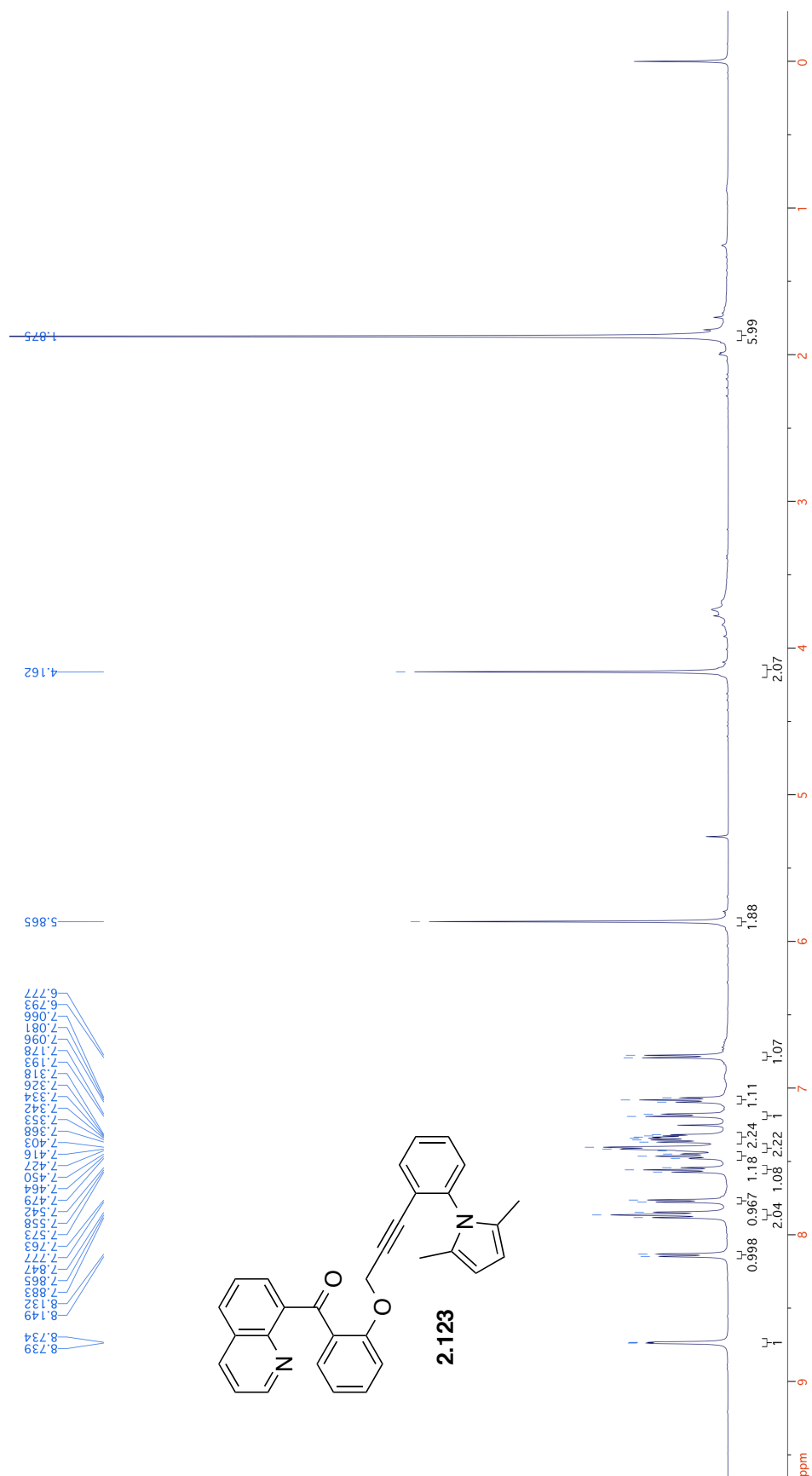


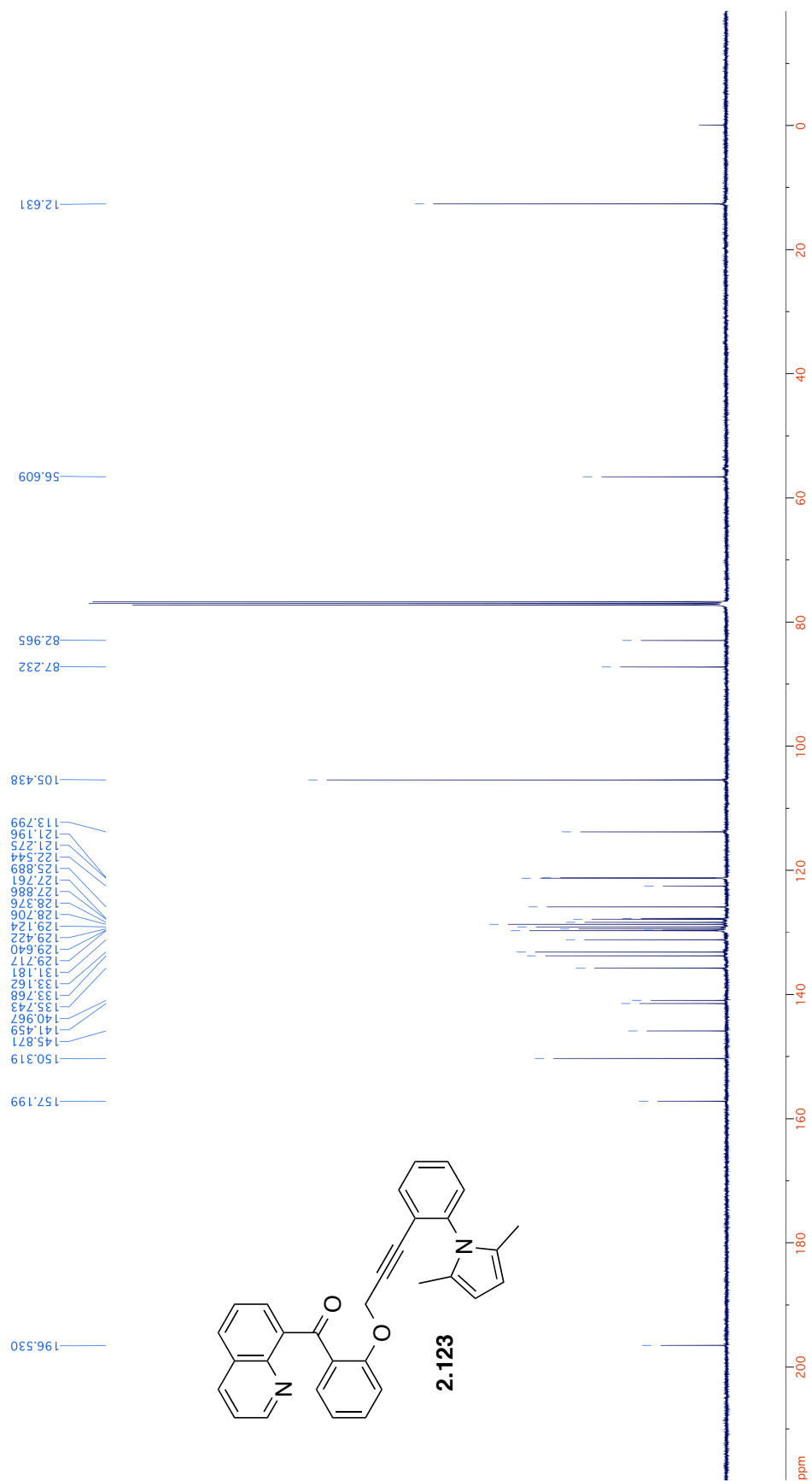


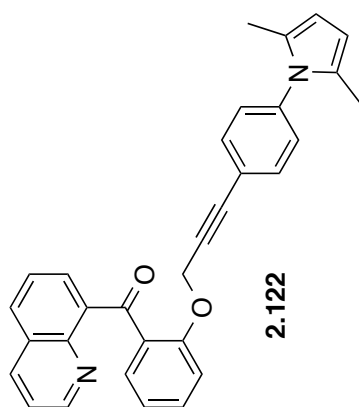








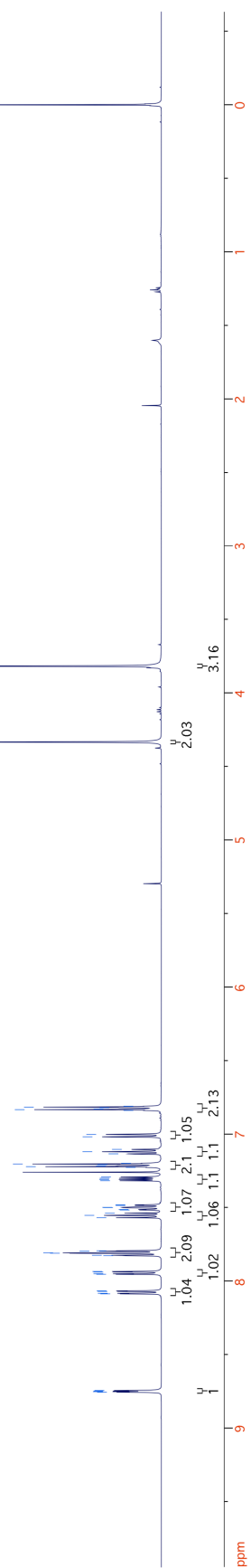


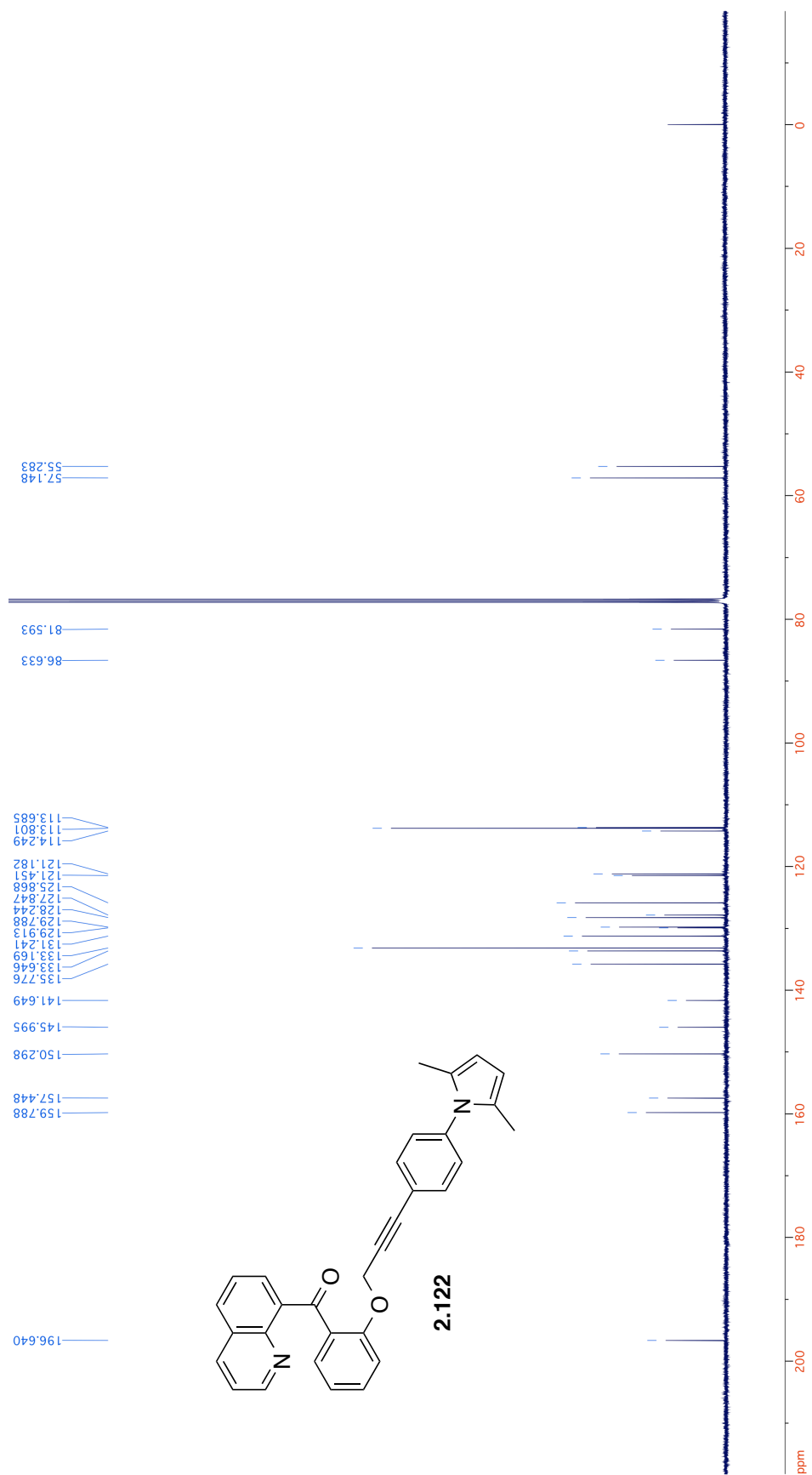


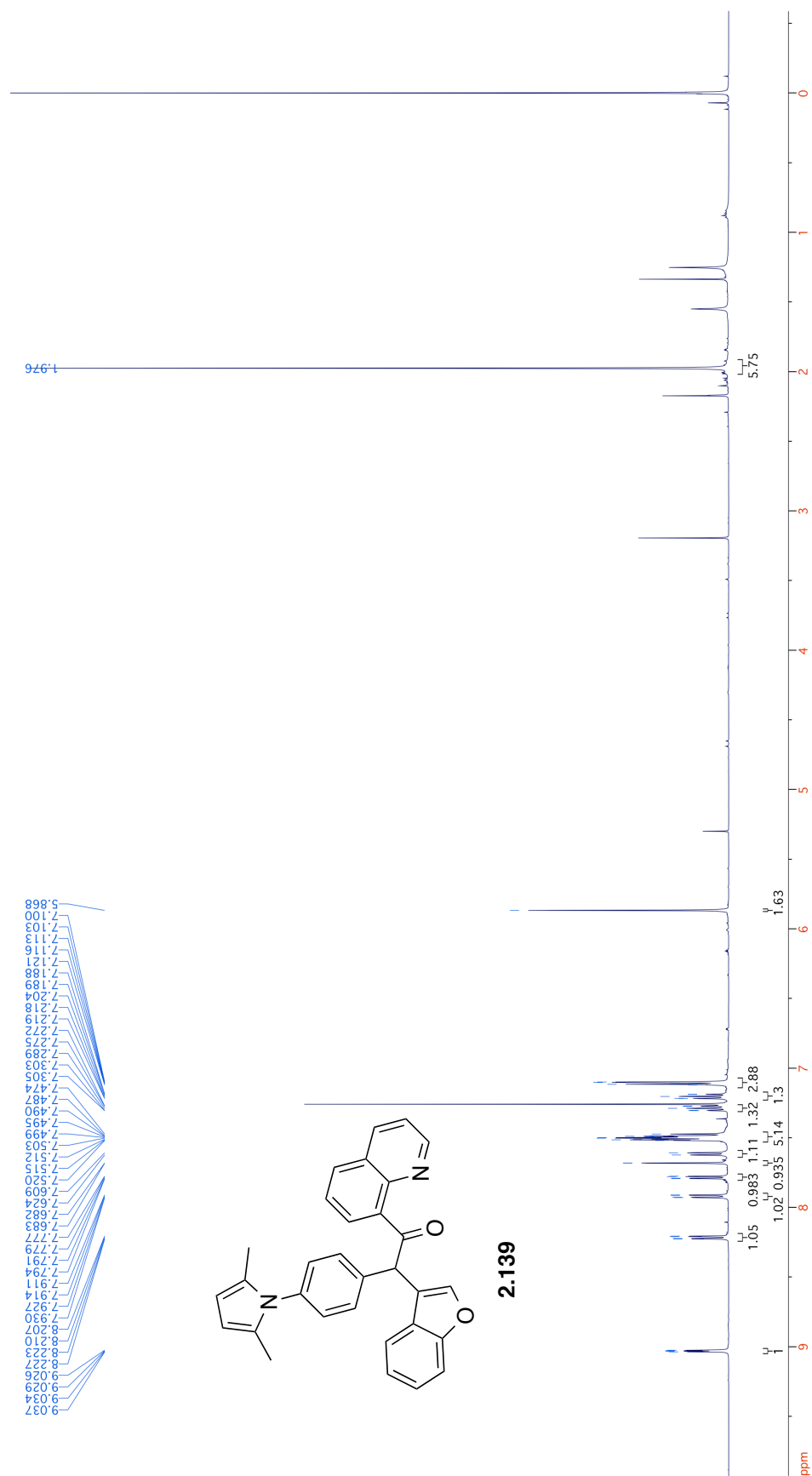
2.122

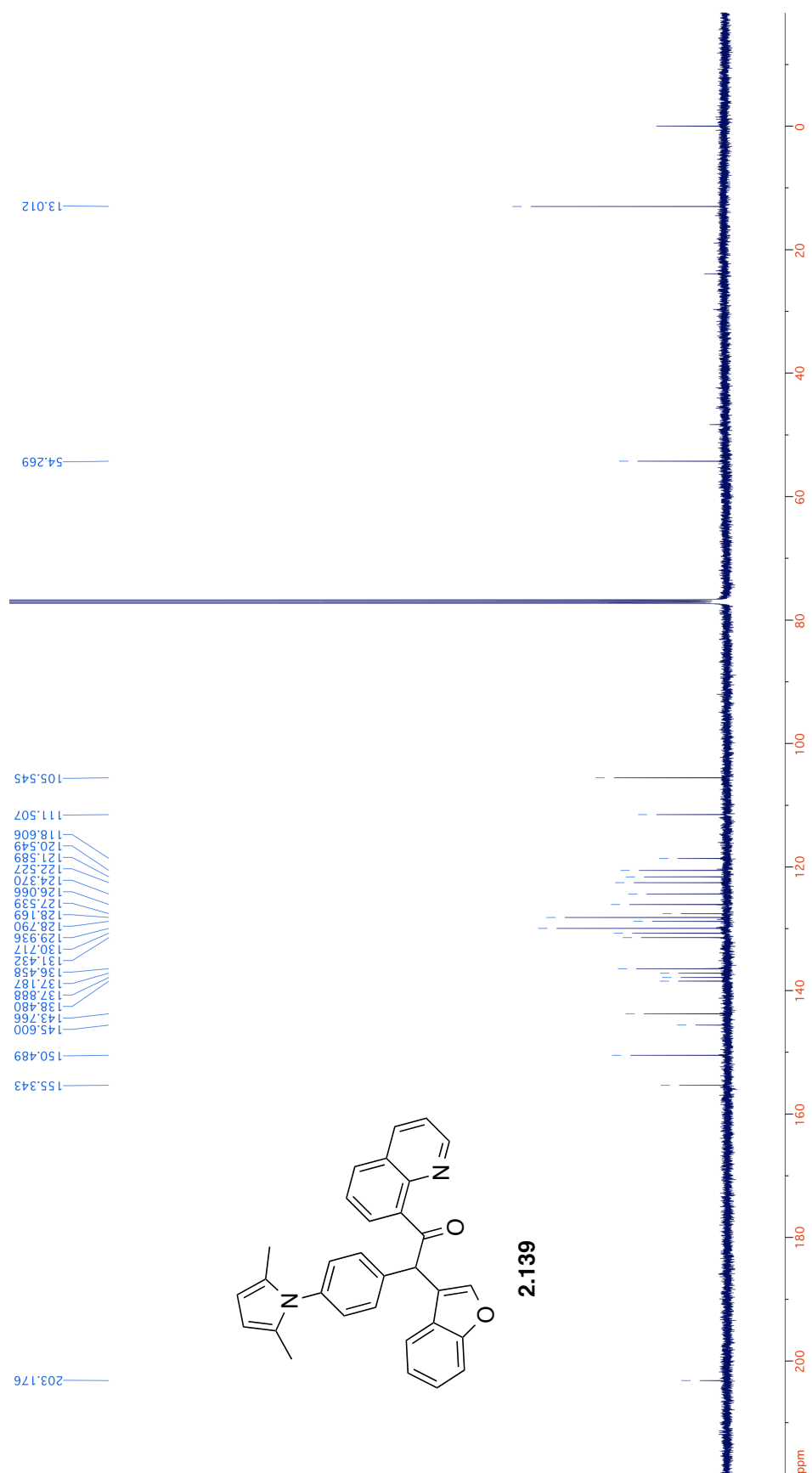
8.756
8.753
8.748
8.745
8.087
8.084
8.071
8.067
7.954
7.951
7.939
7.935
7.828
7.825
7.811
7.809
7.797
7.794
7.569
7.553
7.539
7.517
7.514
7.500
7.486
7.482
7.318
7.309
7.301
7.293
7.227
7.222
7.218
7.208
7.204
7.199
7.135
7.120
7.105
7.019
7.003
6.840
6.834
6.830
6.821
6.817
6.811

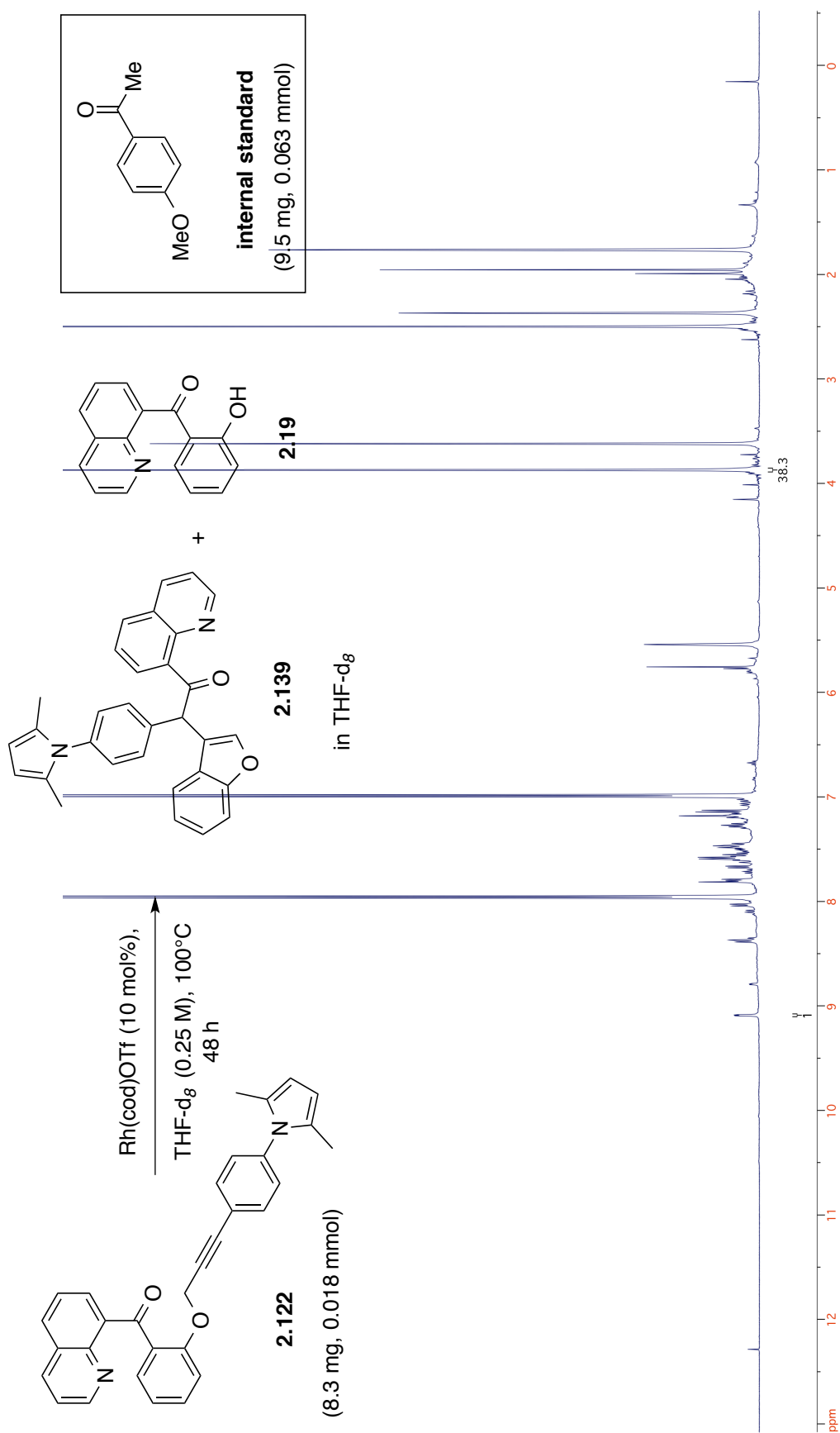
4.334
3.818

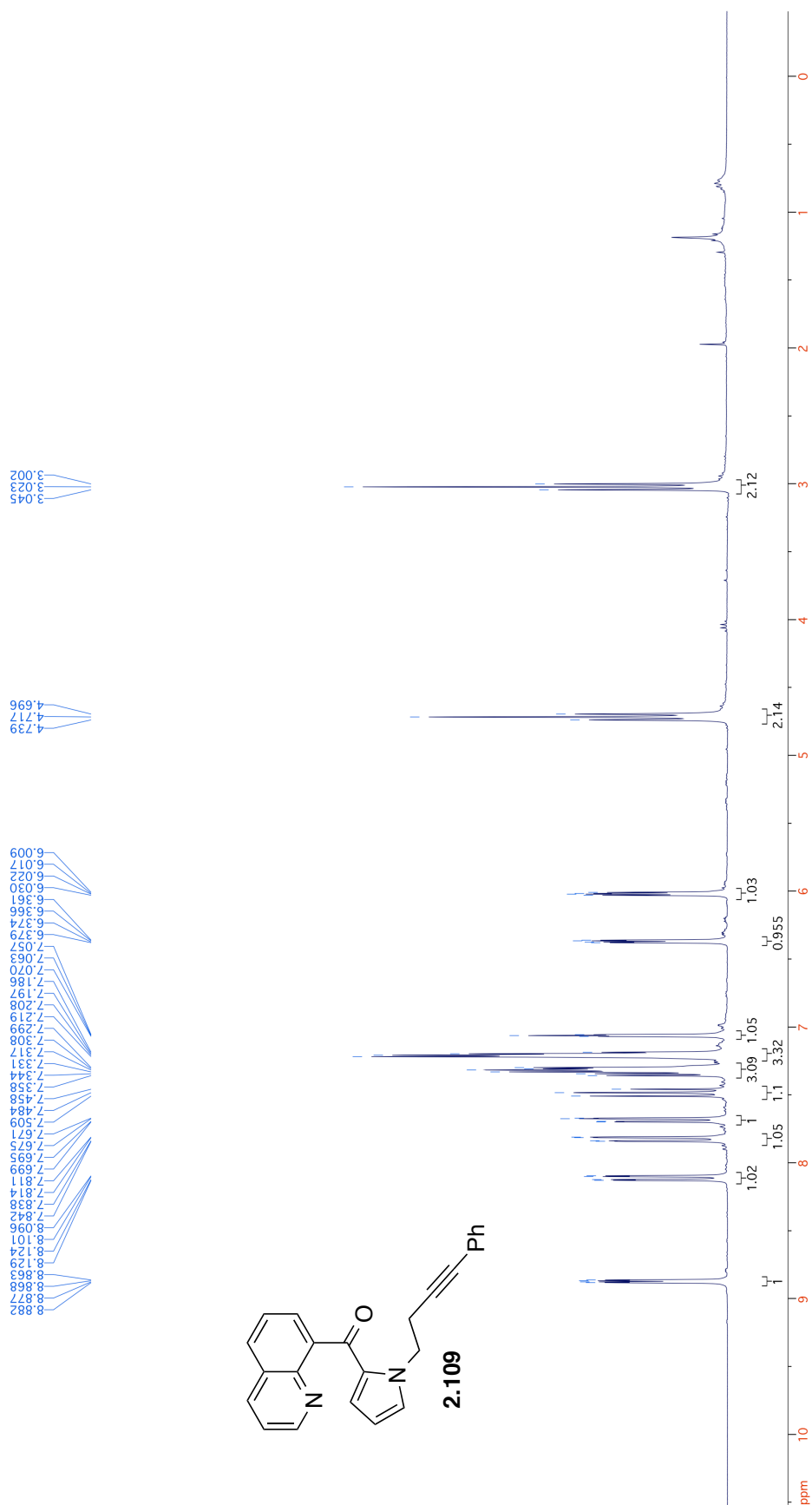
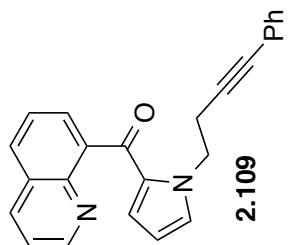


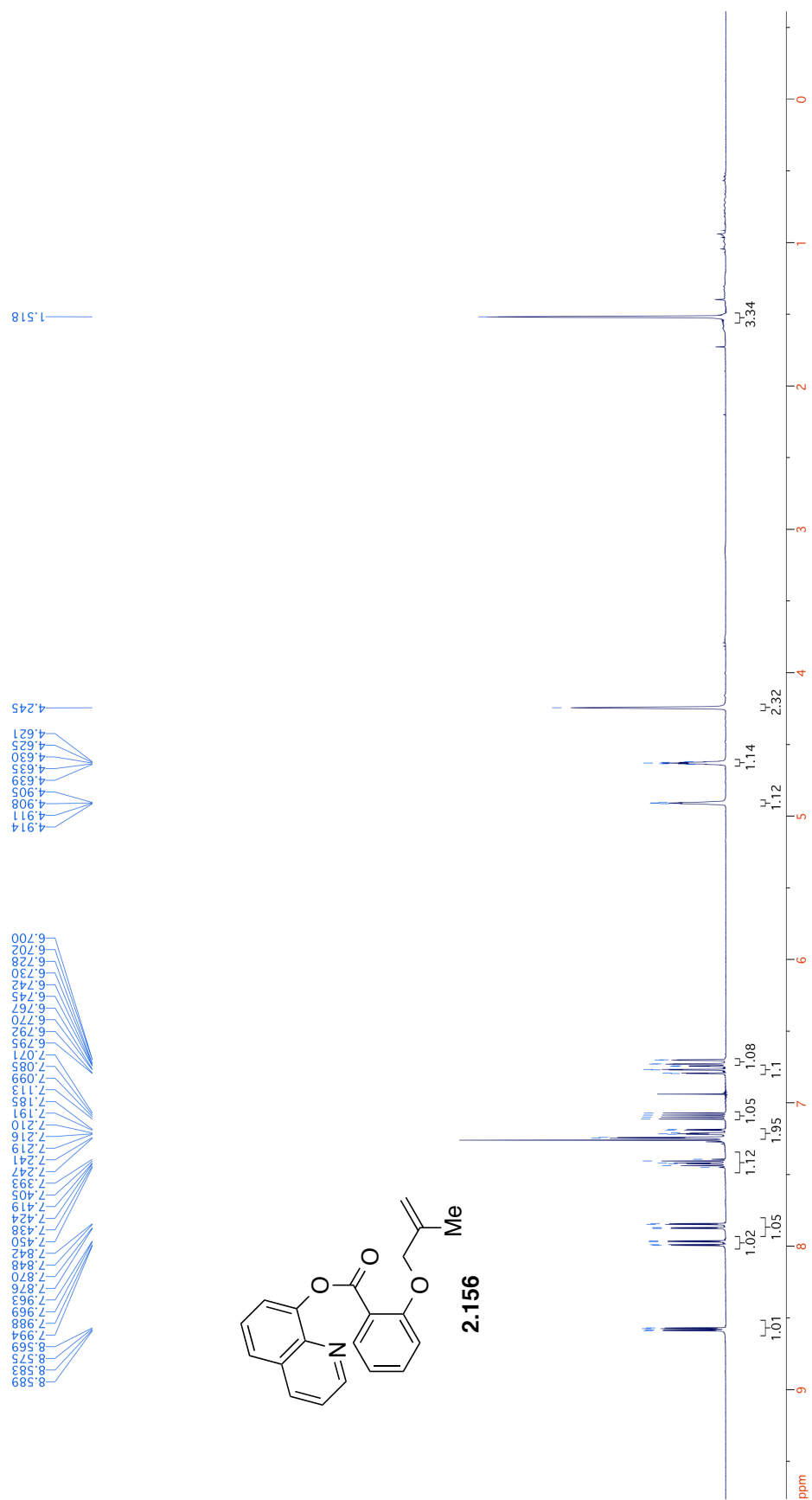
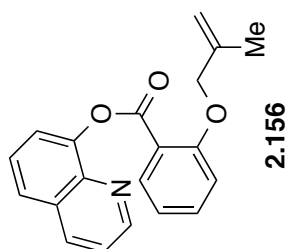


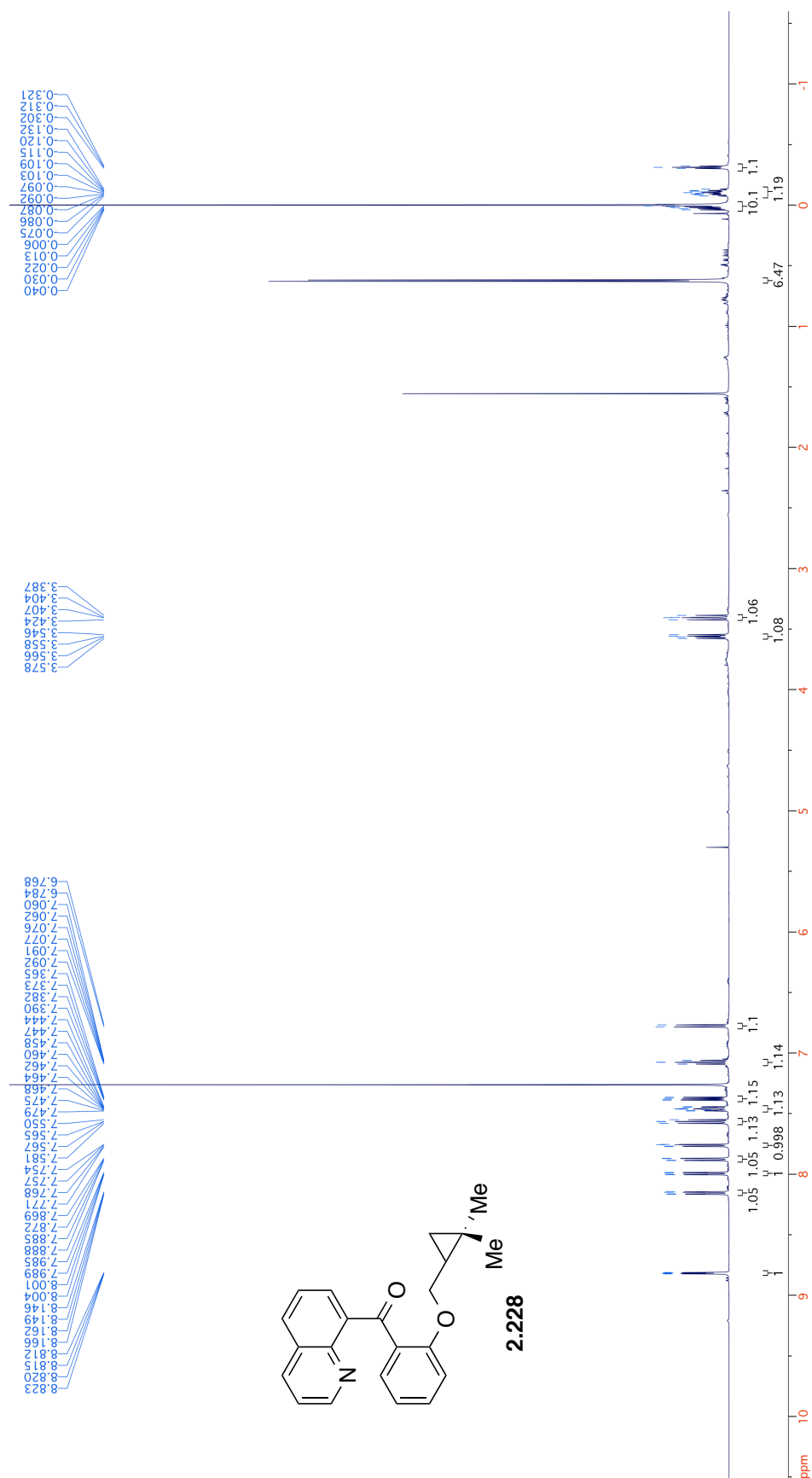


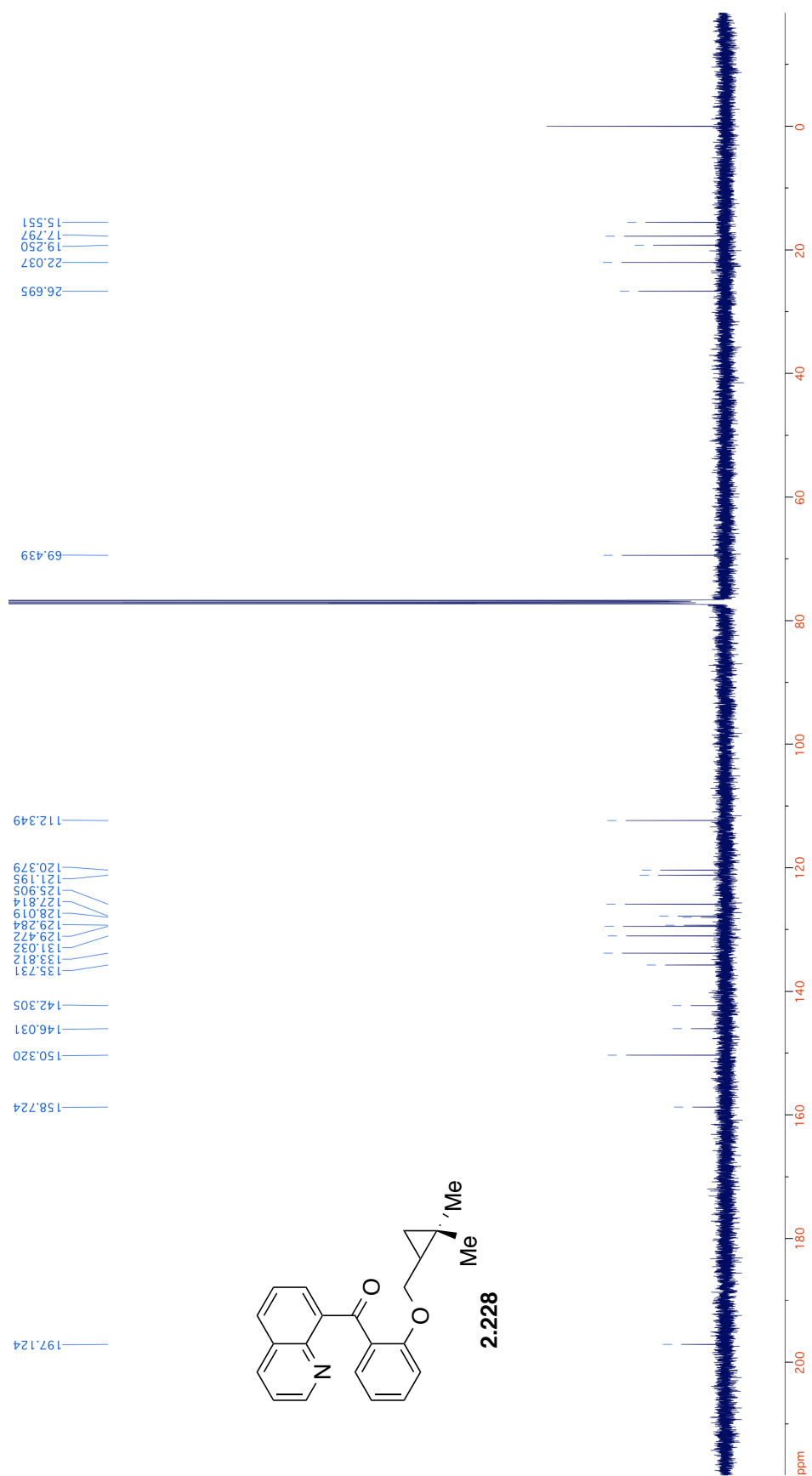


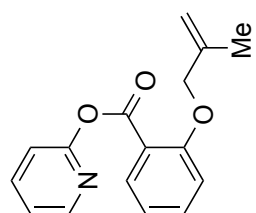




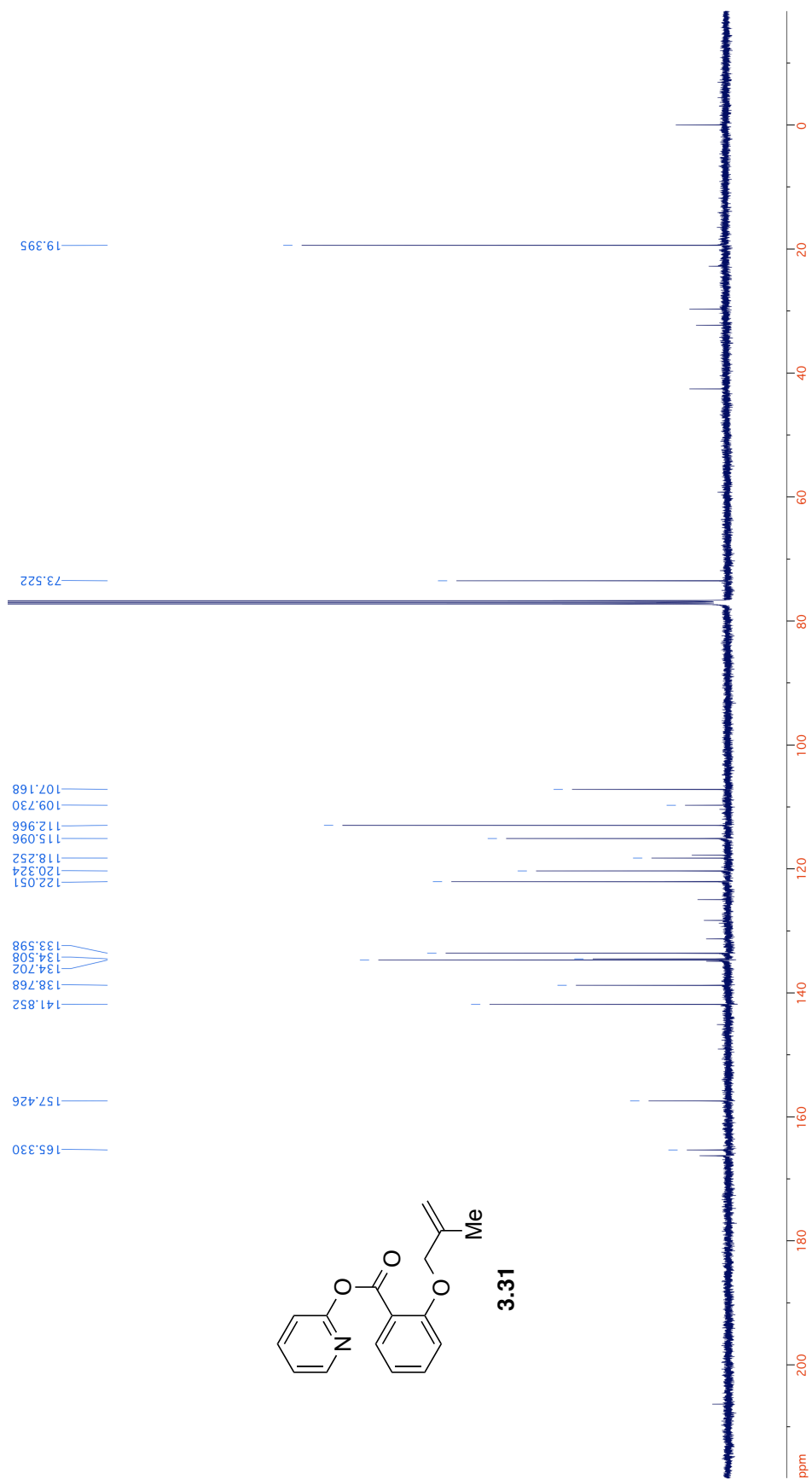


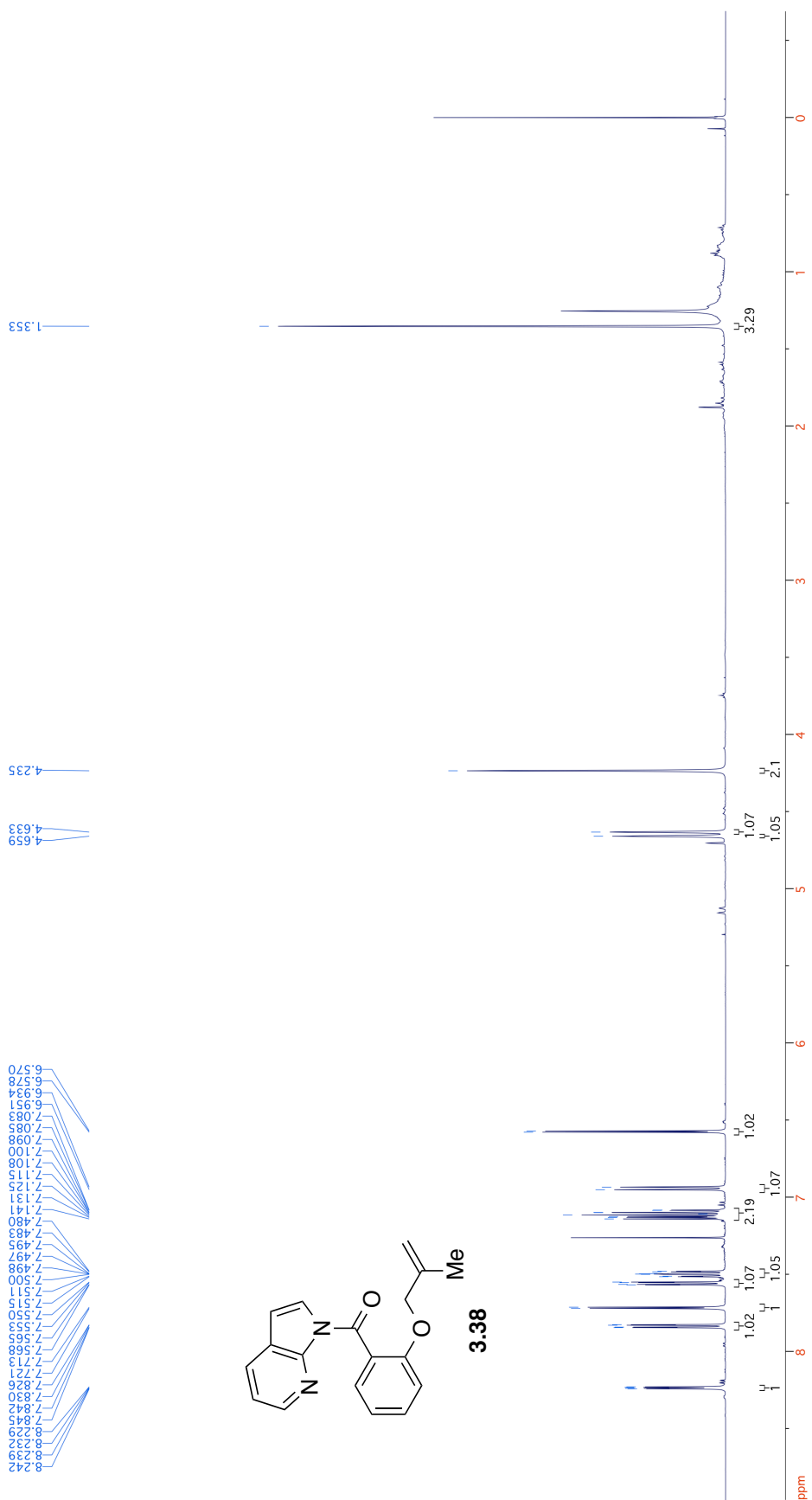
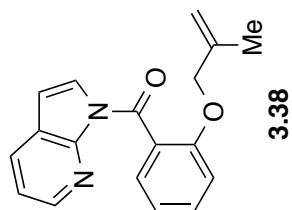


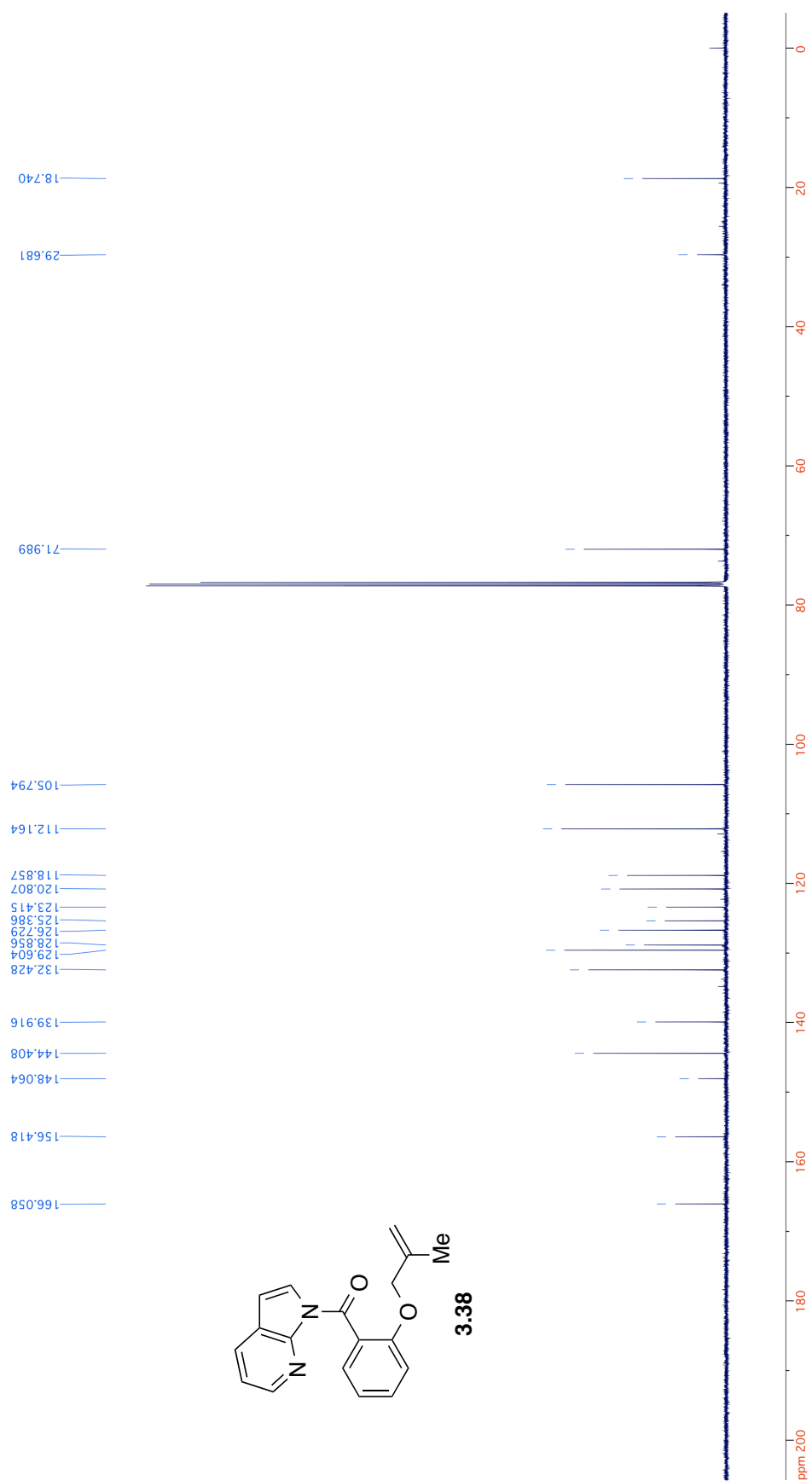


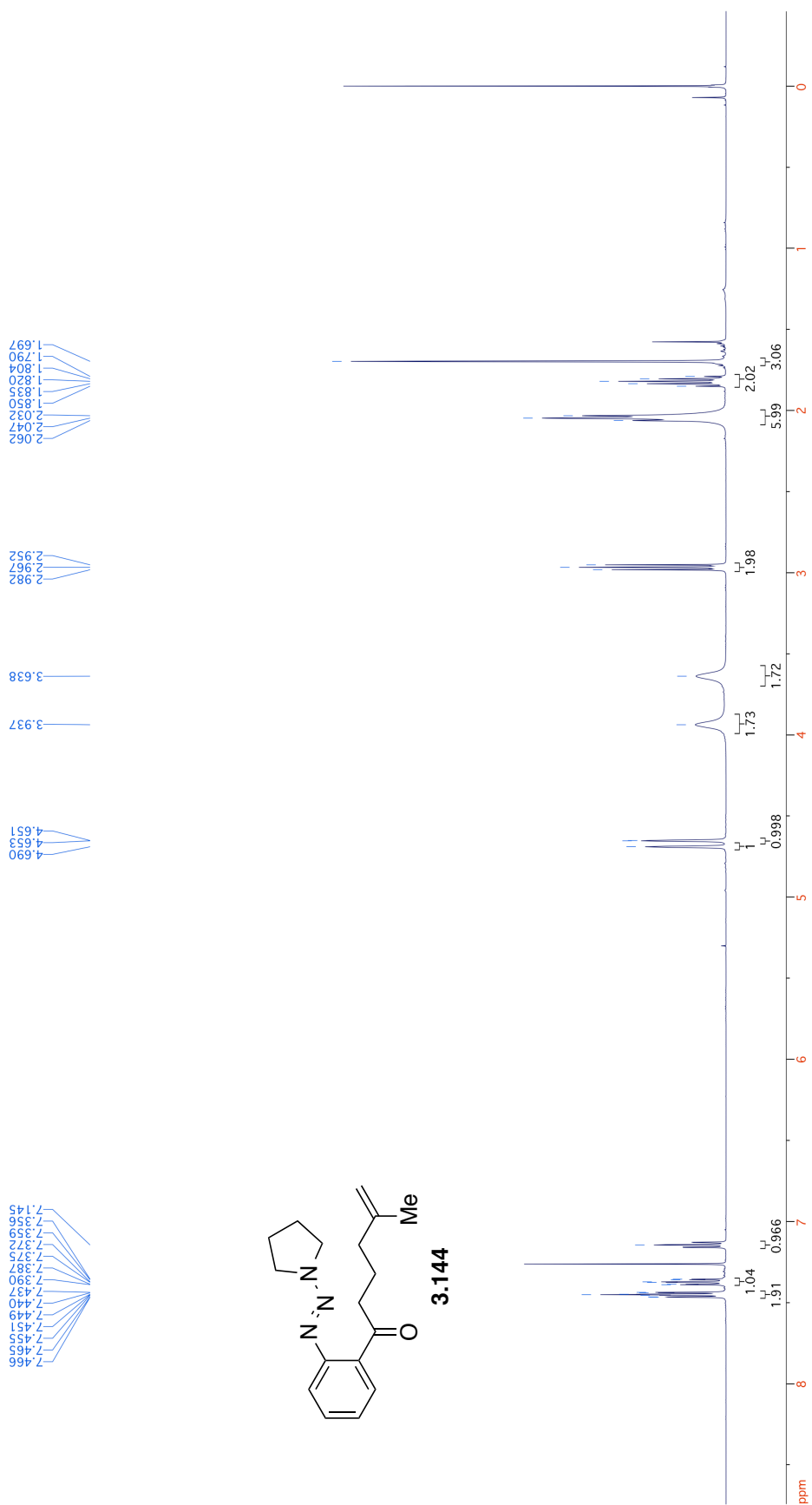
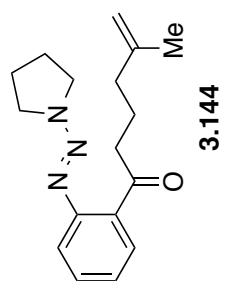


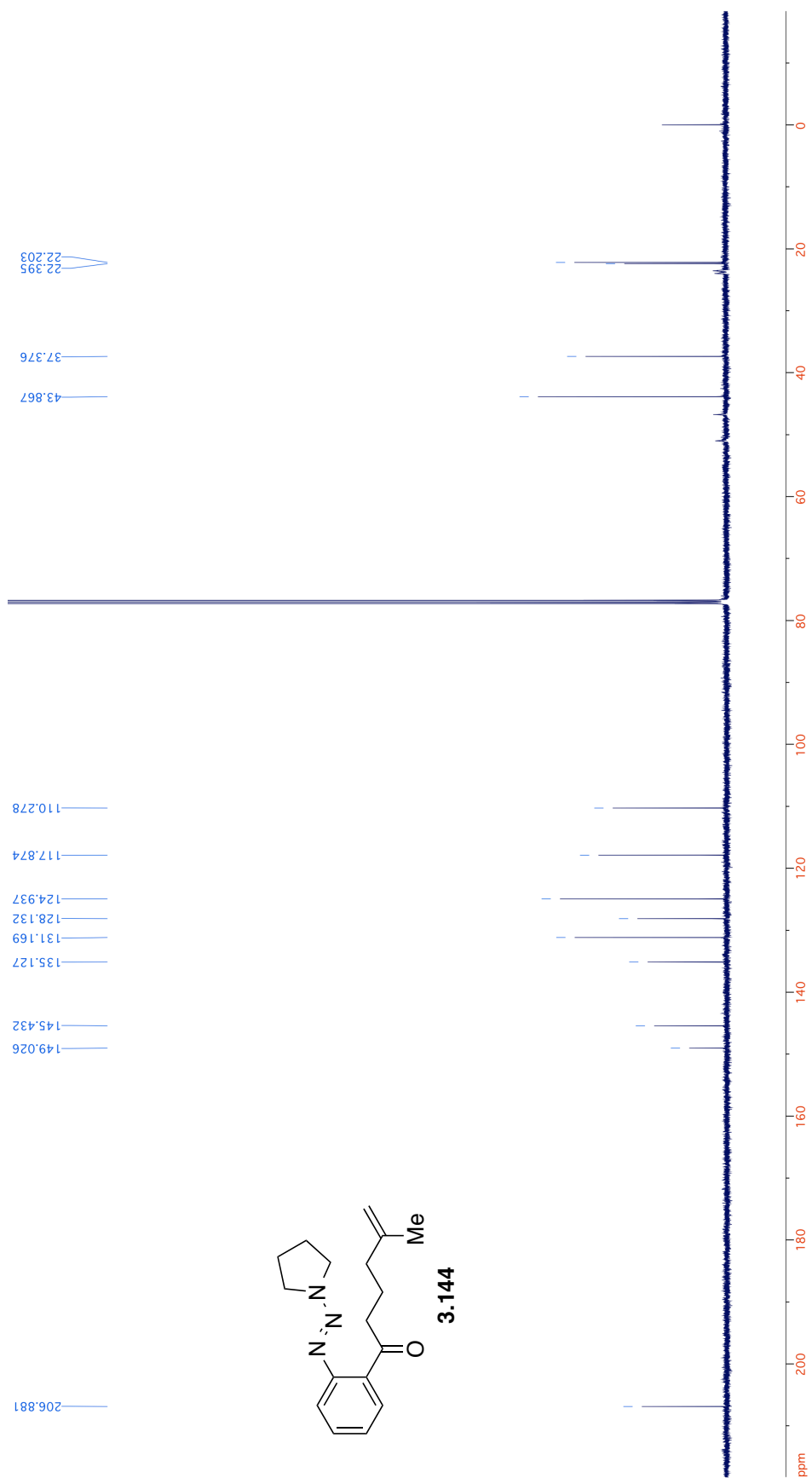
3.31

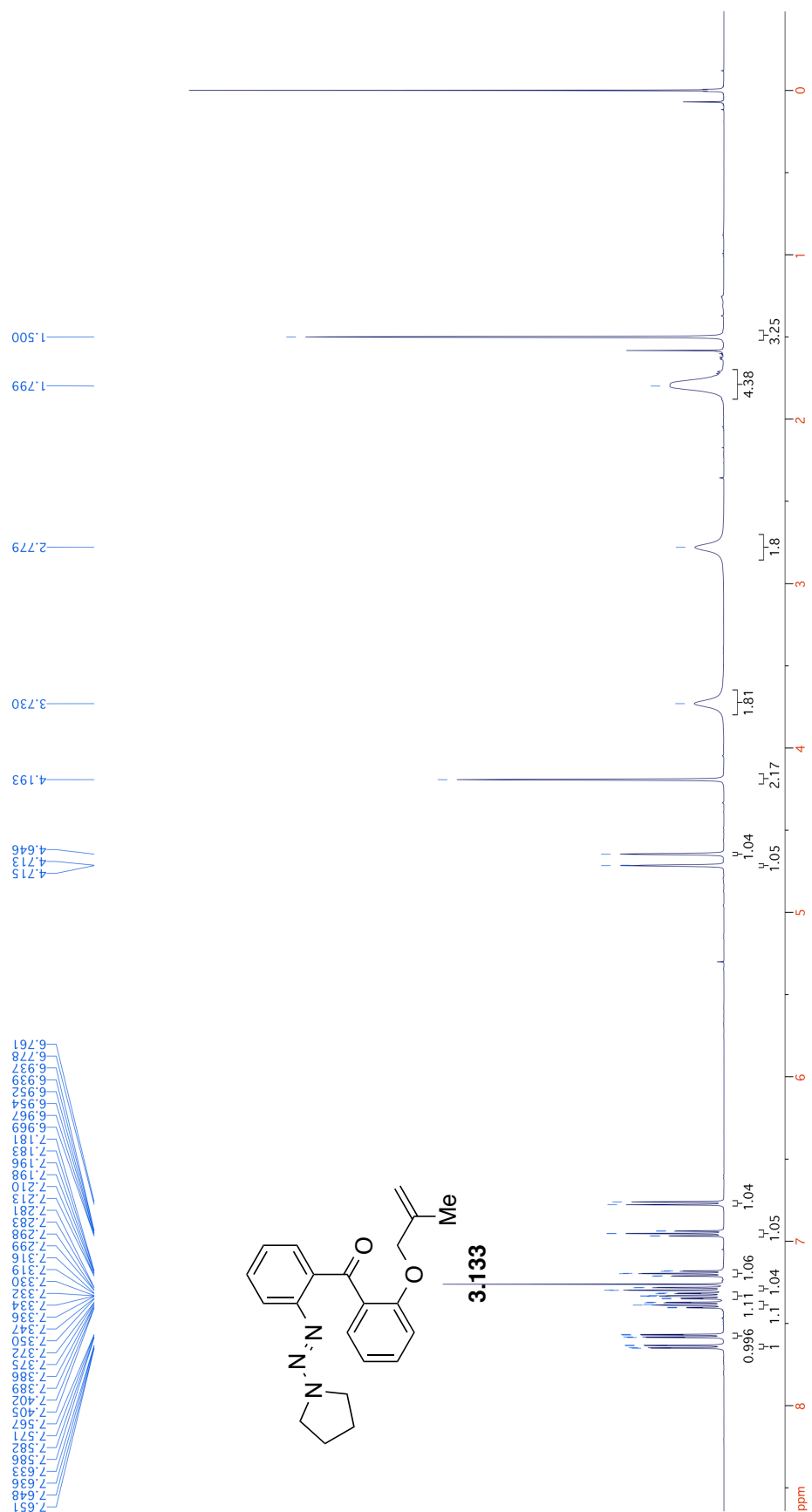


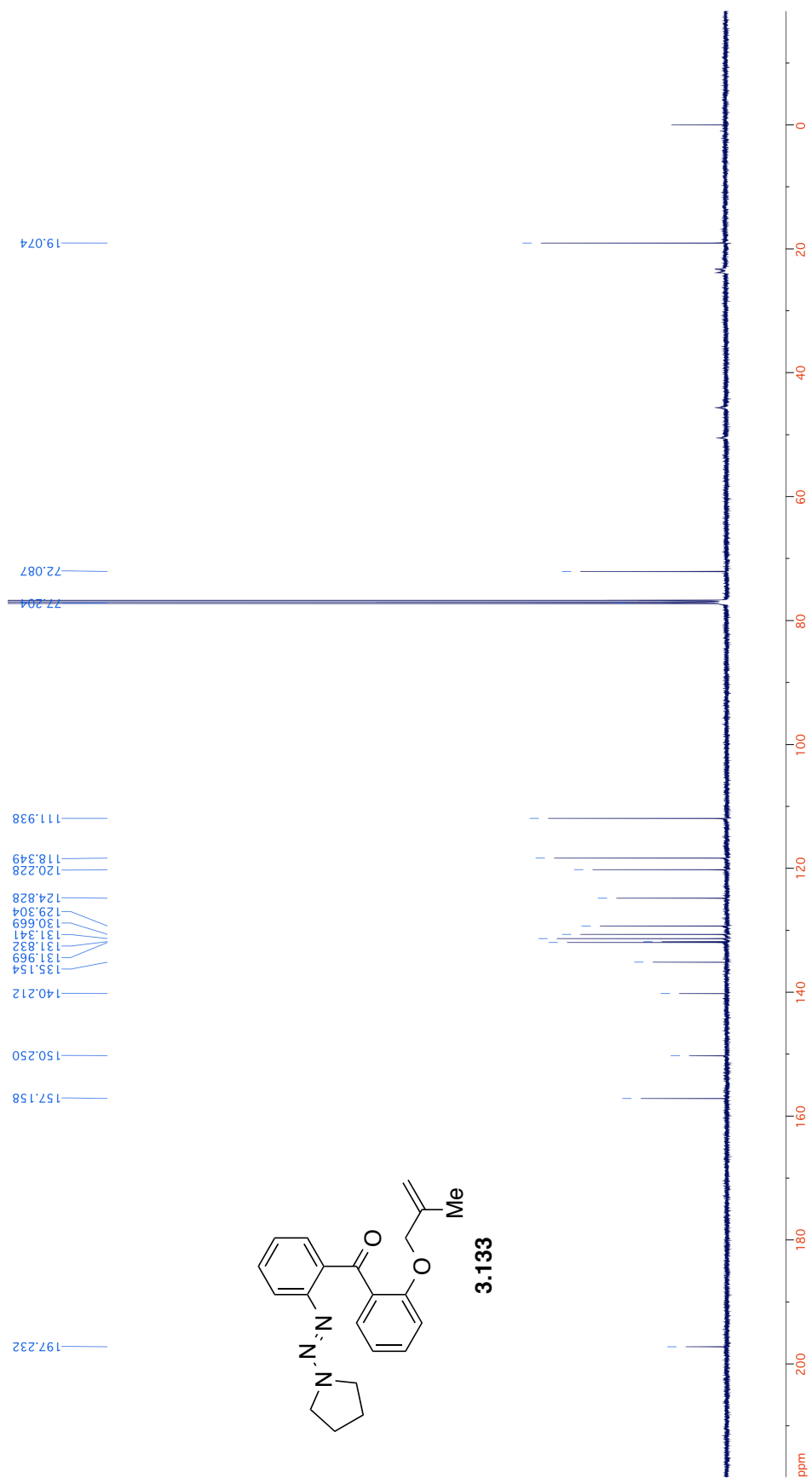
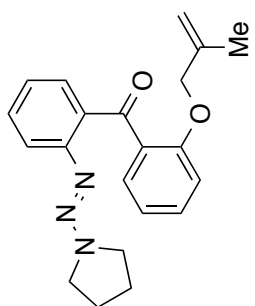


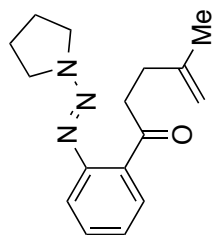




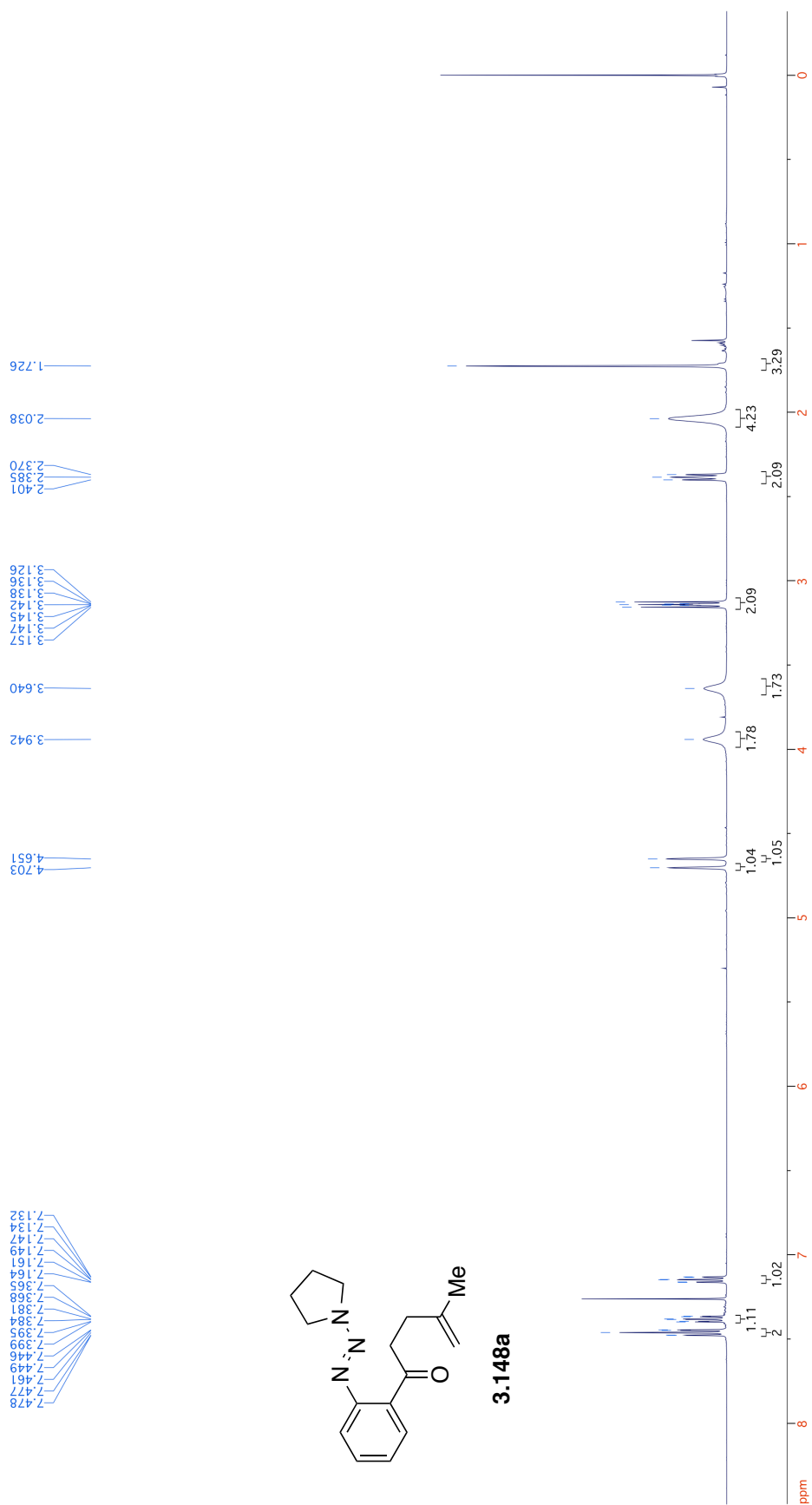


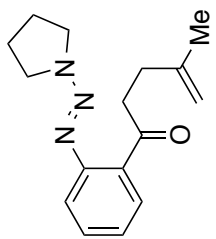




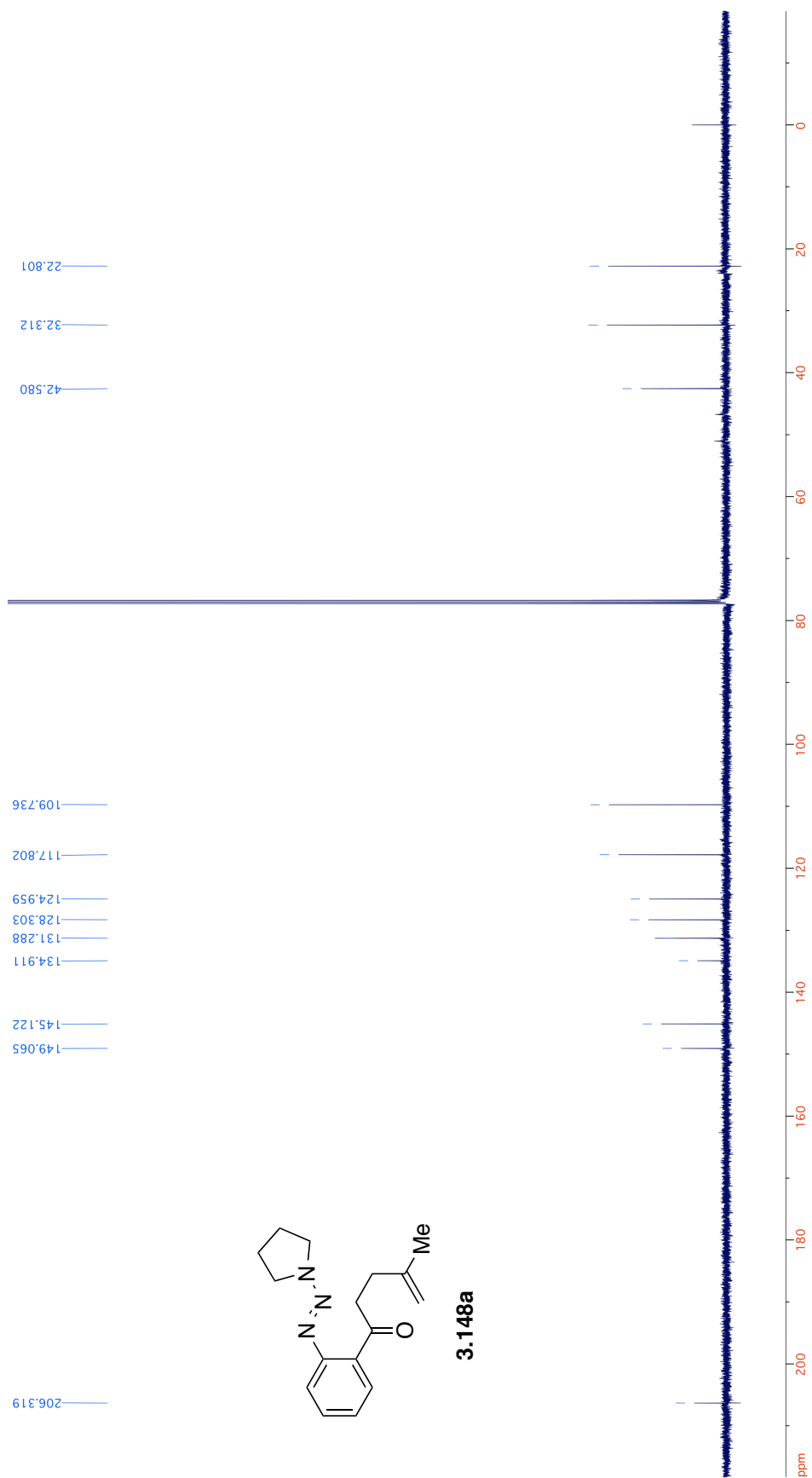


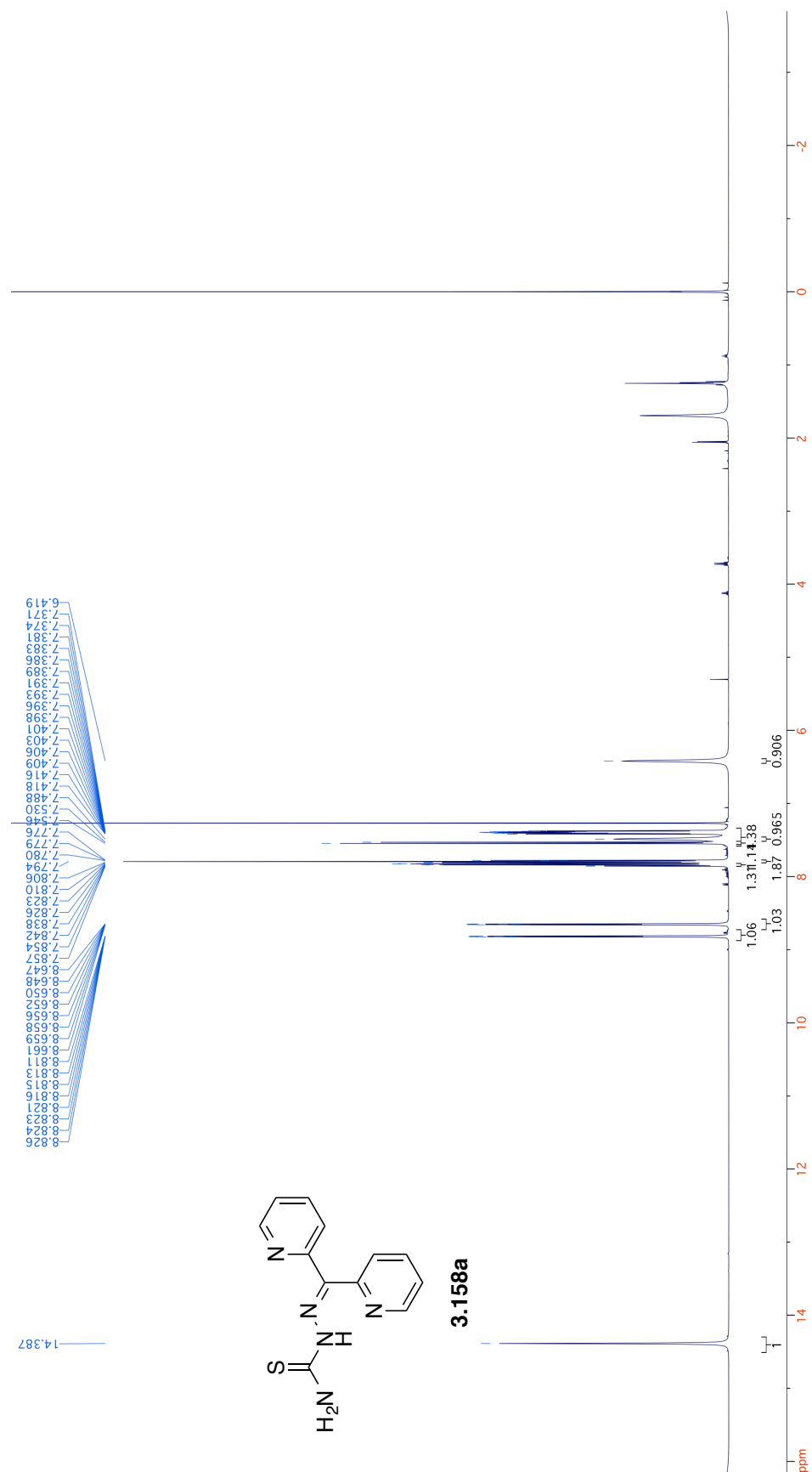
3.148a

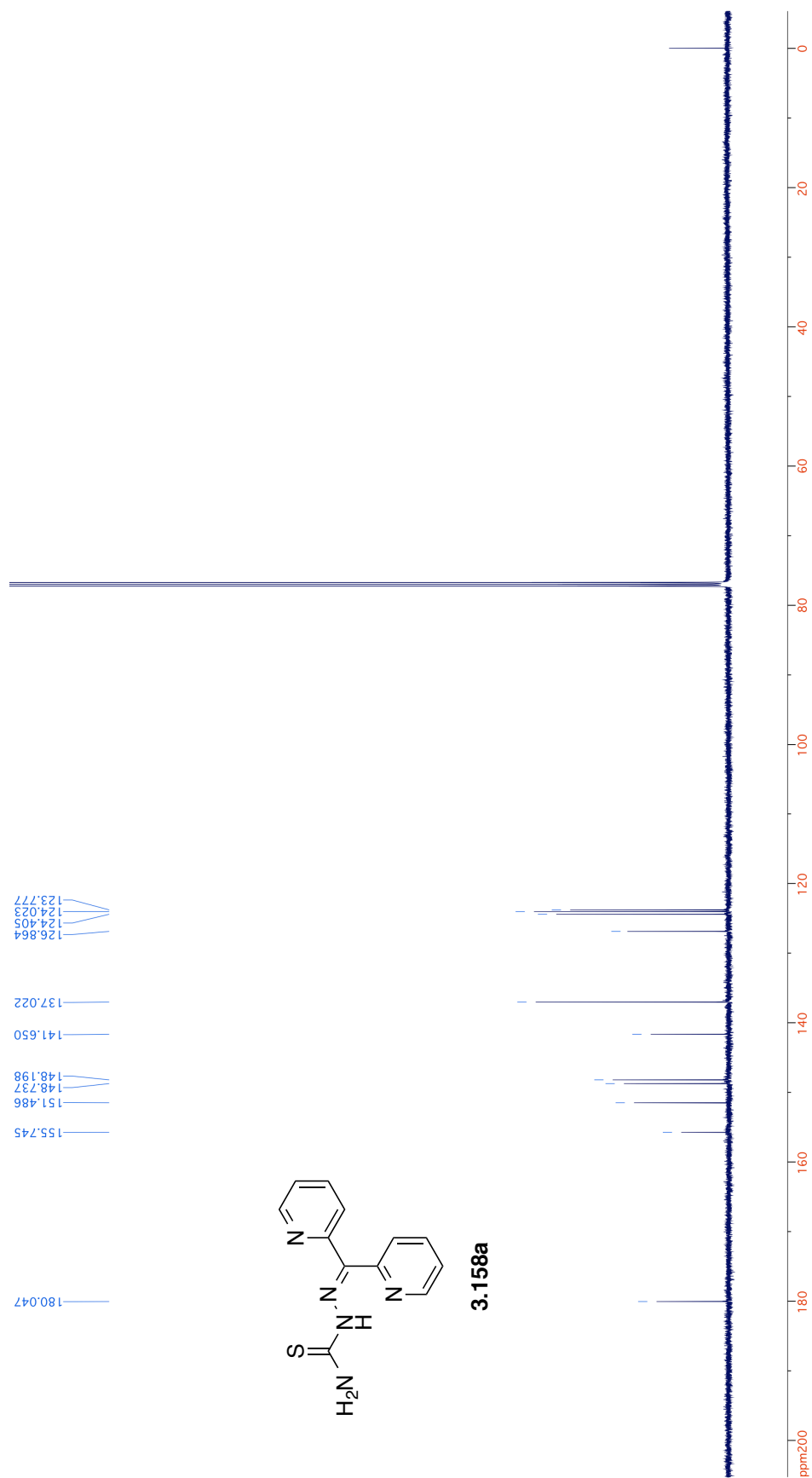


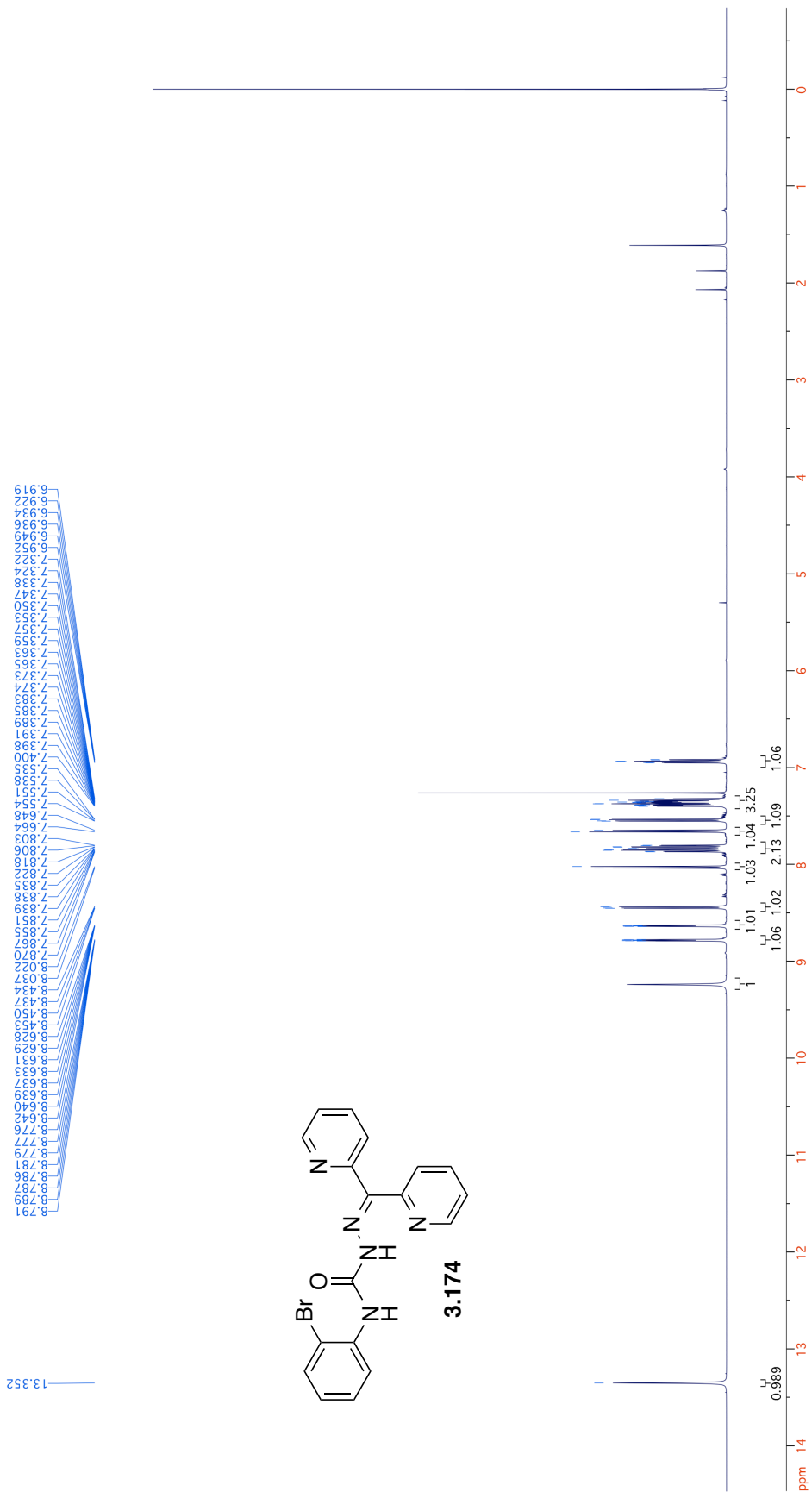


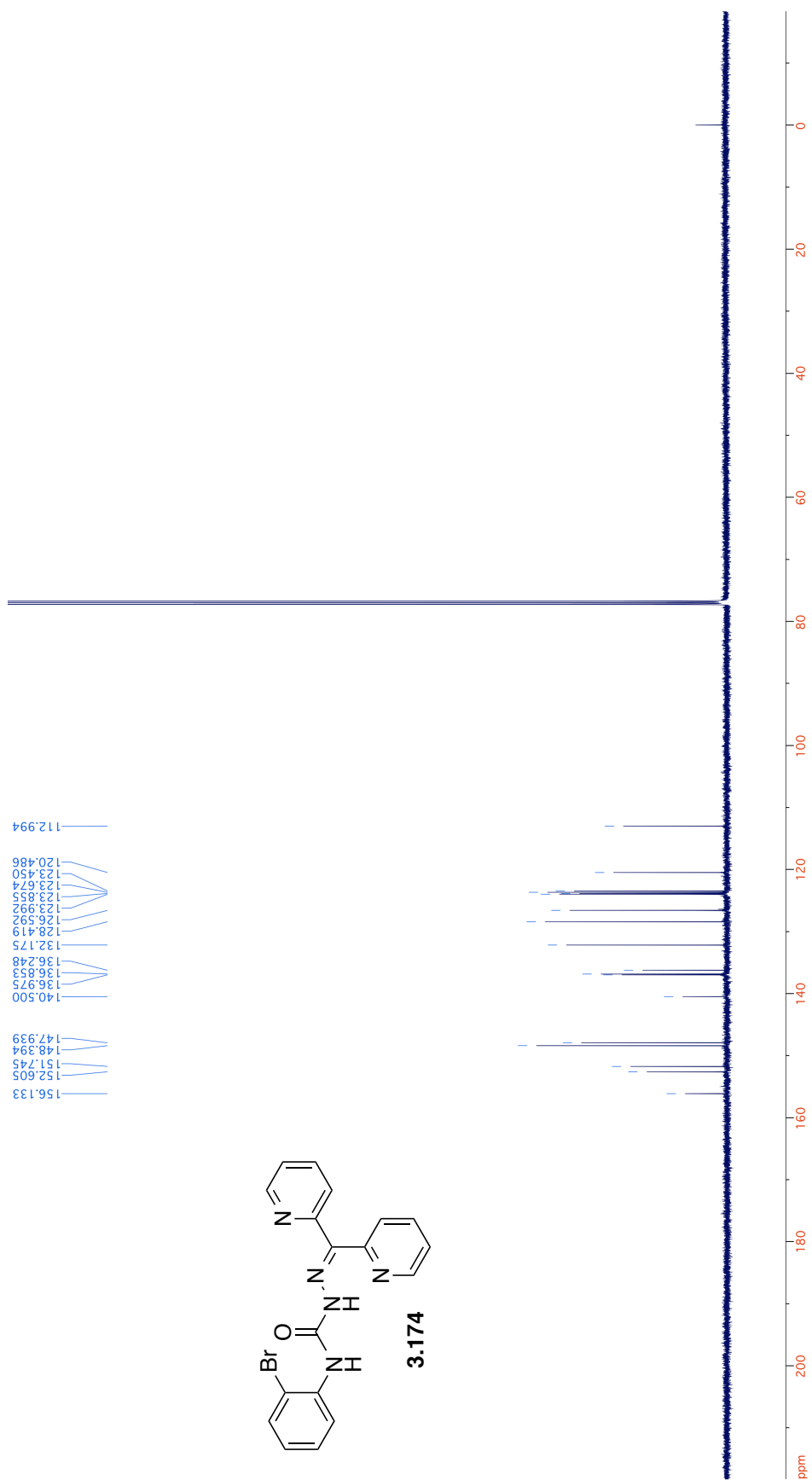
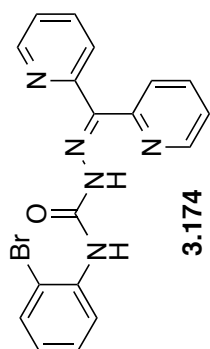
3.148a

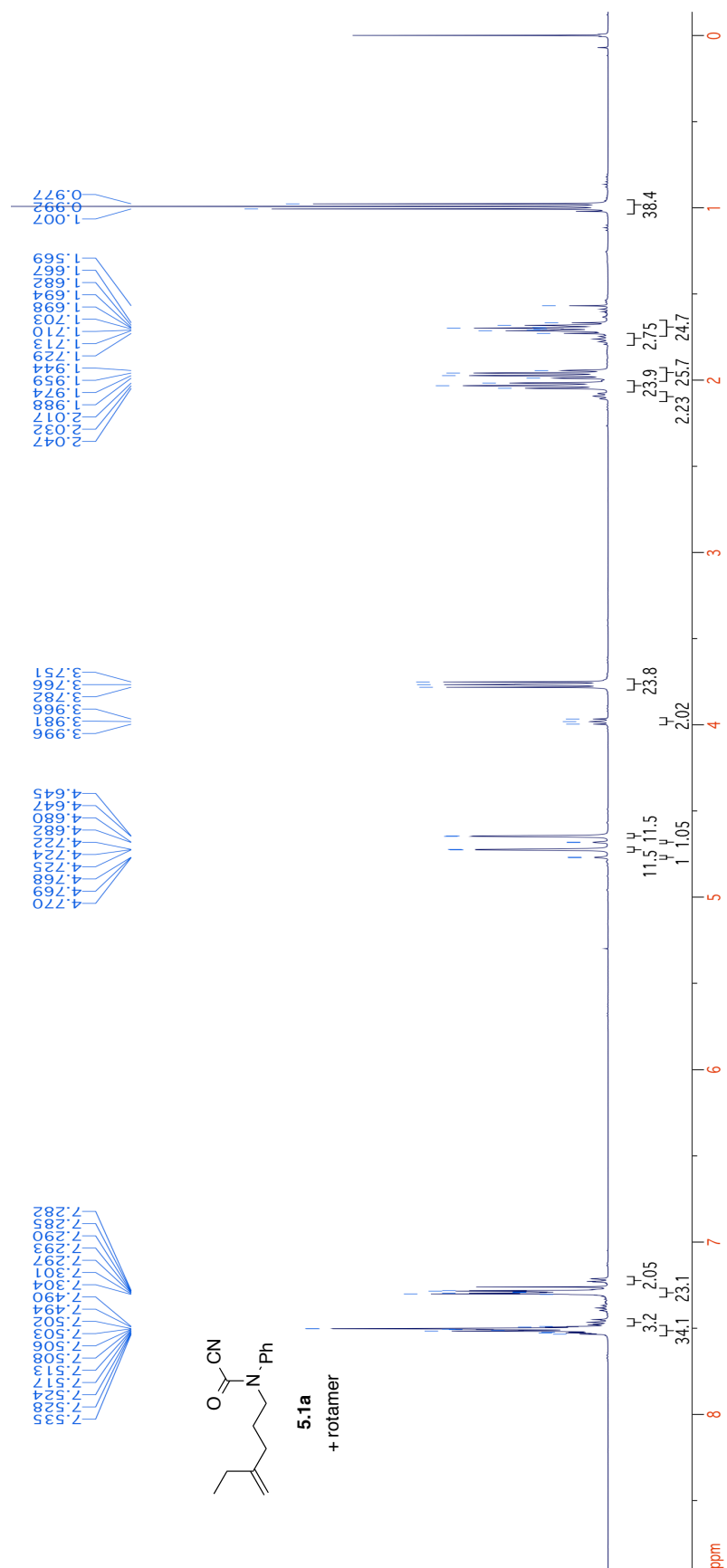


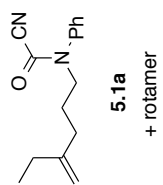
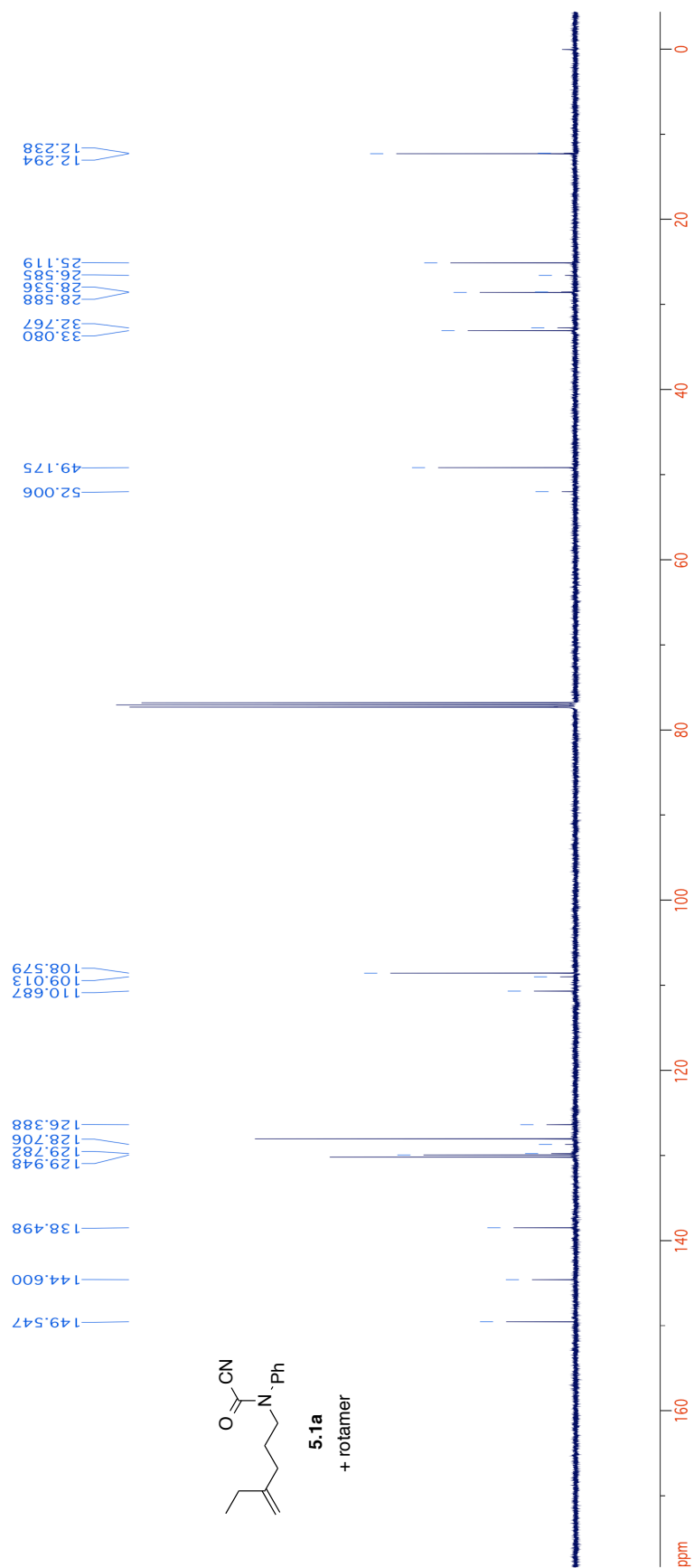


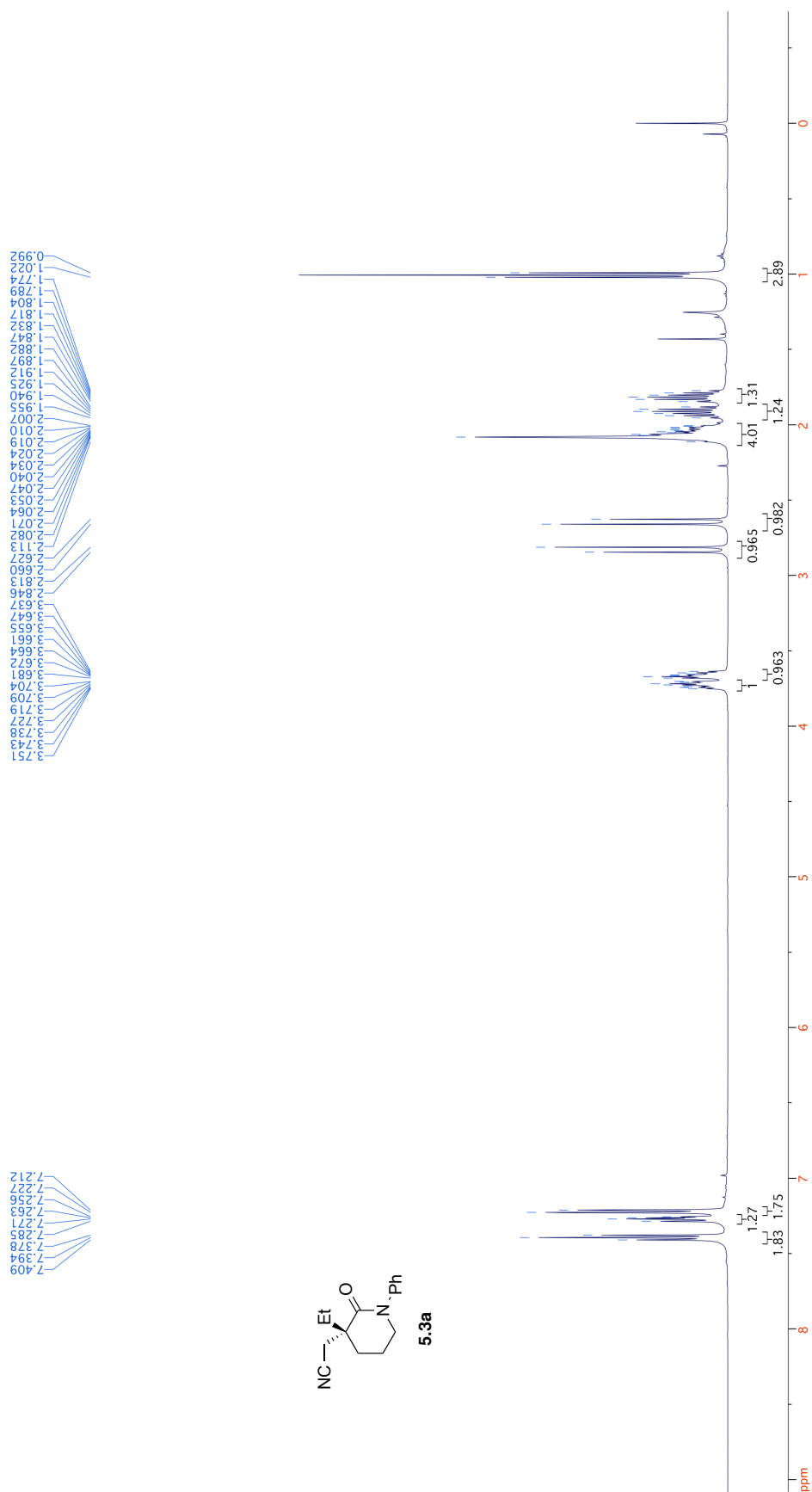
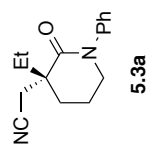


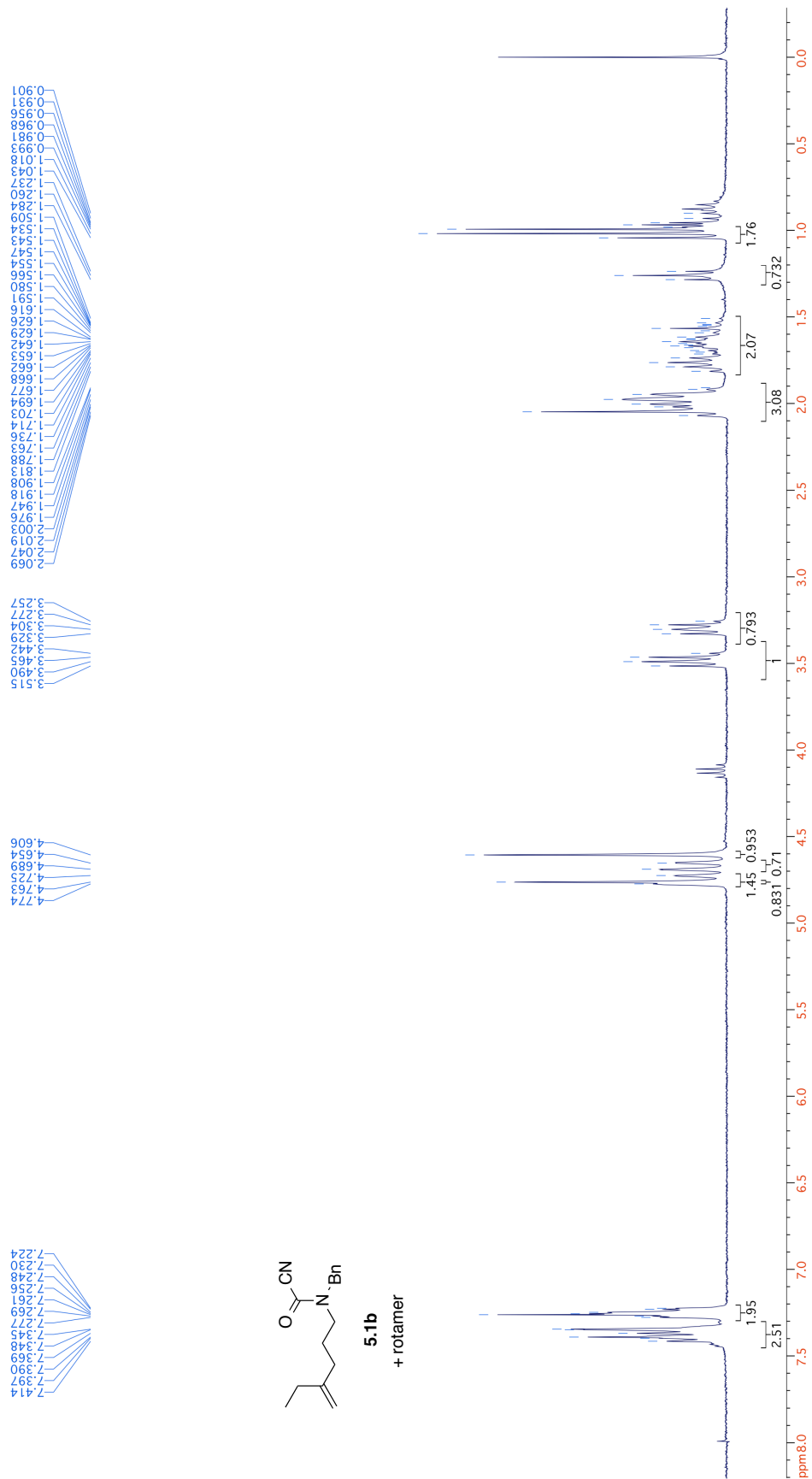
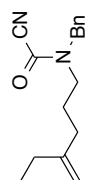


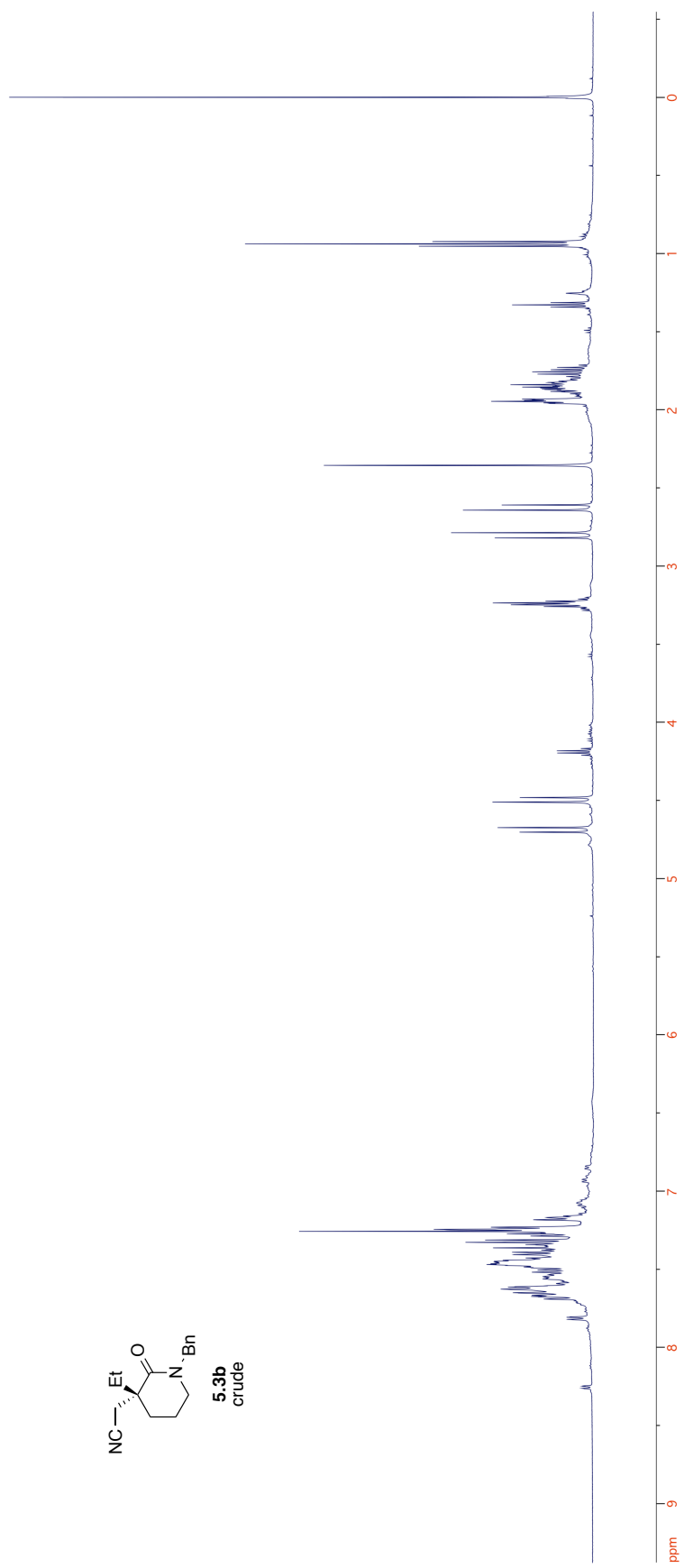
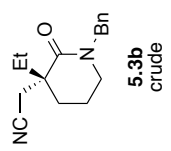


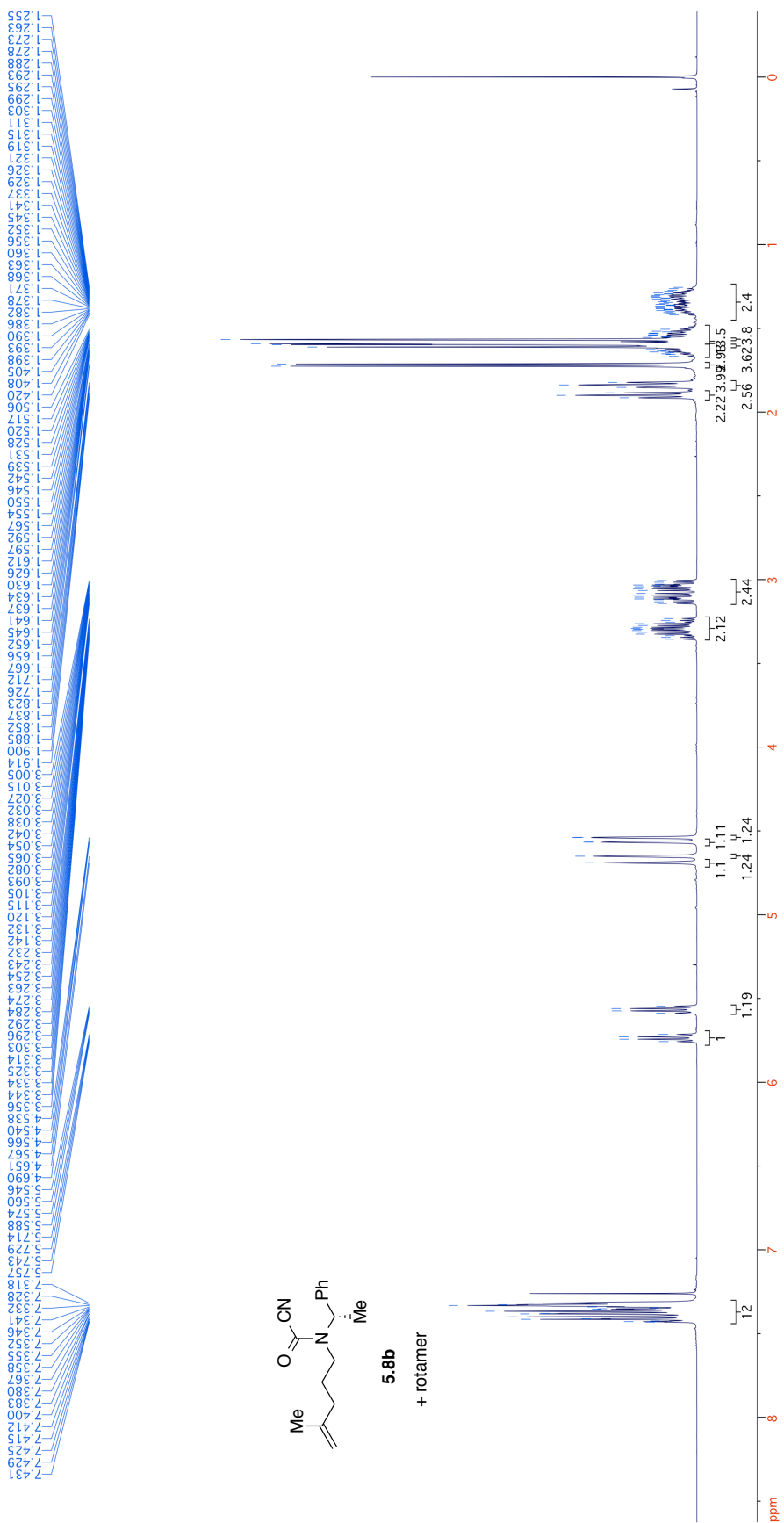
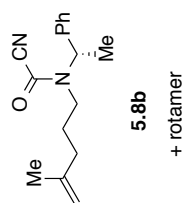


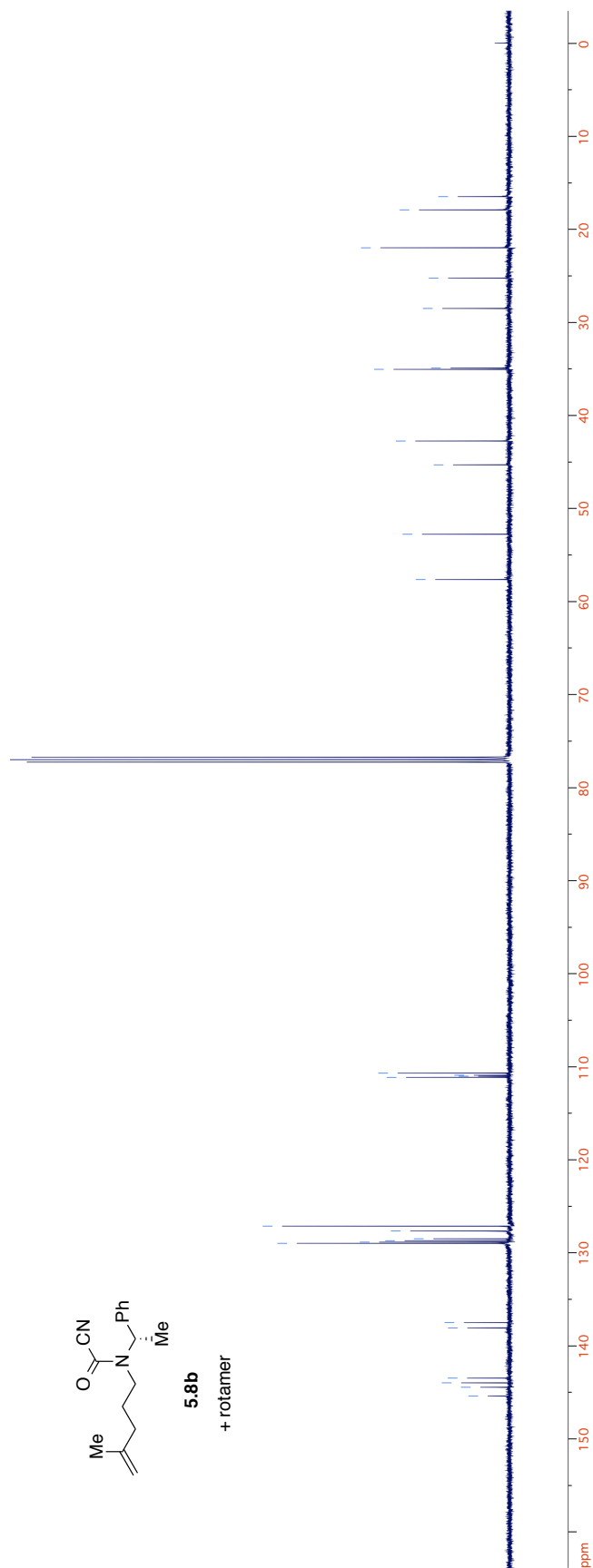
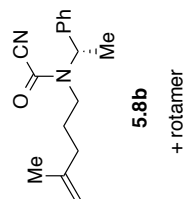


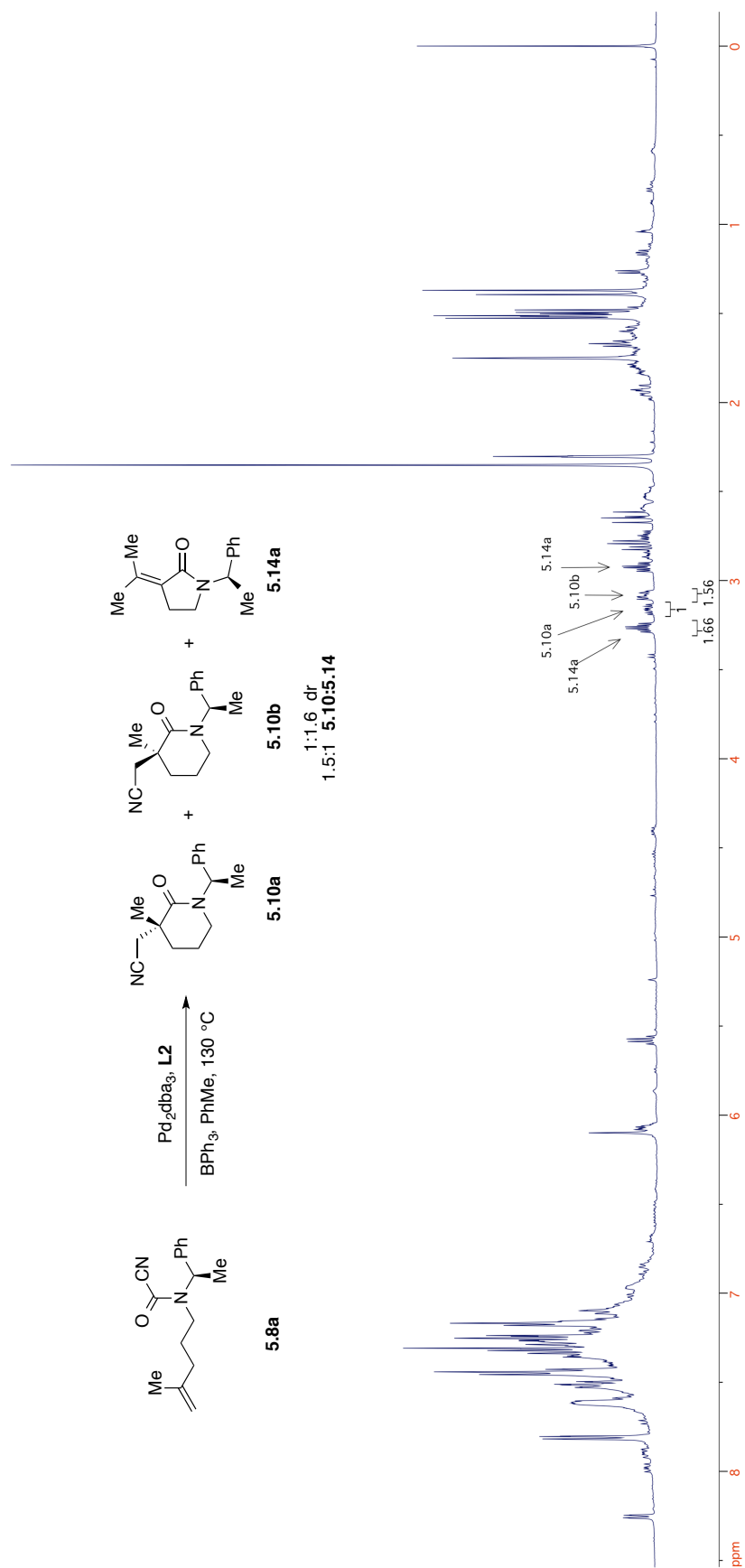


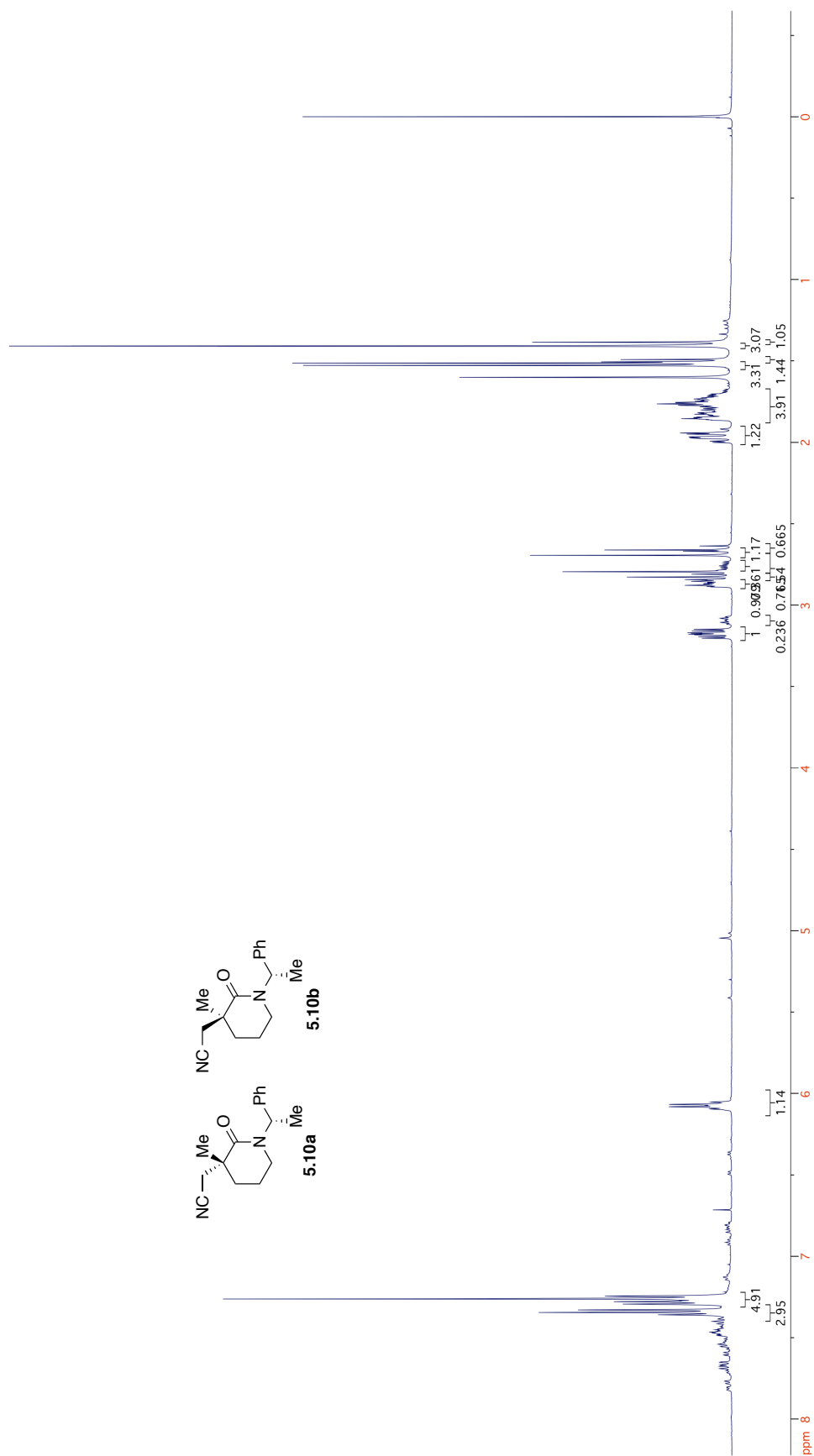
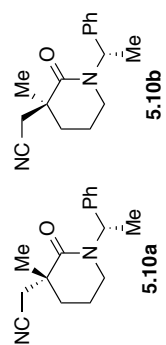


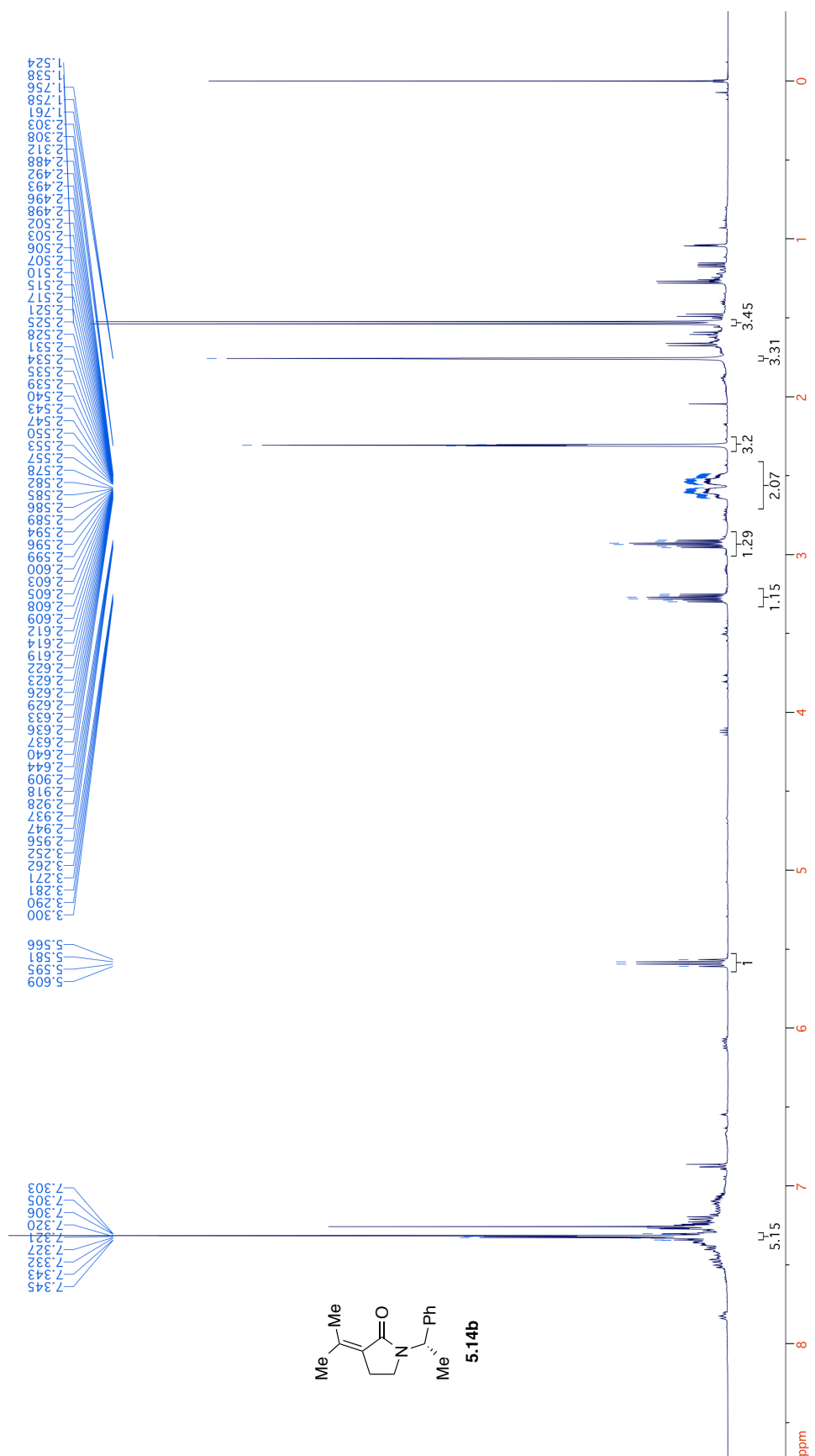


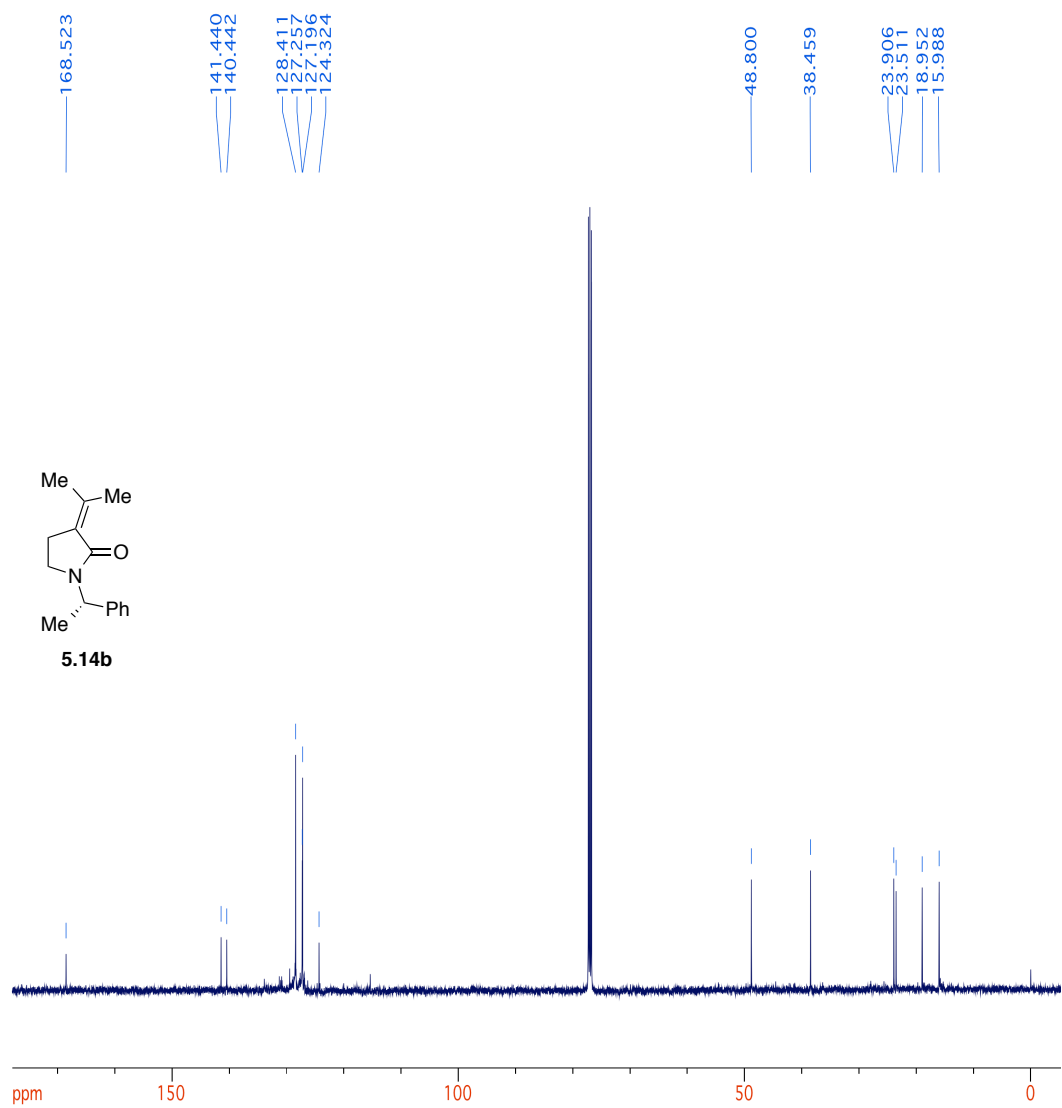


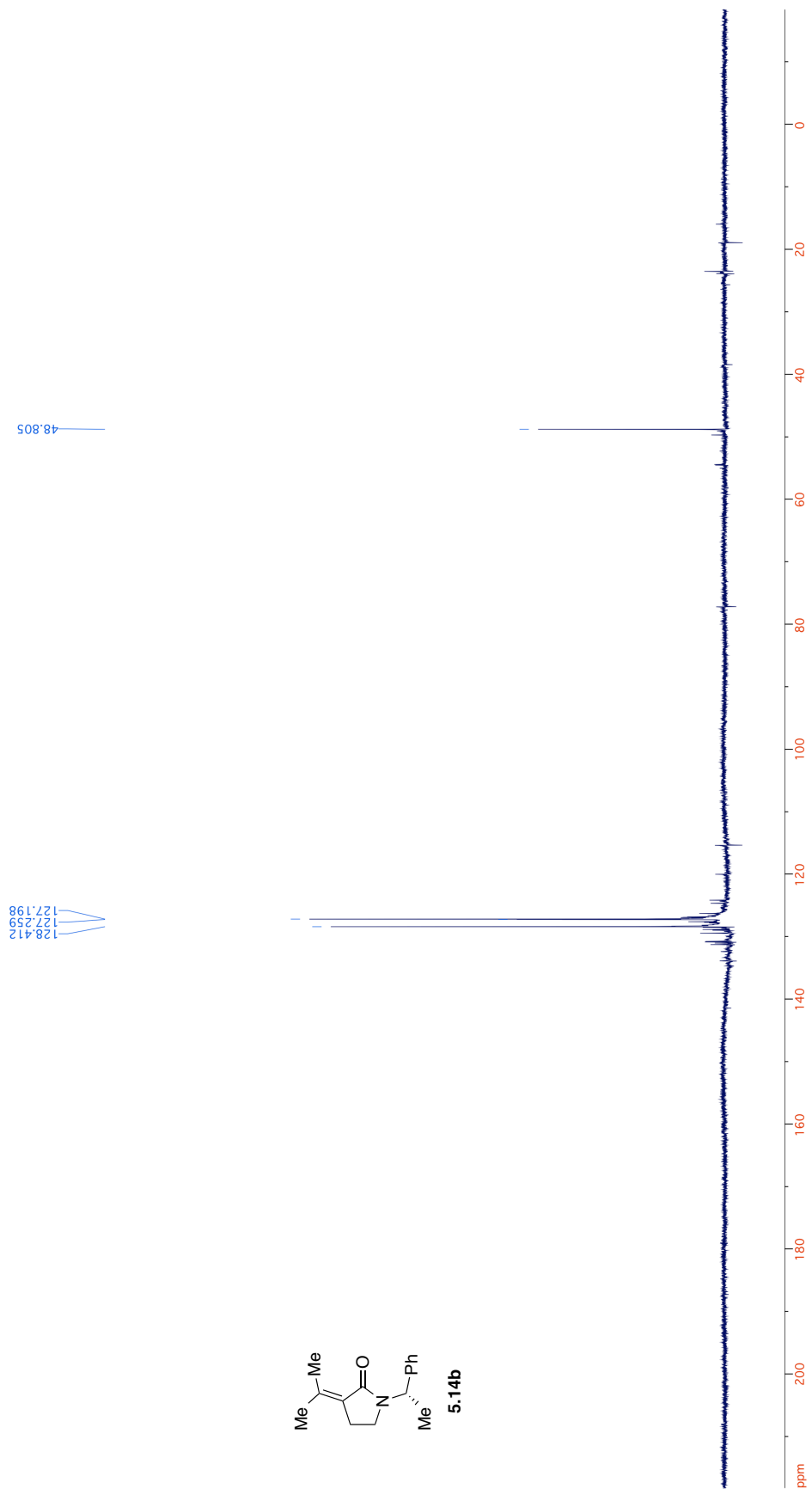
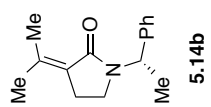


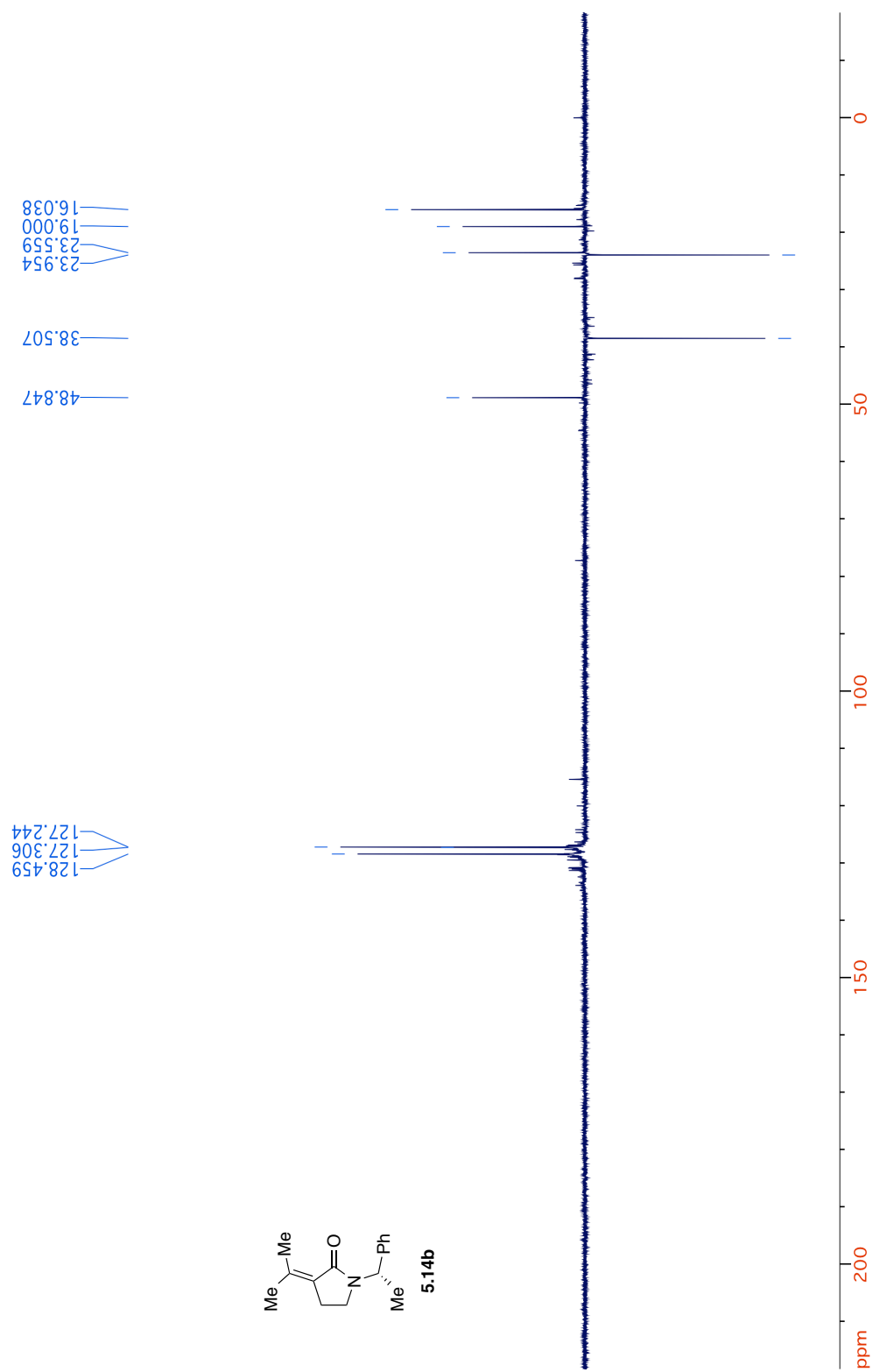
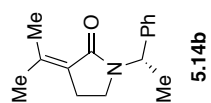


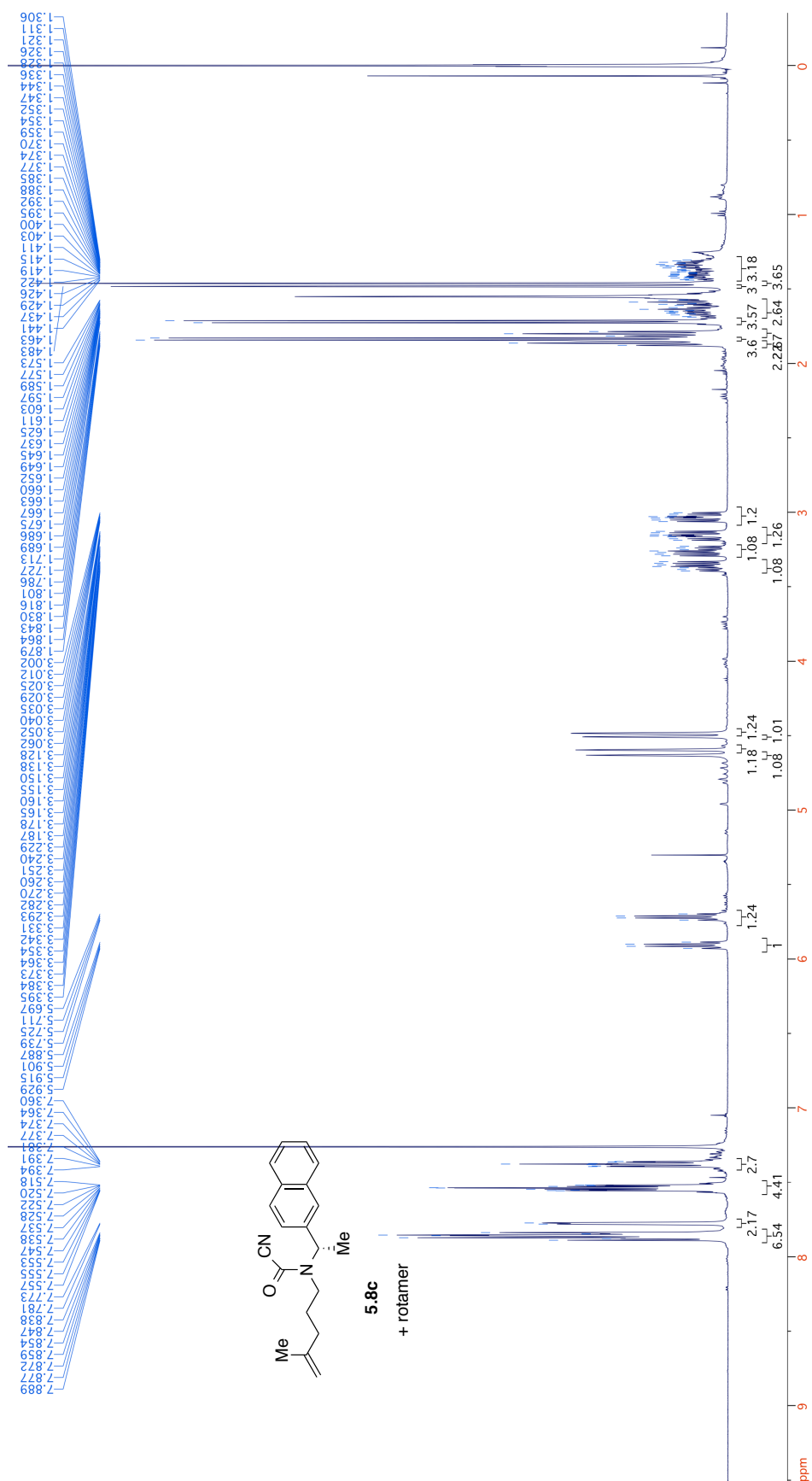


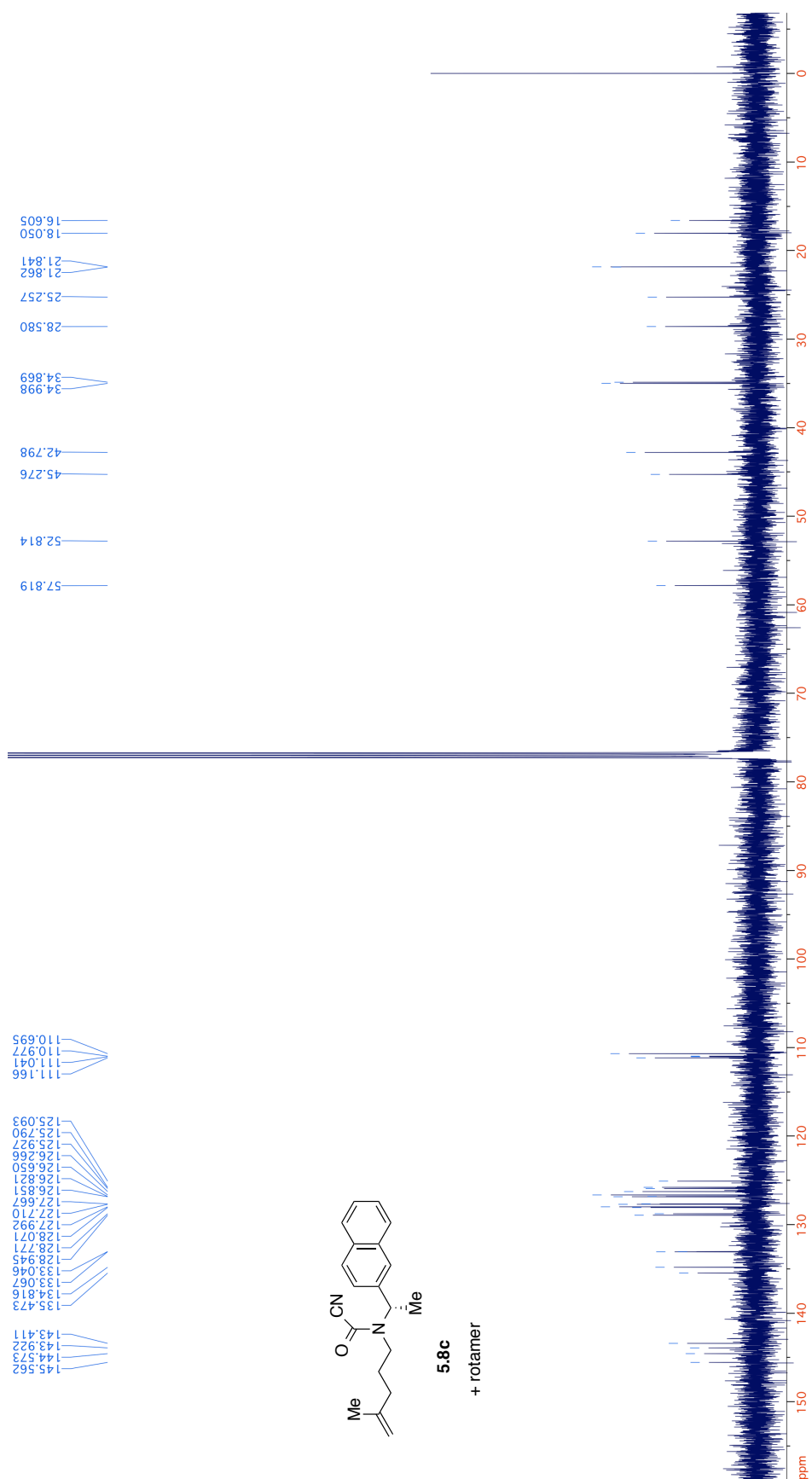


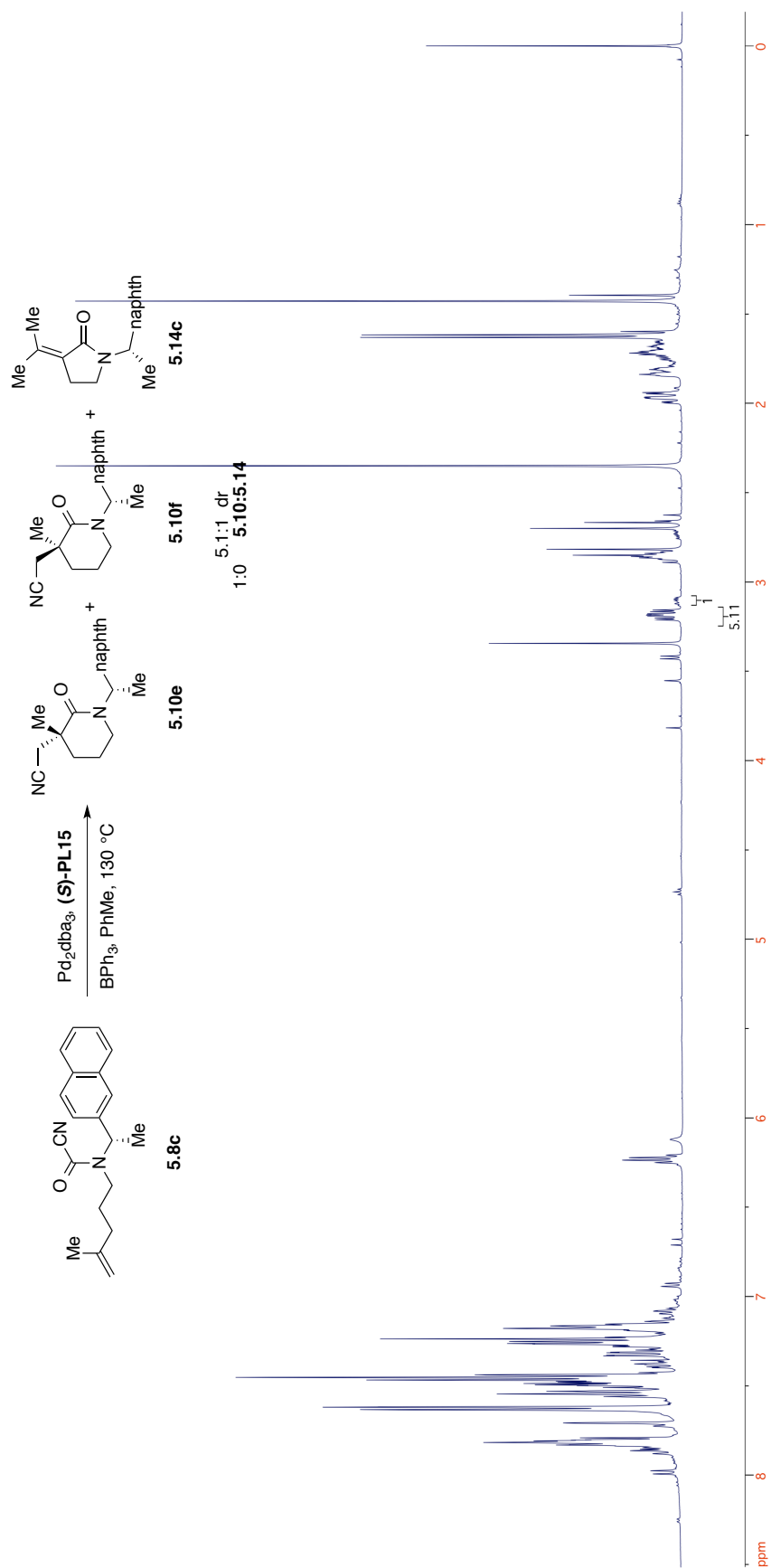


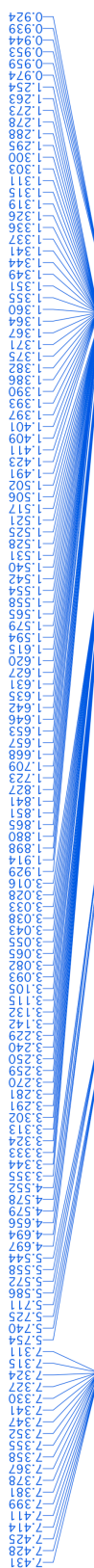
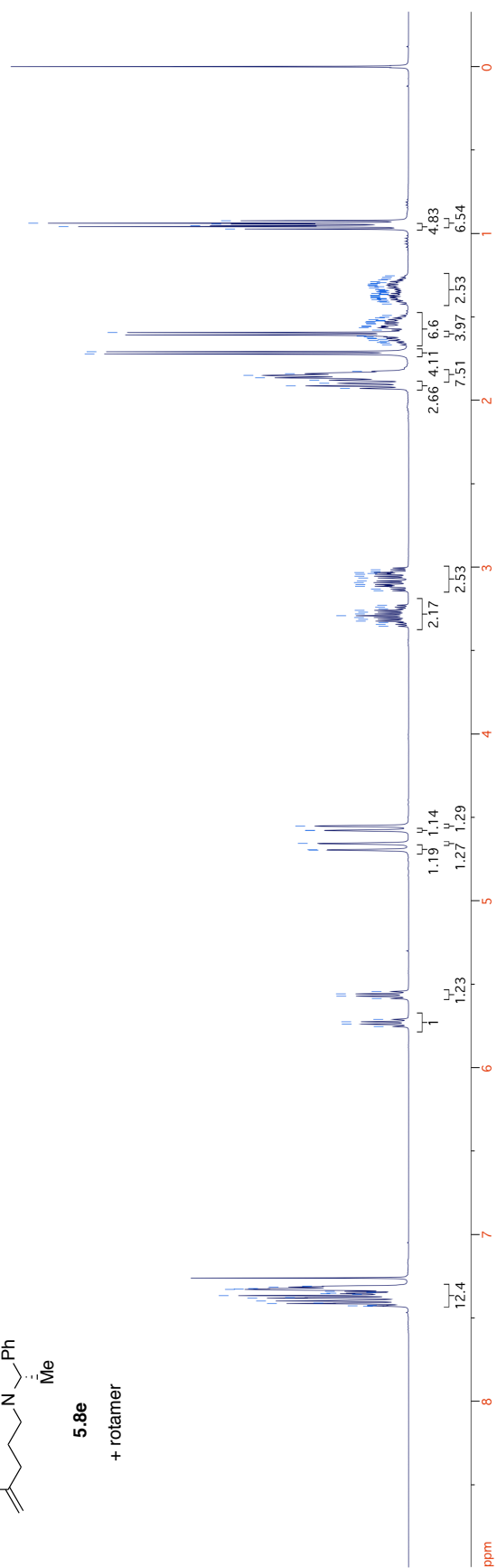
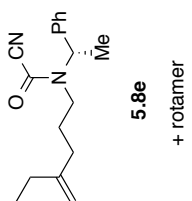


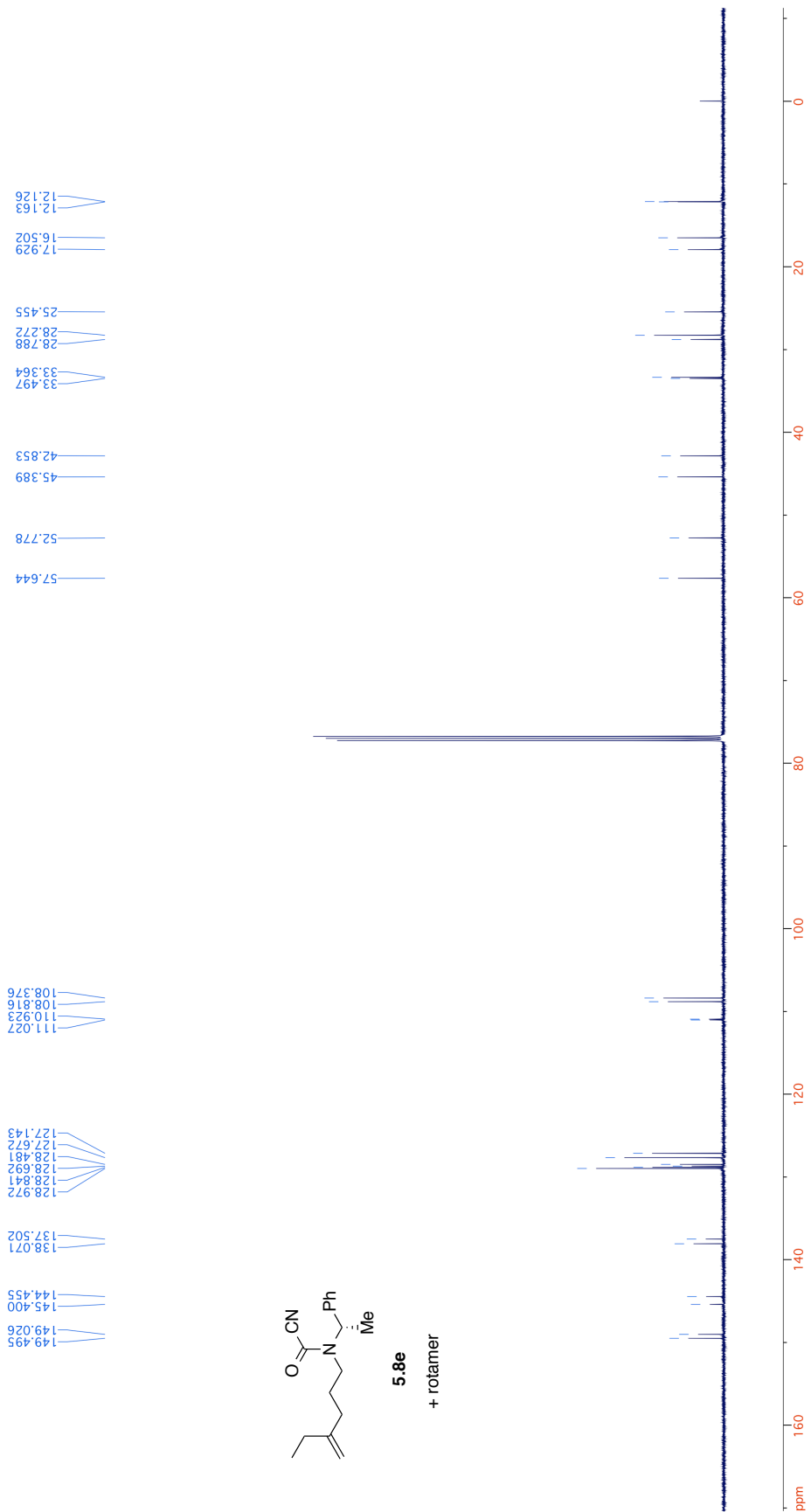
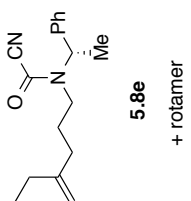


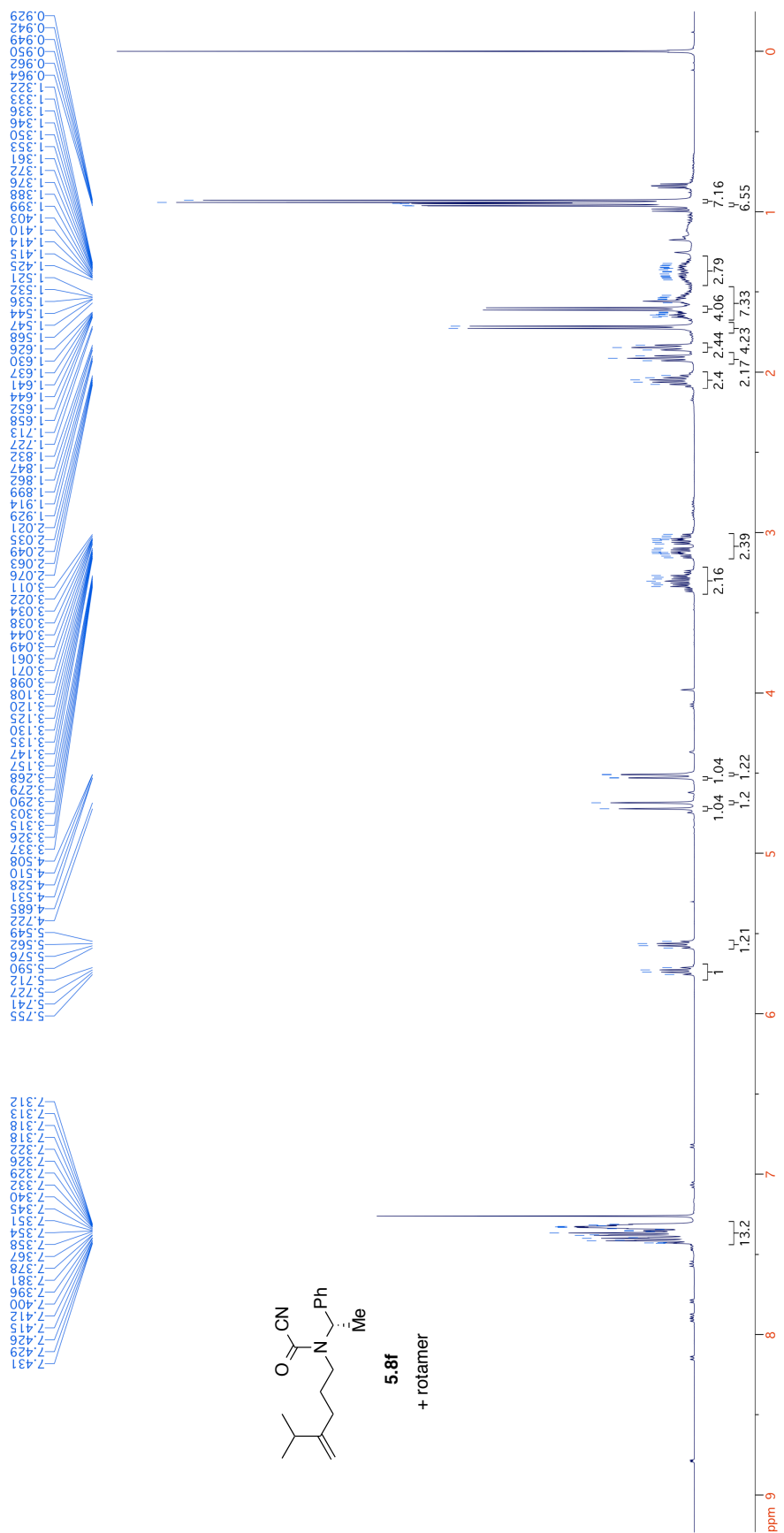


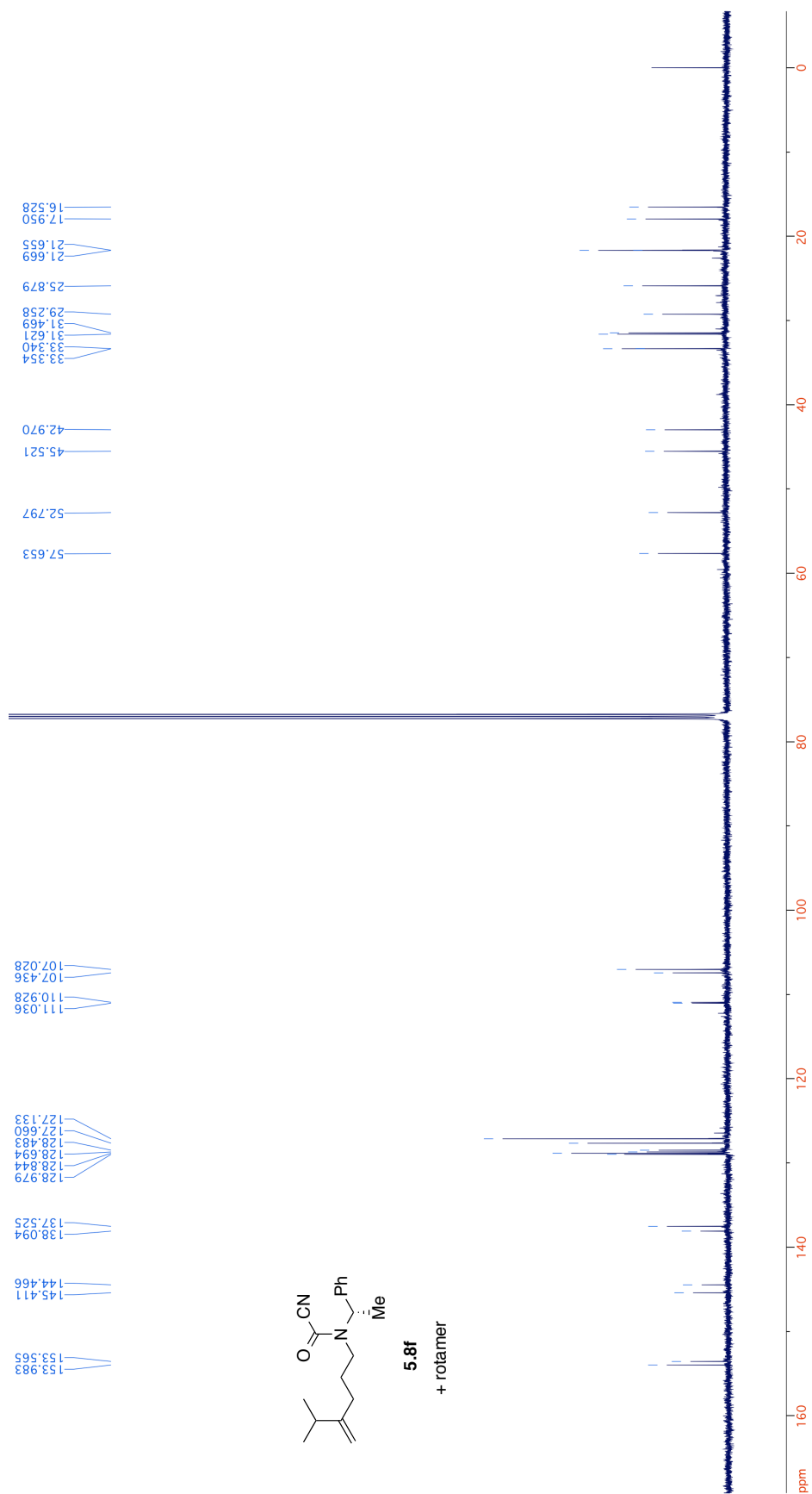


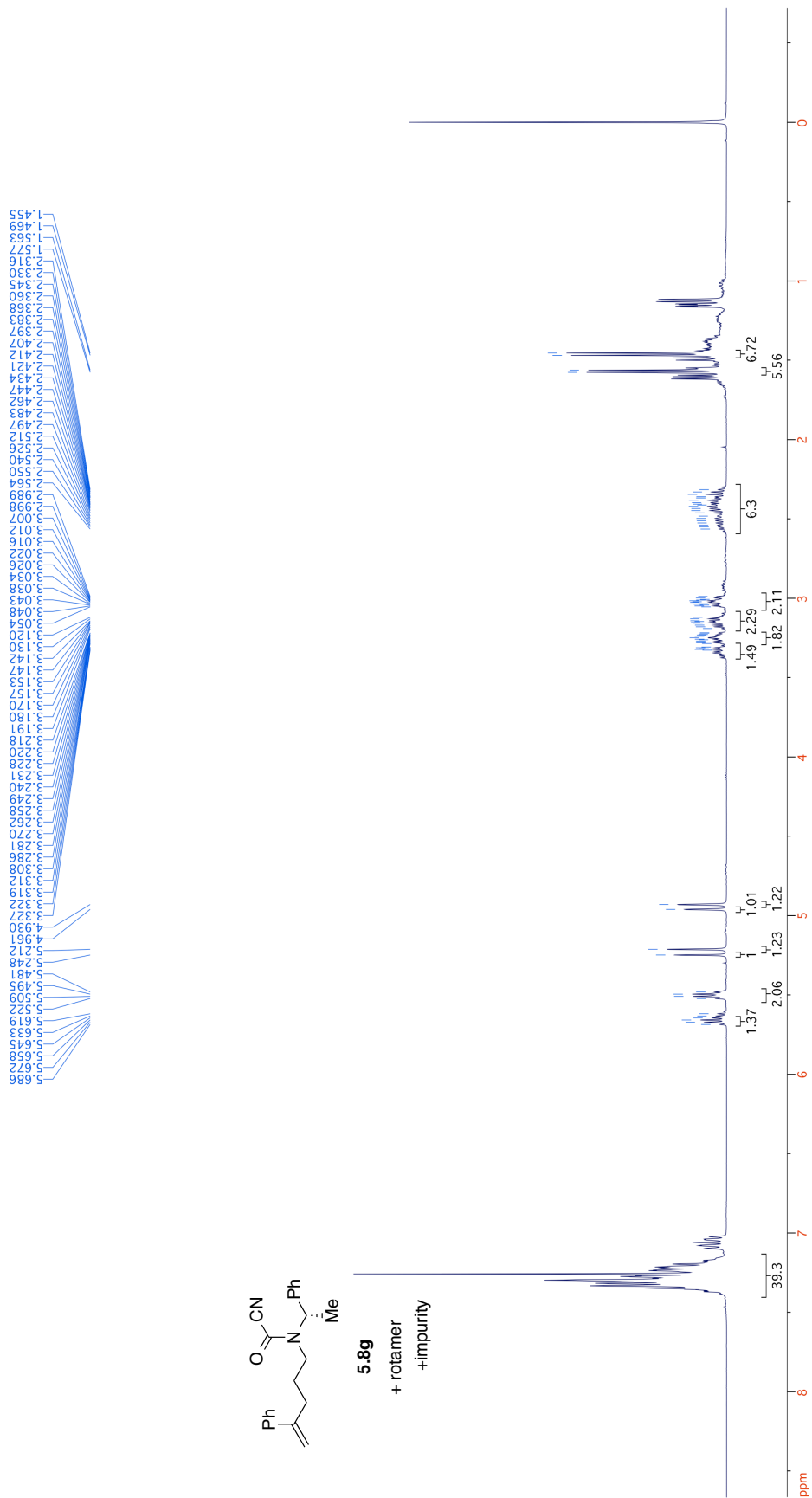
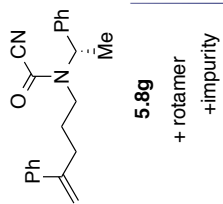


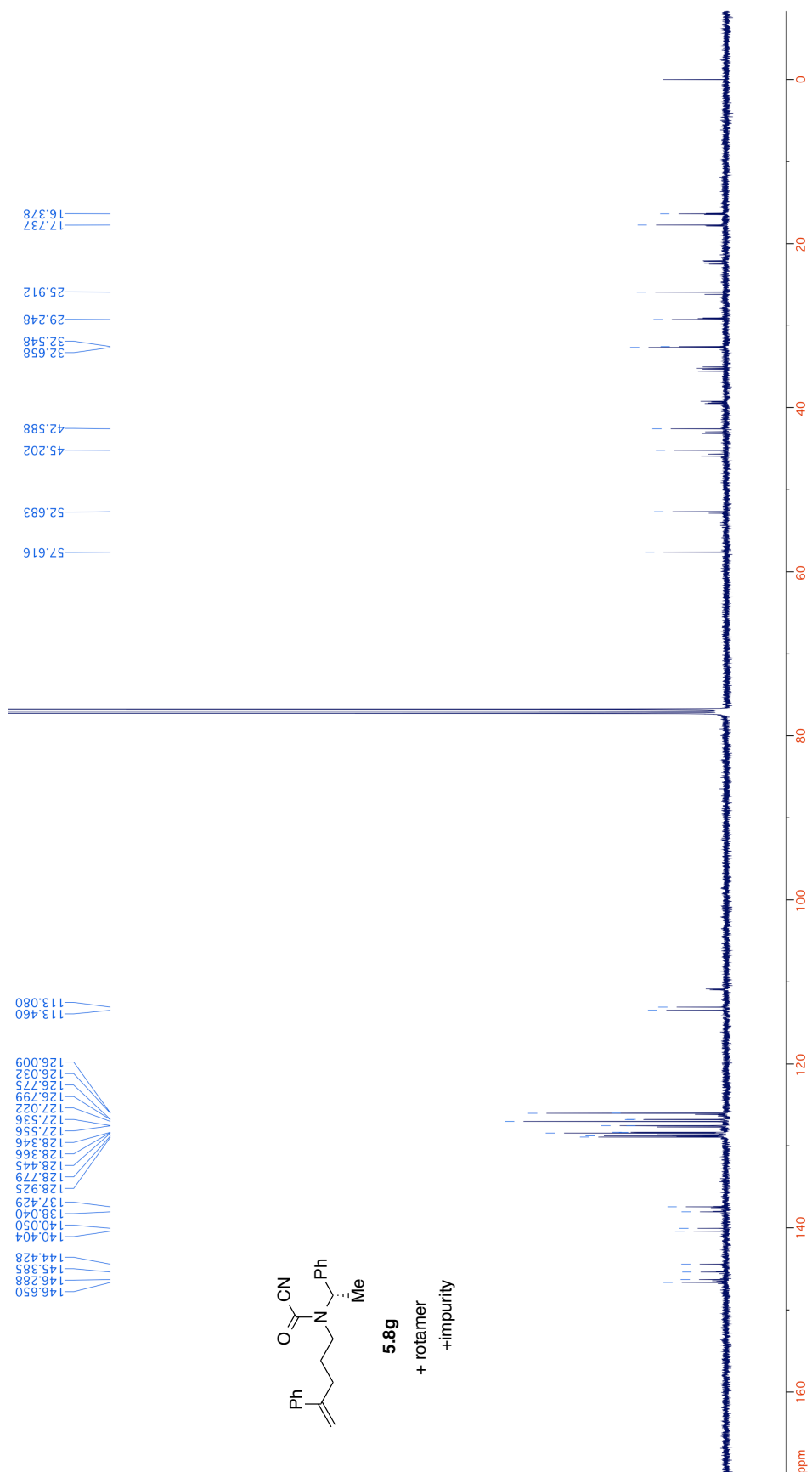


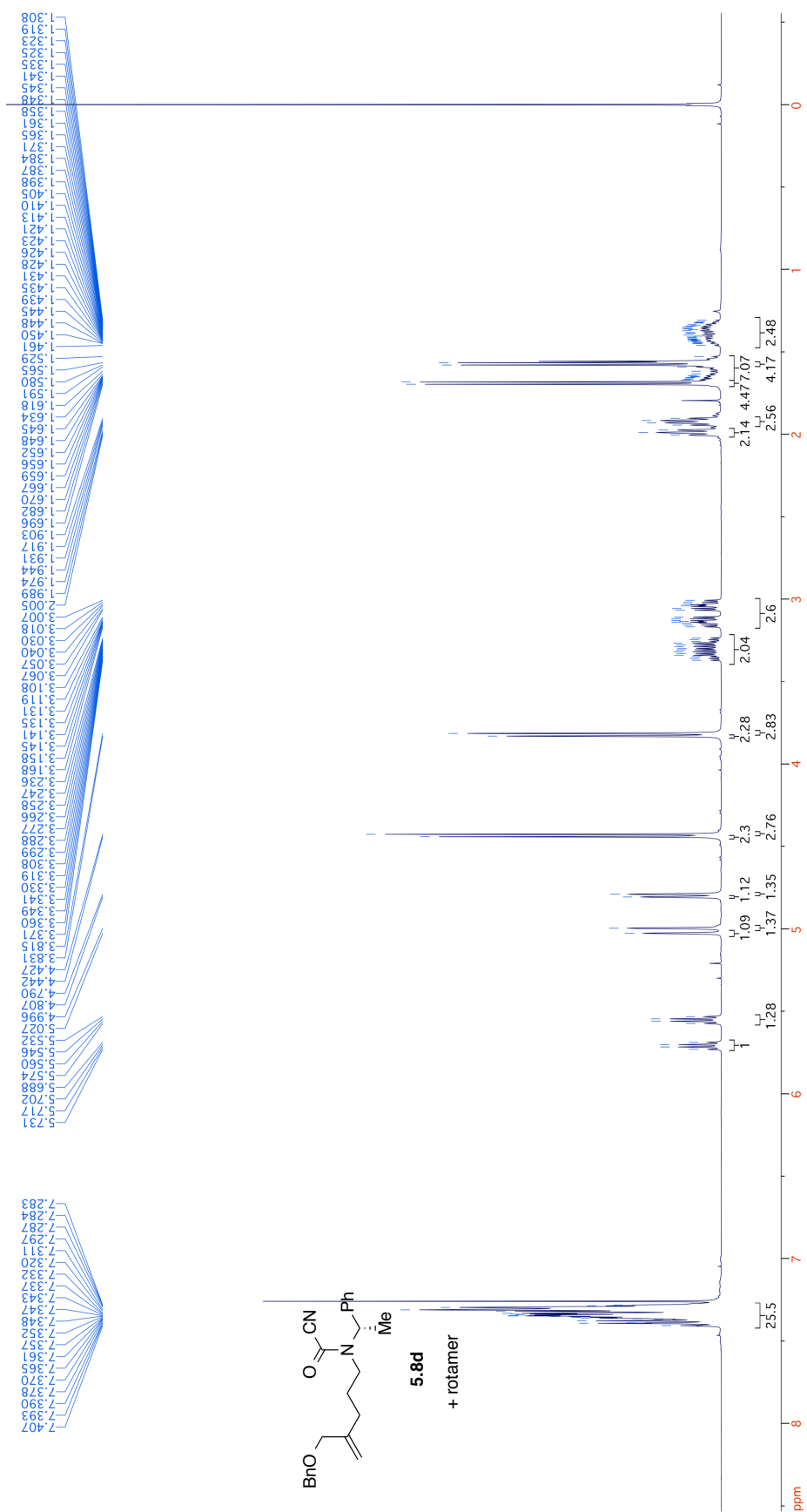


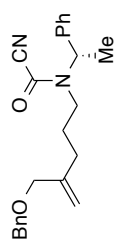












5.8d

+ rotamer

